

Palladium and gold N-heterocyclic carbene complexes: synthesis and catalytic applications

Caroline Magdalene Zinser

A thesis submitted for the degree of PhD
at the
University of St Andrews



2019

Full metadata for this item is available in
St Andrews Research Repository
at:

<http://research-repository.st-andrews.ac.uk/>

Identifier to use to cite or link to this thesis:

DOI: <https://doi.org/10.17630/10023-17066>

This item is protected by original copyright

Candidate's declaration

I, Caroline Magdalene Zinser, do hereby certify that this thesis, submitted for the degree of PhD, which is approximately 70,000 words in length, has been written by me, and that it is the record of work carried out by me, or principally by myself in collaboration with others as acknowledged, and that it has not been submitted in any previous application for any degree.

I was admitted as a research student at the University of St Andrews in September 2014.

I received funding from an organisation or institution and have acknowledged the funder(s) in the full text of my thesis.

Date

Signature of candidate

Supervisor's declaration

I hereby certify that the candidate has fulfilled the conditions of the Resolution and Regulations appropriate for the degree of PhD in the University of St Andrews and that the candidate is qualified to submit this thesis in application for that degree.

Date

Signature of supervisor

Permission for publication

In submitting this thesis to the University of St Andrews we understand that we are giving permission for it to be made available for use in accordance with the regulations of the University Library for the time being in force, subject to any copyright vested in the work not being affected thereby. We also understand, unless exempt by an award of an embargo as requested below, that the title and the abstract will be published, and that a copy of the work may be made and supplied to any bona fide library or research worker, that this thesis will be electronically accessible for personal or research use and that the library has the right to migrate this thesis into new electronic forms as required to ensure continued access to the thesis.

I, Caroline Magdalene Zinser, confirm that my thesis does not contain any third-party material that requires copyright clearance.

The following is an agreed request by candidate and supervisor regarding the publication of this thesis:

Printed copy

Embargo on all of print copy for a period of 5 years on the following ground(s):

- Publication would preclude future publication

Supporting statement for printed embargo request

The work presented in Chapters 4,5,6 and 7 has not been published yet.

Electronic copy

Embargo on all of electronic copy for a period of 5 years on the following ground(s):

- Publication would preclude future publication

Supporting statement for electronic embargo request

The work in Chapters 4,5,6,7 has not been published yet.

Title and Abstract

- I require an embargo on the abstract only.

Date

Signature of candidate

Date

Signature of supervisor

Underpinning Research Data or Digital Outputs

Candidate's declaration

I, Caroline Magdalene Zinser, understand that by declaring that I have original research data or digital outputs, I should make every effort in meeting the University's and research funders' requirements on the deposit and sharing of research data or research digital outputs.

Date

Signature of candidate

Permission for publication of underpinning research data or digital outputs

We understand that for any original research data or digital outputs which are deposited, we are giving permission for them to be made available for use in accordance with the requirements of the University and research funders, for the time being in force.

We also understand that the title and the description will be published, and that the underpinning research data or digital outputs will be electronically accessible for use in accordance with the license specified at the point of deposit, unless exempt by award of an embargo as requested below.

The following is an agreed request by candidate and supervisor regarding the publication of underpinning research data or digital outputs:

Embargo on all of electronic files for a period of 5 years on the following ground(s):

- Publication would preclude future publication

Supporting statement for embargo request

The work in Chapters 4,5,6 and 7 has not been published yet

Title and Description

- I require an embargo on the title and description

Date

Signature of candidate

Date

Signature of supervisor

Acknowledgements

First of all I would like to thank Steven Nolan and Catherine Cazin for given me the opportunity to carry out my PhD under their supervision. Thank you both for all your guidance and support through an unusual PhD journey. A special thanks goes to Paul Kamer, for accepted me into his research group and guidance throughout a difficult time.

I would also like to thank Andy Smith, for all his help and support and letting me finish my PhD in his group.

A very big thank you goes to Fady Nahra, I could have not done it without you! Thank you for all your help and putting up with my chaos. I was very lucky working with you.

My AstraZeneca supervisor Rebecca Meadow, thank you very much for all the support and help.

I was very lucky meeting a lot of amazing very talented people in the four research groups I was a part of.

The Nolan group, thank you all for an amazing first year, especially Fred Izquierdo, Enrico Marelli, Lorenzo Piola, Rik Veenboer and Danila Gasperini. You all became very important to me and I will never forget you!

The Cazin group; Orlando Santoro, Alberto Gomez-Herrera, Mathieu Lesieur and especially Marie Vasseur, you became a dear friend and I am very glad I had the opportunity to get to know you.

The Kamer group; Amanda Jarvis, Ciaran Lahive, Luke Shaw and Yiping Shi, you all helped me so much and I cannot thank you enough for this.

Last but not least The ADS group, my last group. I had such a good time with all of you, thank you so much for accepting me in the group and making my last year unforgettable. A very special thank you to Claire Young for all your help! A big thanks goes to my closest friend Nastja Matviitsuk, I am so glad I met you. I would also like to thank, Stephanie, Jude, Stefania, Calum and Jaci for all the help and fun in the lab. Lastly Sam Lawrence, thank you very much for all the coffee breaks, chats and your friendship.

I would like to thank everyone at the University of St Andrews, who helped me one way or another and AstraZeneca for the funding and the amazing 3 months placement.

The biggest thank you is for my parents, Sonja and Walter, for always believing in me, even when I did not believe in myself. My dearest siblings, Christian, Steffen and Maggy, one way or another, you all contributed to this. My sisters, Cindy and Diana thank you for all your support and laughter.

My best friend and almost sister Claudia Hohmann for always being by my side.

Authors Contribution

The research described in this thesis is partially published in peer-reviewed journals.

Chapter 2:

Caroline M. Zinser, Fady Nahra, Marcel Brill, Rebecca E. Meadows, David B. Cordes, Alexandra M. Z. Slawin, Steven P. Nolan and Catherine S. J. Cazin, *ChemCommun.*, **2017**, *53*, 7990-7993.

David B. Cordes carried out the X-Ray diffraction analysis.

Chapter 3:

Caroline M. Zinser, Katie G. Warren, Rebecca E. Meadows, Fady Nahra, Abdullah M. Al-Majid, d Assem M. Barakat, Mohammad S. Islam, Steven P. Nolan and Catherine S. J. Cazin, *Green Chemistry*, **2018**, manuscript accepted.

Katie Warren was assisting with the base/solvent optimisation.

Chapter 4:

Katie Warren was assisting partially with the base/solvent optimisation.

The synthesis of the biologically interesting substrates was carried out by Abdullah Al.Majid, Assem Barakat and Mohammad Shahidul Islam from King Saud University in Saudi Arabia

Chapter 5:

David B. Cordes carried out the X-Ray diffraction analysis.

Chapter 6:

All work was carried out by myself.

Chapter 7:

David B. Cordes carried out the X-Ray diffraction analysis.

Computational analysis were obtained by Laura Falivene and Luigi Cavallo

Publications not mentioned in this thesis:

Marcel Brill, Fady Nahra, Alberto Gomez-Herrera, Caroline Zinser, David B. Cordes, Alexandra M. Z. Slawin and Steven P. Nolan, *ChemCatChem*, **2017**, *9*, 117-120.

Frederic Izquierdo[#], Caroline Zinser[#], Yury Minenkov, David. B. Cordes, Alexandra M. Z. Slawin, Luigi Cavallo, Fady Nahra, Catherine S. J. Cazin and Steven P. Nolan, *ChemCatChem*, **2018**, *10*, 601-611

Abstract

Palladium and gold-N-heterocyclic carbene (NHC) complexes have been studied in detail, with focus on their synthesis and applications.

Palladium(II)-NHC complexes are known to be highly catalytically active complexes for numerous organic reactions, specifically $[\text{PdCl}(\eta^3\text{-R-allyl})(\text{NHC})]$ complexes are widely used in cross-coupling chemistry. Based on this, an optimised, more facile and most importantly air-stable synthesis was developed (Chapter 2). The preparation of a new class of Pd(II)-NHC complexes, $[\text{NHC}\cdot\text{H}][\text{Pd}(\eta^3\text{-R-allyl})\text{Cl}_2]$, was optimised and applied to a wide range of NHC ligands (Chapter 2). Furthermore, the catalytic activity of $[\text{NHC}\cdot\text{H}][\text{Pd}(\eta^3\text{-R-allyl})\text{Cl}_2]$ was intensely studied in cross-coupling chemistry (Chapter 3-6).

An environmentally friendly protocol was established for the Suzuki-Miyaura reaction using $[\text{NHC}\cdot\text{H}][\text{Pd}(\eta^3\text{-R-allyl})\text{Cl}_2]$ in low catalyst loading. Both, the synthesis of the pre-catalysts as well as the catalysis can be carried out under air and the mild conditions and enabled a diverse substrate scope (Chapter 3).

The formation of C-N bonds is widely studied and of importance due to their appearance in a wide range of molecules, particular in pharmaceutical reagents and natural products. $[\text{IPr}^*\cdot\text{H}][\text{Pd}(\eta^3\text{-cin})\text{Cl}_2]$ was found to be a highly catalytically active pre-catalyst in the Buchwald-Hartwig amination as well as in ketone arylation (Chapter 4). Low catalyst loading, the use of a green solvent and high yields created an efficient protocol.

An extensive study of the effect of different R-allyl ligands was performed for the Mizoroki-Heck reaction (Chapter 5). Different $[\text{NHC}\cdot\text{H}][\text{Pd}(\eta^3\text{-R-allyl})\text{Cl}_2]$ pre-catalysts were tested and the catalysis was optimised resulting in very low catalyst loading (0.1 mol%). Biologically interesting heteroatom-containing aryl bromides were successfully coupled with styrene.

The catalytic activity of $[\text{NHC}\cdot\text{H}][\text{Pd}(\eta^3\text{-R-allyl})\text{Cl}_2]$ was further extended to the C-H activation of terminal alkynes with aryl bromides (Chapter 6). The catalysis tolerated substrates containing electron donating and withdrawing substituents. Furthermore the dimerization of terminal alkynes to 1,3-enynes was investigated resulting in excellent yields.

Transition-Novel Au(I)-NHC complexes, namely $[\text{Au}(\text{Bpin})(\text{NHC})]$ were synthesised and fully characterised. In total, four complexes bearing different NHCs were synthesised and their reactivity studied, revealing unique characteristics (Chapter 7).

Abbreviations

$\%V_{\text{Bur}}$	Percent Buried Volume
ν_{CO}	CO stretching frequency
ν_{av}	average stretching frequency
acac	acetylacetonate
Amphos	4-di- <i>tert</i> -butylphosphino- <i>N,N'</i> -dimethylaniline
B ₂ pin ₂	bis(pinacolato)diboron
BDE	bond dissociation enthalpy
BSE	bond snapping energy
2-Br-pyr	2-bromopyridine
BrettPhos	2-di(cyclohexylphosphino)3,6-dimethoxy-2',4',6'- triisopropyl-1-1'-biphenyl
cin	cinnamyl
cod	1,5-cyclooctadiene
CPME	cyclopentylmethyl ether
<i>c</i>	speed of light
DavePhos	2-dicyclohexylphosphine-2'-(<i>N,N</i> - dimethylamino)biphenyl
DABCO	1,4-diazabicyclo(2,2,2)octane
dba	dibenzylideneacetone
DMA	dimethylacetamide
DMI	1,3-dimethyl-2-imidazolidinone
DME	1,2-dimethoxyethane
DMF	dimethylformamide
DMS	dimethyl sulfide
DMSO	dimethyl sulfoxide
dppe	1,2-bis(diphenylphosphino)ethane
EDA	energy decomposition analysis
ΔE_{elstat}	electrostatic interaction term
HBpin	4,4,5,5-tetramethyl-1,3,2-dioxaborolane

HOMO	highest occupied molecular orbital
IAd	<i>N,N'</i> -bis-(adamantyl)imidazol-2-ylidene
IBiox	bioxazoline-derived carbene
I ^t Bu	<i>N,N'</i> -(di- <i>tert</i> -butyl)imidazol-2-ylidene
IHept	<i>N,N</i> -bis-[2,6-bis(di- <i>iso</i> -heptylyl)phenyl]imidazol-2-ylidene
IHept ^{Cl}	<i>N,N</i> -bis-[2,6-bis(di- <i>iso</i> -heptylyl)phenyl-4,5-dichloro]imidazol-2-ylidene
IHept ^{OMe}	<i>N,N'</i> -bis(2,6-di-4-heptyl-4-methoxyphenyl)imidazol-2-ylidene
IMe	<i>N,N'</i> -dimethylimidazol-2-ylidene
IMes	<i>N,N'</i> -bis-[2,4,6-(trimethyl)phenyl]imidazol-2-ylidene
INon	<i>N,N</i> -bis-[2,6-bis(di- <i>iso</i> -nonyl)phenyl]imidazol-2-ylidene
IPent	<i>N,N</i> -bis-[2,6-bis(di- <i>iso</i> -pentylyl)phenyl]imidazol-2-ylidene
IPent ^{Cl}	<i>N,N</i> -bis-[2,6-bis(di- <i>iso</i> -pentylyl)phenyl-4,5-dichloro]imidazol-2-ylidene
IPr	<i>N,N'</i> -bis-[2,6-(di- <i>iso</i> -propyl)phenyl]imidazol-2-ylidene
IPr ^{Cl}	<i>N,N</i> -bis-[2,6-(di- <i>iso</i> -propyl)phenyl-4,5-dichloro]imidazol-2-ylidene
IPr*	<i>N,N</i> -bis-[2,6-bis(diphenylmethyl)-4-methylphenyl]imidazol-2-ylidene
IPr* ^{2-Np}	<i>N,N</i> -bis-[2,6-bis(dinaphtalene)-4-methylphenyl]imidazol-2-ylidene
IPr* ^{OMe}	<i>N,N</i> -bis-[2,6-bis(diphenyl)-4-methoxyphenyl]imidazol-2-ylidene
<i>i.e.</i>	Id est
Ind ^{tBu}	1- <i>tert</i> -butyl-1H-indene
LUMO	lowest unoccupied molecular orbital
L	ligand
MAO	monoamine oxidase

m	corrected mass
m_0	non-relativistic mass
M	metal
nbd	norbornadiene
NHC	N-heterocyclic carbene
NMP	<i>N</i> -methyl-2-pyrrolidinone
NTf ₂	bis-(trifluoromethane sulfonyl)imide
ΔE_{int}	orbital interaction
OTf	trifluoromethanesulfonate
PEPPSI	Pyridine-Enhanced Precatalyst Preparation, Stabilisation and Initiation
ppm	parts per million
pyr	pyridine
ΔE_{Pauli}	Pauli repulsion term
RuPhos	2-dicyclohexylphosphino-2',6'-diisopropoxybiphenyl
SI ^t Bu	<i>N,N'</i> -(di- <i>tert</i> -butyl)imidazolidin-2-ylidene
SIPr	<i>N,N</i> -bis-[2,6-(di- <i>iso</i> -propyl)phenyl]imidazolidin-2-ylidene
SIMes	<i>N,N</i> -bis-(2,4,6-trimethylphenyl)imidazolidin-2-ylidene
SPhos	2-dicyclohexylphosphino-2'-6'-dimethoxybiphenyl
ΔE_0	steric interaction
TEP	Tolman electronic parameter
TEA	triethylamine
THF	tetrahydrofuran
TON	turnover number
TOF	turnover frequency
TBA	<i>tetra</i> -butylammonium
<i>t</i> -BuBrettPhos	2-(di- <i>tert</i> -butylphosphino)-2',4',6'-triisopropyl-3,6-dimethoxy-1,1'-biphenyl
Tol-BINAP	2,2'-bis (di- <i>p</i> -tolyl)phosphinol-1,1'-binaphthyl
TBAE	2-(<i>tert</i> -butylamino)ethanol

TBAB	tetrabutylammonium bromide
TBAOAc	tetrabutylammonium acetate
TM	Transition metal
TMEDA	<i>N,N,N',N'</i> -tetramethylethylenediamine
v	velocity
WOLEDs	white organic light-emitting devices
XPhos	2-dicyclohexylphosphino,2',4',6'-triisopropylbiphenyl
Xantphos	4,5-bis(diphenyl)phosphino-9,9-dimethylxanthene
Z	atomic number

Table of Content

Declaration	i
Acknowledgements	iv
Authors contribution	v
Abstract	iv
Chapter 1: Introduction	1
1.1. N-Heterocyclic Carbenes.....	1
1.1.1. Electronic and Steric Features.....	4
1.1.2. Synthesis.....	8
1.2. Palladium-NHC Complexes.....	12
1.2.1. Introduction and General Synthesis	12
1.2.2. Applications of Pd-NHC Complexes.....	16
1.3. References.....	26
Chapter 2: A straightforward synthesis of [PdCl(η^3-R-allyl)(NHC)] complexes	31
2.1. Introduction to [PdCl(η^3 -R-allyl)(NHC)] Complexes.....	31
2.2. General Synthesis of [PdCl(η^3 -R-allyl)(NHC)] Complexes	32
2.2 Optimisation of the Synthesis of [PdCl(η^3 -R-allyl)(NHC)] Complexes	35
2.3 Synthesis of [NHC·H][Pd(η^3 -allyl)Cl ₂] Complexes	41
2.4 Conclusion	46
2.5 References.....	47
Chapter 3: Investigation into the catalytic activity of [NHC·H][Pd(R)Cl₂] complexes in the Suzuki-Miyaura reaction	50
3.1 The Suzuki-Miyaura Reaction.....	50
3.2 Initial catalytic tests using [NHC·H][Pd(R)Cl ₂] complexes.	59
3.3 Optimisation of the Suzuki-Miyaura reaction using [IPr·H][Pd(η^3 -cin)Cl ₂] as pre-catalyst ...	64
3.4 Conclusion	71
3.5 References.....	72
Chapter 4: Highly catalytically active Pd-NHC pre-catalyst for the formation of C-N and C-C bonds	74
4.1 The Buchwald-Hartwig reaction.....	74
4.2 Optimisation of the Buchwald-Hartwig Reaction using [IPr*·H][Pd(η^3 -cin)Cl ₂]	81
4.3 Using [IPr*·H][Pd(η^3 -cin)Cl ₂] in the α -Ketone Arylation Reaction.....	91
4.3.1. Results and Discussion	94

4.4 Conclusion	95
4.5 References	96
Chapter 5: Study of different throw-away ligands of [NHC-H][Pd(L)Cl₂] complexes and its effect in the Mizoroki-Heck reaction	100
5.1 The Mizoroki-Heck Reaction	100
5.2 Results and Discussion	109
5.3 Conclusion	122
5.4 References.....	123
Chapter 6: Palladium catalysed C-H activation of alkynes with aryl halides.....	126
6.1 The Sonogashira Reaction	126
6.2. Results and Discussion	135
6.3. Catalytic Dimerisation of Terminal Alkynes	144
6.4. Conclusion	147
6.5 References	148
Chapter 7: Synthesis and application of [Au(NHC)(Bpin)] complexes	150
7.1 Introduction to Gold Chemistry	150
7.1.1 Reactivity of Gold Complexes.....	150
7.2 Introduction to Au(I)- NHC complexes	153
7.2.1 Synthesis of Cationic Au(I)-NHC Complexes.....	153
7.2.2 Synthesis of Neutral Au(I)-NHC Complexes.....	154
7.2.3. Catalytic Applications of Au(I)-NHC Complexes	155
7.3 Introduction to Transition Metal-Boron Complexes	161
7.4 Synthesis of [Au(NHC)(Bpin)] Complexes	165
7.5 Initial reactivity studies of [Au(NHC)(Bpin)]	168
7.6 Computational Studies of [Au(IPr)(Bpin)]	170
7.7 Investigation into the reactivity of [Au(IPr)(Bpin)].....	174
7.7.1. Reactivity with Lewis bases and H ₂ activation	174
7.7.2. Reactivity with Lewis acids.....	175
7.7.3 Reactivity with alky/aryl iodide.	180
7.8 Conclusion	183
7.9 References	184
Chapter 8: Conclusion and Future Work	190
Chapter 9: Experimental Section	193
9.1 General Information.....	193
9.2 Chapter 2.....	194

9.3 Chapter 3	214
9.4 Chapter 4	238
9.5 Chapter 5	266
9.6 Chapter 6	284
9.7 Chapter 7	302
9.8 References	318

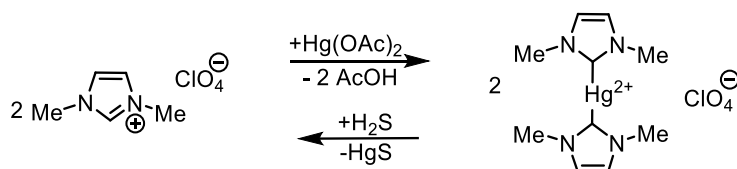
Chapter 1

Introduction

1.1 N-heterocyclic carbenes

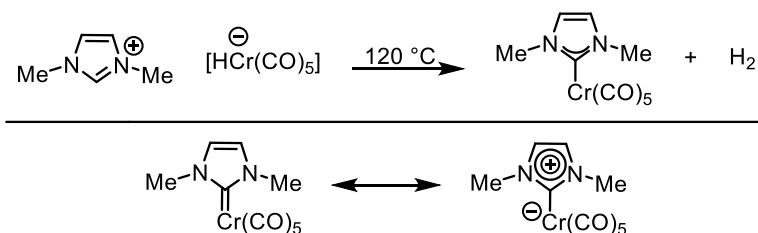
Since their discovery N-heterocyclic carbenes (NHCs) have been evolved an important role in modern chemistry.¹ Their unique characteristics enabled them to become widely used ligands in organometallic chemistry² as well as organocatalysts³ on their own. The many applications of NHCs have led to increasing interest throughout the chemistry community, resulting in NHCs being extensively studied.⁴⁻⁶ The next subchapter will introduce the history of NHCs followed by their unique steric and electronic features. The general synthesis of imidazolylidene and imidazolidinylidene will be discussed.

The pioneering work from Wanzlick^{7,8} and Öfele⁹⁻¹¹ started in the 1960s with their reports of breakthroughs in carbene chemistry. Wanzlick studied the formation of a free carbene using chloroform and subsequently its dimer formation, concluding the nucleophilic character of NHCs.⁷ This was followed by the study of the synthesis of NHC-metal complexes. By treating 1,3-diphenylimidazolium perchlorate with mercury (II) acetate in dimethyl sulfoxide (DMSO), Wanzlick prepared the first reported NHC-Hg complex (Scheme 1.1).⁸



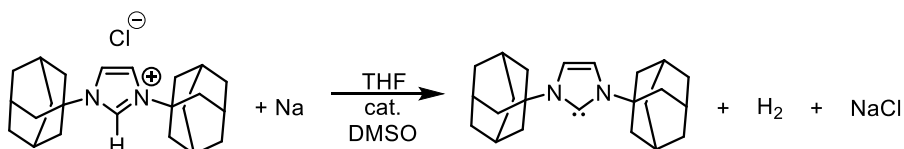
Scheme 1.1: Synthesis of the first NHC-Hg complex.⁸

In parallel, Öfele reported the formation of a surprisingly air stable $[\text{Cr}(\text{IME})(\text{CO})_5]$ (IME = *N,N'*-dimethylimidazol-2-ylidene) complex by heating a chromium imidazolium salt, $[\text{IME}][\text{HCr}(\text{CO})_5]$ (Scheme 1.2).⁹ After the report of the similar $[\text{Fe}(\text{IME})(\text{CO})_5]$ complex and further investigation into these complexes, it was concluded that the stability and characteristics of these NHC-M complexes originate from their aromatic character.¹⁰



Scheme 1.2: Synthesis and proposed aromaticity of $[\text{Cr}(\text{IMe})(\text{CO})_5]$.^{9,10}

Arduengo reported the first crystalline carbene: IAd (IAd = *N,N'*-bis-(adamantyl)imidazol-2-ylidene) (Scheme 1.3). This tremendous breakthrough was thoroughly studied, showing the stability in the absence of oxygen and moisture as well as X-Ray structures which were studied in detail.¹²



Scheme 1.3: Synthesis of IAd.¹²

Further studies were conducted focusing on the halogenation of the backbone of the NHC, this resulted in a change of electronic and steric characteristics.¹³ Arduengo later reported the synthesis of imidazolylidenes and imidazolidinylidene, which will be discussed in section 1.1.3.¹⁴ Since then many different NHCs have been synthesised and reported. Figure 1.1 summarises the diversity of NHCs.¹⁵

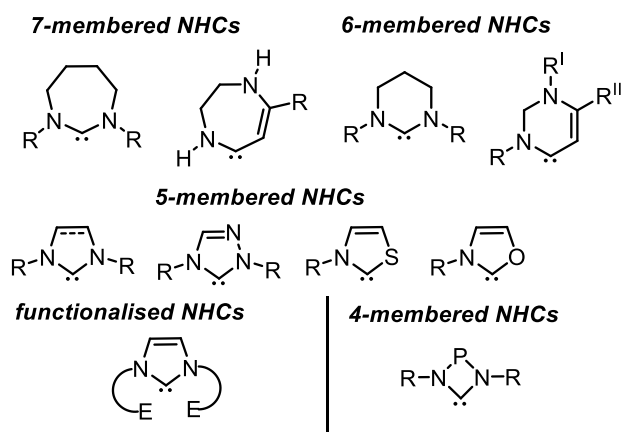


Figure 1.1: Different NHCs ligands found in literature.¹⁵

The most common NHCs used as ligands in organometallic chemistry are 5-membered NHCs. Early research as well as the amount published about 5-membered NHC reflects on their role and importance in organometallic chemistry. Imidazolylidene and Imidazolidinylidene are common ligands used in many different organometallic complexes and catalysis. This

introduction will focus mainly on symmetrical imidazole and imidazolidine as these are used in the following chapters (Figure 1.2).¹⁵

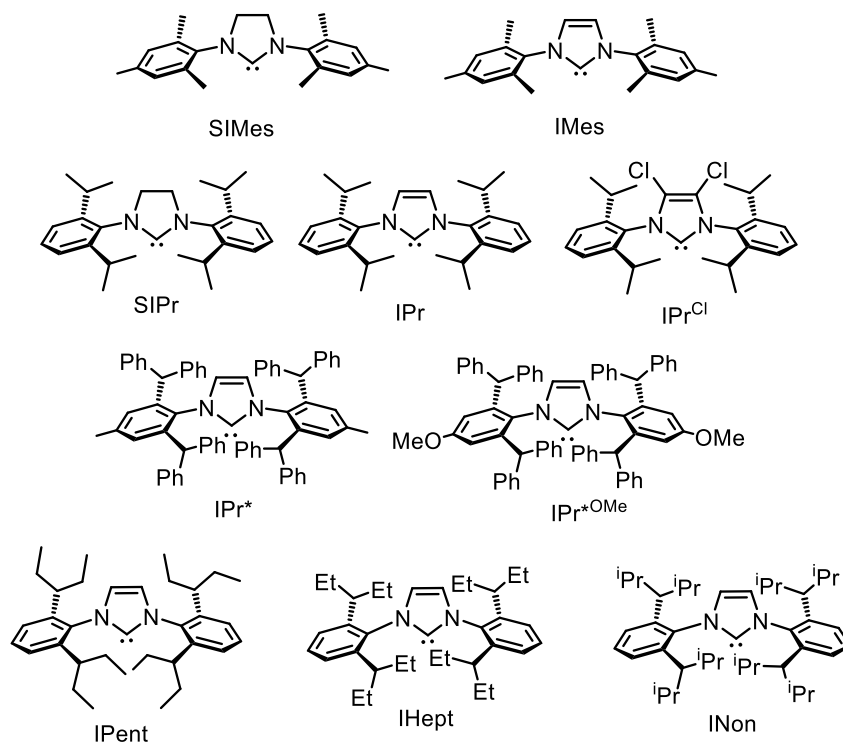


Figure 1.2: Most common 5-membered NHCs ligands used.¹⁵

The stability of NHCs was studied intensively soon after the first stable carbene was isolated.¹³ The general description of a carbene is a neutral compound bearing six valence electrons, in which two of the electrons are not involved in bonding.¹⁶ Early reports suggested the steric bulk of the IAd ligand to be responsible for its stability.¹² After the isolation of smaller NHCs it was clear that steric bulk can play a role but it is not the sole feature of its stability. The ground state spin multiplicity for a $S = 1$ system can either split into a singlet or a triplet state (Figure 1.3).¹⁷ In a singlet state the two non-bonding electrons are in the same orbital ($\sigma^2 p_{\pi}^0$, $^1A^1$).¹⁸ Fischer and co-worker reported and characterised the singlet carbene in 1964. In a triplet state the two non-bonding electrons are in two different orbitals with parallel spin ($\sigma^1 p_{\pi}^1$, $^3B^1$).¹⁸ The first high oxidation state metal alkylidene complex bearing a triplet state carbene was reported by Schrock and co-workers soon after.¹⁶ The HOMO-LUMO gap (HOMO = highest occupied molecular orbital; LUMO = lowest unoccupied molecular orbital), or singlet-triplet gap, defines the ground state spin multiplicity. The singlet state is favoured if the singlet-triplet gap is larger than 2 eV, while if the gap is smaller than 2 eV the triplet state will be favoured. Most NHCs adapt the singlet state.¹⁵ The HOMO-LUMO gap can be manipulated by the substituents on the carbene.

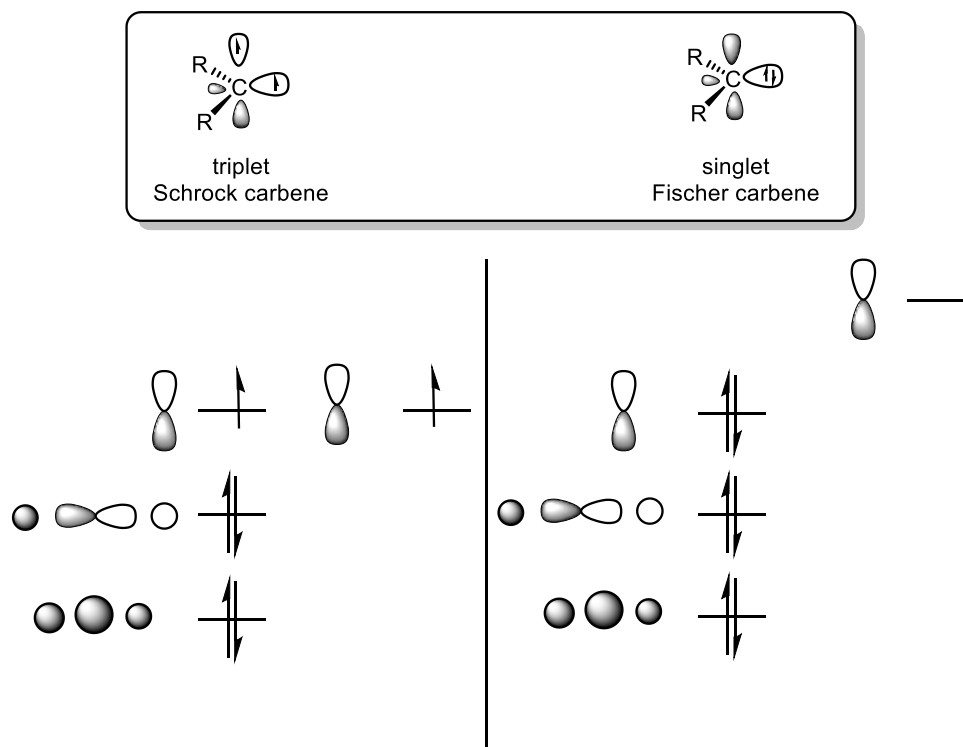


Figure 1.3: Molecular orbital diagram of Fischer and Schrock carbene.^{16–18}

The inductive effect for example through the use of electronegative substituents, *i.e.* nitrogen atoms, can lower the energy of the σ orbital without influencing the p_{π} orbital and thus increase the HOMO-LUMO gap. The mesomeric effect using π -donor substituent can strongly bend the carbene and raise the p_{π} orbital, which also increases the HOMO-LUMO gap.

This remarkable stability of NHCs is used to synthesise stable organometallic complexes in catalysis. The singlet state of the carbene ligand can form an exceptional strong NHC-metal bond resulting in unique organometallic complexes. The next section will go into detail of the electronic and steric features of NHC and subsequently their behaviour as ligands.

1.1.1. Electronic and steric features

The electronic features can be defined as σ -basic/ π^* acidic.^{19–22} The lone pair in the σ orbital on the carbene gives the σ -basic characteristic, as the π^* acidity arises from the possibility for the NHC to accept electron density from the metal into the π^* orbital (Figure 1.4).

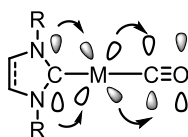


Figure 1.4: The back-donation of the metal to the NHC.¹⁵

The ability of the NHC to donate electron density to the metal increases the strength of the NHC-metal bond, resulting in more stable complexes. Due to the electronic features playing such an important role in the characteristics and properties of NHCs different ways have been developed to measure them. The Tolman electronic parameter (TEP) was widely used to measure the electronic of different ligands such as phosphine and NHC ligands.²³

The IR stretching frequency of the C-O bond (ν_{CO}) in $[\text{Ni}(\text{NHC})(\text{CO})_3]$ is measured in order to determine the electronic characteristics of the NHC. In theory the more electron density donated to the metal centre by the NHC, the stronger the metal-carbon bond (π^* back-donation) of M-CO. This results in a weaker C-O bond (more π^* back-donation) and a lower IR stretching frequency for C=O. Therefore more electron donating NHCs have a smaller ν_{CO} value. This method is widely used to measure the electron-donating abilities of NHCs but it does have several drawbacks, such as difficulties in the synthesis of these complexes and severe toxicity issues of the Ni complex. In order to prevent these drawbacks a new complex was synthesised: $[\text{Ir}(\text{NHC})(\text{CO})_2\text{Cl}]$ which was found to be a less toxic alternative.²⁴ The change to the electronic features of the NHC ligand can change the characteristics of the corresponding complex and ideally can improve the catalytic activity. There are three different ways to achieve this. Firstly by altering the substituents of the backbone of the NHC *i.e.* on C⁴ and C⁵. Bielawski and co-workers later reported the change of the IR stretching frequency of the C-O bond in $[\text{Rh}(\text{NHC})(\text{CO})_2\text{Cl}]$ when the substituents of the C⁴ and C⁵ position of the NHC were changed (Figure 1.5).²⁵ A clear difference can be seen going from hydrogen to cyanide.

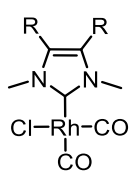
	Complex	ν_{av} (cm ⁻¹)
	R = H	2046
	R = Cl	2051
	R = NO ₂	2053
	R = CN	2058

Figure 1.5: $[\text{Rh}(\text{NHC})(\text{CO})_2\text{Cl}]$ and the ν_{av} values for different NHCs.²⁵

Secondly changes to the skeleton of the NHC (saturated/unsaturated backbone) were investigated. The difference in electronic properties between IMes/SIMes (IMes = *N,N*-bis-[2,4,6-(trimethyl)phenyl]imidazol-2-ylidene, SIMes = *N,N*-bis-(2,4,6-trimethylphenyl)imidazolidin-2-ylidene) and IPr/SIPr (IPr = *N,N'*-bis-[2,6-(di-*iso*-propyl)phenyl]imidazol-2-ylidene, SIPr = *N,N*-bis-[2,6-(di-*iso*-propyl)phenyl]imidazolidin-2-ylidene) was investigated but it was concluded that only minimal change in the electronic parameter can be seen²⁶ and that the change in the skeleton is most likely to influence the steric rather than the electronic properties of the complex. Lastly changing

the substituents on the nitrogens has shown a significant change. The ν_{av} value increases when an alkyl substituent is replaced by an aryl substituent (Figure 1.6).^{15,26} Therefore NHCs bearing alkyl substituents have better donating character.

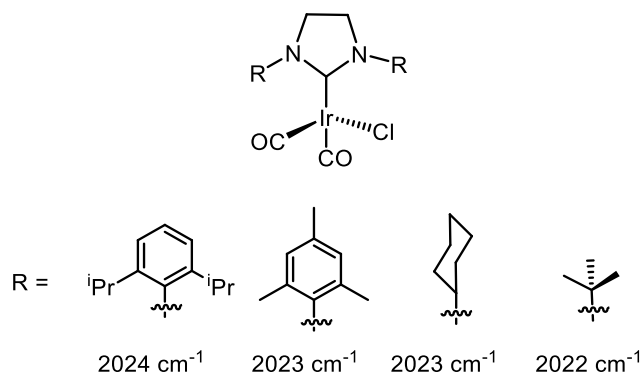


Figure 1.6: Comparison of aryl and alkyl substituents of the nitrogen in NHCs.^{15,26}

These unique electronic properties result in the ability of the NHC to have different bonding modes with a metal (Figure 1.7). The lone pair of electrons in the σ orbital of the carbene can form a bond with an empty d orbital of the metal, *i.e.* $\sigma \rightarrow d$ bonding mode. The NHC can also accept electron density from the metal's filled d orbital into its empty π^* orbital. Furthermore in the case of an electron deficient metal, the NHC can donate electron density from a combination of filled and empty π orbitals into an empty d orbital from the metal.

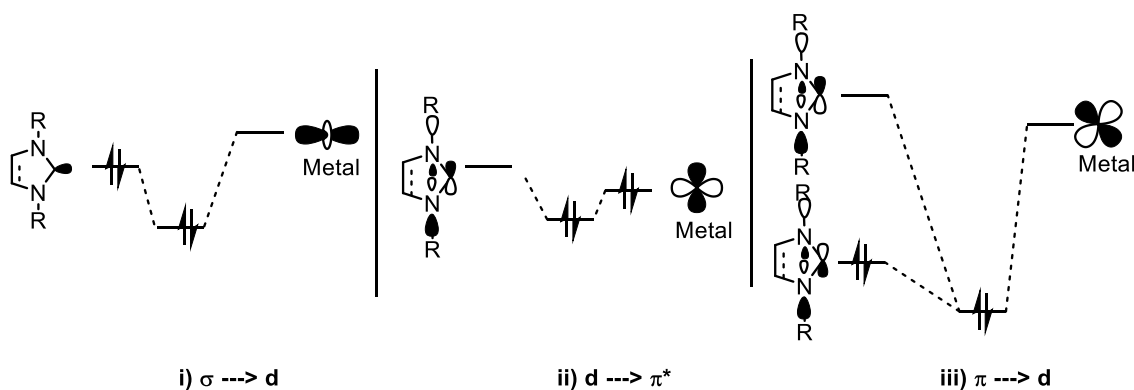


Figure 1.7: $\sigma \rightarrow d$ bonding (i), $d \rightarrow \pi^*$ bonding mode (ii) and $\pi \rightarrow d$ bonding mode (iii).¹⁵

The electronic and steric features define the characteristics and main advantages of NHCs. The steric bulk of the NHC as well can influence its character as a ligand on an organometallic complex as their electronic properties and so the measurement of steric parameters is of immense importance.

The Tolman Cone Angle is widely used to measure the sterics of different phosphine ligands.²³ However, due to the difference in symmetry of phosphine ligands (C^3 symmetry) and NHC

ligands (C^2 symmetry), the Tolman Cone Angle cannot be applied to NHCs. The importance of NHCs as ligands in organometallic chemistry has led to the introduction of a new model that can be applied to NHCs. The Percent Buried Volume ($\%V_{Bur}$) is the measurement of the volume of the first coordination sphere of the metal occupied by the ligand (Figure 1.8).²⁷ This model can be used for most common ligands used in organometallic chemistry, such as phosphine based ligands, cyclopentadienyl based ligands and NHCs.²⁷

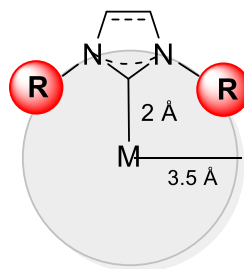


Figure 1.8: Illustration of $\%V_{Bur}$ of NHCs.¹⁵

The $\%V_{Bur}$ can be obtained by using the free web application SambVca and crystallographic data (Figure 1.8).²⁷ SambVca was tested against the binding energy of NHC ligands in $[RuClCp^*(NHC)]$ complexes in terms of sterics and electronics, this resulting in an almost linear correlation between the $\%V_{Bur}$ and the bond dissociation energy. This concluded that the binding character of NHC ligands develop mainly from its steric parameter. Comparing the steric parameter of saturated NHCs to unsaturated NHCs a slight but significant difference can be found. In saturated NHCs the $\%V_{Bur}$ is slightly bigger, this is due to the different N-C-N angle of the NHC skeleton.¹⁵ The N-C-N angle is 4-5° greater in saturated NHCs, resulting in the N-substituents being bent towards the metal centre (Figure 1.9). This steric change can affect the reactivity and catalytic activity of the organometallic complex significantly.²⁸ Therefore it can be reasoned that changing the substituents on C^4 and C^5 can influence the steric parameter and hence the catalytic reactivity. Recent developments have refined the model by introducing the dihedral angles ϕ_1 and ϕ_2 (Figure 1.9).²⁹

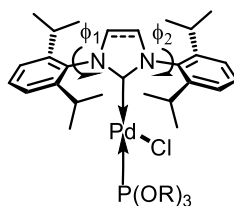


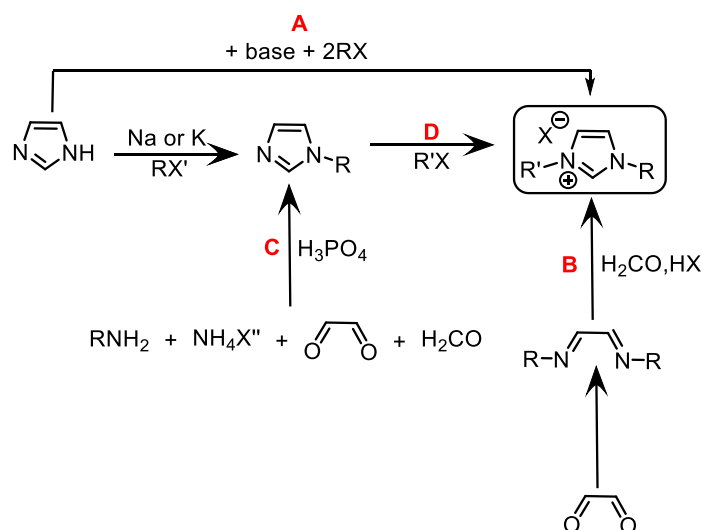
Figure 1.9: Example of dihedral angles ϕ_1 and ϕ_2 .²⁹

The angles ϕ_1 and ϕ_2 were investigated for the $[\text{PdCl}_2(\text{NHC})\{\text{P}(\text{OR})_3\}]$ complexes.²⁹ Computational modelling showed the bulkiness of the NHC can change depending on the bulkiness of its co-ligand. For example $[\text{PdCl}_2(\text{IPr})\{\text{P}(\text{OMe})_3\}]$ has a $\%V_{\text{Bur}}$ of 36.3, but changing the phosphite ligand to $\text{P}(\text{OPh})_3$, $[\text{PdCl}_2(\text{NHC})\{\text{P}(\text{OPh})_3\}]$, the $\%V_{\text{Bur}}$ changes to 32.4. This highlights the immense flexibility of NHC ligands.³⁰

1.1.2. Synthesis

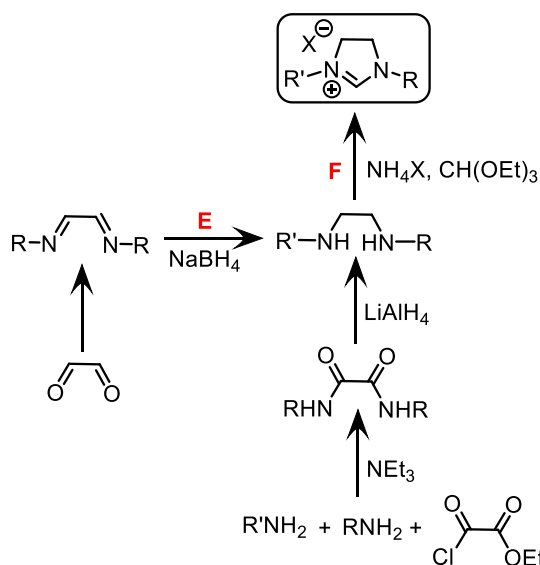
In this section the synthesis of imidazolylidene and imidazolidinylidenes will be described and the general synthesis of NHC-M complexes will be discussed. Firstly the syntheses of symmetrically and unsymmetrically *N*-substituted imidazolylidene are described.

There are two main routes; Route **A** starts from the imidazole which is reacted with a base and two RX to form the corresponding imidazolium salt. Alternatively (Route **B**) glyoxal is condensed with two equivalents of amine to form the α -diimine or diazobutadiene, followed by a cyclisation with formaldehyde in the presence of a Brønsted acid to form the corresponding imidazolium salt. For the synthesis of unsymmetrically *N*-substituted imidazolylidenes, the imidazole has to be functionalised, this can be achieved via two routes. Following Route **C**, glyoxal is reacted with a primary amine, an ammonium salt and formaldehyde. Route **D** starts from the imidazole, which is deprotonated by sodium or potassium followed by RX. The *N*-functionalised imidazole then can be alkylated or arylated to the corresponding imidazolium salt. The synthesis of symmetrically *N*-substituted imidazolidinylidenes starts from the α -diimine (condensation of the amine with glyoxal) which is reduced using NaBH_4 followed by a cyclisation using triethyl orthoformate and ammonium salt (Route **F**).



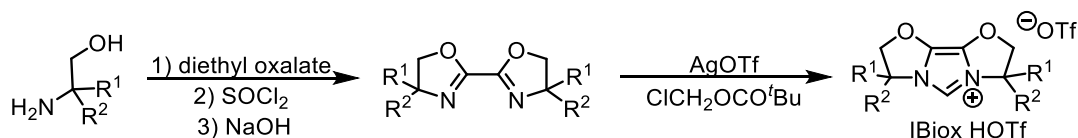
Scheme 1.4: General Synthesis of imidazolium salts.¹⁵

In the case of the unsymmetrically *N*-substituted imidazolidinylidene the synthesis starts from ethyl-2-chloro-2-oxoacetate, which is reacted with two different primary amines to form the corresponding oxalamide. Next the oxalamide is reduced using LiAlH₄ to the diamine which then undergoes cyclisation to the corresponding imidazolidinium salt (Route F).



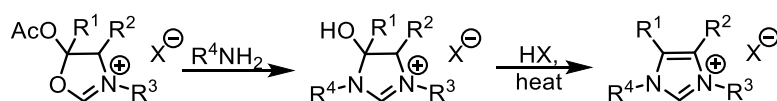
Scheme 1.5: General Synthesis of imidazolidinium salts.¹⁵

Different syntheses of more challenging NHCs have also been developed. In 2008, Glorius and co-workers introduced the tricyclic IBiox ligand (bioxazoline-derived carbene) (Scheme 1.6).³¹ The synthesis differs at the cyclisation step from the previous discussed routes. Silver triflate and butyl chloromethyl were used to install the C2 of the imidazolium instead of the formaldehyde.



Scheme 1.6: Synthesis of IBiox·HOTf.³¹

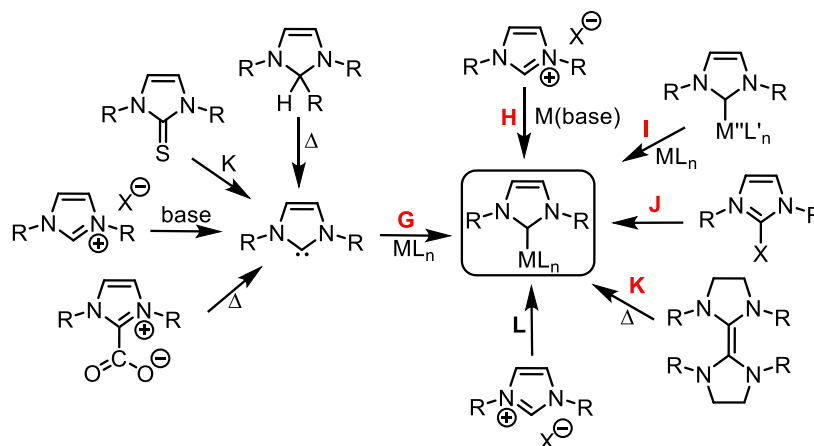
In 2006, Lehmann and co-workers reported the synthesis of imidazolium salts with substituted backbones.³² The synthesis begins with oxazolium acetals which are reacted with primary amines resulting in imidazolidinium salts (Scheme 1.7). After the elimination of water, the imidazolium salt is obtained.



Scheme 1.7: Synthesis of NHC salts with substituted backbones.³²

1.1.2.1 Synthesis of metal-NHC complexes

The most common and widely used to synthesis M-NHC complexes is the free carbene route (Scheme 1.8, **G**). The free carbene is most commonly generated by deprotonation of the corresponding salt. It can also be generated by desulfurisation, by thermal α -elimination or by decarboxylation. The free carbene then can coordinate to a metal centre (Route **G**). Alternatively a metal precursor can be used containing a base as a ligand, which then can deprotonate the NHC salt (Route **H**). The transmetallation route (Route **I**) has a carbene transfer reagent delivering the NHC to the second metal centre. Route **J** proceeds through C-H activation via oxidative addition, which is less often used than the other routes discussed above. Route **K** starts from the dimerised imidazolidinylidene which, via C=C activation, will result in the corresponding M-NHC complex.



Scheme 1.8: Main synthesis of NHC-M complexes.¹⁵

Overall NHCs are highly stable ligands, with diverse steric and electronic properties. The syntheses of NHC are facile and straight forward. The procedure for the formation of NHC-metal complexes is widely studied in the literature resulting in a simple and fast outcome.

1.2 Palladium-NHC complexes

1.2.1. Introduction and general synthesis

Palladium is one of the most versatile metals, with a wide array of applications. There are many advantages of using palladium in organometallic chemistry such as its tolerance to many different functional groups in catalysis.³³ Most palladium reagents are air and moisture stable, which eases the handling and storage.³³ Toxicity has not been a serious problem as well, allowing many different industries to use palladium reagents. Palladium can form stable complexes with many different ligands, such as mono and bidentate phosphines or NHC ligands.^{34,35} The most common oxidation state for Pd-NHC complexes is II, but oxidation states of 0 and I are also known (Figure 1.10). Hazari and co-workers reported Pd-NHC dimers which have an oxidation state of I.³⁶ Nolan and Cazin reported Pd-NHC complexes bearing two L-ligands resulting in an oxidation state of 0.³⁷ In the next chapters the Pd-NHC complexes bearing the oxidation state of II will be mainly used and discussed.

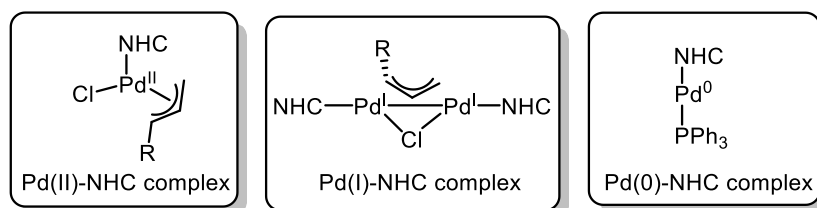
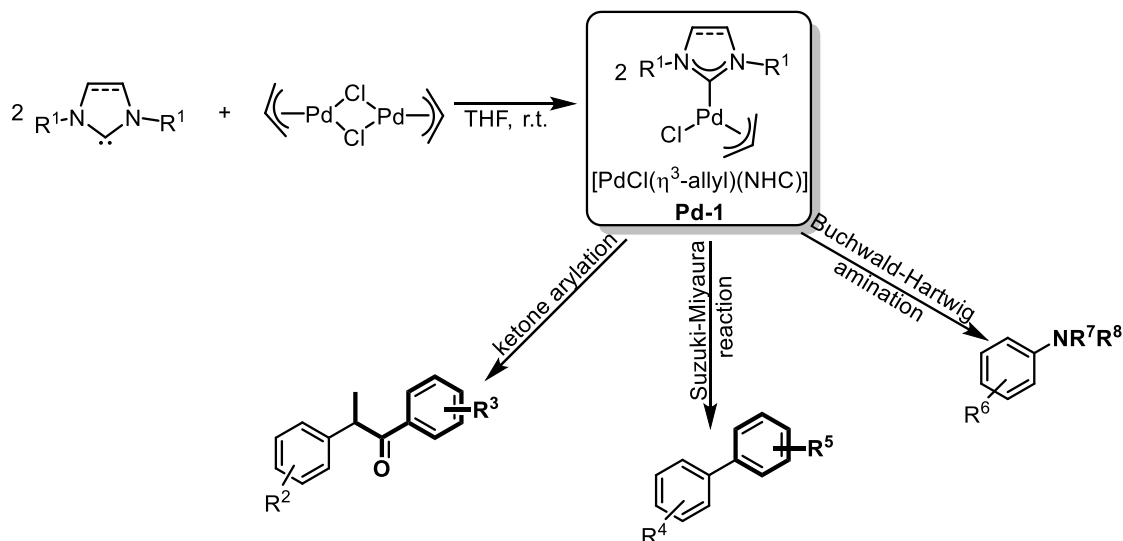


Figure 1.10: Pd-NHC complexes bearing different oxidation states.^{36–38}

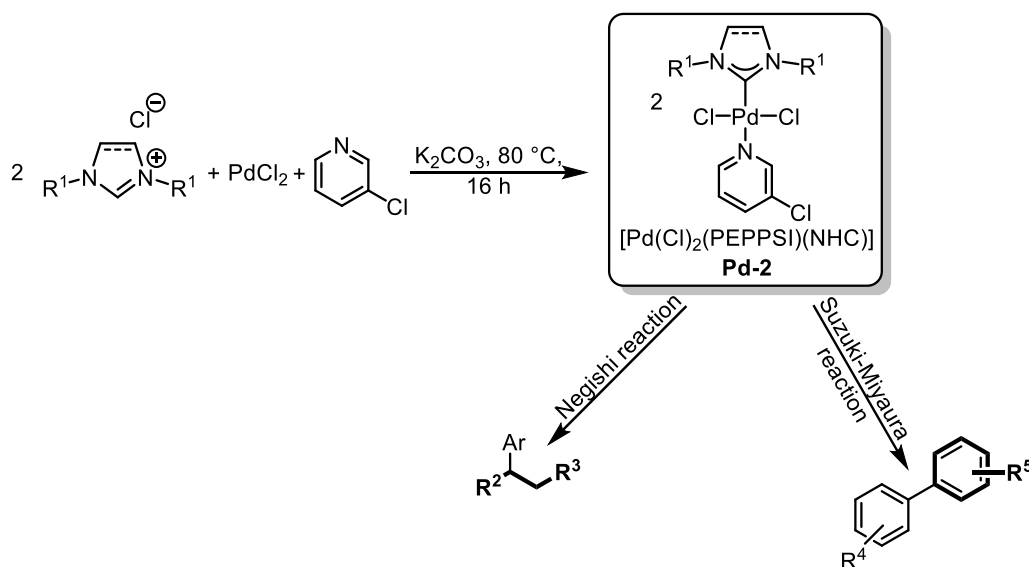
The first Pd-NHC complex was reported by Herrmann and co-workers in 1995.³⁹ In this report the synthesis and catalysis of these newly found species was studied.^{40,41} Herrmann investigated their catalytic activity early on using the Mizoroki-Heck reaction, which concluded the highly catalytic activity of Pd-NHC complexes.³⁹ Early results showed the high stability of Pd-NHC complexes, with most being air-, moisture- and thermally stable. Furthermore the decoordination of the NHC from the palladium was never observed, illustrating the strength of the bond.²²

In 2002 Nolan and co-workers reported the synthesis of a well-defined $[\text{PdCl}(\eta^3\text{-allyl})(\text{NHC})]$ complex, which was tested in different catalytic reactions (Scheme 1.9).^{38,42} The complexes showed high catalytic activity in the ketone arylation,³⁸ Buchwald-Hartwig amination and the Suzuki-Miyaura reaction.⁴²



Scheme 1.9: Synthesis and application in cross-coupling chemistry of $[\text{PdCl}(\eta^3\text{-allyl})(\text{NHC})]$.^{38,42}

As the interest in these new species grew many different research groups started to investigate the unique properties of Pd-NHC complexes. Organ and co-workers reported a detailed study about *in situ* generated Pd-NHC complexes and their catalytic reactivity in the Negishi reaction.⁴³ A year later the synthesis of $[\text{Pd}(\text{Cl})_2(\text{PEPPSI})(\text{IPr})]$ was reported (PEPPSI = Pyridine-Enhanced Precatalyst Preparation, Stabilisation and Initiation).⁴⁴ Organ's PEPPSI catalysts have shown very high catalytic reactivity in many cross-coupling reactions, such as the Negishi reaction and the Suzuki-Miyaura reaction (Scheme 1.10).^{45,46}



Scheme 1.10: Synthesis and application in cross-coupling chemistry of $[\text{Pd}(\text{Cl})_2(\text{PEPPSI})(\text{NHC})]$.³⁵

In 2002, Beller reported a monoligated NHC-Pd complex, **Pd-3**, in the telomerization of 1,3-dienes with alcohols.⁴⁷ Aerobic alcohol oxidation using a stable Pd(II)-NHC complex, **Pd-4**, was demonstrated in a report from Sigman.⁴⁸ Nolan's [PdCl(acac)(NHC)] (acac = acetylacetonate) pre-catalyst, **Pd-5**, showed high catalytic activity in the Buchwald-Hartwig amination as well as in ketone arylation.⁴⁹ Herrmann reported the synthesis of NHC substituted phosphapalladacycles, **Pd-6**, in the Mizoroki-Heck reaction (Figure 1.11).⁵⁰

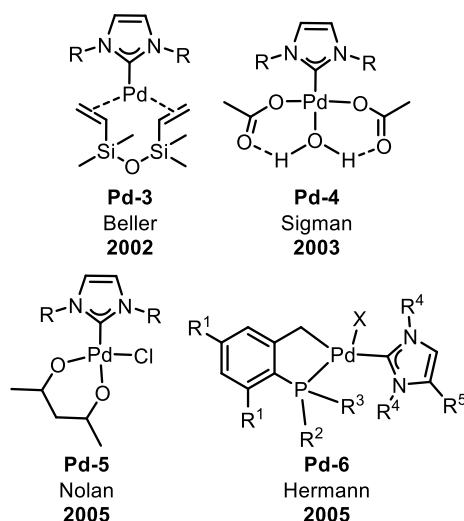
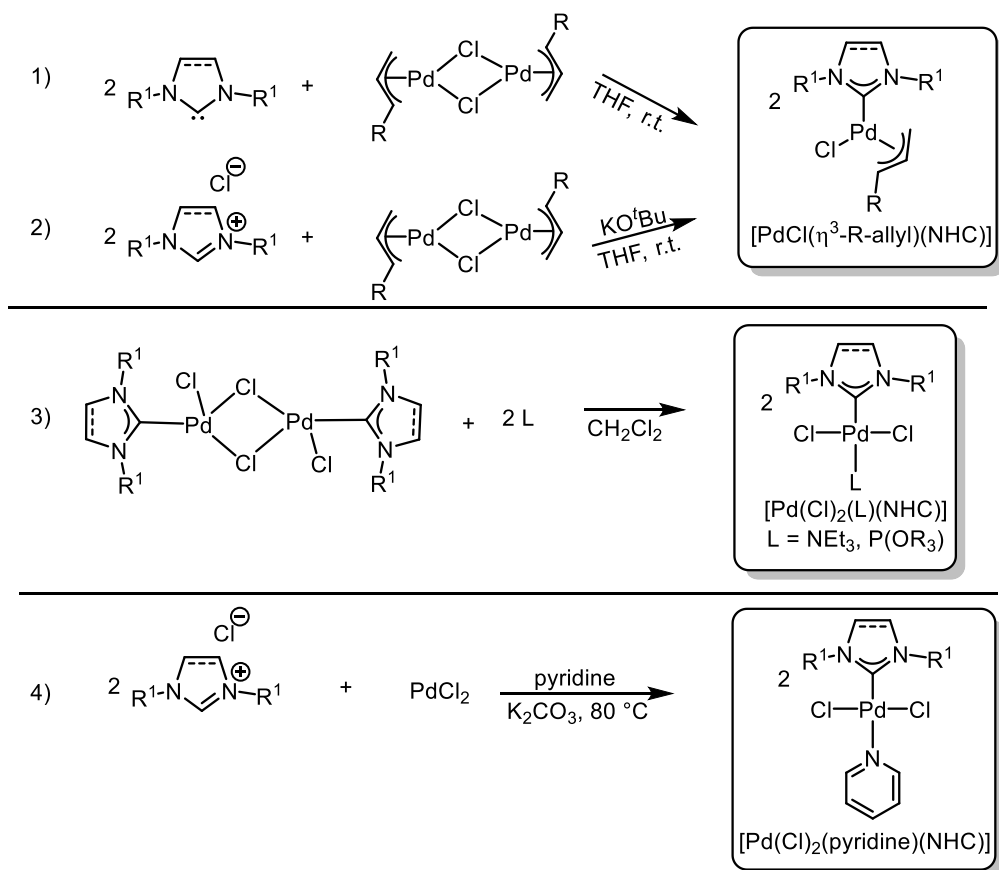


Figure 1.11: Examples of Pd-NHC complexes.^{47–50}

The synthesis of metal-NHC complexes was introduced in section 1.1.3. The specific synthesis of Pd-NHC complexes correlates to the general synthesis. The most applied synthesis, as before is the free carbene route. This route starts from the free NHC and a palladium dimer, which can be applied to many different complexes and has been used to synthesise the above mentioned complexes by Herrmann,⁵⁰ Beller⁴⁷ and Nolan^{38,49} (Scheme 1.11, eq. 1). As the free carbene is not stable under aerobic conditions, the one-pot route is commonly used as well. This starts from the NHC salt which is deprotonated usually by base, often KO^tBu in tetrahydrofuran (THF) (Scheme 1.11, eq. 2).⁵¹ In the same mixture the palladium dimer is added resulting in a well-defined Pd-NHC complex. Alternatively a pre-synthesised [Pd(μ-Cl)Cl(NHC)]₂ dimer can be mixed with a ligand such as triethylamine (TEA) for example on the synthesis of Navarro's [Pd(NHC)(TEA)Cl₂] complex (Scheme 1.11, eq. 3),⁵² the [Pd(μ-Cl)Cl(IPr)]₂ dimer was also used in the synthesis of Sigman's **Pd-4** complex.⁴⁸ To synthesise Organ's PEPPSI complex, PdCl₂ is used as palladium source. PdCl₂ is heated with the corresponding NHC salt and an excess of K₂CO₃ in 3-chloropyridine for 16 hours (Scheme 1.11, eq. 4).⁵³

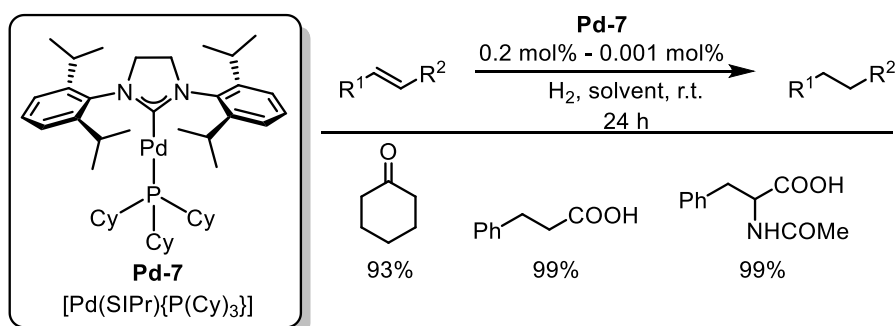
Scheme 1.11: Most common syntheses of Pd-NHC complexes.^{38,51,52,54}

1.2.2 Applications of Pd-NHC complexes

Pd-NHC complexes have found many different applications in homogeneous and heterogeneous catalysis.^{55–59} Due to the vast amount of research reported, the focus of this introduction will be on homogeneous catalysis. Pd-NHC complexes have emerged as highly active catalysts in a wide range of organic reactions such as hydrogenation reactions,⁶⁰ cross-coupling reactions⁶¹ and polymer chemistry.⁶² Their use in synthesising important organic molecules and materials underlies their importance in the chemistry community. Examples of different catalytic reactions using Pd-NHC complexes will be given in this section, outlining their significance.

1.2.2.1 Hydrogenation of alkynes and alkenes

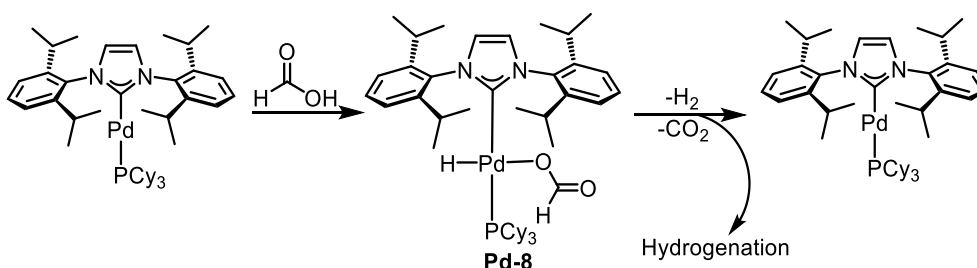
Mixed phosphine/NHC complexes, $[\text{Pd}(\text{NHC})\{\text{P}(\text{OR})_3\}]$ have been studied in the hydrogenation of alkynes and alkenes.⁶⁰ $[\text{Pd}(\text{SIPr})\{\text{P}(\text{Cy})_3\}]$, **Pd-7**, has shown high catalytic activity with catalyst loading as low as 0.001 mol%.⁶⁰ The hydrogenation of a wide range of alkynes and alkenes with an exceptional functional group tolerance was successfully reported under mild conditions such as room temperature and low hydrogen pressure (Scheme 1.12).



Scheme 1.12: Hydrogenation of alkenes using $[\text{Pd}(\text{SIPr})\{\text{P}(\text{Cy})_3\}]$.⁶³

Further investigations were conducted optimising the hydrogen source. Finding an alternative to the use of hydrogen gas is very important due to the high safety risk which accompanies the use of hydrogen gas. The use of ammonia borane as hydrogen source was reported using **Pd-7** with low catalyst loading in an alcohol solvent.⁶⁴ Ammonia borane dehydrogenation was observed with **Pd-7** forming the $[\text{Pd}(\text{H})_2(\text{SIPr})\{\text{P}(\text{Cy})_3\}]$ complex, which consequently resulted in the release of hydrogen gas.⁶⁴ A detailed study was reported using formic acid and $[\text{Pd}(\text{IPr})\{\text{P}(\text{Cy})_3\}]$ in an hydrogenation reaction of alkynes and alkenes. The mechanism was studied in detail showing the formation of hydridoformatopalladium complex **Pd-8** (Scheme 1.13), which was isolated and characterised.⁶³ The tandem sequence allowed the semi-

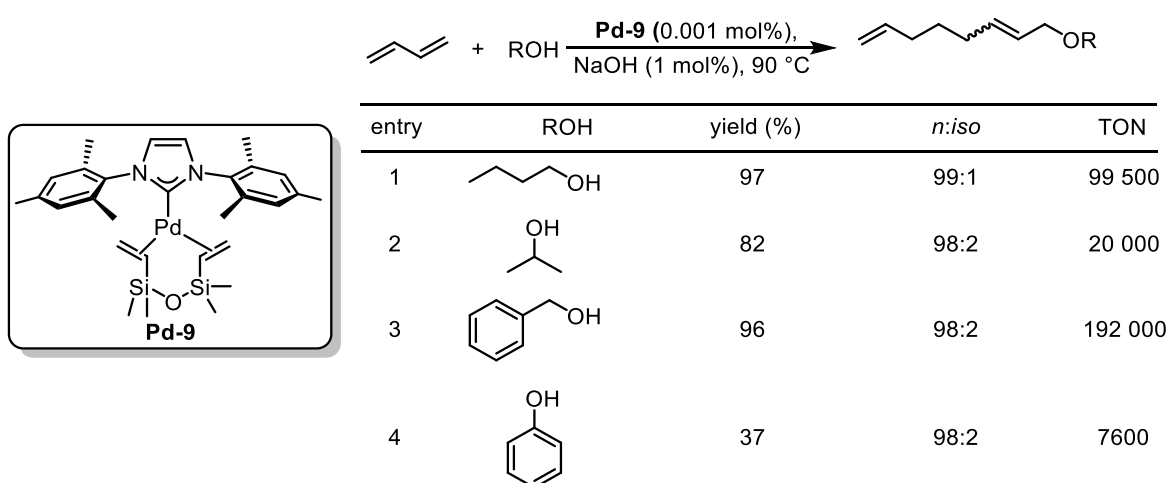
hydrogenation of aromatic and aliphatic internal alkynes to the corresponding Z-alkenes under mild conditions.



Scheme 1.13: Proposed mechanism of the hydrogenation reaction using $[\text{Pd}(\text{IPr})\{\text{P}(\text{Cy})_3\}]$ and formic acid.⁶³

1.2.2.2 Telomerization reactions

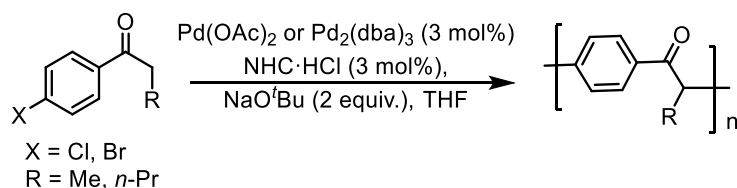
The homogeneous catalysed telomerisation reaction is the dimerization of two molecules, for example 1,3-dienes under the addition of nucleophilic compounds.⁶⁵ The telomerization between butadiene and water was first reported using an *in situ* system of palladium and an arylphosphine ligand.⁶⁶ The ligand was later changed to a NHC ligand, which improved the regioselectivity, yield and selectivity of the reaction.⁶⁷ Beller and co-workers reported the use of a well-defined Pd(0)-NHC complex **Pd-9** as a highly active catalyst in the telomerisation of butadiene with methanol (Scheme 1.14).⁴⁷ High yields (98%) and turnover numbers (TONs) of 98 000 were obtained. **Pd-9** was further investigated and aliphatic alcohols and phenols were successfully applied in the catalysis (Scheme 1.14). Furthermore high TON (up to 1500 000) and turnover frequency (TOF) (100 000 h⁻¹) were achieved.⁶⁸ Many examples can be found in the literature nowadays using Pd-NHC catalysts in different telomerisation reactions.⁶⁹



Schemed 1.14: Telomerisation of butadiene with ROH.⁷⁰

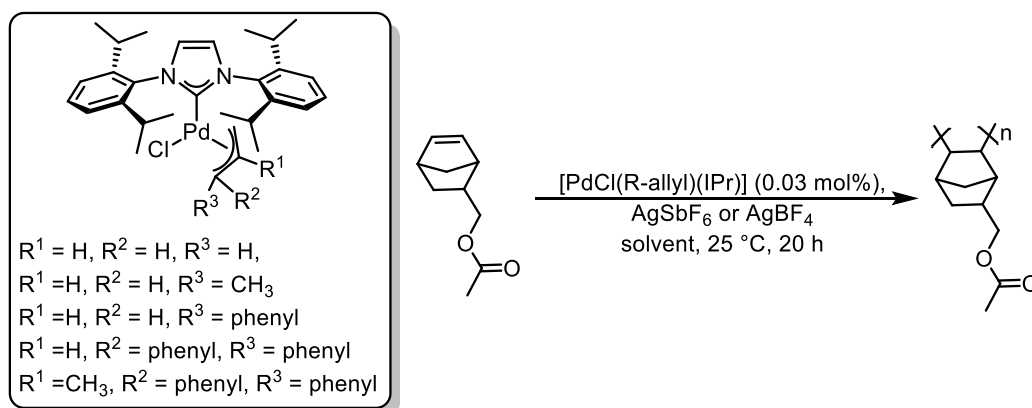
1.2.2.3 Polymerisation reactions

Matsubara and co-workers illustrated the use of NHCs as ligands in the polycondensation reaction of haloarylketones.⁷¹ The polymerisation was successfully performed using Pd(OAc)₂ or Pd₂(dba)₃ (dba = dibenzylidene acetone) in combination with a NHC·HCl and NaO^tBu as base (Scheme 1.15). Better reactivity was observed when NHCs as ligands were used rather than phosphine ligands, furthermore the catalyst loading could be reduced when NHCs were used.



Scheme 1.15: Polymerisation of haloarylketones.⁷¹

The polymerisation of norbornene and polar functionalised norbornene were carried out using [PdCl(η³-R-allyl)(NHC)] with AgSbF₆ or AgBF₄.⁶² The substituents on the allyl ligand was varied and compared in the polymerisation, where better results were observed the bulkier the allyl ligand (Scheme 1.16).⁶²



Scheme 1.16: Polymerisation of norbornene using [PdCl(η³-R-allyl)(NHC)].⁶²

1.2.2.4 Pd-NHC complexes as electrocatalysts

Wolf and co-workers reported the use of Pd-bis(NHC) pincer complexes as electrocatalysts in the reduction of CO₂ to CO.⁷² 2,2,2-trifluoroethanol, acetic acid or 2,2,2-trifluoroacetic acid was used as proton source. Furthermore the one-electron reduction of **Pd-10** and **Pd-11** is chemically reversible, therefore avoiding the decomposition into a bimetallic species, which is reported for Pd triphosphine electrocatalysts. (Figure 1.12).⁷²

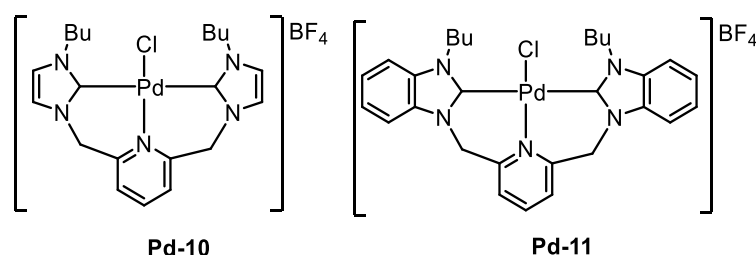
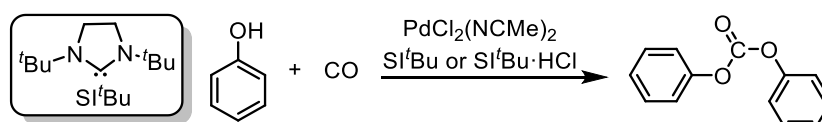


Figure 1.12: Pd-NHC complexes **Pd-10** and **Pd-11**.⁷²

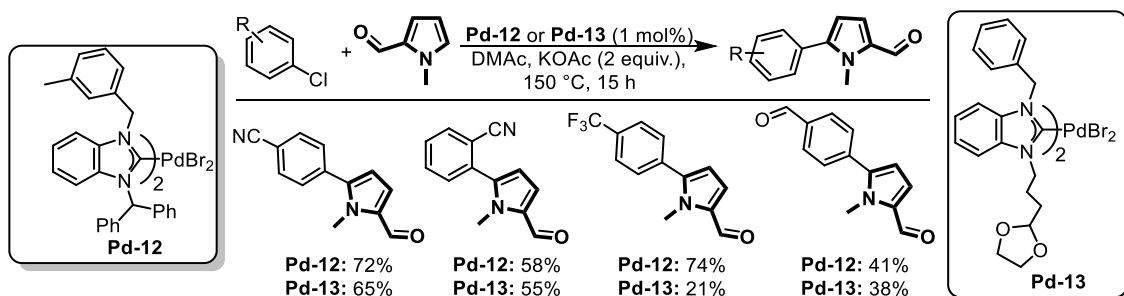
An *in situ* system using [PdCl₂(CH₃CN)₂] and a NHC as ligand is used for the electrocarbonylation of phenol with CO to generate diphenyl carbonate.⁷³ Different free NHCs and their corresponding NHC·HCl salts were tested resulting in up to 80% electrochemical formation of diphenyl carbonate. The best performing NHC was Si^tBu (*N,N'*-(di-*tert*-butyl)imidazolidin-2-ylidene) with the corresponding Si^tBu·HCl (Scheme 1.17). It was reasoned that the stronger electron donating ability of the NHC compared to phosphine ligands is aids the reaction.⁷³



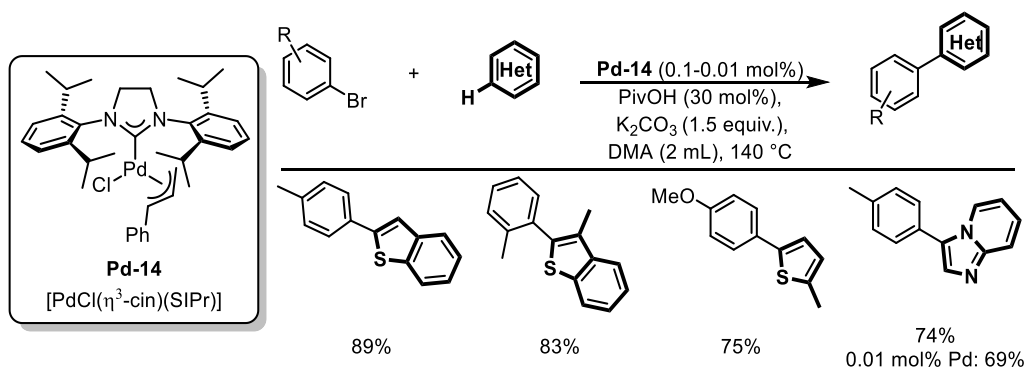
Scheme 1.17: Electrocarbonylation using an *in-situ* Pd:NHC catalyst.⁷³

1.2.2.5 Direct C-H arylation using Pd-NHC complexes.

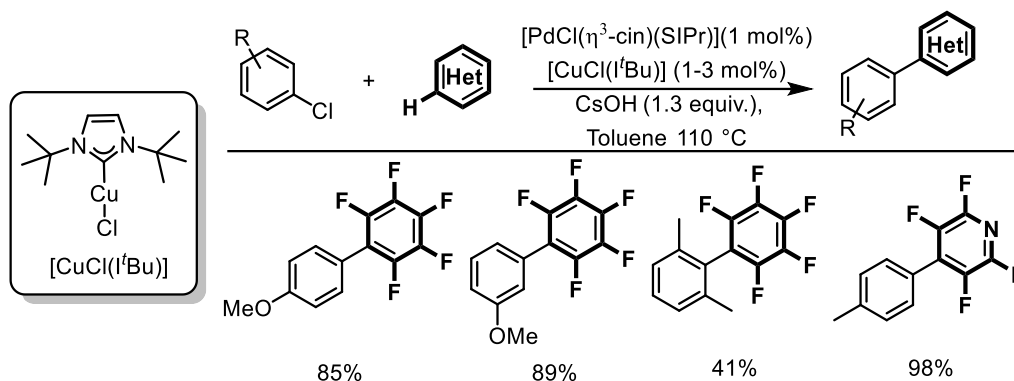
The direct C-H arylation is an atom-economical coupling reaction, receiving more and more attention.⁷⁴ The main challenges are the unreactive nature of the C-H bond, the homocoupling of the aryl halide as well as the selective arylation. Özdemir and Doucet reported the synthesis of the new air-stable Pd-NHC complexes **Pd-12** and **Pd-13**, which were tested in the C-H arylation of pyrrols with electron-withdrawing aryl chlorides (Scheme 1.18).⁷⁵ The bulky *N*-substituents on the catalysts were favourable for the reaction, resulting in moderate yield.

Scheme 1.18: Direct C-H arylation of pyrroles.⁷⁵

[PdCl(η^3 -cin)(SIPr)], **Pd-14** was used in the direct arylation of heterocycles at low catalyst loading (0.1 mol%). The catalyst loading could even be reduced to 0.01 mol% for selected examples (Scheme 1.19).⁷⁶ The highly active system was applied to a small scope using K₂CO₃ as a base in DMA (dimethylacetamide) at 140 °C.⁷⁶

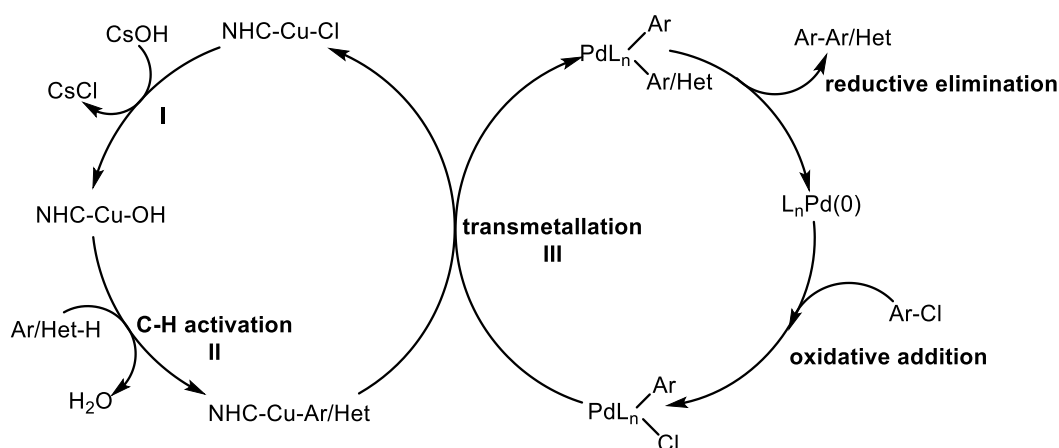
Scheme 1.19: Direct arylation of heterocycles.⁷⁶

Cazin and co-workers reported an improved protocol using the same catalyst **Pd-14** but added a copper co-catalyst, [Cu(Cl)(I^tBu)] (I^tBu = *N,N'*-(di-*tert*-butyl)imidazol-2-ylidene), to the system.⁷⁷ The catalyst loading of **Pd-14** was increased to 1 mol% but the direct C-H arylation of a range of aromatic and heteroaromatic substrates was achieved without the need of a directing group. Furthermore Cazin and co-workers assembled a scope using aryl bromides and chlorides (Scheme 1.20).⁷⁷



Scheme 1.20: Direct C-H arylation of aryl chlorides.⁷⁷

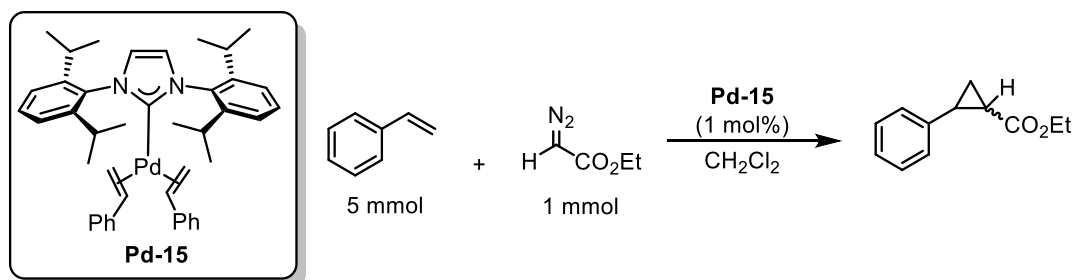
Mechanistic studies suggested a dual catalytic cycle. In the copper cycle $[\text{Cu}(\text{Cl})(\text{I}^t\text{Bu})]$ reacts with CsOH to generate $[\text{Cu}(\text{OH})(\text{I}^t\text{Bu})]$ *in situ*. This activates the C-H of the corresponding aryl or heteroaryl substrates via an acid/base reaction (Scheme 1.21, II), followed by a transmetalation to the palladium to deliver the aryl/heteroaryl fragment (Scheme 1.21, III).⁷⁷



Scheme 1.21: Proposed mechanism of the direct C-H arylation using a dual Pd/Cu system.⁷⁷

1.2.2.6 Cyclopropanation of alkenes

Belderrain and co-workers reported the palladium catalysed cyclopropanation of alkenes using a Pd(0)-NHC catalyst.⁷⁸ **Pd-15** was synthesised starting from $[\text{PdCl}(\eta^3\text{-allyl})(\text{IPr})]$, in the presence of KO^tBu in *iso*-propanol with an excess of styrene.⁷⁸ Initial experiments were conducted using **Pd-15** in low catalyst loading (1 mol%), for the cyclopropanation of ethyl diazoacetate with styrene, resulting in 98% yield (Scheme 1.22).⁷⁸ Based on the promising result the authors changed the alkene to 1-hexene, which resulted in 95% and cyclooctene (58%).

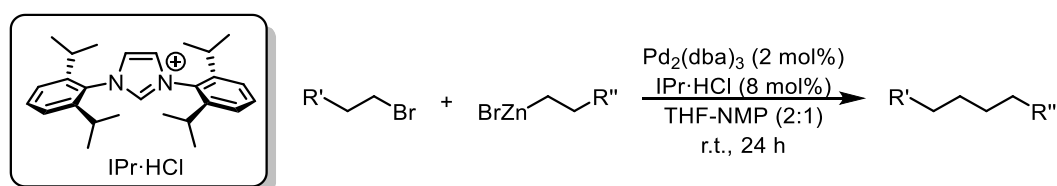
Scheme 1.22: Cyclopropanation of styrene.⁷⁸

1.2.2.7 Cross-coupling chemistry

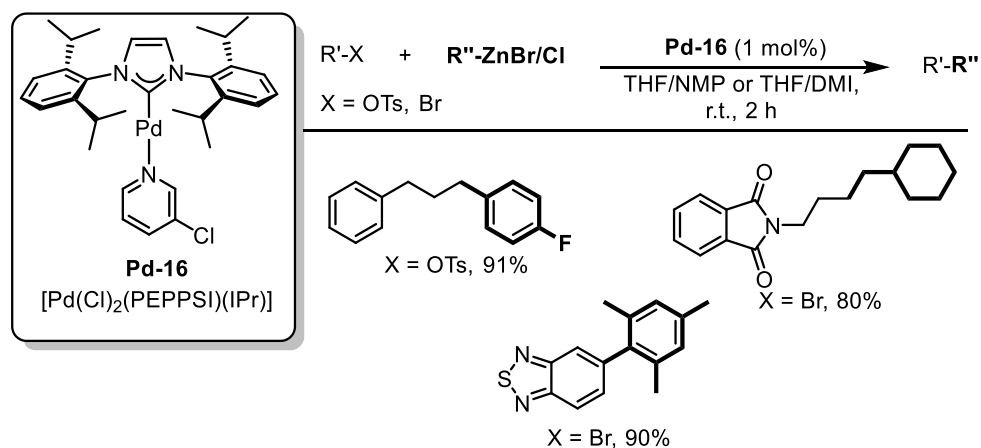
Cross-coupling chemistry is by far the most known and applied field for Pd-NHC complexes.⁶¹ The first Pd-NHC complexes synthesised by Herrmann were tested in a Mizoroki-Heck reaction.⁷⁹ From then onwards, Pd-NHC complexes have been successfully applied to a wide number of different cross-coupling reactions. The following coupling reactions will be discussed in detail in the relevant chapters: The Suzuki-Miyaura reaction (Chapter 3), The Buchwald-Hartwig amination (Chapter 4), the α -ketone arylation (Chapter 4), the Mizoroki-Heck (Chapter 5) and the Sonogashira (Chapter 6) reaction. Two more important examples will be given in the next section, namely the Negishi reaction and the C-S coupling reaction.

1.2.2.7.1 The Negishi reaction

Negishi and co-workers reported the carbon-carbon bond formation starting from an organozinc reagent and an organic nucleophile in 1977.⁸⁰ The use of Pd-NHC complexes in the Negishi reaction as catalysts was minimal in the literature with little success until 2005.⁸¹ The major breakthrough in this area was reported by Organ and co-workers, starting with an *in situ* system of $\text{Pd}_2(\text{dba})_3$ and $\text{IPr}\cdot\text{HCl}$.⁸² The coupling of unactivated primary bromides and alkyl organozinc reagents was performed at room temperature.⁸² This was not only the first Negishi reaction forming alkyl-alkyl bonds, it proceeded under very mild conditions (room temperature) resulting in good to high yields (61-92%) (Scheme 1.23).⁸²

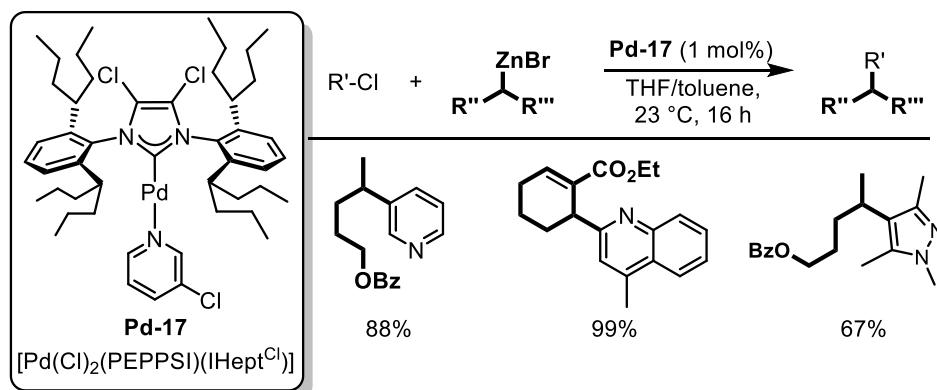
Scheme 1.23: The Negishi coupling of alkyl bromides and alkyl zinc reagents.⁸²

One year later Organ and co-workers achieved a major breakthrough in this field as they reported the use of an air stable, well-defined Pd NHC precatalyst, namely $[\text{Pd}(\text{Cl})_2(\text{PEPPSI})(\text{IPr})]$, which showed extraordinary reactivity in the Negishi reaction.⁵⁴ The coupling of several aryl and alkyl halides/pseudohalides (*i.e.* chlorides, bromides, iodides, triflates, tosylates, mesityl) was achieved.⁵⁴ Steric hindrance was widely tolerated in the catalysis as well as heteroaromatic substrates (Scheme 1.24).⁵⁴



Scheme 1.24: Negishi coupling using $[\text{Pd}(\text{Cl})_2(\text{PEPPSI})(\text{IPr})]$ (NMP = *N*-methyl-2-pyrrolidinone, DMI = 1,3-dimethyl-2-imidazolinone).⁵⁴

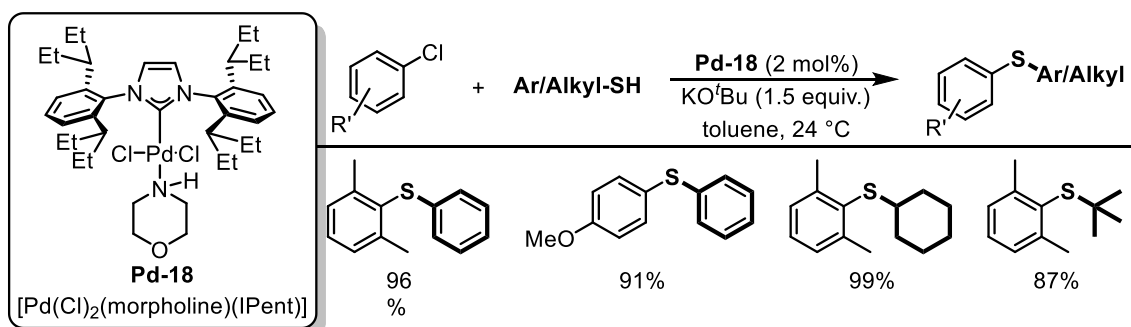
Based on this success, the Organ group investigated the use of different NHCs as ligands in the $[\text{Pd}(\text{Cl})_2(\text{PEPPSI})(\text{NHC})]$ scaffold.^{83,84} In 2012, $[\text{Pd}(\text{Cl})_2(\text{PEPPSI})(\text{IPent}^{\text{Cl}})]$ (IPent^{Cl} = *N,N*-bis-[2,6-bis(di-*iso*-pentylyl)phenyl-4,5-dichloro]imidazol-2-ylidene) was reported concentrating on the coupling of secondary organozinc reagents (Scheme 1.25).⁸³ The use of the bulky IPent^{Cl} was favoured in the Negishi reaction and an efficient protocol for the coupling of secondary organozinc reagents was obtained. Three years later, the Organ group improved this system even further, concentrating on coupling five and six-membered heterocycles with secondary organozinc reagents using $[\text{Pd}(\text{Cl})_2(\text{PEPPSI})(\text{IHept}^{\text{Cl}})]$, **Pd-17** (IHept^{Cl} = *N,N*-bis-[2,6-bis(di-*iso*-heptylyl)phenyl-4,5-dichloro]imidazol-2-ylidene) (Scheme 1.24).⁸⁴



Scheme 1.25: Negishi coupling of secondary alkyl organozinc reagents.⁸⁴

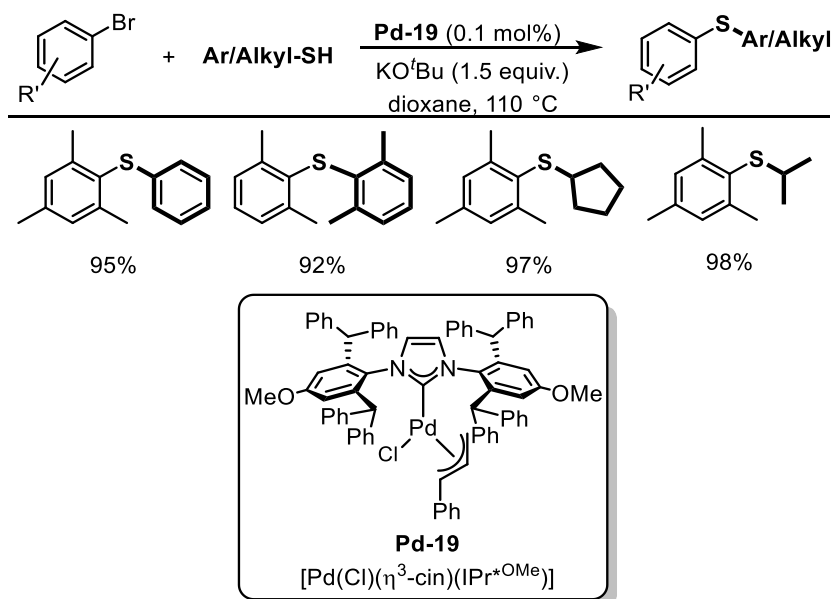
1.2.2.7 2 Carbon-Sulfur cross-coupling reactions

The thioether motif is abundant in natural products and drug molecules.^{85,86} The synthesis of thioethers can be performed using cross-coupling chemistry, starting from an aryl or alkyl thiol and an aryl halide. Organ and co-workers reported the C-S coupling of both aryl and alkyl thiols with aryl chlorides using a Pd-NHC pre-catalyst, [Pd(Cl)₂(morpholine)(IPent)], **Pd-18** (IPent = *N,N'*-bis-[2,6-bis(*di-iso*-pentyl)phenyl]imidazol-2-ylidene), in 2 mol% catalyst loading.⁸⁷ The catalytic reaction was performed at room temperatures, showing the high catalytic activity of the pre-catalyst, resulting in high yields (Scheme 1.26).



Scheme 1.26: C-S bond formation using [Pd(Cl)₂(morpholine)(IPent)].⁸⁷

Nolan and co-workers reported the C-S bond formation using [Pd(Cl)(η^3 -cin)(IPr^{*OMe})], **Pd-19** (IPr^{*OMe} = *N,N*-bis-[2,6-bis(diphenyl)-4-methoxyphenyl]imidazol-2-ylidene) as pre-catalyst.⁸⁸ The catalyst loading was significantly reduced to 0.1 mol% using aryl bromides as coupling substrates. Several aryl and alkyl thiols were coupled with unactivated and/or sterically hindered aryl bromides in good to excellent yield (Scheme 1.27).



Scheme 1.27: C-S bond formation using [Pd(Cl)(η³-cin)(IPr*OMe)].⁸⁸

In conclusion, Pd-NHC complexes have been extensively studied and used as catalysts in a wide range of reactions. This section summarises only a part of the capability of Pd-NHC complexes. Based on their prevalence the synthesis and application of Pd-NHC complexes is an ongoing and very active research field. This thesis described our efforts towards new Pd(II)-NHC complexes, by focusing on environmental friendly protocols for the synthesis and catalysis.

1.3. References

- (1) Hopkinson, M. N.; Richter, C.; Schedler, M.; Glorius, F. *Nature* **2014**, *510*, 485–496.
- (2) Herrmann, W. A. *Angew. Chem. Int. Ed.* **2002**, *41*, 1290–1309.
- (3) Flanigan, D. M.; Romanov-Michailidis, F.; White, N. A.; Rovis, T. *Chem. Rev.* **2015**, *115*, 9307–9387.
- (4) Peris, E. *Chem. Rev.* **2017**, acs.chemrev.6b00695.
- (5) Hahn, F. E.; Jahnke, M. C. *Angew. Chem. Int. Ed.* **2008**, *47*, 3122–3172.
- (6) Herrmann, W. A.; Köcher, C. *Angew. Chem. Int. Ed.* **1997**, *36*, 2162.
- (7) Wanzlick, H. M. *Angew. Chem. Int. Ed.* **1962**, *1*, 75–80.
- (8) Wanzlick, H. M.; Schönherr, H.-J. *Angew. Chem. Int. Ed.* **1968**, *7*, 141–142.
- (9) Öfele, K. *J. Organomet. Chem.* **1968**, *12*, 42–43.
- (10) Öfele, K. *Angew. Chem.* **1969**, *22*, 936.
- (11) Öfele, K. *J. Organomet. Chem.* **1970**, *22*, C9.
- (12) Arduengo, A. J.; Harlow, R. . I.; Kline, M. *J. Organomet. Chem.* **1991**, *113*, 361–363.
- (13) Arduengo, A.; Davidson, F. *J. Am. Chem. Soc.* **1997**, *119*, 12742–12749.
- (14) Arduengo, A. J.; Krafczyk, R.; Schmutzler, R.; Craig, H. a.; Goerlich, J. R.; Marshall, W. J.; Unverzagt, M. *Tetrahedron* **1999**, *55*, 14523–14534.
- (15) C. Bianchini, D.J. Cole-Hamilton, P.W.N.M. van Leeuwen, C. S. J. C. *N-Heterocyclic carbenes in Transition Metal Catalysis and Organocatalysis*; Cazin, C. S. J., Ed.; Springer, 2011.
- (16) Schrock, R. R. *J. Am. Chem. Soc.* **1974**, *96*, 6796–6797.
- (17) Fischer, E. O.; Maasböl, A. *Angew. Chem. Int. Ed.* **1964**, *3*, 3–4.
- (18) Carter, E. A.; Goddard, W. *J. Phys. Chem.* **1986**, *90*, 998–1001.
- (19) Frenking, G.; Solà, M.; Vyboishchikov, S. F. *J. Organomet. Chem.* **2005**, *690*, 6178–6204.
- (20) Jacobsen, H.; Correa, A.; Costabile, C.; Cavallo, L. *J. Organomet. Chem.* **2006**, *691*, 4350–4358.
- (21) Tonner, R.; Heydenrych, G.; Frenking, G. *Chem. An Asian J.* **2007**, *2*, 1555–1567.
- (22) Jacobsen, H.; Correa, A.; Poater, A.; Costabile, C.; Cavallo, L. *Coord. Chem. Rev.* **2009**, *253*, 687–703.
- (23) Tolman, C. *Chem. Rev.* **1977**, *77*, 313–348.
- (24) Iii, R. A. K.; Clavier, H.; Giudice, S.; Scott, N. M.; Stevens, E. D.; Bordner, J.; Samardjiev, I.; Hoff, C. D.; Cavallo, L.; Nolan, S. P. *Organometallics* **2008**, *27*, 202–210.
- (25) Khramov, D. M.; Lynch, V. M.; Bielawski, C. W. *Organometallics* **2007**, *26*, 6042–6049.

- (26) Dorta, R.; Stevens, E. D.; Scott, N. M.; Costabile, C.; Cavallo, L.; Hoff, C. D.; Nolan, S. P. *J. Am. Chem. Soc.* **2005**, *127*, 2485–2495.
- (27) Poater, A.; Cosenza, B.; Correa, A.; Giudice, S.; Ragone, F.; Scarano, V.; Cavallo, L. *Eur. J. Inorg. Chem.* **2009**, *2009*, 1759–1766.
- (28) Hillier, A. C.; Sommer, W.; Yong, B. S.; Petersen, J. L.; Cavallo, L.; Nolan, S. P. *Organometallics* **2003**, *22*, 4322–4326.
- (29) Diebolt, O.; Jurčik, V.; Correa da Costa, R.; Braunstein, P.; Cavallo, L.; Nolan, S. P.; Slawin, A. M. Z.; Cazin, C. S. J. *Organometallics* **2010**, *29*, 1443–1450.
- (30) Ragone, F.; Poater, A.; Cavallo, L. *J. Am. Chem. Soc.* **2010**, *132*, 4249–4258.
- (31) Würtz, S.; Glorius, F. *Acc. Chem. Res.* **2008**, *41*, 1523–1533.
- (32) Fürstner, A.; Alcarazo, M.; César, V.; Lehmann, C. W. *Chem. Commun.* **2006**, 2176–2178.
- (33) Tsuji, J. *Palladium Reagents and Catalysts*; Tsuji, J., Ed.; John Wiley & Sons, Ltd: Chichester, 2004.
- (34) Surry, D. S.; Buchwald, S. L. *Angew. Chem. Int. Ed.* **2008**, *47*, 6338–6361.
- (35) Kantchev, E. A. B.; O'Brien, C. J.; Organ, M. G. *Angew. Chem. Int. Ed.* **2007**, *46*, 2768–2813.
- (36) Hruszkewycz, D. P.; Balcells, D.; Guard, L. M.; Hazari, N.; Tilset, M. *J. Am. Chem. Soc.* **2014**, *136*, 7300–7316.
- (37) Schmid, T. E.; Jones, D. C.; Songis, O.; Diebolt, O.; Furst, M. R. L.; Slawin, A. M. Z.; Cazin, C. S. J. *Dalton Trans.* **2013**, *42*, 7345–7353.
- (38) Viciu, M. S.; Germaneau, R. F.; Nolan, S. P. *Org. Lett.* **2002**, *4*, 4053–4055.
- (39) Herrmann, W. A.; Elison, M.; Kocher, C.; Artus, G. R. J. *Angew. Chem. Int. Ed.* **1995**, *34*, 2371–2374.
- (40) Herrmann, W. A.; Elison, M.; Fischer, J.; Köcher, C.; Artus, G. R. J. *Chem. -A Eur. J.* **1996**, *2*, 772–780.
- (41) Herrmann, W. A.; Fischer, J.; Öfele, K.; Artus, G. R. J. *J. Organomet. Chem.* **1997**, *530*, 259–262.
- (42) Viciu, M. S.; Germaneau, R. F.; Navarro-fernandez, O.; Stevens, E. D.; Nolan, S. P. *Organometallics* **2002**, *21*, 5470–5472.
- (43) O'Brien, C. J.; Kantchev, E. A. B.; Chass, G. A.; Hadei, N.; Hopkinson, A. C.; Organ, M. G.; Setiadi, D. H.; Tang, T. H.; Fang, D. C. *Tetrahedron* **2005**, *61*, 9723–9735.
- (44) Organ, M. G.; Avola, S.; Dubovyk, I.; Hadei, N.; Kantchev, E. A. B.; O'Brien, C. J.; Valente, C. *Chemistry* **2006**, *12*, 4749–4755.

- (45) Atwater, B.; Chandrasoma, N.; Mitchell, D.; Rodriguez, M. J.; Pompeo, M.; Froese, R. D. J.; Organ, M. G. *Angew. Chem. Int. Ed.* **2015**, *54*, 9502–9506.
- (46) Organ, M. G.; Çalimsiz, S.; Sayah, M.; Hoi, K. H.; Lough, A. J. *Angew. Chem. Int. Ed.* **2009**, *48*, 2383–2387.
- (47) Jackstell, R.; Andreu, M. G.; Frisch, A.; Selvakumar, K.; Zapf, A.; Klein, H.; Spannenberg, A.; Röttger, D.; Briel, O.; Karch, R.; Beller, M. *Angew. Chem. Int. Ed.* **2002**, *41*, 986–989.
- (48) Jensen, D. R.; Schultz, M. J.; Mueller, J. A.; Sigman, M. S. *Angew. Chem. Int. Ed.* **2003**, *42*, 3810–3813.
- (49) Navarro, O.; Marion, N.; Scott, N. M.; González, J.; Amoroso, D.; Bell, A.; Nolan, S. P. *Tetrahedron* **2005**, *61*, 9716–9722.
- (50) Frey, G. D.; Schütz, J.; Herdtweck, E.; Herrmann, W. A. *Organometallics* **2005**, *24*, 4416–4426.
- (51) Clavier, H.; Correa, A.; Cavallo, L.; Escudero-Adán, E. C.; Benet-Buchholz, J.; Slawin, A. M. Z.; Nolan, S. P. *Eur. J. Inorg. Chem.* **2009**, *2009*, 1767–1773.
- (52) Chen, M.; Vivic, D. A.; Turner, M. L.; Navarro, O. *Organometallics* **2011**, *2*, 5052–5056.
- (53) O'Brien, C. J.; Kantchev, E. A. B.; Valente, C.; Hadei, N.; Chass, G. A.; Lough, A.; Hopkinson, A. C.; Organ, M. G. *Chem. Eur. J.* **2006**, *12*, 4743–4748.
- (54) Organ, M. G.; Avola, S.; Dubovyk, I.; Hadei, N.; Kantchev, E. A. B.; Brien, C. J. O.; Valente, C. *Chem. Eur. J.* **2006**, *12*, 4749–4755.
- (55) Hoyos, M.; Guest, D.; Navarro, O. In *N-Heterocyclic Carbenes: Effective Tools for Organometallic Synthesis*; Nolan, S. P., Ed.; Wiley-VCH Verlag GmbH & Co. KGaA, 2014; pp. 85–110.
- (56) Pahlevanneshan, Z.; Moghadam, M.; Mirkhani, V.; Tangestaninejad, S.; Mohammadpoor-Baltork, I.; Loghmani-Khouzani, H. *J. Organomet. Chem.* **2016**, *809*, 31–37.
- (57) Collinson, J. M.; Wilton-Ely, J. D. E. T.; Díez-González, S. *Catal. Commun.* **2016**, *87*, 78–81.
- (58) Begum, T.; Mondal, M.; Borpuzari, M. P.; Kar, R.; Kalita, G.; Gogoi, P. K.; Bora, U. *Dalt. Trans.* **2017**, *46*, 539–546.
- (59) Budagumpi, S.; Haque, R. A.; Salman, A. W. *Stereochemical and structural characteristics of single- and double-site Pd(II)-N-heterocyclic carbene complexes: Promising catalysts in organic syntheses ranging from CC coupling to olefin polymerizations*; Elsevier B.V., 2012; Vol. 256.

- (60) Jurčík, V.; Nolan, S. P.; Cazin, C. S. J. *Chem. Eur. J.* **2009**, *15*, 2509–2511.
- (61) Fortman, G. C.; Nolan, S. P. *Chem. Soc. Rev.* **2011**, *40*, 5151–5169.
- (62) Jung, I. G.; Lee, Y. T.; Choi, S. Y.; Choi, D. S.; Kang, Y. K.; Chung, Y. K. *J. Organomet. Chem.* **2009**, *694*, 297–303.
- (63) Broggi, J.; Jurčík, V.; Songis, O.; Poater, A.; Cavallo, L.; Slawin, A. M. Z.; Cazin, C. S. J. *J. Am. Chem. Soc.* **2013**, *135*, 4588–4591.
- (64) Hartmann, C. E.; Jurčík, V.; Songis, O.; Cazin, C. S. J. *Chem. Commun.* **2013**, *49*, 1005–1007.
- (65) Behr, A.; Becker, M.; Beckmann, T.; Johnen, L.; Leschinski, J.; Reyer, S. *Angew. Chem. Int. Ed.* **2009**, *48*, 3598–3614.
- (66) Schaart, B. J.; Pelt, H. L.; Jacobson, G. B. (Dow C. C. US5254782A1, 1993.
- (67) Jackstell, R.; Frisch, A.; Beller, M.; Röttger, D.; Malaun, M.; Bildstein, B. *J. Mol. Catal. A Chem.* **2002**, *185*, 105–112.
- (68) Jackstell, R.; Harkal, S.; Jiao, H.; Spannenberg, A.; Borgmann, C.; Röttger, D.; Nierlich, F.; Elliot, M.; Niven, S.; Cavell, K.; Navarro, O.; Viciu, M. S.; Nolan, S. P.; Beller, M. *Chem. Eur. J.* **2004**, *10*, 3891–3900.
- (69) Clement, N. D.; Routaboul, L.; Grotevendt, A.; Jackstell, R.; Beller, M. *Chem. Eur. J.* **2008**, *14*, 7408–7420.
- (70) Maluenda, I.; Chen, M.-T.; Guest, D.; Mark Roe, S.; Turner, M. L.; Navarro, O. *Catal. Sci. Technol.* **2015**, *5*, 1447–1451.
- (71) Matsubara, K.; Okazaki, H.; Senju, M. *J. Organomet. Chem.* **2006**, *691*, 3693–3699.
- (72) Therrien, J. a; Wolf, M. O.; Patrick, B. O.; Therrien, a; Wolf, M. O.; Patrick, B. O. *Inorg. Chem.* **2014**, *53*, 12962–12972.
- (73) Kanega, R.; Hayashi, T.; Yamanaka, I. *ACS Catal.* **2013**, *3*, 389–392.
- (74) Crabtree, R. H.; Lei, A. *Chem. Rev.* **2017**, *117*, 8481–8482.
- (75) Özdemir, I.; Gürbüz, N.; Kaloğlu, N.; Doğan, Ö.; Kaloğlu, M.; Bruneau, C.; Doucet, H. *Beilstein J. Org. Chem.* **2013**, *9*, 303–312.
- (76) Martin, A. R.; Chartoire, A.; Slawin, A. M. Z.; Nolan, S. P. *Beilstein J. Org. Chem.* **2012**, *8*, 1637–1643.
- (77) Lesieur, M.; Lazreg, F.; Cazin, C. S. J. *Chem. Commun.* **2014**, *50*, 8927–8929.
- (78) Martín, C.; Molina, F.; Alvarez, E.; Belderrain, T. R. *Chem. Eur. J.* **2011**, *17*, 14885–14895.
- (79) A. Herrmann, W.; Reisinger, C. P.; Spiegler, M. *J. Organomet. Chem.* **1998**, *557*, 93–96.
- (80) King, A. O.; Okukado, N.; Negishi, E. *J. Chem. Soc. Chem. Commun.* **1977**, 683.

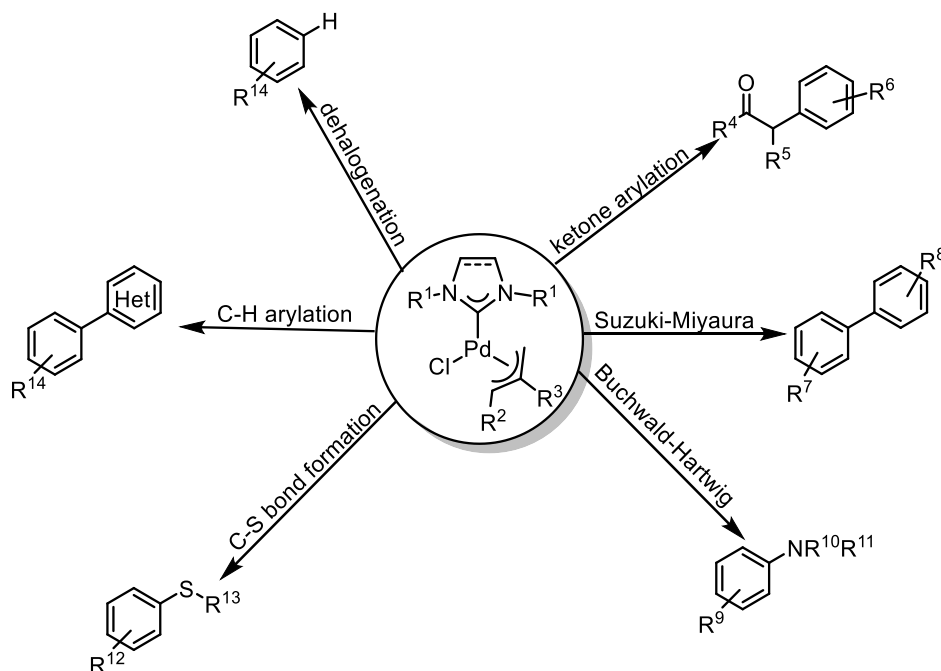
- (81) Organ, M. G.; Chass, G. A.; Fang, D. C.; Hopkinson, A. C.; Valente, C. *Synthesis* **2008**, 2776–2797.
- (82) Hadei, N.; Kantchev, E. A. B.; O'Brien, C. J.; Organ, M. G. *Org. Lett.* **2005**, 7, 3805–3807.
- (83) Pompeo, M.; Froese, R. D. J.; Hadei, N.; Organ, M. G. *Angew. Chem. Int. Ed.* **2012**, 51, 11354–11357.
- (84) Atwater, B.; Chandrasoma, N.; Mitchell, D.; Rodriguez, M. J.; Organ, M. G. *Chem. Eur. J.* **2016**, 22, 14531–14534.
- (85) Bagley, M. C.; Davis, T.; Dix, M. C.; Fusillo, V.; Pigeaux, M.; Rokicki, M. J.; Kipling, D. J. *Org. Chem.* **2009**, 74, 8336–8342.
- (86) De Martino, G.; Edler, M. C.; La Regina, G.; Coluccia, A.; Barbera, M. C.; Barrow, D.; Nicholson, R. I.; Chiosis, G.; Brancale, A.; Hamel, E.; Artico, M.; Silvestri, R. *J. Med. Chem.* **2006**, 49, 947–954.
- (87) Farmer, J. L.; Pompeo, M.; Lough, A. J.; Organ, M. G. *Chem. Eur. J.* **2014**, 20, 15790–15798.
- (88) Bastug, G.; Nolan, S. P. *J. Org. Chem.* **2013**, 78, 9303–9308.

Chapter 2

A straightforward synthesis of $[\text{PdCl}(\eta^3\text{-R-allyl})(\text{NHC})]$ complexes

2.1. Introduction to $[\text{PdCl}(\eta^3\text{-R-allyl})(\text{NHC})]$ complexes

As discussed in Chapter 1, Pd-NHC complexes can be used in a wide range of applications, in particular $[\text{PdCl}(\eta^3\text{-R-allyl})(\text{NHC})]$ complexes have emerged as highly active pre-catalysts in many different organic reactions such as cross-coupling chemistry (Scheme 2.1). In a seminal example, Nolan reported the ketone arylation using $[\text{PdCl}(\eta^3\text{-allyl})(\text{NHC})]$ as pre-catalyst, resulting in a wide scope in good to excellent yields.¹ Soon after, these complexes were tested in several cross-coupling reactions, such as the Suzuki-Miyaura^{2,3} and the Buchwald-Hartwig amination.⁴ The direct C-H arylation was successfully carried out using $[\text{PdCl}(\eta^3\text{-cin})(\text{NHC})]$ ⁵ (cin = cinnamyl) and C-S bond formation was demonstrated in low catalyst loading using $[\text{PdCl}(\eta^3\text{-R-allyl})(\text{NHC})]$ as pre-catalyst.^{6,7} Diez-González and co-workers reported the dehalogenation reaction using $[\text{PdCl}(\eta^3\text{-R-allyl})(\text{NHC})]$ (1 mol%) with a modified NHC backbone.⁸

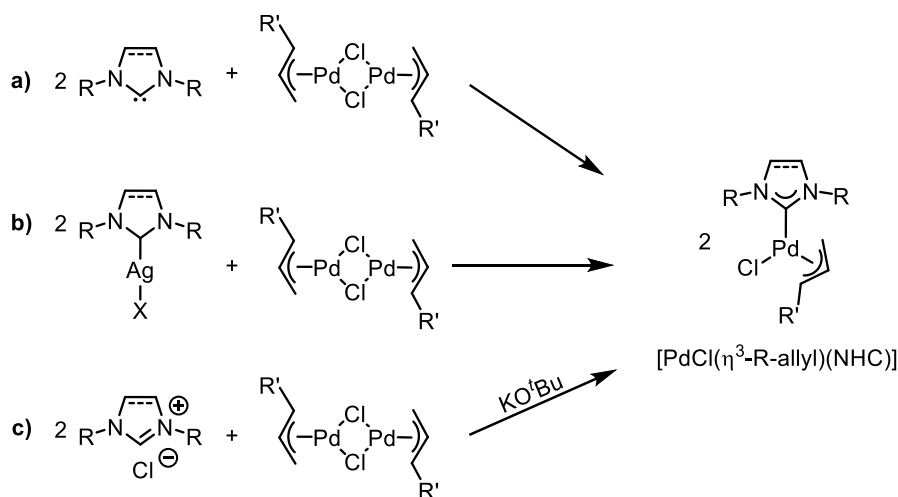


Scheme 2.1: Applications of $[\text{PdCl}(\eta^3\text{-R-allyl})(\text{NHC})]$ complexes.¹⁻⁹

Cross-coupling chemistry is widely used in many research fields, such as natural product synthesis,¹⁰ polymer chemistry,¹¹ pharmaceutical-¹² and the fine-chemical industry¹³ amongst others. This illustrates the importance of cross-coupling reactions to the chemistry community and hence the importance of developing highly active pre-catalysts to perform these reactions efficiently.

2.2. General synthesis of $[\text{PdCl}(\eta^3\text{-R-allyl})(\text{NHC})]$ complexes

There are several published routes for the synthesis of $[\text{PdCl}(\eta^3\text{-R-allyl})(\text{NHC})]$ complexes.^{14–20} However three main synthetic methods are typically used. The direct addition of free carbenes to metal precursors is one of the most common strategies, giving good to excellent yields for various $[\text{PdCl}(\eta^3\text{-R-allyl})(\text{NHC})]$ complexes in short reaction times (1-4 hours) at room temperature (Scheme 2.2a).^{1,2}

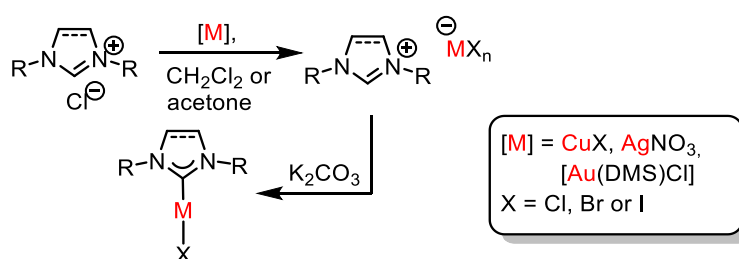


Scheme 2.2: General Synthesis of $[\text{PdCl}(\eta^3\text{-R-allyl})(\text{NHC})]$ complexes.¹⁶

Less commonly used is the transmetallation route, where the NHC ligand is introduced *via* a transmetallation agent such as silver or copper complexes (Scheme 2.2b). Silver complexes are widely used, although, due to being light sensitive and prone to dimerization, copper complexes are now more conveniently used.^{21,22} Mangeney and co-workers have reported the synthesis of chiral diaminocarbene palladium allyl complexes¹⁵ by treating diaminocarbene silver halide complexes with $[\text{Pd}(\eta^3\text{-allyl})(\mu\text{-Cl})_2]$ achieving good yields in short reaction times (0.5 hours). Since the transmetallation route is not an economically-friendly process to introduce the NHC ligand, it is less commonly used nowadays.

A much more common route is the “one-pot” procedure. In that context, the NHC salt, *i.e.* NHC \cdot HCl, is deprotonated using a strong inorganic base such as KO^tBu to generate the free NHC *in situ*. The following complexation of $[Pd(\eta^3\text{-R-allyl})(\mu\text{-Cl})_2]$ affords the desired complex (Scheme 2.2c).^{14,23} The use of the NHC salt in lieu of the free carbene is generally favoured as the NHC salt is air and moisture stable as well as thermally stable, which eases storage and handling. Nevertheless, the free carbene is generated *in situ* forcing inert reaction conditions.

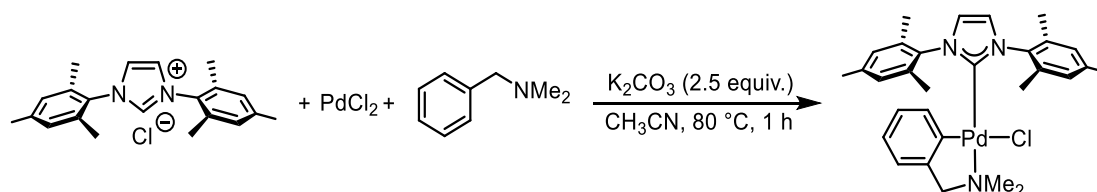
All published routes so far have shown several disadvantages such as inert atmosphere or the use of a strong inorganic base and harmful/environmentally unfriendly solvents. An air and moisture stable synthesis would make these complexes much more accessible to the wider chemistry community as highly active pre-catalysts for various organic reactions. Initial investigations started by taking a closer look into the air- and moisture-stable syntheses of different NHC-transition metal complexes, such as the method generating gold-, silver- and copper-NHC complexes using a weak inorganic base in air (Scheme 2.3).^{24–26} Nolan and Gimeno independently published a similar route generating $[AuX(NHC)]$ (X = Cl, Br, I) complexes using K₂CO₃ as base and acetone (Nolan)²⁴ or dichloromethane (Gimeno)²⁶ as solvent. A range of different NHC ligands were tested in the synthesis, resulting in excellent yields in short reaction times (1-4 hours). Cazin and co-workers applied this route to the synthesis of $[CuX(NHC)]$ (X = Cl, Br, I) complexes, using various saturated and unsaturated NHCs, on small and large scales.²⁵ Plenio and co-workers reported the synthesis of $[MX(cod)(NHC)]$ (M = Rh and Ir, X = Cl, I, cod = 1,5-cyclooctadiene) using K₂CO₃ in acetone. The resulting complexes were isolated in excellent yield.²⁷



Scheme 2.3: Synthesis of different transition metal-NHC complexes

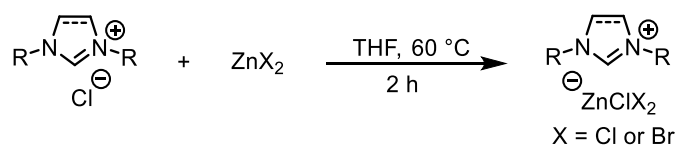
(DMS = dimethyl sulfide).^{24–26}

Ying and co-workers reported the synthesis of a NHC-ligated cyclopalladated *N,N*-dimethylbenzylamine complex in a one-pot fashion in air, starting from PdCl_2 , *N,N*-dimethylbenzylamine and NHC·HCl in acetonitrile in the presence of K_2CO_3 (Scheme 2.4).^{28,29} The resulting complexes were isolated in good to excellent yields.



Scheme 2.4: Synthesis of the IMes-ligated cyclopalladated *N,N*-dimethylbenzylamine complex (IMes = *N,N*-bis-[2,4,6-(trimethyl)phenyl]imidazol-2-ylidene).²⁸

Furthermore, Cazin and co-workers investigated this route with zinc to generate zinc-NHC complexes. Interestingly, the synthesis was unsuccessful towards the zinc(II)-NHC complexes; however, zincate complexes, $[\text{NHC}\cdot\text{H}][\text{ZnXY}_3]$ (X, Y = Br, Cl), were successfully obtained, (Scheme 2.5).³⁰ These zincate complexes showed catalytic activity in the methylation of amines with CO_2 and phenylsilane. These “ate” complexes have been previously reported for gold and copper as intermediates in the reaction mechanism.^{24,31}

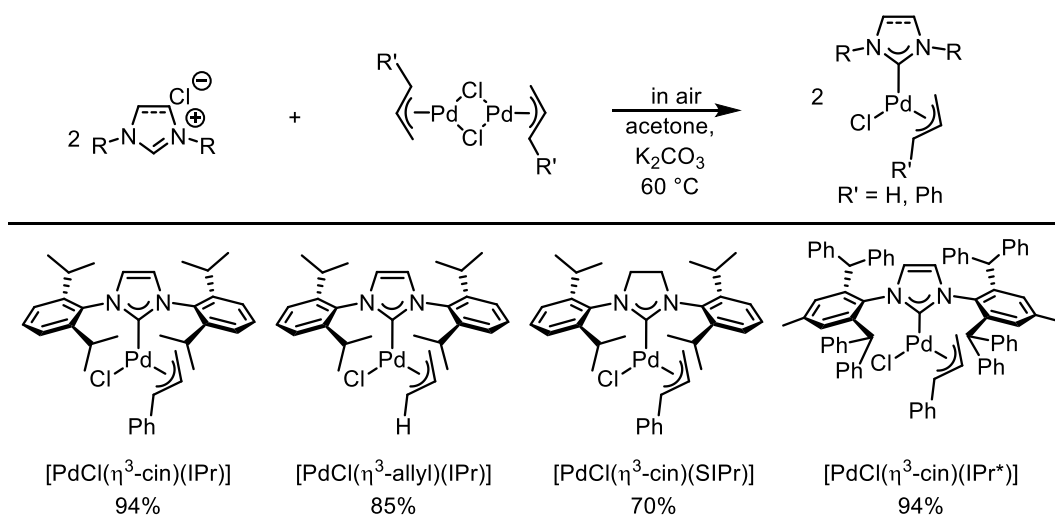


Scheme 2.5: Synthesis of $[\text{NHC}\cdot\text{H}][\text{ZnXY}_3]$ complexes.³⁰

Since the NHC salt will react with the metal source in the absence of base to generate these “ate” complexes, Nolan and Cazin have studied the formation and fully characterised these “ate” intermediates for gold and copper.^{24,25} Furthermore, Nolan postulated that the formation of this intermediate is important before the base is added to achieve high yields.²⁴ Considering the success in literature for many different NHC-metal complexes, it was applied to the synthesis of $[\text{PdCl}(\eta^3\text{-R-allyl})(\text{NHC})]$ complexes, in order to establish an air- and moisture-stable synthesis.

2.2 Optimisation of the synthesis of $[\text{PdCl}(\eta^3\text{-R-allyl})(\text{NHC})]$ complexes

The investigation began with the attempted synthesis of complexes of relevance to cross-coupling catalysis, namely $[\text{PdCl}(\eta^3\text{-cin})(\text{IPr})]$ (IPr = *N,N*-bis-[2,6-(di-*iso*-propyl)phenyl]imidazol-2-ylidene), $[\text{PdCl}(\eta^3\text{-cin})(\text{SIPr})]$ (SIPr = *N,N*-bis-[2,6-(di-*iso*-propyl)phenyl]imidazolidin-2-ylidene), $[\text{PdCl}(\eta^3\text{-allyl})(\text{IPr})]$ and $[\text{PdCl}(\eta^3\text{-cin})(\text{IPr}^*)]$ (IPr* = *N,N*-bis-[2,6-bis(diphenylmethyl)-4-methylphenyl]imidazol-2-ylidene) using the weak base approach (K_2CO_3). Two different palladium sources were tested; $[\text{Pd}(\eta^3\text{-allyl})(\mu\text{-Cl})_2]$ and $[\text{Pd}(\eta^3\text{-cin})(\mu\text{-Cl})_2]$ as well as three different NHC salts (IPr·HCl, SIPr·HCl and IPr*·HCl), which are electronically and sterically different as well as being the most widely used in catalytic processes (Scheme 2.6).



Scheme 2.6: Synthesis of $[\text{PdCl}(\eta^3\text{-R-allyl})(\text{NHC})]$ complexes using the weak base approach. Reaction conditions: In air, NHC·HCl (2 equiv.), $[\text{Pd}(\eta^3\text{-allyl})(\mu\text{-Cl})_2]$ (0.048 mmol) or $[\text{Pd}(\eta^3\text{-cin})(\mu\text{-Cl})_2]$ (0.048 mmol), K_2CO_3 (4 equiv.), acetone (0.28 M), 60 °C, 5 h. Work up: Filtration through silica; isolated yields.

Our main goal was to develop a green and efficient synthesis of these well-defined Pd-NHC complexes using the weak base approach. Another important aspect was to establish a simple, practical and fast work up, while maintaining high yields and high degrees of purity. Under the optimised conditions for copper and gold systems, the palladium dimers $[\text{Pd}(\eta^3\text{-allyl})(\mu\text{-Cl})_2]$ and $[\text{Pd}(\eta^3\text{-cin})(\mu\text{-Cl})_2]$ were reacted with the NHC·HCl of the corresponding NHC ligands, IPr, its saturated analogue SIPr and the sterically more encumbered congener IPr* in acetone in the

presence of K_2CO_3 in air. All reactions were successful, and the optimised conditions of each target complex are summarised in Table 2.1. Following this, several different $[\text{PdCl}(\eta^3\text{-R-allyl})(\text{NHC})]$ complexes were synthesised and optimised through this new route (Table 2.1). Noteworthy is the establishment of two variations, depending on the bulk of the corresponding NHC salt. Firstly when “less” bulky NHC salts were used, such as IPr (Table 2.1, entry 1 and 2), SIPr (Table 2.1, entry 3) or SIMes (SIMes = *N,N*-bis-(2,4,6-trimethylphenyl)imidazolidin-2-ylidene) (Table 2.1, entry 6), a slight excess of 2.4 equivalent of the corresponding NHC salt was the optimal amount to achieve high yields. During the optimisation an increase in the amount of K_2CO_3 led to an acceleration of the reaction but also led to an increased formation of side-products, therefore two equivalents of K_2CO_3 was found to be the optimal amount. The NHC salt and the palladium dimer were pre-mixed in acetone at room temperature, followed immediately by the addition of K_2CO_3 , then heated for 5 hours at 60 °C (Further optimisation result can be found in the experimental chapter).

Table 2.1: Summary of the optimised condition for the scope.

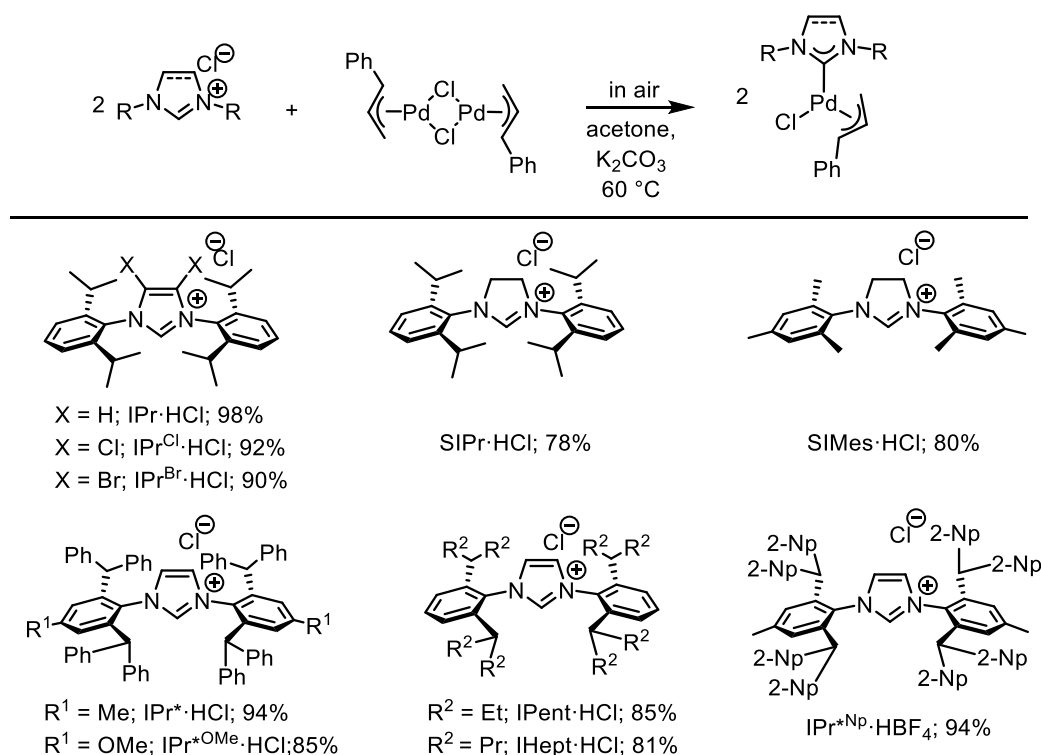
$$2 \text{ NHC} \cdot \text{HCl} + [\text{Pd}(\eta^3\text{-R-allyl})(\mu\text{-Cl})]_2 \xrightarrow[60^\circ\text{C}]{\text{acetone, } \text{K}_2\text{CO}_3} [\text{PdCl}(\eta^3\text{-R-allyl})(\text{NHC})]$$

Entry	Complex	NHC·HCl (equiv.)	K_2CO_3 (equiv.)	t (h)	Yield (%)
1	$[\text{PdCl}(\eta^3\text{-cin})(\text{IPr})]$	2.4	2	5	98
2	$[\text{PdCl}(\eta^3\text{-allyl})(\text{IPr})]$	2.4	2	5	85
3	$[\text{PdCl}(\eta^3\text{-cin})(\text{SIPr})]$	2.4	2	5	78
4	$[\text{PdCl}(\eta^3\text{-cin})(\text{IPr}^{\text{Cl}})]$	2.4	2	5	92
5	$[\text{PdCl}(\eta^3\text{-cin})(\text{IPr}^{\text{Br}})]$	2.4	2	5	90
6	$[\text{PdCl}(\eta^3\text{-cin})(\text{SIMes})]$	2.4	2	5	80
7	$[\text{PdCl}(\eta^3\text{-cin})(\text{IPr}^*)]$	2	4	24	94
8	$[\text{PdCl}(\eta^3\text{-cin})(\text{IPr}^{\text{OMe}})]$	2	4	24	85
9	$[\text{PdCl}(\eta^3\text{-cin})(\text{IPr}^{\text{Np}})]$	2	4	24	94
10	$[\text{PdCl}(\eta^3\text{-cin})(\text{IPent})]$	2	4	24	85
11	$[\text{PdCl}(\eta^3\text{-cin})(\text{IHept})]$	2	4	24	81

Reaction conditions: NHC·HCl (0.1 to 0.3 mmol), $[\text{Pd}(\eta^3\text{-R-allyl})(\mu\text{-Cl})]_2$ (1 equiv.), K_2CO_3 and acetone at 60 °C, for the indicated time. Isolated yields are average of two reactions.

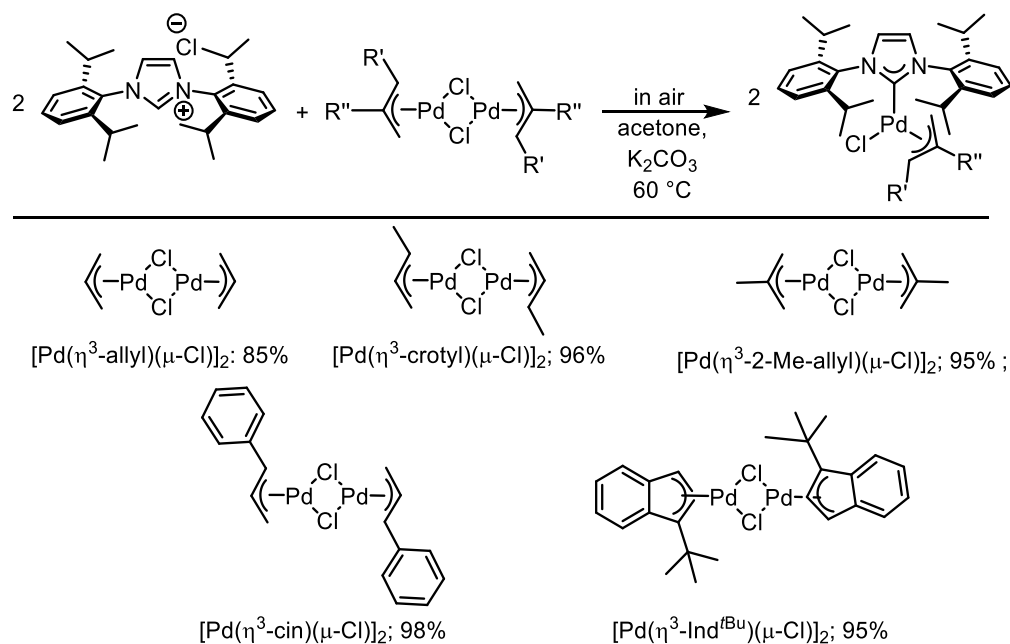
This variation was successfully applied to Table 2.1, entries 1-6. The optimisation of larger NHCs, such as IPr* (Table 2.1, entry 7), revealed interesting insights into the reaction mechanism. The ideal ratio of NHC·HCl and $[\text{Pd}(\eta^3\text{-cin})(\mu\text{-Cl})]_2$ was found to be 2:1 but four equivalent of K_2CO_3 were required to reach excellent yields after 24 hours. The acetone concentration was also an

important factor to reduce side-product formation. By reducing the molar concentration several side-products were detected via ^1H NMR spectroscopy. Interestingly the ideal concentration in acetone was found to be the same for all complexes (0.23 M). More interestingly in this variation, the NHC·HCl and the palladium dimer had to be pre-mixed in acetone for 1 hour at 60 °C, followed by the addition of K_2CO_3 and further heating at 60 °C for 24 hours. The pre-mixing of the two starting materials was necessary in order to obtain high yields but more importantly to prevent the formation of side-products. Therefore, it was postulated that the formation of a palladate intermediate has to be done before the base is added.



Scheme 2.7: The scope of $[\text{PdCl}(\eta^3\text{-cin})(\text{NHC})]$ complexes, illustrating the different NHC·HCl used. Reaction conditions: NHC·HCl (0.1 to 0.3 mmol), $[\text{Pd}(\eta^3\text{-cin})(\mu\text{-Cl})_2]$ (1 equiv.), K_2CO_3 (1st row: 2 equiv.; 2nd row 4 equiv.) and acetone at 60 °C, for 1st row: 5 h and 2nd row 24 h. Isolated yields are average of two reactions.

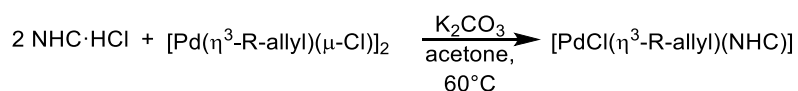
To highlight the efficiency of the system, different commercially available palladium dimers were reacted with IPr·HCl under the optimised conditions, resulting in good to excellent yields. Changing the substituent on the allyl ligand was widely accepted (Scheme 2.8). The newly synthesised $[\text{Pd}(\eta^3\text{-Ind}^{\text{tBu}})(\mu\text{-Cl})_2]$ dimer (Ind^{tBu} = 1-*tert*-butyl-1H-indene), was successfully applied in the synthesis of $[\text{PdCl}(\eta^3\text{-Ind}^{\text{tBu}})(\text{IPr})]$, which is a very active pre-catalyst for the Suzuki-Miyaura reaction.³²



Scheme 2.8: The scope of [PdCl(η³-R-allyl)(IPr)] complexes, illustrating the different Pd dimers used. Reaction conditions: IPr·HCl (0.1 mmol), [Pd(η³-R-allyl)(μ-Cl)]₂ (1 equiv.), K₂CO₃ (1st row: 2 equiv.) and acetone at 60 °C, for 5h. Isolated yields are average of two reactions.

It should be stated that [Pd(IPr)(η³-cin)Cl], [Pd(IPr)(η³-allyl)Cl] and [Pd(IPr*)(η³-cin)Cl] could be scaled up to multi-gram quantities with excellent yields (Table 2.2).

Table 2.2: The large scale reaction of [PdCl(η³-R-allyl)(NHC)] complexes.



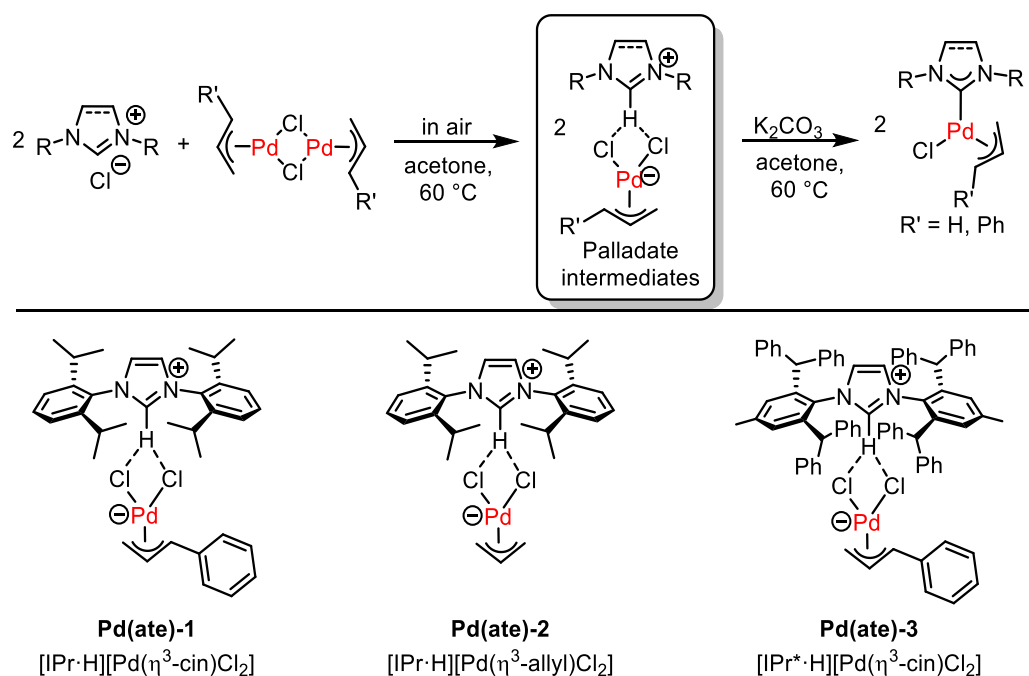
Entry	Complex	t (h)	Yield % (g)
1	[PdCl(η ³ -cin)(IPr)]	10	97 (4.9)
2	[PdCl(η ³ -allyl)(IPr)]	10	92 (2.9)
3	[PdCl(η ³ -cin)(IPr*)]	24	98 (4.2)

Reaction conditions: NHC·HCl (2.2 equiv. for entries 1-2 and 2 equiv. for entry 3), [Pd(η³-R-allyl)(μ-Cl)]₂ (1 equiv.), K₂CO₃ (2 equiv. for entries 1-2 and 4 equiv. for entry 3) and acetone at 60 °C for the indicated time. Isolated yield.

Further optimisation of the synthesis was conducted by varying the base from a weak inorganic base, K₂CO₃, to a stronger organic base NEt₃. The model synthesis of [PdCl(η³-cin)(IPr)] was performed under the optimised reaction conditions using triethylamine as base. Consequently, the desired complex was acquired in a lower yield than expected. The ¹H NMR spectrum of the crude showed traces of side-products, which required an extra recrystallisation step in the work up of the complex.

As for looking into the possibility of using different solvents our interest was set on ethanol as a greener alternative to acetone.³³ Delightfully the reaction proceeded smoothly, using the optimised reaction conditions, only changing from acetone to ethanol (0.23 M).

$[\text{PdCl}(\eta^3\text{-cin})(\text{IPr})]$ was isolated in 64% yield. From simple examination of these results it was clear that steric bulk (such as that found in $\text{IPr}^*\cdot\text{HCl}$, $\text{IPr}^{*\text{OMe}}\cdot\text{HCl}$ ($\text{IPr}^{*\text{OMe}} = N,N\text{-bis-[2,6-bis(diphenyl)-4-methoxyphenyl]imidazol-2-ylidene}$), $\text{IPr}^{*2\text{-Np}}\cdot\text{HBF}_4$ ($\text{IPr}^{*2\text{-Np}} = N,N\text{-bis-[2,6-bis(dinaphthalene)-4-methylphenyl]imidazol-2-ylidene}$), $\text{IPent}\cdot\text{HCl}$ ($\text{IPent} = N,N\text{-bis-[2,6-bis(di-iso-pentyl)phenyl]imidazol-2-ylidene}$) and $\text{IHept}\cdot\text{HCl}$ ($\text{IHept} = N,N\text{-bis-[2,6-bis(di-iso-heptyl)phenyl]imidazol-2-ylidene}$) played an important role not just in the formation of the product but also in the possible formation of an intermediate. To confirm our suspicion about the presence of an “ate” intermediate and how rapidly this may form as a function of steric bulk of the imidazolium salt, these intermediates were targeted for isolation (Scheme 2.9). To obtain the intermediate the synthesis was performed without the addition of the base. The isolated compounds were obtained in a straightforward manner, by simple removal of solvent, in quantitative yields and characterised by NMR spectroscopy and elemental analysis. The ^1H NMR data revealed the presence of an imidazol(idin)ium proton. In the case of $[\text{IPr}\cdot\text{H}][\text{Pd}(\eta^3\text{-cin})\text{Cl}_2]$, the ^1H NMR spectrum was compared with $\text{IPr}\cdot\text{HCl}$, showing a drastic upfield shift of the imidazolium proton from 10.08 ppm for $\text{IPr}\cdot\text{HCl}$ to 9.26 ppm for $[\text{IPr}\cdot\text{H}][\text{Pd}(\eta^3\text{-cin})\text{Cl}_2]$ (Figure 2.1).



Scheme 2.9: Proposed reaction mechanism.

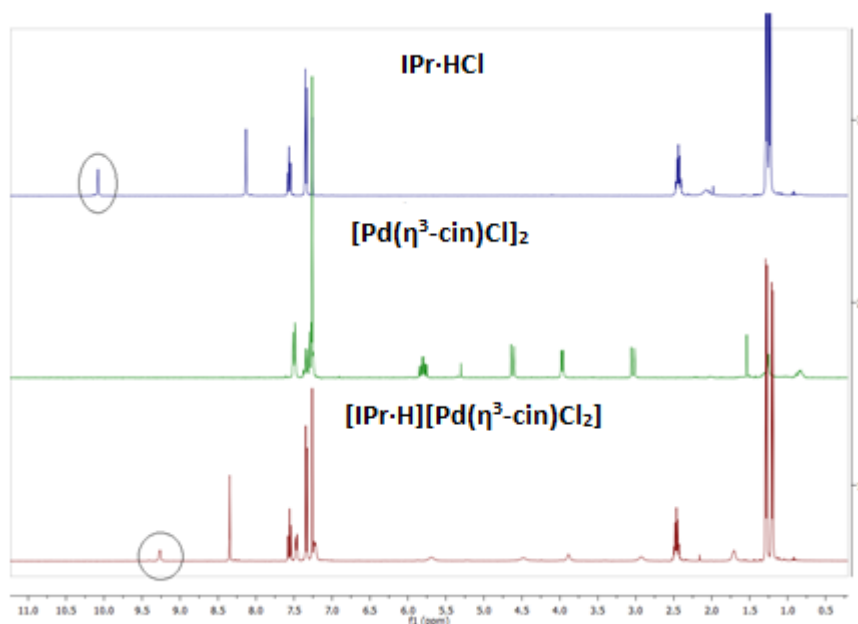


Figure 2.1: Comparison of the ^1H NMR spectra of $[\text{IPr}\cdot\text{H}][\text{Pd}(\eta^3\text{-cin})\text{Cl}_2]$ with its starting material.

X-Ray diffraction on single crystal confirmed the identity of these intermediate as palladates associated with imidazol(idin)ium counterions. By simply mixing the NHC·HCl and the palladium dimer in acetone at $60\text{ }^\circ\text{C}$ for 1 hour the isolation of $[\text{IPr}\cdot\text{H}][\text{Pd}(\eta^3\text{-cin})\text{Cl}_2]$, $[\text{IPr}\cdot\text{H}][\text{Pd}(\eta^3\text{-allyl})\text{Cl}_2]$, $[\text{SIPr}\cdot\text{H}][\text{Pd}(\eta^3\text{-cin})\text{Cl}_2]$ and $[\text{IPr}^*\cdot\text{H}][\text{Pd}(\eta^3\text{-cin})\text{Cl}_2]$ were achieved. The crystal structures of both $[\text{IPr}\cdot\text{H}][\text{Pd}(\eta^3\text{-cin})\text{Cl}_2]$ and $[\text{IPr}^*\cdot\text{H}][\text{Pd}(\eta^3\text{-cin})\text{Cl}_2]$ showed H-bonding interactions between the most acidic proton on the imidazolium heterocycle (C-2 position) and both the chloride ligands of the palladate counter ion, confirming the formation of a strong ion-pair in solid state (Figure 2.2). It can be reasoned that the stabilising interaction prevents decomposition of the palladate species as these complexes are air and moisture stable. In the case of $[\text{IPr}\cdot\text{H}][\text{Pd}(\eta^3\text{-cin})\text{Cl}_2]$ the distance between the C-2 hydrogen (H1) and the Cl1 is 2.740 \AA and Cl2 is 2.558 \AA . The isolation of such palladates bearing various $\eta^3\text{-allyl}$ fragments supports the general pathway to neutral Pd-NHC, involving their intermediary role. The formation of an imidazolium palladate salt such as $[\text{NHC}\cdot\text{H}][\text{Pd}(\eta^3\text{-R-allyl})\text{Cl}_2]$ from the NHC·HCl and corresponding palladium dimer is illustrated in Scheme 2.9. The addition of K_2CO_3 to the palladate intermediate results in the formation of the previously reported $[\text{PdCl}(\eta^3\text{-R-allyl})(\text{NHC})]$ complex (Scheme 2.9).

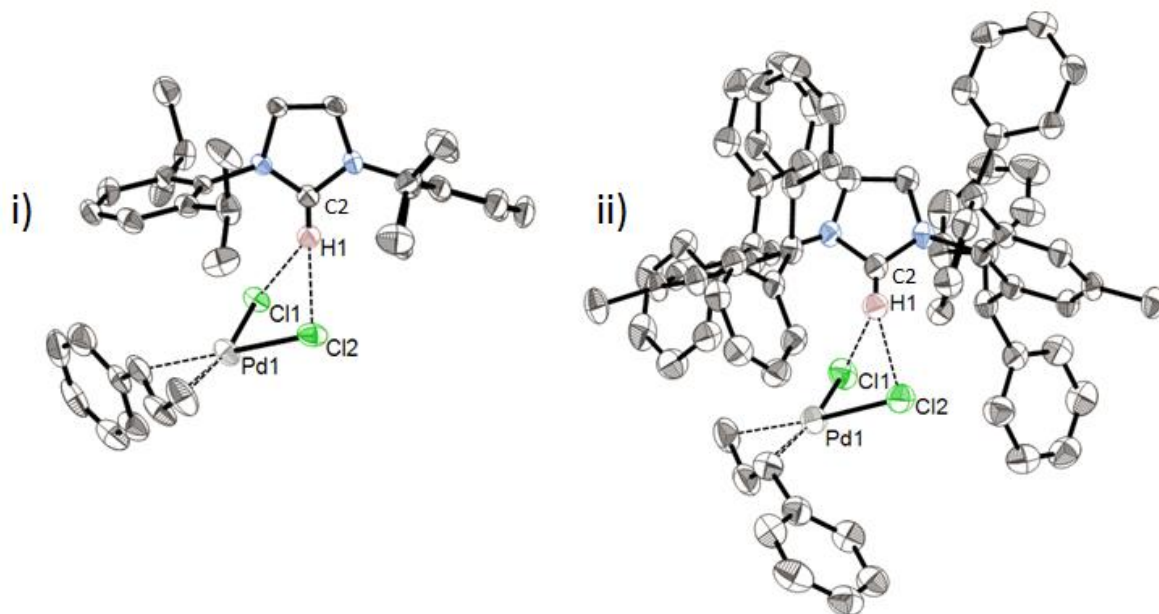
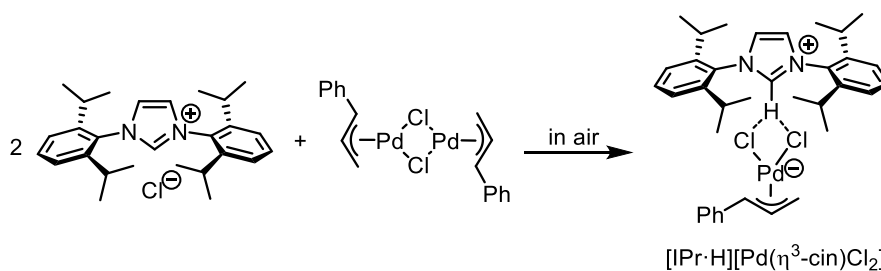


Figure 2.2 Crystal structures of $[IPr\cdot H][Pd(\eta^3\text{-cin})Cl_2]$ (i) and $[IPr^*\cdot H][Pd(\eta^3\text{-cin})Cl_2]$ (ii).

2.3 Synthesis of $[NHC\cdot H][Pd(\eta^3\text{-R-allyl})Cl_2]$ Complexes

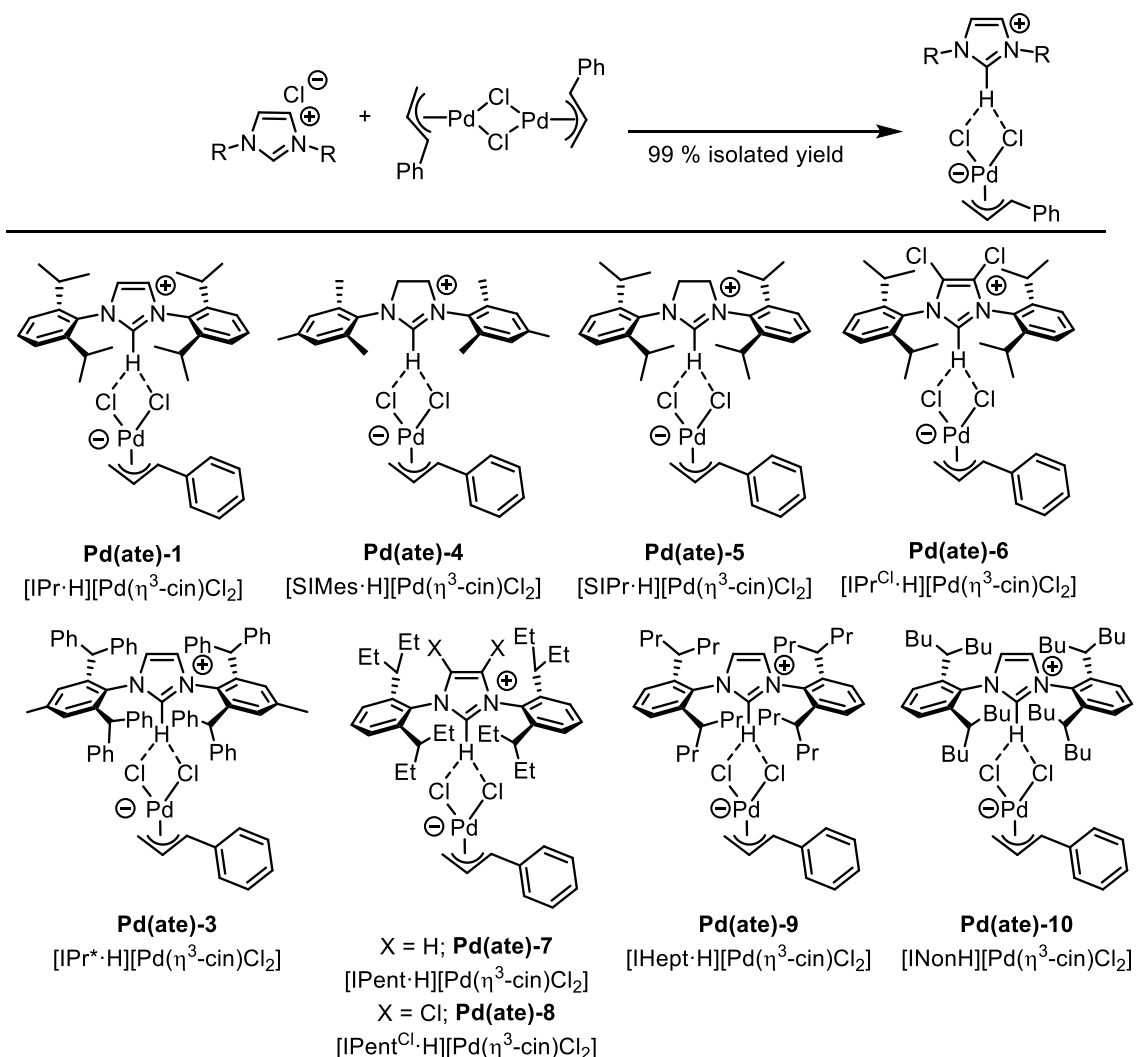
As these newly synthesised complexes showed very interesting characteristics, a closer look into the synthesis was taken. Firstly, the synthesis as mentioned before was carried out in air and resulted in air and moisture stable complexes. Furthermore, by simply removing the solvent the complex can be obtained in quantitative yield as an analytically pure complex. No additives were needed, and the original synthesis was carried out in acetone at 60 °C. The model complex used for the investigation was $[IPr\cdot H][Pd(\eta^3\text{-cin})Cl_2]$, starting from $IPr\cdot HCl$ and $[Pd(\eta^3\text{-cin})(\mu\text{-Cl})_2]$. Different solvents were tested and the focus was drawn to environmentally-friendly solvents. A total of 8 solvents were tested; all reactions resulted in quantitative yield of $[IPr\cdot H][Pd(\eta^3\text{-cin})Cl_2]$ (Table 2.3). This suggested that the polarity of the solvent does not play a role in the reaction. What was most interesting was the successful reaction in solvents such as water and ethanol in which the starting materials were not fully soluble. Considering this finding, a solvent-free synthesis was conducted between the two solids; $IPr\cdot HCl$ and $[Pd(\eta^3\text{-cin})(\mu\text{-Cl})_2]$. By simply grinding the two starting materials using a pestle and mortar $[IPr\cdot H][Pd(\eta^3\text{-cin})Cl_2]$ was obtained analytically pure, eliminating any kind of work up.

Table 2.3: Solvent optimisation of $[IPr\cdot H][Pd(\eta^3\text{-}cin)Cl_2]$.

Entry	Solvent	Yield (%)
1	Acetone	>99
2	Cyclopentylmethyl ether	>99
3	Pentane	>99
4	Dichloromethane	>99
5	Chloroform	>99
6	Water	>99
7	Ethyl acetate	>99
8	Ethanol	>99
9	No solvent	>99

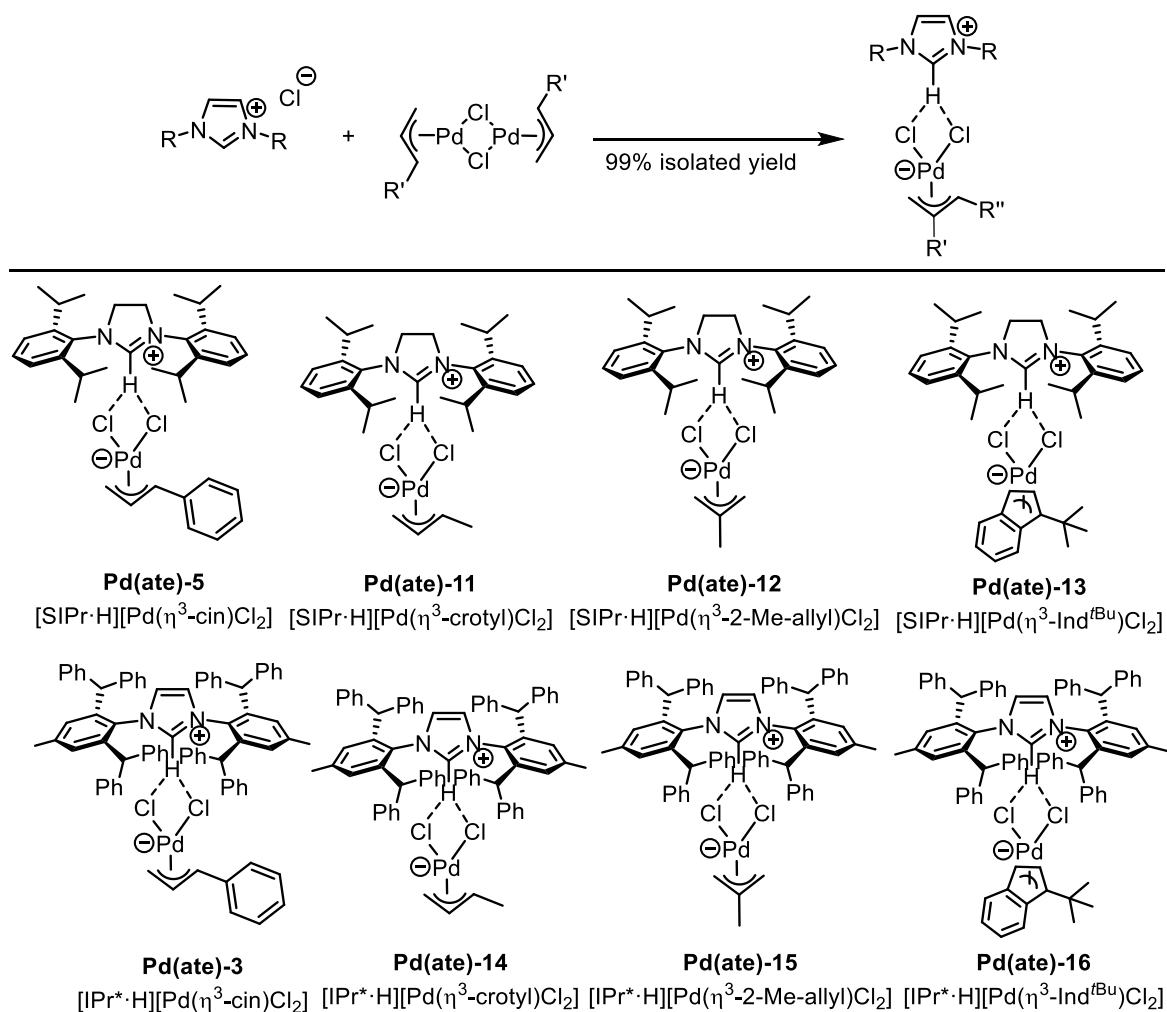
Reaction conditions: In air, $IPr\cdot HCl$ (2 equiv.), $[Pd(\eta^3\text{-}cin)(\mu\text{-}Cl)_2]$ (1 equiv.) and a magnetic stir bar were charged in a vial and solvent (1 mL) was added. The mixture was stirred at 60 °C for 1 hour. The reaction was allowed to cool for 1 min and the sample was concentrated to 1/3 of the original volume under reduced pressure. Microcrystalline product collected by filtration and washed with minimum amount of cold acetone or ethanol if necessary. The Solid was dried under vacuum. For entry 9: In air, the $IPr\cdot HCl$ (2 equiv.) and $[Pd(\eta^3\text{-}cin)(\mu\text{-}Cl)_2]$ (1 equiv.) were added to a mortar. The two solids were mixed and ground using a pestle for 5 min. The product was obtained as a crystalline solid in quantitative yield.

Considering this very simple and fast synthesis of new organometallic complexes, the scope was conducted. In that context, various NHC salts, bearing different electronic and steric properties, were tested with $[Pd(\eta^3\text{-}cin)(\mu\text{-}Cl)_2]$ (Scheme 2.10). The smaller NHC, $IMes\cdot HCl$ resulted in quantitative yield, similarly $SIPr\cdot HCl$ and $IPr^{Cl}\cdot HCl$ ($IPr^{Cl} = N,N$ -bis-[2,6-(di-*iso*-propyl)phenyl-4,5-dichloro]imidazol-2-ylidene) followed the same trend. Increasing the steric bulk, $IPr^*\cdot HCl$ and the ITent series; $IPent\cdot HCl$, $IHept\cdot HCl$ and $INon\cdot HCl$ ($INon = N,N$ -bis-[2,6-bis(di-*iso*-nonyl)phenyl]imidazol-2-ylidene) did not show any decrease in reactivity. All resulting complexes were isolated in quantitative yield and fully characterised using NMR spectroscopy and elemental analysis.



Scheme 2.10: Scope of $[\text{NHC}\cdot\text{H}][\text{Pd}(\eta^3\text{-cin})\text{Cl}_2]$; Part 1. Reaction conditions: In air, the corresponding NHC·HCl (2 equiv.) and $[\text{Pd}(\eta^3\text{-cin})(\mu\text{-Cl})_2]$ (1 equiv.) were added to a mortar. The two solids were mixed and ground using a pestle for 5 min. The product was obtained as a crystalline solid in quantitative yield.

Next, different palladium sources were investigated. Two NHC salts were chosen, bearing different electronic and steric properties, namely SIPr·HCl and IPr*·HCl (Scheme 2.11). Four palladium dimers were used; $[\text{Pd}(\eta^3\text{-cin})(\mu\text{-Cl})_2]$ as the “model” dimer investigated previously; $[\text{Pd}(\eta^3\text{-crotyl})(\mu\text{-Cl})_2]$ where the phenyl ring on the allyl ligand is exchanged to a methyl group; $[\text{Pd}(\eta^3\text{-2-Me-allyl})(\mu\text{-Cl})_2]$, swapping position of the substituent on the allyl. The previously mentioned $[\text{Pd}(\eta^3\text{-Ind}^{\text{tBu}})(\mu\text{-Cl})_2]$ dimer reported by Hazari and co-workers was used as an alternative to the allyl derivatives. Yet again, all complexes were successfully synthesised and isolated in quantitative yield as well as fully characterised.



Scheme 2.11: Scope of $[NHC\cdot H][Pd(\eta^3\text{-R-allyl})Cl_2]$; Part 2. Reaction conditions: In air, the corresponding NHC-HCl (2 equiv.) and $[Pd(\eta^3\text{-R-allyl})(\mu\text{-Cl})_2]$ (1 equiv.) were added to a mortar. The two solids were mixed and grinded using a pestle for 5 min. A crystalline solid was obtained in quantitative yield.

Crystal structures were obtained for $[SiPr\cdot H][Pd(\eta^3\text{-2-Me-allyl})Cl_2]$, $[SiPr\cdot H][Pd(\eta^3\text{-crotyl})Cl_2]$ and $[SiPr\cdot H][Pd(\eta^3\text{-Ind}^{tBu})Cl_2]$. A similar structure configuration was observed where the most acidic proton on the imidazolium salt (C-2 position) has a close interaction with the chloride ligands on the palladium (Figure 2.3).

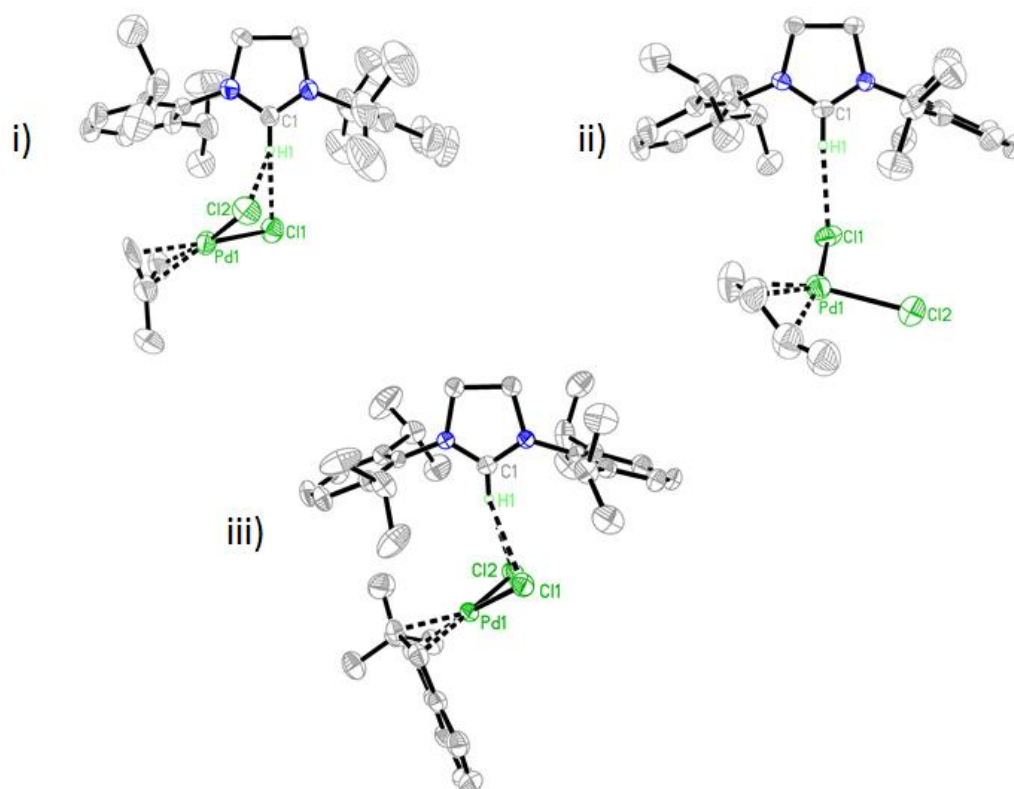


Figure 2.3: X-ray single crystal structures of $[SIPr\cdot H][Pd(\eta^3\text{-2-Me-allyl})Cl_2]$ (i), $[SIPr\cdot H][Pd(\eta^3\text{-crotyl})Cl_2]$ (ii) and of $[SIPr\cdot H][Pd(\eta^3\text{-Ind}^{tBu})Cl_2]$ (iii).

All palladate complexes synthesised were air and moisture stable complexes. The first three synthesised complexes $[IPr\cdot H][Pd(\eta^3\text{-cin})Cl_2]$, $[IPr\cdot H][Pd(\eta^3\text{-allyl})Cl_2]$ and $[IPr^*\cdot H][Pd(\eta^3\text{-cin})Cl_2]$ were kept on the bench for 2 years without any sign of decomposition. This was confirmed by 1H NMR spectroscopy and elemental analysis. This is illustrating the stability of these newly synthesised Pd-NHC complexes.

2.4 Conclusion

A simple and efficient synthesis for an important class of palladium-NHC pre-catalysts $[PdCl(\eta^3\text{-R-allyl})(NHC)]$ was developed. The synthesis was optimised resulting in the use of a mild inorganic base and an inexpensive solvent. Furthermore, the synthesis can be carried out in air without the need of dry solvents. It was shown that the reaction proceeds *via* the formation of a palladate intermediate and the rate of formation of the latter is principally affected by the steric bulk of the NHC salt. The efficiency and simplicity of this protocol ensured the reliable scale up of previously developed complexes and will most likely facilitate the development of new congeners of this frequently used class of cross-coupling pre-catalysts. Additionally, the palladate species found as intermediate in the synthesis of $[PdCl(\eta^3\text{-R-allyl})(NHC)]$ was isolated and fully characterised. A closer look towards their synthesis was taken, resulting in a solvent-free synthesis. A scope was conducted by firstly changing the NHC salts bearing many variations of electronic and steric properties, followed by changing the palladium dimer. All complexes were synthesised in air and are air and moisture stable complexes.

In the following chapters the catalytic activity of the palladate complexes will be discussed, focusing on cross-coupling chemistry.

2.5 References

- (1) M. S. Viciu, R. F. Germaneau and S. P. Nolan, *Org. Lett.*, **2002**, *4*, 4053–4055.
- (2) M. S. Viciu, R. F. Germaneau, O. Navarro-Fernandez, E. D. Stevens and S. P. Nolan, *Organometallics*, **2002**, *21*, 5470–5472.
- (3) O. Navarro, N. Marion, J. Mei and S. P. Nolan, *Chem. Eur. J.*, **2006**, *12*, 5142–5148.
- (4) A. Chartoire, X. Frogneux and S. P. Nolan, *Adv. Synth. Catal.*, **2012**, *354*, 1897–1901.
- (5) A. R. Martin, A. Chartoire, A. M. Z. Slawin and S. P. Nolan, *Beilstein J. Org. Chem.*, **2012**, *8*, 1637–43.
- (6) G. Bastug and S. P. Nolan, *J. Org. Chem.*, **2013**, *78*, 9303–9308.
- (7) F. Izquierdo, A. Chartoire and S. P. Nolan, *ACS Catal.*, **2013**, *3*, 2190–2193.
- (8) J. M. Collinson, J. D. E. T. Wilton-Ely and S. Díez-González, *Catal. Commun.*, **2016**, *87*, 78–81.
- (9) A. Chartoire, M. Lesieur, L. Falivene, A. M. Z. Slawin, L. Cavallo, C. S. J. Cazin and S. P. Nolan, *Chem. Eur. J.*, **2012**, *18*, 4517–21.
- (10) A. B. Dounay and L. E. Overman, *Chem. Rev.*, **2003**, *103*, 2945–2963.
- (11) M. H. Majeed, P. Shayesteh, R. Wallenberg, A. R. Persson, N. Johansson, L. Ye, J. Schnadt and O. F. Wendt, *Chem. Eur. J.*, **2017**, *23*, 8457–8465.
- (12) P. E. Tessier, A. J. Penwell, F. E. S. Souza and A. G. Fallis, *Org. Lett.*, **2003**, *5*, 2989–2992.
- (13) A. Zapf and M. Beller, *Top. Catal.*, **2002**, *19*, 101–109.
- (14) M. S. Viciu, O. Navarro, R. F. Germaneau, R. A. K. Iii, W. Sommer, N. Marion, E. D. Stevens, L. Cavallo and S. P. Nolan, *Organometallics*, **2004**, *23*, 1629–1635.
- (15) S. Roland, M. Audouin and P. Mangeney, *Organometallics*, **2004**, *23*, 3075–3078.
- (16) H. Clavier, A. Correa, L. Cavallo, E. C. Escudero-Adán, J. Benet-Buchholz, A. M. Z. Slawin and S. P. Nolan, *Eur. J. Inorg. Chem.*, **2009**, *2009*, 1767–1773.
- (17) S. Dastgir, K. S. Coleman, A. R. Cowley and M. L. H. Green, *Organometallics*, **2010**, *29*, 4858–4870.
- (18) B. R. Dible, R. E. Cowley and P. L. Holland, *Organometallics*, **2011**, *30*, 5123–5132.
- (19) T. Terashima, S. Inomata, K. Ogata and S. I. Fukuzawa, *Eur. J. Inorg. Chem.*, **2012**, 1387–1393.
- (20) A. Winkler, K. Brandhorst, M. Freytag, P. G. Jones and M. Tamm, *Organometallics*, **2016**, *35*, 1160–1169.
- (21) P. L. Arnold, *Heteroat. Chem.*, **2002**, *13*, 534–539.
- (22) M. R. L. Furst and C. S. J. Cazin, *Chem. Commun.*, **2010**, *46*, 6924–6925.

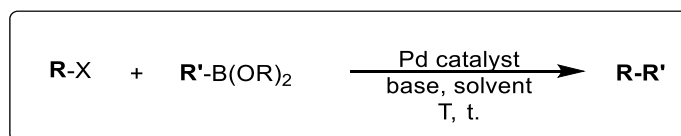
- (23) M. J. Cawley, F. G. N. Cloke, R. J. Fitzmaurice, S. E. Pearson, J. S. Scott and S. Caddick, *Org. Biomol. Chem.*, **2008**, *6*, 2820–2825.
- (24) A. Collado, A. Gómez-Suárez, A. R. Martín, A. M. Z. Slawin and S. P. Nolan, *Chem. Commun.*, **2013**, *49*, 5541.
- (25) N. H. C. N-heterocyclic, X. Cl, O. Santoro, A. Collado, A. M. Z. Slawin, S. P. Nolan and C. S. J. Cazin, *Chem. Commun.*, **2013**, *49*, 10483–10485.
- (26) R. Visbal, A. Laguna and M. C. Gimeno, *Chem. Commun.*, **2013**, *49*, 5642.
- (27) R. Savka and H. Plenio, *Dalt. Trans.*, **2015**, *44*, 891–893.
- (28) G.-R. Peh, E. A. B. Kantchev, C. Zhang and J. Y. Ying, *Org. Biomol. Chem.*, **2009**, *7*, 2110–2119.
- (29) G. R. Peh, E. A. B. Kantchev, J. C. Er and J. Y. Ying, *Chem. Eur. J.*, **2010**, *16*, 4010–4017.
- (30) O. Santoro, F. Nahra, D. B. Cordes, A. M. Z. Slawin, S. P. Nolan and C. S. J. Cazin, *J. Mol. Catal. A Chem.*, **2016**, *423*, 85–91.
- (31) O. Santoro, A. Collado, A. M. Z. Slawin, S. P. Nolan and C. S. J. Cazin, *Chem. Commun.*, **2013**, *49*, 10483–5.
- (32) P. R. Melvin, A. Nova, D. Balcells, W. Dai, N. Hazari, D. P. Hruszkewycz, H. P. Shah and M. T. Tudge, *ACS Catal.*, **2015**, *5*, 3680–3688.
- (33) D. Prat, J. Hayler and A. Wells, *Green Chem.*, **2014**, *16*, 4546–4551.

Chapter 3

Investigation into the catalytic activity of [NHC·H][Pd(R)Cl₂] complexes in the Suzuki-Miyaura reaction

3.1 The Suzuki-Miyaura reaction

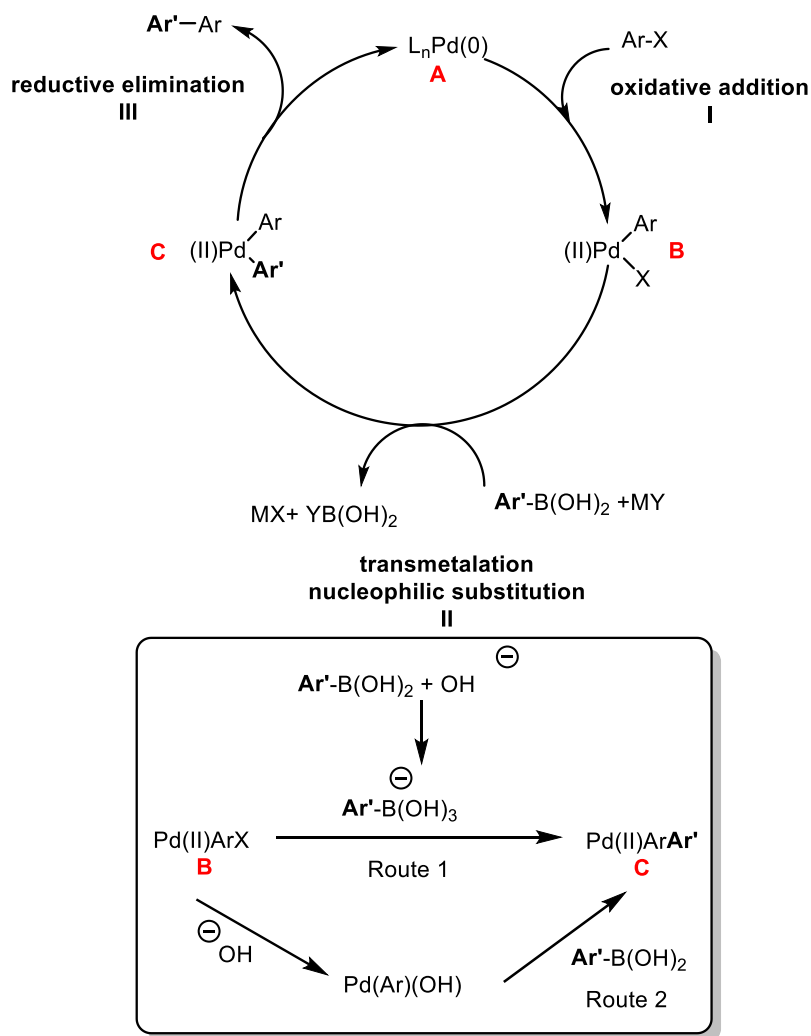
The formation of C-C bonds is one of the most important and common reactions in modern synthetic chemistry.¹⁻³ Using an organopalladium complex as catalyst has revolutionized this field and the area was rewarded with the 2010 Nobel Prize in Chemistry. Palladium complexes are nowadays widely used for this purpose.⁴ As the area affects the polymer, fine chemical and pharmaceutical industries, research continues to be focused on improving existing methodologies and developing novel transformations using this metal-catalyzed strategy.⁵⁻⁷ In 1979, Akira Suzuki and Norio Miyaura published the reaction of 1-alkenylboranes with 1-alkenyl or 1-alkynyl halides using a catalytic amount of a palladium catalyst.⁸ The principle feature of the newly reported cross-coupling reactions was the catalytic amount of palladium complex needed (Scheme 3.1).



Scheme 3.1: The Suzuki-Miyaura reaction.⁸

Different palladium complexes have been reported as pre-catalysts in the Suzuki-Miyaura reaction, such as Pd(OAc)₂, [PdCl₂(PPh₃)] and [Pd(PPh₃)₄].⁸ The catalytic cycle of the Suzuki-Miyaura reaction was discussed in depth by Miyaura and Suzuki,⁸ concluding three main steps: the oxidative addition, transmetalation and the reductive elimination. The oxidative addition of an alkyl/aryl halide to a Pd(0) species to form Pd(II)_{L_n}ArX is the first step (Scheme 3.2, I). This is thought of the rate determining step of the catalysis but widely depends on the palladium catalyst.^{8,9} The rate of the oxidative reaction can be influenced by the halide or pseudo-halide used and is decreasing in the order I > OTf > Br >> Cl.⁸ This is due to the bond dissociation enthalpy (BDE) of the alkyl/aryl-halide bond. For example comparing the BDE of Cl = 95.5 ± 1.5 kcal mol⁻¹ and I = 65.0 ± 1.0 kcal mol⁻¹. The next step in the catalytic cycle is the transmetalation step (Scheme 3.2, II). Two routes are possible and studied in the literature.^{10,11} In the first route

the organoboron reagent reacts with a base to form a nucleophilic boronate species. This species is then reacting with $L_nPd(II)ArX$ (**B**) to give $L_nPd(II)ArAr'$ (**C**) (Scheme 3.2). In the second route **B** reacts with the base to form a palladium hydroxo complex, which then reacts with a neutral organoboron reagent to give **C**. The reductive elimination is the last step in the catalytic cycle, releasing the product and generating the active $Pd(0)$ species (Scheme 3.2 III).



Scheme 3.2: Catalytic cycle of the Suzuki-Miyaura reaction.^{8,10,11}

Nowadays the Suzuki-Miyaura reaction dominates the synthesis of biaryls and substituted aromatic compounds. Mild reaction conditions are leading the list of the many advantages that this reaction provides. Others include the exceptional functional group tolerance and the use of environmental friendly and cheap organoboron reagents.¹² The use of organoboron reagents bears many advantages as they are generally thermally stable and inert to water and oxygen. Furthermore the ease of handling organoboron reagents can be illustrated by the low toxicity and the ease of removal. The diversity of the Suzuki-Miyaura reaction is illustrated by the wide

range of products and their use in many different fields, such as natural product synthesis or pharmaceutical synthesis.¹³ Many different conditions have been developed and reformed since its discovery due to the enormous amount not all of the possibilities will be discussed.

The approach to catalyst formation has been refined over the last 15 years.² Initially a palladium source and a ligand (or ligand precursor) were used to generate the active complex *in situ*. Bulky and electron rich phosphine ligands have found to be beneficial in cross-coupling reactions.¹⁴ Buchwald and co-workers have reported the synthesis of tetra-*ortho*-substituted biaryls using hindered biaryl phosphine ligands (Figure 3.1).¹⁵

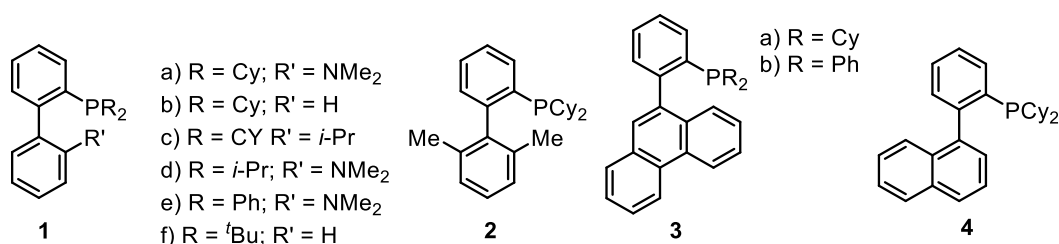
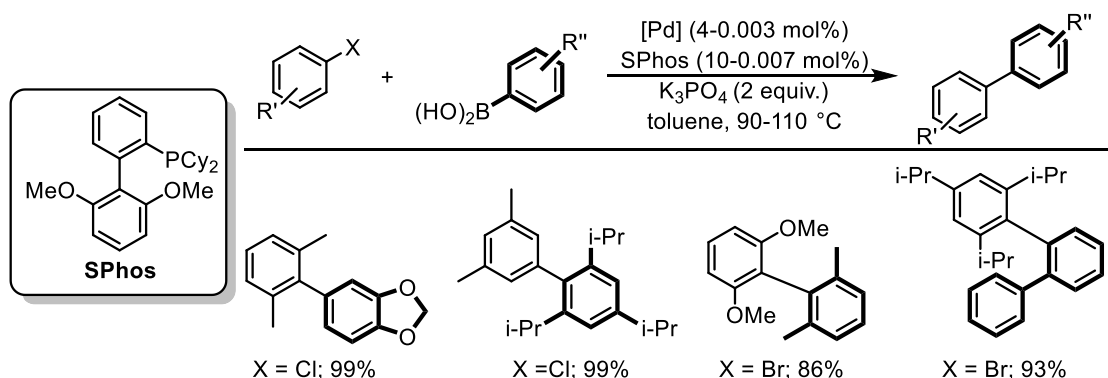


Figure 3.1: Examples of hindered biarylphosphine ligands.¹⁵

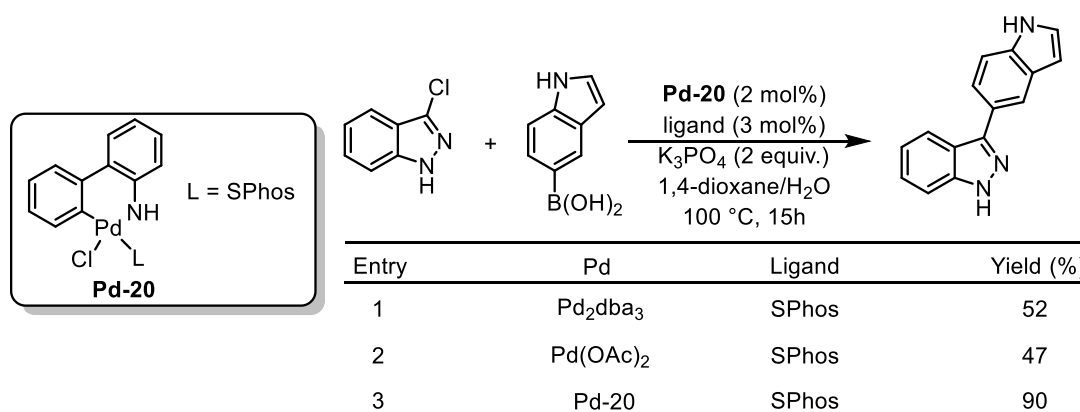
Organophosphines as ligands are strong π -acceptors as well as bearing σ -donor properties allowing the formation of stable complexes with high valent metals.¹⁶ The *in situ* formation of the catalyst generally consists of $[Pd_2(dba)_3]$ (dba = dibenzylideneacetone) or $[Pd(OAc)_2]$ as palladium source, combined with bulky phosphines such as P^tBu_3 , PCy_3 or PAd^tBu .¹⁶ The monoligated SPhos (2-dicyclohexylphosphino-2'-6'-dimethoxybiphenyl) ligand was tested in the Suzuki-Miyaura reaction and was able to couple very hindered *ortho*-,*ortho'*-substituted aryl halides (Scheme 3.3).¹⁷ Although high reaction temperatures (90–110 °C) were needed to achieve high yields.



Scheme 3.3: The Suzuki-Miyaura reaction using SPhos as ligand.¹⁷

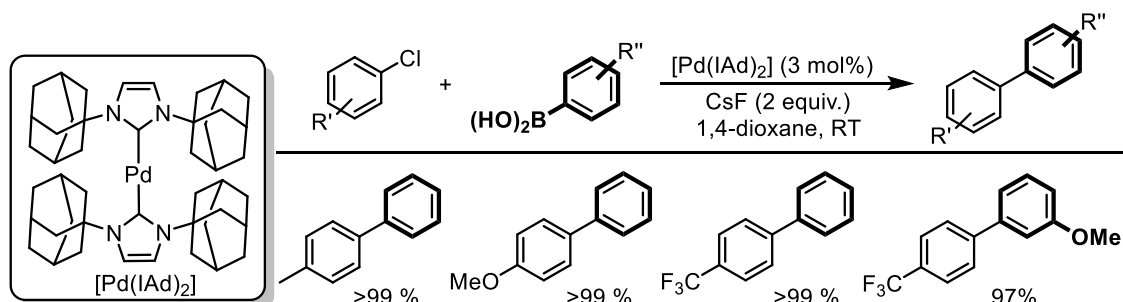
A second generation pre-catalyst containing SPhos as a ligand was reported by Buchwald, this time as a well-defined complex (Table 3.1). It was possible to couple a wide variety of unprotectedazole halides using mild conditions.¹⁸ A clear improvement in catalytic activity was observed when comparing the previously used *in situ* system to the second-generation well-defined complex.

Table 3.1: The comparison of a well-defined pre-catalyst with an *in situ* system in the Suzuki-Miyaura reaction.¹⁸



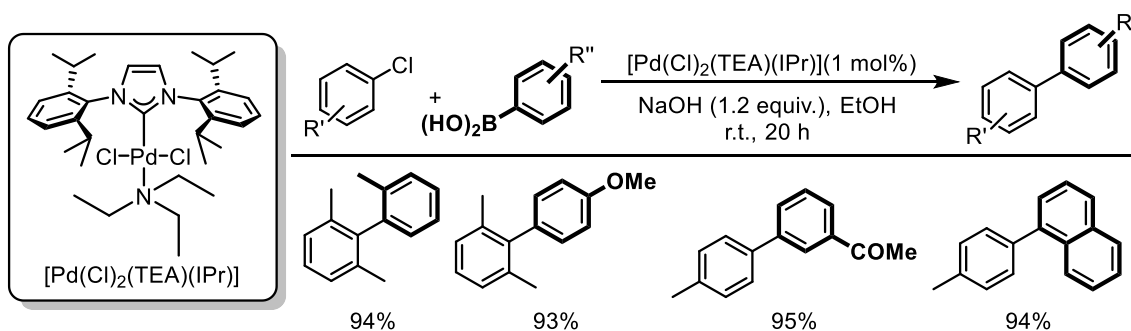
High yields were obtained using a weak inorganic base, K_3PO_4 , coupling a variety of heterocyclic substrates and accommodating sensitive functional groups. The well-defined approach using complexes having a known metal-to-ligand ratio (usually 1:1) permitted the formation of a putative L-Pd active species.¹⁹ This approach has offered simpler operational protocols, leading to improved catalytic performance. The latest developments have focused on the nature of the throw-away ligand in palladium(II) precursors.^{20,21} In the quest to improve the catalytic system for the Suzuki-Miyaura reaction, N-heterocyclic carbenes (NHCs) as ligands were tested in several different palladium scaffoldings.

One of the first examples using NHC-Pd complexes was reported by Herrmann in 2002.²² The $[Pd(IAd)_2]$ (IAd = *N,N'*-bis-(adamantyl)imidazol-2-ylidene) was used as a highly catalytic active catalyst to couple deactivated aryl chlorides in excellent yield (Scheme 3.4). Most interestingly, this reaction was successfully performed at room temperature.



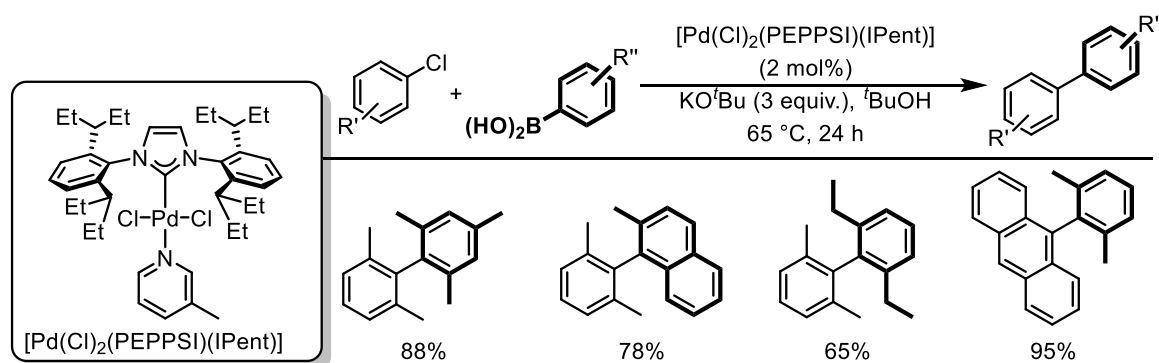
Scheme 3.4: One of the first examples using Pd-NHC pre-catalyst.²²

This very early example is illustrating the high catalytic activity of Pd-NHC complexes in the Suzuki-Miyaura reaction at this time. Since then a wide range of different Pd-NHC catalysts have been reported for the Suzuki-Miyaura reaction. $[Pd(Cl)_2(TEA)(IPr)]$ ($IPr = N,N'$ -bis-[2,6-(di-*iso*-propyl)phenyl]imidazol-2-ylidene, TEA = triethylamine) was reported by Navarro and co-workers and is part of many different Pd-NHC complexes bearing an amine derivative as “throw-away” ligand.²³ This air and moisture stable complex was synthesised in high yield in air and successfully employed in the Suzuki-Miyaura reaction (Scheme 3.5). Sterically hindered substrates were coupled in excellent yield at room temperature, highlighting the high catalytic activity of this protocol.



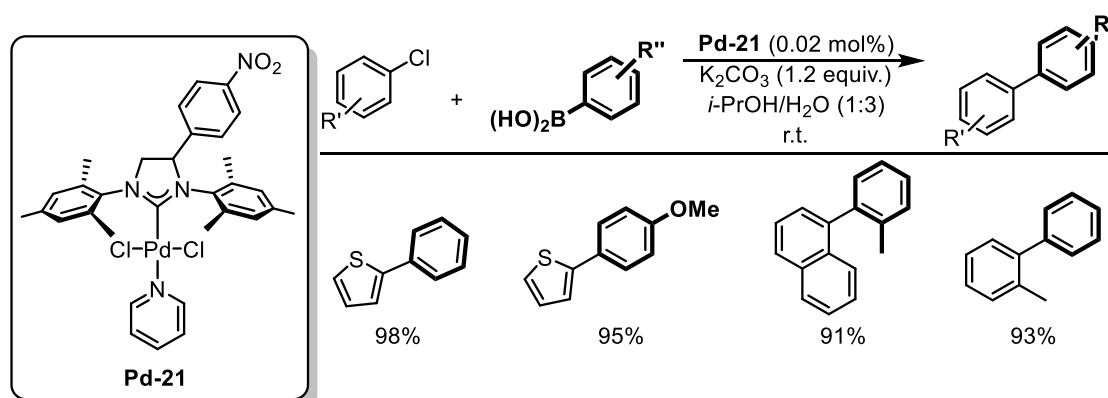
Scheme 3.5: The use of $[Pd(Cl)_2(TEA)(IPr)]$ in the Suzuki-Miyaura reaction.²³

Organ and co-workers reported the synthesis of air-stable, highly active, well-defined pre-catalysts $[Pd(Cl)_2(PEPPSI)(NHC)]$ (PEPPSI = Pyridine-Enhanced Precatalyst, Preparation, Stabilization and Initiation), firstly reported for the Negishi reaction²⁴ but later tested in the Suzuki-Miyaura reaction (Scheme 3.6).²⁵ $[Pd(Cl)_2(PEPPSI)(IPent)]$ ($IPent = N,N$ -bis-[2,6-bis(di-*iso*-pentyl)phenyl]imidazol-2-ylidene) was used to synthesise sterically demanding tetra-*ortho* substituted biaryls in excellent yield (Scheme 3.6).²⁵ It was postulated that the steric bulk of the IPent ligand enhanced the coupling of sterically hindered substrates.²⁵



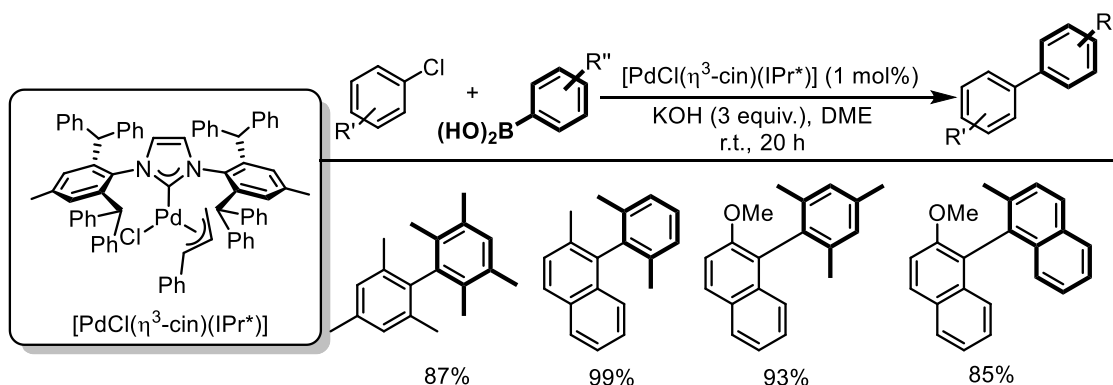
Scheme 3.6: The Suzuki-Miyaura reaction using $[Pd(Cl)_2(PEPPSI)(IPent)]$.²⁵

Thiel and co-worker reported the synthesis of a new Pd(II)-NHC complex bearing a functionalised NHC with a nitrobenzene in the backbone, **Pd-21** (Scheme 3.7).²⁶ Similar to Navarro and Organ, an amine-derived “throw-away” ligand was used (pyridine). The complex showed high catalytic activity in the Suzuki-Miyaura reaction. Very low catalyst loading was needed (0.02 mol%) in order to couple a wide range of different aryl chlorides. The mild reaction conditions must be stressed as the reaction was carried out in an aqueous medium at room temperature.²⁶



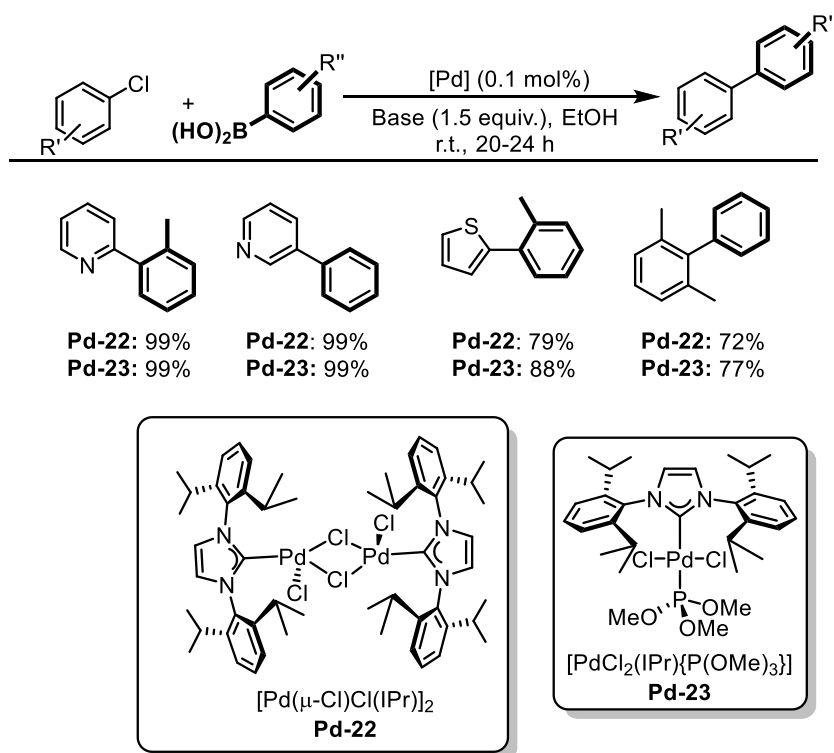
Scheme 3.7: The Suzuki-Miyaura reaction catalysed by a functionalised NHC-Pd complex.²⁶

This trend of “flexible steric bulk” was further reported by Fukuzawa²⁷ and co-workers using 1,2,3-triazol-5-ylidene and by Nolan using IPr^* (N,N -bis-[2,6-bis(diphenylmethyl)-4-methylphenyl]imidazol-2-ylidene) in the $[PdCl(\eta^3-cin)(NHC)]$ scaffold, where they showed successful coupling of hindered substrates in the Suzuki-Miyaura reaction.²⁸ In Nolan’s protocol mild reaction conditions were used, *i.e.* room temperature, and an inexpensive base; KOH. Furthermore, 1 mol% catalyst loading was efficient to obtain good to excellent yields (67-99%) (Scheme 3.8).²⁸



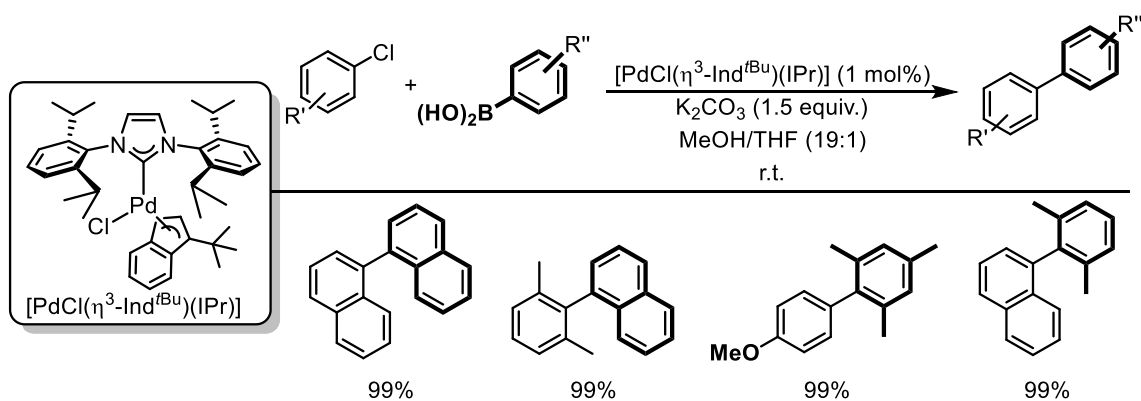
Scheme 3.8: The use of $[\text{PdCl}(\eta^3\text{-cin})(\text{IPr}^*)]$ in the Suzuki-Miyaura reaction.²⁸

The Pd-allyl synthon, $[\text{Pd}(\eta^3\text{-R-allyl})(\mu\text{-Cl})_2]$ has emerged as a widely used structure in cross-coupling chemistry.²⁹ A number of synthetic protocols using either well-defined or *in situ* generated palladium catalysts have recently been disclosed using either $[\text{Pd}(\eta^3\text{-R-allyl})(\mu\text{-Cl})_2]$ or its allyl-substituted derivatives.³⁰ Of note, Johnson Matthey now offers a family of well-defined Pd-allyl complexes bearing biaryl-based phosphine ligands.³¹ The $[\text{Pd}(\mu\text{-Cl})\text{Cl}(\text{IPr})_2]$ dimer reported by Cazin and co-workers was used to couple a range of different hindered substrates and heteroatom containing substrates in mild conditions (Scheme 3.9).³² It should be highlighted that a very low catalyst loading is needed (0.1 mol%). Cazin and co-workers continued the investigation into the Suzuki-Miyaura reaction and reported the synthesis of mixed phosphite/NHC-complexes.^{33,34} These complexes were fully characterised and subsequently tested in the Suzuki-Miyaura reaction. As before a very low catalyst loading (0.1 mol%) was required to successfully couple aryl, benzyl and heterocyclic chlorides (Scheme 3.9).



Scheme 3.9: The use of $[Pd(\mu\text{-Cl})Cl(IPr)]_2$ and mixed phosphite/NHC-complexes in the Suzuki-Miyaura reaction.³²⁻³⁴

Hazari and co-workers recently reported the synthesis of a new Pd(II) dimer; $[Pd(\eta^3\text{-R-Ind})(\mu\text{-Cl})_2]_2$, which is now commercially available.³⁵ These new dimers were compared to the $[Pd(\eta^3\text{-R-allyl})(\mu\text{-Cl})_2]$ dimers mentioned before. Different well-defined Pd(II) complexes were synthesised using phosphine ligands and NHCs. $[PdCl(\eta^3\text{-Ind}^{tBu})(IPr)]$ (Ind^{tBu} = 1-*tert*-butyl-1H-indene) in particular showed very high catalytic activity in the Suzuki-Miyaura reaction using mild reaction conditions (Scheme 3.10).³⁵ It was argued that the inability to form an unreactive Pd(I) dimer during the catalysis is what gives this protocol its high catalytic activity.³⁵



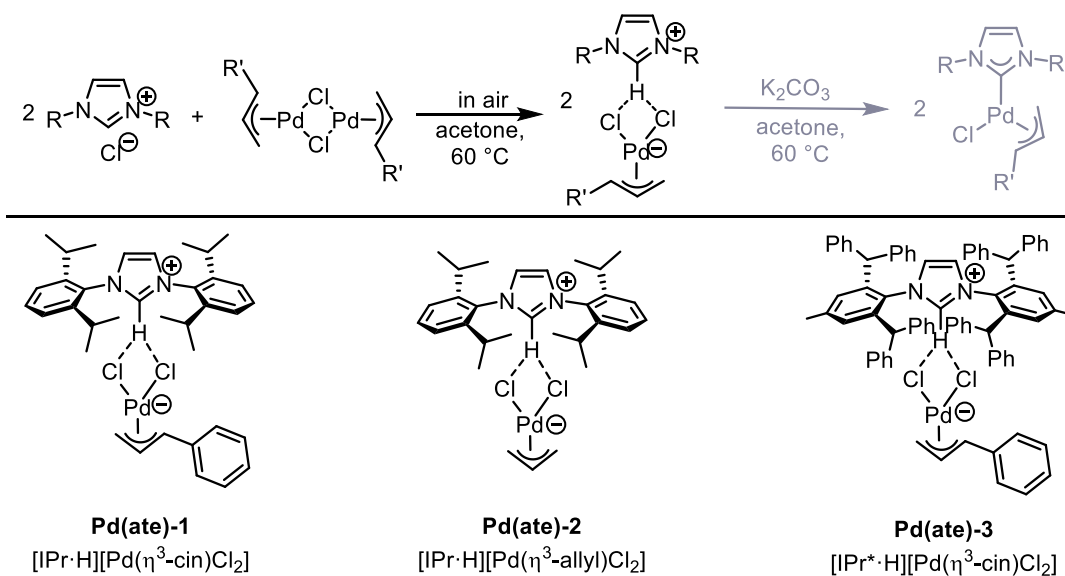
Scheme 3.10: The use of $[PdCl(\eta^3\text{-Ind}^{tBu})(IPr)]$ in the Suzuki-Miyaura reaction.³⁵

3.2 Initial catalytic tests using $[\text{NHC}\cdot\text{H}][\text{Pd}(\text{R})\text{Cl}_2]$ complexes

Since the newly synthesised palladate salts $[\text{NHC}\cdot\text{H}][\text{Pd}(\text{R})\text{Cl}_2]$ (see Chapter 2) shown many attractive characteristics, such as being air- and moisture stable as well as having a facile synthesis resulting in quantitative yield, it was proposed that their use as pre-catalysts could be extremely valuable. Furthermore, since the palladates are easily obtained in ethanol, we considered the possibility of their direct use in cross-coupling catalysis. Koszinowski and co-workers have investigated the reduction of Pd(II) to Pd(0), where an anionic palladate complex $[\text{L}_n\text{PdR}_3]^-$ was observed.³⁶ It was argued that this species plays a crucial role in the catalytic cycle of cross-coupling chemistry.³⁶ Different palladate complexes bearing NHC ligands have been reported by various research groups.^{37,38} For example a NHC-palladate complex, $[\text{TBA}][(\text{NHC})\text{PdCl}_3]$, (TBA = *tetra*-butylammonium) was reported by Navarro and co-workers and consequently employed in the Mizoroki-Heck reaction.³⁹ The computational and mechanistic studies concluded an Amatore-Jutand type reaction mechanism. Where an anionic palladium species is formed *in situ*, which undergoes the oxidative addition with an aryl halide to form a short lived anionic penta-coordinated aryl palladium(II) complex, followed by a *syn* migratory insertion, *syn*- β -hydride elimination and reductive elimination.

Since other “ate” complexes were capable of this transformation and ethanol has been shown compatible with the Suzuki-Miyaura reaction,³⁵ we reasoned that the palladate could prove efficient in this transformation.

The catalytic activity of these $[\text{NHC}\cdot\text{H}][\text{Pd}(\eta^3\text{-R-allyl})\text{Cl}_2]$ complexes was then expanded upon using three palladates, $[\text{IPr}\cdot\text{H}][\text{Pd}(\eta^3\text{-cin})\text{Cl}_2]$ (**Pd(ate)-1**) (cin = cinnamyl), $[\text{IPr}\cdot\text{H}][\text{Pd}(\eta^3\text{-allyl})\text{Cl}_2]$ (**Pd(ate)-2**) and $[\text{IPr}^*\cdot\text{H}][\text{Pd}(\eta^3\text{-cin})\text{Cl}_2]$ (**Pd(ate)-3**) (Scheme 3.11). These three complexes are intermediates in the synthesis of the well-defined $[\text{PdCl}(\eta^3\text{-cin})(\text{IPr})]$, $[\text{PdCl}(\eta^3\text{-allyl})(\text{IPr})]$ and $[\text{PdCl}(\eta^3\text{-cin})(\text{IPr}^*)]$ respectively. All of the well-defined Pd(II)-NHC complexes are commercially available and have shown high catalytic activity in many cross-coupling reactions.^{28,40}

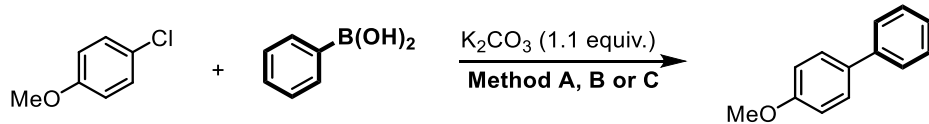


Scheme 3.11: $[\text{NHC}\cdot\text{H}][\text{Pd}(\eta^3\text{-R-allyl})\text{Cl}_2]$ complexes used in the preliminary catalytic reactions.

Preliminary experiments of the palladates, $[\text{NHC}\cdot\text{H}][\text{Pd}(\eta^3\text{-R-allyl})\text{Cl}_2]$, were performed using the conditions previously reported for their well-defined counterparts.⁴¹ This is in light of recent reports that have highlighted the use of a weak inorganic base as an operational base in the Suzuki-Miyaura reaction using a NHC-Pd catalyst. It was postulated that the base could potentially play multi-faceted role in such reactions, using the palladates as pre-catalysts. The base serves initially to convert the palladate into a neutral NHC-Pd complex and in a second step, it triggers the activation of Pd(II) species to the active Pd(0) species, and finally it acts as the operational base in the Suzuki-Miyaura reaction.

4-Chloroanisole and phenyl boronic acid were used as model substrates for the investigation. **Pd(ate)-1**, **Pd(ate)-2** and **Pd(ate)-3** were tested and compared with the well-defined counterparts and the *in situ* reaction (Table 3.2). Following the reported reaction conditions,⁴² only the well-defined complexes showed catalytic activity (Table 3.2, entries 1-3). Considering these disappointing results, milder conditions were used; the solvent was switched to ethanol instead of an ethanol/water mixture and the reaction was carried out at room temperature instead of 80 °C. Again, only the well-defined complexes gave moderate to good yields (Table 3.2, method B). A significant difference between the Suzuki-Miyaura using the palladate pre-catalysts to the well-defined NHC-Pd pre-catalysts was the instant colour change after the addition of the coupling substrates.

Table 3.2: Investigation into the Suzuki-Miyaura reaction using different Pd-NHC pre-catalysts.

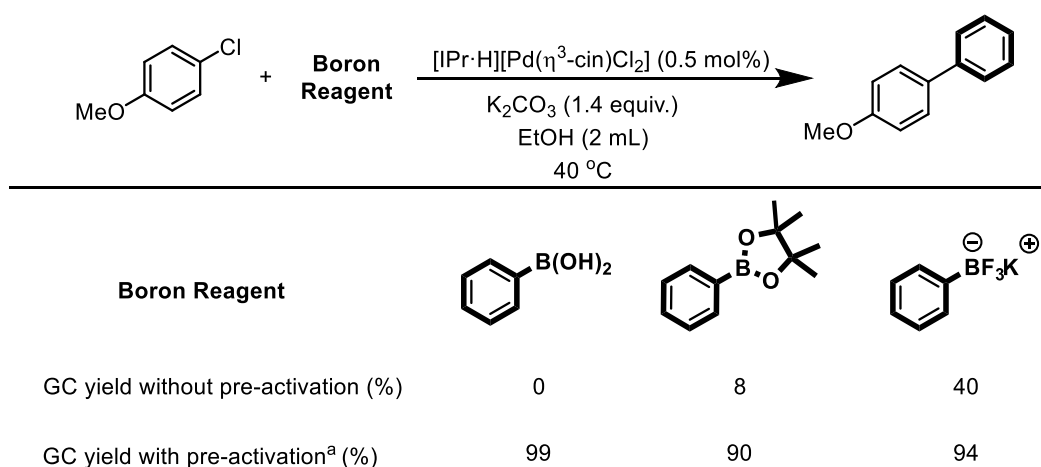


Entry	Catalysts (0.3 mol%)	Meth. A (conv. %)	Meth. B (conv. %)	Meth. C (conv. %)		
				C1	C2	C3
1	$[PdCl(\eta^3\text{-cin})(IPr)]$	71	82			
2	$[PdCl(\eta^3\text{-allyl})(IPr)]$	61	58			
3	$[PdCl(\eta^3\text{-cin})(IPr^*)]$	70	73			
4	$[IPr\cdot H][Pd(\eta^3\text{-cin})Cl_2]$	NR	NR	82	9	43
5	$[IPr\cdot H][Pd(\eta^3\text{-allyl})Cl_2]$	NR	NR	50	NR	13
6	$[IPr^*\cdot H][Pd(\eta^3\text{-cin})Cl_2]$	NR	NR	83	28	97
7	$[Pd(\eta^3\text{-cin})(\mu\text{-Cl})_2] + 2 IPr\cdot HCl$	NR	NR	NR		
8	$[Pd(\eta^3\text{-allyl})(\mu\text{-Cl})_2] + 2 IPr\cdot HCl$	NR	NR	NR		
9	$[Pd(\eta^3\text{-cin})(\mu\text{-Cl})_2] + 2 IPr^*\cdot HCl$	NR	NR	NR		

Reaction conditions: 4-chloroanisole (0.5 mmol), phenylboronic acid (1 equiv.), K_2CO_3 (1.1 equiv.) in 1 mL of solvent. The reactions were all charged under inert atmosphere and all reagents and catalysts were charged initially except for methods C1 and C3. Method A: ethanol/water (1:1) at 80 °C for 4 h. Method B: ethanol at room temperature for 20 h. Method C: palladate pre-catalysts (entries 4-6) (or Pd dimer, 0.15 mol% and NHC·HCl, 0.3 mol% for entries 7-9), K_2CO_3 and ethanol were heated for; 1 h at 60 °C (C1) or 30 min at 60 °C (C3), then the coupling partners were added and the reaction was left stirring at room temperature for 20 h. C2: all reagents and catalysts were added from the start and heated for 1 h at 60 °C then stirred at room temperature for 20 h. Conversion determined by GC. NR: no reaction.

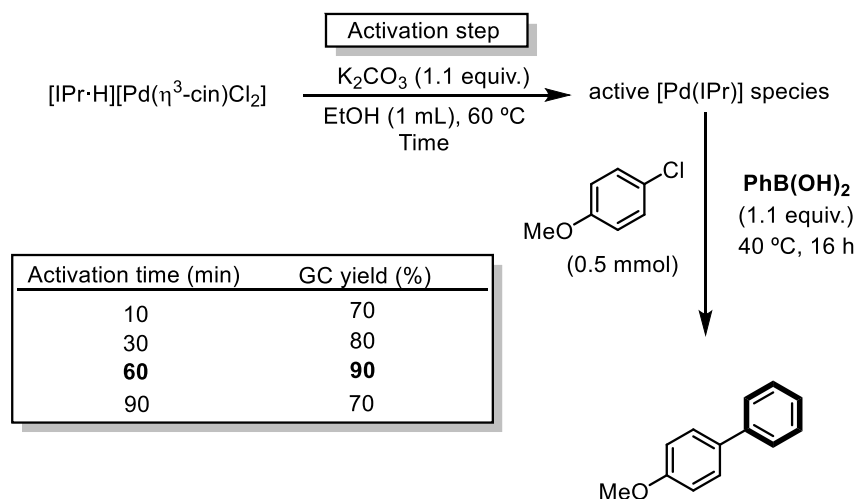
For the reaction using the palladates as pre-catalysts the reaction mixture turned black instantly after the addition of the substrates, this suggested the formation of palladium black (elemental palladium). We reasoned that the missing Pd-NHC bond could be the cause of this lack of reactivity.^{29,40} The absence of this bond in the palladate species could account for shutting down the catalysis or not initiating it at all. These observations suggested that the palladate complex might require conversion *in situ* into the Pd-NHC complex prior to the addition of the coupling partners. For this reason, the palladate complex and K_2CO_3 (1.1 equiv.) were stirred for 1 hour followed by the addition of both coupling partners and stirring at room temperature for 20 hours. Under these conditions, the desired product was obtained in similar yields to the well-defined Pd-NHC complexes (Table 3.2, method C1). It should be noted that when all reagents and catalysts were added from the start, heated for 1 hour at 60 °C and then stirred at room temperature for 20 hours, no to low yield of coupling product were formed (Table 3.2, method C2). Interestingly, when using a combination of the NHC·HCl and $[Pd(\eta^3\text{-R-allyl})(\mu\text{-Cl})_2]$ instead of the well-defined palladates, no reaction was observed in all Suzuki-Miyaura reactions, thus confirming the importance of preforming the palladate intermediates (Table 3.2, entries 7-9). Changing the activation period, drastically affected the yields (Table 3.2, method C3).

Three different boron sources were investigated in order to better understand the transmetallation step (Scheme 3.12). Performing the reaction using phenyl boronic pinacol ester instead of phenyl boronic acid resulted in low yield and decomposition as evidenced by the reaction colour evolving to black. When potassium phenyltrifluoroborate was used, the yield reached 40%. In order to form the desired Pd-NHC bond, an activation step was introduced. The palladate pre-catalyst and the base were heated together in solution for one hour before the coupling substrates were added. Introducing an activation step did result in a significant increase in yield (Scheme 3.12).



Scheme 3.12: Nature of the boron reagent in the Suzuki-Miyaura reaction. Reaction conditions: $[\text{IPr}\cdot\text{H}][\text{Pd}(\eta^3\text{-cin})\text{Cl}_2]$ (0.5 mol%) and K_2CO_3 (0.7 mmol) in ethanol (1 mL). (^a when indicated, activation is performing at this point by heating at 60 °C for 1 h). 4-chloroanisole (0.5 mmol) and the aryl boron reagent (0.55 mmol) were added as an ethanol solution (1 mL). The reaction was left to stir at 40 °C for 16 h. Yield determined by GC using mesitylene (0.1 mmol) as internal standard.

This finding supports the hypothesis that the $\text{PhB}(\text{OR})_3^-$ species may be the culprit of this decomposition. The activation step appears necessary and is independent of the boron source. To our delight, results improved drastically when this activation step was used. All three palladate species previously tested showed catalytic activity, with $[\text{IPr}\cdot\text{H}][\text{Pd}(\eta^3\text{-cin})\text{Cl}_2]$ and $[\text{IPr}^*\cdot\text{H}][\text{Pd}(\eta^3\text{-cin})\text{Cl}_2]$ displaying high catalytic activity (80-90% yield).⁴³ The optimal time for the activation step of the pre-catalyst is one hour. When the activation time was lowered, the yield of the cross-coupling product decreased (Scheme 3.13).

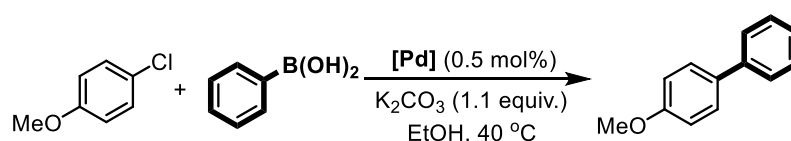


Scheme 3.13: Optimisation of the activation time. Reaction conditions: $[IPr\cdot H][Pd(\eta^3\text{-cin})Cl_2]$ (0.5 mol%) and K_2CO_3 (0.55 mmol) in ethanol (1 mL). The mixture was heated at 60 °C for the given time. 4-chloroanisole (0.5 mmol) and phenyl boronic acid (0.55 mmol) were added as an ethanol solution (1 mL). The reaction was left to stir at 40 °C for 16 h. The GC yield was determined using mesitylene (0.1 mmol) as internal standard and is the average of at least two runs.

3.3 Optimisation of the Suzuki-Miyaura reaction using $[IPr\cdot H][Pd(\eta^3\text{-cin})Cl_2]$ as pre-catalyst

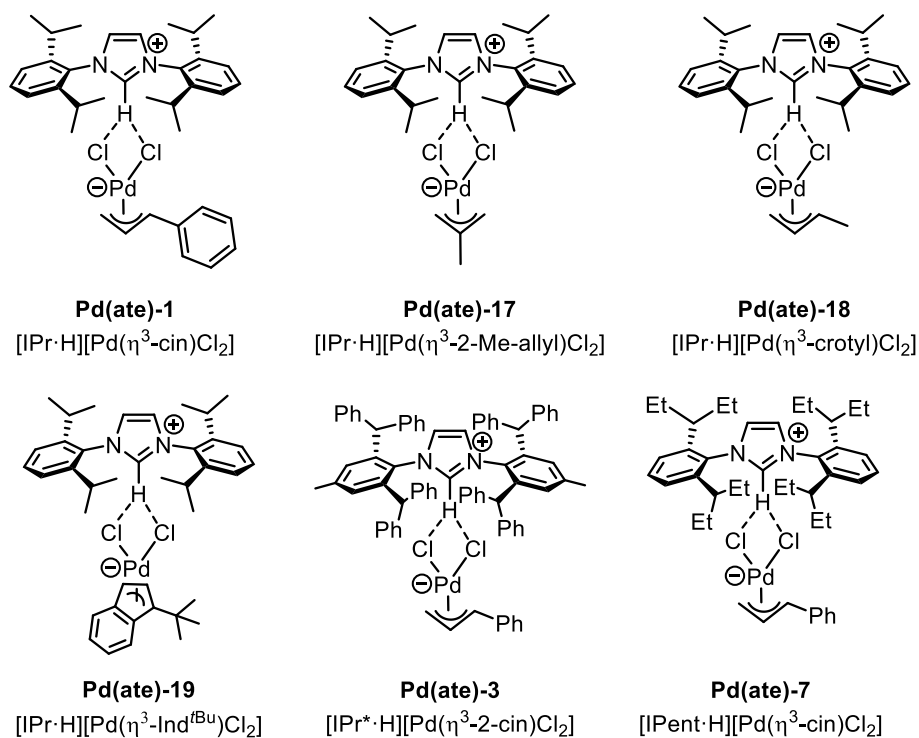
Based on the need for this activation step, a detailed catalyst optimization was conducted in air. Several palladates (Table 3.3, entries 1-7) were synthesized according to the optimal procedure described above. The ease and speed in synthesizing these pre-catalysts should be stressed. Among the palladate complexes tested, the best proved to be $[IPr\cdot H][Pd(\eta^3\text{-cin})Cl_2]$ (Table 3.3, entry 1) giving excellent yield and high turnover numbers (TON).

Table 3.3: Catalyst optimization^[a]



Entry	Palladate pre-catalyst	GC yield ^[a]	TON ^[b]
1	$[IPr\cdot H][Pd(\eta^3\text{-cin})Cl_2]$	93	310,000
2	$[IPr\cdot H][Pd(\eta^3\text{-2-Me-allyl})Cl_2]$	80	266,667
3	$[IPr\cdot H][Pd(\eta^3\text{-crotyl})Cl_2]$	8	26,667
4	$[IPr\cdot H][Pd(\eta^3\text{-Ind}^{tBu})Cl_2]$	n.r.	-
5	$[SIPr\cdot H][Pd(\eta^3\text{-cin})Cl_2]$	30	100,000
6	$[IPent\cdot H][Pd(\eta^3\text{-cin})Cl_2]$	n.r.	-
7	$[IPr^*\cdot H][Pd(\eta^3\text{-cin})Cl_2]$	88	293,334

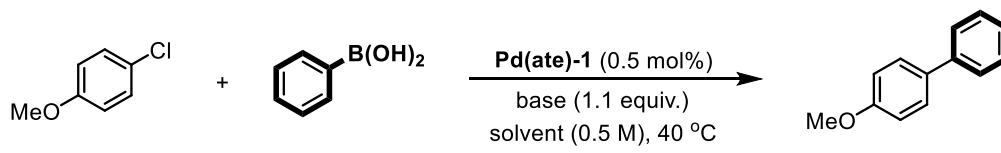
Palladate pre-catalyst (0.5 mol%) and K_2CO_3 (0.7 mmol) in ethanol (1 mL) was heated at 60 °C for 1 h. Then 4-chloroanisole (0.5 mmol) and phenylboronic acid (0.55 mmol) were added as an ethanol solution (1 mL). The reaction was left to stir at 40 °C for 16 h. ^[a]The GC yield was determined using mesitylene (0.1 mmol) as internal standard and is the average of at least two runs. ^[b]TON = mol of product/mol of catalyst



Scheme 3.14: Palladate complexes used in this investigation.

The optimization of base and solvent was next carried out. The best conversions were obtained when alcohol solvents were used (Table 3.4). Ethanol, *iso*-propanol and *n*-butanol gave moderate to excellent conversion. Different solvents with varying polarities were tested but mainly resulted in low to no conversion.

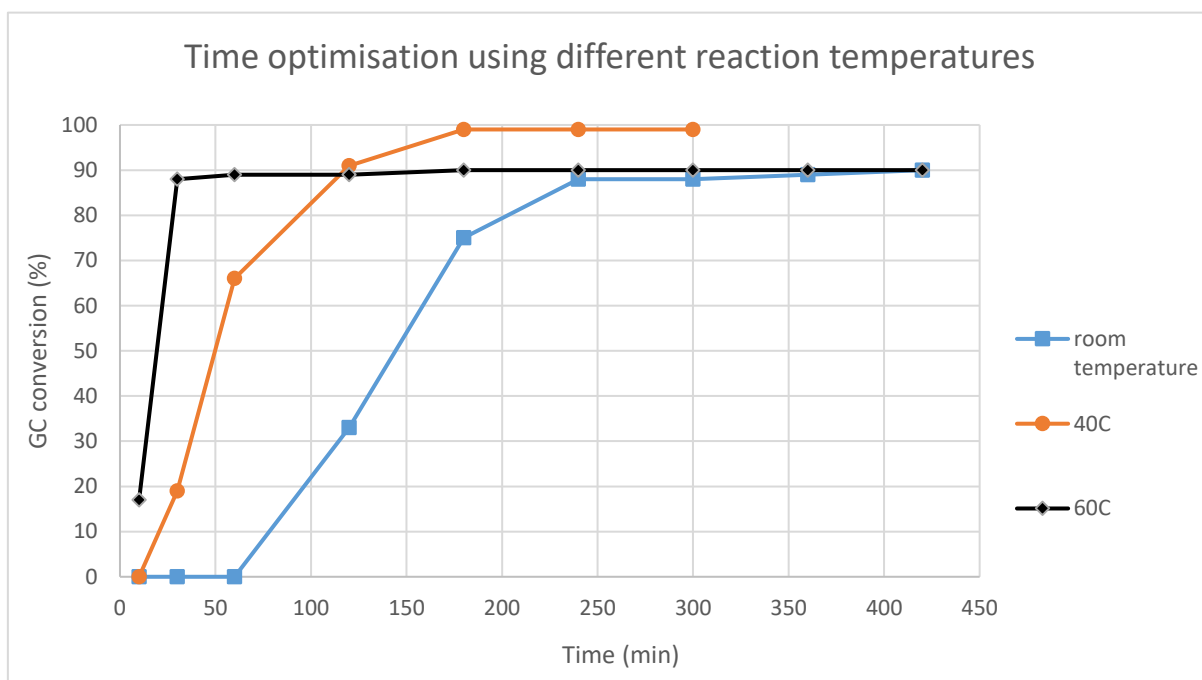
Table 3.4: Part of the solvent/base optimisation



Entry	Solvent (0.5 M)	Base (1.1 equiv.)	GC yield
1	ethanol	K ₂ CO ₃	93
2	ethanol	K ₃ PO ₄	40
3	ethanol	KOH	72
4	ethanol	KO ^t Bu	75
5	<i>iso</i> -propanol	K ₂ CO ₃	47
6	<i>iso</i> -propanol	K ₃ PO ₄	55
7	<i>iso</i> -propanol	KOH	55
8	<i>iso</i> -propanol	KO ^t Bu	72
9	<i>n</i> -butanol	K ₂ CO ₃	53
10	<i>n</i> -butanol	K ₃ PO ₄	traces
11	<i>n</i> -butanol	KOH	65
12	<i>n</i> -butanol	KO ^t Bu	70

Reaction conditions: $[IPr\cdot H][Pd(\eta^3\text{-cin})Cl_2]$ (0.5 mol%) and the corresponding base (0.55 mmol) and corresponding solvent (1 mL) was heated at 60 °C for 1 h. Then 4-chloroanisole (0.5 mmol) and phenylboronic acid (0.55 mmol) were added as a solvent solution (1 mL). The reaction was left to stir at 40 °C for 16 h. The GC yield was determined using mesitylene (0.1 mmol) as internal standard and is the average of at least two runs.

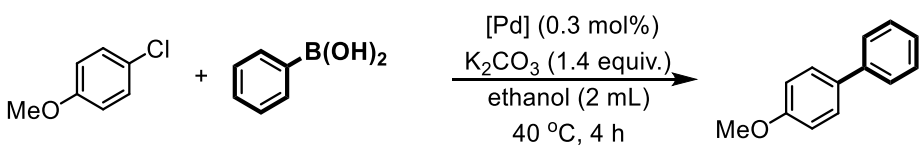
A range of inorganic bases were tested in the three best solvents; ethanol, *iso*-propanol and *n*-butanol (Table 3.4). Interestingly, weaker inorganic bases such as K₂CO₃ and K₃PO₄ gave similar conversion to stronger bases such as KOH and KO^tBu. The best solvent/base system was ethanol/K₂CO₃. The extensive base/solvent optimization gave an insight into the high catalytic activity of **Pd(ate)-1**; clearly, alcohol solvents are very important for the catalysis to achieve good conversions and a variety of different inorganic bases can be used, most resulting in moderate to high yields. The activation of the palladates from Pd(II) to Pd(0) must be similar to the activation of the well-defined complexes $[PdCl(\eta^3\text{-R-allyl})(NHC)]$ but requiring the additional step of palladate to Pd-NHC conversion.⁹ Time optimization for the catalysis was conducted using three different temperatures at 0.5 mol% of **Pd(ate)-1** in ethanol (Scheme 3.15). The reaction was completed after 4 h at 40 °C whereas at room temperature, the reaction required 16 h to reach completion. The reaction at 60 °C never reached completion, which suggests catalyst deactivation over time might be an issue at elevated temperatures (60 °C and higher).



Graph 3.1: Time optimisation of the Suzuki-Miyaura reaction using different reaction temperatures. Reaction Conditions: $[IPr\cdot H][Pd(\eta^3\text{-cin})Cl_2]$ (0.5 mol%) and K_2CO_3 (0.55 mmol) and ethanol (1 mL) was heated at 60 °C for 1 h. Then 4-chloroanisole (0.5 mmol) and phenylboronic acid (0.55 mmol) were added as a solvent solution (1 mL). The reaction was left to stir at the corresponding temperature. The GC yield was determined using mesitylene (0.1 mmol) as internal standard and is the average of at least two runs.

In order to prove the efficiency of the optimised system, the optimised reaction conditions were tested with different Pd(II)-NHC pre-catalysts. All bearing IPr as ligand for consistency. Four different pre-catalysts were selected namely $[Pd(Cl)_2(PEPPSI)(IPr)]$ (Table 3.5, entry 2), $[PdCl(acac)(IPr)]$ (acac = acetylacetonate) (Table 3.5, entry 3), $[PdCl(\eta^3\text{-allyl})(IPr)]$ (Table 3.5, entry 4) and $[PdCl(\eta^3\text{-cin})(IPr)]$ (Table 3.5, entry 5). All introduced before, showing high catalytic activity in the Suzuki-Miyaura reaction.

Table 3.5: Comparisons of different Pd(II)-IPr pre-catalyst in the optimised protocol.

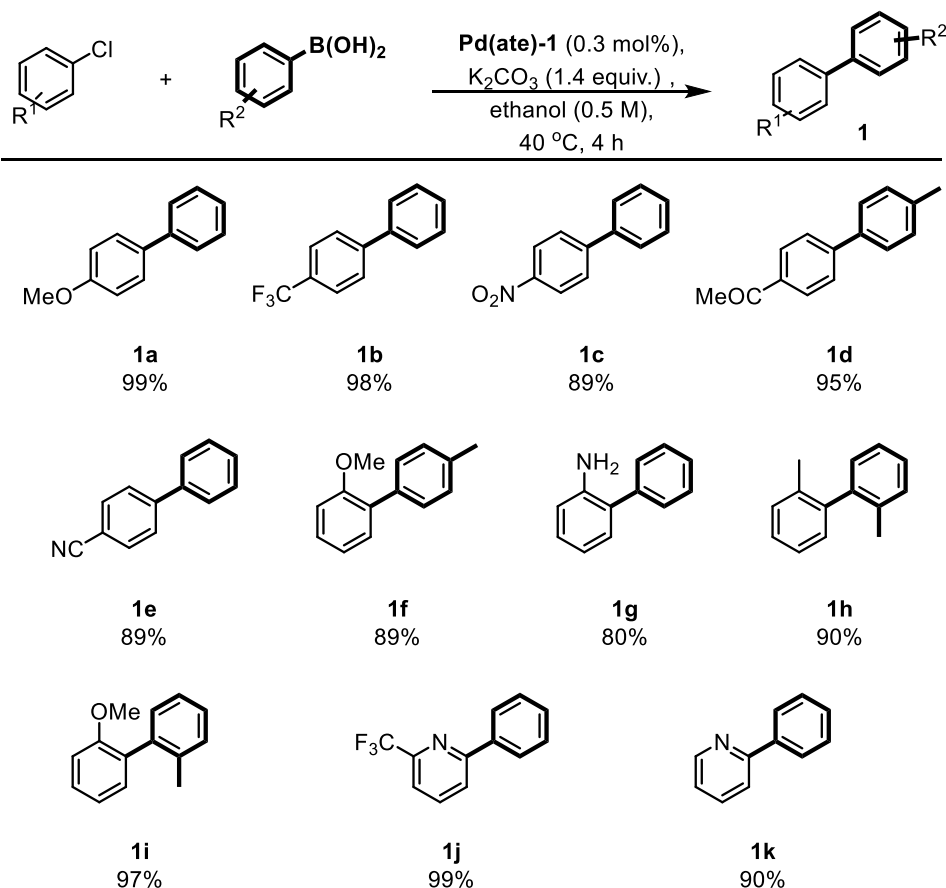


entries	pre-catalyst	GC yield (%) ^a
1	$[IPr\cdot H][Pd(\eta^3\text{-cin})Cl_2]$	99
2	$[Pd(Cl)_2(PEPPSI)(IPr)]$	79
3	$[PdCl(acac)(IPr)]$	75
4	$[PdCl(\eta^3\text{-allyl})(IPr)]$	74
5	$[PdCl(\eta^3\text{-cin})(IPr)]$	80

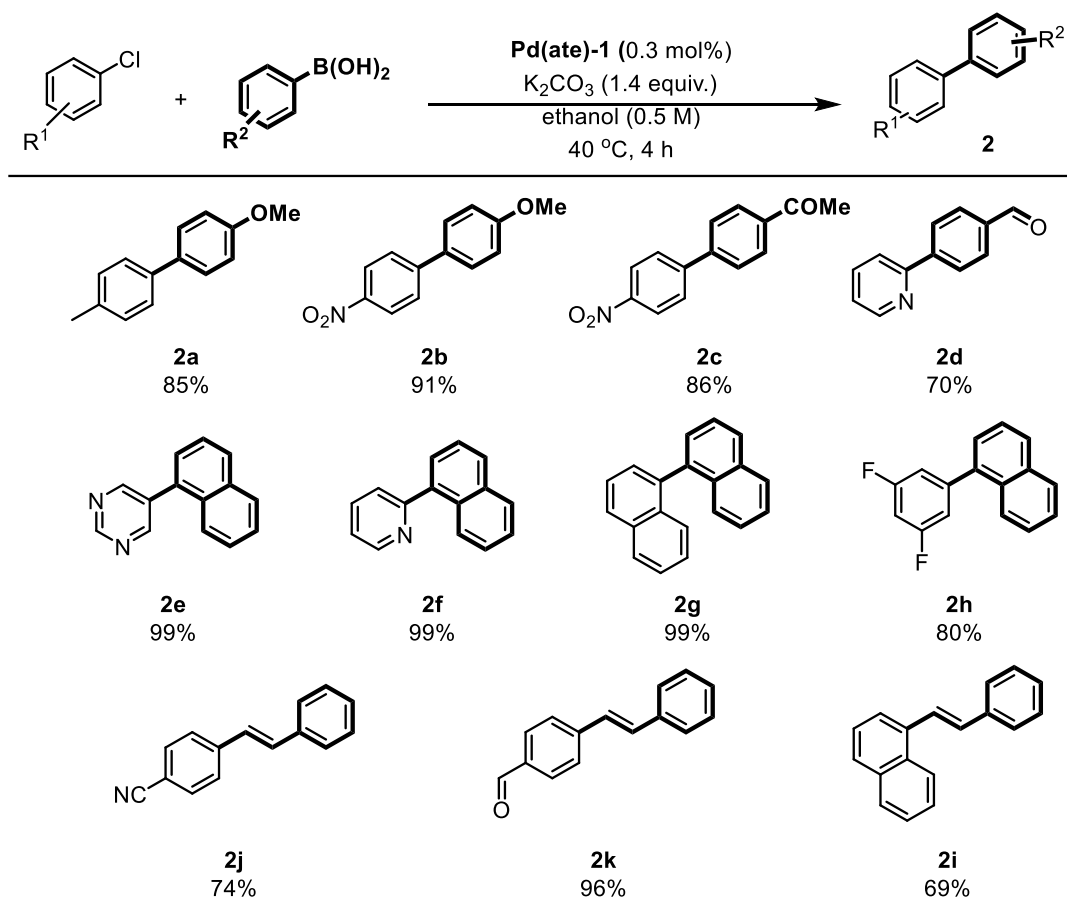
^aThe GC yield was determined using mesitylene (0.1 mmol) as internal standard and is the average of at least two runs.

All pre-catalysts showed good catalytic activity, but the palladate pre-catalyst gave the highest conversion (Table 3.5, entry 1). The comparison shows that the newly developed palladate complex can compete with the reported systems and is an improvement for Pd(II)-NHC catalyst systems in the Suzuki-Miyaura reaction.

A reaction scope was examined to probe the catalytic activity of the palladate as a pre-catalyst (Scheme 3.15 and 3.16). A range of aryl chlorides were used containing electron withdrawing and electron donating groups. Sterically hindered substrates were tested giving high yields. 2-Methoxy-4-methylbiphenyl was synthesized in 89% yield (Scheme 3.15, entry 6). 2-Aminobiphenyl was synthesized in 80% yield (Scheme 3.15, entry 7) from 2-chloroaniline and phenylboronic acid. The more hindered 2,2'-dimethylbiphenyl (Scheme 3.15, entry 8) and 2-methoxy-2-methylbiphenyl (Scheme 3.15, entry 9) were synthesized in 90% and 97% yields, respectively. In order to test the limits and use of this catalytic system, aryl chlorides containing heteroatoms were examined as their use in agrochemicals and pharmaceuticals is widespread (Scheme 3.16).⁶



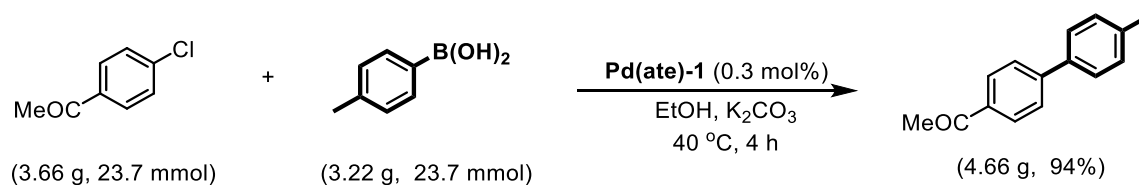
Scheme 3.15: Scope of the Suzuki-Miyaura reaction; Part 1. Reaction conditions: $[IPr\cdot H][Pd(\eta^3-cin)Cl_2]$ (0.3 mol%) and the K_2CO_3 (0.55 mmol) in ethanol (0.5 M) was heated at 60 °C for 1 h. Then the corresponding aryl chloride (0.5 mmol) and the corresponding aryl boronic acid (0.55 mmol) were added as a solvent solution (0.5 M). The reaction was left to stir at the 40 °C. Average of two runs.



Scheme 3.16: Scope of the Suzuki-Miyaura reaction; Part 2. Reaction conditions: $[\text{IPr-H}][\text{Pd}(\eta^3\text{-cin})\text{Cl}_2]$ (0.3 mol%) and the K_2CO_3 (0.55 mmol) in ethanol (1 mL) was heated at 60°C for 1 h. Then the corresponding aryl chloride (0.5 mmol) and the corresponding aryl boronic acid (0.55 mmol) were added as a solvent solution (1 mL). The reaction was left to stir at the 40°C . Average of two runs.

First the electronic properties on the aryl boronic acids were studied using 4-methoxyphenyl boronic acid (Scheme 3.16, **2a** and **2b**), 4-acetylphenyl boronic acid (scheme 16, **2c**) and 4-formylphenyl boronic acid (Scheme 3.16, **2d**). Changing from electron-withdrawing to electron-donating groups on the aryl boronic acid resulted in no loss of activity. Bulky boronic acids such as 1-naphthalene boronic acid were coupled with challenging aryl chlorides such as 5-chloropyrimidine (Scheme 3.16, **2e**) and 1-chloronaphthalene (Scheme 3.16, **2g**) resulting in quantitative yields in both cases. Lastly, styryl boronic acid was also tested and moderate to high yields of coupled products were obtained (Scheme 3.16, **2j**, **2k** and **2i**). The reaction scope highlights the high catalytic activity of $\text{Pd}(\text{ate})\text{-1}$ irrespective of the electronics of the aryl chlorides and of the steric nature of the substrates. The involvement of heteroatom-containing substrates, which can be difficult to couple due to possible coordination to the metal centre, displayed no drop of activity and led to high yields. As we were interested in highlighting the

versatility and scalability of the method, a test reaction was successfully scaled-up to yield 4.66 g of product in 94% isolated yield (Scheme 3.17). Noteworthy, a 1:1 aryl chloride to boronic acid ratio was used in the larger scale reaction, establishing that an excess of boronic acid, a common operational practice, is not required.



Scheme 3.17: Large scale reaction of the Suzuki-Miyaura reaction using $[IPr\cdot H][Pd(\eta^3\text{-cin})Cl_2]$.

3.4 Conclusion

A newly synthesized class of Pd(II) pre-catalysts was studied, focusing on its synthesis and its catalytic activity under mild reaction conditions while using environmentally acceptable conditions (solvent and base). The reaction of the pre-catalyst itself with coupling substrates was examined. A wide reaction scope was demonstrated, where various classes of substrates were investigated and proved compatible with this simple catalytic protocol. Furthermore, the Suzuki-Miyaura reaction and the pre-catalyst synthesis can both be scaled up without loss of yield. The palladate and neutral Pd-NHC syntheses are easy to carry out, even in air. The use of ethanol affords a green alternative as a reaction medium in pre-catalyst synthesis and as solvent to perform the Suzuki-Miyaura reaction. The role of these palladates in related transformations is presently being investigated.

3.5 References

- (1) Corbet, J. P.; Mignani, G. *Chem. Rev.* **2006**, *106*, 2651–2710.
- (2) Johansson Seechurn, C. C. C.; Kitching, M. O.; Colacot, T. J.; Snieckus, V. *Angew. Chem. Int. Ed.* **2012**, *51*, 5062–5085.
- (3) Li, H.; Johansson Seechurn, C. C. C.; Colacot, T. J. *ACS Catal.* **2012**, *2*, 1147–1164.
- (4) Nicolaou, K. C.; Bulger, P. G.; Sarlah, D. *Angew. Chem. Int. Ed.* **2005**, *44*, 4442–4489.
- (5) Magano, J.; Dunetz, J. R. *Chem. Rev.* **2011**, *111*, 2177–2250.
- (6) Ruiz-Castillo, P.; Buchwald, S. L. *Chem. Rev.* **2016**, *116*, 12564–12649.
- (7) Würtz, S.; Glorius, F. *Acc. Chem. Res.* **2008**, *41*, 1523–1533.
- (8) Miyaura, N.; Suzuki, A. *Chemistry* **1995**, *95*, 2457–2483.
- (9) Navarro, O.; Marion, N.; Oonishi, Y.; Kelly, R. A.; Nolan, S. P. *J. Org. Chem.* **2006**, *71*, 685–692.
- (10) Carrow, B. P.; Hartwig, J. F. *J. Am. Chem. Soc.* **2011**, *133*, 2116–2119.
- (11) Lennox, A. J. J.; Lloyd-Jones, G. C. *Angew. Chem. Int. Ed.* **2013**, *52*, 7362–7370.
- (12) Suzuki, A. *J. Organomet. Chem.* **1999**, *576*, 147–168.
- (13) Gujral, S. S.; Khatri, S.; Riyal, P.; Gahlot, V. *Indo Glob. J. Pharm. Sci.* **2012**, *2*, 351–367.
- (14) Martin, R.; Buchwald, S. L. *Acc. Chem. Res.* **2008**, *41*, 1461–1473.
- (15) Yin, J.; Rainka, M. P.; Zhang, X.; Buchwald, S. L. *J. Am. Chem. Soc.* **2002**, *124*, 1162–1163.
- (16) Lavallo, V.; Canac, Y.; Präsang, C.; Donnadieu, B.; Bertrand, G. *Angew. Chem. Int. Ed.* **2005**, *44*, 5705–5709.
- (17) Walker, S. D.; Barder, T. E.; Martinelli, J. R.; Buchwald, S. L. *Angew. Chem. Int. Ed.* **2004**, *43*, 1871–1876.
- (18) Düfert, M. A.; Billingsley, K. L.; Buchwald, S. L. *J. Am. Chem. Soc.* **2013**, *135*, 12877–12885.
- (19) Viciu, M. S.; Iii, R. a K.; Stevens, E. D.; Studer, M.; Nolan, S. P. *Org. Lett.* **2003**, *5*, 1479–1482.
- (20) Navarro, O.; Kelly, R. a.; Nolan, S. P. *J. Am. Chem. Soc.* **2003**, *125*, 16194–16195.
- (21) O'Brien, C. J.; Kantchev, E. A. B.; Valente, C.; Hadei, N.; Chass, G. A.; Lough, A.; Hopkinson, A. C.; Organ, M. G. *Chem. Eur. J.* **2006**, *12*, 4743–4748.
- (22) Gstöttmayr, C. W. K.; Böhm, V. P. W.; Herdtweck, E.; Grosche, M.; Herrmann, W. A. *Angew. Chem. Int. Ed.* **2002**, *41*, 1363–1365.
- (23) Chen, M.; Viciu, D. A.; Turner, M. L.; Navarro, O. *Organometallics* **2011**, *2*, 5052–5056.
- (24) Organ, M. G.; Avola, S.; Dubovyk, I.; Hadei, N.; Kantchev, E. A. B.; O'Brien, C. J.; Valente,

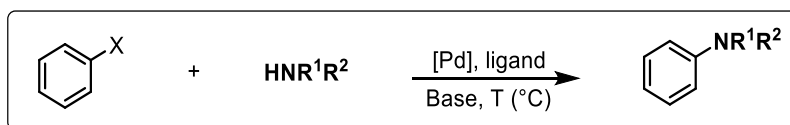
- C. Chemistry* **2006**, *12*, 4749–4755.
- (25) Organ, M. G.; Çalimsiz, S.; Sayah, M.; Hoi, K. H.; Lough, A. J. *Angew. Chem. Int. Ed.* **2009**, *48*, 2383–2387.
- (26) Rajabi, F.; Thiel, W. R. *Adv. Synth. Catal.* **2014**, *356*, 1873–1877.
- (27) Terashima, T.; Inomata, S.; Ogata, K.; Fukuzawa, S. I. *Eur. J. Inorg. Chem.* **2012**, 1387–1393.
- (28) Chartoire, A.; Lesieur, M.; Falivene, L.; Slawin, A. M. Z.; Cavallo, L.; Cazin, C. S. J.; Nolan, S. P. *Chem. Eur. J.* **2012**, *18*, 4517–4521.
- (29) Viciu, M. S.; Germaneau, R. F.; Nolan, S. P. *Org. Lett.* **2002**, *4*, 4053–4055.
- (30) Chartoire, A.; Lesieur, M.; Slawin, A. M. Z.; Nolan, S. P.; Cazin, C. S. J. *Organometallics* **2011**, *30*, 4432–4436.
- (31) DeAngelis, A. J.; Gildner, P. G.; Chow, R.; Colacot, T. J. *J. Org. Chem.* **2015**, 150602123838004.
- (32) Diebolt, O.; Braunstein, P.; Nolan, S. P.; Cazin, C. S. J. *Chem. Commun.* **2008**, 3190–3192.
- (33) Schmid, T. E.; Jones, D. C.; Songis, O.; Diebolt, O.; Furst, M. R. L.; Slawin, A. M. Z.; Cazin, C. S. J. *Dalton Trans.* **2013**, *42*, 7345–7353.
- (34) Diebolt, O.; Jurčík, V.; Correa da Costa, R.; Braunstein, P.; Cavallo, L.; Nolan, S. P.; Slawin, A. M. Z.; Cazin, C. S. J. *Organometallics* **2010**, *29*, 1443–1450.
- (35) Melvin, P. R.; Nova, A.; Balcells, D.; Dai, W.; Hazari, N.; Hruszkewycz, D. P.; Shah, H. P.; Tudge, M. T. *ACS Catal.* **2015**, *5*, 3680–3688.
- (36) Kolter, M.; Koszinowski, K. *Chem. Eur. J.* **2016**, 1–8.
- (37) Huynh, H. V.; Han, Y.; Ho, J. H. H.; Tan, G. K. *Organometallics* **2006**, *25*, 3267–3274.
- (38) Zamora, M. T.; Ferguson, M. J.; McDonald, R.; Cowie, M. *Organometallics* **2012**, *31*, 5463–5477.
- (39) Guest, D.; Menezes Da Silva, V. H.; De Lima Batista, A. P.; Roe, S. M.; Braga, A. A. C.; Navarro, O. *Organometallics* **2015**, *34*, 2463–2470.
- (40) Izquierdo, F.; Corpet, M.; Nolan, S. P. *Eur. J. Org. Chem.* **2015**, 1920–1924.
- (41) Amatore, C.; Jutand, A.; Le Duc, G. *Chemistry* **2012**, *18*, 6616–6625.
- (42) Izquierdo, F.; Chartoire, A.; Nolan, S. P. *ACS Catal.* **2013**, *3*, 2190–2193.
- (43) Zinser, C. M.; Nahra, F.; Brill, M.; Meadows, R. E.; Cordes, D. B.; Slawin, A. M. Z.; Nolan, S. P.; Cazin, C. S. J. *Chem. Commun.* **2017**, *53*, 7990–7993.

Chapter 4

Highly catalytically active Pd-NHC pre-catalysts for the formation of C-N and C-C bonds

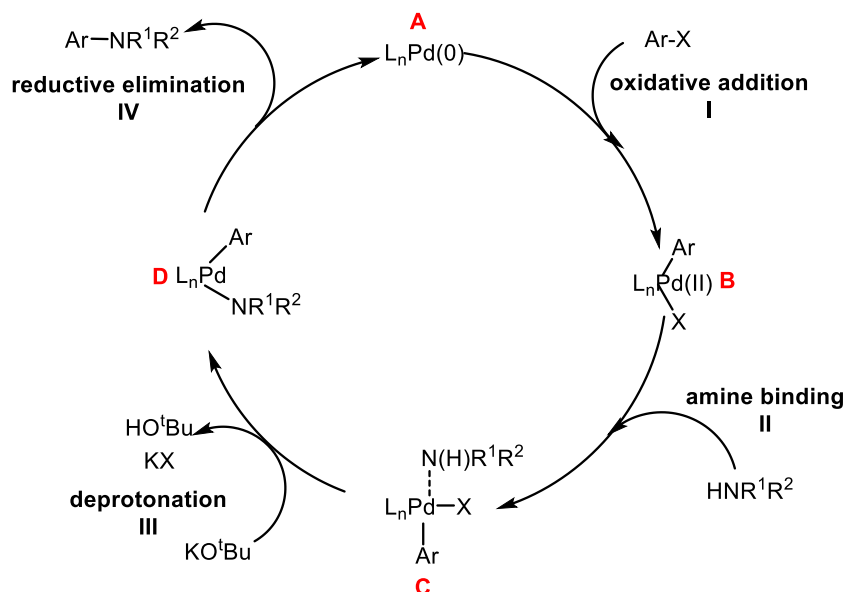
4.1 The Buchwald-Hartwig Reaction

A wide range of research fields are involved in the investigation and improvement of the carbon-heteroatom bond formation reactions.¹⁻³ Carbon-nitrogen bonds, in particular can be found in many molecules, ranging from pharmaceutical agents and natural products to agrochemicals.⁴⁻⁸ Such as the Buchwald-Hartwig amination reaction has become one of the most studied and important cross-coupling reactions in modern chemistry, resulting in the facile synthesis of a wide variety of molecules with a diverse range of academic and industrial applications.⁹⁻¹⁸ Due to the importance of this reaction, numerous catalytic systems have been developed over the years to enable this transformation.



Scheme 4.1: The Buchwald-Hartwig amination.¹⁹

Buchwald²⁰ and Hartwig^{21,22} simultaneously reported the catalytic palladium-mediated C-N bond formation in 1998. Buchwald and co-workers illustrated a broad substrate scope by cross-coupling of amines with aryl bromides, chlorides, iodides and sulfonates. Hartwig and co-workers on the other hand firstly reported the mechanistic studies of the coupling of aryl bromides and tin amides.²² Two years later, Hartwig reported the coupling of aryl amides, sulfides and ethers using a palladium catalyst.²¹ Both research groups proposed and mechanistically investigated a catalytic cycle shown in Scheme 4.2.



Scheme 4.2: Catalytic cycle of the Buchwald-Hartwig amination.^{20–22}

The first step in the catalytic cycle consists of the oxidative addition of the aryl halide to the active Pd(0) species forming a Pd(II) intermediate (Scheme 4.2, I). At this step a bulky and electron-donating ligand on the palladium favours oxidative addition of the palladium centre and prevents the formation of an inactive palladium dimer. Buchwald and co-workers reported the use of BrettPhos ((2-dicyclohexylphosphino)3,6-dimethoxy-2',4',6'-triisopropyl-1-1'-biphenyl),²³ XPhos (2-dicyclohexylphosphino,2',4',6'-triisopropylbiphenyl)²⁴ and RuPhos (2-dicyclohexylphosphino-2',6'-diisopropoxybiphenyl)¹⁰ as efficient ligands in the C-N bond formation as these bulky ligands favour the formation of the active Pd(0) species hence accelerating the oxidative addition, which allowed the coupling of unactivated aryl chlorides and the use of low reaction temperatures.

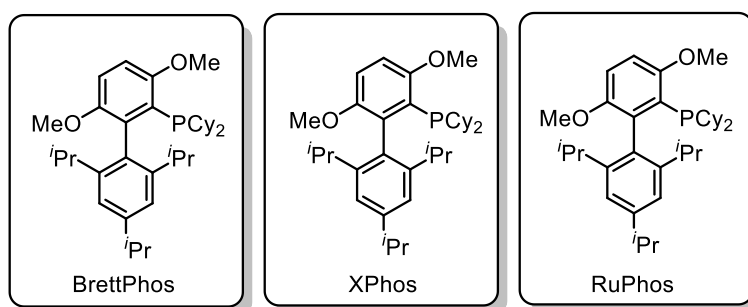
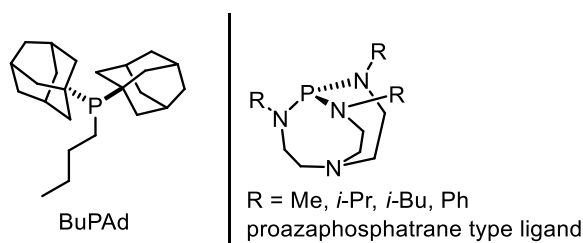


Figure 4.1: Illustrating BrettPhos, XPhos and RuPhos ligands.^{23,24}

The next step in the cycle is the amine binding, or nucleophilic attack (Scheme 4.2, II), where the amine coordinates to the Pd(II) intermediate, followed by the deprotonation by a base to the

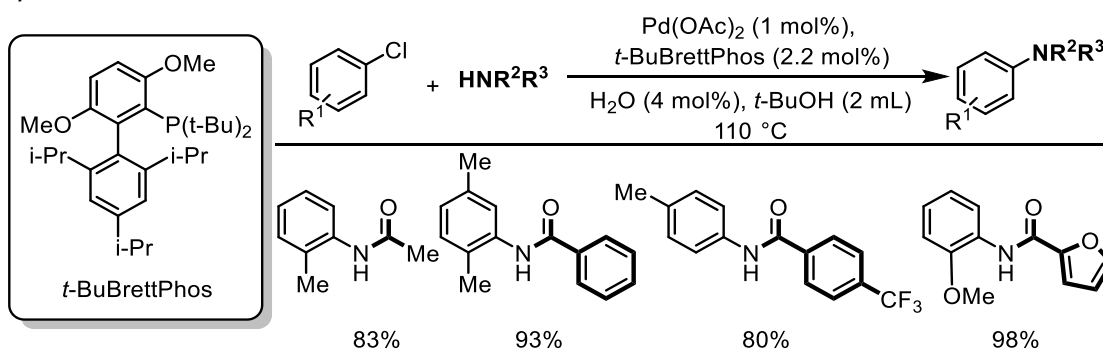
$\text{Pd}(\text{Ar})(\text{NR}^1\text{R}^2)$ species (Scheme 4.2, III). In the reductive elimination step the final product is released alongside the $\text{Pd}(0)$ species (Scheme 4.2, IV).

Catalysts generated *in situ* have shown high catalytic activity.^{6,11,25,26} Strongly electron-donating, monodentate ligands were studied for the C-N coupling. Beller and co-workers reported diadamantylalkylphosphine ligands (such as the BuPAd ligand), which resulted in the coupling of unactivated aryl chlorides (Scheme 4.3).²⁷ Verkade and co-workers designed triaminophosphine ligands, similarly to Beller. These ligands were bulky, electron-donating monoligated phosphines which showed high catalytic activity in C-N coupling reactions (Scheme 4.3).²⁸⁻³⁰ The disadvantages of these ligands was the lack of control of the coordination sphere around the palladium.



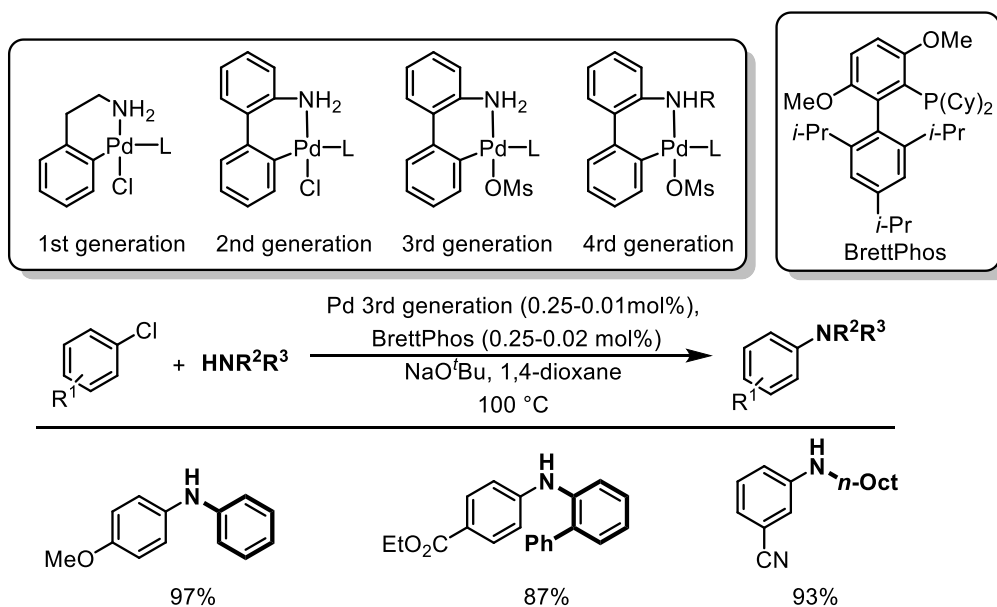
Scheme 4.3: Examples of bulky, monoligated phosphine ligands.²⁷⁻³⁰

As discussed in Chapter 3, dialkylbiarylphosphine ligands are widely studied in cross-coupling chemistry. Buchwald and co-workers have studied these ligands in depth (as well as designing a family of such bulky and electron-donating ligands), especially for C-N coupling reactions.³¹ The increased bulk on both of the aryl rings results in many advantages such as increased stability, prevention of cyclometalation and retardation of oxidation by O_2 .³¹ Increased electron density at the phosphorus promotes oxidative addition, overall resulting in a highly catalytic active system.



Scheme 4.4: Example of the use of *t*-BuBrettPhos (2-(di-*tert*-butylphosphino)-2',4',6'-triisopropyl-3,6-dimethoxy-1,1'-biphenyl) in C-N coupling.³²

Many disadvantages of the *in situ* systems still remain when compared to the well-defined pre-catalyst bearing a metal:ligand stoichiometry of 1:1.⁸ The fast and simple activation of well-defined pre-catalysts to the active Pd(0)L species, as well as the air- and moisture-stability, makes them very attractive candidates to study in cross-coupling catalysis.³³⁻³⁵ Well-defined palladacycles have shown promising reactivity in the C-N coupling reactions and several have been reported to-date.^{31,36} The air and moisture stable palladacycles shown in Scheme 4.5 have been extensively studied with the focus directed towards the activation to Pd(0) in cross-coupling chemistry. The activation of Pd(II) to Pd(0) requires a Brønsted base in order to deprotonate the ligated amine, followed by the reductive elimination of the nitrogen containing heterocycle.³⁷ The 1st generation was highly active but required very harsh conditions, an issue that was resolved in the 2nd and 3rd generation catalysts by introduction of a biaryl.¹² The 3rd generation was a highly active pre-catalyst for the C-N bond formation, coupling primary and secondary amines in low catalyst loading (Scheme 4.5).¹²

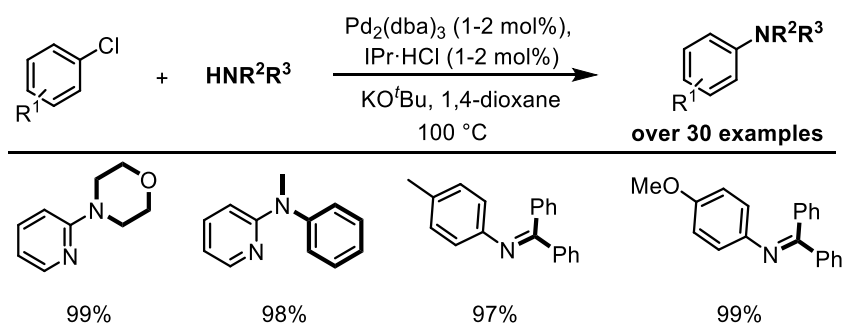


Scheme 4.5: C-N coupling using the 3rd generation palladacycle.¹²

The main disadvantage was the formation of an equivalent of carbazole during the activation step to Pd(0). As the carbazole side-product is a potential carcinogen.¹² This formation of a 2nd cyclic amine was, however, prevented by the development of the 4th generation, where the NH₂ group was exchanged to a NHMe or NPh group.^{38,39} Although the high catalytic activity of the well-defined palladacycle, a disadvantage of excess phosphine ligands remains (Scheme 4.5).

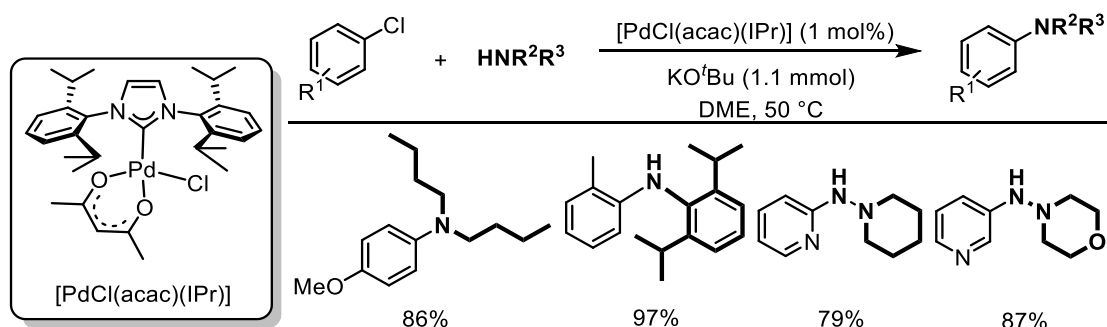
Our interest focused on N-heterocyclic carbenes (NHCs) as supporting ligands.^{40,41} The combination of a Pd source and a NHC ligand in cross-coupling catalysis was studied very early

after the first isolation of a free carbene showing promising results.⁴² The difference in electronic and steric properties of NHCs compared to the traditionally used phosphine ligands generated new possibilities and improved conditions.⁴³ An early example of the use of NHCs as ligands was conducted as an *in situ* system using Pd₂(dba)₃ and IPr·HCl (IPr = *N,N'*-bis-[2,6-(di-*iso*-propyl)phenyl]imidazol-2-ylidene).⁴⁴ Although harsh conditions were used such as KO^tBu and 100 °C, a wide substrate scope was reported. (Scheme 4.6).



Scheme 4.6: C-N coupling using an *in situ* Pd/NHC-HCl protocol.⁴⁴

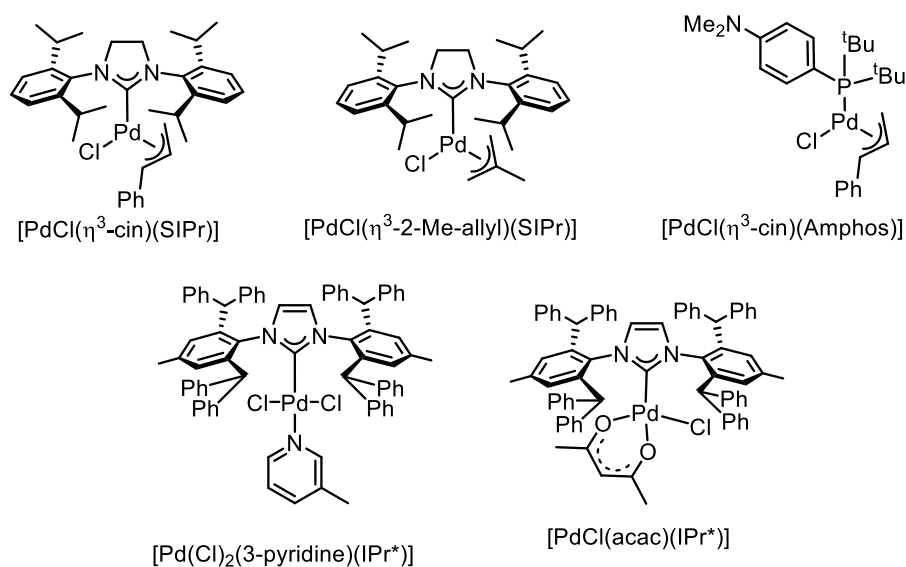
Following the promising results, Nolan and co-workers reported the highly active and well-defined [PdCl(acac)(IPr)] (acac = acetylacetonate) pre-catalyst.⁴⁵ This air and moisture stable Pd(II) complex was efficiently and quickly synthesised in quantitative yield (>95%). A wide scope of secondary and tertiary amines was obtained, featuring unactivated, sterically hindered and heterocyclic aryl chlorides (Scheme 4.7).



Scheme 4.7: The use of [PdCl(acac)(IPr)] as pre-catalyst in C-N coupling reaction.⁴⁵

The [Pd(η^3 -R-allyl)(μ -Cl)]₂ scaffold has been widely used in a number of cross-coupling reactions as *in situ* systems as well as in well-defined protocols. Similarly, the family of [PdCl(η^3 -R-allyl)(IPr)] pre-catalysts have shown high catalytic activity in a variety of cross-coupling reactions such as carbon-carbon,^{46,47} carbon-nitrogen^{13,18,48-51} and carbon-sulfur^{52,53} bond formation, as well as for ketone arylation.⁵⁴ A main advantage of the use of these pre-catalysts is in the low catalyst loadings required and the milder reaction conditions such as environmentally friendly solvents.^{55,56} Nolan and co-workers reported the use of [PdCl(η^3 -cin)(SIPr)] (SIPr = *N,N'*-bis-[2,6-

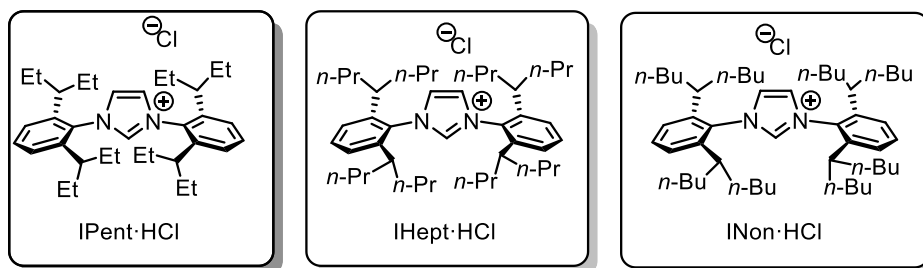
(di-*iso*-propyl)phenyl]imidazolidin-2-ylidene, cin = cinnamyl) for C-N coupling of unactivated aryl chlorides. A wide scope was conducted with low catalyst loading (1 mol%) at room temperature.^{49,57} Furthermore the catalyst loading could be reduced to as low as 10 ppm when the reaction temperature was increased to 80 °C. Caddick and co-workers reported a similar protocol using $[\text{PdCl}(\eta^3\text{-2-Me-allyl})(\text{SIPr})]$.³⁵ In this report the catalyst loading of 3 mol% was significantly higher than the cinnamyl analogue. This trend was thoroughly discussed by Nolan and co-workers.⁴⁹ Caddick reported a wide scope for different primary and secondary alkyl amines, where the use of bulky substrates was limited in this system.³⁵



Scheme 4.8: Examples of well-defined Pd(II) pre-catalysts in C-N coupling reactions.^{33,35,48,49,58,59}

Nolan and Cazin reported the efficient synthesis of $[\text{PdCl}(\eta^3\text{-cin})(\text{Amphos})]$ (Amphos = 4-(di-*tert*-butyl)phosphino-*N,N'*-dimethylaniline), a highly active pre-catalyst for C-N coupling.⁴⁸ Very low catalyst loading was used (0.1-0.3 mol%), featuring a wide range of substrates for example the coupling of unactivated aryl chlorides with cyclic dialkylamines. Steric hindrance was widely tolerated; for example 2,6-dimethylchlorobenzene was successfully coupled with 2,6-diisopropylaniline in 94% isolated yield with only 0.2 mol% catalyst loading.⁴⁸ It was shown that the supporting ligand on the palladium plays a key role in C-N coupling reactions and can influence different steps in the catalytic cycle. A more bulky ligand can stabilize the Pd(0) species during the catalysis as well as shielding the coordination shell of palladium from harmful binding of unwanted ligands.⁴⁸ Therefore Nolan and co-workers reported the synthesis and reactivity of bulkier variants, $[\text{PdCl}_2(3\text{-Cl-pyridine})(\text{IPr}^*)]$ ⁵⁸ and $[\text{PdCl}(\text{acac})(\text{IPr}^*)]$ ⁵⁹ (IPr* = *N,N'*-bis-[2,6-bis(diphenylmethyl)-4-methylphenyl]imidazol-2-ylidene) in the C-N coupling reaction (Scheme 4.8). Both pre-catalysts are highly active, requiring low catalyst loading and tolerating a wide

range of cross-coupling substrates. $[\text{Pd}(\text{Cl})_2(3\text{-Cl-pyridine})(\text{IPr}^*)]$ was extensively optimised,⁵⁸ focusing on milder reaction conditions, very low catalyst loading (0.05 mol%) could be used when the reaction was refluxed in toluene. Although the reaction could be conducted at room temperature with catalyst loading of 2 mol%, the optimised conditions were determined to be 0.4 mol% catalyst loading at 110 °C in 1,4-dioxane.⁵⁸ The $[\text{PdCl}(\text{acac})(\text{NHC})]$ family was further investigated by changing the NHC ligand to the ITent ligand.^{17,60}

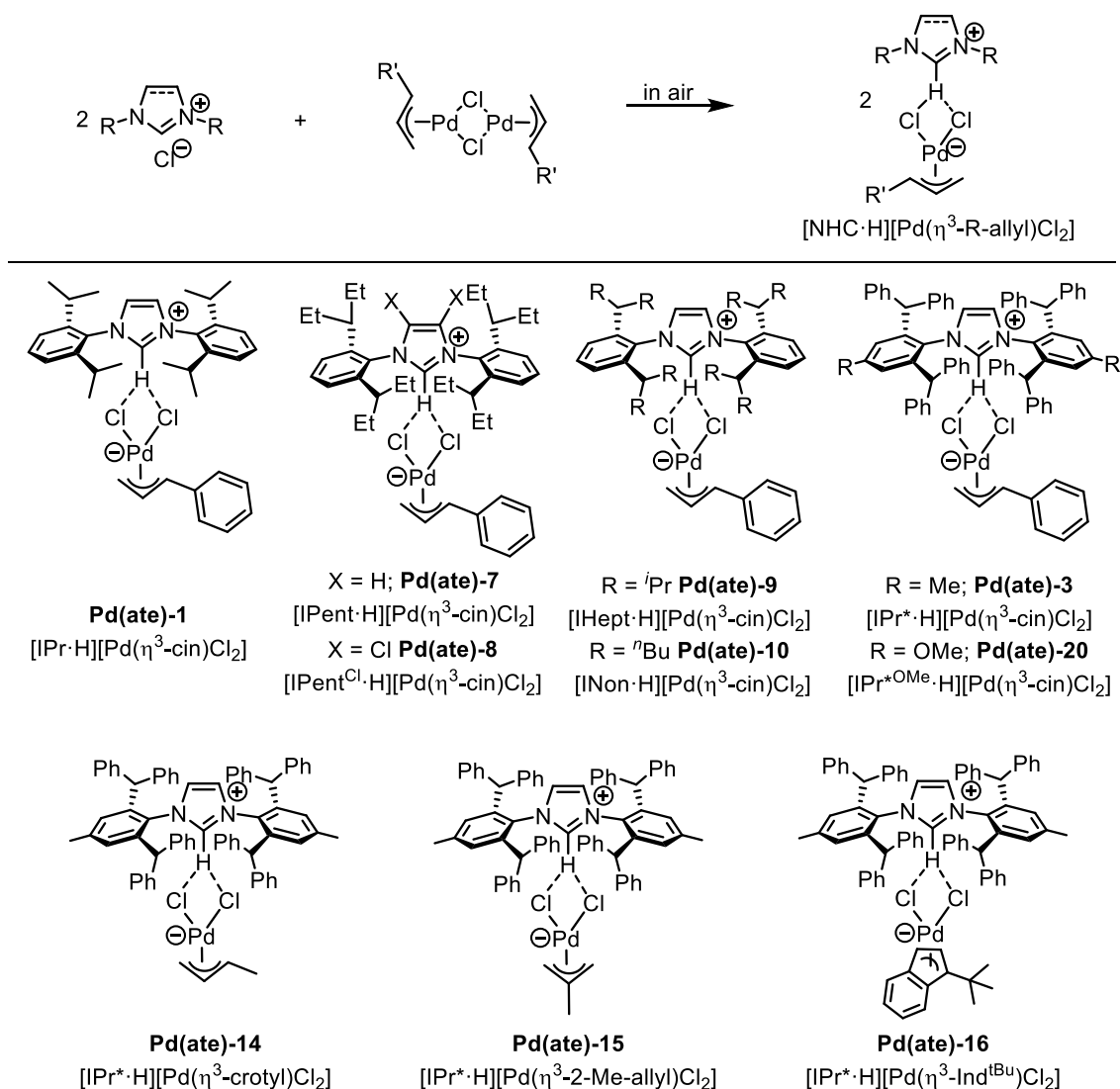


Scheme 4.9: The ITent ligands.⁶⁰

It was postulated that ITent ligands are effective because steric bulk was favourable for the catalysis as discussed above, while the flexibility of the alkane chain minimises hindrance to the reactive palladium centre.⁶⁰ $[\text{PdCl}(\text{acac})(\text{IHept}^{\text{OMe}})]$ ($\text{IHept}^{\text{OMe}} = N,N'$ -bis(2,6-di-4-heptyl-4-methoxyphenyl)imidazol-2-ylidene) was found to be the ideal pre-catalyst successfully coupling a range of different substrates at low catalyst loading (0.05-0.2 mol%).¹⁷ As these flexible bulky NHC ligands displayed very promising results, they were applied to the $[\text{PdCl}(\eta^3\text{-R-allyl})(\text{NHC})]$ family. Nolan reported the use of $[\text{PdCl}(\eta^3\text{-cin})(\text{IPr}^{*\text{OMe}})]$ ($\text{IPr}^{*\text{OMe}} = N,N'$ -bis-(2,6-diphenylmethyl)-4-methoxyphenyl)imidazol-2-ylidene⁶¹ and $[\text{PdCl}(\eta^3\text{-cin})(\text{INon})]$ ($\text{INon} = N,N'$ -bis-[2,6-bis(di-*iso*-nonyl)phenyl]imidazol-2-ylidene)¹⁸ in C-N coupling reactions, with low catalyst loading required (as low as 0.1 mol%).

4.2 Optimisation of the Buchwald-Hartwig Reaction using $[\text{IPr}^*\cdot\text{H}][\text{Pd}(\eta^3\text{-cin})\text{Cl}_2]$

The task of developing a more efficient and greener system for the Buchwald-Hartwig amination was our next focus. Previously reported palladate precatalyst, $[\text{IPr}\cdot\text{H}][\text{Pd}(\eta^3\text{-cin})\text{Cl}_2]$,⁶² showed very high catalytic activity in the Suzuki-Miyaura reaction (Chapter 3) resulting in a wide scope with a broad functional group tolerance as well as the use of a mild inorganic base and green solvent. In addition the synthesis of $[\text{NHC}\cdot\text{H}][\text{Pd}(\eta^3\text{-R-allyl})\text{Cl}_2]$ complexes can be obtained quantitatively without solvent or work-up, making these complexes very interesting pre-catalysts (Chapter 2) for cross-coupling chemistry (Chapter 3, 5 and 6). Herein the palladate complexes, $[\text{NHC}\cdot\text{H}][\text{Pd}(\eta^3\text{-R-allyl})\text{Cl}_2]$ were investigated as pre-catalysts for the Buchwald-Hartwig amination and ketone arylation. A range of $[\text{NHC}\cdot\text{H}][\text{Pd}(\eta^3\text{-R-allyl})\text{Cl}_2]$ complexes were prepared using the synthesis described in Chapter 2 and a catalyst screening for the C-N coupling was conducted (Scheme 4.10). In previous reports $[\text{PdCl}(\eta^3\text{-allyl})(\text{NHC})]$ pre-catalysts were used in the Buchwald-Hartwig amination, bulkier NHC ligands such as the ITent series⁶⁰ and IPr* analogues led to the best performance.^{59,63,64} Therefore the attention was set on more bulky ligands, this was confirmed as complexes bearing IPr* as ligand showed the best conversion. Next palladate complexes bearing different palladium dimers, such as $[\text{Pd}(\eta^3\text{-crotyl})(\mu\text{-Cl})_2]$ or $[\text{Pd}(\eta^3\text{-Ind}^{\text{tBu}})(\mu\text{-Cl})_2]$ (Ind^{tBu} = 1-*tert*-butyl-1H-indene) were synthesised (Scheme 4.10).



Scheme 4.10: Palladate pre-catalysts used in this study.

To gain better understanding of the inner workings of these new pre-catalysts in the Buchwald-Hartwig amination reaction, a catalyst screening was conducted. The model system involved the coupling of 4-chloroanisole (0.5 mmol) with 4-fluoroaniline (1.1 equiv.) as coupling substrates. The catalysis was carried out in 1,4-dioxane (0.5 M) at 110 °C for 16 hours, using KO^tAm (1.1 equiv.) as base. The palladate pre-catalysts bearing ITent ligands showed good conversions; [IPent·H][Pd(η³-cin)Cl₂] (IPent = *N,N'*-bis-[2,6-bis(di-*iso*-pentyl)phenyl]imidazol-2-ylidene) resulted in 86% conversion (Table 4.1, entry 1), a similar conversion was seen for [IHept·H][Pd(η³-cin)Cl₂] (IHept = *N,N'*-bis-[2,6-bis(di-*iso*-heptyl)phenyl]imidazol-2-ylidene) with 88% conversion (Table 1, entry 2), and [INon·H][Pd(η³-cin)Cl₂] with 93% conversion (Table 4.1, entry 3). The conversion to the cross-coupling product was moderate when [IPr·H][Pd(η³-cin)Cl₂] (Table 4.1, entry 7) was used as pre-catalyst, illustrating that a significant steric bulk on the NHC ligand is

needed. Changing the ancillary ligand on the palladium lowered the conversion (Table 4.1, entries 8-10), especially when the catalyst loading was reduced to 0.2 mol% (Table 4.1, entries 12-14). [IPr*·H][Pd(η^3 -cin)Cl₂] was determined as the optimum pre-catalyst showing full conversion to the desired cross-coupling product (Table 4.1, entry 4), even at 0.2 mol% catalyst loading (Table 4.1, entry 11).

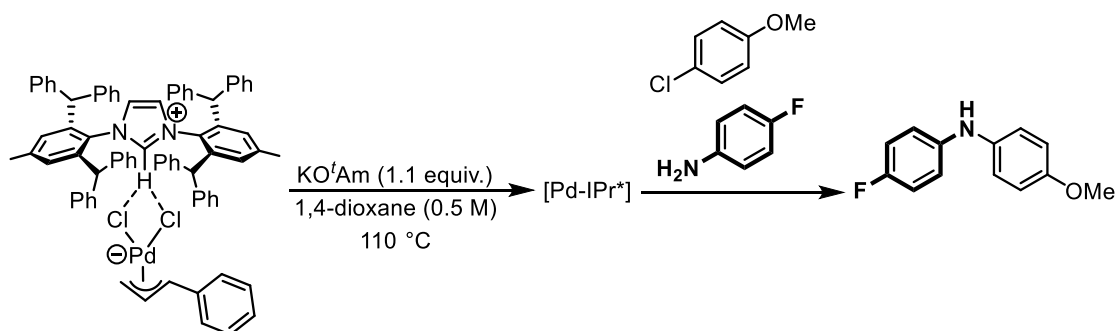
Table 4.1: Catalyst screening

Entry	Pre-catalyst	mol%	GC conversion (%)
1	[IPent·H][Pd(η^3 -cin)Cl ₂]	0.5	86
2	[IHept·H][Pd(η^3 -cin)Cl ₂]	0.5	88
3	[INon·H][Pd(η^3 -cin)Cl ₂]	0.5	93
4	[IPr*·H][Pd(η^3 -cin)Cl ₂]	0.5	99
5	[IPr* ^{OMe} ·H][Pd(η^3 -cin)Cl ₂]	0.5	95
6	[IPent ^{Cl} ·H][Pd(η^3 -cin)Cl ₂]	0.5	87
7	[IPr·H][Pd(η^3 -cin)Cl ₂]	0.5	63
8	[IPr*·H][Pd(η^3 -crotyl)Cl ₂]	0.5	96
9	[IPr*·H][Pd(η^3 -2-Me-allyl)Cl ₂]	0.5	95
10	[IPr*·H][Pd(η^3 -Ind ^{tBu})Cl ₂]	0.5	87
11	[IPr*·H][Pd(η^3-cin)Cl₂]	0.2	99
12	[IPr*·H][Pd(η^3 -crotyl)Cl ₂]	0.2	90
13	[IPr*·H][Pd(η^3 -2-Me-allyl)Cl ₂]	0.2	88
14	[IPr*·H][Pd(η^3 -Ind ^{tBu})Cl ₂]	0.2	56
15	[INon·H][Pd(η^3 -cin)Cl ₂]	0.2	83

Reaction conditions: In an inert atmosphere the pre-catalyst, K^tOAm (1.1 equiv.), 1,4-dioxane (0.5 M) was let to stir at the 110 °C for the stated time (1 h, activation time). The sample was removed from the heating block and 4-fluoroaniline (1.1 equiv.) was added followed by the 4-chloroanisole (0.5 mmol). The reaction was left to stir (910 rpm) for 16 h at 110 °C. Average of two runs. GC conversion based on 4-chloroanisole.

The activation of the pre-catalysts was next investigated. As discussed in the Suzuki-Miyaura reaction in Chapter 3, the palladate pre-catalysts can react with the cross-coupling substrates and shut down the catalysis. Therefore preliminary experiments were conducted first to establish if the activation step is required in the Buchwald-Hartwig amination. Two cross-coupling reactions were set up, one with an activation step and the other without. In the activation step, the pre-catalyst and base were left to stir at 60 °C for 1 hour before the substrates were added

(Scheme 4.11). Without the activation step the yield dropped to 70%, compared to the 99% isolated yield when the activation step was initially performed.



Scheme 4.11: Illustration of the activation step in the catalysis.

Next the activation temperature and the experimental temperature were optimised. Different temperatures for both activation and experimental temperatures were tested (Table 4.2). Increasing the experimental temperature is beneficial but interestingly the activation temperature plays an important role in obtaining full conversion of the product. The ideal activation temperature was determined to be 60 °C, above this temperature a decrease in the conversion is observed.

Table 4.2: Optimisation of the activation temperature.

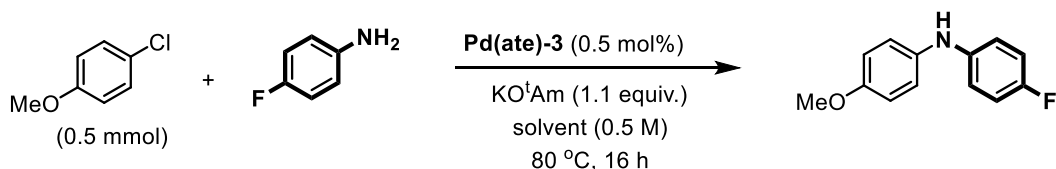
Entry	Time (min)	GC conversion (%)
1	10	88
2	30	80
3	60	99

Reaction conditions: [IPr*·H][Pd(η^3 -cin)Cl₂] (0.5 mol%), KO^tAm (1.1 equiv.), 1,4-dioxane (0.5 M) was let to stir at 110 °C for the corresponding time. The sample was removed from the heating block and 4-fluoroaniline (1.1 equiv.) was added followed by the 4-chloroanisole (0.5 mmol). The reaction was left to stir for 16 h at the 110 °C. GC conversion based on 4-chloroanisole. An average of two reactions.

The optimisation of the reaction was further focused on the use of green and non-toxic solvents,^{65,66} and therefore a wide range of solvent was tested in the model system (Table 4.2) resulting in cyclopentylmethyl ether (CPME) as the most promising medium (Table 4.3). CPME is an alternative to the more toxic, hazardous ether solvents such as tetrahydrofuran (THF), diethyl ether or 1,4-dioxane. The stability of the solvent under acidic and basic conditions as well as the

suppression of the formation of peroxide are some of its many advantages.⁶⁷ The recovery of CPME, due to its low solubility in water eases the use in large scale reactions, especially looking towards industrial applications.⁶⁷

Table 4.3: Solvent optimisation.

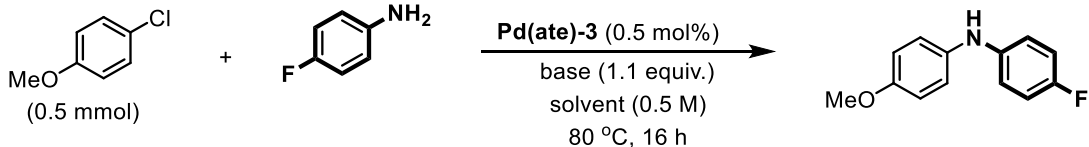


Entry	Solvent	GC conversion (%)
1	ethanol	n.r.
2	<i>iso</i> -propanol	19
3	cyclohexane	94
4	2-methyltetrahydrofuran	87
5	1,4-dioxane	90
6	cyclopentylmethylether	97

Reaction conditions: [IPr*·H][Pd(η^3 -cin)Cl₂] (0.5 mol%), KO^tAm (1.1 equiv.), the corresponding solvent (0.5 M) was let to stir at 60 °C for 1 h. The sample was removed from the heating block and 4-fluoroaniline (1.1 equiv.) was added followed by the 4-chloroanisole (0.5 mmol). The reaction was left to stir for 16 h at 80 °C. GC conversion based on 4-chloroanisole. An average of two reactions.

Several inorganic bases were tested ranging from weak inorganic bases (K₂CO₃, K₃PO₄) to stronger inorganic bases such as hydroxide and alkoxide bases. Cross experiments were performed with the three best solvents and the five best bases, determining the ideal conditions for the protocol (Table 4.4).

Table 4.4: Base and solvent screening

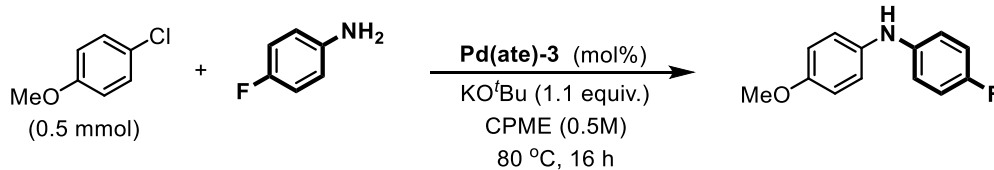


Base	GC conversion (%)		
	1,4-dioxane	cyclohexane	cyclopentylmethylether
KO ^t Am	99	94	99
KO ^t Bu	93	86	99
KOH	57	12	42
NaOH	45	<1	32
CsOH	22	n.r.	38

Reaction conditions: [IPr*·H][Pd(η^3 -cin)Cl₂], the corresponding base (1.1 equiv.), the corresponding solvent (0.5 M) was let to stir at 60 °C for 1 h. The sample was removed from the heating block and 4-fluoroaniline (1.1 equiv.) was added followed by the 4-chloroanisole (0.5 mmol). The reaction was left to stir (910 rpm) for 16 h at 80 °C. GC conversion based on 4-chloroanisole. An average of two reactions.

After establishing the ideal conditions (CPME as ideal solvent in the combination with KO^tBu), the catalyst loading and reaction time were optimised. The catalyst loading could be reduced to 0.2 mol%, (Table 4.5, entry 3).

Table 4.5: Optimisation of the catalyst loading.



Entry	[Pd] mg	[Pd] mol%	GC conversion %	TON
1	3	0.5	99	196
2	1.8	0.3	99	350
3	1.2	0.2	99	490
4	0.6	0.1	50	490

Reaction conditions: [IPr*·H][Pd(η^3 -cin)Cl₂], KO^tBu (1.1 equiv.) and CPME (0.5 M) was let to stir at 60 °C for 1 h. The sample was removed from the heating block and 4-fluoroaniline (1.1 equiv.) was added followed by the 4-chloroanisole (0.5 mmol). The reaction was left to stir for 16 h at 80 °C. GC conversion based on 4-chloroanisole. An average of two reactions.

Furthermore the reaction time could be reduced to two hours.

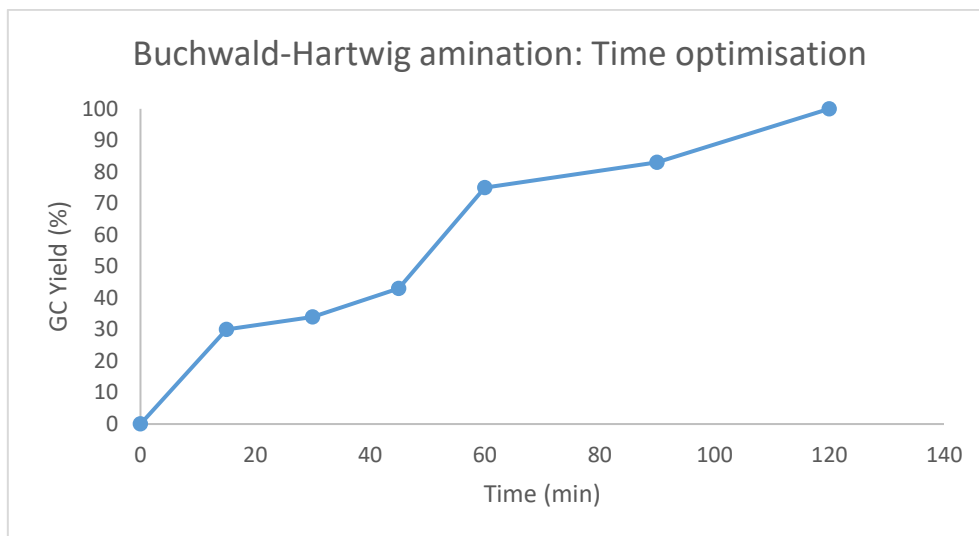
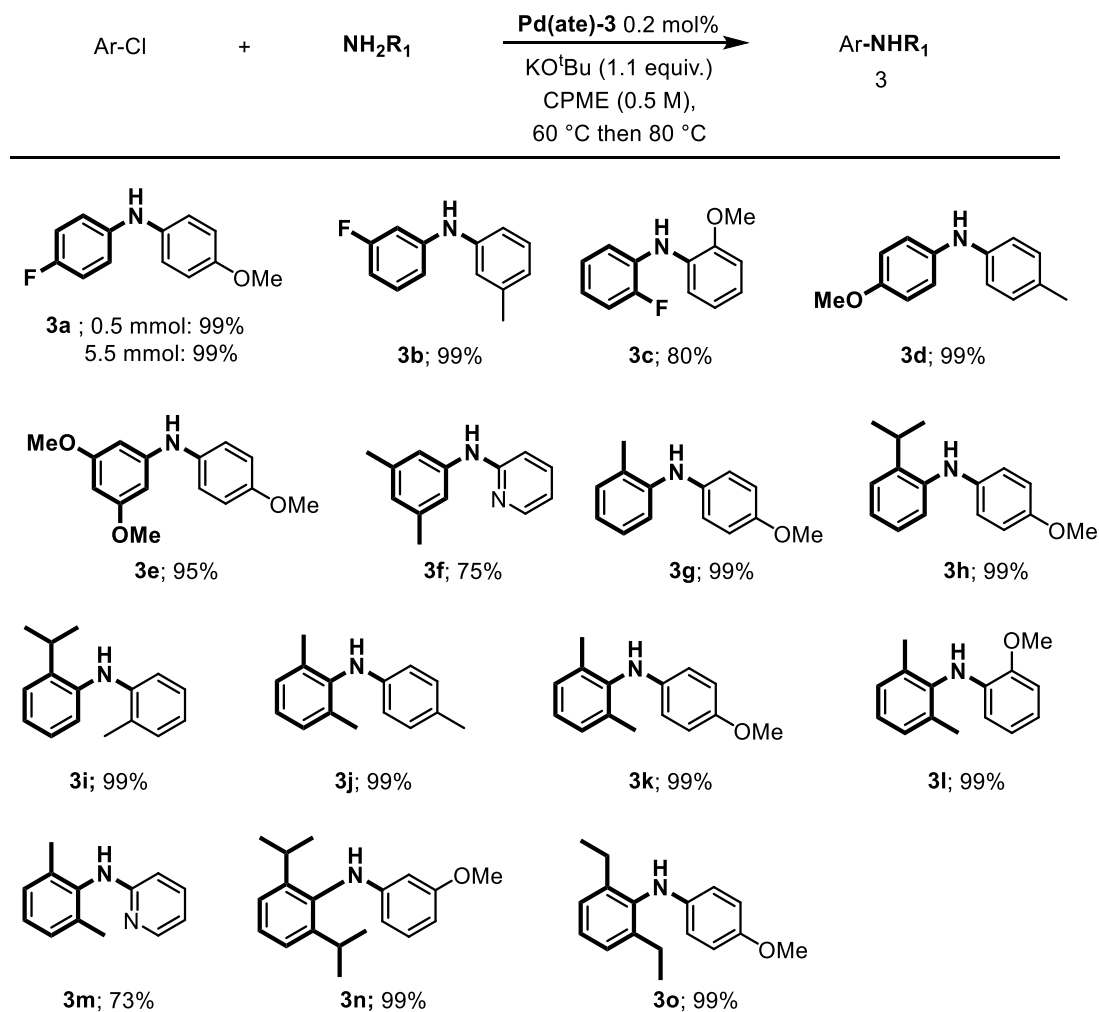


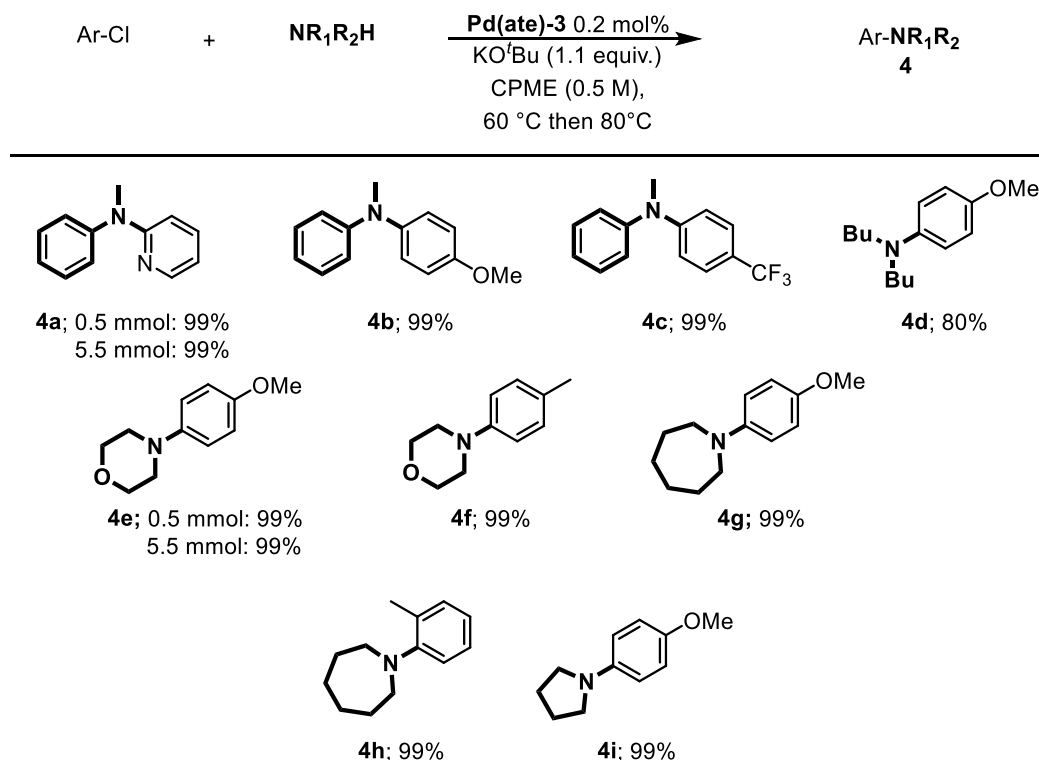
Figure 1: Time optimisation for the Buchwald-Hartwig amination. Reaction conditions: [IPr*·H][Pd(η^3 -cin)Cl₂], KO^tBu (1.1 equiv.), and CPME (0.5 M) was let to stir at 60 °C for 1 h. The sample was removed from the heating block and 4-fluoroaniline (1.1 equiv.) was added followed by the 4-chloroanisole (0.5 mmol). The reaction was left to stir at 80 °C. GC conversion based on 4-chloroanisole. An average of two reactions.

The newly established catalytic system was tested firstly using a variety of primary amines with aryl chlorides. Our attention was drawn to the positions of functional groups on the aryl chlorides and aryl amines. It was possible to couple substrates with substituents on *para*, *meta* or *ortho* position without loss of reactivity (Scheme 4.12, **3a**, **3b** and **3c**) and **3a** was successfully scaled up to a 5.5 mmol scale. Election-donating groups on the primary amine were tolerated resulting in high yields (Scheme 4.12, **3d** and **3e**). 2-Chloropyridine was successfully coupled with 3,5-methylaniline in 75% isolated yield (Scheme 4.12, **3f**). Sterically hindered anilines were tested, such as 2-tolyaniline (Scheme 4.12, **3g**), 2-isopropylaniline (Scheme 4.12, **3h** and **3i**) and 2,6-dimethyl aniline (Scheme 4.12, **3j**, **3k**, **3l** and **3m**) were successfully coupled with a range of aryl chlorides. More sterically hindered anilines such as 2,6-diisopropylaniline (Scheme 4.12, **3n**) and 2,6-diethylaniline (Scheme 4.12, **3o**) resulting in excellent isolated yield. Due to the high conversions, all of the products were isolated after simple filtration over silica with no need for flash chromatography.



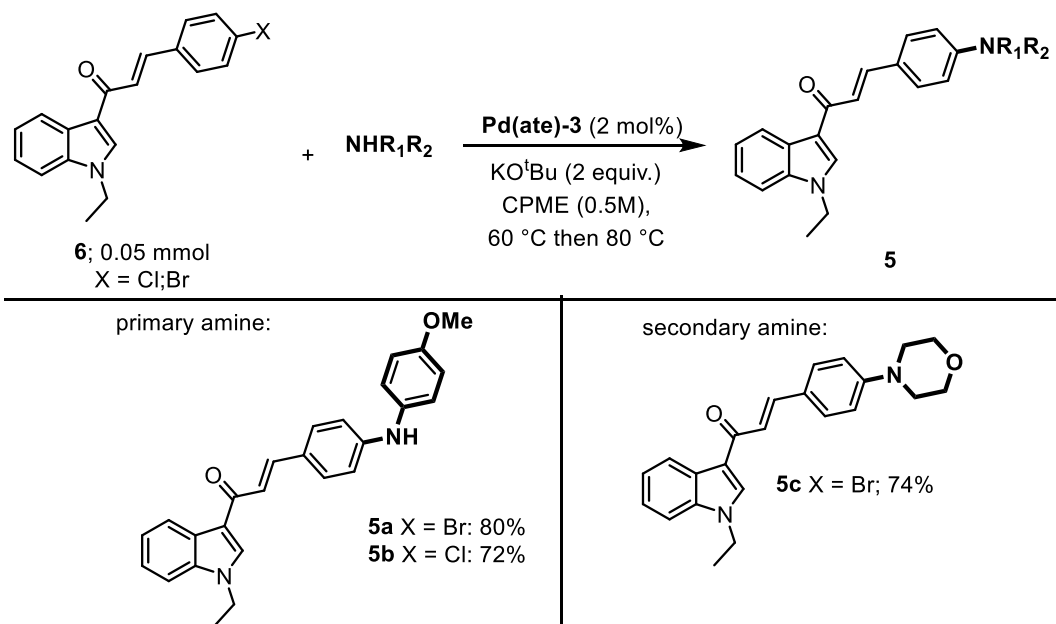
Scheme 4.12: Scope of the Buchwald-Hartwig amination of primary amines. Reaction conditions: [IPr*·H][Pd(η^3 -cin)Cl₂] (0.2 mol%), KO^tBu (1.1 equiv.) and CPME (0.5 M) was let to stir at 60 °C for 1 h. The mixture was removed from the heating block and the corresponding aniline (1.1 equiv.) was added followed by the aryl chloride (0.5 mmol). The reaction was left to stir for 2 h at the 80 °C. The product was isolated via a filtration over silica gel. An average of two reactions.

The coupling of secondary amines was addressed next. Different aliphatic and aromatic amines were tested. *N*-methylaniline was coupled with 2-chloropyridine (Scheme 4.13, **4a**), 4-chloroanisole (Scheme 4.13, **4b**) and 1-chloro-4-(trifluoromethyl)benzene (Scheme 4.13, **4c**) in high yield. Dibutylamine was coupled with 4-chloroanisole (Scheme 4.13, **4d**) in 80% yield. Morpholine was successfully coupled with 4-chloroanisole (Scheme 4.13, **4e**) and 4-chlorotoluene (Scheme 4.13, **4f**). A 7-membered ring; azepane, (Scheme 4.13, **4g** and **4h**) as well as pyrrolidine, (Scheme 4.13, **4i**) were coupled, resulting in excellent yield.



Scheme 4.13: Scope of the Buchwald-Hartwig amination of secondary amines. Reaction conditions: [IPr*·H][Pd(η^3 -cin)Cl₂] (0.2 mol%), KO^tBu (1.1 equiv.) and CPME (0.5 M) was let to stir at 60 °C for 1 h. The sample was removed from the heating block and the corresponding aniline (1.1 equiv.) was added followed by the aryl chloride (0.5 mmol). The reaction was left to stir (910 rpm) for 2 h at the 80 °C. The product was isolated via a filtration over silica gel. An average of two reactions.

The cross-coupling of heteroatom-containing aryl halides remains a challenge, especially at low catalyst loading used. The coupling of amines with aryl chlorides containing one heteroatom has been studied and reported by several groups.^{12,48,68–70} Successful amination of aryl chlorides containing more than one heteroatom, on the other hand is still a challenge and rarely reported. *N*-ethylindolylphenylpropenones were synthesised for testing in the new developed protocol. The chosen scaffold offers challenges in the form of two heteroatoms and an alkene.



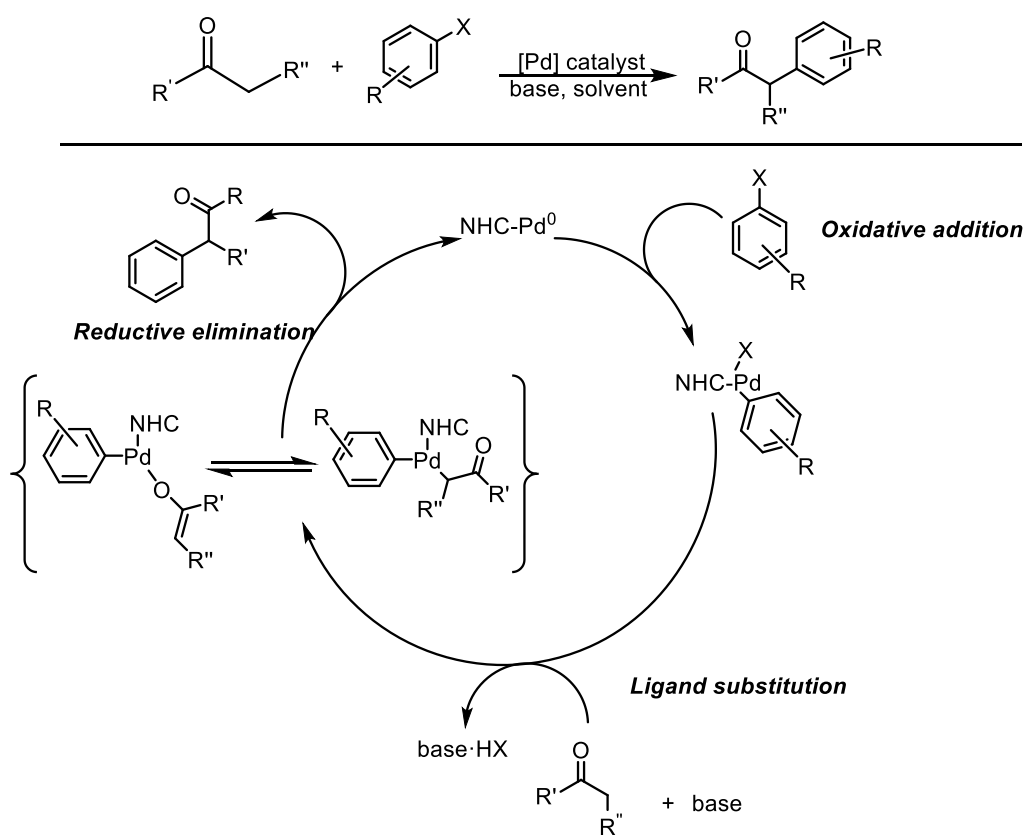
Scheme 4.14: Buchwald-Hartwig amination of biologically interesting substrates. Reaction conditions: $[\text{IPr}^*\cdot\text{H}][\text{Pd}(\eta^3\text{-cin})\text{Cl}_2]$ (2 mol%), KO^tBu (2 equiv.) and CPME (0.5 M) was let to stir at 60 °C for 1 h. The sample was removed from the heating block and the corresponding amine (1.1 equiv.) was added followed by the aryl halide (0.05 mmol). The reaction was left to stir (910 rpm) for 4 h at the 80 °C. The product was isolated via flash chromatography. An average of two reactions.

The successful syntheses of **5a**, **5b** and **5c** are reported; both primary and secondary amines were coupled, resulting in good yields of the desired product. Many of these analogues have been studied in anti-cancer research and have shown promising results.⁷¹ Being able to couple more challenging aryl halides opens the door to a new range of biologically active compounds.

4.3 Using [IPr*·H][Pd(η³-cin)Cl₂] in the α-Ketone Arylation Reaction

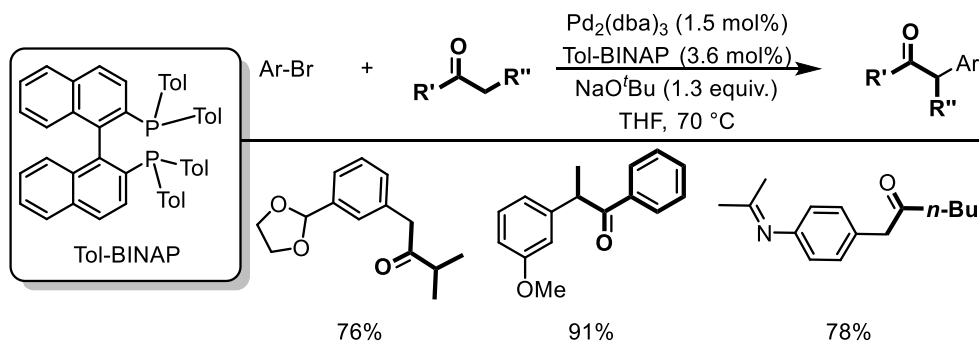
The newly developed system was next used to test and optimise a ketone arylation reaction. The coupling of enolizable ketones and aryl chlorides is important in the synthesis of natural products and synthetic intermediates for pharmaceuticals.⁷²⁻⁷⁴ First reported by Hartwig,⁷⁵ Buchwald¹⁹ and Miura,⁷⁶ the α-arylation of ketones is now a powerful and widely used tool in synthetic chemistry.

The catalytic cycle consists of three steps (Scheme 4.15): i) the oxidative addition of the aryl halide to the Pd(0), ii) the substitution of the halide by the *in situ* formed enolate and iii) the reductive elimination.



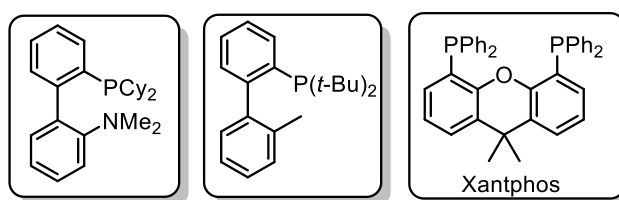
Scheme 4.15: General ketone arylation and proposed catalytic cycle.⁵⁴

In a seminal report from Palucki and Buchwald, the coupling of a different ketones with a wide range of aryl bromides was described using Pd₂dba₃ and Tol-BINAP (2,2'-bis (di-*p*-tolyl)phosphinol-1,1'-binaphthyl) (Scheme 4.16).¹⁹ The resulting α-arylated ketones were obtained in good to excellent yields, showing a wide functional group tolerance.¹⁹



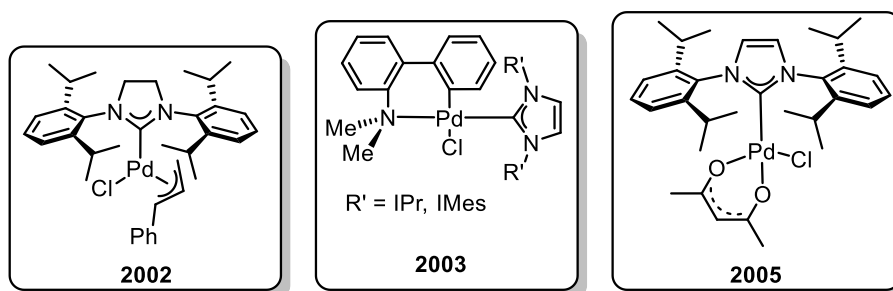
Scheme 4.16: Arylation using Pd_2dba_3 and Tol-BINAP.¹⁹

The use of bulky electron-rich biaryl phosphine ligands was found to be beneficial in the arylation of ketones.⁷⁷ The advantages of bulky electron-rich ligands were later confirmed by Buchwald who tested a range of different ligands in the arylation of ketones (Scheme 4.17).^{77,78} In particular Xantphos (4,5-bis(diphenyl)phosphino-9,9-dimethylxanthene) with $\text{Pd}(\text{OAc})_2$ was used in low catalyst loading (1.0-0.2 mol%) coupling a variety of aryl chlorides and bromides with ketones in good yields.⁷⁸



Scheme 4.17: Examples of bulky electron-rich ligands used in the arylation of ketones.^{77,78}

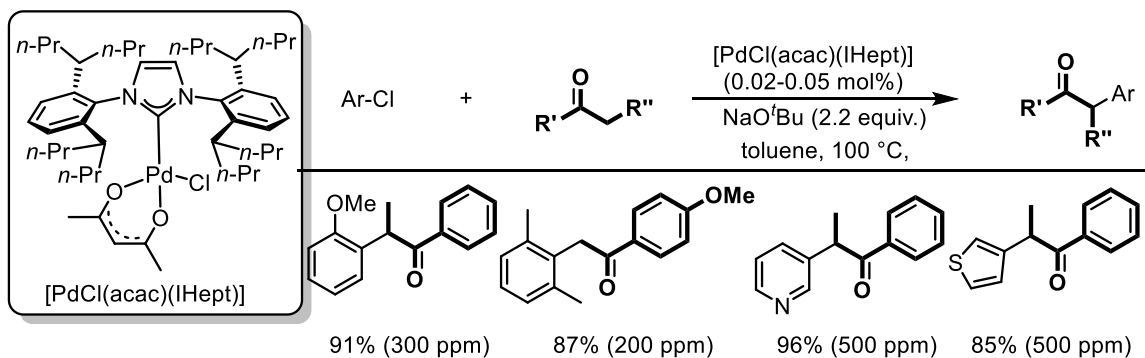
Several well-defined Pd(II)-NHC complexes have been reported and studied in the ketone arylation by Nolan and co-workers (Scheme 4.18).^{45,54,79-81} The use of NHCs as ligands allowed Nolan and co-workers to couple different aryl bromides, triflates and chlorides with ketones in good to excellent yields.⁷⁹



Scheme 4.18: Well-defined Pd(II)-NHC complexes reported for the ketone arylation.^{45,54,80,82}

The high catalytic activity of $[\text{PdCl}(\text{acac})(\text{IPr})]$ was illustrated by the coupling of unactivated, sterically hindered and heterocyclic aryl chlorides in 1 mol% catalyst loading.⁴⁵ Good to excellent yields were achieved in moderate heating (60 °C) in short reaction time (1-4 hours). By changing

the NHC from IPr to IHept in the [PdCl(acac)(NHC)] scaffold, Nolan and co-workers developed a highly catalytically active protocol for the ketone arylation.⁸³ The catalyst loading was as low as 0.02-0.05 mol%. A good functional group tolerance was possible, resulting in good to excellent yields (Scheme 4.19).⁸³ The synthesis of the [PdCl(acac)(NHC)] pre-catalysts is straightforward by simply refluxing the corresponding NHC·HCl and Pd(acac)₂ in 1,4-dioxane, but not as facile and convenient as the [NHC·H][Pd(η³-cin)Cl₂] pre-catalysts.



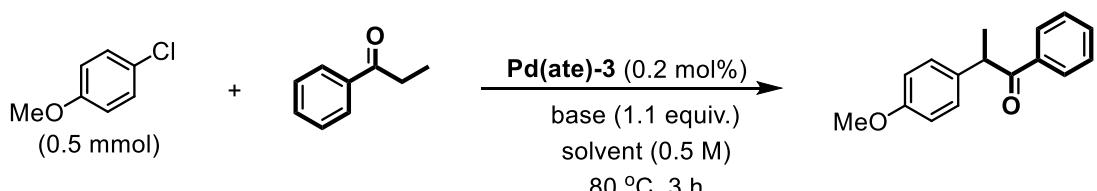
Scheme 4.19: The ketone arylation using [PdCl(acac)(IHept)].⁸³

The exceptional reaction conditions established showed the potential for Pd(II)-NHC complexes in the ketone arylation.

4.3.1. Results and Discussion

A smaller optimisation was conducted, based on the already optimised Buchwald-Hartwig amination condition as the two reactions are mechanistically linked. The reaction was carried out at 80 °C for three hours and the combination of NaO^tBu (1.1 equiv.) as base and CPME as solvent was found to be most efficient with 4-chloroanisole (0.5 mmol) and propiophenone (1.1 equiv.) as model substrates (Table 4.6).

Table 4.6: Optimisation: base and solvent

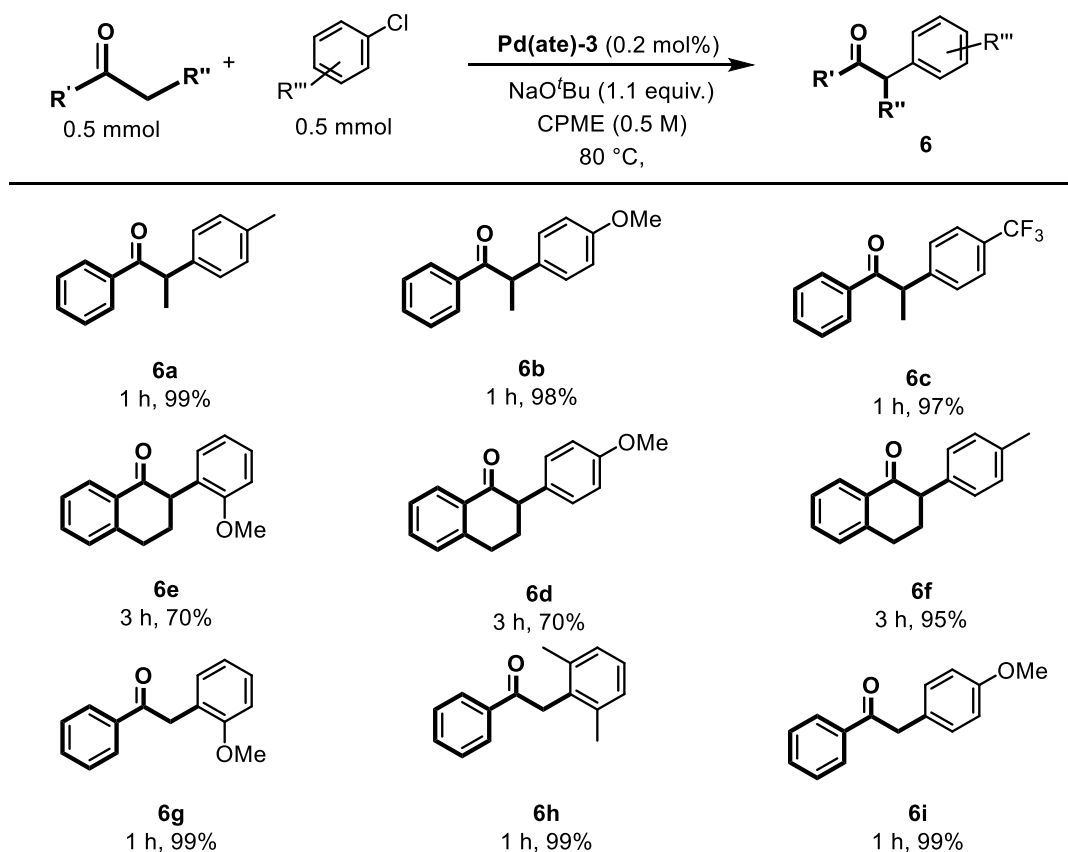


Base	GC conversion (%)			
	1,4-dioxane	tetrahydrofuran	toluene	cyclopentylmethylether
KO ^t Bu	11	n.r.	72	n.r.
LiO ^t Bu	n.r.	traces	5	31
NaO ^t Bu	11	31	91	99
KOH	n.r.	n.r.	n.r.	n.r.
NaOH	n.r.	n.r.	n.r.	n.r.

Reaction conditions: [IPr*·H][Pd(η³-cin)Cl₂] (0.2 mol%), the corresponding base (1.1 equiv.) and the corresponding solvent (0.5 M) was let to stir at 60 °C for 1 h. The sample was removed from the heating block and the propiophenone (1.1 equiv.) was added followed by 4-chloroanisole (0.05 mmol). The reaction was left to stir for 3 h at the 80 °C. GC conversion based on 4-chloroanisole. An average of two reactions.

Cross experiments were conducted with the four best solvents, determined for the Buchwald-Hartwig amination and five inorganic bases. When NaO^tBu was used as base, the best conversions were achieved, resulting in NaO^tBu as the ideal base in combination with CPME. The reaction was carried out in air with no need for a dry solvent and the low catalyst loading (0.2 mol%) was maintained.

Propiophenone was coupled with unsubstituted- (Scheme 4.16, **6a**), electron-donating (Scheme 4.16, **6b**) and electron-withdrawing (Scheme 4.16, **6c**) aryl chloride with no loss of reactivity. Sterically hindered aryl chlorides were successfully coupled with the more challenging α-tetralone (Scheme 4.16, **6e**) and acetophenone (Scheme 4.16, **6g** and **6h**).



Scheme 4.16: Scope of the ketone arylation. **Reaction conditions:** $[\text{IPr}^*\cdot\text{H}][\text{Pd}(\eta^3\text{-cin})\text{Cl}_2]$ (1.2 mg, 0.2 mol%), NaO^tBu (53 mg, 0.55 mmol) and CPME (0.5 M) was let to stir at the $60\text{ }^\circ\text{C}$ for 1 h. The vial was removed from the heating block and the corresponding solution of aryl ketone and aryl chloride in CPME (1 mL) was added. The reaction was left to stir (910 rpm) for the corresponding time at $80\text{ }^\circ\text{C}$.

4.4 Conclusion

A range of different NHC-Pd pre-catalysts were synthesized following a facile and environmental friendly synthesis. The pre-catalysts were tested in the Buchwald-Hartwig amination and the ketone arylation reactions. A highly user-friendly catalytic protocol was established for both reactions using low catalyst loadings and a green solvent (CPME). Challenging biologically relevant substrates were coupled in the Buchwald-Hartwig aminations pushing the limits of the developed protocol. High yields were achieved for all substrates tested in both reactions, making this a highly active and efficient protocol. All experiments are conducted under air, starting from the synthesis of the pre-catalyst and ending with the catalysis.

4.5 References

- (1) Corbet, J. P.; Mignani, G. *Chem. Rev.* **2006**, *106*, 2651–2710.
- (2) Johansson Seechurn, C. C. C.; Kitching, M. O.; Colacot, T. J.; Snieckus, V. *Angew. Chem. Int. Ed.* **2012**, *51*, 5062–5085.
- (3) Colacot, T. J.; Matthey, J. *Platin. Met. Rev.* **2011**, *55*, 84–90.
- (4) Nicolaou, K. C.; Bulger, P. G.; Sarlah, D. *Angew. Chem. Int. Ed.* **2005**, *44*, 4442–4489.
- (5) Magano, J.; Dunetz, J. R. *Chem. Rev.* **2011**, *111*, 2177–2250.
- (6) Ruiz-Castillo, P.; Buchwald, S. L. *Chem. Rev.* **2016**, *116*, 12564–12649.
- (7) Würtz, S.; Glorius, F. *Acc. Chem. Res.* **2008**, *41*, 1523–1533.
- (8) Hazari, N.; Melvin, P. R.; Beromi, M. M. *Nat. Rev. Chem.* **2017**, *1*, 25.
- (9) Klingensmith, L. M.; Strieter, E. R.; Barder, T. E.; Buchwald, S. L. *Organometallics* **2006**, *25*, 82–91.
- (10) Surry, D. S.; Buchwald, S. L. *Angew. Chem. Int. Ed.* **2008**, *47*, 6338–6361.
- (11) Fors, B. P.; Davis, N. R.; Buchwald, S. L. *J. Am. Chem. Soc.* **2009**, *131*, 5766–5768.
- (12) Bruno, N. C.; Tudge, M. T.; Buchwald, S. L. *Chem. Sci.* **2013**, *4*, 916–920.
- (13) Pommella, A.; Tomaiuolo, G.; Chartoire, A.; Caserta, S.; Toscano, G.; Nolan, S. P.; Guido, S. *Chem. Eng. J.* **2013**, *223*, 578–583.
- (14) Chartoire, A.; Boreux, A.; Martin, A. R.; Nolan, S. P. *RSC Adv.* **2013**, *3*, 3840.
- (15) Sunesson, Y.; Lime, E.; Lill, S. O. N.; Meadows, R. E.; Norrby, P. J. *Org. Chem.* **2014**, *79*, 11961–11969.
- (16) Zhang, Y.; César, V.; Storch, G.; Lugan, N.; Lavigne, G. *Angew. Chem. Int. Ed.* **2014**, *53*, 6482–6486.
- (17) Le Duc, G.; Meiries, S.; Nolan, S. P. *Organometallics* **2013**, *32*, 7547–7551.
- (18) Marelli, E.; Chartoire, A.; Le Duc, G.; Nolan, S. P. *ChemCatChem* **2015**, *7*, 4021–4024.
- (19) Palucki, M.; Buchwald, S. L. *J. Am. Chem. Soc.* **1997**, *119*, 11108–11109.
- (20) Wolfe, J. P.; Wagaw, S.; Marcoux, J. F.; Buchwald, S. L. *Acc. Chem. Res.* **1998**, *31*, 805–818.
- (21) Hartwig, J. F. *Acc. Chem. Res.* **1998**, *31*, 852–860.
- (22) Louie, J.; Paul, F.; Hartwig, J. F. *Organometallics* **1996**, *15*, 2794–2805.
- (23) Fors, B. P.; Watson, D. A.; Biscoe, M. R.; Buchwald, S. L. *J. Am. Chem. Soc.* **2008**, *3*, 3–5.
- (24) Fors, B. P.; Dooleweerd, K.; Zeng, Q.; Buchwald, S. L. *Tetrahedron* **2009**, *65*, 6576–6583.
- (25) Sorribes, I.; Junge, K.; Beller, M. *J. Am. Chem. Soc.* **2014**, *136*, 14314–14319.
- (26) Meadows, R. E.; Woodward, S. *Tetrahedron* **2008**, *64*, 1218–1224.

- (27) Zapf, A.; Ehrentraut, A.; Beller, M. *Angew. Chem. Int. Ed.* **2000**, *39*, 4153–4155.
- (28) Urgaonkar, S.; Nagarajan, M.; Verkade, J. G. *Org. Lett.* **2003**, *5*, 815–818.
- (29) Urgaonkar, S.; Verkade, J. G. *J. Org. Chem.* **2004**, *69*, 9135–9142.
- (30) Urgaonkar, S.; Xu, J. H.; Verkade, J. G. *J. Org. Chem.* **2003**, *68*, 8416–8423.
- (31) Surry, D. S.; Buchwald, S. L. *Chem. Sci.* **2011**, *2*, 27–50.
- (32) Arrechea, P. L.; Buchwald, S. L. *J. Am. Chem. Soc.* **2016**, *138*, 12486–12493.
- (33) Marion, N.; Navarro, O.; Mei, J.; Stevens, E. D.; Scott, N. M.; Nolan, S. P. *J. Am. Chem. Soc.* **2006**, *128*, 4101–4111.
- (34) Marion, N.; Navarro, O.; Stevens, E. D.; Ecarnot, E. C.; Bell, A.; Amoroso, D.; Nolan, S. P. *Chem. Asian J.* **2010**, *5*, 841–846.
- (35) Cawley, M. J.; Cloke, F. G. N.; Fitzmaurice, R. J.; Pearson, S. E.; Scott, J. S.; Caddick, S. *Org. Biomol. Chem.* **2008**, *6*, 2820–2825.
- (36) Ingoglia, B. T.; Buchwald, S. L. *Org. Lett.* **2017**, *19*, 2853–2856.
- (37) Biscoe, M. R.; Fors, B. P.; Buchwald, S. L. *J. Am. Chem. Soc.* **2008**, *130*, 6686–6687.
- (38) Friis, S. D.; Skrydstrup, T.; Buchwald, S. L. *Org. Lett.* **2014**, *16*, 4296–4299.
- (39) Bruno, N. C.; Niljianskul, N.; Buchwald, S. L. *J. Org. Chem.* **2014**, *79*, 4161–4166.
- (40) Scott, N. M.; Nolan, S. P. *Eur. J. Inorg. Chem.* **2005**, *2005*, 1815–1828.
- (41) Herrmann, W. A. *Angew. Chem. Int. Ed.* **2002**, *41*, 1290–1309.
- (42) Herrmann, W. A.; Elison, M.; Köcher, C.; Artus, G. R. J. *Angew. Chem. Int. Ed.* **1995**, *34*, 2371–2374.
- (43) Herrmann, W. A.; Köcher, C. *Angew. Chem. Int. Ed.* **1997**, *36*, 2162–2187.
- (44) Grasa, G. a; Viciu, M. S.; Huang, J.; Nolan, S. P. *J. Org. Chem.* **2001**, *66*, 7729–7737.
- (45) Marion, N.; Ecarnot, E. C.; Navarro, O.; Amoroso, D.; Bell, A.; Nolan, S. P. *J. Org. Chem.* **2006**, *71*, 3816–3821.
- (46) Chartoire, A.; Lesieur, M.; Falivene, L.; Slawin, A. M. Z.; Cavallo, L.; Cazin, C. S. J.; Nolan, S. P. *Chem. Eur. J.* **2012**, *18*, 4517–4521.
- (47) Martin, A. R.; Chartoire, A.; Slawin, A. M. Z.; Nolan, S. P. *Beilstein J. Org. Chem.* **2012**, *8*, 1637–1643.
- (48) Chartoire, A.; Lesieur, M.; Slawin, A. M. Z.; Nolan, S. P.; Cazin, C. S. J. *Organometallics* **2011**, *30*, 4432–4436.
- (49) Navarro, O.; Marion, N.; Mei, J.; Nolan, S. P. *Chem. Eur. J.* **2006**, *12*, 5142–5148.
- (50) Navarro, O.; Kaur, H.; Mahjoor, P.; Nolan, S. P. *J. Org. Chem.* **2004**, *69*, 3173–3180.
- (51) Chartoire, A.; Claver, C.; Corpet, M.; Krinsky, J.; Mayen, J.; Nelson, D.; Nolan, S. P.; Pen

- Afiel, I.; Woodward, R.; Meadows, R. E. *Org. Process Res. Dev.* **2016**, *20*, 551–557.
- (52) Bastug, G.; Nolan, S. P. *J. Org. Chem.* **2013**, *78*.
- (53) Izquierdo, F.; Chartoire, A.; Nolan, S. P. *ACS Catal.* **2013**, *3*, 2190–2193.
- (54) Viciu, M. S.; Germaneau, R. F.; Nolan, S. P. *Org. Lett.* **2002**, *4*, 4053–4055.
- (55) Izquierdo, F.; Corpet, M.; Nolan, S. P. *European J. Org. Chem.* **2015**, 1920–1924.
- (56) Hruszkewycz, D. P.; Balcells, D.; Guard, L. M.; Hazari, N.; Tilset, M. *J. Am. Chem. Soc.* **2014**, *136*, 7300–7316.
- (57) Marion, N.; Navarro, O.; Mei, J.; Stevens, E. D.; Scott, N. M.; Nolan, S. P. *J. Am. Chem. Soc.* **2006**, *128*, 4101–4111.
- (58) Chartoire, A.; Frogneux, X.; Boreux, A.; Slawin, A. M. Z.; Nolan, S. P. *Organometallics* **2012**, *31*, 6947–6951.
- (59) Meiries, S.; Chartoire, A.; Slawin, A. M. Z.; Nolan, S. P. *Organometallics* **2012**, *31*, 3402–3409.
- (60) Meiries, S.; Le Duc, G.; Chartoire, A.; Collado, A.; Speck, K.; Athukorala Arachchige, K. S.; Slawin, A. M. Z.; Nolan, S. P. *Chemistry* **2013**, *19*, 17358–17368.
- (61) Bastug, G.; Nolan, S. P. *Organometallics* **2014**, *33*, 1253–1258.
- (62) Zinser, C. M.; Nahra, F.; Brill, M.; Meadows, R. E.; Cordes, D. B.; Slawin, A. M. Z.; Nolan, S. P.; Cazin, C. S. J. *Chem. Commun.* **2017**, *53*, 7990–7993.
- (63) Marelli, E.; Chartoire, A.; Le Duc, G.; Nolan, S. P. *ChemCatChem* **2015**, *7*, 4021–4024.
- (64) Bastug, G.; Nolan, S. P. *Organometallics* **2014**, *33*, 1253–1258.
- (65) Slater, C. S.; Savelski, M. *J. Environ. Sci. Heal. Part A* **2007**, *42*, 1595–1605.
- (66) Henderson, R. K.; Jiménez-González, C.; Constable, D. J. C.; Alston, S. R.; Inglis, G. G. a.; Fisher, G.; Sherwood, J.; Binks, S. P.; Curzons, A. D. *Green Chem.* **2011**, *13*, 854–862.
- (67) Watanabe, K.; Yamagiwa, N.; Torisawa, Y. *Org. Process Res. Dev.* **2007**, *11*, 251–258.
- (68) Zhang, Y.; Lavigne, G.; César, V. *J. Org. Chem.* **2015**, *80*, 7666–7673.
- (69) Brusoe, A. T.; Hartwig, J. F. *J. Am. Chem. Soc.* **2015**, *137*, 8460–8468.
- (70) Ge, S.; Green, R. A.; Hartwig, J. F. *J. Am. Chem. Soc.* **2014**, *136*, 1617–1627.
- (71) Martel-Frchet, V.; Kadri, M.; Boumendjel, A.; Ronot, X. *Bioorganic Med. Chem.* **2011**, *19*, 6143–6148.
- (72) Johansson, C. C. C.; Colacot, T. J. *Angew. Chem. Int. Ed.* **2010**, *49*, 676–707.
- (73) Edmondson, S.; Danishefsky, S. J.; Sepp-Lorenzino, L.; Rosen, N. *J. Am. Chem. Soc.* **1999**, *121*, 2147–2155.
- (74) Goehring, R. R.; Sachdeva, Y. P.; Pisipati, J. S.; Sleevi, M. C.; Wolfe, J. F. *J. Am. Chem. Soc.*

- 1985**, *107*, 435–443.
- (75) Hamann, B. C.; Hartwig, J. F. *J. Am. Chem. Soc.* **1997**, *119*, 12382–12383.
- (76) Tetsuya, S.; Kawamura, Y.; Miura, M.; Nomura, M. *Angew. Chem. Int. Ed.* **1997**, *36*, 1740–1742.
- (77) Old, D. W.; Wolfe, J. P.; Buchwald, S. L. *J. Am. Chem. Soc.* **1998**, *120*, 9722–9723.
- (78) Fox, J. M.; Huang, X.; Chieffi, A.; Buchwald, S. L. *J. Am. Chem. Soc.* **2000**, *122*, 1360–1370.
- (79) Viciu, M. S.; Germaneau, R. F.; Navarro-Fernandez, O.; Stevens, E. D.; Nolan, S. P. *Organometallics* **2002**, *21*, 5470–5472.
- (80) Viciu, M. S.; Iii, R. a K.; Stevens, E. D.; Studer, M.; Nolan, S. P. *Org. Lett.* **2003**, *5*, 1479–1482.
- (81) Navarro, O.; Marion, N.; Oonishi, Y.; Kelly, R. A.; Nolan, S. P. *J. Org. Chem.* **2006**, *71*, 685–692.
- (82) Navarro, O.; Marion, N.; Scott, N. M.; González, J.; Amoroso, D.; Bell, A.; Nolan, S. P. *Tetrahedron* **2005**, *61*, 9716–9722.
- (83) Marelli, E.; Corpet, M.; Davies, S. R.; Nolan, S. P. *Chem. Eur. J.* **2014**, *20*, 17272–17276.

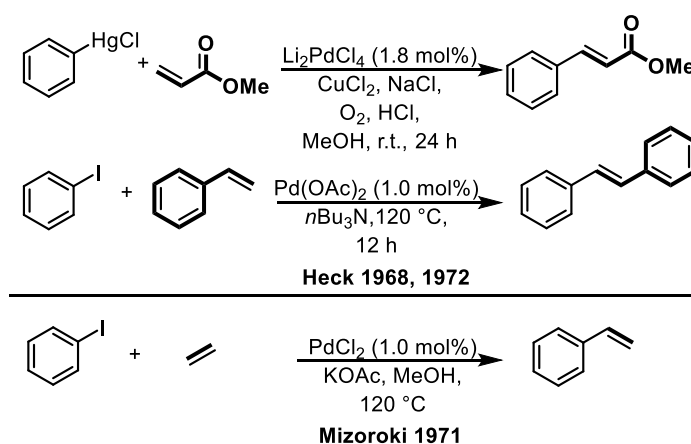
Chapter 5

Study of different throw-away ligands of $[NHC\cdot H][Pd(L)Cl_2]$ complexes and their effect in the Mizoroki-Heck reaction

5.1 Mizoroki-Heck reaction

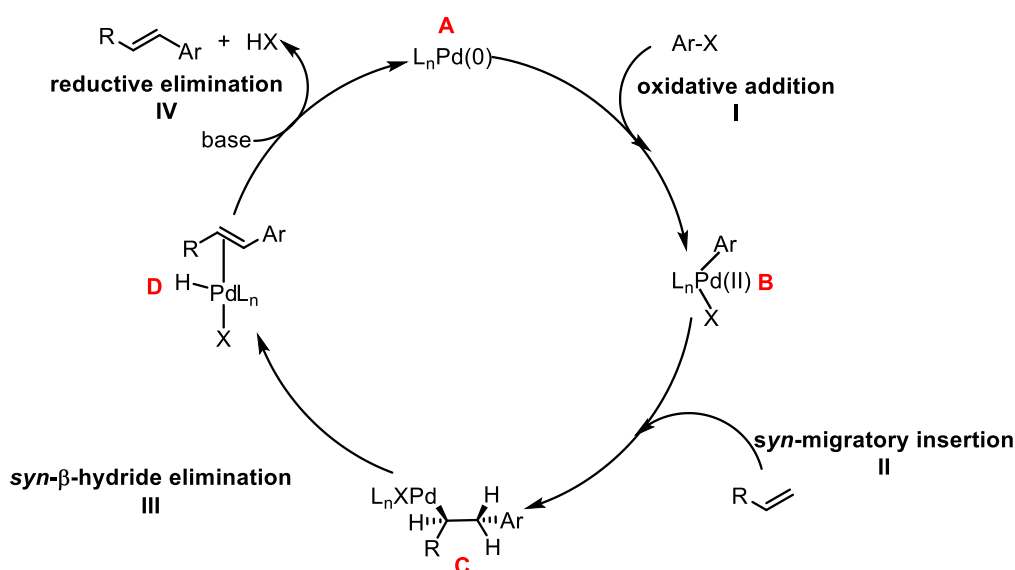
Cross-coupling reactions have been demonstrated as effective methods for carbon-carbon bond formation. Despite this there is a need for more active catalysts, which can operate under milder conditions. The Mizoroki-Heck reaction is a very useful synthetic tool widely used in medicinal,^{1,2} fine-chemical,³ natural product⁴ and polymer chemistry.⁵ The direct cross-coupling of an alkene and aryl/alkyl halide allows rapid access to important intermediates for the synthesis of drug molecules and natural products. Jiang and co-workers illustrated this with the synthesis of a retinoid x receptor antagonist, diazepinylbenzoic acid, which employed a Mizoroki-Heck coupling as a key step in the synthetic route.⁶ Initial reports required high temperatures, phase-transfer additives and toxic solvents. The use of palladium catalysts has improved the cross-coupling of alkenes significantly.

Mizoroki and Heck simultaneously reported the cross-coupling reaction between an alkene and an aryl halide using a palladium catalyst in the early 1970s (Scheme 5.1).^{7,8} The first report by Mizoroki and co-workers in 1971 described the cross-coupling of ethylene and iodobenzene using catalytic amounts of Pd(II).⁷ The reaction needed a slight excess of base in order to achieve high yields. Heck's first report described the alkene arylation coupling an aryl mercury halide with an alkene using a lithium palladium chloride catalyst (Scheme 5.1).⁹⁻¹⁵



Scheme 5.1: Early example of the Mizoroki-Heck reaction.^{7,8,12}

The general catalytic cycle was proposed in 1972.⁸ The reaction proceeds via oxidative addition (Scheme 5.2,I) between the active Pd(0) and aryl halide to form Pd(II)ArX (Scheme 5.2,B). This is followed by the *syn* insertion of the alkene, resulting in a α -alkyl Pd(II) halide (Scheme 5.2;II). This step is also referred to as carbopalladation. If necessary a bond rotation occurs as a β hydrogen in a *syn* position relative to the palladium is needed. As the next step is the *syn*- β -hydride elimination, which gives the hydropalladium(II) halide ligated to the arylated alkene (Scheme 5.2;III). The dissociation of the new arylated alkene and the reductive elimination of the hydropalladium(II) halide to the Pd(0) species is closing the cycle (Scheme 5.2;IV).

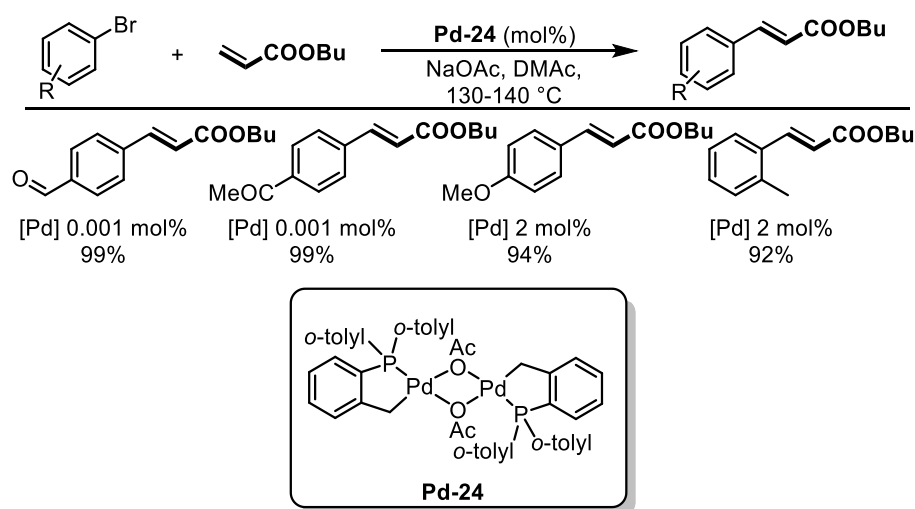


Scheme 5.2: Catalytic cycle of the Mizoroki-Heck reaction.⁸

Over the years significant improvements have been made in the reaction conditions and widening the substrate scope.¹⁶ Due to the enormous amount of research in this field, only an overview of the most relevant examples will be given.

The first examples reported by Heck all operated as *in situ* systems, consisting of bulky phosphine ligands such as PPh_3 or $P(o\text{-tolyl})_3$ and $Pd(PPh_3)_2(OAc)_2$ or $Pd(OAc)_2$.¹⁷ Herrmann and Beller reported the use of **Pd-24** in the Mizoroki-Heck reaction (Scheme 5.3).^{18,19} The pre-catalyst was synthesised efficiently from $Pd(OAc)_2$ and *ortho*-methyl substituted aryl phosphines. Several aryl bromides were successfully coupled with *n*-butyl acrylate in the presence of sodium acetate. For activated aryl bromides the reaction proceeded at low catalyst loadings although high reaction temperatures were needed. Compared to aryl bromides, some examples of aryl chlorides were reported, but the yield and TON dropped significantly compared to aryl

bromides. Following these initial results, several groups investigated the use of palladacycles in the Mizoroki-Heck reaction, such as Shaw,²⁰ Mason²¹ and Bedford.²²



Scheme 5.3: Mizoroki-Heck reaction using **Pd-24**.^{18,19}

Different PCP pincer ligands were reported for the Mizoroki-Heck reactions.²³ Pincer ligands are chelators which bind to three adjacent sites on a metal centre, a PCP ligand possesses a central carbon with two phosphine *ortho* to it for binding.²⁴ The PCP complex reported by Milstein and co-workers showed high catalytic activity for aryl iodides and aryl bromides as coupling substrates (Figure 5.1).²³ Unfortunately for all systems harsh conditions, such as high reaction temperature, were needed.^{23,25}

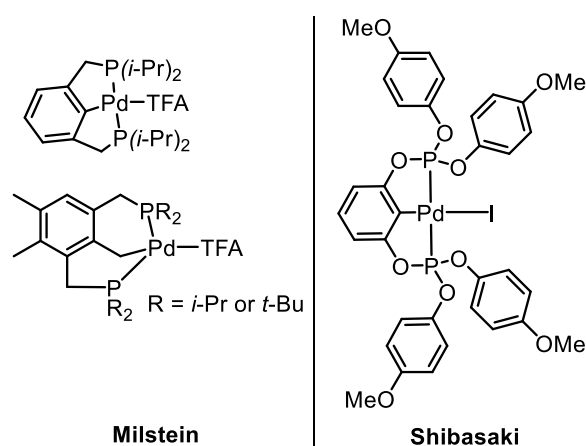


Figure 5.1: Examples of PCP ligands used in the Mizoroki-Heck reaction.^{23,25}

Herrmann and co-workers reported the synthesis of air and moisture stable NHC-Pd(II) pre-catalysts, **Pd-25** and **Pd-26** which they tested in the Mizoroki-Heck reaction (Figure 5.2).²⁶ These complexes showed high thermal stability as well as high catalytic activity, successfully coupling

a range of aryl bromides and activated aryl chlorides using low catalyst loadings (0.5 mol%). The use of bulkier, electron-donating ligands enabled the use of aryl chlorides in the Mizoroki-Heck reaction.²⁶

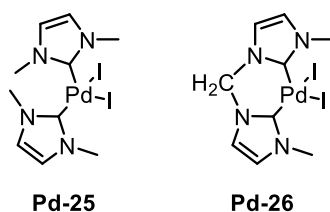
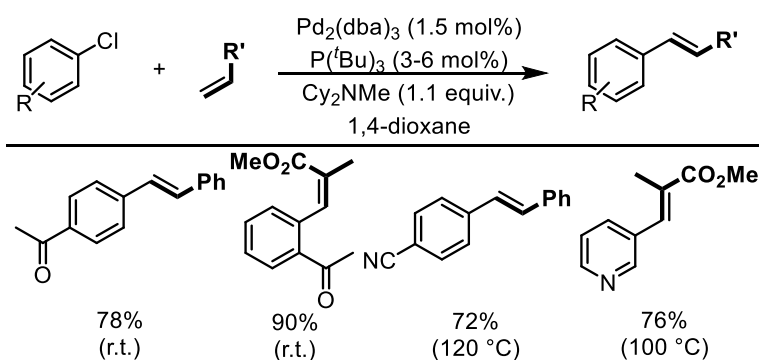


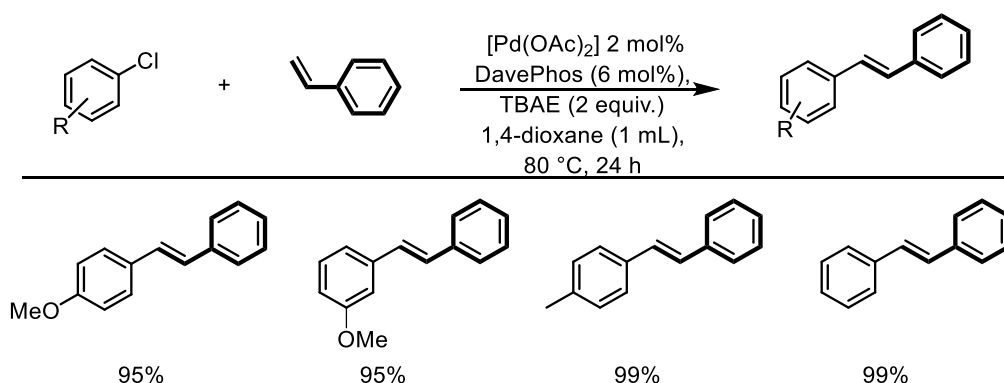
Figure 5.2: Pd-NHC pre-catalysts, **Pd-25** and **Pd-26** used in the Mizoroki-Heck reaction.²⁶

Herrmann and co-workers then tested a range of different NHC-substituted phosphapalladacycles in the Mizoroki-Heck reaction.²⁷ The combination of the palladacycle with the electron-donicity of the NHC enabled the coupling of 4-chloroacetophenone with styrene in high turnover number (TON).²⁷ Fu and co-workers demonstrated on the use of $P(tBu)_3$ and PCy_3 in the Mizoroki-Heck reaction, which enabled them to successfully couple aryl chlorides using Cs_2CO_3 as base, although the reaction temperature was still high (100 °C).²⁸ The reaction conditions were further investigated by Fu and co-workers, in order to lower the reaction temperature. Simply swapping the base to Cy_2NMe allowed the authors to couple activated aryl chlorides with alkenes (Scheme 5.4).²⁹ Unfortunately unactivated aryl chlorides again needed high reaction temperatures (100-120 °C).²⁹



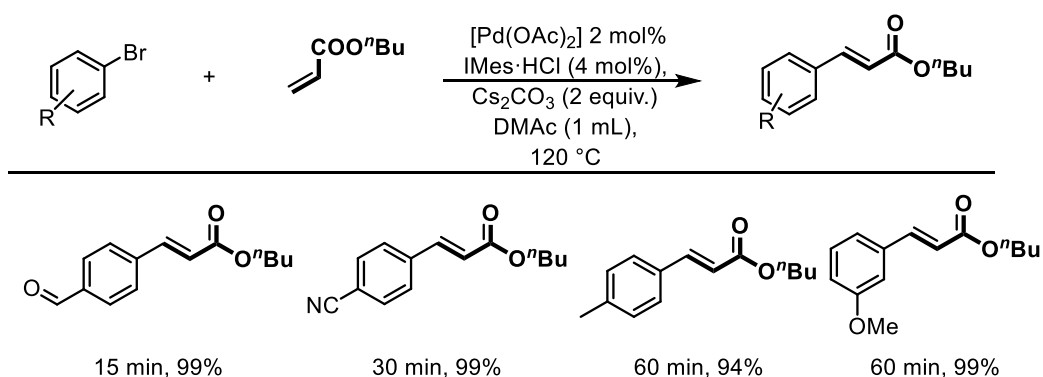
Careful selection of ligand and base by Xu and co-workers facilitated a reduction in the reaction temperature for unactivated aryl chlorides.³⁰ Electron-rich DavePhos (2-dicyclohexylphosphine-2'-(*N,N*-dimethylamino)biphenyl) was chosen as ligand in combination with $Pd(OAc)_2$, and the use of an organic ionic base, TBAE (2-(*tert*-butylamino)ethanol), was reasoned to be an

important factor.³⁰ Unactivated aryl chlorides were successfully coupled at 80 °C in 1,4-dioxane (Scheme 5.5).



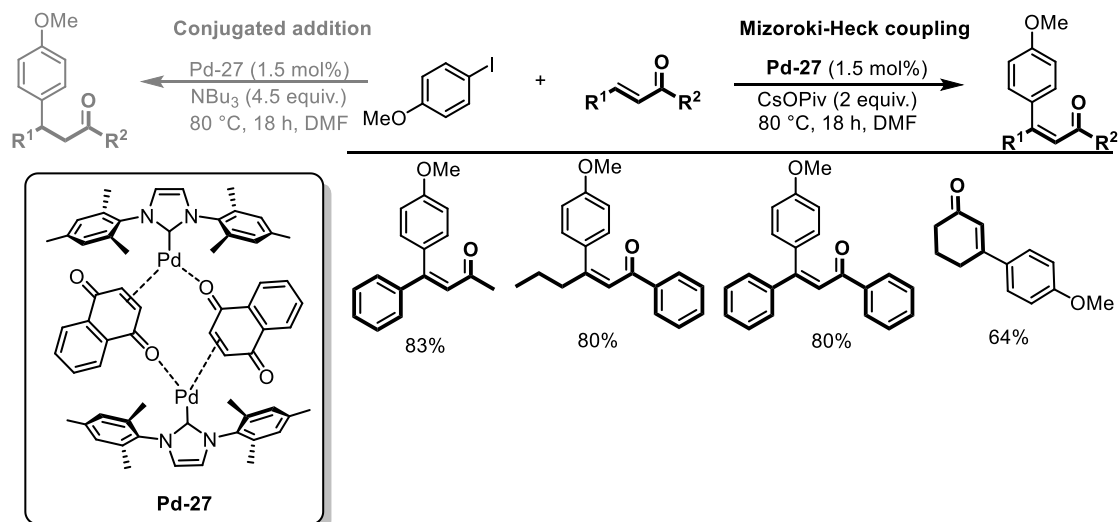
Scheme 5.5: Coupling of unactivated aryl chlorides using Pd(OAc)₂ and DavePhos.³⁰

Nolan and co-workers reported an *in situ* system consisting of Pd(OAc)₂ and IMes·HCl (*N,N'*-bis-[2,4,6-(trimethyl)phenyl]imidazol-2-ylidene).³¹ The coupling of different aryl bromides with *n*-butyl acrylate was reported in short reaction time. 4-Bromobenzaldehyde was coupled with *n*-butyl acrylate in 99% yield in just 15 min (Scheme 5.6).³¹



Scheme 5.6: The coupling of *n*-butyl acrylate with different aryl bromides using an *in situ* system of [Pd(OAc)₂] and IMes·HCl.³¹

The use of a Pd(0)-NHC complex in the Mizoroki-Heck reaction was reported by de Vries and Minnaard, coupling 4-iodoanisole with a variation of different Michael acceptors (Scheme 5.7).³² As the Pd(0)-NHC complex is a well-defined complex, the Pd:ligand ratio is 1:1, eliminating the need for excess ligand. CsOPiv was used as base at 80 °C in dimethylformamide (DMF). Interestingly by switching the base to NBU₃, a conjugated addition of the aryl halide with the Michael acceptor was observed (Scheme 5.7).³²



Scheme 5.7: The use of a Pd(0)-NHC catalyst in the Mizoroki-Heck reaction.³²

Using the same NHC ligand, Ying and Kantchev reported a cyclopalladated complex (**Pd-28**) with *N,N*-dimethylbenzylamine and IMes (IMes = *N,N'*-bis-(2,4,6-trimethylphenyl)imidazol-2-ylidene) as ligands, it is easily accessed by a one-pot reaction of *N,N*-dimethylbenzylamine, $PdCl_2$ and IMes·HCl (Figure 5.3).³³ Unlike the Pd(0)-NHC mentioned before, this complex and catalyst is air and moisture stable. This eases not only the procedure for catalysis but also the handling and storage of the pre-catalyst. Very low catalyst loading was needed, ranging from 10 ppm to 2 mol%. Mild inorganic bases such as carbonate bases (K_2CO_3) were used for most substrates. A wide scope was established coupling aryl bromides, iodides and triflates with a range of different acrylate derivatives (nitrile, *tert*-butyl ester and amides) as well as styrene derivatives.³³ A *para*-pyridine linked NHC palladium complex (**Pd-29**) was reported by Sun and Ong, coupling fused polyaromatic bromides with styrene (Figure 5.3).³⁴ The resulting cross-coupling products are used in optoelectronic chemistry and devices. Low catalyst loading was needed (0.1 mol%) with a mild inorganic base resulting in moderate to high yield.³⁴

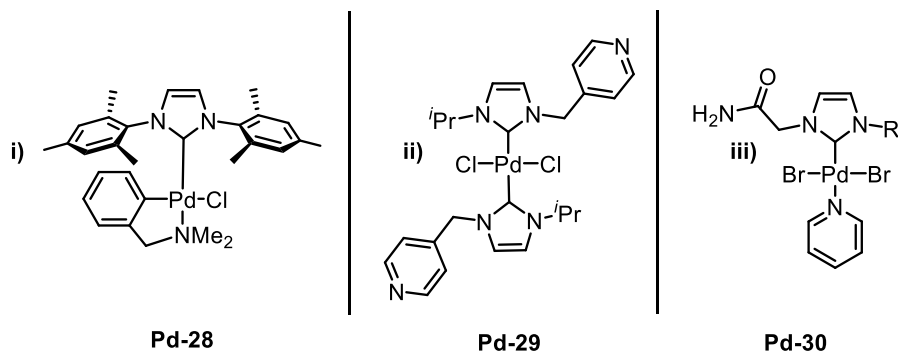
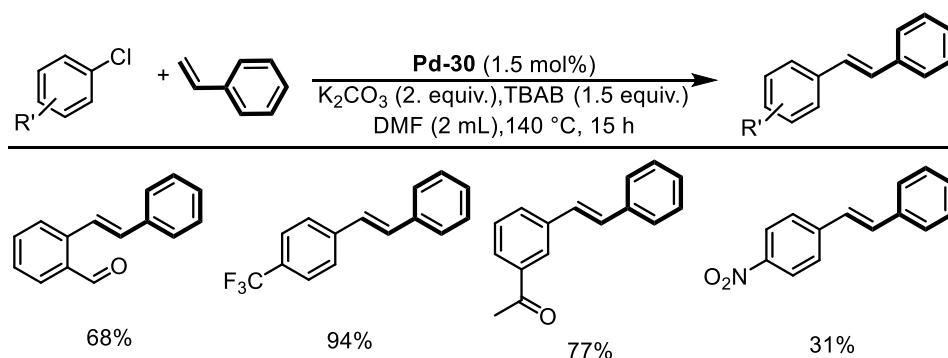


Figure 5.3: Pd-NHC complexes by Kantchev and Ying (i)³³, Sun and Ong (ii)³⁴ and Liu and Lin (iii).³⁵

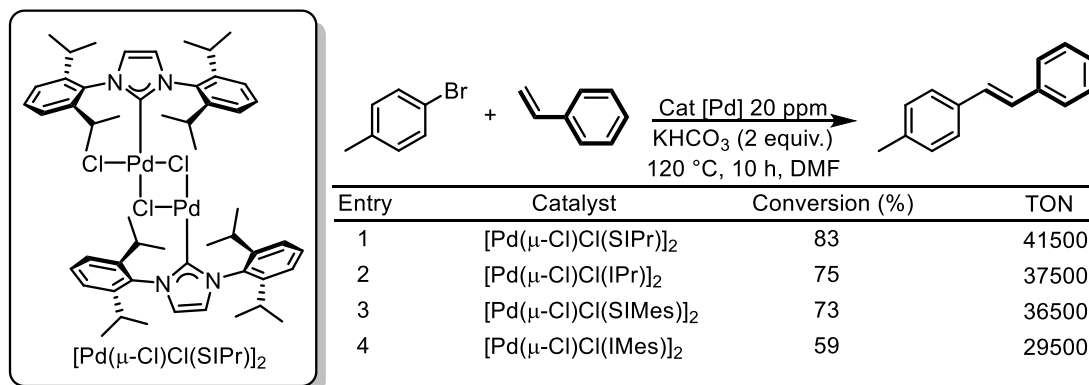
$[PdBr_2(NHC)PEPPSI]$, **Pd-30** (Figure 5.3, iii) was used for the coupling of aryl chlorides with styrene in DMF (Scheme 5.8).³⁵ K_2CO_3 was used as a base in combination with a phase transfer reagent, tetrabutylammonium bromide (TBAB). Moderate to good yields were obtained but high temperatures (140 °C) were needed, as well as a reaction time of 15 hours. Interestingly the formation of nanoparticles was observed and proven by using dynamic light scattering, transmission electron microscopy and the mercury poisoning test.³⁵ It was postulated that these nanoparticles can influence the catalytic reaction, it was not specified if this was hindering or aiding the Mizoroki-Heck reaction.³⁵



Scheme 5.8: Pd-30 as pre-catalyst for the coupling of aryl chlorides in the Mizoroki-Heck reaction.³⁵

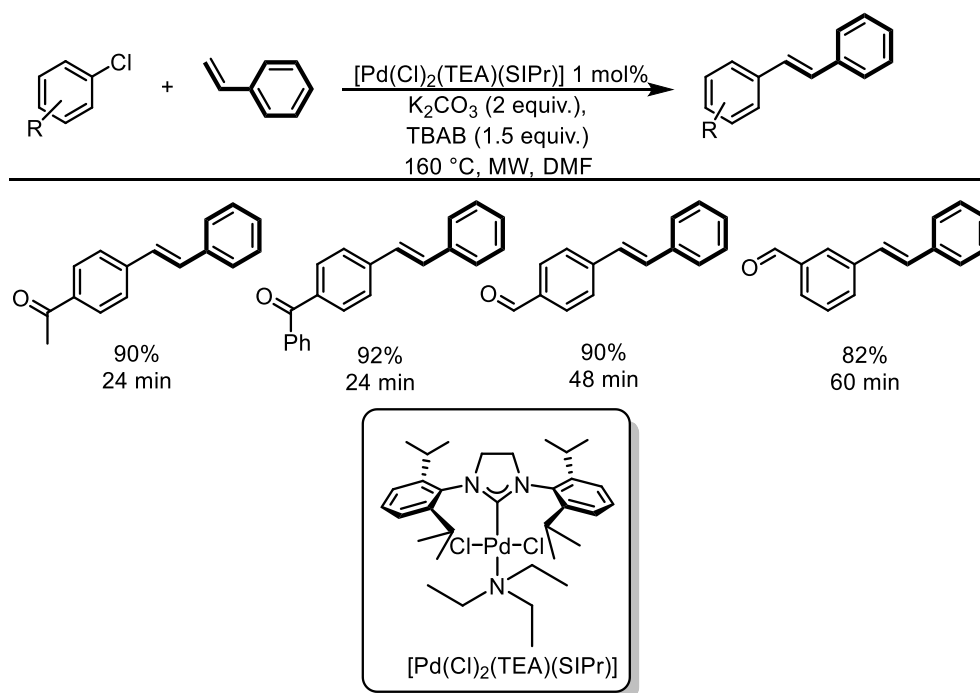
The $[Pd(\mu-Cl)Cl(NHC)]_2$ complexes from Cazin, introduced in Chapter 3, were also successfully tested in the Mizoroki-Heck reaction.³⁶ Four different pre-catalysts were initially tested with very low catalyst loading (20 ppm) (Scheme 5.9). 4-Bromotoluene and styrene were coupled in good yield using two equivalents of $KHCO_3$ in DMF at 120 °C. The most active pre-catalyst was $[Pd(\mu-Cl)Cl(SiPr)]_2$, which coupled a range of activated, deactivated and sterically hindered aryl

bromides with styrene.³⁶ Examples included, heteroaromatic substrates such as 3-bromopyridine and 3-bromoquinoline, which were coupled with styrene in good to excellent yield. The catalyst loading was increased to 200 ppm, which still represented a very low catalyst loading in comparison with previous reports, but the reaction temperature was increased to 140 °C.³⁶



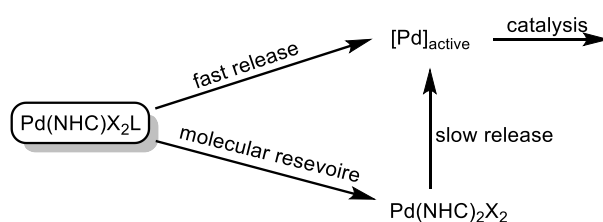
Scheme 5.9: The use of $[Pd(\mu\text{-Cl})Cl(NHC)]_2$ complexes in the Mizoroki-Heck reaction.³⁶

Navarro and co-workers carried out a Mizoroki-Heck reaction with $[Pd(Cl)_2(TEA)(SIPr)]$ using microwave radiation in order to reduce the reaction time as much as possible (Scheme 5.10).³⁷ The investigation firstly focused on the coupling of aryl bromides and chlorides to styrene. The optimal conditions for the case of aryl bromides required normal heating at 140 °C, 1 mol% catalyst loading and K_2CO_3 as base in combination with TBAB as phase-transfer reagent. The catalysis was carried out in air, demonstrating the stability of the catalyst and the robustness protocol. The scope was extended to aryl chlorides.³⁷ By applying microwave conditions a variety of different aryl chlorides were coupled in good to excellent yield as well as very short reaction time (12 min to 60 min).



Scheme 5.10: The use of microwave irradiation in the Mizoroki-Heck reaction.³⁷

The behaviour of NHC-M species in the presence of aliphatic amines was explored in a recent study from Ananikov and co-workers.³⁸ The activation of $Pd(II)(NHC)X_2L$ to $Pd(0)$ was studied and the effect in the Mizoroki-Heck reaction. Two transformations were proposed: (i) the formation of metal clusters or nanoparticles and azolium salt and (ii) the formation of bis NHC complexes, $M(NHC)_2X_2$ from $M(NHC)X_2L$ (Scheme 5.11). The formed metal species from (i) is a highly catalytic active $Pd(0)$ species which enters the catalytic cycle. The formed bis-NHC metal complex in transformation (ii) was described as a molecular reservoir, where the complex decomposed over time to release the active metal species. This was described as a dynamic catalytic system having a fast release of active species in combination with a slow release.³⁸



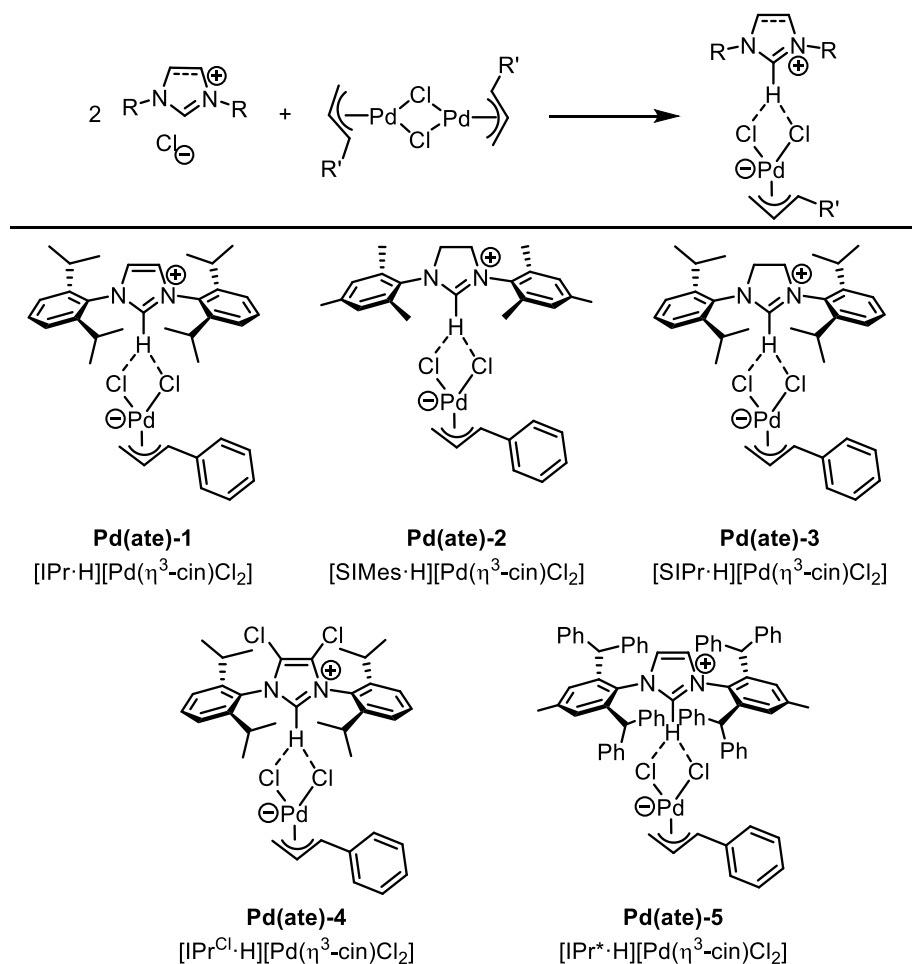
Scheme 5.11: Dynamic catalytic system, illustrating the fast and slow release of the active species.³⁸

Although the Mizoroki-Heck reaction is widely used in academia and industry the lack of mild reaction conditions and low catalyst loading in combination remains. We were interested if the

previously introduced palladate complexes could solve this problem. As mentioned in Chapter 3 and 4 these complexes are highly active pre-catalysts for several cross-coupling reactions, resulting in low catalyst loading and mild reaction conditions.

5.2 Results and discussion

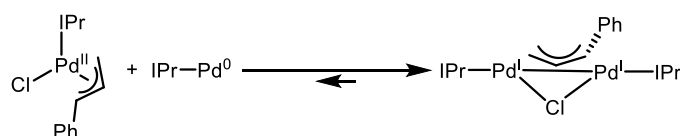
Based on the previously discussed positive results of $[\text{NHC}\cdot\text{H}][\text{Pd}(\eta^3\text{-R-allyl})\text{Cl}_2]$ complexes in the Suzuki-Miyaura, Buchwald-Hartwig and ketone arylation reactions, an investigation into the catalytic activity of $[\text{NHC}\cdot\text{H}][\text{Pd}(\eta^3\text{-R-allyl})\text{Cl}_2]$ in the Mizoroki-Heck reaction was undertaken. Previous reports highlight the importance of the electronic properties of the NHC ligand towards catalytic activity, thus $[\text{NHC}\cdot\text{H}][\text{Pd}(\eta^3\text{-R-allyl})\text{Cl}_2]$ complexes bearing NHC ligands with different steric and electronic properties were synthesised. In total five different NHC ligands were used in the $[\text{NHC}\cdot\text{H}][\text{Pd}(\eta^3\text{-cin})\text{Cl}_2]$ skeleton (Scheme 5.12).



Scheme 5.12: $[\text{NHC}\cdot\text{H}][\text{Pd}(\eta^3\text{-R-allyl})\text{Cl}_2]$ complexes bearing five different NHC ligands used in this study.

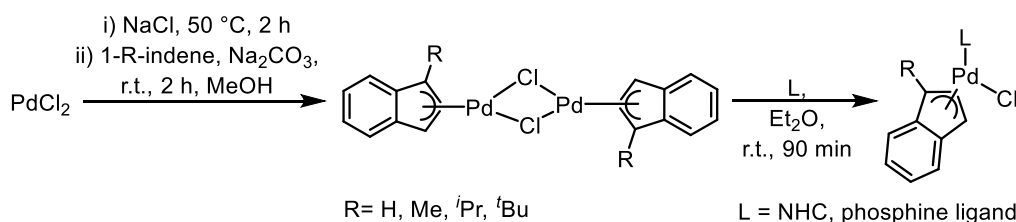
The effect of the substitution of the allyl ligand is known to be an important factor in the activation step of the pre-catalyst to the active species in cross-coupling reactions. It was postulated by Nolan and co-workers that the substitution on the allyl moiety can decrease the stability of the palladium complex.³⁹ This can be due to the steric bulk around the palladium centre and by decreasing the back-bonding from the palladium to the alkene. Furthermore if the allyl moiety is less tightly bound to the palladium, it will be more prone to nucleophilic attack or reductive elimination, depending which activation pathway is considered.⁴⁰

Hazari and co-workers studied the activation of $[PdCl(\eta^3\text{-R-allyl})(NHC)]$ complexes and the effect of the substitution of the allyl ligand, experimentally and computationally.⁴¹ The activation pathway found featured a comproportionation step of $[PdCl(\eta^3\text{-R-allyl})(NHC)]$ and $I\text{Pr-Pd}(0)$, which resulted in the dimer formation, $[Pd_2(\mu\text{-Cl})(I\text{Pr})_2(\text{allyl})]$ (Scheme 5.13). It is postulated that these dimer complexes are present during the catalysis and decreased the amount of the active species $I\text{Pr-Pd}(0)$.⁴¹ Further studies into this pathway reveal that steric bulk on the 1-position of the allyl ligand, such as crotyl and cinnamyl can increase the kinetic barrier to comproportionation and therefore hinder the dimer formation.⁴¹



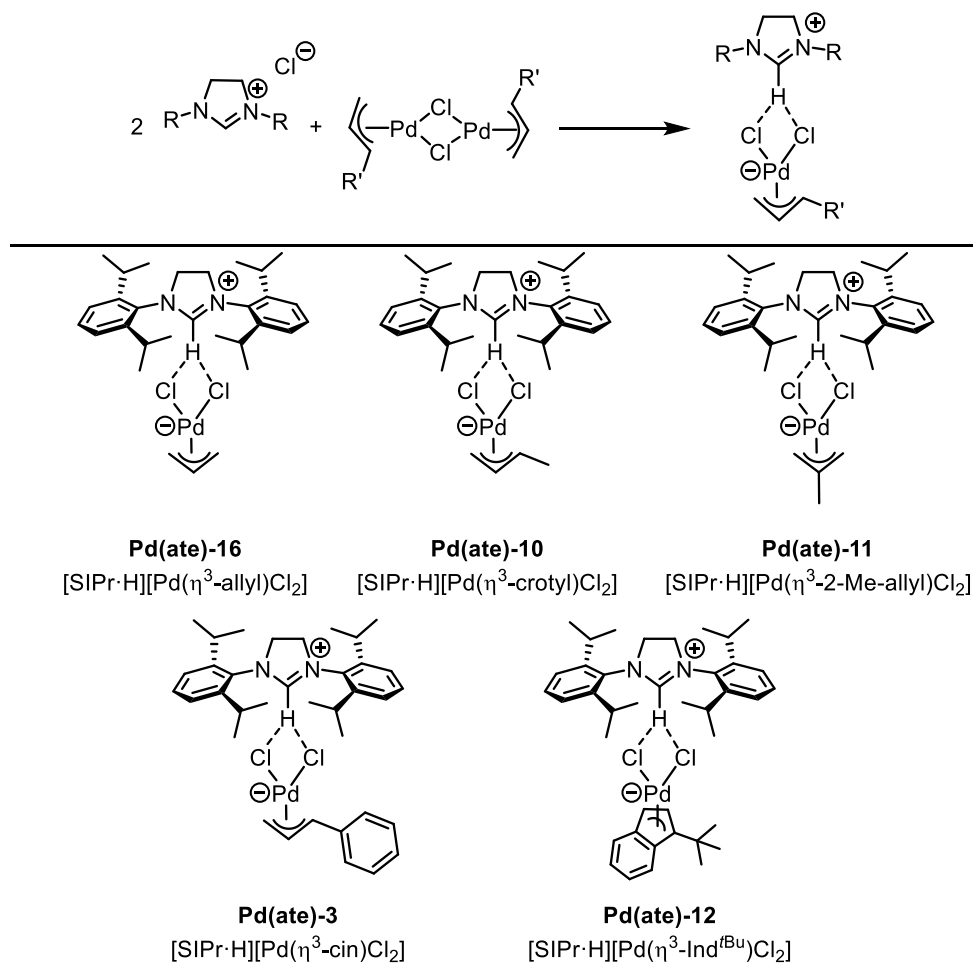
Scheme 5.13: Comproportionation of $[PdCl(\eta^3\text{-R-allyl})(I\text{Pr})]$ and $I\text{Pr-Pd}(0)$.⁴¹

Further investigations focused on the substituent on the 2-position of the allyl ligand, and its role in catalysis.⁴² A detailed study was carried out using different substituents on the 2-position.⁴² Interestingly it was postulated that the speed of activation of $Pd(II)$ is not solely responsible for the catalytic activity. Moreover the stability of the $Pd(I)$ dimer is of importance. A $Pd(II)$ pre-catalyst that forms a thermodynamically destabilised $Pd(I)$ dimer is more catalytically active than a $Pd(II)$ pre-catalyst that forms a thermodynamically stabilised $Pd(I)$ dimer.⁴² Hazari and co-workers used the newly acquired knowledge to develop a pre-catalyst scaffold, namely $[Pd(\eta^3\text{-1-}^t\text{Bu-indenyl})(\mu\text{-Cl})_2]$ (Scheme 15.14).⁴³



Scheme 5.14: Synthesis of $[Pd(\eta^3\text{-1-}^t\text{Bu-indenyl})(\mu\text{-Cl})_2]$ and $[PdCl(\eta^3\text{-1-}^t\text{Bu-indenyl})(L)]$.⁴³

The new Pd dimer is compatible with NHC ligands as well as with phosphine ligands.⁴³ The absence of the Pd(I) dimer formation is reasoned to be responsible for its high catalytic activity. Pre-catalysts bearing the η^3 -1-*t*Bu-indenyl ligand were tested in the Suzuki-Miyaura and Buchwald-Hartwig amination reactions and gave high catalytic activity.⁴⁴ With this in mind, different ancillary ligands were tested in the palladate scaffold: $[Pd(\eta^3\text{-allyl})(\mu\text{-Cl})_2]$, $[Pd(\eta^3\text{-crotyl})(\mu\text{-Cl})_2]$, $[Pd(\eta^3\text{-2-Me-allyl})(\mu\text{-Cl})_2]$, $[Pd(\eta^3\text{-cin})(\mu\text{-Cl})_2]$ and $[Pd(\eta^3\text{-1-}t\text{Bu-indenyl})(\mu\text{-Cl})_2]$ (Scheme 5.15).

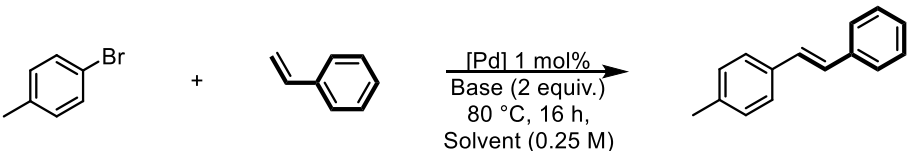


Scheme 5.15: $[NHC\cdot H][Pd(\eta^3\text{-R-allyl})Cl_2]$ pre-catalysts bearing different ancillary ligands on the palladium.

The catalytic investigation was started using 4-bromotoluene (0.5 mmol) and styrene (1.5 equiv.) as model substrates. Initial cross experiments were conducted using seven different palladate pre-catalysts, namely $[SiMes\cdot H][Pd(\eta^3\text{-cin})Cl_2]$ **Pd(ate)-2** (SiMes = *N,N'*-bis-(2,4,6-trimethylphenyl)imidazolidin-2-ylidene), $[SIPr\cdot H][Pd(\eta^3\text{-cin})Cl_2]$ **Pd(ate)-3** (SIPr = *N,N'*-bis-[2,6-(di-*iso*-propyl)phenyl]imidazolidin-2-ylidene), $[IPr^Cl\cdot H][Pd(\eta^3\text{-cin})Cl_2]$ **Pd(ate)-4** (IPr^Cl = *N,N'*-bis-

[2,6-(di-*iso*-propyl)phenyl-4,5-dichloro]imidazol-2-ylidene), $[IPr^*\cdot H][Pd(\eta^3\text{-cin})Cl_2]$ **Pd(ate)-5** ($IPr^* = N,N'$ -bis-[2,6-bis(diphenylmethyl)-4-methylphenyl]imidazol-2-ylidene), $[SIPr\cdot H][Pd(\eta^3\text{-crotyl})Cl_2]$ **Pd(ate)-10**, $[SIPr\cdot H][Pd(\eta^3\text{-2-Me-allyl})Cl_2]$ **Pd(ate)-11** and $[SIPr\cdot H][Pd(\eta^3\text{-Ind}^{tBu})Cl_2]$ **Pd(ate)-12**, plus **Pd(ate)-3** with TBAB as additive. Furthermore four commonly used inorganic bases were selected; K_2CO_3 , K_3PO_4 , KOH and KO^tBu in combination with three different solvents; *n*-BuOH, Me-THF and toluene (Table 5.1).

Table 5.1: Initial studies for the Mizoroki-Heck reaction



Pre-catalysts	Bases	Solvents
$[SiMes\cdot H][Pd(\eta^3\text{-cin})Cl_2]$	K_2CO_3	<i>n</i> -butanol
$[IPr^{Cl}\cdot H][Pd(\eta^3\text{-cin})Cl_2]$	K_3PO_4	2-methyl tetrahydrofuran
$[SIPr\cdot H][Pd(\eta^3\text{-cin})Cl_2]$	KOH	toluene
$[IPr^*\cdot H][Pd(\eta^3\text{-cin})Cl_2]$	KO^tBu	
$[SIPr\cdot H][Pd(\eta^3\text{-crotyl})Cl_2]$		
$[SIPr\cdot H][Pd(\eta^3\text{-2-Me-allyl})Cl_2]$		
$[SIPr\cdot H][Pd(\eta^3\text{-Ind}^{tBu})Cl_2]$		

Reaction conditions: In the glovebox, a vial was charged with the pre-catalyst, base (2 equiv.), solvent (0.25 M) and a magnetic stir bar and sealed with a screw cap. 4-bromotoluene (0.5 mmol) was added followed by styrene (1.5 equiv.). The reaction was left to stir (910 rpm) for 16 h at 80 °C. Average of two runs, mesitylene (0.01 mmol) was used as internal standard.

The resulting 96 experiments helped to gain insight into the most ideal reaction conditions (See Chapter 9.5.5.3, Table S-36). Interestingly for the Mizoroki-Heck reaction, the activation step, which was essential for the Suzuki-Miyaura (Chapter 3) and Buchwald-Hartwig amination reactions (Chapter 4) is not needed. 1H NMR experiments showed no reaction between the palladate and the styrene in solution. This means the activation of the palladate pre-catalyst can occur in the presence of the coupling substrates, without the coupling substrates interfering.

The best pre-catalysts from this study were identified as **Pd(ate)-10**, **Pd(ate)-11** and **Pd(ate)-12**. Crystal structures of these complexes were obtained from single-crystal x-ray diffraction and as discussed in Chapter 2, these three palladate complexes showed similar configuration in space.



Figure 5.4: Single crystal structure of **Pd(ate)-10** (left) and **Pd(ate)-11** (right)

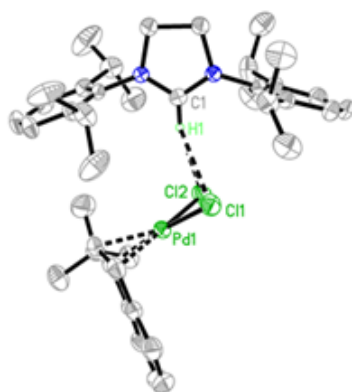
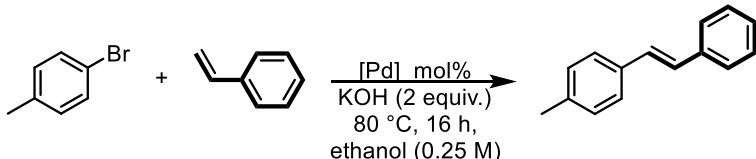


Figure 5.5: Single crystal of **Pd(ate)-12**

In the conditions screened, the best conversions were obtained in alcohol solvent in combination with carbonate and hydroxide bases. A second set of experiments were set up using the three best palladates, four different alcohol solvents: *iso*-propanol, 2-butanol, ethanol and 2-methyl-butan-2-ol, four different carbonate bases: K_2CO_3 , $KHCO_3$, Cs_2CO_3 , Na_2CO_3 , and four different hydroxide bases: $LiOH\cdot H_2O$, $NaOH$, KOH and $KOAc$. The resulting 96 experiments (See Chapter 9.5.5.3, Table S-37) gave very promising results, illustrating the high catalytic activity of the palladate pre-catalyst in the Mizoroki-Heck reaction, as most experiments resulted in high or full conversion (>90%). Unfortunately most of the experiments showed homo-coupling of the aryl bromide by gas chromatography analysis.

Before continuing the base/solvent optimisation, the ideal pre-catalyst was determined (Table 5.2). The three pre-catalysts gave full conversion when KOH in ethanol was used, therefore these conditions were used, and the catalyst loading was gradually dropped (Table 5.2). Four different catalyst loadings were tested and $[SIPr\cdot H][Pd(\eta^3\text{-}2\text{-Me-allyl})Cl_2]$ maintained excellent reactivity at 0.3 mol% .

Table 5.2: Optimisation of the catalyst loading.

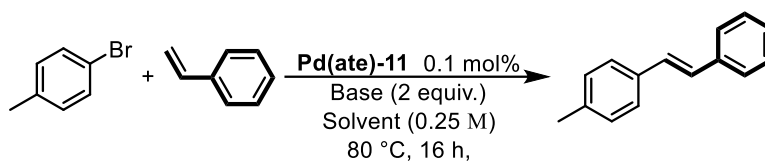


Entry	Pre-catalyst	Catalyst loading mol%	GC yield(%)
1	$[SiPr\cdot H][Pd(\eta^3\text{-2-Me-allyl})Cl_2]$	1	99
2	$[SiPr\cdot H][Pd(\eta^3\text{-crotyl})Cl_2]$	1	99
3	$[SiPr\cdot H][Pd(\eta^3\text{-Ind}^{tBu})Cl_2]$	1	99
4	$[SiPr\cdot H][Pd(\eta^3\text{-2-Me-allyl})Cl_2]$	0.5	99
5	$[SiPr\cdot H][Pd(\eta^3\text{-crotyl})Cl_2]$	0.5	99
6	$[SiPr\cdot H][Pd(\eta^3\text{-Ind}^{tBu})Cl_2]$	0.5	86
7	$[SiPr\cdot H][Pd(\eta^3\text{-2-Me-allyl})Cl_2]$	0.3	99
8	$[SiPr\cdot H][Pd(\eta^3\text{-crotyl})Cl_2]$	0.3	78
9	$[SiPr\cdot H][Pd(\eta^3\text{-Ind}^{tBu})Cl_2]$	0.3	86
10	$[SiPr\cdot H][Pd(\eta^3\text{-2-Me-allyl})Cl_2]$	0.1	45
11	$[SiPr\cdot H][Pd(\eta^3\text{-crotyl})Cl_2]$	0.1	35
12	$[SiPr\cdot H][Pd(\eta^3\text{-Ind}^{tBu})Cl_2]$	0.1	35

Reaction conditions: In air, a vial was charged with the pre-catalyst, KOH (2equiv.), ethanol (0.25 M) and a magnetic stir bar and sealed with a screw cap. 4-bromotoluene (0.5 mmol) was added followed by styrene (1.5 equiv.). The reaction was left to stir (910 rpm) for 16 h at 80 °C. Average of two runs, mesitylene (0.01 mmol) was used as internal standard.

With these preliminary conditions determined, an extensive optimisation was conducted. Firstly focusing on the optimal base and solvent combination. Four bases, K_2CO_3 , NaOH, KOH and Cs_2CO_3 were selected as all previously shown high conversions and no homo-coupling, in combination with *iso*-propanol, 1-butanol, ethanol and 2-methyl-but-2-ol (Table 5.3). Five base/solvent combinations showed high conversions; NaOH/1-butanol (Table 5.3, entry 6), KOH/*iso*-propanol (Table 5.3, entry 9), KOH/ ethanol (Table 5.3, entry 12), Cs_2CO_3 /*iso*-propanol and Cs_2CO_3 /1-butanol (Table 5.3, entry 14). The five entries were rerun decreasing the catalyst loading from 0.3 mol% to 0.1 mol%, revealing the best combination to be KOH/*iso*-propanol as full conversion was obtained, even at 0.1 mol%.

Table 5.3: Base/Solvent screening.

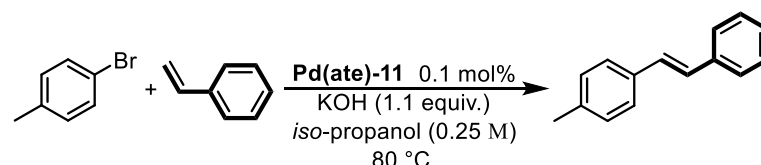


Entry	Base (2 equiv.)	Solvent (0.25 M)	GC yield(%)
1	K ₂ CO ₃	<i>iso</i> -propanol	n.r.
2	K ₂ CO ₃	1-butanol	n.r.
3	K ₂ CO ₃	2-methyl-but-2-ol	18
4	K ₂ CO ₃	ethanol	70
5	NaOH	<i>iso</i> -propanol	n.r.
6	NaOH	1-butanol	99
7	NaOH	2-methyl-but-2-ol	n.r.
8	NaOH	ethanol	74
9	KOH	<i>iso</i> -propanol	99
10	KOH	1-butanol	80
11	KOH	2-methyl-but-2-ol	80
12	KOH	ethanol	99
13	Cs ₂ CO ₃	<i>iso</i> -propanol	95
14	Cs ₂ CO ₃	1-butanol	90
15	Cs ₂ CO ₃	2-methyl-but-2-ol	37
16	Cs ₂ CO ₃	ethanol	70

Reaction conditions: In air, a vial was charged with the pre-catalyst, base (2 equiv.), solvent (0.25 M) and a magnetic stir bar and sealed with a screw cap. 4-bromotoluene (0.5 mmol) was added followed by styrene (1.5 equiv.). The reaction was left to stir (910 rpm) for 16 h at 80 °C. Average of two runs, mesitylene (0.01 mmol) was used as internal standard.

The optimal base equivalence was determined, being able to reduce the number of equivalents from 2 to 1.1 without any loss of reactivity. Next, the optimal stoichiometry of styrene was determined, being able to reduce the number of equivalents to 1.1 from the original 1.5. A time optimisation was conducted following the reaction over 5 hours (Table 5.4). After 4 hours the reaction reached full conversion.

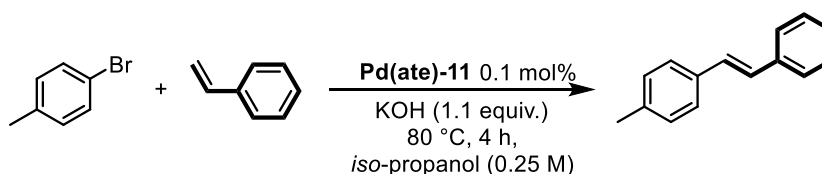
Table 5.4: Time optimisation



Entry	Time (min)	GC yield(%)
1	15	20
2	30	25
3	45	50
4	60	72
5	120	85
6	180	91
7	240	99
8	300	99

Reaction conditions: In air, a vial was charged with the **Pd(ate)-11**, KOH (1.1 equiv.), *iso*-propanol (0.25 M) and a magnetic stir bar and sealed with a screw cap. 4-bromotoluene (0.5 mmol) was added followed by styrene (1.1 equiv.). The reaction was left to stir (910 rpm) for the corresponding time at 80 °C. Average of two runs, mesitylene (0.01 mmol) was used as internal standard.

Lastly the reaction temperature was investigated. However, gradually lowering the reaction temperature resulted in loss of reactivity, therefore 80 °C was kept. The optimal conditions are shown in Scheme 5. 16.



Scheme 5.16: Optimised conditions for the Mizoroki-Heck reaction.

Noteworthy is the catalyst loading of **Pd(ate)-11** which could be lowered to 0.1 mol%, in combination with reaction temperature of 80 °C. Although very low catalyst loading and moderate reaction temperatures have been reported before, in combination it is rare. With the optimal conditions in hand the pre-catalyst was examined. The catalyst screening was divided in two parts. Firstly, a range of SIPr containing palladate complexes were tested, bearing different ancillary ligands. All five entries showed good to excellent conversion, although homo-coupling was observed in the GC spectrum using $[SIPr\cdot H][Pd(\eta^3\text{-crotyl})Cl_2]$ (Table 5.5; entry 3) and

$[\text{SIPr}\cdot\text{H}][\text{Pd}(\eta^3\text{-cin})\text{Cl}_2]$ (Table 5.5; entry 4). Therefore the best ancillary ligand was determined to be 2-Me-allyl.

Table 5.5: Catalyst screening; Part 1.

Entry	Pre-catalyst	GC conversion (%)
1	Pd(ate)-16	91
2	Pd(ate)-11	99
3	Pd(ate)-10	97*
4	Pd(ate)-3	97*
5	Pd(ate)-12	87

Pd(ate)-16
[SIPr·H][Pd(η^3 -allyl)Cl₂]

Pd(ate)-10
[SIPr·H][Pd(η^3 -crotyl)Cl₂]

Pd(ate)-11
[SIPr·H][Pd(η^3 -2-Me-allyl)Cl₂]

Pd(ate)-3
[SIPr·H][Pd(η^3 -cin)Cl₂]

Pd(ate)-12
[SIPr·H][Pd(η^3 -Ind^{tBu})Cl₂]

*Homocoupling was observed in the GC spectrum. Reaction conditions: In air, a vial was charged with the pre-catalyst (0.1 mol%), KOH (1.1 equiv.), *iso*-propanol (0.25 M) and a magnetic stir bar and sealed with a screw cap. 4-bromotoluene (0.5 mmol) was added followed by styrene (1.1 equiv.). The reaction was left to stir (910 rpm) for 4 h at 80 °C. Average of two runs, mesitylene (0.01 mmol) was used as internal standard.

The second part of the catalyst screening involved changing the NHC ligand on the palladate. Five NHC with varying electronic and steric properties were chosen and the corresponding palladates were synthesised. All pre-catalysts showed excellent reactivity in the Mizoroki-Heck reaction. Furthermore the previously chosen $[SiPr\cdot H][Pd(\eta^3\text{-2-Me-allyl})Cl_2]$ pre-catalyst shown to be the ideal choice (Table 5.6, entry 1).

Table 5.6: Catalyst screening; Part 2.

Entry	Pre-catalyst	GC conversion (%)
1	Pd(ate)-11	99
2	Pd(ate)-14	99*
3	Pd(ate)-18	97*
4	Pd(ate)-20	92
5	Pd(ate)-21	93

Pd(ate)-11
[SiPr·H][Pd(η^3 -2-Me-allyl)Cl₂]

Pd(ate)-18
[IPr·H][Pd(η^3 -2-Me-allyl)Cl₂]

Pd(ate)-14
[IPr*·H][Pd(η^3 -2-Me-allyl)Cl₂]

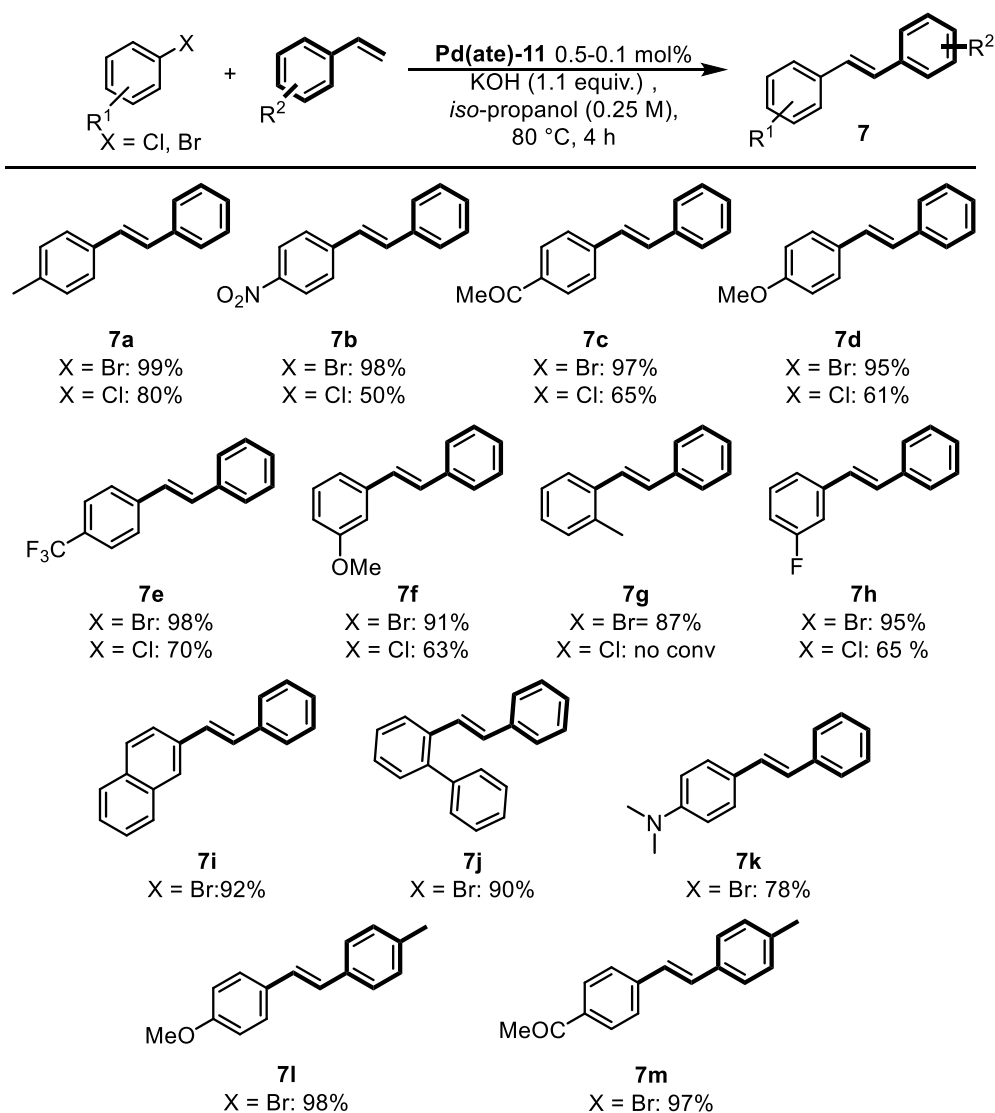
Pd(ate)-20
[IHept·H][Pd(η^3 -2-Me-allyl)Cl₂]

Pd(ate)-21
[IPent·H][Pd(η^3 -2-Me-allyl)Cl₂]

*Homocoupling was observed in the GC spectrum. Reaction conditions: In air, a vial was charged with the pre-catalyst (0.1 mol%), KOH (1.1 equiv.), *iso*-propanol (0.25 M) and a magnetic stir bar and sealed with a screw cap. 4-bromotoluene (0.5 mmol) was added followed by styrene (1.1 equiv.). The reaction was left to stir (910 rpm) for 4 h at 80 °C. Average of two runs, mesitylene (0.01 mmol) was used as internal standard.

The substrate scope was then explored. Firstly electronically different aryl bromides and chlorides were coupled with styrene. Excellent yields were obtained for the aryl bromide entries, independently of the electronic properties (Scheme 5.18, **7a-7e**).

The aryl chloride containing entries resulted in moderate to good yield, although the reactivity dropped drastically as soon as steric bulk was introduced as seen for 2-chlorotoluene (Scheme 5.17, **7g**). Pleasingly this was not the case for aryl bromides, where steric bulk was not an issue. 2-Bromotoluene (Scheme 5.17, **7g**), 3-bromoanisole (Scheme 5.17, **7f**) and 1-bromo-3-fluorobenzene (Scheme 5.17, **7h**) were all coupled to styrene in good to excellent yield. More bulky coupling substrates such as 2-bromonaphthalene and 2-bromobiphenyl were also coupled with styrene in excellent yield (Scheme 5.17, **7i,7j**). Considering the promising results, more challenging substrates were next considered.

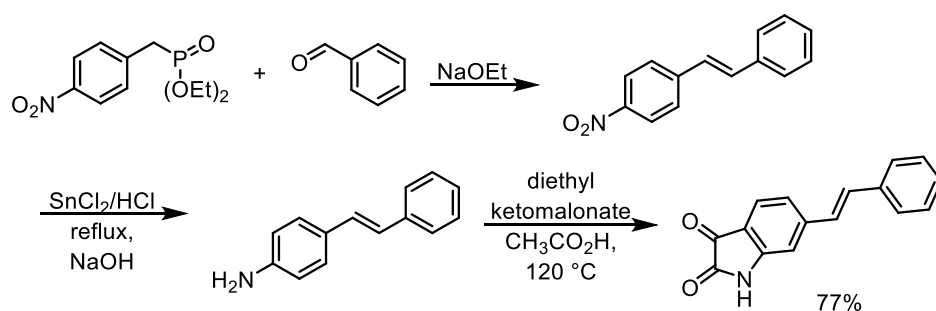


Scheme 5.17: Scope of the Mizoroki-Heck reaction; Part 1. Reaction conditions: In air, a vial was charged with $[SiPr-H][Pd(\eta^3-2-Me-allyl)Cl_2]$ (0.1 mol%), KOH (1.1 equiv.), *iso*-propanol (0.25 M) and a magnetic stir bar and sealed with a screw cap. The corresponding aryl halide (0.5 mmol) was added followed by the corresponding alkene (1.1 equiv.). The reaction was left to stir (910 rpm) for 4 h at 80 °C. Average of two runs. Isolated yields.

Heteroatom containing substrates are widely desired as these motifs are seen in a variety of drug molecules, natural products and polymers.

Therefore, the coupling of these substrates is very important to study. The main challenge is the possible coordination of heteroatoms such as nitrogen or oxygen to the palladium centre. This can, in the worst case, completely hinder the catalysis. *E*-6-styrylisatin is known to be a reversible inhibitor of human monoamine oxidase (MAO) A and B.⁴⁵ A relationship between the MAO-B enzyme and neuropsychiatric/degenerative disorders was found, therefore a development of inhibitors of MAO-B is a major interest as it could treat a number of neurological diseases.⁴⁶ The

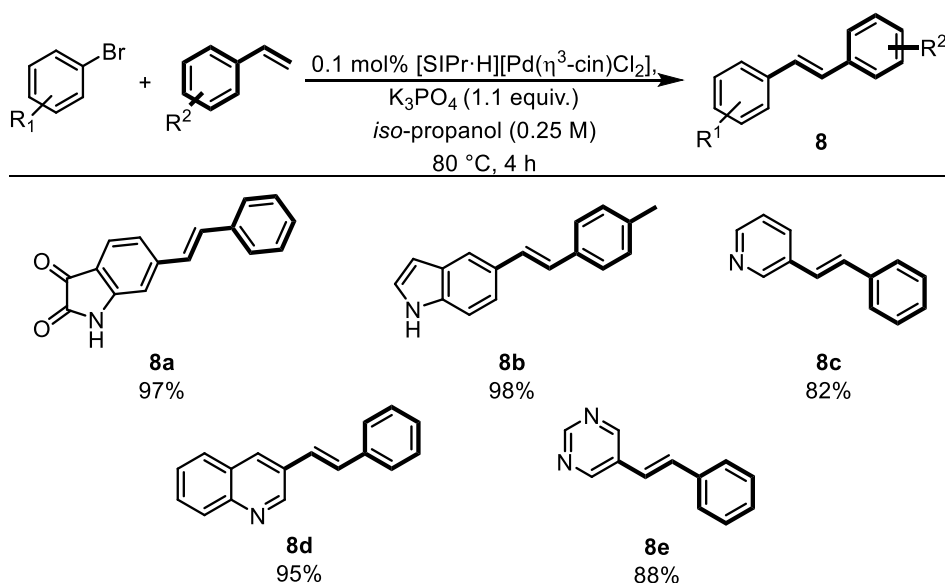
only published synthesis of *E*-6-Styrylisatin contains three steps. The starting substrate is diethyl-4-nitrobenzylphosphonate which is reacted with benzaldehyde to form 4-nitrostilbene. Next reduction of a nitro group is performed using $SnCl_2/HCl$ to yield aminostilbene. Treatment of aminostilbene with diethyl ketomalonate in the presence of acetic acid, followed by the oxidative decarboxylation of the resulting 3-hydroxy-2-oxindoyl intermediate yields the product, *E*-6-styrylisatin in 77% yield (Scheme 5.18).



Scheme 5.18: Reported synthesis of *E*-6-styrylisatin.⁴⁷

Using the established protocol for the Mizoroki-Heck reaction *E*-6-styrylisatin was synthesised in 97% yield from two commercially available starting material in 4 hours using mild reaction conditions (Scheme 5.19, **8a**).

A range of heteroaryl bromides could be coupled including 5-bromoindole to give *E*-5-(4-methylstyryl)-1H-indole (Scheme 5.19, **8b**). This is an intermediate in the synthesis of novel small molecule inhibitors of 25-hydroxyvitamin D-25-hydroxylase.⁴⁸ Further demonstrating the synthetic utility of the developed protocol, 3-bromopyridine (**8c**, 82%), 3-bromoquinoline (**8d**, 95%) and 5-bromopyrimidine (**8e**, 88%) were also coupled with styrene in good to excellent yield.



Scheme 5.19: Scope of the Mizoroki-Heck; Part 2. Reaction conditions: In air, a vial was charged with $[SIPr\cdot H][Pd(\eta^3\text{-2-Me-allyl})Cl_2]$ (0.1 mol%), KOH (1.1 equiv.), *iso*-propanol (0.25 M) and a magnetic stir bar and sealed with a screw cap. The corresponding aryl halide (0.5 mmol) was added followed by the corresponding alkene (1.1 equiv.). The reaction was left to stir (910 rpm) for 4 h at 80 °C. Average of two runs. Isolated yields.

5.3 Conclusion

An extensive investigation was conducted into the catalytic activity of the palladate pre-catalysts in the Mizoroki-Heck reaction. Different palladates were tested bearing electronically and sterically different NHC ligands. The use of different allyl ligands was investigated, resulting in 2-Me-allyl being identified as optimal. Many different common solvents were tested, showing a clear favour for alcohol solvents. Base/solvent cross experiments were conducted to establish the ideal protocol. Very low catalyst loading was needed to achieve high yield in a variation of substrates. Overall different aryl bromides and chlorides were tested. Steric bulk on the aryl bromide was tolerated, without loss of reactivity. Biologically interesting heteroatom-containing aryl bromides were successfully coupled with styrene using the optimised protocol including a significant improvement in the synthesis of *E*-6-styrylisatin. Overall $[SIPr\cdot H][Pd(\eta^3\text{-2-Me-allyl})Cl_2]$ was a highly catalytic active pre-catalyst for the Mizoroki-Heck reaction using low catalyst loading (0.1 mol%) under mild conditions and moderate temperatures. The coupling of challenging substrates was possible and more investigation into similar substrates should follow.

5.4 Reference

- (1) Zhang, Y.; Lv, Z.; Zhong, H.; Zhang, M.; Zhang, T.; Zhang, W.; Li, K. *Tetrahedron* **2012**, *68*, 9777–9787.
- (2) Ding, Y. H.; Fan, H. X.; Long, J.; Zhang, Q.; Chen, Y. *Bioorganic Med. Chem. Lett.* **2013**, *23*, 6087–6092.
- (3) de Vries, J. G. *Can. J. Chem.* **2001**, *79*, 1086–1092.
- (4) Dounay, A. B.; Overman, L. E. *Chem. Rev.* **2003**, *103*, 2945–2963.
- (5) Sato, T.; Takata, T. *Polym. J.* **2009**, *41*, 470–476.
- (6) Jiang, X.; Lee, G. T.; Prasad, K.; Repic, O. *Org. Process Res. Dev.* **2008**, *12*, 1137–1141.
- (7) Mizoroki, T.; Mori, K.; Ozaki, A. *Bull. Chem. Soc. Jpn.* **1971**, *44*, 581–581.
- (8) Heck, R. F.; Nolley, J. P. *J. Org. Chem.* **1972**, *37*, 2320–2322.
- (9) Heck, R. F. *J. Am. Chem. Soc.* **1968**, *90*, 5518–5526.
- (10) Heck, R. F. *J. Am. Chem. Soc.* **1968**, *90*, 5526–5531.
- (11) Heck, R. F. *J. Am. Chem. Soc.* **1968**, *90*, 5531–5534.
- (12) Heck, R. F. *J. Am. Chem. Soc.* **1968**, *90*, 5535–5538.
- (13) Heck, R. F. *J. Am. Chem. Soc.* **1968**, *90*, 5538–5542.
- (14) Heck, R. F. *J. Am. Chem. Soc.* **1968**, *90*, 5542–5546.
- (15) Heck, R. F. *J. Am. Chem. Soc.* **1968**, *90*, 5546–5548.
- (16) de Meijere, A.; Meyer, F. E. *Angew. Chem. Int. Ed.* **1994**, *33*, 2379–2411.
- (17) Ziegler, C. B.; Heck, R. F. *J. Org. Chem.* **1978**, *43*, 2941–2946.
- (18) Herrmann, W. A.; Brossmer, C.; Reisinger, C.-P.; Riermeier, T. H.; Öfele, K.; Beller, M. *Chem. Eur. J.* **1997**, *3*, 1357–1364.
- (19) Hermann, W. A.; Brossmer, C.; Öfele, K.; Reisinger, C.; Riermeier, T.; Beller, M.; Fischer, H. *Angew. Chem. Int. Ed.* **1995**, *34*, 1844–1848.
- (20) Shaw, B. L. *Chem. Commun.* **1998**, 1361–1362.
- (21) Gainsford, G. J.; Mason, R. *J. Organome* **1974**, *80*, 395–406.
- (22) Albisson, D. A.; Bedford, R. B.; Scully, P. N. *Tetrahedron Lett.* **1998**, *39*, 9793–9796.
- (23) Ohff, M.; Ohff, A.; Van der Boom, M. E.; Milstein, D. *J. Am. Chem. Soc.* **1997**, *119*, 11687–11688.
- (24) Lawrence, M. A. W.; Green, K. A.; Nelson, P. N.; Lorraine, S. C. *Polyhedron* **2017**, 1–17.
- (25) Miyazaki, F.; Yamaguchi, K.; Shibasaki, M. *Tetrahedron Lett.* **1999**, *40*, 7379–7383.
- (26) Herrmann, W. A.; Elison, M.; Köcher, C.; Artus, G. R. J. *Angew. Chem. Int. Ed.* **1995**, *34*, 2371–2374.

- (27) Frey, G. D.; Schütz, J.; Herdtweck, E.; Herrmann, W. A. *Organometallics* **2005**, *24*, 4416–4426.
- (28) Littke, A. F.; Fu, G. C. *J. Org. Chem.* **1999**, *64*, 10–11.
- (29) Littke, A. F.; Fu, G. C. *J. Am. Chem. Soc.* **2001**, *123*, 6989–7000.
- (30) Xu, H. J.; Zhao, Y. Q.; Zhou, X. F. *J. Org. Chem.* **2011**, *76*, 8036–8041.
- (31) Yang, C.; Nolan, S. P. *Synlett* **2001**, *10*, 1539–1542.
- (32) Gottumukkala, A. L.; de Vries, J. G.; Minnaard, A. J. *Chem. Eur. J.* **2011**, *17*, 3091–3095.
- (33) Peh, G.-R.; Kantchev, E. A. B.; Zhang, C.; Ying, J. Y. *Org. Biomol. Chem.* **2009**, *7*, 2110–2119.
- (34) Links, D. A.; Liu, Y.; Lin, Y.; Chen, W.; Cheng, J.; Chen, Y.; Yap, G. P. A.; Sun, S.; Ong, T. *Dalton Trans.* **2012**, *41*, 7382–7389.
- (35) Lin, Y.; Hsueh, H.; Kanne, S.; Chang, L.; Liu, F.; Lin, I. J. B. *Organometallics* **2013**, *32*, 3859–3869.
- (36) Tessin, U. I.; Bantreil, X.; Songis, O.; Cazin, C. S. J. *Eur. J. Inorg. Chem.* **2013**, 2007–2010.
- (37) Gallop, C.; Zinser, C.; Guest, D.; Navarro, O. *Synlett* **2014**, *25*, 2225–2228.
- (38) Khazipov, O. V.; Shevchenko, M. A.; Chernenko, A. Y.; Astakhov, A. V.; Pasyukov, D. V.; Eremin, D. B.; Zubavichus, Y. V.; Khrustalev, V. N.; Chernyshev, V. M.; Ananikov, V. P. *Organomet. Chem.* **2018**, 10.1021/acs.organomet.8b0012.
- (39) Clavier, H.; Correa, A.; Cavallo, L.; Escudero-Adán, E. C.; Benet-Buchholz, J.; Slawin, A. M. Z.; Nolan, S. P. *Eur. J. Inorg. Chem.* **2009**, 2009, 1767–1773.
- (40) Marion, N.; Navarro, O.; Mei, J.; Stevens, E. D.; Scott, N. M.; Nolan, S. P. *J. Am. Chem. Soc.* **2006**, *128*, 4101–4111.
- (41) Hruszkewycz, D. P.; Balcells, D.; Guard, L. M.; Hazari, N.; Tilset, M. *J. Am. Chem. Soc.* **2014**, *136*, 7300–7316.
- (42) Hruszkewycz, D. P.; Guard, L. M.; Balcells, D.; Feldman, N.; Hazari, N.; Tilset, M. *Organometallics* **2014**, *34*, 381–394.
- (43) Melvin, P. R.; Nova, A.; Balcells, D.; Dai, W.; Hazari, N.; Hruszkewycz, D. P.; Shah, H. P.; Tudge, M. T. *ACS Catal.* **2015**, *5*, 3680–3688.
- (44) Melvin, P. R.; Hazari, N.; Lant, H. M. C.; Peczak, I. L.; Shah, H. P. *Beilstein J. Org. Chem.* **2015**, *11*, 2476–2486.
- (45) Manley-King, C. I.; Bergh, J. J.; Petzer, J. P. *Bioorganic Med. Chem.* **2011**, *19*, 261–274.
- (46) Carradori, S.; Silvestri, R. *J. Med. Chem.* **2015**, *58*, 6717–6732.
- (47) Langenbeck, W.; Ruhlmann, K.; Reif, H.; Stolze, F. *J. für Prakt. Chemie* **1956**, *4*, 136–146.

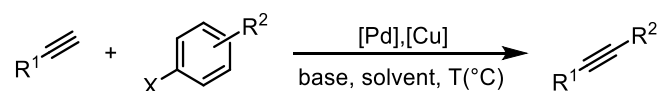
- (48) Ferla, S.; Goma, M. S.; Brancale, A.; Zhu, J.; Ochalek, J. T.; DeLuca, H. F.; Simons, C. *Eur. J. Med. Chem.* **2014**, *87*, 39–51.
- (49) Zhang, Y.; Zhang, Y.; Chen, Z.; Wu, W.; Su, W. *J. Org. Chem.* **2013**, *78*, 12494–12504.
- (50) Guo, T.; Wei, X.-N.; Wang, H.-Y.; Zhu, Y.-L.; Zhao, Y.-H.; Ma, Y.-C. *Org. Biomol. Chem.* **2017**, *15*, 9455–9464.
- (51) Katritzky, A. R.; Tymoshenko, D. O.; Monteux, D.; Vvedensky, V.; Nikonov, G.; Cooper, C. B.; Deshpande, M. *J. Org. Chem.* **2000**, *65*, 8059–8062.

Chapter 6

Palladium catalysed C-H activation of alkynes with aryl halides

6.1 The Sonogashira Reaction

The catalytic coupling of aryl/vinyl halides with terminal acetylenes is widely known as the Sonogashira reaction. First reported by Heck¹ and Cassar² in 1975, it included the coupling of aryl halides with alkynes using catalytic amounts of palladium without the need of copper, but high reaction temperatures (100 °C) and led to low to moderate yields. The initial report of Sonogashira, Tohda and Hagihara in 1975³ however described the sp²-sp carbon-carbon bond formation catalysed at room temperature by PdCl₂(PPh₃)₂ and CuI as a co-catalyst, with the addition of copper improving the coupling yields immensely.

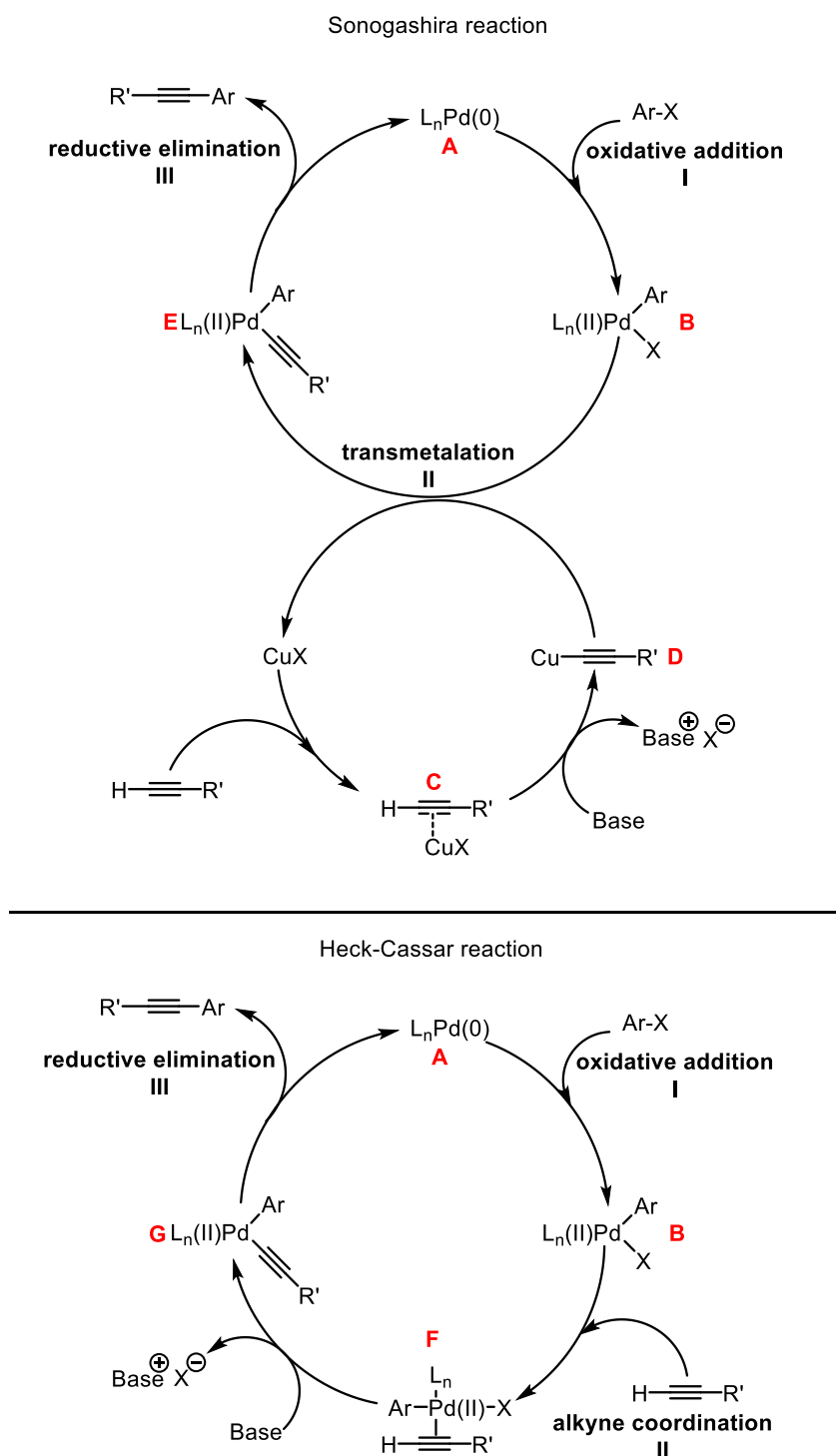


Scheme 6.1: General Sonogashira reaction.³

The Sonogashira reaction is now widely used in many important transformations such as for example in the synthesis of biologically important compounds^{4,5} and electro-optical devices.⁶ Furthermore the Sonogashira reaction is used for the synthesis of many pharmacologically interesting cyclic peptides.^{7,8}

The mechanism of the reaction consists of two cycles, the palladium cycle and the copper cycle. The catalysis starts in the palladium cycle with the active Pd(0) species, **A**, undergoing an oxidative addition with the aryl halide (Scheme 6.2, **I**) forming L_nPd(II)ArX, species **B**. Followed by transmetalation of the copper acetylide species **D** to generate **E**, which then undergoes reductive elimination (**III**) and liberates the product. The copper cycle starts with the coordination of a terminal alkyne to a Cu species, **C**. The abstraction of the terminal hydrogen by the base generates the copper acetylide species **D**, which enters the palladium cycle. The “copper-free Sonogashira”, or better described as the Heck-Cassar reaction, follows a similar mechanism.⁹ The cycle starts with an oxidative addition of the aryl halide and the Pd(0) species (Scheme 6.2, **I**). Followed by π-coordination of alkyne to the Pd(II) species **F**. Deprotonation of

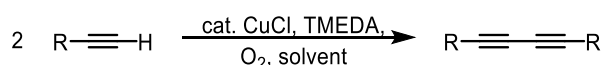
the terminal hydrogen of the terminal alkyne by the base generates **G**, which releases the coupling product and generates the active Pd(0) species **A**.



Scheme 6.2: Catalytic cycles of the Sonogashira reaction, with and without copper.¹⁰

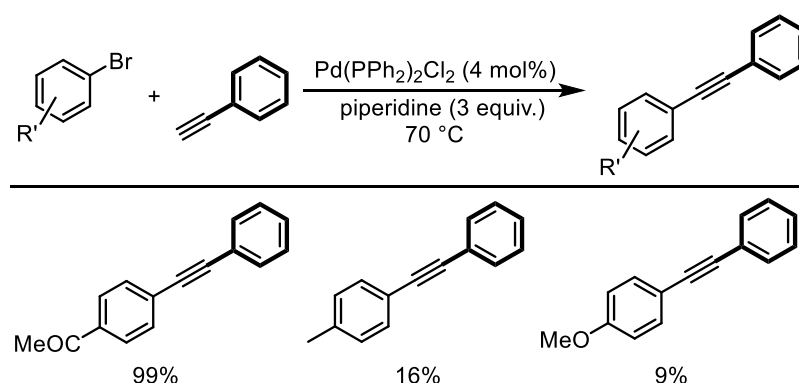
In 1977 seminal papers by Hagihara and co-workers reported the use of Pd-phosphine catalysts, such as $Pd(PPh_3)_4$, $Pd(PPh_3)_2Cl_2$ or $Pd(dppe)Cl_2$ ($dppe = 1,2$ -bis(diphenylphosphino)ethane), in

high catalyst loadings (5-10 mol%) in combination with large amounts of copper salt, copper(I) iodide (up to 15 mol%) for the Sonogashira reaction.¹⁰⁻¹² The main bases used are organic bases, such as NEt_3 , which are also commonly used as solvents.¹⁰ Although the addition of copper has many advantages such as low reaction temperatures, it bears many disadvantages as well, such as economic and environmental issues.¹⁰ Furthermore in the presence of copper, the reaction has to be performed under inert atmosphere in order to prevent the Glaser coupling of the terminal alkynes (Scheme 6.3).^{13,14}



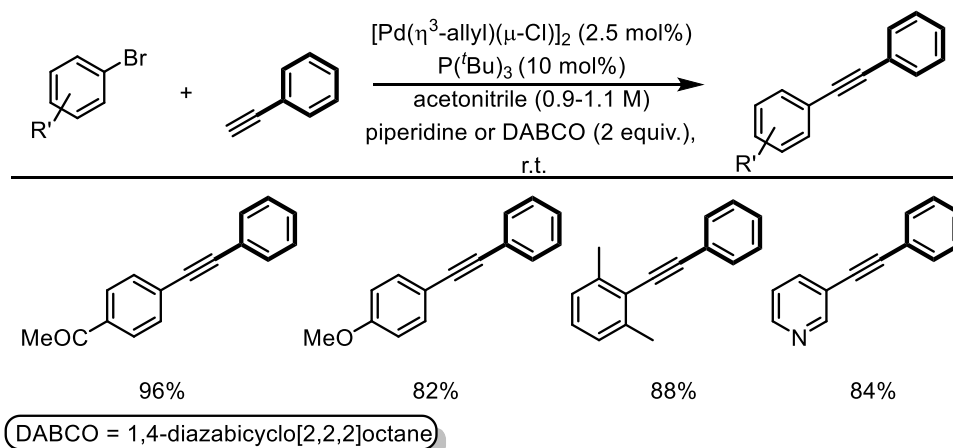
Scheme 6.3: General Glaser coupling reaction (TMEDA = *N,N,N',N'*-tetramethylethylenediamine).^{13,14}

In 2003, Leadbeater and co-workers reported the use of $\text{Pd}(\text{PPh}_3)_2\text{Cl}_2$ in a copper-free Sonogashira coupling, although 4 mol% catalyst loading was needed at 70 °C.¹⁵ The substrate scope was very restricted and, as depicted in Scheme 6.4, electron-withdrawing groups on the aryl halide were needed in order to achieve high yields.



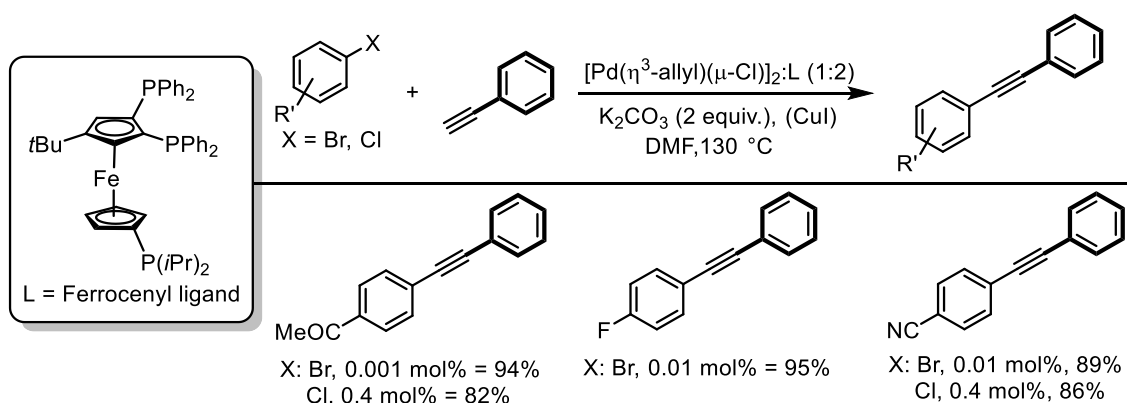
Scheme 6.4: The Sonogashira reaction catalysed by $\text{Pd}(\text{PPh}_3)_2\text{Cl}_2$.¹⁵

In the same year, Hughes and co-workers overcame that issue by using a bulkier phosphine ligand, namely P^tBu_3 in combination with 2.5 mol% of $[\text{Pd}(\eta^3\text{-allyl})(\mu\text{-Cl})_2]$ in acetonitrile.¹⁶ The catalysis was conducted at room temperature, without the need of a copper co-catalyst. The obtained products illustrated the tolerance towards aryl halides bearing electron-donating groups (Scheme 6.5).



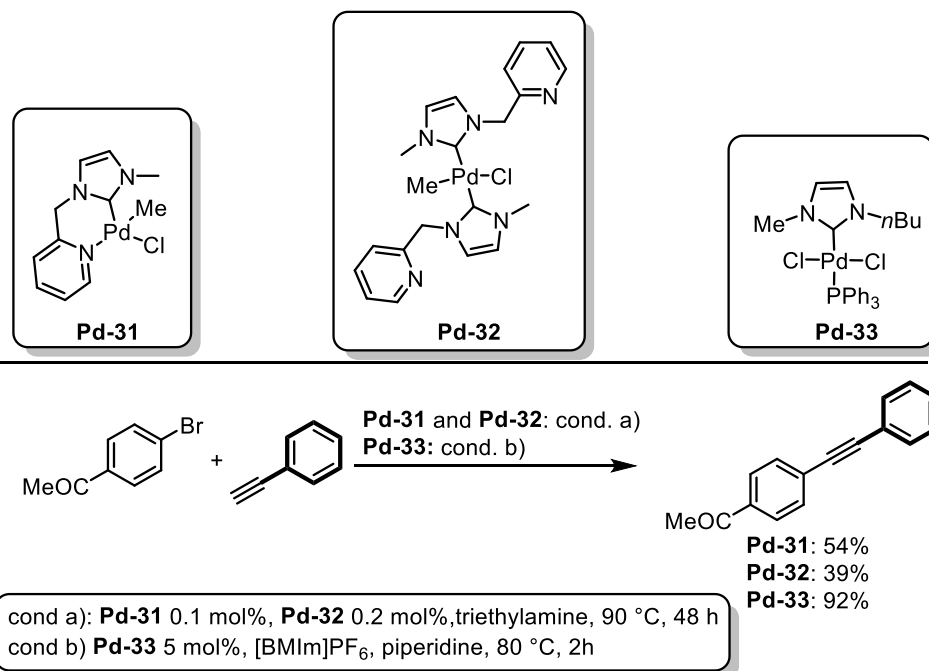
Scheme 6.5: The Sonogashira reaction catalysed by $[Pd(\eta^3\text{-allyl})(\mu\text{-Cl})_2]$ and $P(t\text{Bu})_3$.¹⁶

By changing the ligand to a multidentate ferrocenyl phosphine ligand, Meunier and co-workers established a protocol using very low catalyst loading (0.1 mol%-0.001 mol%).¹⁷ Several aryl bromides and chlorides were tested under these conditions, although CuI had to be used when coupling aryl chlorides to obtain high yields (Scheme 6.6).¹⁷

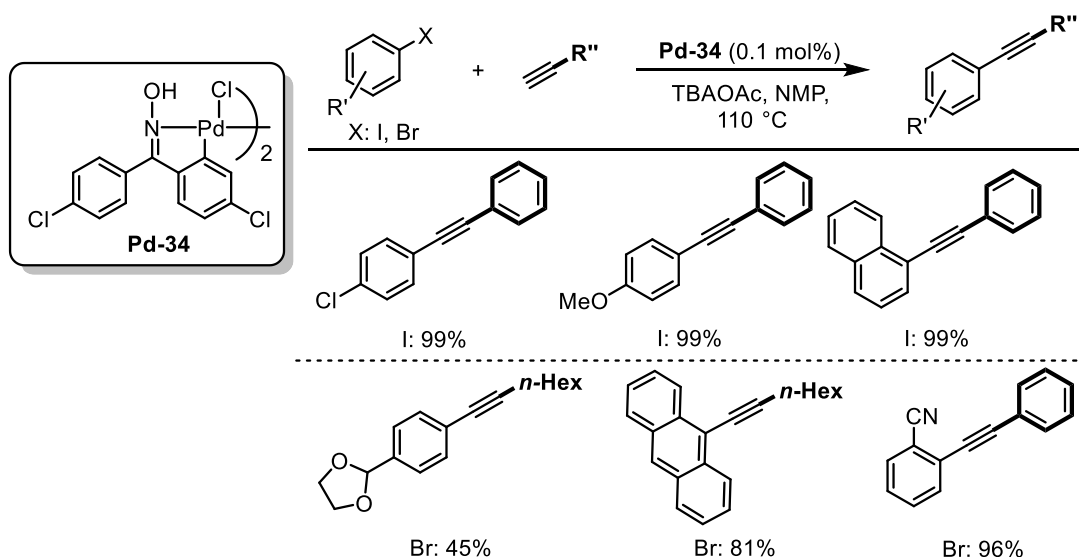


Scheme 6.6: The use of a multidentate ferrocenyl ligand in the Sonogashira reaction.¹⁷

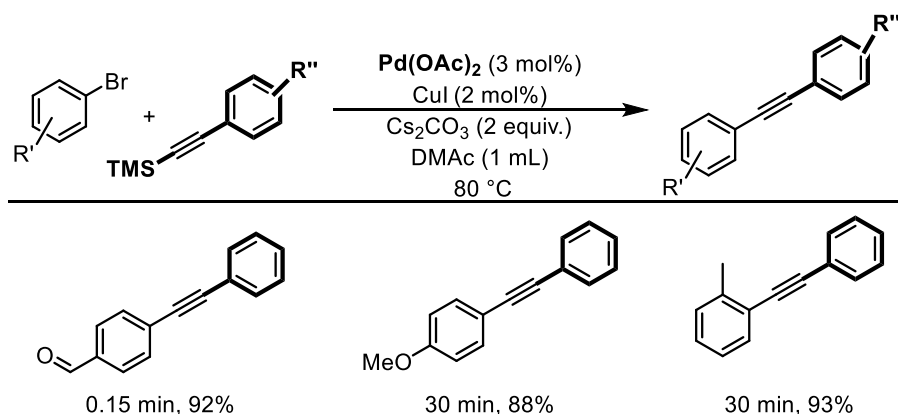
The effect of NHC ligands in the Sonogashira reaction was studied by Cavell and co-worker in 2000.¹⁸ The palladacycle **Pd-31** and the monodentate NHC-Pd complex **Pd-32** were tested under the same reaction conditions, coupling 4-bromoacetophenone and phenylacetylene using triethylamine as solvent and base at 90 °C (Scheme 6.7).¹⁸ Low catalyst loadings were used, revealing **Pd-31** as the more active catalyst compared to **Pd-32**, although only moderate yields were obtained in both experiments. **Pd-33** was investigated in the Sonogashira reaction using ionic liquids, resulting in high yields but a high catalyst loading (5 mol%) was needed.¹⁹

Scheme 6.7: Pd-NHC complexes in the Sonogashira reaction.¹⁸

The oxime derived palladacycle **Pd-34** reported by Pacheco in 2002 was used at low catalyst loading (0.1 mol%) to couple aryl iodides and bromides with a series of different terminal alkynes.^{20,21} *N*-methylpyrrolidinone (NMP) was used as solvent and together with tetrabutylammonium acetate (TBAOAc) as additive at 110 °C, resulting in moderate to high yield in air, without the use of copper as a co-catalyst (Scheme 6.8).

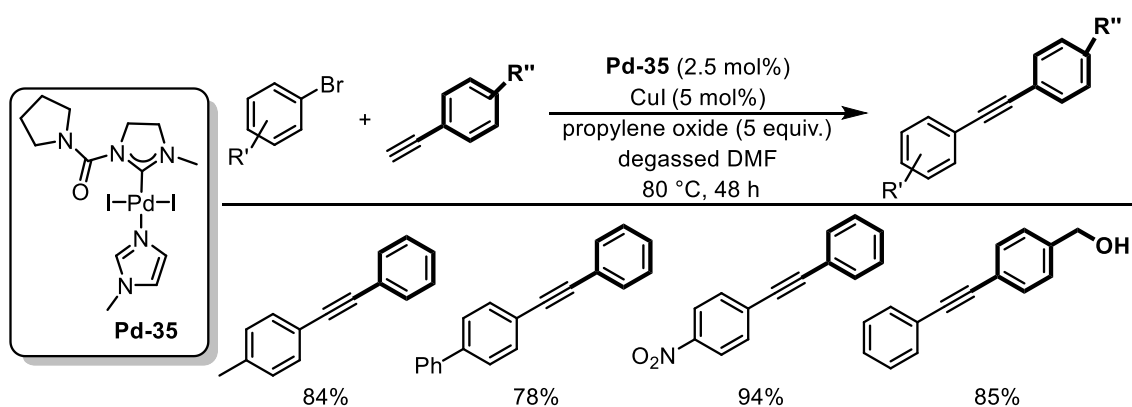
Scheme 6.8: Sonogashira coupling using an oxime-derived palladacycle.^{20,21}

Nolan and co-workers reported the coupling of aryl bromides with alkynylsilanes using an *in situ* system consisting of Pd(OAc)₂ (3 mol%) and IMes·HCl (6 mol%).²² The established system showed high reactivity in a short reaction time (15 min–60 min), furthermore the catalysis proceeded without a copper source, although CuI was used to enhance the rate of the reaction (Scheme 6.9).²²



Scheme 6.9: Coupling of aryl bromides with alkynylsilanes using Pd(OAc)₂ with IMes·HCl.²²

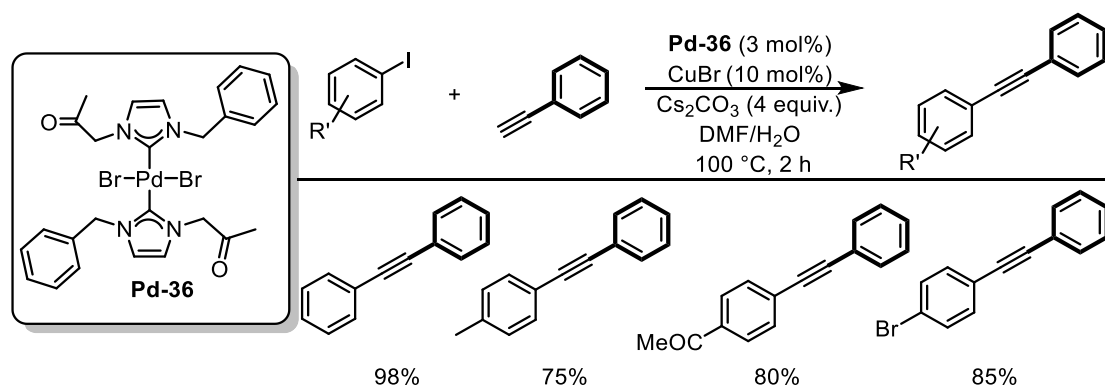
The well-defined Pd-NHC complex **Pd-35**, was used in a base-free Sonogashira reaction coupling aryl bromides with alkynes reported by Zhai in 2008.²³ The acid scavenger propylene oxide was used instead of a base, which allowed the use of base-sensitive groups on the cross-coupling substrates (Scheme 6.10). Although a wider substrate scope could be used with this protocol a catalyst loading of 2.5 mol% was needed in combination with CuI. Furthermore high reaction temperatures (80 °C) and long reaction times (48 h) were needed.



Scheme 6.10: Base-free Sonogashira.²³

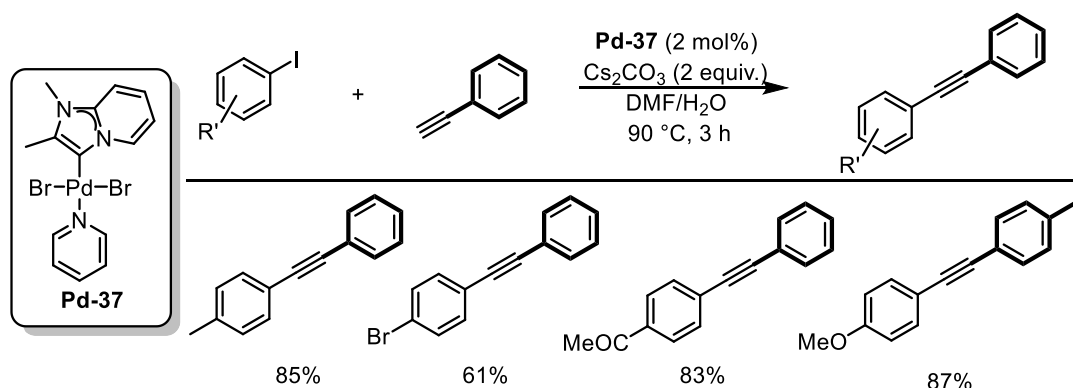
Ghosh and co-workers reported an example of the Sonogashira reaction using a bis-NHC-Pd complex, **Pd-36**, making the palladium centre very electron-rich.²⁴ The reactions were conducted

in air in mixture of DMF and water, making the procedure more convenient. A range of different aryl iodides were coupled with phenylacetylene using 3 mol% of **Pd-36** in the presence of CuBr (10 mol%) (Scheme 6.11). Increased reaction temperatures (100 °C) resulted in a short reaction time of 2 hours.



Scheme 6.11: The Sonogashira reaction using **Pd-36**.²⁴

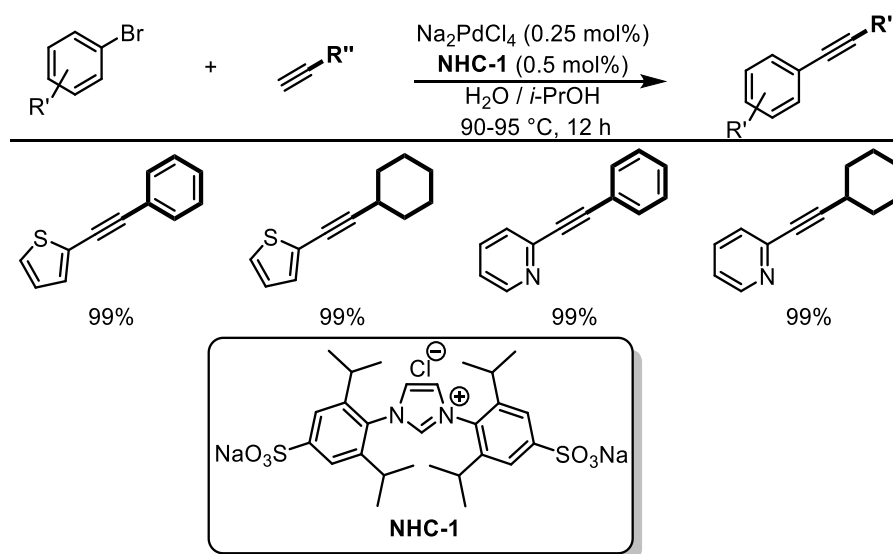
Further investigations of Ghosh and co-workers followed in 2009, introducing copper-free conditions for the Sonogashira reaction.²⁵ A well-defined Pd(II) complex bearing an abnormal NHC and a PEPPSI (Pyridine-Enhanced Precatalyst Preparation, Stabilisation and Initiation) ligand was introduced (Scheme 6.12). Ghosh and co-workers postulated that the strong donating character of the abnormal NHC ligand weakened the Pd-N bond from the PEPPSI ligand, aiding the reduction of Pd(II) to Pd(0) as well as the catalysis.²⁵ Furthermore the base loading was reduced from 4 to 2 equivalents of Cs₂CO₃.



Scheme 6.12: "Copper-free" Sonogashira.²⁵

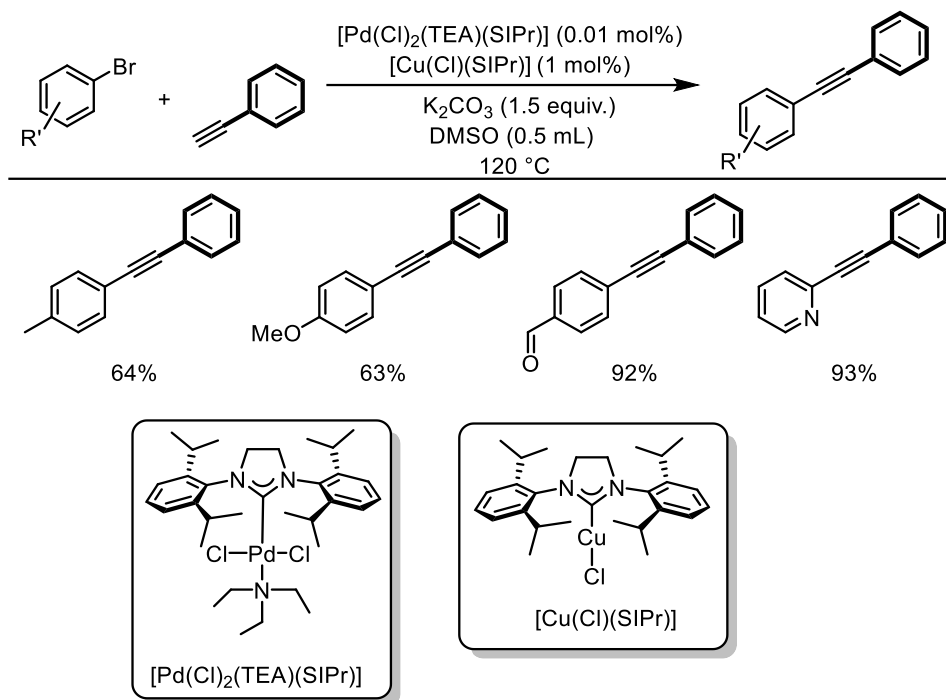
In 2010 Plenio and co-workers reported an example of aqueous Sonogashira reaction, catalysed by an *in situ* catalytic system of PdNa₂Cl₄ and disulfonated NHC ligand, **NHC-1** (Scheme 6.13).²⁶ No copper was needed in this protocol; furthermore a low catalyst loading (0.25 mol% of Pd)

was required. The developed protocol was successfully applied and aryl bromides and chlorides were coupled with aryl and alkyl acetylenes in good to excellent yield.



Scheme 6.13: Example of aqueous Sonogashira reaction.²⁶

Navarro and co-workers reported an example of a Sonogashira reaction using the $[\text{Pd}(\text{Cl})_2(\text{TEA})(\text{SIPr})]$ (TEA = triethylamine, SIPr = *N,N'*-bis-[2,6-(di-*iso*-propyl)phenyl]imidazolidin-2-ylidene) pre-catalyst, introduced in Chapter 3, in combination with $[\text{Cu}(\text{Cl})(\text{SIPr})]$ (Scheme 6.14).²⁷ Both catalysts were used in very low catalyst loading (Pd: 0.01 mol%, Cu: 1 mol%). A wide scope was conducted in air using electron-donating and electron-withdrawing aryl bromides, although high reaction temperatures were needed.



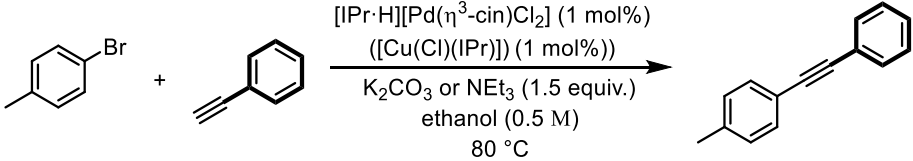
Scheme 6.14: The Sonogashira reaction catalysed by $[\text{Pd}(\text{Cl})_2(\text{TEA})(\text{SIPr})]$.²⁷

Based on the promising results of Pd-NHC pre-catalysts in the Sonogashira, an investigation was conducted using the palladate pre-catalysts.

6.2 Results and Discussion

Preliminary reaction conditions were chosen; [IPr·H][Pd(η^3 -cin)Cl₂] (IPr = *N,N'*-bis-[2,6-(di-*iso*-propyl)phenyl]imidazol-2-ylidene) (1 mol%) was chosen as palladate pre-catalyst, K₂CO₃ or triethylamine (1.5 equiv.) as bases in ethanol. [Cu(Cl)(IPr)] was used as copper source (Table 6.1). 4-Bromotoluene and phenylacetylene were chosen as model substrates (Table 6.1). Firstly the need of an activation step was investigated. When the reaction was set up without an activation step, *i.e.* heating the pre-catalyst with the base, the catalysis did not proceed. The reaction mixture instantly turned black from yellow after the addition of phenylacetylene. It was proposed as seen in Chapter 3, that the palladate can react with the coupling substrates, in this case with phenylacetylene. After the introduction of the activation step, the need of a copper co-catalyst was assessed. Two bases were used for these experiments; triethylamine (a widely used base in the Sonogashira) and an inorganic base, K₂CO₃. When NEt₃ was used no conversion towards the coupling product was observed. This could be an influence of the activation step of the palladate complexes, where the Pd-NHC bond is formed, as NEt₃ may not be suitable for this step. In the case of K₂CO₃, 40% GC conversion was obtained, with or without copper. Based on these experiments, the investigation was conducted without the use of copper as a co-catalyst.

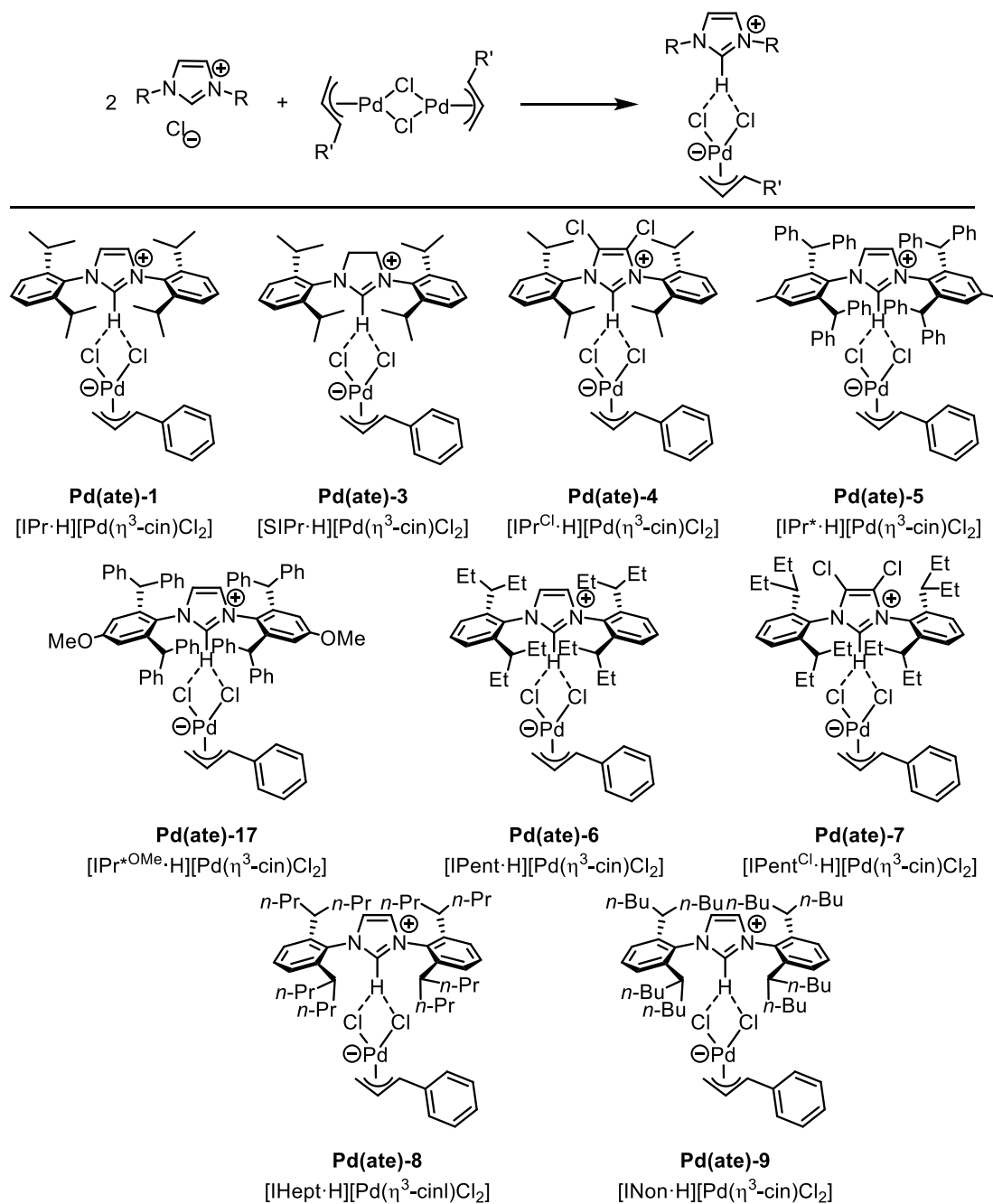
Table 6.1 Preliminary reaction conditions for the Sonogashira.



entry	[Cu]	base	GC conversion (%)
1	no	K ₂ CO ₃	40
2	yes	K ₂ CO ₃	40
3	no	NEt ₃	n.r.
4	yes	NEt ₃	n.r.

Reaction conditions: In the glovebox, a vial was charged with the [IPr·H][Pd(η^3 -cin)Cl₂] (1 mol%), [CuCl(IPr)] (1 mol%) for entry 2 and 4, K₂CO₃ or NEt₃ (1.5 equiv.), ethanol (0.5 M) and a magnetic stir bar and sealed with a screw cap. The mixture was let to stir at 80 °C for 1 hour. The sample was removed from the heating block and 4-bromotoluene (0.5 mmol) was added followed by the phenylacetylene (0.75 mmol). The reaction was left to stir for 16 h at the 80 °C. GC conversion based on 4-bromotoluene. An average of two reactions.

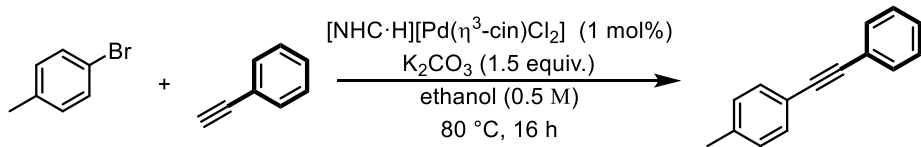
In order to find the optimum catalytic system, a variety of palladate complexes, $[\text{NHC}\cdot\text{H}][\text{Pd}(\eta^3\text{-cin})\text{Cl}_2]$ were synthesised following the procedure discussed in Chapter 2. Different NHC ligands were used with varying electronic and steric parameters (Scheme 6.14). The ITent series was used to exploit their “flexible steric bulk” as well as IPr^* (*N,N'*-bis-[2,6-bis(diphenylmethyl)-4-methylphenyl]imidazol-2-ylidene) and $\text{IPr}^{*\text{OMe}}$ (*N,N'*-bis-[2,6-bis(diphenyl)-4-methoxyphenyl]imidazol-2-ylidene) as the most bulky ligands in this investigation.



Scheme 6.14: Palladate pre-catalysts used in the catalyst optimisation, Part 1.

Using K_2CO_3 as base, the palladate pre-catalysts were tested in the Sonogashira reaction. Changing the electron-donating properties from IPr to its saturated analogue, SIPr and the chlorinated analogue IPr^{Cl} (N,N' -bis-[2,6-(di-*iso*-propyl)phenyl-4,5-dichloro]imidazol-2-ylidene), caused a decrease in conversion (Table 6.2, entries 1-3). A large increase in conversion was observed when $[IPent^{Cl}\cdot H][Pd(\eta^3\text{-cin})Cl_2]$ ($IPent^{Cl}$ = N,N' -bis-[2,6-bis(di-*iso*-penty)phenyl-4,5-dichloro]imidazol-2-ylidene) (Table 6.2, entry 5) was used, whereas pre-catalysts bearing IPent (N,N' -bis-[2,6-bis(di-*iso*-penty)phenyl]imidazol-2-ylidene) (Table 6.2, entry 4), IHept (N,N' -bis-[2,6-bis(di-*iso*-hepty)phenyl]imidazol-2-ylidene) (Table 6.2, entry 6) and INon (N,N' -bis-[2,6-bis(di-*iso*-nonyl)phenyl]imidazol-2-ylidene) (Table 6.2, entry 7) gave low conversions. It was postulated that steric bulk on the NHC can be an advantage as $[IPr^*\cdot H][Pd(\eta^3\text{-cin})Cl_2]$ (IPr^* = N,N' -bis-[2,6-bis(diphenylmethyl)-4-methylphenyl]imidazol-2-ylidene) (Table 6.2, entry 8) and $[IPr^{*OMe}\cdot H][Pd(\eta^3\text{-cin})Cl_2]$ (IPr^{*OMe} = N,N' -bis-[2,6-bis(diphenyl)-4-methoxyphenyl]imidazol-2-ylidene) (Table 6.2, entry 9) gave moderate conversions.

Table 6.2: Pre-catalyst optimisation, Part 1



entry	pre-catalyst	GC conversion (%)
1	$[IPr\cdot H][Pd(\eta^3\text{-cin})Cl_2]$	40
2	$[SIPr\cdot H][Pd(\eta^3\text{-cin})Cl_2]$	29
3	$[IPr^{Cl}\cdot H][Pd(\eta^3\text{-cin})Cl_2]$	15
4	$[IPent\cdot H][Pd(\eta^3\text{-cin})Cl_2]$	30
5	$[IPent^{Cl}\cdot H][Pd(\eta^3\text{-cin})Cl_2]$	73
6	$[IHept\cdot H][Pd(\eta^3\text{-cin})Cl_2]$	34
7	$[INon\cdot H][Pd(\eta^3\text{-cin})Cl_2]$	32
8	$[IPr^*\cdot H][Pd(\eta^3\text{-cin})Cl_2]$	64
9	$[IPr^{*OMe}\cdot H][Pd(\eta^3\text{-cin})Cl_2]$	53

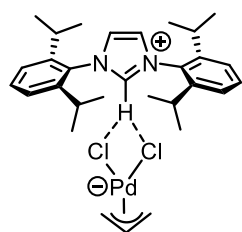
Reaction conditions: In the glovebox, the pre-catalyst, K_2CO_3 (1.5 equiv.), ethanol (0.5 M) was heated at 60 °C for 1 h. Then 4-bromotoluene (0.5 mmol) was added followed by phenylacetylene (1.5 equiv.). The reaction was left to stir for 16 h at 80 °C. Average of two runs.

The effect of the R-allyl ligand was next investigated. Different $[IPr\cdot H][Pd(\eta^3\text{-R-allyl})Cl_2]$ pre-catalysts were tested in the reaction to determine the most suitable R-allyl ligand. Interestingly changing from cinnamyl (Table 6.3, entry 4) to crotyl (Table 6.3, entry 2) decreased the conversion significantly. Similar effects were obtained when changing to allyl (Table 6.3, entry 1) and 1-*tert*-butylindenyl (Table 6.3, entry 5). A large increase in conversion was observed for

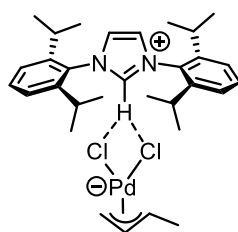
[IPr·H][Pd(η^3 -2-Me-allyl)Cl₂] (Table 6.3, entry 4). The large increase indicates that the R-allyl ligand is either involved in the activation step of Pd(II) to Pd(0) or in the catalysis as ligand on the active Pd(0) species.

Table 6.3: Pre-catalyst optimisation, Part 2

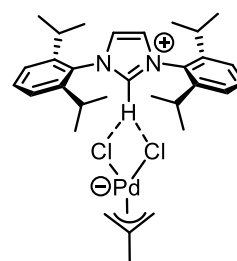
entry	pre-catalyst	GC conversion (%)
1	Pd(ate)-16	25
2	Pd(ate)-22	22
3	Pd(ate)-18	90
4	Pd(ate)-1	40
5	Pd(ate)-23	15



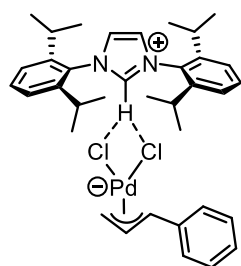
Pd(ate)-16
[IPr·H][Pd(η^3 -allyl)Cl₂]



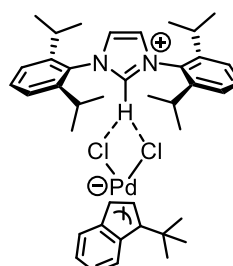
Pd(ate)-22
[IPr·H][Pd(η^3 -crotyl)Cl₂]



Pd(ate)-18
[IPr·H][Pd(η^3 -2-Me-allyl)Cl₂]



Pd(ate)-1
[IPr·H][Pd(η^3 -cin)Cl₂]



Pd(ate)-23
[IPr·H][Pd(η^3 -Ind^{tBu})Cl₂]

Reaction conditions: In the glovebox, the pre-catalyst, K₂CO₃ (1.5 equiv.), ethanol (0.5 M) was heated at 60 °C for 1 h. Then 4-bromotoluene (0.5 mmol) was added followed by phenylacetylene (1.5 equiv.). The reaction was left to stir (910 rpm) for 16 h at 80 °C. Average of two runs.

Based on optimisation results, further pre-catalysts were synthesised and tested in the Sonogashira reaction, namely [IPr*·H][Pd(η^3 -2-Me-allyl)Cl₂], [IPr*·H][Pd(η^3 -crotyl)Cl₂] and

[IPent^{Cl}·H][Pd(η³-2-Me-allyl)Cl₂]. Very promising results were obtained as all experiments resulted in high conversions (Table 6.4). Furthermore when [IPr*·H][Pd(η³-2-Me-allyl)Cl₂] was used as pre-catalyst, full conversion and an isolated yield of 98% were obtained.

Table 6.4: Pre-catalyst optimisation; Part 3.

entry	pre-catalyst	GC conversion (%)
1	Pd(ate)-14	99
2	Pd(ate)-15	87
3	Pd(ate)-26	88

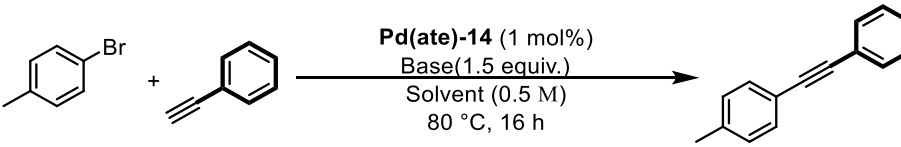
Pd(ate)-14
[IPr*·H][Pd(η³-2-Me-allyl)Cl₂]

Pd(ate)-15
[IPr*·H][Pd(η³-2-crotyl)Cl₂]

Pd(ate)-26
[IPent^{Cl}·H][Pd(η³-2-Me-allyl)Cl₂]

Reaction conditions: In the glovebox, the pre-catalyst, K₂CO₃ (1.5 equiv.), ethanol (0.5 M) was heated at 60 °C for 1 h. Then 4-bromotoluene (0.5 mmol) was added followed by phenylacetylene (1.5 equiv.). The reaction was left to stir (910 rpm) for 16 h at 80 °C. Average of two runs.

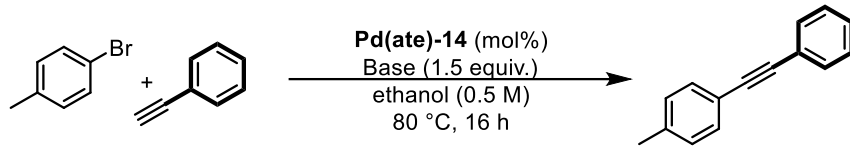
Pd(ate)-14 was used as pre-catalyst from this point onwards and the base/solvent optimisation was conducted next. In total eight inorganic bases were tested with 10 different solvent systems. Cross experiments were conducted where the best bases were tested against the best solvent (Chapter 9.6.6).

Table 6.5: Bases and solvents used in the optimisation.


Base	Solvent
K ₂ CO ₃	EtOH
Cs ₂ CO ₃	EtOH/H ₂ O (1:1)
Na ₂ CO ₃	MeOH
KOH	<i>iso</i> -PrOH
CsOH	<i>n</i> -BuOH
NaOH	1,4-Dioxane
KO ^t Bu	Toluene
NaO ^t Bu	CPME
	2-Me-THF
	Cyclohexane

Reaction conditions: In the glovebox, [IPr*·H][Pd(η^3 -2-Me-allyl)Cl₂] (1 mol%), the base (1.5 equiv.) and solvent (0.5 M) was heated at 60 °C for 1 h. Then 4-bromotoluene (0.5 mmol) was added followed by phenylacetylene (1.5 equiv.). The reaction was left to stir (910 rpm) for 16 h at 80 °C. Average of two runs.

The use of hydroxide bases such as NaOH and alkoxide bases, NaO^tBu and KO^tBu in ethanol resulted in full conversion. Therefore the catalyst loading in these conditions was lowered in an attempt to find which base was optimal. The catalyst loading was halved to 0.5 mol% for NaOH, NaO^tBu, KO^tBu and K₃PO₄ (Table 6.6, entries 1-4), again resulting in full conversion for all bases. The catalyst loading was then further reduced to 0.2 mol% and NaOMe was added as sodium based bases showed promising results. Yet again, NaOH (Table 6.6, entry 5) and NaO^tBu (Table 6.6, entry 6) resulted in full conversion, as well as NaOMe (Table 6.6, entry 9). A further reduction of the catalyst loading to 0.1 mol% determined the three best bases in this system, namely NaOH (Table 6.6, entry 10), NaO^tBu (Table 6.6, entry 11) and NaOMe (Table 6.6, entry 12).

Table 6.6: Optimisation of the pre-catalyst loading.


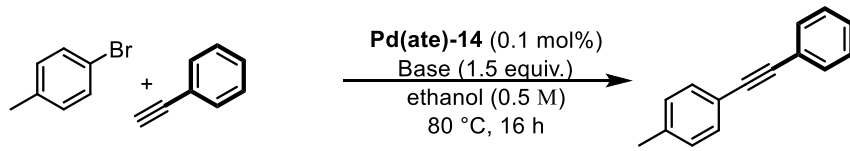
entry	base	pre-catalyst loading (mol%)	GC yield (%)
1	NaOH	0.5	99
2	NaO ^t Bu	0.5	99
3	KO ^t Bu	0.5	99
4	K ₃ PO ₄	0.5	99

5	NaOH	0.2	99
6	NaO ^t Bu	0.2	99
7	KO ^t Bu	0.2	73
8	K ₃ PO ₄	0.2	63
9	NaOMe	0.2	99

10	NaOH	0.1	79
11	NaO ^t Bu	0.1	82
12	NaOMe	0.1	81

Reaction conditions: In the glovebox, [IPr*·H][Pd(η^3 -2-Me-allyl)Cl₂] (mol%), the base (1.5 equiv.) and ethanol (0.5 M) was heated at 60 °C for 1 h. Then 4-bromotoluene (0.5 mmol) was added followed by phenylacetylene (1.5 equiv.). The reaction was left to stir (910 rpm) for 16 h at 80 °C. Average of two runs.

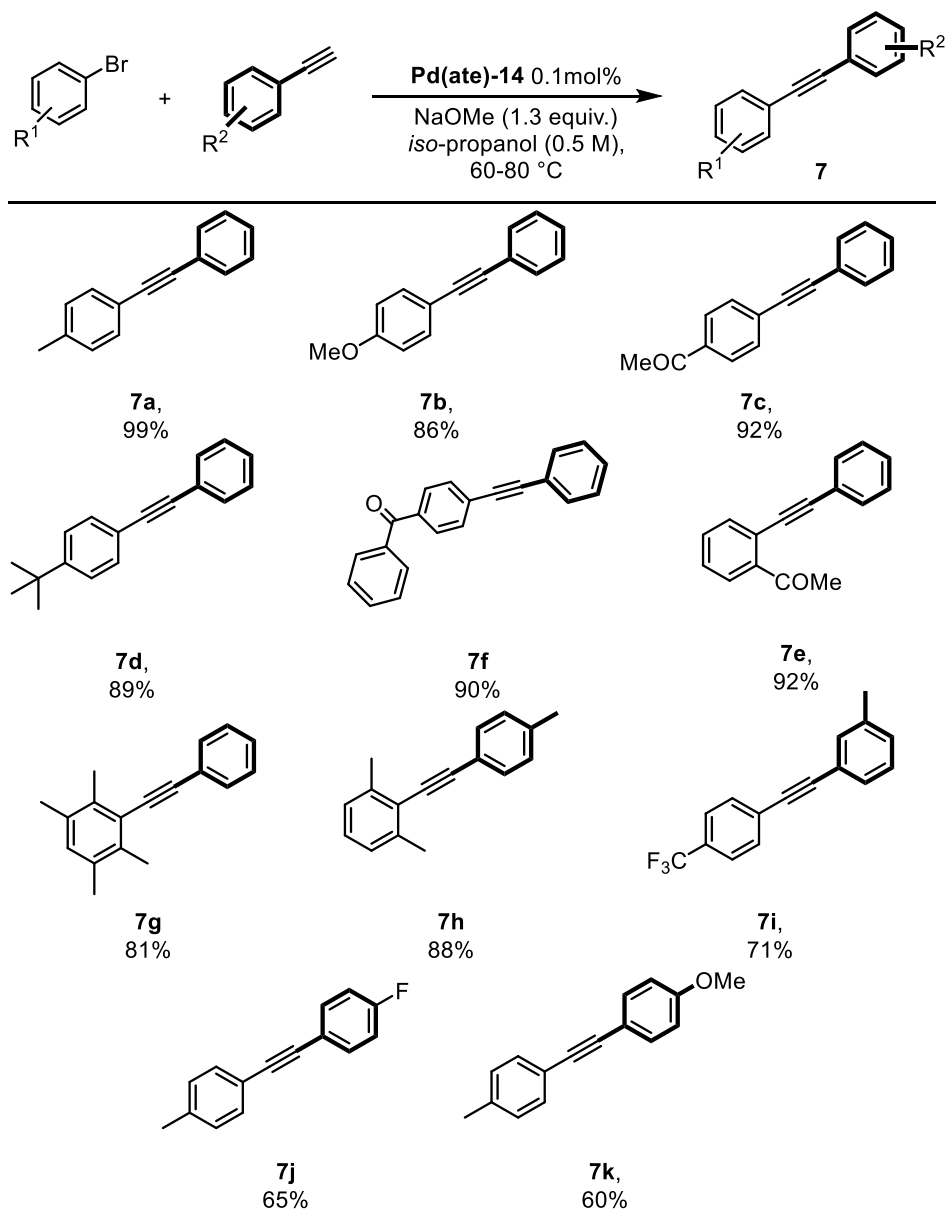
The resulting three bases were then used in a solvent screen. For NaOH and NaO^tBu, the best solvent was ethanol and the highest conversion achieved are illustrated in Table 6.7. NaOMe in combination with *iso*-propanol resulted in 87% GC yield.

Table 6.7: Summary of the optimal base/solvent systems.


entry	base	solvent	GC yield (%)
1	NaOH	ethanol	79
2	NaO ^t Bu	ethanol	82
3	NaOMe	<i>iso</i> -propanol	87

Reaction conditions: In the glovebox, [IPr*·H][Pd(η^3 -2-Me-allyl)Cl₂] (0.1 mol%), base (1.5 equiv.) and ethanol (0.5 M) heated at 60 °C for 1 h. Then 4-bromotoluene (0.5 mmol) was added followed by phenylacetylene (1.5 equiv.). The reaction was left to stir (910 rpm) for 16 h at 80 °C. Average of two runs.

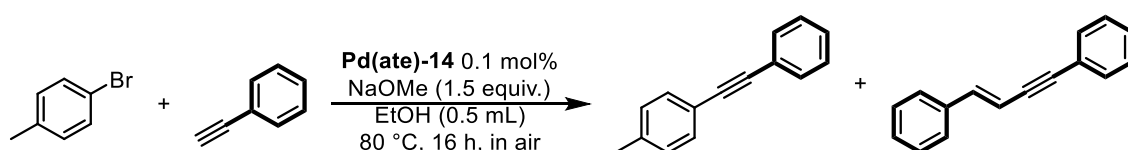
Furthermore by reducing the stoichiometry of NaOMe from 1.5 to 1.1 equivalents the GC yield was increased to >99%. In summary, the optimal conditions are [IPr*·H][Pd(η^3 -2-Me-allyl)Cl₂] using a very low catalyst loading of 0.1 mol%, NaOMe (1.1 equiv.) as base in *iso*-propanol (0.25 M) at 80 °C. Lastly the reaction time was optimised to 2.5 h. To test the diversity of this system a substrate scope was conducted. Firstly phenylacetylene was coupled with a variety of aryl bromides (Scheme 6.16, **7a-g**). High yields were obtained using electron-neutral groups on the aryl bromide such as 4-bromotoluene (Scheme 6.16, **7a**) and 1-bromo-4-*tert*-butylbenzene (Scheme 6.16, **7d**). Electron-donating (Scheme 6.16, **7b**) and electron-withdrawing aryl bromides (Scheme 6.16, **7c** and **7f**) resulted in high conversion, with no significant difference in yields. Sterically hindered aryl bromides such as bromodurene (Scheme 6.16, **7g**) was successfully coupled with phenylacetylene in good yield (81%). Next substituted acetylenes were investigated. *Para*-tolylacetylene was coupled with the sterically challenging 2-bromo-*m*-xylene in 88% isolated yield (Scheme 6.16, **7h**). Changing the substituent on tolylacetylene in the *meta* position was possible and **7i** was isolated in 71% yield. Changing the electronics of substituent on the acetylene was also possible, 4-fluorophenylacetylene and 4-methoxyphenylacetylene were coupled with 4-bromotoluene in moderate yield (Scheme 6.16 **7j** and **7k**). 4-chlorotoluene was tested with the optimised conditions but resulted in no conversion.



Scheme 6.16: Scope of the Sonogashira reaction. Reaction conditions: In the glovebox, [IPr*·H][Pd(η^3 -2-Me-allyl)Cl₂] (0.1 mol%), NaOMe (1.3 equiv.) and *iso*-propanol (0.5 M) was heated at 60 °C for 1 h. Then the corresponding aryl bromide (0.5 mmol) was added followed by the corresponding acetylene (1.1 equiv.). The reaction was left to stir (910 rpm) for 2.5 h at 80 °C. Average of two runs. Isolated yield.

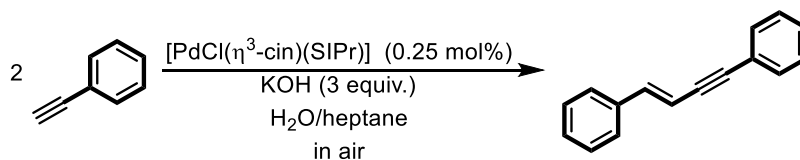
6.3 Catalytic dimerisation of terminal alkynes

During the optimisation of the Sonogashira reaction, a side-product was detected by GC analysis. Firstly the dimerization of the phenylacetylene was proposed as it is a known side-product formation in the Sonogashira reaction, although this is mainly reported when copper is used as a co-catalyst and known as the Glaser coupling.¹⁴ As our system is copper-free, the side-product identified was not obvious and so it was isolated and fully characterised. ¹H and ¹³C {¹H} NMR analysis confirmed a conjugated 1,3-enyne (Scheme 6.17).



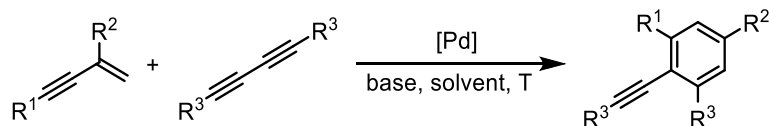
Scheme 6.17: The Sonogashira reaction illustrating the side-product.

This product results from the head to head catalysed dimerization of phenylacetylene. As this was at first an unwanted side-product, the system was modified to suppress its formation. It was found that if the catalysis was carried out under an inert atmosphere using dry, degassed solvent, this side-product formation was minimised as only traces (or less) could be detected in the crude reaction procedure. If the catalysis was carried out using the same conditions but in air using technical grade *iso*-propanol the side-product was almost exclusively obtained.



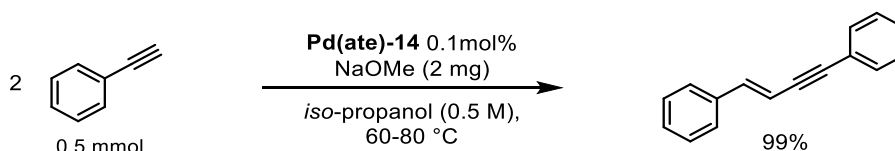
Scheme 6.17: Dimerisation of phenylacetylene using [PdCl(η³-cin)(SIPr)]

Interestingly the synthesis of (*E*)-1,3-enynes has been published using Pd-NHC catalysts.^{28,29} Furthermore enynes are useful building blocks in organic synthesis, such as the [4+2] benzannulation reaction between an enyne and a enynophile (Scheme 6.18).³⁰ They are also used in the synthesis of white organic light-emitting devices (WOLEDs)³¹ and can be converted into conjugated polymers.³²



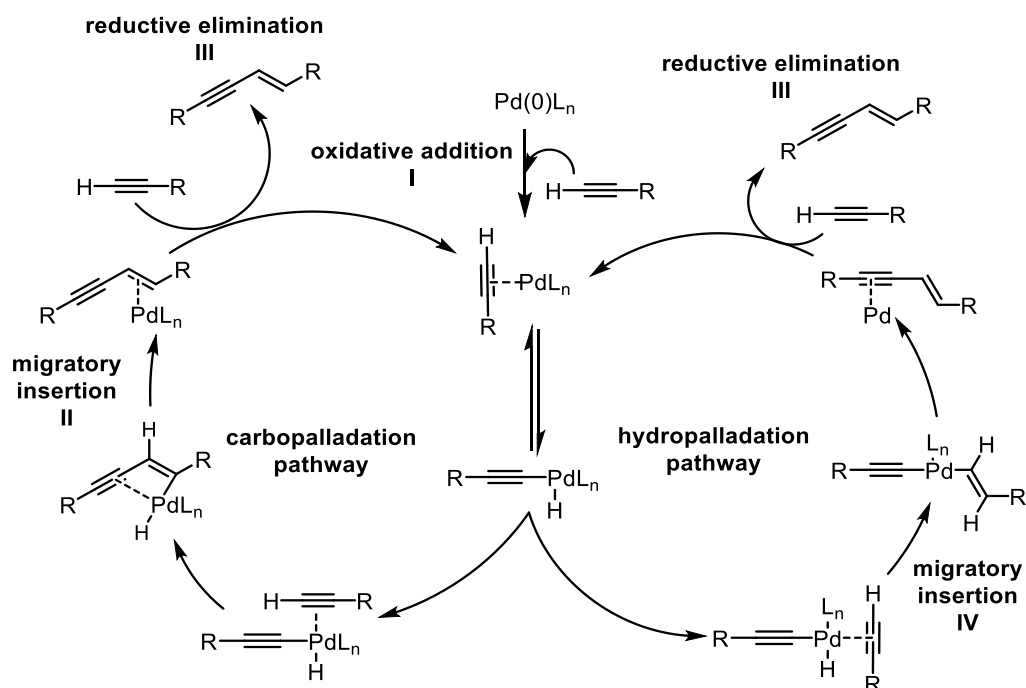
Scheme 6.18: [4+2] benzannulation reaction.³⁰

As enynes have been shown to be useful organic substrates and the optimised catalysis can achieve full conversion towards the dimerization product by just changing the atmosphere, an investigation was started. Initial experiments were conducted using phenylacetylene as model substrate. Control experiments revealed that only catalytic amounts of base were needed in the reactions. Scheme 6.19 is showing the conditions used in this study.



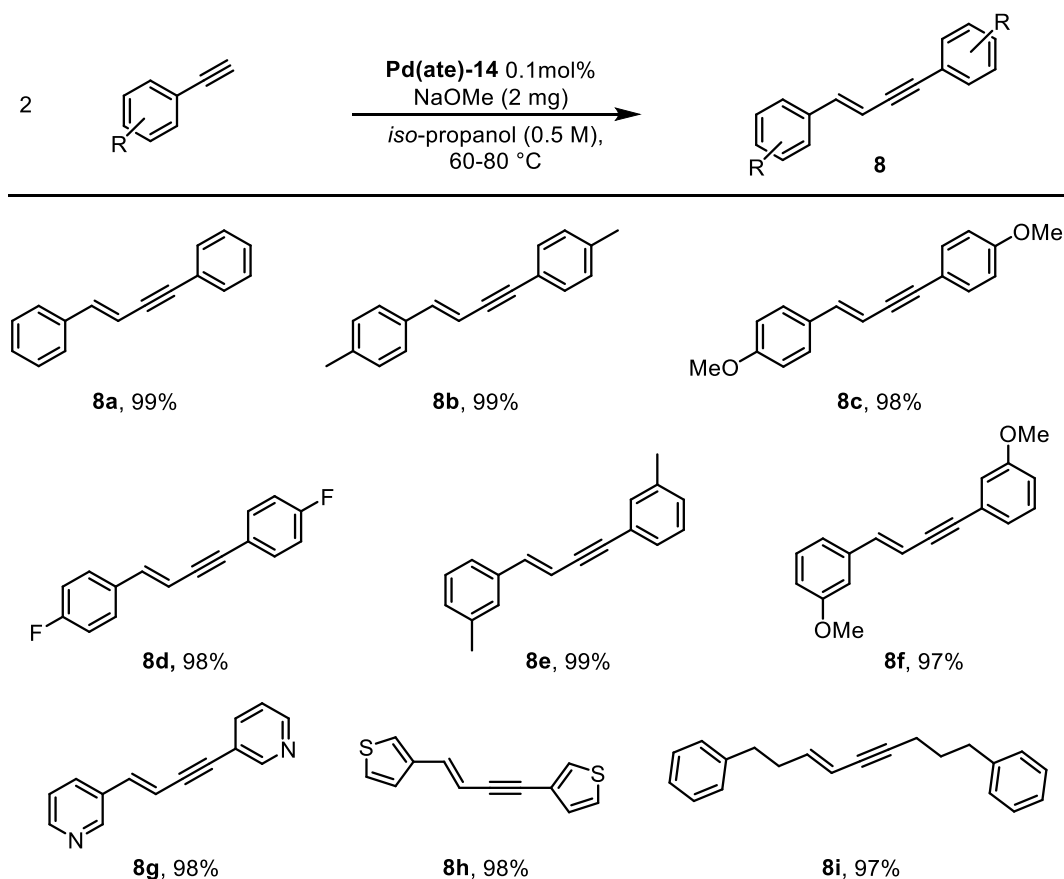
Scheme 6.19: Conditions for the dimerisation of terminal alkynes.

A closer look at the catalytic cycle was taken.²⁸ Trost and co-workers firstly reported the dimerization of terminal alkynes in 1987, where two different catalytic pathways were proposed,³³ namely the “carbopalladation” or “hydropalladation” pathway. The carbopalladation pathway for the dimerization of terminal alkynes was hypothesised by Toste and co-workers.³⁴ The catalytic cycle starts with the oxidative addition of the terminal alkynes with the Pd(0) species (Scheme 6.20, **I**). This is followed by the addition of the second terminal alkyne and the migratory insertion into the Pd-C bond (Scheme 6.20, **II**). The product is released *via* the reductive elimination and the incoming of a terminal alkyne (Scheme 6.20, **III**). Hagihara and co-workers reported the oligomerisation of terminal acetylene, hypothesising an hydropalladation pathway.³⁵ The main difference from the carbopalladation pathway is the migratory insertion. In the hydropalladation pathway, the second terminal alkyne will be migratory inserted into the Pd-H bond (Scheme 6.20, **IV**).²⁸ In the discussed system, both pathways are possible and further mechanistic studies would be required to reveal the pathway followed in this reaction.



Scheme 6.20: Proposed mechanism for the dimerisation of terminal alkynes.²⁸

A scope was conducted, starting with different *para* substituents on the aryl ring. Firstly *para*-tolylacetylene was tested, resulting in full conversion to the enyne (Scheme 6.21, **8b**). When changing to an electron-donating group (Scheme 6.21, **8c**) no drop of reactivity was observed, similar results were obtained when electron-withdrawing groups (Scheme 6.21, **8d**) were used. Changing the position of the substituent to the *meta* position was well tolerated as well (Scheme 6.21, **8e** and **8f**). Substituents in the *ortho* position of the aryl ring although is not tolerated and results in no conversion. Heteroaromatic substrates, such as 3-ethynylpyridine (Scheme 6.21, **8g**) and 3-ethynylthiophene (Scheme 6.21, **8h**) did result in full conversion and 98% isolated yield. 1-Methyl-4-vinyl benzene was dimerised successfully resulting in 97% isolated yield, indicating that aryl substituent of the alkyne starting material is not necessary for reactivity.



Scheme 6.21: Scope of the dimerization of terminal alkynes Reaction conditions: In air, [IPr*·H][Pd(η^3 -2-Me-allyl)Cl₂] (0.1 mol%), NaOMe (2 mg) and *iso*-propanol (0.5 M) was heated at 60 °C for 1 h. Then the corresponding acetylene (0.5 mmol) was added. The reaction was left to stir (910 rpm) for 2 h at 80 °C. Average of two runs. Isolated yield.

6.4 Conclusion

The applications of [NHC·H][Pd(R- η^3 -allyl)Cl₂] pre-catalysts were extended to the Sonogashira reactions. A wide optimisation was conducted, synthesising and testing different [NHC·H][Pd(R- η^3 -allyl)Cl₂] pre-catalysts. [IPr*·H][Pd(η^3 -2-Me-allyl)Cl₂] was shown to be the optimal pre-catalyst. A very highly catalytic activity protocol was established with very low catalyst loadings (0.1 mol%). A scope was established, showing no significant loss of reactivity when changing the electronic properties of the aryl bromides. Electronically different substituents were allowed on the acetylene, resulting in moderate yields. The dimerization of 1,3-enynes was successfully studied using [IPr*·H][Pd(η^3 -2-Me-allyl)Cl₂] as pre-catalyst. Excellent yields were obtained in the scope.

6.5 References

- (1) Dieck, H. A.; Heck, F. R. *J. Organomet. Chem.* **1975**, *93*, 259–263.
- (2) Cassar, L. J. *Organomet. Chem.* **1975**, *93*, 253–257.
- (3) Sonogashira, K.; Tohda, Y.; Hagihara, N. *Tetrahedron Lett.* **1975**, *16*, 4467–4470.
- (4) Corona, C.; Bryant, B. K.; Arterburn, J. B. *Org. Lett.* **2006**, *8*, 1883–1886.
- (5) Tessier, P. E.; Penwell, A. J.; Souza, F. E. S.; Fallis, A. G. *Org. Lett.* **2003**, *5*, 2989–2992.
- (6) Nagy, A.; Novák, Z.; Kotschy, A. J. *Organomet. Chem.* **2005**, *690*, 4453–4461.
- (7) Spivey, A. C.; McKendrick, J.; Srikanan, R.; Helm, B. A. *J. Org. Chem.* **2003**, *68*, 1843–1851.
- (8) Ten Brink, H. T.; Rijkers, D. T. S.; Liskamp, R. M. J. *J. Org. Chem.* **2006**, *71*, 1817–1824.
- (9) Chinchilla, R.; Najera, C. *Chem. Soc. Rev.* **2011**, *40*, 5084–5121.
- (10) Chinchilla, R.; Najera, C. *Chem. Rev.* **2007**, *107*, 874–922.
- (11) Tohida, Y.; Sonogashira, K.; Hagihara, N. *Tetrahedron Lett.* **1977**, 777–778.
- (12) Takahashi, S.; Kuroyama, Y.; Sonogashira, K.; Hagihara, N. *Synthesis* **1980**, 627–630.
- (13) Glaser, C. *Berichte der Dtsch. Chem. Gesellschaft* **1869**, *2*, 422.
- (14) Glaser, C. *Ann. Chem. Pharm.* **1870**, *154*, 137.
- (15) Leadbeater, N. E.; Tominack, B. J. *Tetrahedron Lett.* **2003**, *44*, 8653–8656.
- (16) Soheili, A.; Albaneze-Walker, J.; Murry, J. A.; Dormer, P. G.; Hughes, D. L. *Org. Lett.* **2003**, *5*, 4191–4194.
- (17) Hierso, J. C.; Fihri, A.; Amardeil, R.; Meunier, P.; Doucet, H.; Santelli, M.; Ivanov, V. V. *Org. Lett.* **2004**, *6*, 3473–3476.
- (18) McGuinness, D. S.; Cavell, K. J. *Organometallics* **2000**, *19*, 741–748.
- (19) Rahman, M. T.; Fukuyama, T.; Ryu, I.; Suzuki, K.; Yonemura, K.; Hughes, P. F.; Nokihara, K. *Tetrahedron Lett.* **2006**, *47*, 2703–2706.
- (20) Alonso, D. A.; Nájera, C.; Pacheco, M. C. *Tetrahedron Lett.* **2002**, *43*, 9365–9368.
- (21) Alonso, D. A.; Nájera, C.; Pacheco, M. C. *Adv. Synth. Catal.* **2003**, *345*, 1146–1158.
- (22) Yang, C.; Nolan, S. P. *Organometallics* **2002**, *21*, 1020–1022.
- (23) Tong, Z.; Gao, P.; Deng, H.; Zhang, L.; Xu, P. F.; Zhai, H. *Synlett* **2008**, *1*, 3239–3241.
- (24) Ray, L.; Barman, S.; Shaikh, M. M.; Ghosh, P. *Chemistry* **2008**, *14*, 6646–6655.
- (25) John, A.; Shaikh, M. M.; Ghosh, P. *Dalt. Trans.* **2009**, 10581.
- (26) Roy, S.; Plenio, H. *Adv. Synth. Catal.* **2010**, *352*, 1014–1022.
- (27) Gallop, C. W. D.; Chen, M.; Navarro, O. *Org. Lett.* **2014**, *16*, 3724–3727.
- (28) Jahier, C.; Zatulochnaya, O. V.; Zvyagintsev, N. V.; Ananikov, V. P.; Gevorgyan, V. *Org.*

- Lett.* **2012**, *14*, 2846–2849.
- (29) Morozov, O. S.; Asachenko, A. F.; Antonov, D. V.; Kochurov, V. S.; Paraschuk, D. Y.; Nechaev, M. S. *Adv. Synth. Catal.* **2014**, *356*, 2671–2678.
- (30) Zatolochnaya, O. V.; Galenko, A. V.; Gevorgyan, V. *Adv. Synth. Catal.* **2012**, *354*, 1149–1155.
- (31) Liu, Y.; Nishiura, M.; Wang, Y.; Hou, Z. *J. Am. Chem. Soc.* **2006**, *128*, 5592–5593.
- (32) Pasquini, C.; Fratoddi, I.; Bassetti, M. *European J. Org. Chem.* **2009**, *2*, 5224–5231.
- (33) Trost, B. M.; Chan, C.; Rühler, G. *J. Am. Chem. Soc.* **1987**, *109*, 3486–3487.
- (34) Trost, B. M.; Sorum, M. T.; Chan, C.; Harms, A. E.; Rühler, G. *J. Am. Chem. Soc.* **1997**, *119*, 698–708.
- (35) Tohda, Y.; Sonogashira, K.; Hagihara, N. *J. Organomet. Chem.* **1976**, *110*, C53–C56.

Chapter 7

Synthesis and application of [Au(NHC)(Bpin)] complexes

7.1 Introduction to gold chemistry

Gold has been present since the dawn of civilisation as one of the first metals known to mankind, its use was mainly in form of money and jewellery, representing power and beauty. Although gold has played such an important role in history, the knowledge of the chemistry of gold was minimal.¹ The main area of interest was the recovery and purification of elemental gold.¹

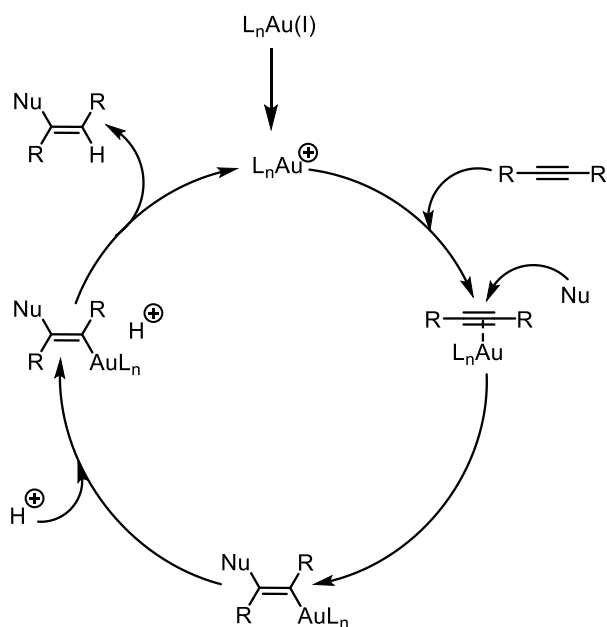
The most common oxidation states of gold are +1 and +3, although less common ones are known; -1,² +2³ and +5.⁴ In this introduction the main focus will be on Au(I) complexes, which will be expanded in Chapter 7. The unique reactivity of gold can be explained through the relativistic effect.^{4,5} This effect is seen for atoms with a large atomic number, ($Z > 50$) such as gold $Z = 79$. In a simplified explanation, the increase in velocity of electrons in the s orbital lead to an increase of their mass, thus a relativistic contraction of the s orbitals occurs. Furthermore, the contraction of s orbitals shields greatly the nuclear charge for the electrons on d and f orbitals, which diffuse in to larger orbitals. The relativistic effects reflect greatly on the coordination chemistry of gold. The energy difference between the s, p and d orbital is very small, which results to the efficient formation of linear two-coordinate complexes in Au(I).⁶ The reactivity is also affected as it results in the lowest unoccupied molecular orbital being relatively low and hence gives the gold its associated high Lewis acidity.⁷

7.1.1 Reactivity of gold complexes

Gold complexes were seen as inert and catalytically inactive until the early 1970s, when Bond and co-workers reported the hydrogenation of alkenes over a supported gold catalyst.⁸ After initial studies on the carbophilic properties of gold, reports of gold as catalysts started to emerge.^{8,9}

Nowadays gold is seen as a potent “soft” carbophilic Lewis acid, with the ability to activate π -systems such as alkynes, alkenes and allenes towards the addition of a nucleophile under very mild conditions.⁷ For example; the electrophilic gold complex withdraws electron density from the alkyne via coordination, elongating the C-C bond, making the alkyne more electrophilic and

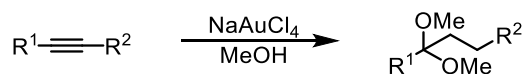
hence more desirable for an attack of a nucleophile (Scheme 7.1). In detail, the gold complex coordinates to the alkyne, followed by the attack of a nucleophile, which then undergoing a deprotonation-reprotonation sequence, releasing the gold complex and subsequently the desired product (Scheme 7.1).¹⁰



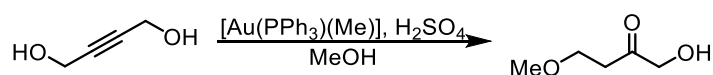
Scheme 7.1: Reactivity of gold complexes.⁷

Ito and co-workers showed in a seminal report that a chiral ferrocenylphosphine-Au(I) complex could catalyse asymmetric aldol reactions in gold yield and enantioselectivity.¹¹ Noteworthy examples are the work from Utimoto⁹ and Teles¹² demonstrating the functionalisation of alkynes using a gold catalyst (Scheme 7.2). Utimoto reported the use of a gold(III) salt, NaAuCl₄.⁹ Teles and co-workers used a cationic gold(I) complex for the catalytic addition of alcohols to alkynes (Scheme 7.2).¹²

Utimoto and co-workers:

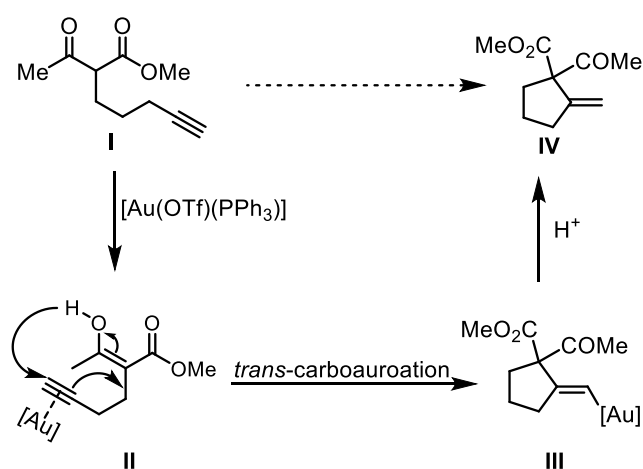


Teles and co-workers:



Scheme 7.2: Early example of the catalytic activity of gold complexes.^{9,12}

From then onwards, the interest in gold complexes and their catalytic activity in organic synthesis was sparked. Toste and co-workers reported the Conia-ene cyclisation of α,β -ketoesters using an Au(I) catalyst.¹³ The Conia-ene reaction is the cyclisation of ketones onto alkynes to give α -vinylated ketones, however high reaction temperature is normally needed.¹³ By using [Au(OTf)(PPh₃)] as a catalyst, Toste and co-workers performed the Conia-ene reaction at ambient temperature and neutral conditions, *i.e.* no use of strong acids. A mechanism was proposed starting from the nucleophilic attack on the Au(I)alkyne complex, by the enol form of the ketoester (Scheme 7.3, II). This results in the vinyl-Au(I) intermediate (Scheme 7.3, III). The product is formed after the protodeauration of III.



Scheme 7.3: Gold catalyzed Conia-ene reaction.¹³

The use of mild conditions such as low catalyst loading (1 mol%) in neutral media at room temperature, is a clear advantage, as the usually used Brønsted acids need harsh conditions, resulting in possible numerous side-reactions of the carbocationic intermediate.¹⁴ Furthermore gold catalyzed reactions are seen to be operationally safe, simple and practical, with no need for an inert atmosphere.¹⁴ The use of gold catalysis enabled the conversion of simple starting materials through an array of transformations into products with significantly increased complexity in an atom-efficient manner.¹⁴

These days, Au(I) complexes find valuable applications in the synthesis of pharmaceuticals,^{15,16} liquid crystals,¹⁷ chemical vapour deposition¹⁸ and optical devices.¹⁹

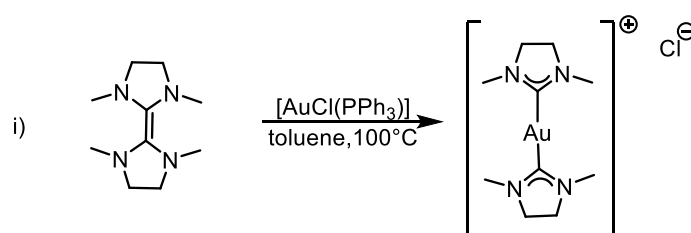
7.2 Introduction to Au(I)- NHC complexes

The use of well-defined Au(I) complexes bearing monodentate ancillary ligands has been extensively studied.²⁰ The active species in catalytic reactions is believed to be a cationic, mono-ligated gold species, where the use of N-heterocyclic carbene (NHC) ligands comes in favour as the σ -donating nature of the carbenes can stabilise the catalytically active gold species.²¹ The Au(I)-NHC bond is a three-centre four-electron hyperbond, where the NHC ligand can donate electron-density to the 6s orbital of the gold. The NHC-metal bond was discussed in Section 1.1, where it was stated that σ -bonding is the main bonding between the NHC and the metal, with partial π -back donation of the metal to the NHC.

Au(I)-NHC complexes can show high back donation with a π -acceptance of around 50%, this was intensely studied by Zuccaccia and co-workers.²² It was postulated that the Au-NHC bond can adapt in a reaction depending on the substrates present, allowing the gold to undergo bond cleavage or formation with different substrates during the catalysis.²² Nowadays gold-NHC complexes are widely studied and reviewed.^{21,23}

7.2.1 Synthesis of cationic Au(I)-NHC complexes

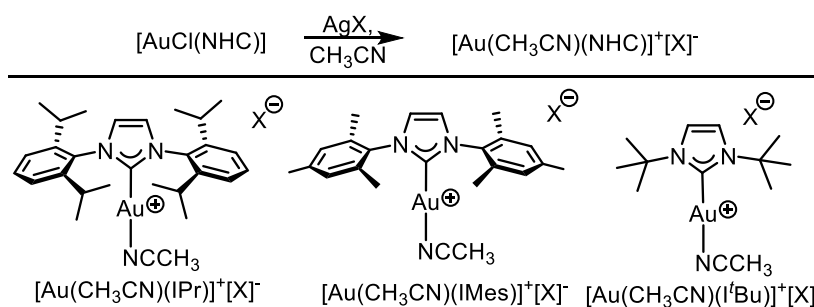
Several syntheses have been reported for cationic Au(I)-NHC complexes; Lappert and co-workers reported in 1974 the synthesis of a cationic $[\text{Au}(\text{NHC})_2]^+$ species from cleavage of a dimeric saturated NHC and $[\text{AuCl}(\text{PPh}_3)]$ (Scheme 7.4).²⁴ However, only saturated NHCs can form dimers, which limits the synthesis.²⁵



Scheme 7.4: Synthesis of $[\text{Au}(\text{IME})_2]^+[\text{Cl}]^-$ (IME = *N,N'*-dimethylimidazol-2-ylidene).²⁴

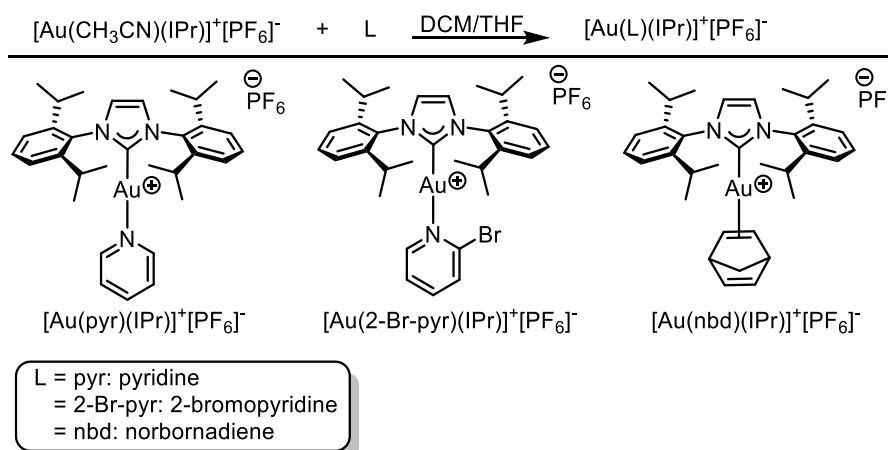
The synthesis of $[\text{Au}(\text{MeCN})(\text{IPr})^+[\text{X}]^-$ (IPr = *N,N'*-bis-[2,6-(di-*iso*-propyl)phenyl]imidazol-2-ylidene, X = PF_6 , BF_4) was reported by Nolan and co-workers in 2006 (Scheme 7.5).²⁶ The facile synthesis started from the well-defined $[\text{AuCl}(\text{IPr})]$ complex and stoichiometric amounts of AgPF_6 or AgBF_4 in acetonitrile as solvent (Scheme 7.5). The cationic complexes were air stable white solids, and fully described in their solution and solid state.²⁶ The synthesis of $[\text{Au}(\text{MeCN})(\text{NHC})^+[\text{X}]^-$ complexes was expanded using different NHCs, such as IMes (*N,N'*-bis-

[2,4,6-(trimethyl)phenyl]imidazol-2-ylidene), $t^t\text{Bu}$ (N,N' -(di-*tert*-butyl)imidazol-2-ylidene) and IAd (N,N' -bis-(adamantyl)imidazol-2-ylidene).²⁷



Scheme 7.5: Synthesis and examples of $[\text{Au}(\text{MeCN})(\text{NHC})]^+[\text{X}]^-$ complexes.^{26,27}

Furthermore, these complexes were used to synthesise a range of different cationic Au(I)-NHC complexes,²⁷ by addition of other coordinating organic substrates such as substituted pyridines and norbornadiene (Scheme 7.6). Again, all obtained complexes were air-stable, white complexes and obtained in good to excellent yield.²⁷

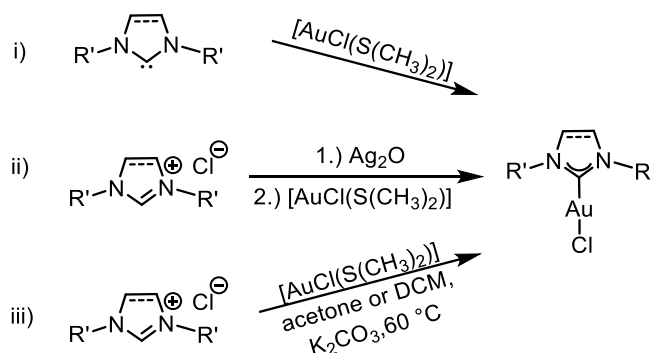


Scheme 7.6: Synthesis and examples of $[\text{Au}(\text{L})(\text{IPr})]^+[\text{PF}_6]^-$.²⁷

7.2.2 Synthesis of neutral Au(I)-NHC complexes

Three main routes are used for the synthesis of neutral Au(I)-NHC complexes: The free carbene route, is a common and widely applied synthesis for $[\text{AuCl}(\text{NHC})]$ complexes, starting from $[\text{AuCl}(\text{S}(\text{CH}_3)_2)]$ and the corresponding free NHC, which can be generated from its NHC salt, *via* deprotonation of a strong inorganic base (KO^tBu) (Scheme 7.7, i).²³ Lin and co-workers developed the transmetalation route for $[\text{AuCl}(\text{NHC})]$, starting from the corresponding silver-NHC complex as transmetalation agent (Scheme 7.7, ii).^{28,29} Nolan and co-workers applied this method to synthesise a variety of different $[\text{AuCl}(\text{NHC})]$ complexes.³⁰ A straightforward and

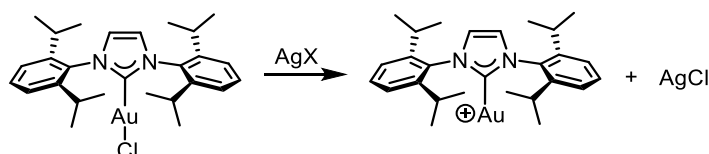
facile synthesis of [AuCl(NHC)] complexes was reported simultaneously by Nolan³¹ and Gimeno³² in 2013 starting from the corresponding NHC salt and [AuCl(S(CH₃)₂)] or [AuCl(tht)] (tht = tetrahydrothiophene). The synthesis was performed in air using a weak inorganic base (K₂CO₃) (Scheme 7.7, iii).^{31,32} Of note, using these syntheses allows the preparation of [AuCl(NHC)] complexes bearing a wide range of NHC ligands bearing different electronic and steric character.³¹



Scheme 7.7: Synthesis of Au(I)-NHC complexes.^{23,24,28–32}

7.2.3. Catalytic applications of Au(I)-NHC complexes

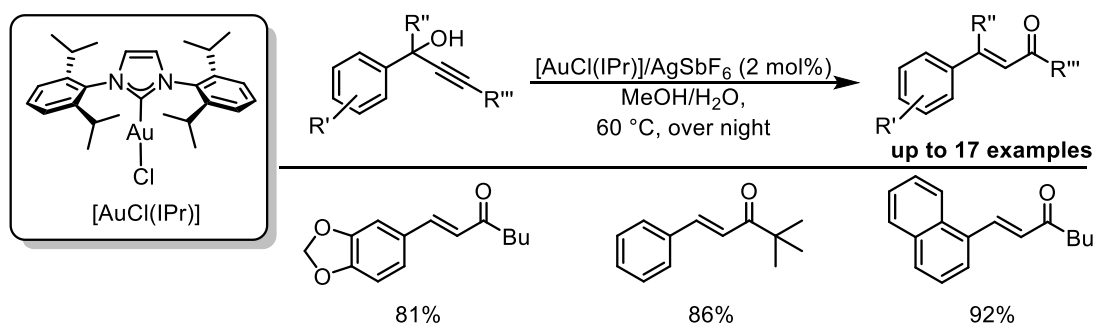
Au(I)-NHC complexes are very active catalysts in a wide range of different organic reactions,^{10,21,23,33–37} due to the size of this field only selected examples were give. After the successful synthesis of [AuCl(NHC)] complexes, different catalytic reactions were tested, such as cycloisomerization reactions³⁸ and rearrangement reactions.^{21,39} For the neutral [AuCl(NHC)] pre-catalyst, usually an activation step has to be introduced to release active species *in situ* prior to catalysis. The activation of [AuCl(NHC)] to its catalytic active species can be achieved using a silver(I) salt with a non-coordinating anion such as BF₄⁻, OTf⁻ or SbF₆⁻, which undergoes a salt metathesis to form the catalytically active species [Au(NHC)]⁺ and silver chloride (Scheme 7.8).⁴⁰ [Au(NHC)]⁺ then can coordinate to the organic substrate and start the catalysis, however the actual structure of the active species is not known as the activation is done *in situ*.⁴¹ Although this is a facile process, the silver salt showed catalytic properties that could co-catalyse or interfere in the chosen reaction.⁴²



Scheme 7.8: Proposed activation of [AuCl(NHC)] complexes.⁴¹

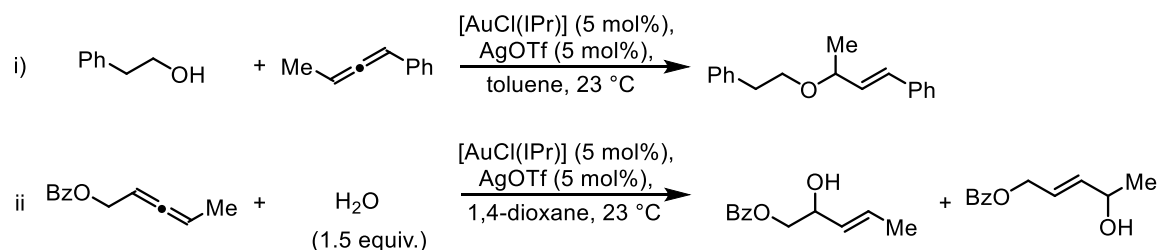
Therefore, the elimination of silver(I) salts did improve the understanding of pure gold catalysis. Examples of the silver-free gold catalysed reactions will be given in this section.

Nolan and co-workers reported the Meyer-Schuster rearrangement of propargylic alcohols, catalysed by [AuCl(IPr)], in the presence of a silver(I) salt.⁴³ The synthesis of α,β -unsaturated ketones was reported using low catalyst loading (2 mol%) to achieve high yields (Scheme 7.9).⁴³ Challenging substrates such as tertiary- and sterically hindered alcohols were allowed in the rearrangement.



Scheme 7.9: The Meyer-Schuster rearrangement of propargylic alcohols catalysed by [AuCl(IPr)].⁴³

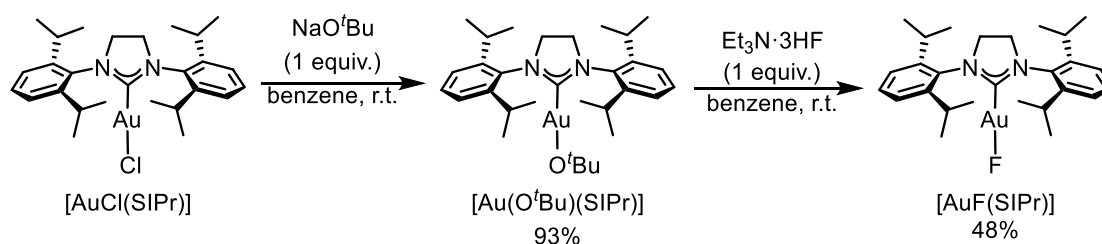
Widenhöfer and co-worker described the intermolecular hydroalkoxylation of allenes with alcohols to yield alkyl allylic ethers using [AuCl(IPr)] as catalyst.⁴⁴ The reaction was regio- and stereoselective and a wide scope was obtained by using also 1,1- and 1,3-disubstituted allenes as well as *tri*- and *terta*-substituted allenes as starting materials (Scheme 7.10, i).⁴⁴ The same group reported the hydration of allenes to form (*E*)-allylic alcohols using [AuCl(IPr)] in the presence of AgOTf (Scheme 7.10, ii).⁴⁵ Control experiments were conducted to prove the need of both catalysts, *i.e.* the gold and silver species. Furthermore, the reaction proceeded in good yield when a water miscible solvent was used.



Scheme 7.10: Hydroalkoxylation and hydration of allenes catalysed by [AuCl(IPr)] complex.^{44,45}

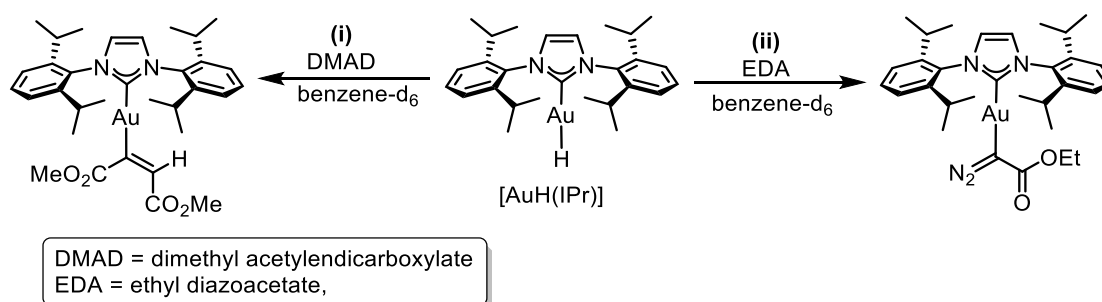
The unique properties of NHCs as ligand in organometallic complexes was mentioned in Section 1.1. The NHC ligand in a gold complex, stabilises generally unstable Au(I) species and allows the isolation of new Au(I) species. This was illustrated by Sadighi and co-workers in 2005, as the first

isolable Au(I) fluoride complex was reported.⁴⁶ The metal-F bond is of interest due to π -donating nature of fluoride ions, which can lead to a destabilising interaction with filled d-orbitals on gold. This potentially can result in synthetically very interesting complexes, with unique reactivity such as a potential C-F bond formation.^{47–50} [AuCl(SIPr)] was reacted with one equivalence of NaO^tBu to give [Au(O^tBu)(SIPr)] in high yield, followed by the addition of one equivalence of HF in the form of triethylamine tri(hydrofluoride) to give [AuF(SIPr)] (Scheme 7.11).⁴⁶



Scheme 7.11: Synthesis of [AuF(SIPr)].⁴⁶

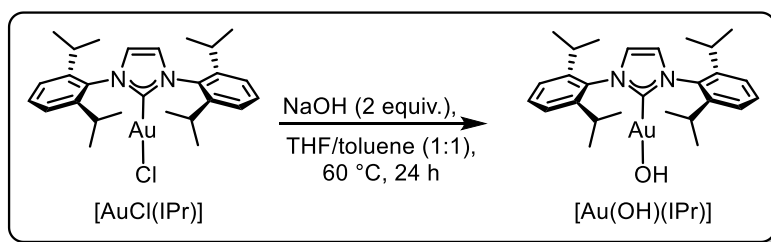
The same group reported three years later the synthesis of a monomeric terminal hydride Au(I) complex bearing a NHC ligand.⁵¹ This, again was the first isolated Au(I) hydride complex, furthermore [AuH(IPr)] was fully characterised.⁵¹ Gold hydride complexes have been discussed before in the literature as intermediates in gold catalysed reactions, but they had never been isolated.⁵² The reactivity of [AuH(IPr)] was investigated as well, which revealed a *trans* addition to an electrophilic alkyne (Scheme 7.12, i) and deprotonation of a diazo compound to the α -aurated derivative (Scheme 7.12, ii).⁵¹



Scheme 7.12: Reactivity of [AuH(IPr)].⁵¹

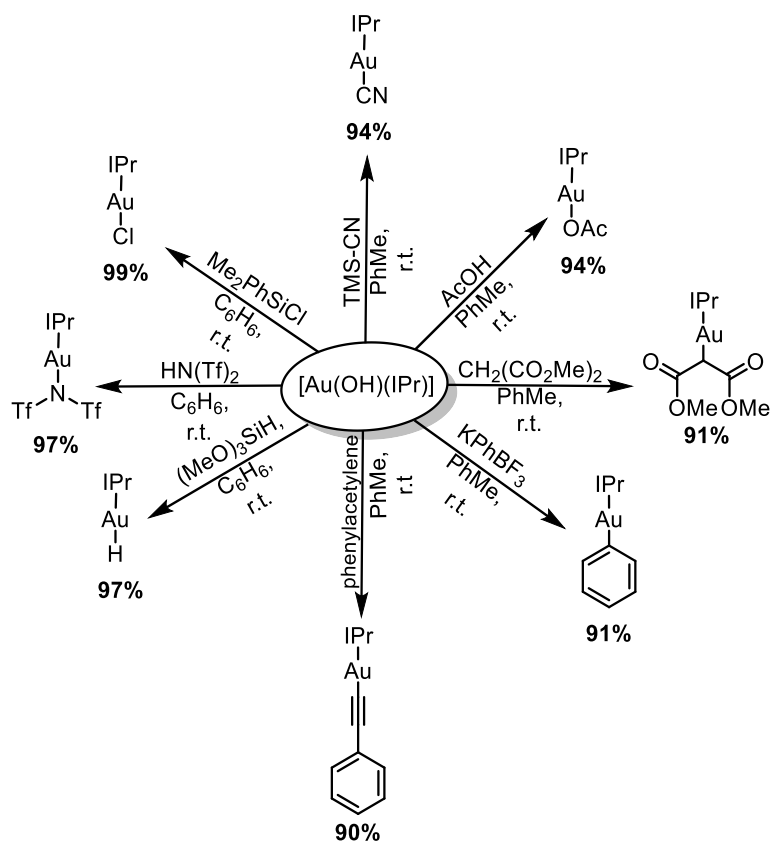
In 2010, Nolan and co-workers reported the synthesis of [Au(OH)(IPr)],⁵³ firstly reported as an *in-situ* generated catalytic species in the catalysis of α,β -unsaturated carbonyl compounds.⁵⁴ It was reasoned that a gold hydroxide complex could be used in a more environmentally friendly way, therefore the synthesis was attempted starting from [AuCl(IPr)].⁵³ A metathesis reaction was performed using different alkali metals such as CsOH, NaOH and KOH.⁵³ [Au(OH)(IPr)] was isolated in high yields, and the reaction proceeded in air with technical grade solvent, showing

an unprecedented robustness of this synthesis.⁵³ The synthesis was later applied to different [AuCl(NHC)] complexes, bearing a wide range of NHC ligands (Scheme 7.13).⁵⁵



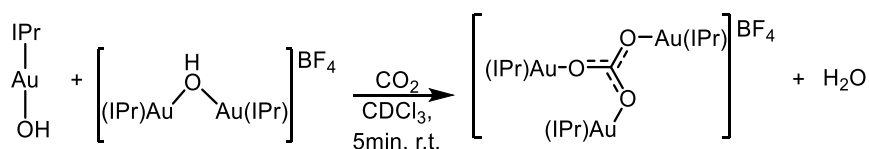
Scheme 7.13: Synthesis of [Au(OH)(IPr)] from [AuCl(IPr)].⁵³

This new air-stable Au(I) hydroxide complex was studied by Nolan and co-workers. The treatment with an acid such as HCl, gave the precursor [AuCl(IPr)].⁵³ [Au(OH)(IPr)] was treated with different organic reagents, such as trimethylsilyl cyanide, which lead to [Au(CN)(IPr)] in high yield. Furthermore protonolysis with acetic acid resulted in the formation of [Au(OAc)(IPr)], similarly the treatment with malonate gave [Au(CH(CO₂Me)₂)(IPr)] in excellent yield. The Gagosz-type complex [Au(NTf₂)(IPr)]^{56,57} (NTf₂ = bis-(trifluoromethane sulfonyl)imidate) was synthesised starting from HN(Tf)₂ in benzene in good yield. In Scheme 7.14, the vast applications of [Au(OH)(IPr)] are presented.



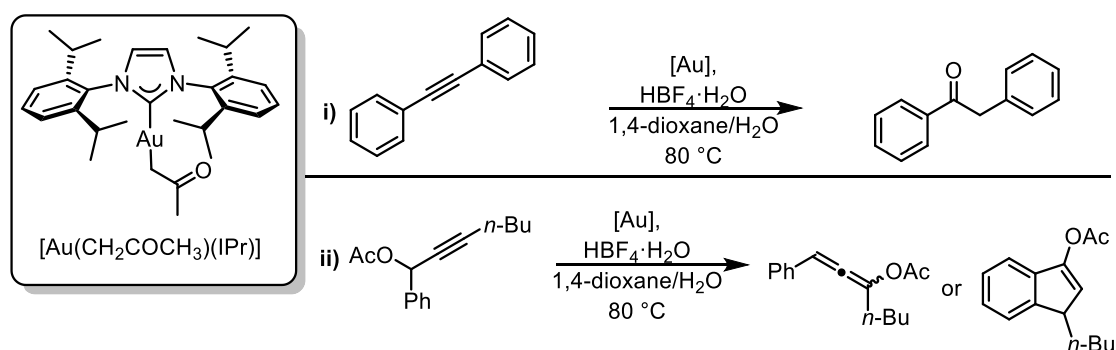
Scheme 7.14: Reactivity of [Au(OH)(IPr)] complexes.⁵³

The reactivity of [Au(OH)(NHC)] was evaluated extensively. Gold hydroxide complexes have the ability to fix CO₂,⁵⁸ this was illustrated with [Au(OH)(NHC)] in combination with the digold hydroxide complex, [{Au(IPr)}₂(μ-OH)][BF₄]. The digold hydroxide complexes can be synthesised in a straightforward manner starting from [Au(OH)(NHC)] and HBF₄ in aqueous media.⁵⁹ Interestingly [{Au(IPr)}₂(μ-OH)][BF₄] showed high catalytic activity in the Meyer-Schuster rearrangement enabling low catalyst loading (2 mol%). The CO₂ feedstock is abundant and cheap and therefore the storage of CO₂ is very interesting. By exposing [Au(OH)(NHC)] and [{Au(IPr)}₂(μ-OH)][BF₄] to CO₂ a trigold carbonate complex was formed (Scheme 7.15).⁵⁸ This reaction was reversible and the newly obtained complex behaved with two basic and one cationic gold centres.



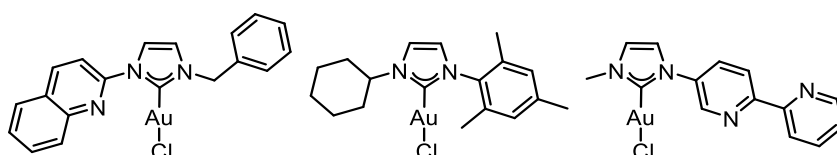
Scheme 7.15: Trapping of CO₂ with gold(I) hydroxide and digold OH complexes.⁵⁸

The synthesis of novel gold(I)-acetyl complexes $[\text{Au}(\text{CH}_2(\text{O})\text{CH}_3)(\text{IPr})]$ were investigated by Nolan and co-workers, by reacting Au precursors with acetone in K_2CO_3 (Scheme 7.16).⁶⁰ Firstly seen as side-products, these Au(I)-NHC complexes showed many interesting reactivities.⁶⁰ The authors illustrated three synthetic routes to obtain these complexes in good yield. All routes start from NHC·HCl, but three different gold precursors such as $[\text{AuCl}(\text{S}(\text{CH}_3)_2)_2]$, $[\text{AuCl}(\text{NHC})]$ or $[\text{Au}(\text{OH})(\text{NHC})]$.⁶⁰ A library of different Au(I)-acetyl complexes bearing different NHCs was synthesised. These complexes can be used as precursors for different Au(I)-NHC complexes such as the Gasgosz complex $[\text{Au}(\text{NTf}_2)(\text{NHC})]$ or $[\text{AuH}(\text{NHC})]$.⁶⁰ Furthermore, $[\text{Au}(\text{CH}_2(\text{O})\text{CH}_3)(\text{IPr})]$ showed catalytic activity in the hydration of alkynes to ketones (Scheme 7.16, i) and the rearrangements of propargylic acetate to substituted indene or allenes varying the reaction times (Scheme 7.16, ii).⁶⁰



Scheme 7.16: Catalytic reactivity of $[\text{Au}(\text{CH}_2(\text{O})\text{CH}_3)_2(\text{IPr})]$.⁶⁰

Lastly, a very recent example will be discussed. Earlier this year Hemmert and Gornitzka reported a series of $[\text{AuCl}(\text{NHC})]$ complexes with functionalised NHC ligands (Scheme 7.17). The complexes were synthesised using the transmetalation route with Ag_2O in good to excellent yields.⁶¹ Furthermore these complexes were screened *in vitro* for antileishmanial activities. Leishmania is a parasitic diseases, which is currently threatening 350 million people all around the world.⁶¹ Promising results were obtained showing that $[\text{AuCl}(\text{NHC})]$ could be potential metallodrugs, showing selective action against the pathologically relevant form of Leishmania.



Scheme 7.17: Examples of $[\text{AuCl}(\text{NHC})]$ complexes synthesised by Hemmert and Gornitzka.⁶¹

Several papers were published in the last years investigating Au(I)-NHC complexes in medicinal chemistry.⁶² Rigobello, Kühn and Casini reported a series of Au(I) complexes bearing sulfonated

bis(NHC) ligands and hydroxylated Au(I) mono(NHC) complexes as promising anticancer reagents.⁶³ These complexes were tested as potent thioredoxin reductase inhibitors, showing promising results.⁶³ The group of Veige reported the synthesis of cationic Au(I)-NHC complexes and the study for anti-tumour activities, resulting in highly cytotoxic Au(I)-NHC complexes.⁶⁴

In conclusion, the use of NHCs as ligands for the synthesis of novel Au(I) complexes is an active and vibrant field in organometallic chemistry, shown by the examples in this introduction. Furthermore Au(I)-NHC complexes shown interesting and unique catalytic reactivity. Therefore the synthesis of new Au(I)-NHC complexes could reveal novel organometallic complexes together with new catalytic transformations.

7.3 Introduction to transition metal-boron complexes

Metal boron bonds have been extensively studied experimentally and theoretically in the last decades to understand their structure and reactivity.^{65–69} Initially reported in 1963,⁷⁰ metal-boron complexes are important intermediates in catalytic hydroboration, diboration and selective C-H bond activation. Nonetheless, the first proven metal-boron complex was reported thirty years later.^{65,71–73} There are three different coordination modes for metal-boron complexes, namely metal-borane-, metal borylene- and metal boryl complexes (Figure 7.18).⁷⁴ Transition-metal-boryl complexes have especially been investigated as intermediates in many organic/organometallic reactions,^{75,76} such as in the Suzuki-Miyaura reaction. Thomas and Denmark reported three different species containing a palladium-oxygen-boron linkage as possible intermediates in the Suzuki-Miyaura reaction.⁷⁷ The synthesis of copper(I) β -boryl complexes from alkene insertion into [Cu(IPr)(Bpin)] was shown by Sadighi and co-worker.⁷⁸ Miyaura and co-workers reported the synthesis of nucleophilic β -boryl copper species starting from B₂pin₂. α - β -unsaturated carbonyl compounds and terminal alkynes were added to the boryl copper species in order to afford new access to β -boryl carbonyl compounds and alkenylboronates.⁷⁹

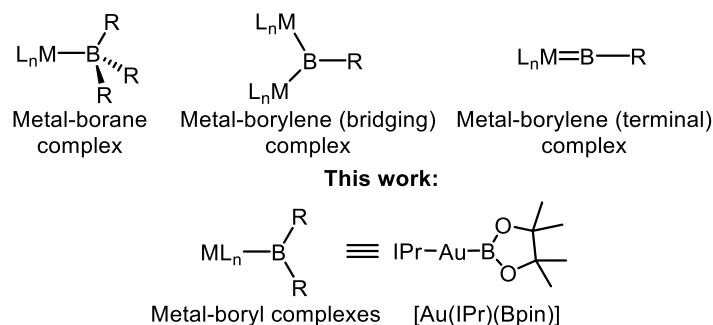
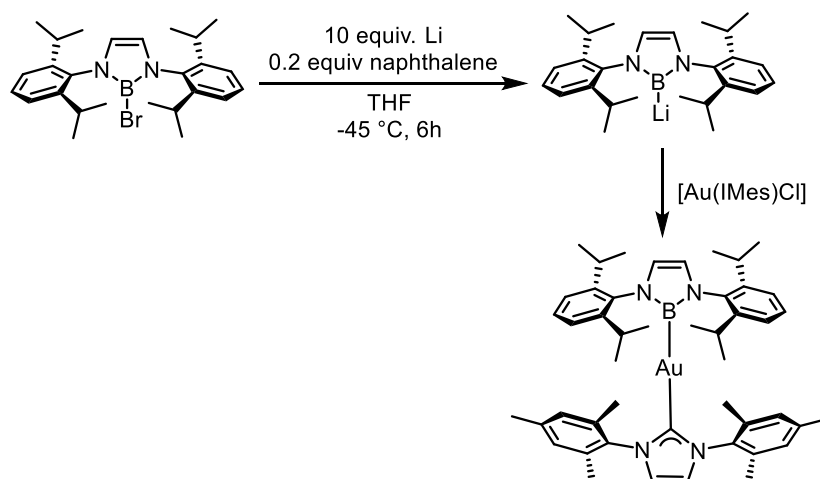


Figure 7.18: Examples of different metal-boron complexes.⁷⁴ (M = metal, L_n = ligand, R = rest)

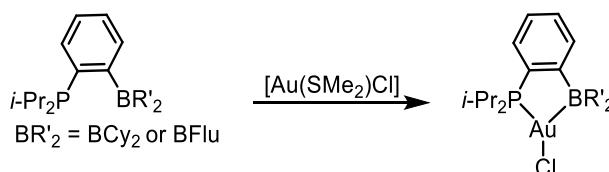
A metal boryl complex has a boron ligand with a coordination number of three, linking a BR₂ group to a metal centre. The bond between the transition-metal and the boron can be described as a two electron two centre bond. The M-BR₂ bond is understood as having a weak π component and a strong σ -donating component due to the strong *trans* influence of the boryl ligand. The electronics of the boryl ligand can be altered by changing the nature of the substituents on the boron atom, this means the boryl ligand can either have an electrophilic character or a nucleophilic character.⁸⁰

Gold-boron complexes have only rarely occurred in the literature until 2006. The main issue was the challenge of the insufficient reducing strength of Au(I) or nucleophilicity to break boron-halide bonds or to donate to a nonbridging Lewis acidic borane. There are four main syntheses to introduce a boron ligand; 1) The salt elimination of an anionic metal carbonyl complex followed by the reaction with a haloborane.⁷⁰ 2) The oxidative addition of a boron-heteroatom bond to a low-valent transition metal.⁸¹ 3) The σ -bond metathesis reaction either between an alkyl metal complex and a hydroborane⁸² or an oxygen-substituted metal complex and a diborane.^{79,83,84} 4) The nucleophilic substitution by boryl lithium compounds on metal chloride complexes. The latter was reported by Yamashita and Nozaki, who synthesised the first boryl anion; a boryl lithium compound, which can react with several electrophiles including metal complexes (Scheme 7.19).^{68,85-88} This was the first report of a boryl gold complex with a two centre two electron metal-boron bond.



Scheme 7.19: Synthesis of a boryl gold complex reported by Yamashita and Nozaki.⁸⁵

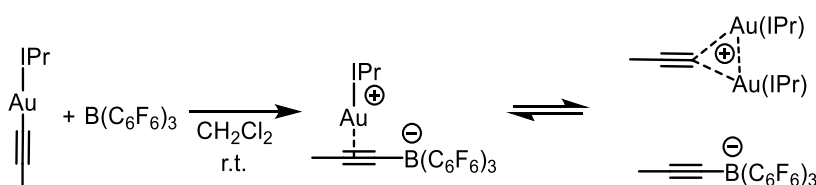
As Yamashita and Nozaki concentrated on the boryl gold (Au-B) interaction, Bourissou and co-workers were more interested in the borane gold interaction.^{76,89–91} A borane gold complex was synthesised containing a monophosphine-borane ligand, which behaved like a bidentate ambiphilic ligand. This resulted in a P to M to B interaction (Scheme 7.20).⁹²



Scheme 7.20: Monophosphine borane gold complex.⁹²

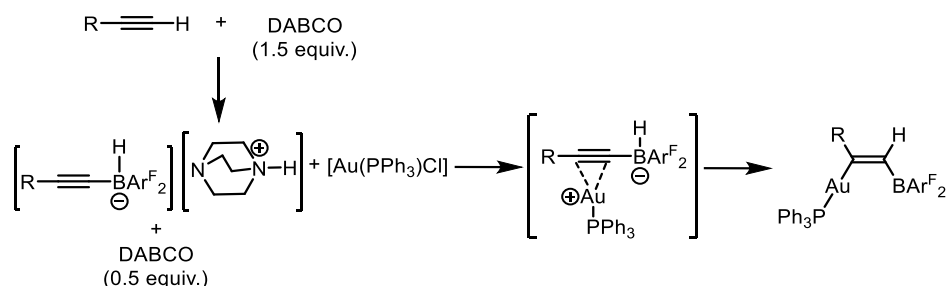
These donor (Au) to acceptor (B) contribution interactions were previously not reported for 14 electron complexes.

Hashmi and co-workers on the other hand reported the synthesis of a stable zwitterionic π -alkyne gold complex containing a borate moiety.⁹³ This was synthesised by reacting gold acetylides with $\text{B}(\text{C}_6\text{F}_6)_3$ in CH_2Cl_2 . Interestingly this can then form a *gem*-diaurated complex with a borate counterion (Scheme 7.21).



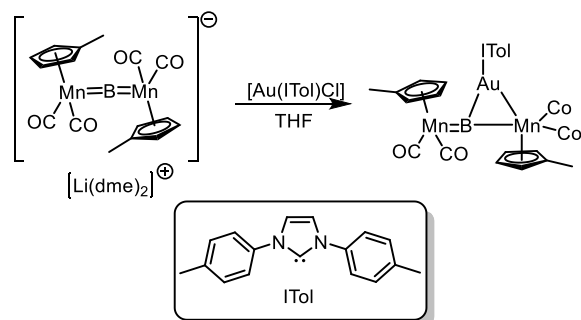
Scheme 7.21: Reaction of a zwitterionic π -alkyne gold complex containing a borate moiety.⁹³

A similar intermediate formation was reported by Li and Wang in the reaction between an ammonium alkynylhydridoborate salt and [Au(PPh₃)Cl] (Scheme 7.22).⁹⁴ The gold-alkyne π -intermediate, then undergoes concerted 1,2-hydride migration and the formation of an Au-C σ -bond.



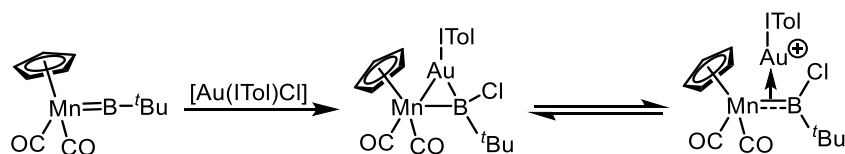
Scheme 7.22: Boroauration of terminal alkynes.⁹⁴

A unique bonding pattern was reported by Braunschweig and co-workers, in the form of an unprecedented Mn-B-Au bonding in a trimetallic dimanganese boryl gold complex (Scheme 7.23).⁶⁹



Scheme 7.23: Dimanganese boryl gold complex.⁶⁹

By changing from [Li(dme)₃][{(η⁵-C₅H₄Me)(OC)₂Mn}₂B] to [(η⁵-C₅H₅)(OC)₂Mn=B^tBu] Braunschweig and co-workers synthesised an anionic σ -coordinated metal-haloboryl complex, where the gold cation is coordinating by a transition metal-B single bond.⁹⁵ As depicted in Scheme 7.24, [(η⁵-C₅H₅)(OC)₂Mn=B^tBu] was reacted with [Au(PPh₃)Cl] in a stoichiometric amount to form the product via halide transfer from Au(I) to boron.⁹⁵



Scheme 7.24: Synthesis of an anionic σ -coordinated metal-haloboryl complex.⁹⁵

In order to get a better understanding of the nature of the transition metal boron bond, it was attempted to synthesis a stable transition metal boron complex. Our attention was drawn to Au-NHC complexes in order to synthesis a NHC-gold-boron complex specifically [Au(NHC)(Bpin)].

7.4 Synthesis of [Au(NHC)(Bpin)] complexes

The conditions for the synthesis of [Cu(Bpin)(IPr)] reported by Sadighi and co-workers⁹⁶ used using B₂pin₂ as boron source. Sadighi started the investigation by using [CuF(SIPr)], but changed the copper source to [Cu(O^tBu)(SIPr)] due to an unwanted side-reaction, limiting the yield to 50%. Having this in mind different gold complexes (Figure 7.2) were reacted with excess of B₂pin₂.

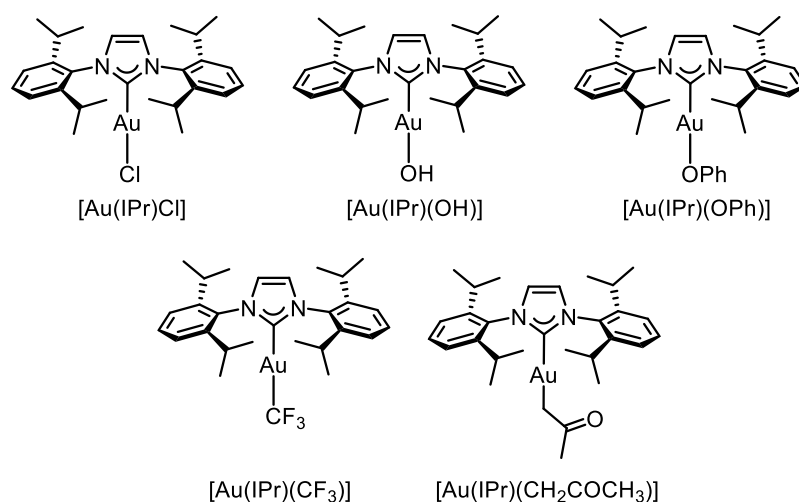
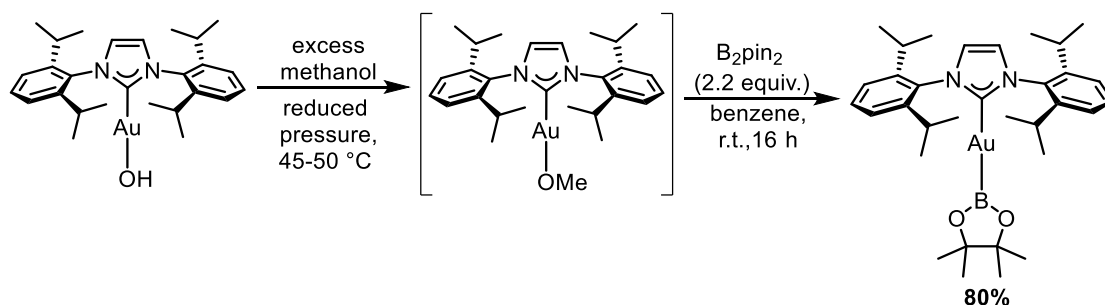


Figure 7.2: Complexes used in the synthesis of [Au(IPr)(Bpin)].

Firstly the complexes were mixed with B₂pin₂ at room temperature for 16 hours and analysed via ¹H NMR spectroscopy. All complexes were fully recovered after the reaction. Harsher conditions were applied, gradually heated to 60 °C for 1 hour but unfortunately no change in the ¹H NMR spectrum was observed. As the stability of the targeted [Au(IPr)(Bpin)] complex was not known, we tried to avoid conditions that are too harsh due to the possibility of decomposition of the new complex. In the final attempt, the complexes were heated at 60 °C for 16 hours. The mixture showed slight decomposition of the gold complexes and no formation of a new species. Since all complexes could be recovered after reaction, with a slight loss of the formation of gold nanoparticles, it was postulated that a more labile bond could favour the formation of the Au-Bpin bond. To test this hypothesis, the relatively unstable [Au(OMe)(IPr)] was formed *in situ* by dissolving [Au(OH)(IPr)] in anhydrous methanol. The solvent was then

removed under reduced pressure at 45-50 °C. The resulting [Au(OMe)(IPr)] complex was not isolated but directly dissolved in benzene under inert atmosphere, followed by the addition of excess B₂pin₂. The reaction was left to stir at room temperature for 16 hours resulting in the formation of the desired [Au(IPr)(Bpin)] complex (Scheme 7.25).



Scheme 7.25: Synthesis of [Au(IPr)(Bpin)].

The amount of B₂pin₂ was optimised to 1.1 equivalent resulting in 84% isolated yield. The newly synthesised complex was analysed using ¹H NMR, ¹¹B NMR and ¹³C {¹H} NMR spectroscopy and elemental analysis. Interestingly the chemical shift of the C2(carbene) in the ¹³C {¹H} NMR spectrum is at 216.7 ppm. For a transition metal-NHC complex, this is significantly shifted downfield and resembled more the shift of a free NHC than a metal bound one. This characteristic was also observed for Yamashita and Nozaki's reported gold boryl complexes.⁸⁵ Single crystals were grown of [Au(IPr)(Bpin)] by diffusion of dichloromethane in pentane under inert atmosphere. The X-ray analysis showed an almost linear structure with a Au-B bond length of 2.065(8) Å and an Au-C(carbene) bond length of 2.079(6) Å (Figure 7.3).

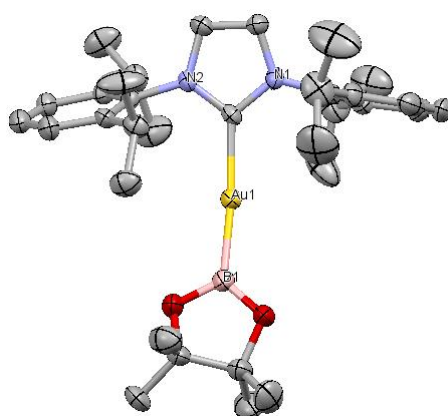
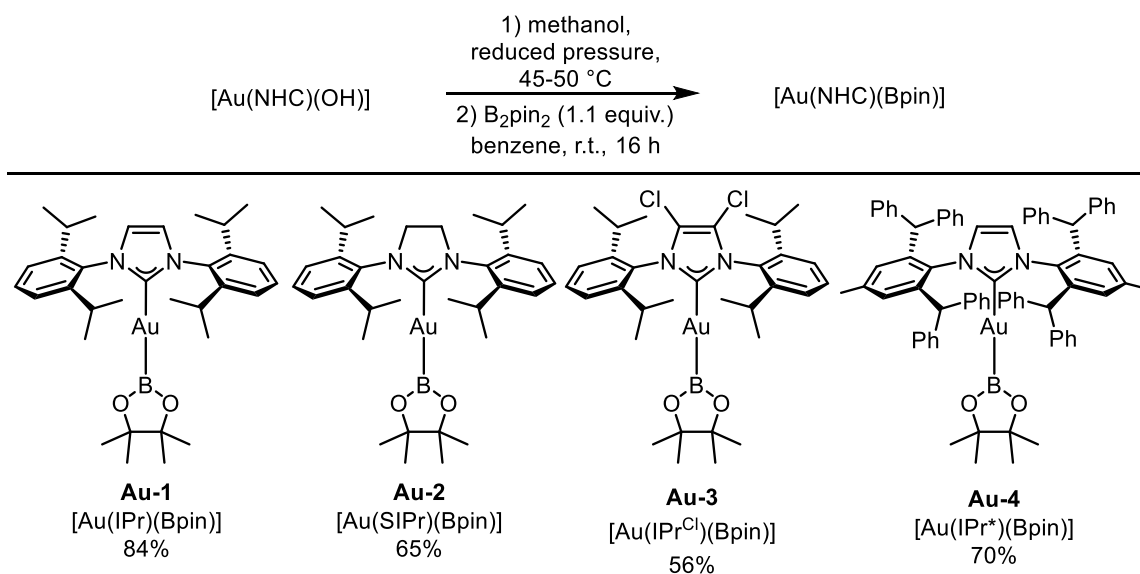


Figure 7.3: Crystal structures of [Au(IPr)(Bpin)], Hydrogen atoms are omitted for clarity.

The synthesis of [Au(NHC)(Bpin)] complexes bearing different NHC ligands was attempted next. [Au(IPr^{*})(Bpin)] (70% yield), [Au(IPr^{cl})(Bpin)] (56% yield) and [Au(SIPr)(Bpin)] (65% yield) were

successfully synthesised using the developed synthesis (Scheme 7.8). Pleasingly, crystal structures were also obtained for [Au(IPr^{Cl})(Bpin)] and [Au(IPr^{*})(Bpin)] (Figure 7.3).



Scheme 7.26: Scope of [Au(NHC)(Bpin)] complexes.

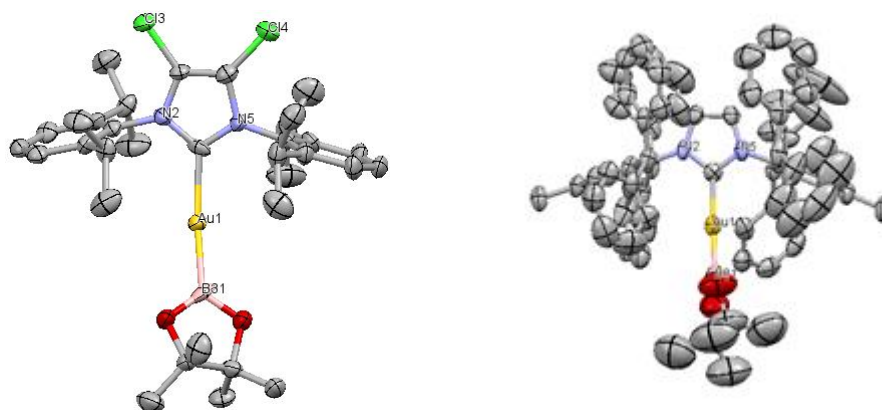
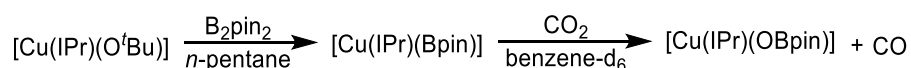


Figure 7.3: Crystal structures of Au(IPr^{Cl})(Bpin)] (left) and [Au(IPr^{*})(Bpin)] (right). Hydrogen atoms are omitted for clarity.

Surprisingly, all four complexes were air- and moisture-stable which readily enabled their full characterisation.

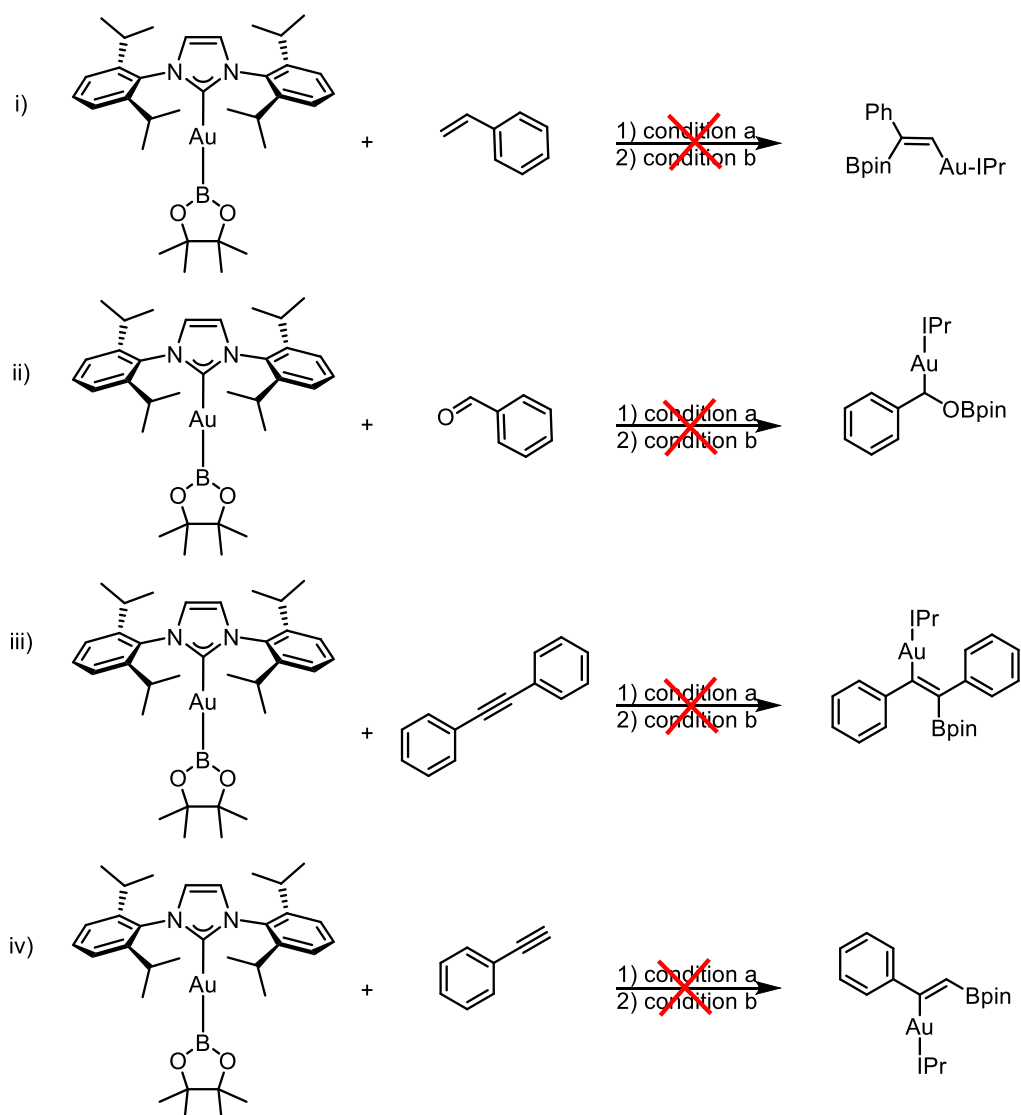
7.5 Initial reactivity studies of [Au(IPr)(Bpin)]

Initially, all reactivity studies were conducted using [Au(IPr)(Bpin)] under inert atmosphere. [Cu(IPr)(Bpin)] was used as a guideline for the initial reactivity of [Au(IPr)(Bpin)]. Sadighi and co-workers reported the catalytic reduction of CO₂ to CO using [Cu(IPr)(Bpin)].⁹⁶ It was shown that [Cu(IPr)(Bpin)] reacted with CO₂ under atmospheric pressure in benzene within minutes to form [Cu(IPr)(OBpin)] and CO as side-product (Scheme 7.27).⁹⁶ This reactivity is not observed in the case of [Au(IPr)(Bpin)] as it is air stable and does not react with CO₂.



Scheme 7.27: Synthesis and reactivity of [Cu(IPr)(Bpin)] by Sadighi and coworkers.⁹⁶

Furthermore, Sadighi and co-workers reported the alkene insertion into [Cu(IPr)(Bpin)]⁹⁷ as well as the catalytic diboration of aldehydes.⁷⁸ The copper-boron bond in [Cu(IPr)(Bpin)] is prone to react with electron-rich organic molecules, a similar reactivity was expected for the [Au(IPr)(Bpin)] complex. Therefore, preliminary experiments were conducted using electron-rich organic molecules such as alkene, alkynes and aldehydes (Scheme 7.28).



Scheme 7.28: Preliminary experiments with [Au(IPr)(Bpin)]. Reaction conditions: [Au(IPr)(Bpin)] (0.11 mmol, 8 mg) was transferred to a NMR tube inside the glovebox, benzene- d_6 was added followed by the substrate (0.11 mmol). Condition a: The NMR tube was stirred at room temperature for 16 min, then ^1H NMR spectrum was taken. Conditions b: The NMR tube was heated to 60 °C for 16 h, then ^1H NMR spectrum was taken.

Styrene (Scheme 7.28, i), benzaldehyde (Scheme 7.28, ii), diphenylacetylene (Scheme 7.28, iii) and phenylacetylene (Scheme 7.28, iv) were separately mixed with **Au-1** in benzene- d_6 in a 1:1 ratio; however, no reactivity was observed resulting in recovery of all starting materials. No decomposition of the starting materials was observed, even after 24 hours. Afterwards, harsher conditions were applied; starting with an excess of the organic substrates (2-3 equivalents). Yet again, no reactivity nor decomposition was observed. Lastly, high temperatures (60 °C, overnight) were applied to the all reactions (Scheme 7.28, i-iv).

Interestingly when heated, **Au-1** did not react with the organic substrates, demonstrating an unexpected high stability. After extensive heating for 24 hours, slight decomposition is detected in form of gold nanoparticles. As mentioned in the introduction, gold is prone to react with π -bonds, this made us conclude that this new complex is not behaving as expected based on literature precedents. To investigate this Au-Bpin bond and therefore elucidate its properties, computational studies were conducted by our collaborators.

7.6 Computational studies of [Au(IPr)(Bpin)]

The electronic structure of **Au-1** was investigated by Dr. Laura Falivene and Prof. Luigi Cavallo. The Gaussian09 package was used for the study (for more information, see experimental section). **Au-1** was compared with two reported and widely studied Au(I)-NHC complexes, namely [AuF(IPr)] and [Au(OH)(IPr)] (Figure 7.5).

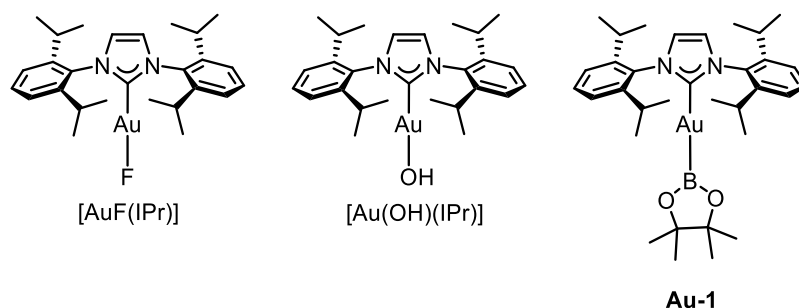


Figure 7.5: NHC-Au complexes used in the computational studies.

Firstly, the accurate dissociation free energy in CH_2Cl_2 of the anionic L ligand ($\text{L} = \text{Bpin}^-$, F^- , OH^-) and of IPr from the IPr-Au-L system was calculated. This was computed as the free energy difference between the fully optimised IPr-Au-L complexes and the optimised fragments, *i.e.* IPr-Au⁺ and L⁻, for the anionic bond as well as IPr and Au-L for the Au-IPr bond. The energy to dissociate the anionic L ligand increases in the order F^- (212 kJ/mol) < OH^- (263 kJ/mol) < **Bpin** (376 kJ/mol). Looking at the dissociation free energy of IPr, it decreases in the order F^- (272 kJ/mol) > OH^- (236 kJ/mol) > **Bpin** (105 kJ/mol). Straight away a significant difference between **Au-1** and [Au(IPr)F] and [Au(IPr)(OH)] was noticed. The weakening of the Au-IPr bond by the Bpin ligand was a remarkable feature, since it is widely known that the NHC-TM bond is a very strong bond;⁹⁸⁻¹⁰⁰ however, it is somewhat expected due to the significant *trans* effect of boryl ligand.

Energy decomposition analysis (EDA) was performed to further investigate and understand the difference between Au-Bpin, Au-F and Au-OH bonds, as well as to investigate the impact of the

L ligand (Bpin, F and OH) on the IPr-Au bond. In these calculations, the geometry of the metal fragment was kept rigid and the heterolytic BSE was calculated, which means fragmenting the complex into cationic and anionic fragments. The BSE consists of two main components; the steric interaction ΔE_0 and the orbital interaction ΔE_{int} (Equ. 1).

$$\diamond \text{ BSE} = -[\Delta E_0 + \Delta E_{\text{int}}] \text{ (Equ. 1)}$$

$$\diamond \Delta E_0 = \Delta E_{\text{elstat}} + \Delta E_{\text{Pauli}} \text{ (Equ. 2)}$$

$$\diamond \Delta E_{\text{int}} = \sum_{\tau} \Delta E_{\text{int}}^{\tau} \text{ (Equ. 3)}$$

The steric interaction term ΔE_0 can be divided into an electrostatic interaction term ΔE_{elstat} and a Pauli repulsion term ΔE_{Pauli} (Equ. 2).

ΔE_{elstat} functions as the stabilising contribution whereas the Pauli repulsion is the destabilising contribution and it is the relative size of the electrostatic interaction. The Pauli repulsion is directly related to the two orbital electron interaction between the occupied orbitals on both fragments. Therefore, ΔE_{Pauli} is the one determining the overall character of ΔE_0 . The orbital interaction term ΔE_{int} consists of the orbital interaction within the various irreducible representations τ of the overall symmetry group of the system. All molecules studied herein possess C_s symmetry; the NHC and the L ligand are located in the σ_{xy} mirror plane of the molecule. This means that A' contributes to the orbital interaction energy representing σ -bonding, whereas A'' is representing the orbital interaction energy of π -bonding. It is further divided into both σ/π donation and σ/π backdonation.

As expected, electrostatic interaction is the most important attractive bonding force since the fragments are ions. The total steric interaction ΔE_0 is stabilizing, indicating that the attractive electrostatic interaction overcompensates the Pauli repulsive term (-1740 vs +1320 kJ/mol for the Au-Bpin bond).

Studying the Au-Bpin bond in the [Au(IPr)(Bpin)] system, it was found that the orbital term is mainly σ -interaction, consisting of 60% ligand to metal σ -donation and the remaining 40% derived from metal to ligand σ -backdonation. The π -interactions consists of 55% ligand to metal π -donation and 45% of metal to ligand π -backdonation. The overall bond strength of this system was determined to be almost 50:50 shared between the steric (420 KJ/mol) and orbital (418 KJ/mol) terms (Table 7.1).

Table 7.1: Bond decomposition analysis (in KJ/mol) for **Au-1**, [Au(IPr)F] and [Au(IPr)(OH)].

	IPr-Au-Bpin	IPr-Au-F	IPr-Au-OH	IPr-Au-Bpin	IPr-Au-F	IPr-Au-OH
ΔE_{elstat}	-1740	-800	-947	-619	-923	-882
ΔE_{Pauli}	1320	408	-547	620	887	877
ΔE_0	-420	-392	-399	52	-36	-5
$\Delta E_{\text{int}(\sigma)}$	-366	-243	-276	-188	-264	-249
$\Delta E_{\text{int}(\pi)}$	-52	-62	-81	-34	-71	-71
ΔE_{int}	-418	-305	-357	-22	-335	-320
BSE	-838	-696	-756	-170	-371	-325

As comparison, the [AuF(IPr)] and the [Au(OH)(IPr)] systems were considered and the BSE analysis of the Au-F and Au-OH bonds was performed (Table 7.1). The decreased strength of the Au-L (L = F, OH; 696 and 756 kJ/mol, respectively) bonds, compared to the Au-BPin bond, 838 kJ/mol, is mainly ascribed to the much lower orbital interaction term ΔE_{int} , which is 113 and 61 kJ/mol weaker for the Au-F and the Au-OH bonds, respectively; while the steric term ΔE_0 is substantially the same for both systems (oscillating in a 20 kJ/mol window). Interestingly, despite the similar magnitude in ΔE_0 , the ΔE_{elstat} and ΔE_{Pauli} components of ΔE_0 are remarkably lower in the Au-F and Au-OH bonds, which indicate that these bonds are less polarized than the Au-Bpin bond.

This result is confirmed by the Hirshfeld charge analysis showing a charge of -0.71e and -0.38e on F and OH, respectively, versus a charge of **-0.82e** on BPin. Correspondingly, the positive charge on Au is larger in the [Au(IPr)(F)] and the [Au(IPr)(OH)] systems (0.75e and 0.52e, respectively) than in the BPin system (**0.83e**). As for the orbital interaction term, the π contribution is marginally larger in the Au-F and Au-OH systems, while the σ term is clearly larger in the Au-Bpin system due to the strong σ -back-donation from the Au to the Bpin (the first empty σ orbital on Bpin⁻ is clearly more stable than that on F⁻ and OH⁻). Overall, these results suggest that the increased strength of the Au-Bpin bond is consequence of its high ionic character, leading to stronger electrostatic interaction, and of increased orbital interaction correlated to a stronger σ -backdonation from the metal to the ligand.

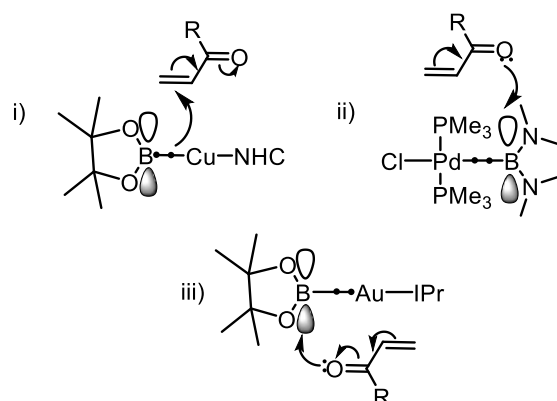
Moving to the Au-IPr bond, a bond decomposition analysis was performed by fragmenting the complex into the neutral [Au-L] and [IPr] fragments. The BSE analysis shows the opposite trend relative to the one reported above for the [(IPr)Au]-L bond. In fact, the Au-IPr bond is 200 and 155 kJ/mol stronger in the [AuF(IPr)] and the [Au(OH)(IPr)] complexes, relative to the [Au(IPr)(Bpin)] system. The clearly weaker IPr-Au bond in presence of Bpin is almost equally

distributed in the overall steric interaction term ΔE_0 and the overall orbital interaction term ΔE_{Int} (Table 7.1).

The HOMO and LUMO analysis showed that the LUMO is almost identical for all three systems and that the main difference is with the HOMO. The HOMO differs significantly. The most surprising finding was the large Au contribution of 47.6% in the Bpin system, compared to the Au contribution of 31.5% and 19.4% in the F and OH systems, respectively. The orbitals involved for **Au-1** are mainly Au $d_{x^2-y^2}$, with a small contribution of Au d_{z^2} . This resulted in a strong bonding interaction from the Au centre to the O-B-O moiety with the B atom mainly participating with s and p_y orbitals. On the other hand, the HOMO in [AuF(IPr)] or [Au(OH)(IPr)] corresponds to an anti-bonding interaction between the Au d_{yz} and the p_z of F or OH.

In conclusion, the data obtained via DFT calculations showed that **Au-1** could offer some new and unique reactivity, which drastically differs from the [Cu(IPr)(Bpin)] complex.

It is widely known that the reactivity of boryl–transition-metal complexes switches depending on the nature of the transition metal. For example, boryl-copper complexes seem to react in a complementary manner to boryl-palladium complexes with α,β -unsaturated ketones (Scheme 7.29). The copper-mediated β -boration to α,β -unsaturated carbonyl compounds was first developed by Miyaura and co-workers⁷⁹ and by Hosomi and co-workers.¹⁰¹ From a theoretical point of view, Lin and Marder provided evidence that the boryl moiety could act as a nucleophile and thus attack at the beta carbon of the substrate, promoting the formation of β -boryl carbonyl compounds (Scheme 7.29).¹⁰² In contrast, the analogous reaction of *trans*-[PdCl{B(NMeCH₂CH₂NMe)}(PMe₂)₂] with an α,β -unsaturated ketone was reported by Onozawa and Tanaka, which suggested that the insertion of the substrate into the Pd-B bond took place with reversed regioselectivity, thereby providing the 1,4-addition product in which the Pd was bonded to the β -carbon atom and the boryl unit was bonded to the oxygen atom (Scheme 7.29).¹⁰³ Compared to both copper and palladium systems, we argued that a reaction between **Au-1** and α,β -unsaturated carbonyl compounds would resemble more the palladium initiation pathway than the copper version. In that manner, the lone pair of the oxygen will react with the empty orbital on the boron, weakening the Au-B bond and resulting with the Au moiety bonded to the β -carbon and the boryl moiety bound to the oxygen.



Scheme 7.29: Proposed reactivity for Cu- and Au-Bpin complexes.

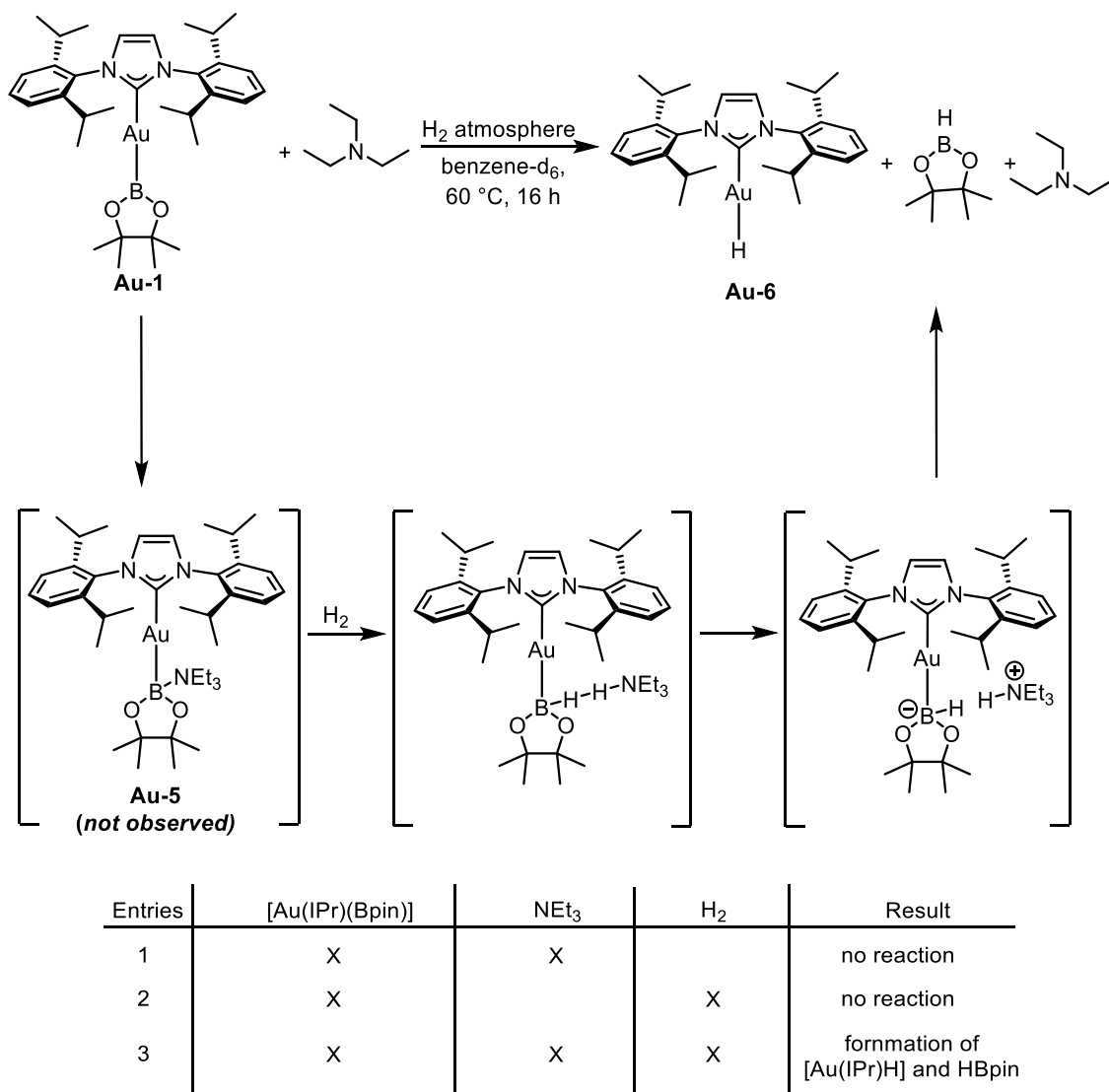
In summary, initially the reactivity of **Au-1** was assumed to be similar to the copper complex, where the boryl moiety initiates the reactivity towards the electron rich organic substrates (Scheme 7.29, i). Although the computational studies showed that the reactivity of **Au-1** is more likely to be initiated by the lone pair of electrons of an organic molecule, which reacts with the empty p orbital on the boron atom. This newly gained knowledge was used to design more appropriate experiments to investigate the reactivity of **Au-1**.

7.7 Investigation into the reactivity of [Au(IPr)(Bpin)]

7.7.1. Reactivity with Lewis bases and H₂ activation

Hydrogen is one of the most important energy resources, mainly due to its abundance and cheapness. H₂ activation is widely studied and used in energy storage,¹⁰⁴ hydrogenation¹⁰⁵ and many more applications.^{106–108} The main challenge is the cleavage of the very strong H-H σ -bond. The d- σ^* back-donation of transition metal complexes into the H₂ bond is widely studied, where the most famous example is the Wilkinson's catalyst, [RhCl(PPh₃)₃].¹⁰⁹ Based on the Au-Bpin bond data, we suggested that the boron moiety can be used as a mild Lewis acid; and by adding the appropriate Lewis base, a FLP (frustrated Lewis pair) system would form that can perform H₂ splitting. In the presence of hydrogen and **Au-1**, phosphines (PPh₃ and PCy₃) were first tried leading to no reaction and/or decomposition. When triethylamine was added to **Au-1** and hydrogen in benzene at 60 °C for 16 hours, we observed the formation of [AuH(IPr)] (**Au-6**) and HBpin in the ¹H NMR spectrum; **Au-6** was isolated in a 97% yield. Interestingly, **Au-1** did not react with H₂, nor with triethylamine by itself to form possible Lewis adduct, such as **Au-5**. In order to

observe H₂ splitting, all three components have to be present in the reaction (Scheme 7.30). It should be noted that conducting the same experiments with CO₂, did not result in any reaction.



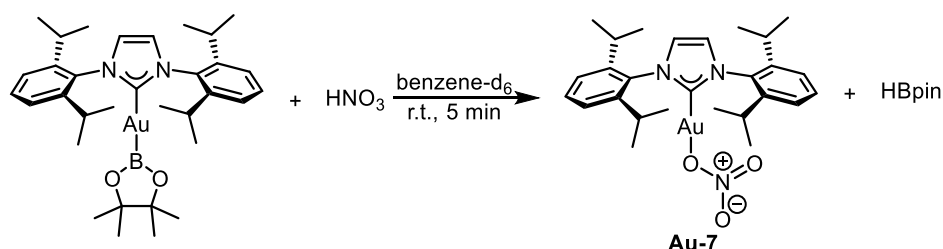
Scheme 7.30: Homoleptic cleavage of H₂ with [Au(IPr)(Bpin)]

7.7.2. Reactivity with Lewis acids

Our group recently reported the synthesis of NHC-Au(I) complexes from different acids such as HNO₃, H₂SO₄, H₃PO₄, HCl and NEt₃·2HF.^{110–112} In these reports, [Au(OH)(IPr)] was reacted with the corresponding acids, where the resulting complexes were tested in various organic transformations, such as hydration, hydrofluorination and hydroalkoxylation of alkynes as well as the Meyer-Schuster rearrangement.^{44,110,111,113,114} Also, different Au(I)-NHC complexes such as

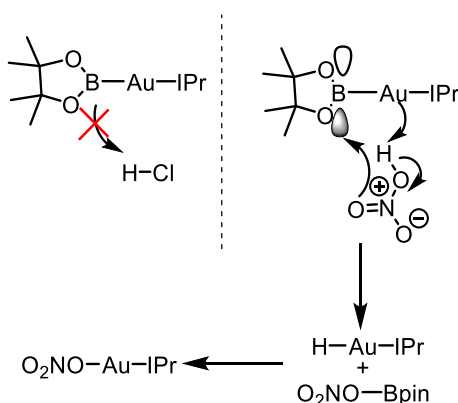
[Au(OH)(IPr)]¹¹⁵ and [Au(OCOCH₃)(IPr)]⁶⁰ have been reacted with carboxylic acids, affording gold carboxylate complexes, [Au(OCOR)(IPr)]. These complexes have been proposed intermediates in carboxylation/decarboxylation reactions.¹¹⁶

So far, experiments and DFT calculations have showed that the Bpin moiety, in these [Au(NHC)(Bpin)] complexes, does not act as a nucleophile. Therefore, we were curious to see if it will at least react as a Brønsted base when in the presence of various acids. When we reacted **Au-1** with HCl in benzene-d₆ at 24 °C for 16 hours, no reaction occurred and the starting material was recovered. This seems to support previous experiments and calculations. However, when **Au-1** was reacted with 1.1 equiv. of HNO₃, the formation of **Au-7** and HBpin was observed (Scheme 7.31). **Au-7** was isolated in 98% yield after just 5 min.



Scheme 7.31: Reaction with nitric acid.

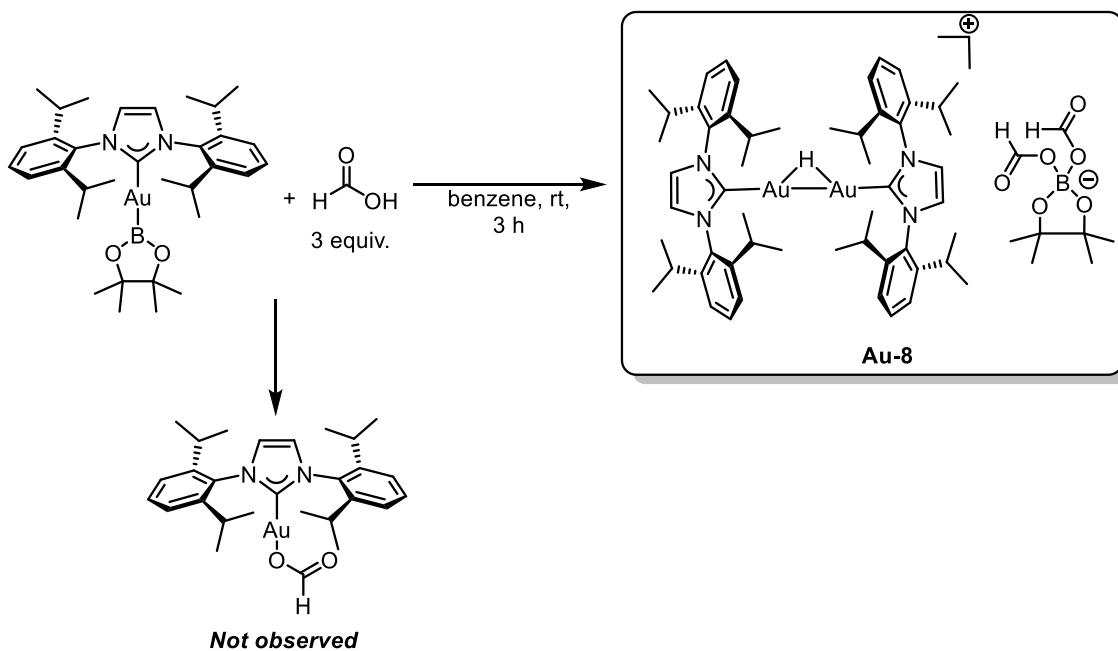
At first glance, it might look like a typical acid-base reaction; however, based on previous experiments and the fact that HNO₃ has a higher pka than HCl, this seemed unlikely. We argued that, in a similar manner to the previously predicted α,β -unsaturated ketone reactivity towards these complexes, it is actually the oxygen-based acid that is initiating the reaction (Scheme 7.32).



Scheme 7.32: Possible mechanism for nitric acid activation using **Au-1**.

The reactivity with acids was further investigated using carboxylic acids. In that manner, **Au-1** was reacted with formic acid at room temperature. After 3 hours, a new species in ¹H NMR

spectrum was detected. This species was fully analysed and a single crystal X-ray structure was obtained. The expected [Au(OCOH)(IPr)] was not observed; instead, a cationic bis(Au-NHC) hydride dimer was obtained with a four-coordinated Bpin-diformato species (Scheme 7.32, **Au-8**). This remarkable dimer species goes to support our initial hypothesis (see Scheme 7.29), since a hydride species is now confirmed as a possible intermediate.



Scheme 7.33: Reaction with formic acid.

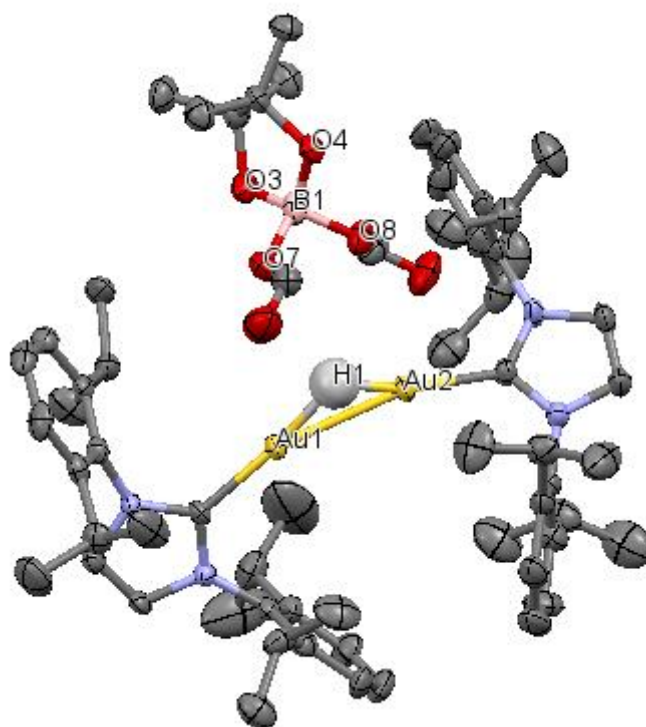
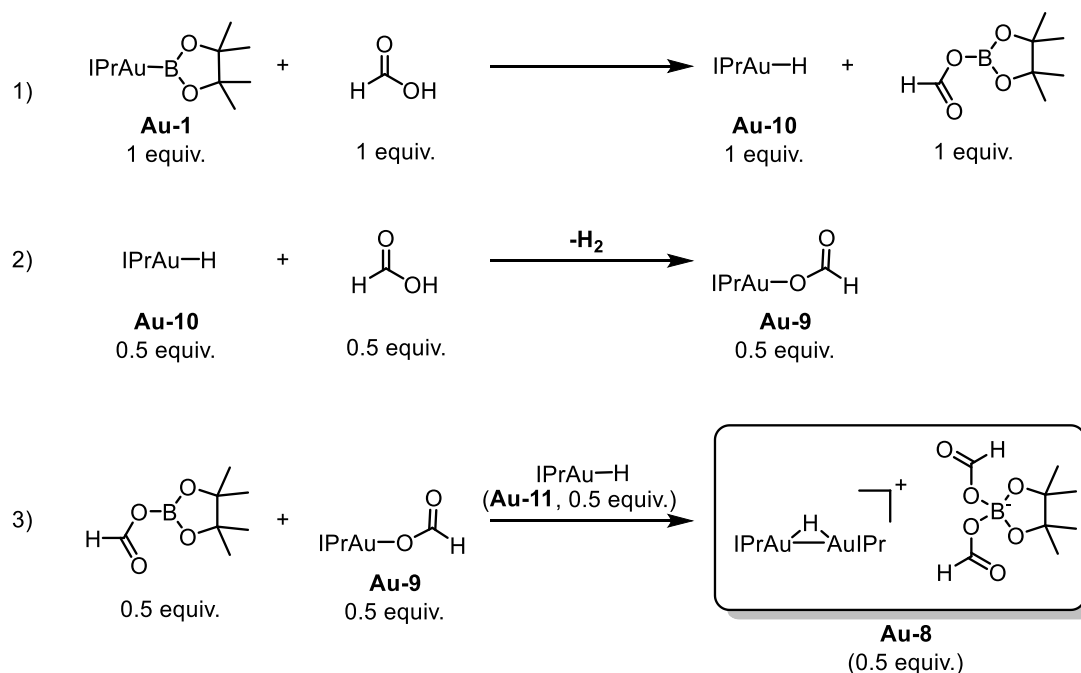


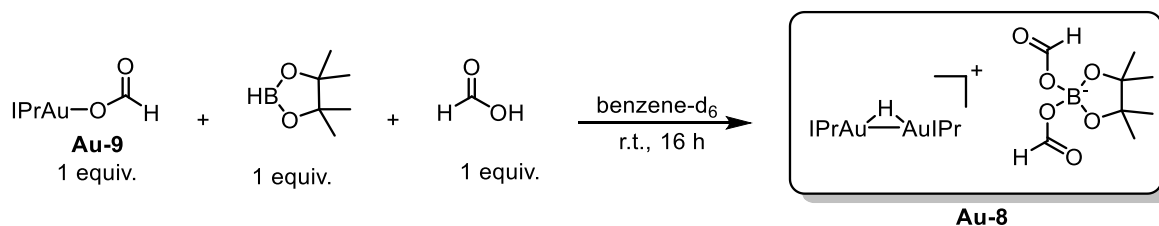
Figure 7.6: Single crystal X-ray structure of **Au-8**.

The cationic hydride-bridged IPr-Au complex was reported by Sadighi and coworkers,⁵¹ firstly by reacting [AuH(IPr)] with a trityl salt, [Ph₃C]⁺[BF₄]⁻, which is a known hydride acceptor, but later by reacting [AuH(IPr)] with [Au(IPr)(OTf)] which affords the gold dimer with a OTf⁻ counterion. Sadighi reported the hydride resonance in the ¹H NMR spectrum at $\delta = 0.42$ ppm, this is in close approximation with the hydride peak in **Au-8** at $\delta = 0.29$ ppm. The short intramolecular separation of the two gold atoms is observed as well, being 2.7500(6) Å. Similar boron diformate species has been reported, by Datta and Mandal¹¹⁷ with an abnormal NHC as counter ion. Also, various boron diformate species have been reported, either as intermediates or as catalysts in the reduction of CO₂.^{118–120}

As this was an unexpected outcome, a closer look towards the mechanism was taken. The proposed mechanism starts with a 1:1 reaction between **Au-1** and HCOOH, forming **Au-10** and (HCOO)₂Bpin in a 1:1 ratio (Scheme 7.34, 1). Next, 0.5 equivalence of **Au-10** react with 0.5 equivalence of HCOOH to form **Au-10** (Scheme 7.34, 2). This then reacts with the previously formed Bpin-formate species to produce IPrAu⁺ and the final Bpin-diformate species, Bpin(OOCH)₂⁻ (Scheme 7.34, 3). Meanwhile, IPrAu⁺ in the presence of **Au-10** will give the Au-IPr hydride dimer, thus affording the final complex, **Au-8**.

Scheme 7.34: Proposed reaction mechanism of **Au-8**.

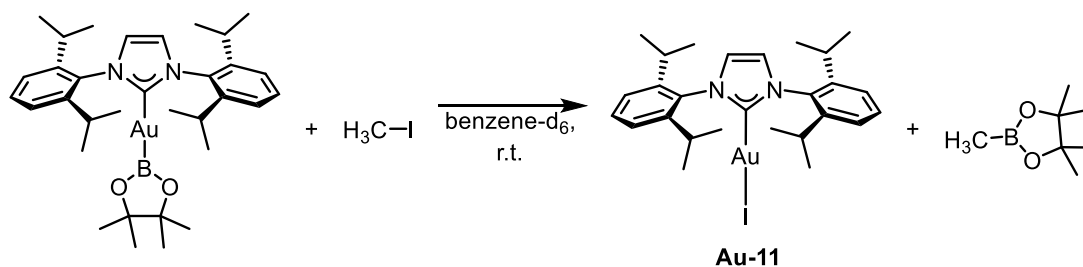
Mechanistic studies were carried out next. Firstly, **Au-9** was synthesised from [Au(OH)(IPr)] and HCOOH (1.1 equiv.) in toluene. **Au-9** was isolated in 97% yield. It should be noted that **Au-9** is also formed when **Au-10** is reacted with formic acid thus confirming step 2 in the proposed mechanism. Then, **Au-9** and HBpin were reacted together in a 1:1 ratio to afford **Au-10** and the Bpin-formate species. This reaction was done to allow us to mimic the formation of the mixture from the first equation of the proposed mechanism (Scheme 7.34, 1), in a controlled manner (the absence of any formic acid, should allow the reaction to stop at this stage). After 5 min, the formation of **Au-10** was clearly observed. Making use of this mixture, we reacted **Au-9**, HBpin and HCOOH in a 1:1:1 ratio. Since we know we are forming the mixture of **Au-10** and the Bpin-formate species (products from the first step of the proposed mechanism) starting from **Au-9** and HBpin, the formic acid present in the reaction mixture should theoretically afford the same hydride dimer **Au-8** that was obtained previously. This was observed experimentally carrying out an ^1H NMR experiment (Scheme 7.35).



Scheme 7.35: Control experiments of the proposed mechanism of **Au-8**.

7.7.3 Reactivity with alkyl/aryl iodide.

The reactivity towards alkyl/aryl iodide was investigated using methyl iodide and tolyl iodide respectively. The Au-B bond in **Au-1** is more polarised than the previously reported Au-NHC complexes, therefore the reactivity towards methyl iodide was not a typical one. **Au-1** and methyl iodide were mixed in a 1:1 ratio in benzene- d_6 at room temperature (Scheme 7.36). Firstly, ^1H NMR experiments were set up, monitoring the reaction over time.



Scheme 7.36: Reaction of **Au-1** with methyl iodide.

The reaction proceeding over 16 hours resulted in the full conversion of **Au-1** to **Au-11**. Both products were isolated and characterised by NMR spectroscopy.

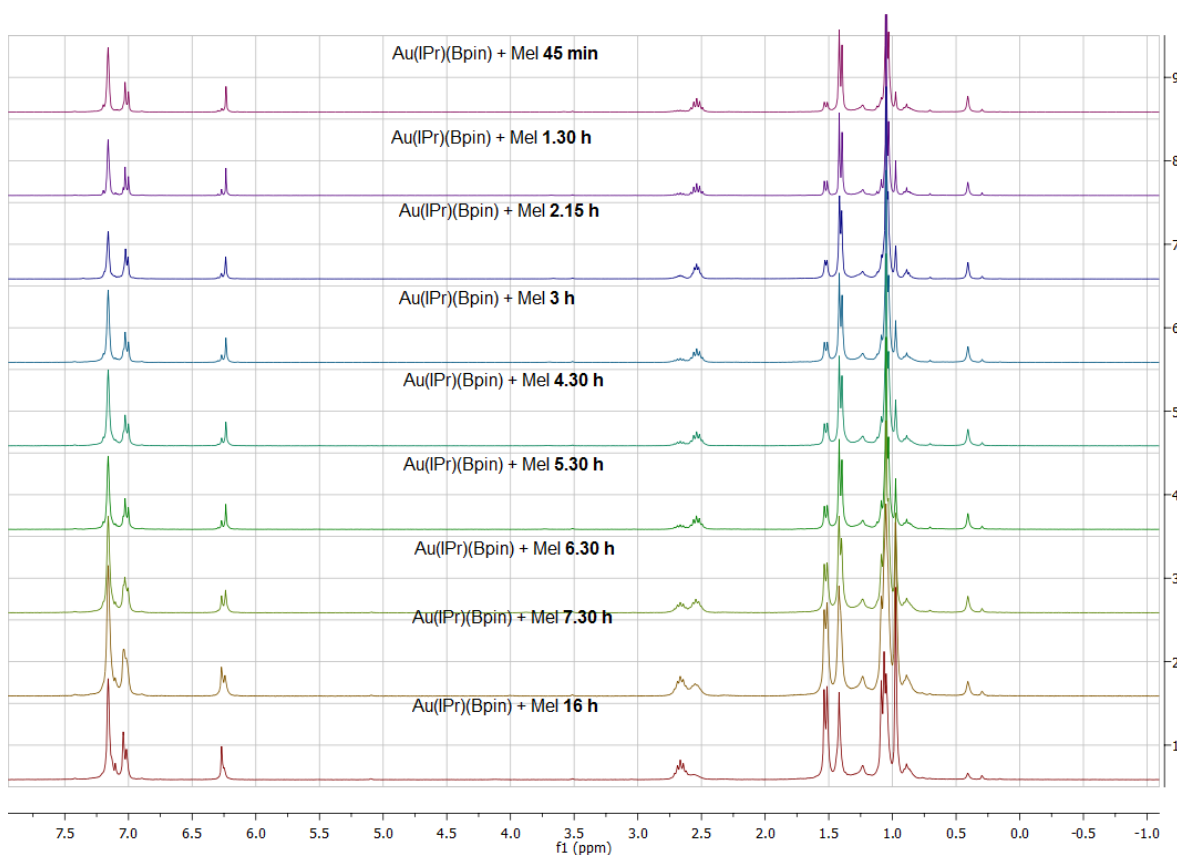
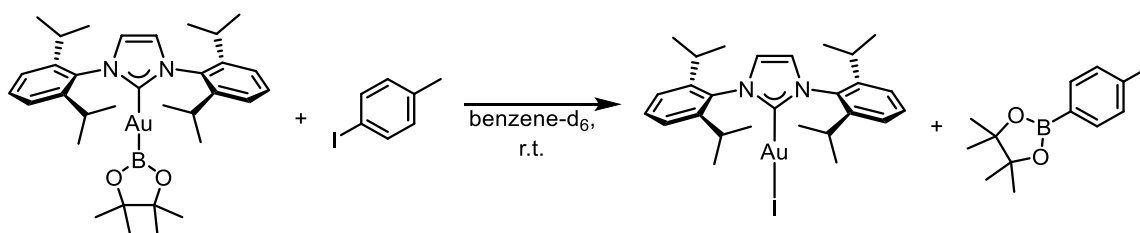


Figure 7.7: Time optimisation for formation of **Au-11**.

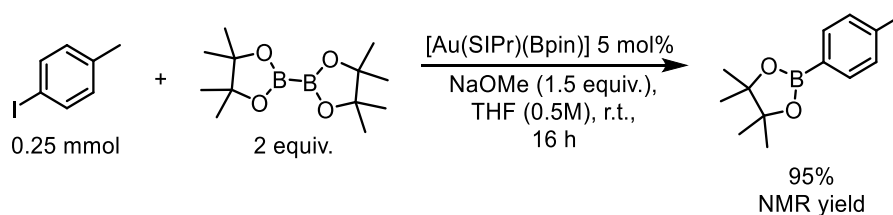
Next, **Au-1** was reacted with tolyl iodide to investigate the difference of alkyl and aryl iodide substrates. Different equivalence of tolyl iodide were reacted with **Au-1**, but no reactivity was observed under inert atmosphere (Scheme 7.37). Surprisingly, the reaction only proceeded under air in 48 hours.



Scheme 7.37: Synthesis of **Au-11** using tolyl iodide.

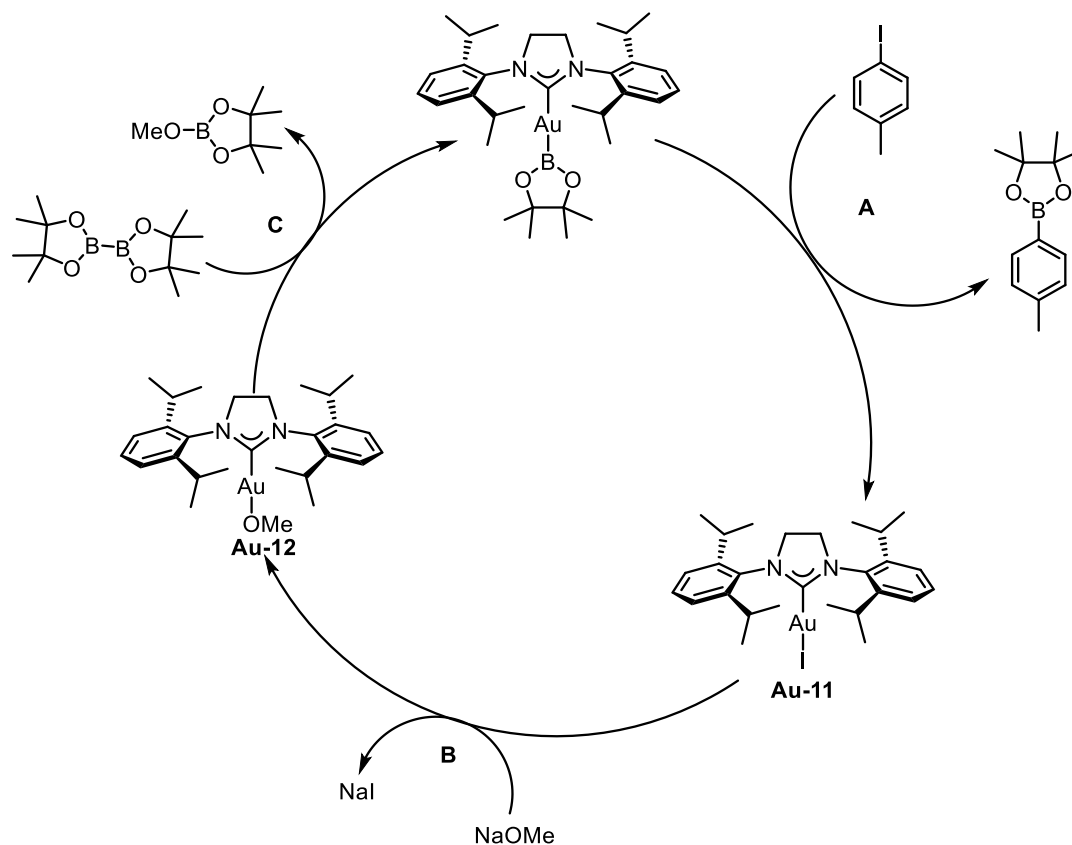
Au-11 and p-tolylpinacolboronate were isolated and characterised via ^1H NMR and $^{13}\text{C}\{^1\text{H}\}$ NMR spectroscopy. Aryl boronates are widely used in organic chemistry. One important example is cross-coupling chemistry, i.e. the Suzuki-Miyaura reaction. Therefore, the preparation of aryl boronates from aryl halides is an interesting approach and has been investigated in the past

using copper catalysts.¹²¹ In that context, we sought to investigate the possible catalytic borylation of tolyl iodide using the newly synthesised [Au(NHC)(Bpin)] complexes (Scheme 7.38).



Scheme 7.38: Preliminary conditions for the borylation of tolyl iodide.

Au-2 was first tested as the SIPr ligand was showed to be the best ligand in the copper system.⁹⁷ A catalytic cycle was proposed (Scheme 7.39), starting with the borylation of tolyl iodide to tolylpinacolboronate and **Au-11**. Next, a base is needed to form an alkoxide species [Au(SIPr)(OR)]. When NaOH and KOH were used, no reaction was observed. This was justified with the fact that **Au-2** cannot be synthesised from [Au(OH)(SIPr)] and B₂pin₂ (as seen previously during the synthesis). To overcome this issue, the base was exchanged to NaOMe to form **Au-12**, as this is the starting complex in the synthesis of **Au-2**. The reported condition from Lin and Marder were used for the initial studies,¹²¹ using THF as solvent at room temperature. The reaction was left to stir for 16 hours, then analysed via ¹H NMR spectroscopy. The crude ¹H NMR spectrum showed full conversion of tolyl iodide to *p*-tolylpinacolboronate, resulting in an isolated yield of 95%. Considering these promising results, **Au-1**, **Au-3** and **Au-4** were tested in the catalysis, resulting in no conversion for **Au-1** and **Au-3** and only 6% GC conversion for **Au-4**. Lastly the catalyst loading was lowered to 3 mol% and 1.5 mol%, resulting in 63% and 52% GC conversion.



Scheme 7.39: Proposed catalytic cycle of the borylation of tolyl iodide using **Au-2**.

7.8 Conclusion

In conclusion four new Au(I)-NHC-Bpin complexes have been synthesised and fully characterised. The reactivity was closely studied including computational studies into their bonding character. Hydrogen splitting was investigated for **Au-1**. Different acids were reacted with **Au-1** showing unique characteristics in the reactivity of these new complexes. Lastly, alkyl/aryl iodides were reacted with **Au-1** and **Au-2** resulting in borylation of both alkyl and aryl iodides. Furthermore the catalytic borylation of tolyl iodide was investigated and successfully established.

7.9 References:

- (1) Gagosz, F. *Adv. Organomet. Chem. Catal. Silver/Gold Jubil. Int. Conf. Organomet. Chem. Celebr. B.* **2014**, 207–225.
- (2) Sommer, A., *Nature*, **1943**, 152, 215.
- (3) Laguna, A.; Laguna, M. *Coord. Chem. Rev.* **1999**, 193, 837–856.
- (4) Bartlett, N. *Gold Bull.* **1998**, 31, 22–25.
- (5) Gorin, D. J.; Toste, F. D. *Nature* **2007**, 446, 395–403.
- (6) Carvajal, M. A.; Novoa, J. J.; Alvarez, S. *J. Am. Chem. Soc.* **2004**, 126, 1465–1477.
- (7) Toste, F. D.; Michelet, V. *Catalytic Science Series Vol 13 Gold Catalysis An Homogeneous Approach*; Hutchings, G. J., Ed.; Imperial College Press, 2014.
- (8) Bond, G. C. *Gold Bull.* **1972**, 5, 11–13.
- (9) Fukuda, Y.; Utimoto, K. *J. Org. Chem.* **1991**, 56, 3729–3731.
- (10) Hashmi, A. S. K.; Rudolph, M. *Chem.Soc.Rev.* **2008**, 37, 1766–1775.
- (11) Ito, Y.; Sawamura, M.; Hayashi, T. *J. Am. Chem. Soc.* **1986**, 108, 6405–6406.
- (12) Teles, J. H.; Brode, S.; Chabanas, M. *Angew. Chem. Int. Ed.* **1998**, 37, 1415–1418.
- (13) Kennedy-Smith, J. J.; Staben, S. T.; Toste, F. D. *J. Am. Chem. Soc.* **2004**, 126, 4526–4527.
- (14) Fürstner, A.; Davies, P. W. *Catalytic carbophilic activation: Catalysis by platinum and gold π acids*; **2007**; Vol. 46.
- (15) Shaw, C. F. *Chem. Rev.* **1999**, 99, 2589–2600.
- (16) Caruso, F.; Rossi, M.; Tanski, J.; Pettinari, C.; Marchetti, F. *J. Med. Chem.* **2003**, 46, 1737–1742.
- (17) Hsu, S. J.; Hsu, K. M.; Leong, M. K.; Lin, I. J. B. *Dalt. Trans.* **2008**, 1924.
- (18) Chen, Y. J.; Yeh, C. T. *J. Catal.* **2001**, 200, 59–68.
- (19) Forward, J. M.; Fackler, J. P.; Assefa, Z. In *Optoelectronic Properties of Inorganic Compounds*; Roundhill, D. M.; Fackler, J. P., Eds.; Springer US: Boston, MA, **1999**; pp. 195–229.
- (20) Gorin, D. J.; Sherry, B. D.; Toste, F. D. *Chem. Rev.* **2008**, 108, 3351–3378.
- (21) Marion, N.; Nolan, S. P. *Chem. Soc. Rev.* **2008**, 37, 1776–1782.
- (22) Marchione, D.; Belpassi, L.; Bistoni, G.; Macchioni, A.; Tarantelli, F.; Zuccaccia, D. *Organometallics* **2014**, 33, 4200–4208.
- (23) Nolan, S. P. *Acc. Chem. Res.* **2011**, 44, 91–100.
- (24) Cetinkaya, B. B.; Dixneuf, P.; Lappert, M. F.; Sciences, M.; Xi, P.; Cetinkaya, R.; Cetinkaya, E.; Lappert, M. F.; Dalton, J. C. S. **1974**, 1827–1833.

- (25) C. Bianchini, D.J. Cole-Hamilton, P.W.N.M. van Leeuwen, C. S. J. C. *N-Heterocyclic carbenes in Transition Metal Catalysis and Organocatalysis*; Cazin, C. S. J., Ed.; Springer, 2011.
- (26) de Frémont, P.; Stevens, E. D.; Fructos, M. R.; Mar Díaz-Requejo, M.; Pérez, P. J.; Nolan, S. P. *Chem. Commun.* **2006**, 2045–2047.
- (27) de Frémont, P.; Marion, N.; Nolan, S. P. *J. Organomet. Chem.* **2009**, *694*, 551–560.
- (28) Wang, H. M. J.; Lin, I. J. B. *Organometallics* **1998**, *17*, 972–975.
- (29) De Frémont, P.; Scott, N. M.; Stevens, E. D.; Ramnial, T.; Lightbody, O. C.; Macdonald, C. L. B.; Clyburne, J. A. C.; Abernethy, C. D.; Nolan, S. P. *Organometallics* **2005**, *24*, 6301–6309.
- (30) De Frémont, P.; Scott, N. M.; Stevens, E. D.; Nolan, S. P. *Organometallics* **2005**, *24*, 2411–2418.
- (31) Collado, A.; Gómez-Suárez, A.; Martin, A. R.; Slawin, A. M. Z.; Nolan, S. P. *Chem. Commun.* **2013**, *49*, 5541.
- (32) Visbal, R.; Laguna, A.; Gimeno, M. C. *Chem. Commun.* **2013**, *49*, 5642–5644.
- (33) Lin, I. J.; Vasam, C. S. *Can. J. Chem.* **2005**, *83*, 812–825.
- (34) Hashmi, A. S. K. *Gold Bull.* **2003**, *36*, 3–9.
- (35) Raubenheimer, H. G.; Cronje, S. *Chem. Soc. Rev.* **2008**, *37*, 1998–2011.
- (36) Dorel, R.; Echavarren, A. M. *Chem. Rev.* **2015**, *115*, 9028–9072.
- (37) Díez-González, S.; Marion, N.; Nolan, S. P. *Chem. Rev.* **2009**, *109*, 3612–3676.
- (38) Marion, N.; de Frémont, P.; Lemièrre, G.; Stevens, E. D.; Fensterbank, L.; Malacria, M.; Nolan, S. P. *Chem. Commun.* **2006**, 2048–2050.
- (39) Marion, N.; Gealageas, R.; Nolan, S. P. *Org. Lett.* **2007**, *9*, 2653–2656.
- (40) Hashmi, A. S. K. *Chem. Rev.* **2007**, *107*, 3180–3211.
- (41) Wurm, T.; Mohamed Asiri, A.; Hashmi, A. S. K. In *N-Heterocyclic Carbenes: Effective Tools for Organometallic Synthesis*; 2014; pp. 243–270.
- (42) Wang, D.; Cai, R.; Sharma, S.; Jirak, J.; Thummanapelli, S. K.; Akhmedov, N. G.; Zhang, H.; Liu, X.; Petersen, J. L.; Shi, X. *J. Am. Chem. Soc.* **2012**, *134*, 9012–9019.
- (43) Ramón, R. S.; Marion, N.; Nolan, S. P. *Tetrahedron* **2009**, *65*, 1767–1773.
- (44) Zhang, Z.; Widenhoefer, R. A. *Org. Lett.* **2008**, *10*, 2079–2081.
- (45) Zhang, Z.; Du Lee, S.; Fisher, A. S.; Widenhoefer, R. A. *Tetrahedron* **2009**, *65*, 1794–1798.
- (46) Laitar, D. S.; Mu, P.; Gray, T. G.; Sadighi, J. P. *Organometallics* **2005**, *24*, 4503–4505.

- (47) Fagnou, K.; Lautens, M. *Angew. Chem. Int. Ed.* **2002**, *41*, 26–47.
- (48) Veltheer, J. E.; Burger, P.; Bergman, R. G. *J. Am. Chem. Soc.* **1995**, *117*, 12478–12488.
- (49) Pilon, M. C.; Grushin, V. V. *Organometallics* **1998**, *17*, 1774–1781.
- (50) Akana, J. A.; Bhattacharyya, K. X.; Müller, P.; Sadighi, J. P. *J. Am. Chem. Soc.* **2007**, *129*, 7736–7737.
- (51) Tsui, E. Y.; Müller, P.; Sadighi, J. P. *Angew. Chem. Int. Ed.* **2008**, *47*, 8937–8940.
- (52) Hashmi, A. S. K.; Hutchings, G. J. *Angew. Chem. Int. Ed.* **2006**, *45*, 7896–7936.
- (53) Gaillard, S.; Slawin, A. M. Z.; Nolan, S. P. *Chem. Commun.* **2010**, *46*, 2742–2744.
- (54) Marion, N.; Carlqvist, P.; Gealageas, R.; De Frémont, P.; Maseras, F.; Nolan, S. P. *Chem. Eur. J.* **2007**, *13*, 6437–6451.
- (55) Patrick, S. R.; Gómez-Suárez, A.; Slawin, A. M. Z.; Nolan, S. P. *Organometallics* **2014**, *33*, 421–424.
- (56) Mézailles, N.; Ricard, L.; Gagosz, F. *Org. Lett.* **2005**, *7*, 4133–4136.
- (57) Ricard, L.; Gagosz, F. *Organometallics* **2007**, *26*, 4704–4707.
- (58) Collado, A.; Gómez-Suárez, A.; Webb, P. B.; Kruger, H.; Bühl, M.; Cordes, D. B.; Slawin, A. M. Z.; Nolan, S. P. *Chem. Commun.* **2014**, *50*, 11321–11324.
- (59) Gaillard, S.; Bosson, J.; Ramón, R. S.; Nun, P.; Slawin, A. M. Z.; Nolan, S. P. *Chem. Eur. J.* **2010**, *16*, 13729–13740.
- (60) Gasperini, D.; Collado, A.; Gómez-Suárez, A.; Cordes, D. B.; Slawin, A. M. Z.; Nolan, S. P. *Chem. Eur. J.* **2015**, *21*, 5403–5412.
- (61) Zhang, C.; Bourgeade Delmas, S.; Fernández Álvarez, Á.; Valentin, A.; Hemmert, C.; Gornitzka, H. *Eur. J. Med. Chem.* **2018**, *143*, 1635–1643.
- (62) Liu, W.; Gust, R. *Coord. Chem. Rev.* **2016**, *329*, 191–213.
- (63) Karaca, Ö.; Scalcon, V.; Meier-Menches, S. M.; Bonsignore, R.; Brouwer, J. M. J. L.; Tonolo, F.; Folda, A.; Rigobello, M. P.; Kühn, F. E.; Casini, A. *Inorg. Chem.* **2017**, *56*, 14237–14250.
- (64) Niu, W.; Teng, I.-T.; Chen, X.; Tan, W.; Veige, A. S. *Dalt. Trans.* **2017**, 120–126.
- (65) Wadepohl, H.; Arnold, U.; Pritzkow, H. *Angew. Chem. Int. Ed.* **1997**, *36*, 974–976.
- (66) Braunschweig, H. *Angew. Chem. Int. Ed.* **1998**, *37*, 1786–1801.
- (67) Braunschweig, H.; Kollann, C.; Rais, D. *Angew. Chem. Int. Ed.* **2006**, *45*, 5254–5274.
- (68) Yamashita, M.; Nozaki, K. *Pure Appl. Chem.* **2008**, *80*, 1187–1194.
- (69) Braunschweig, H.; Brenner, P.; Dewhurst, R. D.; Kaupp, M.; Müller, R.; Östreicher, S. *Angew. Chem. Int. Ed.* **2009**, *48*, 9735–9738.

- (70) Nöth, H.; Schmid, G. *Angew. Chem. Int. Ed.* **1963**, *2*, 623.
- (71) Baker, R. T.; Ovenall, D. W.; Calabrese, J. C.; Westcott, S. a.; Taylor, N. J.; Williams, I. D.; Marder, T. B. *J. Am. Chem. Soc.* **1990**, *112*, 9399–9400.
- (72) Knorr, J. R.; Merola, J. S. *Organometallics* **1990**, *9*, 3008–3010.
- (73) Hartwig, J. F.; De, G. S. R. *J. Am. Chem. Soc.* **1994**, *116*, 3661–3662.
- (74) Braunschweig, H.; Colling, M. *Coord. Chem. Rev.* **2001**, *223*, 1–51.
- (75) Hirner, J. J.; Blum, S. A. *Tetrahedron* **2015**, *71*, 4445–4449.
- (76) Joost, M.; Amgoune, A.; Bourissou, D. *Angew. Chem. Int. Ed.* **2015**, *54*, 15022–15045.
- (77) Thomas, A. A.; Denmark, S. E. *Science* **2016**, *352*, 329–332.
- (78) Laitar, D. S.; Tsui, E. Y.; Sadighi, J. P. *J. Am. Chem. Soc.* **2006**, *128*, 11036–11037.
- (79) Takahashi, K.; Ishiyama, T.; Miyaura, N. *J. Organomet. Chem.* **2001**, *625*, 47–53.
- (80) Cid, J.; Carbó, J. J.; Fernández, E. *Chem. Eur. J* **2012**, *18*, 12794–12802.
- (81) Schmid, G.; Nöth, H. *Zeitschrift für Naturforsch.* **1965**, *20*, 1008–1008.
- (82) Kawano, Y.; Yasue, T.; Shimoi, M. *J. Am. Chem. Soc.* **1999**, *121*, 11744–11750.
- (83) Navarro, O.; Marion, N.; Oonishi, Y.; Kelly, R. A.; Nolan, S. P. *J. Org. Chem.* **2006**, *71*, 685–692.
- (84) Ito, H.; Kawakami, C.; Sawamura, M. *J. Am. Chem. Soc.* **2005**, *127*, 16034–16035.
- (85) Segawa, Y.; Yamashita, M.; Nozaki, K. *Angew. Chem. Int. Ed.* **2007**, *46*, 6710–6713.
- (86) Segawa, Y.; Suzuki, Y.; Yamashita, M.; Nozaki, K. *J. Am. Chem. Soc.* **2008**, *130*, 16069–16079.
- (87) Terabayashi, T.; Kajiwarra, T.; Yamashita, M.; Nozaki, K. *J. Am. Chem. Soc.* **2009**, *131*, 14162–14163.
- (88) Kisu, H.; Sakaino, H.; Ito, F.; Yamashita, M.; Nozaki, K. *J. Am. Chem. Soc.* **2016**, *138*, 3548–3552.
- (89) Sircoglou, M.; Bontemps, S.; Mercy, M.; Saffon, N.; Takahashi, M.; Bouhadir, G.; Maron, L.; Bourissou, D. *Angew. Chem. Int. Ed.* **2007**, *119*, 8737–8740.
- (90) Sircoglou, M.; Bontemps, S.; Bouhadir, G.; Saffon, N.; Miqueu, K.; Gu, W.; Mercy, M.; Chen, C.-H.; Foxman, B. M.; Maron, L.; Ozerov, O. V.; Bourissou, D. *J. Am. Chem. Soc.* **2008**, *130*, 16729–16738.
- (91) Bontemps, S.; Bouhadir, G.; Gu, W.; Mercy, M.; Chen, C. H.; Foxman, B. M.; Maron, L.; Ozerov, O. V.; Bourissou, D. *Angew. Chem. Int. Ed.* **2008**, *47*, 1481–1484.
- (92) Bontemps, S.; Bouhadir, G.; Miqueu, K.; Bourissou, D. *J. Am. Chem. Soc.* **2006**, *128*, 12056–12057.

- (93) Hansmann, M. M.; Rominger, F.; Boone, M. P.; Stephan, D. W.; Hashmi, A. S. K. *Organometallics* **2014**, *33*, 4461–4470.
- (94) Ye, H.; Lu, Z.; You, D.; Chen, Z.; Li, Z. H.; Wang, H. *Angew. Chem. Int. Ed.* **2012**, *51*, 12047–12050.
- (95) Braunschweig, H.; Radacki, K.; Shang, R. *Chem. Commun.* **2013**, *49*, 9905.
- (96) Laitar, D. S.; Müller, P.; Sadighi, J. P. *J. Am. Chem. Soc.* **2005**, *127*, 17196–17197.
- (97) Laitar, D. S.; Tsui, E. Y.; Sadighi, J. P. *Organometallics* **2006**, *25*, 2405–2408.
- (98) Dorta, R.; Stevens, E. D.; Scott, N. M.; Costabile, C.; Cavallo, L.; Hoff, C. D.; Nolan, S. P. *J. Am. Chem. Soc.* **2005**, *127*, 2485–2495.
- (99) Nelson, D. J.; Nolan, S. P. *Chem. Soc. Rev.* **2013**, *42*, 6723–6753.
- (100) Díez-González, S.; Nolan, S. P. *Coord. Chem. Rev.* **2007**, *251*, 874–883.
- (101) Ito, H.; Yamanaka, H.; Tateiwa, J.; Hosomi, A. *Tetrahedron Lett.* **2000**, *41*, 6821–6825.
- (102) Dang, L.; Lin, Z.; Marder, T. B. *Organometallics* **2008**, *27*, 4443–4454.
- (103) Onozawa, S. Y.; Tanaka, M. *Organometallics* **2001**, *20*, 2956–2958.
- (104) Satyapal, S.; Petrovic, J.; Read, C.; Thomas, G.; Ordaz, G. *Catal. Today* **2007**, *120*, 246–256.
- (105) O, W. W. N.; Lough, A. J.; Morris, R. H. *Chem. Commun.* **2010**, *46*, 8240.
- (106) Keaton, R. J.; Blacquiere, J. M.; Baker, R. T. *J. Am. Chem. Soc.* **2007**, *129*, 1844–1845.
- (107) Sattler, A.; Parkin, G. *J. Am. Chem. Soc.* **2011**, *133*, 3748–3751.
- (108) Li, Y.; Hou, C.; Jiang, J.; Zhang, Z.; Zhao, C.; Page, A. J.; Ke, Z. *ACS Catal.* **2016**, *6*, 1655–1662.
- (109) Evans, D.; Osbourne, J. A.; Wilkinson, G. *J. Chem. Soc. A Inorganic, Phys. Theor.* **1968**, *0*, 3133–3142.
- (110) Brill, M.; Nahra, F.; Gómez-Herrera, A.; Zinser, C.; Cordes, D. B.; Slawin, A. M. Z.; Nolan, S. P. *ChemCatChem* **2016**.
- (111) Nahra, F.; Patrick, S. R.; Bello, D.; Brill, M.; Obled, A.; Cordes, D. B.; Slawin, A. M. Z.; O'Hagan, D.; Nolan, S. P. *ChemCatChem* **2015**, *7*, 240–244.
- (112) Nahra, F.; Brill, M.; Gómez-Herrera, A.; Cazin, C. S. J.; Nolan, S. P. *Coord. Chem. Rev.* **2016**, *307*, 65–80.
- (113) Gómez-Suárez, A.; Gasperini, D.; Vummaleti, S. V. C.; Poater, A.; Cavallo, L.; Nolan, S. P. *ACS Catal.* **2014**, *4*, 2701–2705.
- (114) Nun, P.; Ramón, R. S.; Gaillard, S.; Nolan, S. P. *J. Organomet. Chem.* **2011**, *696*, 7–11.
- (115) Dupuy, S.; Lazreg, F.; Slawin, A. M. Z.; Cazin, C. S. J.; Nolan, S. P. *Chem. Commun.* **2011**,

- 47, 5455.
- (116) Dupuy, S.; Nolan, S. P. *Chem. Eur. J.* **2013**, *19*, 14034–14038.
- (117) Sau, S. C.; Bhattacharjee, R.; Vardhanapu, P. K.; Vijaykumar, G.; Datta, A.; Mandal, S. K. *Angew. Chem. Int. Ed.* **2016**, *55*, 15147–15151.
- (118) Das Neves Gomes, C.; Blondiaux, E.; Thuéry, P.; Cantat, T. *Chem. Eur. J.* **2014**, *20*, 7098–7106.
- (119) Chauvier, C.; Tlili, A.; Das Neves Gomes, C.; Thuéry, P.; Cantat, T. *Chem. Sci.* **2015**, *6*, 2938–2942.
- (120) Wang, T.; Stephan, D. W. *Chem. Commun.* **2014**, *50*, 7007–7010.
- (121) Kleeberg, C.; Dang, L.; Lin, Z.; Marder, T. B. *Angew. Chem. Int. Ed.* **2009**, *48*, 5350–5354.

Chapter 8

Conclusions and Future Work

8.1 Conclusions

This thesis described the synthesis and catalytic applications of novel palladium and gold-NHC complexes.

The synthesis of $[\text{PdCl}(\eta^3\text{-R-allyl})(\text{NHC})]$ complexes was improved by establishing an air and moisture stable protocol using mild conditions, making it operationally simple. The synthesis was successfully applied to a range of complexes varying the NHC ligand as well as the allyl ligand, resulting in high yields, comparable or higher than the previous reported syntheses. Furthermore the new preparation can be scaled up to 5 g, which highlights its efficiency.

The procedure was extended to the formation of palladate complexes, $[\text{NHC}\cdot\text{H}][\text{Pd}(\eta^3\text{-R-allyl})\text{Cl}_2]$. These complexes were isolated, fully characterised using NMR spectroscopy, elemental analysis and X-ray diffraction. The synthesis was optimised, resulting in a solvent-free synthesis, with no loss of palladium, which makes it a very atom-economic and environmentally friendly synthesis. This protocol was applied to a wide range of NHC bearing palladate complexes (26 complexes). Eleven NHC·HCl were used ranging from smaller NHCs (SIMes) to bigger NHCs (IPr*, ITent) in combination with five different palladium dimers, $[\text{Pd}(\eta^3\text{-R-allyl})(\mu\text{-Cl})_2]$.

The catalytic activity of the palladate complex was extensively investigated in the Suzuki-Miyaura reaction (Chapter 3); the Buchwald-Hartwig reaction and ketone arylation (Chapter 4); the Mizoroki-Heck reaction (Chapter 5) and the Sonogashira reaction and dimerization of terminal alkynes (Chapter 6).

An environmentally friendly protocol was established for the Suzuki-Miyaura reaction using a mild inorganic base, K_2CO_3 , in ethanol, coupling aryl chlorides with a variety of aryl boronic acids. The substrate scope included sterically hindered as well as heteroatom containing aryl chlorides. The electronic properties of the aryl boronic acid could be varied without significant loss of reactivity.

The catalytic activity of $[\text{IPr}^*\cdot\text{H}][\text{Pd}(\eta^3\text{-cin})\text{Cl}_2]$ was investigated in the Buchwald-Hartwig reaction. A highly efficient system was developed using low catalyst loading (0.2 mol%) and an environmentally friendly solvent (CPME). Primary and secondary amines were coupled in high yields with aryl chlorides. Biologically interesting substrates, namely *N*-ethylindolylphenylpropenones, were successfully coupled with a primary and a secondary amine. Furthermore the established protocol was applied to

the ketone arylation coupling aryl chlorides with different ketones, extending the applications of the palladate pre-catalyst.

The catalytic activity of the palladate pre-catalysts in the Mizoroki-Heck reaction was extensively studied. Several different palladates were tested bearing electronically and sterically different NHC ligands as well as different allyl ligands, resulting in $[\text{SIPr}\cdot\text{H}][\text{Pd}(\eta^3\text{-2-Me-allyl})\text{Cl}_2]$ being the optimal pre-catalyst. Very low catalyst loading (0.1 mol%) was required to achieve high yield in a variety of substrates. Different aryl bromides and chlorides were successfully coupled with styrene. Steric bulk on the aryl bromide is tolerated, without loss of reactivity. Biologically interesting heteroatom-containing aryl bromides were successfully coupled with styrene using the optimised protocol including a significant improvement in the synthesis of *E*-6-styrylisatin.

The coupling of aryl halides with alkynes was investigated where $[\text{IPr}^*\cdot\text{H}][\text{Pd}(\eta^3\text{-2-Me-allyl})\text{Cl}_2]$ was the optimal pre-catalyst. A very efficient protocol was established with very low catalyst loadings (0.1 mol%). The established scope showed no significant loss of reactivity when changing the electronic properties of the aryl bromides. Electronically different substituents were allowed on the acetylene, resulting in moderate yields. The dimerization of 1,3-enynes was successfully studied using $[\text{IPr}^*\cdot\text{H}][\text{Pd}(\eta^3\text{-2-Me-allyl})\text{Cl}_2]$ as pre-catalyst, resulting in excellent yields.

In summary the optimised reaction conditions for the catalytic protocols developed focused on environmentally friendlier reagents, such as mild inorganic bases and green solvents. All catalytic reactions required low catalyst loadings (0.3-0.1 mol%). Heteroatom-containing and biologically interesting substrates were targeted on and several interesting substrates were synthesised using the palladate pre-catalyst in cross-coupling chemistry.

Novel Au(I)-NHC complexes were synthesised and fully characterised. $[\text{Au}(\text{NHC})(\text{Bpin})]$ showed remarkable characteristics, such as being air and moisture stable complexes. The reactivity was closely studied including computational studies into their bonding character. The reactivity of $[\text{Au}(\text{IPr})(\text{Bpin})]$ was studied with Lewis bases, resulting in H_2 activation. The synthesis of a novel Au(I)-NHC complex, $[\text{Au}(\text{IPr})_2\text{H}][\text{Bpin}(\text{OCOH})_2]$ was established starting from $[\text{Au}(\text{IPr})(\text{Bpin})]$ and formic acid. The new complex was fully characterised and initial mechanistic studies were carried out. The reactivity towards alkyl and aryl iodide was investigated, resulting in the catalytic borylation of tolyl iodide.

8.2 Future Work

8.2.1. Investigation of the activation pathway of $[\text{NHC}\cdot\text{H}][\text{Pd}(\eta^3\text{-R-allyl})\text{Cl}_2]$

The activation pathway of $[\text{NHC}\cdot\text{H}][\text{Pd}(\eta^3\text{-R-allyl})\text{Cl}_2]$ pre-catalysts is still unknown. Attempts were made to study this reactions using *in-situ* IR spectroscopy and mass spectroscopy but all results obtained were inconclusive. As the palladate pre-catalysts show different catalytic activity and characteristic to the $[\text{PdCl}(\eta^3\text{-R-allyl})(\text{NHC})]$ pre-catalysts, an investigation into the activation pathway and active species would provide a better understanding of these activity of these complexes. As experimental studies failed so far, computational studies could be beneficial.

8.2.2. Extension of the “mild base approach synthesis”

Earth-abundant metals, such as nickel are of increasing interest in the catalysis community. Several different nickel complexes as catalysts have been studied in different organic reactions, for example in cross-coupling chemistry.¹ The main disadvantages are the instability of many nickel complexes as well as the high catalyst loading used. Nolan and co-workers reported $[\text{NiCl}(\text{R-allyl})(\text{NHC})]$ complexes and its high catalytic activity in the α -ketone arylation.² Taking this into account the synthesis of $[\text{NiX}(\text{L})_2]$ complexes could be improved and the use of these complexes more attractive. The synthesis of NHC based nickelate complexes could be of interest and their potential catalytic activity.

8.2.3. $[\text{Au}(\text{Bpin})(\text{NHC})]$ complexes

The synthesis of Au(I)-NHC complexes bearing different boron ligands could be a interesting extension to the developed Au(I)–NHC complexes. Different commercially available boron dimers can be tested using the optimised synthesis. The different Au(I)-NHC complexes could be used to study the Au-B bond gaining more insides. More reactivity studies should be attempted, focusing on the possible catalytic activity of $[\text{Au}(\text{NHC})(\text{Bpin})]$ complexes.

8.2.4 References

- (1) Hazari, N.; Melvin, P. R.; Beromi, M. M. *Nat. Rev. Chem.* **2017**, *1*, 25.
- (2) Fernández-Salas, J. A.; Marelli, E.; Cordes, D. B.; Slawin, A. M. Z.; Nolan, S. P. *Chem. Eur. J.* **2015**, *21*, 3906–3909.

Chapter 9:

Experimental Section

9.1 General informations

If reactions were carried out under argon, then a glovebox and Schlenk technique were used. All aryl halides and boronic acids were used as received. All bases were used as received (in air) or dried under vacuum at 100 °C (under inert atmosphere). All solvents were used as received when experiments were conducted in air. Degassed solvents were used when experiments were conducted under inert atmosphere. All $[\text{NHC}\cdot\text{H}][\text{Pd}(\eta^3\text{-R-allyl})\text{Cl}_2]$ were prepared from commercially available $\text{NHC}\cdot\text{HCl}$ and $[\text{Pd}(\text{R-allyl})(\mu\text{-Cl})_2]$.

Flash chromatography was performed on silica gel 60 Å pore diameter and 40-63 μm particles size.

^1H , ^{19}F and ^{13}C Nuclear Magnetic Resonance (NMR) spectra were recorded on a Bruker-400 and 500 MHz spectrometers at ambient temperature in CDCl_3 or C_6D_6 , purchased from Acros and dried over molecular sieves. Chemical shifts are expressed in ppm = parts per million and coupling constants, J , are given in Hertz. ^1H NMR spectra were recorded with solvent residual peak (CDCl_3 : 7.26 ppm or C_6D_6 : 7.16 ppm) as internal reference. ^{13}C NMR spectra were recorded with CDCl_3 (77.00 ppm) or C_6D_6 (128.06 ppm) as internal reference. Abbreviations used in the designation of the signals: s = singlet, d = doublet, dd = doublet of doublets, ddd = doublet of doublet of doublets, dt = doublet of triplets, t = triplet, td = triplet of doublets, m = multiplet, br. = broad, hept = heptuplet.

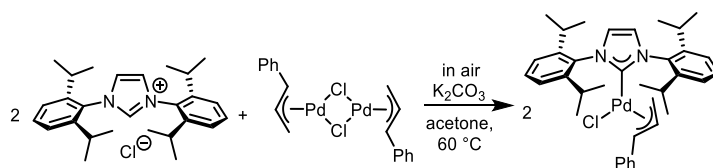
Elemental analyses were performed at London Metropolitan University 166-220 Holloway Road, London, N7 8DB. Mass spectrometry was performed by the EPSRC National Mass Spectrometry Service Centre at Swansea University, Grove Building, Singleton Park, Swansea, SA2 8PP, Wales, UK.

9.2 Chapter 2: A simple and facile synthesis of [PdCl(η^3 -R-allyl)(NHC)] complexes.

9.2.2 General procedure for the synthesis of [PdCl(η^3 -R-allyl)(NHC)]

NHC-HCl, [Pd(η^3 -R-allyl)(μ -Cl)]₂ (1.00 equiv.), a magnetic stir bar and acetone (0.28 M) were charged into a vial or round-bottomed flask, followed by K₂CO₃ (2.00-2.40 equiv.). The mixture was stirred at 60 °C for the corresponding time. After the reaction was complete, the solvent was removed under vacuum. The residue was re-dissolved in CH₂Cl₂ (1.00-2.00 mL) and filtered through a pad of silica. The filter cake was washed with CH₂Cl₂ (20.00 mL). The resulting solution was concentrated and dried under vacuum until a powder was obtained. In some cases, washing with pentane (5.00 mL) was necessary in order to remove the residual CH₂Cl₂. The product was analysed using ¹H NMR and ¹³C {¹H} NMR spectroscopy and elemental analysis.

9.2.3. Synthesis and optimisation of [PdCl(η^3 -cin)(IPr)]



Small scale: Following the general procedure; IPr·HCl (50.00 mg, 0.12 mmol), [Pd(η^3 -cin)(μ -Cl)]₂ (25.30 mg, 0.05 mmol) and K₂CO₃ (13.50 mg, 0.09 mmol) were used. The reaction was left to stir for 5 h. The product was obtained as a microcrystalline material in 98% (60.90 mg) yield.

Large scale: Following the general procedure; IPr·HCl (4.01 g, 9.44 mmol), [Pd(η^3 -cin)(μ -Cl)]₂ (2.04 g, 3.93 mmol) and K₂CO₃ (1.08 g, 7.87 mmol) were used. The reaction was left to stir for 24 h. The product was obtained as a microcrystalline material in 97% (4.94 g) yield.

¹H NMR (400 MHz, CDCl₃): δ (ppm) = δ 7.50 (t, J = 7.7 Hz, 2H), 7.28 (d, J = 7.7 Hz, 4H), 7.19-7.12 (m, 7H), 5.12-5.05 (m, 1H), 4.36 (d, J = 12.9 Hz, 1H), 3.06-2.96 (m, 5H), 1.77 (d, J = 11.4 Hz, 1H), 1.43-1.36 (m, 12H), 1.16 (d, J = 7.1 Hz, 12H).

¹³C {¹H} NMR (100 MHz, CDCl₃): δ (ppm) = δ 184.8 (C_{carbene}), 145.9 (C), 137.7 (C), 135.7 (C), 129.7 (CH) 128.0 (CH), 127.9 (CH), 127.1 (CH), 126.5 (CH), 124.0 (CH), 123.6 (CH), 108.6 (CH), 90.0 (CH), 46.1 (CH₂), 33.9 (CH₂), 28.4 (CH), 26.0 (CH₃), 22.8 (CH₃).

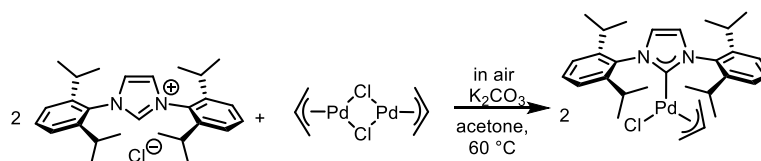
Elemental Analysis: Expected: C 66.66, H 7.15, N 4.32. Found: C 66.73, H 7.27, N 4.38.

Analytical data obtained were in agreement with the reported values.¹

Table S-1: Optimisation of the synthesis of [PdCl(η^3 -cin)(IPr)].

Entries	IPr·HCl (equiv.)	K ₂ CO ₃ (equiv.)	t (h)	Yield (%) ^a
1	1.00	2.00	3	94 [*]
2	1.10	2.00	3	100 [*]
3	1.20	1.10	5	98 [*]
4	1.30	1.10	5	100 [*]
5	1.50	1.10	5	100 [*]
6	1.20	0.90	5	99 [*]
7	1.20	1.00	5	98
8	1.20	1.30	5	100 [*]
9	1.20	1.50	5	96 [*]
10	1.20	0.60	5	65 [*]
11	1.20	0.40	5	69 [*]
12	1.20	0.20	5	52 [*]
13	1.20	1.00	5	94 ^{*b}
14	1.20	1.00	5	99 ^{*c}
15	1.20	1.00	6	99 ^d

^{*}¹H NMR shows impurities in the spectra. ^aIsolated yield after filtration through silica gel using CH₂Cl₂. All reactions were carried out in air using technical grade acetone (0.24 M in respect to IPr·HCl). ^bConcentration = 0.12 M. ^cConcentration = 0.06 M. ^dIPr·HCl and [Pd(η^3 -cin)(μ -Cl)]₂ were stirred in acetone for 1 h at 60 °C, then K₂CO₃ was added and the mixture was left to stir for 5 h at 60 °C.

9.2.4. Synthesis and optimisation of [PdCl(η^3 -allyl)(IPr)]

Small scale: Following the general procedure; IPr-HCl (50.00 mg, 0.12 mmol), [Pd(η^3 -allyl)(μ -Cl)]₂ (17.80 mg, 0.05 mmol) and K₂CO₃ (13.50 mg, 0.09 mmol) were used. The reaction was left to stir for 5 h. The product was obtained as a microcrystalline material in 85% (47.60 mg) yield.

Large scale: Following the general procedure; IPr-HCl (2.70 g, 6.55 mmol), [Pd(η^3 -allyl)(μ -Cl)]₂ (1.00 g, 2.73 mmol) and K₂CO₃ (755.00 mg, 5.47 mmol) were used. The reaction was left to stir for 24 h. The product was obtained as a microcrystalline material in 92% (2.87 g) yield.

¹H NMR (400 MHz, CDCl₃): δ (ppm) = δ 7.42 (t, J = 7.3 Hz, 2H), 7.28-7.25 (m, 4H), 7.15 (s, 2H), 4.86-4.76 (m, 1H), 3.91 (d, J = 5.6 Hz, 1H), 3.16-3.03 (m, 2H), 3.04 (d, J = 6.3 Hz, 1H), 2.89-2.82 (m, 2H), 2.77 (d, J = 13.6 Hz, 1H), 1.59 (d, J = 12.1 Hz, 1H), 1.39 (d, J = 7.1 Hz, 6H), 1.34 (d, J = 6.8 Hz, 6H), 1.18 (d, J = 7.1, 6H), 1.09 (d, J = 7.1 Hz, 6H).

¹³C {¹H} NMR (100 MHz, CDCl₃): δ (ppm) = δ 186.1 (C_{carbene}), 146.0 (C), 145.8 (C), 135.6 (C), 129.7 (CH), 123.9 (CH), 123.7 (CH), 123.6 (CH), 114.0 (CH), 72.3 (CH₂), 49.3 (CH₂), 28.4 (CH₂), 28.3 (CH₂), 26.4 (CH₃), 25.6 (CH₃), 22.7 (CH₃), 22.6 (CH₃).

Elemental Analysis: Expected: C 62.93, H 7.39, N 4.89. Found: C 63.06, H 7.55, N 5.02.

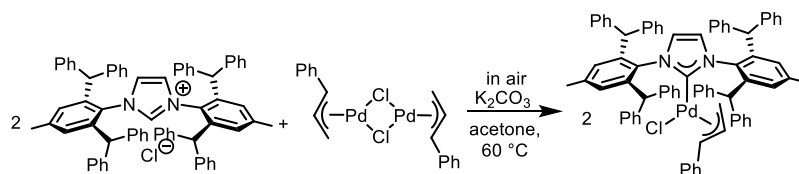
Analytical data obtained were in agreement with the reported values.²

Table S-2: Optimisation of the synthesis of [PdCl(η^3 -allyl)(IPr)]

Entries	IPr-HCl (equiv.)	[Pd(η^3 -allyl)Cl] ₂ (equiv.)	K ₂ CO ₃ (equiv.)	t (h)	Yield (%)
1	1.00	0.50	2	5	85*
2	1.10	0.50	2	5	75*
3	1.00	0.55	1.1	5	60*
4	1.00	0.60	1.1	5	57*
5	1.20	0.50	1	5	85

* ¹H NMR shows impurities in the spectra. ^aIsolated yield after filtration through silica using CH₂Cl₂. All reactions were carried out in air using technical grade acetone (0.23 M).

9.2.5. Synthesis and optimisation of [PdCl(η^3 -cin)(IPr*)]



Small scale: Following the general procedure; IPr*·HCl (110.00 mg, 0.11 mmol), [Pd(η^3 -cin)(μ -Cl)]₂ (30.00 mg, 0.06 mmol) and K₂CO₃ (13.50 mg, 0.09 mmol) were used. The reaction was left to stir for 1 h at 60 °C before the base was added. The product was obtained as a microcrystalline material in 94% (127.00 mg) yield.

Large scale: Following the general procedure; IPr*·HCl (3.00 g, 3.86 mmol), [Pd(η^3 -cin)(μ -Cl)]₂ (1.00 g, 1.93 mmol) and K₂CO₃ (1.07 g, 7.72 mmol) were used. The reaction was left to stir for 30 h. The product was obtained as a microcrystalline material in 98% (4.23 g) yield.

¹H NMR (400 MHz, CDCl₃): δ (ppm) = δ 7.50 (d, J = 7.1 Hz, 2H), 7.41 (t, J = 7.4 Hz, 4H), 7.37-7.18 (m, 16H), 7.13-7.08 (m, 14H), 6.82-6.77 (m, 14H), 6.09 (s, 2H), 5.70 (s, 2H), 5.31 (s, 2H), 5.01-4.96 (m, 1H), 4.64 (d, J = 12.8 Hz, 1H), 2.59 (d, J = 5.8 Hz, 1H), 2.23 (s, 6H).

¹³C {¹H} NMR (100 MHz, CDCl₃): δ (ppm) = δ 182.3 (C_{carbene}), 144.3 (C), 143.5 (C), 143.4 (C), 141.1 (C), 140.3 (C), 138.1 (C), 137.5 (C), 135.6 (C), 130.3 (CH), 130.0 (CH), 129.0 (CH), 128.9 (CH), 128.3 (CH), 128.1 (CH), 127.9 (CH), 127.4 (CH), 126.9 (CH), 126.1 (CH), 126.1 (CH), 123.2 (CH), 108.7 (C), 91.0 (C), 53.3 (CH), 47.1 (CH), 21.7 (CH₃).

Elemental Analysis: Expected: C 79.85, H 5.67, N 2.39. Found: C 79.64, H 5.81, N 2.36.

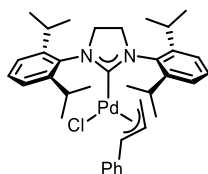
Analytical data obtained were in agreement with the reported values.³

Table S-3: Optimisation of the synthesis of [PdCl(η^3 -cin)(IPr*)]

Entries	IPr*.HCl (equiv.)	K ₂ CO ₃ (equiv.)	t (h)	Yield ^a (%)	Acetone (M)
1	2.00	4.00	5	80 ^{*b}	0.12
2	2.00	4.00	20	81 [*]	0.12
3	2.00	4.00	5	70 [*]	0.12
4	2.20	2.00	5	84 [*]	0.11
5	2.00	4.00	5	74 ^{*c}	0.11
6	2.00	2.00	5	59 [*]	0.11
7	2.00	4.00	5	73 ^{*c}	0.11
8	2.00	2.00	5	60 [*]	0.11
9	2.00	4.00	5	78 ^{*d}	0.11
10	2.00	4.00	20	99 ^d	0.11
11	2.00	4.00	24	94^d	0.23
12	2.00	3.00	20	73 [*]	0.23
13	2.00	4.00	24	93 ^e	0.11
14	2.00	4.00	24	98 [*]	0.06

* ¹H NMR shows impurities in the spectra. ^aIsolated yield after filtration through silica using CH₂Cl₂. All reactions were carried out in air using technical grade acetone. ^bClean NMR spectrum obtained but difficulties in reproducing it. ^cIPr*.HCl and [Pd(η^3 -cin)(μ -Cl)]₂ in acetone were stirred at 60 °C for 7 min, then K₂CO₃ was added and left to stir for 5 h at 60 °C. ^dIPr*.HCl and [Pd(η^3 -cin)(μ -Cl)]₂ in acetone were stirred at 60 °C for 1 h, then K₂CO₃ was added and the mixture was stirred at 60 °C for the indicated time. ^eIPr*.HCl and [Pd(η^3 -cin)(μ -Cl)]₂ in acetone were stirred at 60 °C for 3 h, then K₂CO₃ was added and the mixture was stirred at 60 °C for 24 h.

9.2.6. Synthesis of [PdCl(η^3 -cin)(SIPr)]



Following the general procedure; SIPr-HCl (110.00 mg, 0.23 mmol), [Pd(η^3 -cin)(μ -Cl)]₂ (49.70 mg, 0.09 mmol) and K₂CO₃ (26.90 mg, 0.19 mmol) were used. The product was obtained as a microcrystalline material in 78 % (122.00 mg) yield.

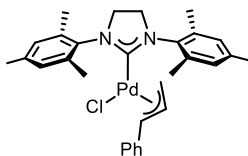
¹H NMR (400 MHz, CDCl₃): δ (ppm) = δ 7.38-7.35 (m, 2H), 7.26 (d, *J* = 7.5 Hz, 4H), 7.14-7.13 (m, 5H), 5.09-5.01 (m, 1H), 4.33 (d, *J* = 13.3 Hz, 1H), 4.02 (s, 4H), 3.78 (s, 1H), 3.44 (br. s, 4H), 2.88 (br.s., 1H), 1.43-1.41 (m, 12H), 1.27 (d, *J* = 6.3 Hz, 12H).

¹³C {¹H} NMR (100 MHz, CDCl₃): δ (ppm) = δ 212.1 (C_{carbene}), 147.2 (C), 137.7 (C), 136.4 (C), 129.1 (C), 128.3 (CH), 127.4 (CH), 126.8 (CH), 124.3 (CH), 109.2 (CH), 91.7 (CH), 54.1 (CH), 46.0 (CH₂), 28.6 (CH₃), 26.7 (CH₃).

Elemental analysis: Expected: C 66.56, H 7.29, N 4.31. Found: C 66.62, H 7.36, N 4.27.

Analytical data obtained were in agreement with the reported values.⁴

9.2.7. Synthesis of [PdCl(η^3 -cin)(SIMes)]



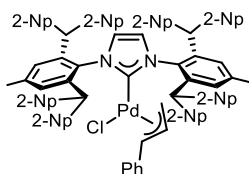
Following the general procedure; SIMes-HCl (100.00 mg, 0.29 mmol), [Pd(η^3 -cin)(μ -Cl)]₂ (62.90 mg, 0.11 mmol) and K₂CO₃ (33.50 mg, 0.24 mmol) were used. The product was obtained as a microcrystalline material in 80% (135.00 mg) yield.

¹H NMR (400 MHz, CDCl₃): δ (ppm) = δ 7.26-7.12 (m, 3H), 7.06-7.04 (m, 2H), 6.96 (s, 2H), 6.93 (s, 2H), 5.30 (s, 1H), 5.12-5.04 (m, 1H), 4.27 (d, *J* = 12.9 Hz, 1H), 3.99 (br.s., 4H), 3.27 (d, *J* = 6.9 Hz, 1H), 2.44 (s, 6H), 2.31 (s, 6H), 1.92 (d, *J* = 12.0 Hz, 6H).

¹³C {¹H} NMR (100 MHz, CDCl₃): δ (ppm) = δ 211.2 (C_{carbene}), 138.3 (C_{Ar}), 138.1 (C_{Ar}), 136.6 (C_{Ar}), 136.5 (C_{Ar}), 136.0 (C_{Ar}), 129.5 (CH), 128.3 (CH), 127.9 (CH), 127.4 (CH), 126.7 (CH), 125.9 (CH), 109.7 (CH_{cin}), 92.4 (CH_{cin}), 90.3 (CH_{cin}), 51.3 (CH_{2(imid.)}), 46.8 (CH_{2(imid.)}), 21.2 (CH_{3(Mes)}), 18.7 (CH_{3(Mes)}), 18.6 (CH_{3(Mes)}).

Elemental analysis: Expected: C 63.72, H 6.24, N 4.95. Found: C 63.84, H 6.35, N 4.96.

9.2.8. Synthesis of [PdCl(η^3 -cin)(IPr*^{2-Np})]



Following the general procedure; IPr*^{2-Np}·HCl (171.20 mg, 0.12 mmol), [Pd(η^3 -cin)(μ -Cl)]₂ (30.00 mg, 0.06 mmol) and K₂CO₃ (32.00 mg, 0.23 mmol) were used. The reaction was left to stir for 1 h at 60 °C before the base was added. The product was obtained as a microcrystalline material in 94% (170.00 mg) yield.

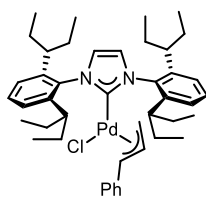
¹H NMR (400 MHz, CDCl₃): δ (ppm) = δ 7.86-7.84 (m, 12H), 7.71 (d, *J* = 6.9 Hz, 2H), 7.62 (d, *J* = 7.8 Hz, 4H), 7.67-7.51 (m, 6H), 7.47-7.41 (m, 10H), 7.39-7.29 (m, 9H), 7.26-7.16 (m, 14H), 7.16 (d, *J* = 15.6 Hz, 4H), 7.12 (s, 4H), 6.94 (d, *J* = 8.0 Hz, 2H), 6.60 (d, *J* = 9.7 Hz, 2H), 5.37 (s, 2H), 5.05 (d, *J* = 12.9 Hz, 1H), 3.15 (d, *J* = 7.1 Hz, 1H), 2.24 (s, 6H), 1.94 (d, *J* = 11.3 Hz, 1H).

¹³C {¹H} NMR (100 MHz, CDCl₃): δ (ppm) = δ 182.0 (C_{carbene}), 141.2 (C), 138.5 (C), 135.9 (C), 133.0 (C), 132.9(C), 132.0 (CH), 131.8 (CH), 130.7 (CH), 129.2 (CH), 128.9 (CH), 128.6 (CH₂), 127.9 (CH₂), 127.8 (CH₂), 127.7 (CH₂), 127.4 (CH₂), 127.3 (CH₂), 127.0 (CH₂), 125.7 (CH₂), 125.6 (CH₂), 125.5 (CH₂), 109.6 (CH₂), 92.1 (CH₂), 51.5 (CH₂), 47.1 (CH₂), 21.7 (CH₃).

Elemental analysis: Expected: C 84.01, H 5.19, N 1.78. Found: C 83.87, H 5.23, N 1.91.

Analytical data obtained were in agreement with the reported values.⁵

9.2.9. Synthesis of [PdCl(η^3 -cin)(IPent)]



Following the general procedure; IPent·HCl (100.00 mg, 0.18 mmol), [Pd(η^3 -cin)(μ -Cl)]₂ (48.20 mg, 0.09 mmol) and K₂CO₃ (51.40 mg, 0.37 mmol) were used. The reaction was left to stir for 1 h at 60 °C before the base was added. The product was obtained as a microcrystalline material in 85% (123.00 mg) yield.

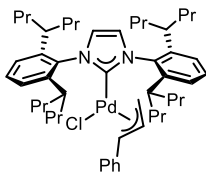
¹H NMR (400 MHz, CDCl₃): δ (ppm) = δ 7.41-7.37 (m, 2H), 7.18-7.09 (m, 11 H), 5.21-5.13 (m, 1H), 4.41 (d, *J* = 13.4 Hz, 1H), 2.58-2.58 (br. m, 4H), 2.34 (br.s. 1H), 2.11-1.97 (m, 4H), 1.76-1.72 (m, 4H), 1.63-1.60 (m, 4H), 1.52-1.43 (m, 4H), 1.26 (s, 1H), 1.01-0.97 (m, 12H), 0.77-0.74 (m, 12H).

^{13}C { ^1H } NMR (100 MHz, CDCl_3): δ (ppm) = δ 181.5 ($\text{C}_{\text{carbene}}$), 143.6 (C), 137.5 (C) 137.5 (C), 128.8 (CH), 128.2 (CH), 127.2 (CH), 126.6 (CH), 124.8 (CH), 124.2 (CH), 108.2 (C), 91.4 (CH), 41.5 (CH), 27.9 (CH_2), 27.2 (CH_2), 12.8 (CH_3), 11.2 (CH_3).

Elemental analysis: Expected: C 69.55, H 8.09, N 3.69. Found: C 69.49, H 8.19, N 3.80.

Analytical data obtained were in agreement with the reported values.⁶

9.2.10. Synthesis of $[\text{PdCl}(\eta^3\text{-cin})(\text{IHept})]$



Following the general procedure; IHept-HCl (100.00 mg, 0.15 mmol), $[\text{Pd}(\eta^3\text{-cin})(\mu\text{-Cl})_2]$ (39.80 mg, 0.07 mmol) and K_2CO_3 (42.50 mg, 0.31 mmol) were used. The reaction was left to stir for 1 h at 60 °C before the base was added. The product was obtained as a microcrystalline material in 81% (109.00 mg) yield.

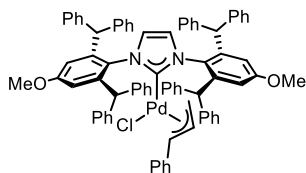
^1H NMR (400 MHz, CDCl_3): δ (ppm) = δ 7.40-7.36 (m, 2H), 7.19-7.13 (m, 9H), 7.06 (s, 2H), 5.18-5.10 (m, 1H), 4.44 (d, J = 13.8 Hz, 1H), 2.61 (br.s., 4H), 1.98-1.91 (m, 4H), 1.56-1.26 (m, 22H), 1.15-1.11 (m, 8H), 0.90-0.80 (m, 24H).

^{13}C { ^1H } NMR (100 MHz, CDCl_3): δ (ppm) = δ 181.4 ($\text{C}_{\text{carbene}}$), 144.2 (C), 137.5 (C), 137.2 (CH_2), 128.9 (CH), 128.1 (CH), 127.3 (CH), 126.5 (CH), 124.7 (CH), 124.2 (CH), 108.1 (C), 91.5 (CH), 39.1 (CH_3), 39.0 (CH), 37.8 (CH_2), 21.4 (CH_2), 20.3 (CH_2), 14.5 (CH_3).

Elemental analysis: Expected: C 71.62, H 8.90, N 3.21. Found: C 71.50, H 8.75, N 3.30.

Analytical data obtained were in agreement with the reported values.⁶

9.2.11. Synthesis of $[\text{PdCl}(\eta^3\text{-cin})(\text{IPr}^*\text{OMe})]$



Following the general procedure; $\text{IPr}^*\text{OMe}\cdot\text{HCl}$ (100.00 mg, 0.10 mmol), $[\text{Pd}(\eta^3\text{-cin})(\mu\text{-Cl})_2]$ (26.70 mg, 0.05 mmol) and K_2CO_3 (28.50 mg, 0.21 mmol) were used. The reaction was left to stir for 1 h at 60 °C before the base was added. The product was obtained as a microcrystalline material in 85% (107.00 mg) yield.

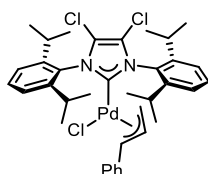
^1H NMR (400 MHz, CDCl_3): δ (ppm) = δ 7.49 (d, J = 7.4 Hz, 2H), 7.40 (t, J = 7.1 Hz, 2H), 7.30-7.19 (m, 22H), 7.10-7.09 (m, 12H), 6.85 (d, J = 7.2 Hz, 4H), 6.80 (d, J = 6.6 Hz, 4H), 6.55 (s, 4H), 6.07 (s, 2H), 5.73 (s, 2H), 5.23 (s, 2H), 5.13-5.05 (m, 1H), 4.69-4.66 (m, 1H), 3.57 (s, 6H), 2.67-2.66 (m, 1H).

^{13}C $\{^1\text{H}\}$ NMR (100 MHz, CDCl_3): δ (ppm) = δ 182.9 ($\text{C}_{\text{carbene}}$), 158.6 (C), 144.0 (C), 130.2 (C), 129.0 (C), 128.9 (C), 128.4 (C), 128.1 (C), 128.0 (CH), 127.4 (CH), 127.0 (CH), 126.3 (CH), 126.1 (CH), 123.3 (CH), 114.8 (CH), 114.7 (CH), 108.7 (C), 91.7 (CH), 54.8 (CH_2), 51.4 (CH_3), 47.0 (CH_3).

Elemental analysis: Expected: C 77.80, H 5.44, N 2.33. Found: C 77.59, H 5.35, N 2.36.

Analytical data obtained were in agreement with the reported values.⁷

9.2.12. Synthesis of $[\text{PdCl}(\eta^3\text{-cin})(\text{IPr}^{\text{Cl}})]$



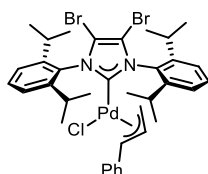
Following the general procedure; $\text{IPr}^{\text{Cl}}\cdot\text{HCl}$ (100.00 mg, 0.20 mmol), $[\text{Pd}(\eta^3\text{-cin})(\mu\text{-Cl})_2]$ (52.20 mg, 0.10 mmol) and K_2CO_3 (55.70 mg, 0.40 mmol) were used. The product was obtained as a microcrystalline material in 92% (113.20 mg) yield.

^1H NMR (400 MHz, CDCl_3): δ (ppm) = δ 7.52 (t, J = 7.7 Hz, 2H), 7.33 (d, J = 7.7 Hz, 4H), 7.16-7.10 (m, 5H), 5.07 (dt, J = 12.6, 9.3 Hz, 1H), 4.34 (d, J = 12.6 Hz, 1H), 3.09 (br.s., 1H), 2.91 (br.s., 4H), 1.84 (bs, 1H), 1.36-1.35 (m, 12H), 1.20 (d, J = 6.8 Hz, 12H)

^{13}C $\{^1\text{H}\}$ NMR (100 MHz, CDCl_3): δ (ppm) = δ 188.6 ($\text{C}_{\text{carbene}}$), 147.0 (C), 137.8 (C), 133.2 (C), 130.9 (CH), 128.4 (CH), 127.7 (CH), 127.1 (CH), 127.1 (CH), 124.6 (CH), 119.9 (C), 109.0 (CH), 90.6 (CH), 49.0 (CH_2), 28.2 (CH), 25.2 (CH_3), 24.1 (CH_3)

Elemental analysis: Expected: C 60.66, H 6.47, N 3.82. Found: C 60.58, H 6.35, N 3.93.

Analytical data obtained were in agreement with the reported values.⁸

9.2.13. Synthesis of [PdCl(η^3 -cin)(IPr^{Br})]

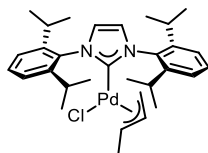
Following the general procedure; IPr^{Br}·HCl (100.00 mg, 0.17 mmol), [Pd(η^3 -cin)(μ -Cl)]₂ (44.20 mg, 0.08 mmol) and K₂CO₃ (47.30 mg, 0.34 mmol) were used. The product was obtained as a microcrystalline material in 90% (103.10 mg) yield.

¹H NMR (400 MHz, CDCl₃): δ (ppm) = δ 7.51 (t, J = 7.8 Hz, 2H), 7.33 (d, J = 7.8 Hz, 4H), 7.16-7.10 (m, 5H), 5.07 (dt, J = 12.6, 9.3 Hz, 1H), 4.34 (d, J = 12.6 Hz, 1H), 3.14-3.02 (m, 1H), 2.93-2.87 (m, 4H), 1.86 (br.s., 1H), 1.36 (d, J = 6.7 Hz, 12H), 1.23 (d, J = 6.7 Hz, 12H).

¹³C {¹H} NMR (100 MHz, CDCl₃): δ (ppm) = δ 190.3 (C_{carbene}), 146.8 (C), 137.7 (C), 134.8 (C), 130.8 (CH), 128.4 (CH), 127.7 (CH), 127.1 (CH), 124.6 (CH), 111.1 (C), 109.0 (CH), 90.8 (CH), 49.4 (CH₂), 28.8 (CH), 25.3 (CH₃), 24.5 (CH₃).

Elemental analysis: Expected: C 52.68, H 5.38, N 3.48. Found: C 52.23, H 5.25, N 3.69.

Analytical data obtained were in agreement with the reported values.⁸

9.2.14. Synthesis of [PdCl(η^3 -crotyl)(IPr)]

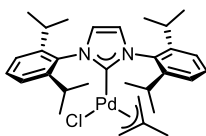
Following the general procedure; IPr·HCl (151.00 mg, 0.35 mmol), [Pd(η^3 -crotyl)(μ -Cl)]₂ (50.00 mg, 0.13 mmol) and K₂CO₃ (35.00 mg, 0.25 mmol) were used. The product was obtained as a microcrystalline material in 82% (121.00 mg) yield.

¹H NMR (400 MHz, CDCl₃): δ (ppm) = δ 7.43 (t, J = 7.8 Hz, 2H), 7.27-7.25 (m, 4H), 7.14 (s, 2H), 4.53 (td, J = 12.0, 6.8 Hz, 1H), 3.48 (dd, J = 12.5, 6.2 Hz, 1H), 3.10 (hept, J = 7.5 Hz, 2H), 2.90 (hept, J = 6.8 Hz, 2H), 2.71 (d, J = 6.2 Hz, 1H), 1.37-1.34 (m, 16H), 1.51 (d, J = 6.9 Hz, 6H), 1.11 (d, J = 6.9 Hz, 6H).

¹³C {¹H} NMR (100 MHz, CDCl₃): δ (ppm) = δ 186.8 (C_{carbene}), 146.2 (C), 146.1 (C), 129.9 (C), 124.7 (CH), 123.9 (CH), 123.9 (CH), 113.2 (CH), 96.1 (C), 44.8 (CH), 28.7 (CH₃), 26.5 (CH₃), 25.9 (CH₃), 23.1 (CH₃), 17.1 (CH₃).

Elemental analysis: Expected: C 63.59, H 7.40, N 4.78. Found: C 63.41, H 7.27, N 4.79.

Analytical data obtained were in agreement with the reported values.⁴

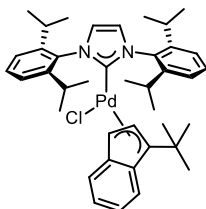
9.2.15. Synthesis of [PdCl(η^3 -2-Me-allyl)(IPr)]

Following the general procedure; IPr·HCl (151.00 mg, 0.36 mmol), [Pd(η^3 -2-Me-allyl)(μ -Cl)]₂ (50.00 mg, 0.13 mmol) and K₂CO₃ (35.00 mg, 0.25 mmol) were used. The product was obtained as a microcrystalline material in 81% yield (120.00 mg).

¹H NMR (400 MHz, CDCl₃): δ (ppm) = δ 7.44 (t, J = 7.8 Hz, 2H), 7.31-7.27 (m, 4H), 7.16 (s, 2H), 5.34-5.34 (m, 1H), 3.71 (d, J = 3.0 Hz, 1H), 3.14 (hept, J = 6.7 Hz, 2H), 2.96 (hept, J = 6.4 Hz, 2H), 2.76 (d, J = 2.9 Hz, 1H), 2.69 (s, 1H), 1.43 (d, J = 6.7 Hz, 6H), 1.32 (d, J = 6.8 Hz, 6H), 1.22 (s, 3H), 1.18 (d, J = 6.9 Hz, 6H), 1.07 (d, J = 6.9 Hz, 6H).

¹³C {¹H} NMR (100 MHz, CDCl₃): δ (ppm) = δ 187.4 (C_{carbene}), 146.3 (C), 146.1 (C), 136.3 (C), 129.9 (CH), 129.1 (CH), 124.2 (CH), 124.0 (CH), 123.9 (CH), 71.5 (C), 53.6 (CH), 49.5 (CH), 28.6 (CH₃), 28.5 (CH₃), 26.6 (CH₃), 26.0 (CH₃), 23.1 (CH₃), 22.8 (CH₃), 22.5 (CH₃).

Elemental analysis: Expected: C 63.59, H 7.40, N 4.78. Found: C 63.62, H 7.56, N 4.90.

9.2.16. Synthesis of [PdCl(η^3 -Ind^{tBu})(IPr)]

Following the general procedure; IPr·HCl (57.00 mg, 0.13 mmol), [Pd(η^3 -Ind^{tBu})(μ -Cl)]₂ (30.00 mg, 0.05 mmol) and K₂CO₃ (13.10 mg, 0.09 mmol) were used. The product was obtained as a microcrystalline material in 84% yield (60.00 mg).

¹H NMR (400 MHz, CDCl₃): δ (ppm) = δ 7.49 (t, J = 7.7 Hz, 2H), 7.36 (d, J = 7.5 Hz, 2H), 7.22 (d, J = 7.7 Hz, 2H), 7.11 (d, J = 7.7 Hz, 1H), 7.09 (s, 2H), 6.72 (t, J = 7.5 Hz, 1H), 6.36 (t, J = 7.5 Hz, 1H), 5.02 (d, J = 2.5 Hz, 1H), 3.18 (dt, J = 13.6, 6.8 Hz, 2H), 2.75 (dt, J = 13.5, 6.7 Hz, 2H), 1.45 (d, J = 6.7 Hz, 6H), 1.26 (d, J = 8.5 Hz, 12H), 1.20 (d, J = 6.8 Hz, 6H), 1.11 (d, J = 6.7 Hz, 6H), 0.96 (d, J = 6.9 Hz, 6H).

¹³C {¹H} NMR (100 MHz, CDCl₃): δ (ppm) = δ 176.3 (C_{carbene}), 146.1 (C), 146.0 (C), 139.0 (C), 138.3 (C), 136.4 (C), 129.8 (CH), 124.7 (CH), 119.0 (CH), 116.6 (CH), 107.3 (C), 63.3 (CH), 34.0 (CH₂), 29.6 (CH₃), 28.8 (CH₃), 28.6 (CH₃), 26.6 (CH₃), 25.5 (CH₃), 23.6 (CH₃), 22.3 (CH₃).

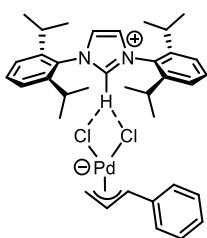
Elemental analysis: Expected: C 68.46, H 7.33, N 3.99. Found: C 68.38, H 7.32, N 4.11.

Analytical data obtained were in agreement with the reported values.⁹

9.2.17. General procedure of [NHC·H][Pd(L)Cl₂]

In air, the corresponding NHC·HCl (2 equiv.) and [Pd(η³-R-allyl)(μ-Cl)]₂ (1 equiv.) were added to a mortar. The two solids were mixed and ground using a pestle for 5 min. A crystalline solid was obtained in quantitative yield.

9.2.17.1 Synthesis of [IPr·H][Pd(η³-cin)Cl₂] Pd(ate)-1

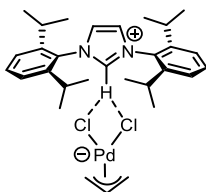


Following the general procedure from IPr·HCl (82.10 mg, 0.19 mmol) and [Pd(η³-cin)(μ-Cl)]₂ (35.30 mg, 0.09 mmol), the product was obtained as a yellow powder in 99% yield (117.00 mg).

¹H NMR (400 MHz, CDCl₃): δ (ppm) = δ 9.19 (s, 1H, C_{NCHN}), 8.32 (d, *J* = 1.6 Hz, 2H, CH_{imid}), 7.54 (t, *J* = 8.1 Hz, 2H, CH_{Ar}), 7.45 (dd, *J* = 7.7, 1.6 Hz, 2H, CH_{Ar(cin)}), 7.33 (d, *J* = 7.9 Hz, 4H, CH_{Ar}), 7.21-7.19 (m, 3H, CH_{Ar(cin)}), 5.69-5.62 (m, 1H, CH_(cin)), 4.46-4.44 (m, 1H, CH_{2(cin)}), 3.86 (d, *J* = 6.6 Hz, 1H, CH_{2(cin)}), 2.90 (d, *J* = 11.9 Hz, 1H, CH_(cin)), 2.48-2.41 (m, 4H, CH_(IPr)), 1.27 (d, *J* = 6.8 Hz, 12H, CH_{3(IPr)}), 1.19 (d, *J* = 6.7 Hz, 12H, CH_{3(IPr)}).

¹³C {¹H} NMR (100 MHz, CDCl₃): δ (ppm) = δ 145.1 (C_{Ar}), 136.9 (CH_{NCHN}), 132.1 (CH_{Ar}), 129.9 (C_{Ar}), 128.7 (CH_{cin}), 127.9 (CH_{cin}), 127.7 (CH_{imid}), 124.7 (CH), 105.2 (CH_{cin}), 81.8 (CH_{cin}), 58.4 (CH_{2(cin)}), 29.0 (CH_(IPr)), 24.7 (CH_{3(IPr)}), 23.9 (CH_{3(IPr)}).

Elemental Analysis: Expected: C 63.02, H 7.05, N 4.08. Found: C 63.11, H 6.95, N 4.14.

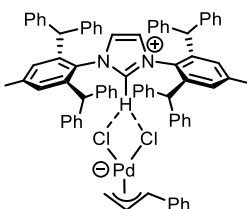
9.2.17.2. Synthesis of [IPr·H][Pd(η^3 -allyl)Cl₂] Pd(ate)-2

Following the general procedure from IPr·HCl (82.04 mg, 0.19 mmol) and [Pd(η^3 -allyl)(μ -Cl)]₂ (35.30 mg, 0.09 mmol), the product was obtained as a yellow powder in 99% yield (117.00 mg).

¹H NMR (400 MHz, CDCl₃): δ (ppm) = 9.16 (s, 1H, C_{NCHN}), 8.28 (d, J = 1.6 Hz, 2H, CH_{imid}), 7.54-7.50 (m, 2H, CH_{Ar}), 7.32 (d, J = 7.2 Hz, 4H, CH_{Ar}), 5.16-5.10 (m, 1H, CH_{allyl}), 3.76 (s, 2H, CH_{allyl}), 2.67 (d, J = 11.6 Hz, 2H, CH_{allyl}), 2.48-2.44 (m, 4H, CH_{IPr}), 1.27 (d, J = 6.8 Hz, 12H, CH_{3(IPr)}), 1.20 (d, J = 7.2 Hz, 12H, CH_{3(IPr)}).

¹³C {¹H} NMR (100 MHz, CDCl₃): δ (ppm) = δ 144.9 (C_{Ar}), 136.8 (CH_{NCHN}), 131.8 (C_{Ar}), 129.7 (C_{Ar}), 127.3 (CH_{Ar}), 124.4 (CH_{allyl}), 108.9 (C_{allyl}), 60.3 (CH_{allyl}), 28.8 (CH_{IPr}), 24.4 (CH_{3(IPr)}), 23.8 (CH_{3(IPr)}).

Elemental analysis: Expected: C 59.07, H 7.27, N 4.59. Found: C 58.90, H 7.17, N 4.57.

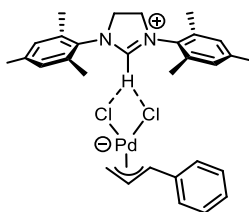
9.2.17.3. Synthesis of [IPr*·H][Pd(η^3 -cin)Cl₂] Pd(ate)-3

Following the general procedure from IPr*·HCl (108.57 mg, 0.12 mmol) and [Pd(η^3 -cin)(μ -Cl)]₂ (30.00 mg, 0.06 mmol), the product was obtained as a yellow powder in 99% yield (147.00 mg).

¹H NMR (400 MHz, CDCl₃): δ (ppm) = δ 12.52 (s, 1H, C_{NCHN}), 7.31-7.23 (m, 20H, CH_{Ar}), 7.19-7.06 (m, 19H, CH_{Ar}), 6.77-6.75 (m, 10H, CH_{Ar}), 5.87-5.75 (br. m, 1H, CH_{cin}), 5.41 (s, 4H, CH_{IPr}), 5.33 (s, 2H, CH_{cin}), 4.60-3.85 (br. m, 2H, CH_{cin}), 2.97-2.58 (m, 1H, CH_{cin}), 2.18 (s, 6H, CH₃).

¹³C {¹H} NMR (100 MHz, CDCl₃): δ (ppm) = δ 142.6 (C_{Ar}), 142.5 (CH_{NCHN}), 142.1 (C_{Ar}), 140.7 (C_{Ar}), 140.6 (C_{Ar}), 130.7 (CH_{Ar}), 130.2 (CH_{Ar}), 129.1 (CH_{Ar}), 128.3 (CH_{Ar}), 127.9 (CH_{Ar}), 126.6 (CH_{Ar}), 126.5 (CH_{Ar}), 122.8 (CH_{imid}), 105.6 (CH_{cin}), 82.2 (CH_{cin}), 59.3 (CH_{cin}), 51.0 (CH_(IPr*)), 21.7(CH_{3(IPr*)}).

Elemental analysis: Expected: C 77.38, H 5.66, N 2.31; Found: C 77.25, H 5.47, N 2.36.

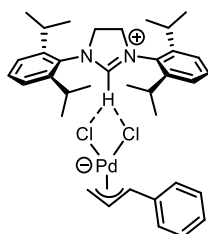
9.2.17.4. Synthesis of [SIMes·H][Pd(η^3 -cin)Cl₂] Pd(ate)-4

Following the general procedure from SIMes·HCl (52.10 mg, 0.11 mmol) and [Pd(η^3 -cin)(μ -Cl)]₂ (40.00 mg, 0.07 mmol), the product was obtained as a yellow powder in 99% yield (91.00 mg).

¹H NMR (400 MHz, CDCl₃): δ (ppm) = δ 8.99 (s, 1H, C_{NCHN}), 7.93 (d, J = 8.7 Hz, 2H, CH_{Imid}), 7.21-7.18 (m, 3H, CH_{Ar}), 6.94 (s, 4H, CH_{2(Imid)}), 5.56 (br.s., 1H, CH_{cin}), 4.51 (br.s., 1H, CH_{cin}), 4.24-4.21 (m, 1H, CH_{cin}), 3.79-3.75 (m, 1H, CH_{cin}), 2.72 (br.s., 1H, CH_{cin}), 2.37 (s, 12H, CH_{3(IMes)}), 2.29 (s, 6H, CH_{3(IMes)}).

¹³C {¹H} NMR (100 MHz, CDCl₃): δ (ppm) = δ 159.9 (CH_{NCHN}), 140.5 (C_{Ar}), 135.5 (C_{Ar}), 130.6 (C_{Ar}), 130.1 (C_{Ar}), 128.7 (CH_{Ar}), 128.0 (CH_{cin}), 127.6 (CH_{cin}), 105.3 (C_{cin}), 58.4 (CH_{2(SIMes)}), 52.2 (CH_{3(SIMes)}), 21.2 (CH_{3(SIMes)}), 18.4 (CH_{3(SIMes)}).

Elemental Analysis: Expected: C 59.86, H 6.03, N 4.65. Found: C 60.05, H 6.15, N 4.65.

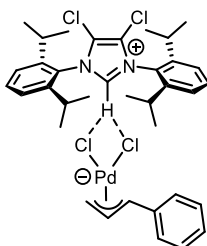
9.2.17.5. Synthesis of [SIPr·H][Pd(η^3 -cin)Cl₂] Pd(ate)-5

Following the general procedure from SIPr·HCl (65.00 mg, 0.15 mmol), [Pd(η^3 -cin)(μ -Cl)]₂ (40.00 mg, 0.07 mmol), the product was obtained as a yellow powder in 99% yield (107.00 mg).

¹H NMR (400 MHz, CDCl₃): δ (ppm) = δ 7.71 (s, 1H, C_{NCHN}), 7.53-7.48 (m, 4H, CH_{Ar(IPr + cin)}), 7.31-7.26 (m, 7H, CH_{Ar(IPr + cin)}), 5.80-5.72 (m, 1H, CH_{cin}), 4.97 (s, 4H, CH_{2(Imid)}), 4.55 (d, J = 11.1 Hz, 1H, CH_{cin}), 3.96 (d, J = 6.7 Hz, 1H, CH_{cin}), 3.15-3.08 (m, 4H, CH_{SIPr}), 3.01 (d, J = 11.9 Hz, 1H, CH_{cin}), 1.42 (d, J = 6.3 Hz, 12H, CH_{3(SIPr)}), 1.23 (d, J = 6.3 Hz, 12H, CH_{3(SIPr)}).

¹³C {¹H} NMR (100 MHz, CDCl₃): δ (ppm) = δ 156.9 (CH_{NCHN}), 146.6 (C_{Ar}), 131.6 (CH_{Ar}), 129.5 (C_{Ar}), 129.1 (CH_{cin}), 128.4 (CH_{cin}), 128.1 (CH_{cin}), 125.1 (CH_{Ar}), 105.9 (CH_{cin}), 81.3 (CH_{cin}), 59.0 (CH_{2(cin)}), 56.0 (CH_{2(imid)}), 29.1 (CH_(IPr)), 25.6 (CH_{3(IPr)}), 24.1 (CH_{3(IPr)}).

Elemental analysis: Expected: C 63.02, H 7.05, N 4.08. Found: C 63.28, H 6.96, N 4.15.

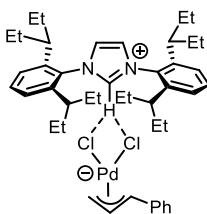
9.2.17.6. Synthesis of [IPr^{Cl}-H][Pd(η^3 -cin)Cl₂] Pd(ate)-6

Following the general procedure from IPr^{Cl}-HCl (75.00 mg, 0.15 mmol) and [Pd(η^3 -cin)(μ -Cl)]₂ (40.00 mg, 0.07 mmol), the product was obtained as a yellow powder in 99% yield (144.00 mg).

¹H NMR (400 MHz, CDCl₃): δ (ppm) = δ 12.85 (s, 1H, C_{NCHN}), 7.63 (t, J = 7.4 Hz, 2H, CH_{Ar}), 7.48-7.44 (m, 3H, CH_{Ar}), 7.38 (d, J = 7.9 Hz, 4H, CH_{Ar}), 7.34 (d, J = 7.8 Hz, 2H, CH_{Ar}), 5.79 (s, 1H, CH_{cin}), 4.60 (s, 1H, CH_{cin}), 3.96 (s, 1H, CH_{cin}), 3.20 (s, 1H, CH_{cin}), 2.37 (quant, J = 7.4 Hz, 4H, CH_{IPr}), 1.37 (d, J = 6.7 Hz, 12H, CH_{3(IPr)}), 1.29 (d, J = 6.9 Hz, 12H, CH_{3(IPr)})

¹³C {¹H} NMR (100 MHz, CDCl₃): δ (ppm) = δ 145.7 (C_{Ar}), 132.9 (CH_{NCHN}), 129.1 (CH_{Ar}), 128.1 (CH_{Ar}), 127.3 (CH_{Ar}), 125.1 (CH_{cin}), 124.6 (CH_{cin}), 121.2 (CH_{cin}), 106.0 (CH_{2(cin)}), 29.9 (CH_{IPr}), 24.9 (CH_{3(IPr)}), 23.5 (CH_{3(IPr)})

Elemental analysis: Expected: C 56.42, H 5.89, N 3.72. Found: C 56.57, H 6.03, N 3.70.

9.2.17.7. Synthesis of [IPent-H][Pd(η^3 -cin)Cl₂] Pd(ate)-7

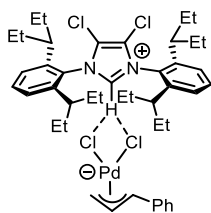
Following the general procedure from IPent-HCl (62.20 mg, 0.12 mmol) and [Pd(η^3 -cin)(μ -Cl)]₂ (30.00 mg, 0.06 mmol), the product was obtained as a yellow powder in 99% (92.00 mg).

¹H NMR (400 MHz, CDCl₃): δ (ppm) = δ 8.43 (d, J = 1.6 Hz, 2H, CH_{Imid}), 8.37 (br. s, 1H, C_{NCHN}), 7.60 (t, J = 7.9 Hz, 2H, CH_{Ar}), 7.50 (d, J = 7.5 Hz, 2H, CH_{Ar(cin)}), 7.27-7.25 (m, 7H, CH_{Ar}), 5.75 (br. s, 1H, CH_{cin}), 4.60 (br. s, 1H, CH_{2(cin)}), 3.93 (br. s, 1H, CH_{2(cin)}), 3.00 (br. s, 1H, CH_{cin}), 1.96 (sept, J = 8.1 Hz, 4H, CH_{IPent}), 1.75-1.60 (m, 16H, CH_{2(IPent)}), 0.86 (t, J = 7.1 Hz, 12H, CH_{3(IPent)}), 0.76 (t, J = 7.4 Hz, 12H, CH_{3(IPent)}).

¹³C {¹H} NMR (100 MHz, CDCl₃): δ (ppm) = δ 142.7 (C_{Ar}), 134.9 (CH_{NCHN}), 132.8 (C_{Ar}), 132.0 (CH_{Ar}), 129.2 (CH_{cin}), 128.9 (CH_{cin}), 128.3 (C_{cin}), 128.1 (CH_{imid}), 125.4 (CH_{Ar}), 105.6 (CH_{cin}), 81.2 (CH_{cin}), 59.2 (CH_{2(cin)}), 43.5 (CH_{IPent}), 29.4 (CH_{2(IPent)}), 28.5 (CH_{2(IPent)}), 12.6 (CH_{3(IPent)}), 12.4 (CH_{3(IPent)}).

Elemental analysis: Expected: C 65.07, H 7.85, N 3.52. Found: C 64.77, H 7.94, N 3.68.

9.2.16.8. Synthesis of [IPent^{Cl}·H][Pd(η³-cin)Cl₂] Pd(ate)-8



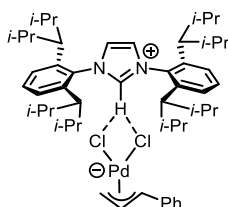
Following the general procedure from IPent^{Cl}·HCl (50.00 mg, 0.08 mmol) and [Pd(η³-cin)(μ-Cl)]₂ (21.00 mg, 0.04 mmol), the product was obtained as a yellow powder in 99% yield (71.00 mg).

¹H NMR (400 MHz, CDCl₃): δ (ppm) = δ 12.41 (s, 1H, C_{NCHN}), 7.60 (t, *J* = 7.7 Hz, 2H, CH_{Ar}), 7.48 (d, *J* = 7.3 Hz, 2H, CH_{Ar(cin)}), 7.29 (d, *J* = 7.7 Hz, 4H), 7.24-7.23 (m, 3H, CH_{Ar(cin)}), 5.74 (br. s, 1H, CH_(cin)), 4.56 (br. s, 1H, CH_{2(cin)}), 3.92 (br. s, 1H, CH_{2(cin)}), 2.97 (br. s, 1H, CH_(cin)), 1.96-1.95 (m, 4H, CH_(IPentCl)), 1.86-1.78 (m, 8H, CH_{2(IPentCl)}), 1.69-1.63 (m, 8H, CH_{2(IPentCl)}), 0.89-0.84 (m, 24H, CH_{3(IPentCl)}).

¹³C {¹H} NMR (100 MHz, CDCl₃): δ (ppm) = δ 143.4 (C_{Ar}), 142.8 (C_{Climid}), 137.3 (CH_{NCHN}), 132.2 (CH_{Ar}), 129.6 (CH_{Ar}), 128.1 (CH_{Ar}), 126.1 (CH_{Ar}), 121.1 (C_{Ar}), 105.9 (CH_{cin}), 81.9 (CH_{cin}), 59.2 (CH_{2(cin)}), 43.4 (CH_(IPentCl)), 29.3 (CH_{2(IPentCl)}), 27.2 (CH_{2(IPentCl)}), 12.4 (CH_{3(IPentCl)}), 11.9 (CH_{3(IPentCl)}).

Elemental analysis: Expected: C 61.08, H 6.99, N 3.24. Found: C 60.90, H 6.78, N 3.14.

9.2.16.9. Synthesis of [IHept·H][Pd(η³-cin)Cl₂] Pd(ate)-9



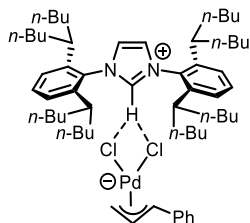
Following the general procedure from IHept·HCl (50.00 mg, 0.08 mmol) and [Pd(η³-cin)(μ-Cl)]₂ (20.00 mg, 0.04 mmol), the product was obtained as a yellow powder in 96% yield (67.00 mg).

¹H NMR (400 MHz, CDCl₃): δ (ppm) = δ 8.51 (s, 2H, CH_{imid}), 7.95 (s, 1H, C_{NCHN}), 7.60 (t, *J* = 7.8 Hz, 2H, CH_{Ar}), 7.49 (d, *J* = 9.1 Hz, 2H, CH_{Ar(cin)}), 7.27-7.25 (m, 4H, CH_{Ar}), 7.21-7.19 (m, 3H, CH_{Ar(cin)}), 5.68 (br. s, 1H, CH_(cin)), 4.47 (br. s, 1H, CH_{2(cin)}), 3.88 (d, *J* = 6.0 Hz, 1H, CH_{2(cin)}), 2.94 (d, *J* = 11.6 Hz, 1H, CH_(cin)), 2.08-2.01 (m, 4H, CH_(IHept)), 1.65-1.49 (m, 16H, CH_{2(IPent)}), 1.34-1.25 (m, 4H, CH_{2(IHept)}), 1.11-0.95 (m, 12H, CH_{2(IHept)}), 0.89-0.81 (m, 24H, CH_{3(IHept)}).

¹³C {¹H} NMR (100 MHz, CDCl₃): δ (ppm) = δ 143.1 (C_{Ar}), 134.2 (CH_{NCHN}), 132.0 (CH_{Ar} + C_{Ar}), 129.3 (CH_{imid}), 128.6 (CH_{cin}), 128.0 (CH_{cin}), 125.3 (CH_{Ar}), 105.1 (CH_{cin}), 68.9 (CH_{cin}), 58.1 (CH_{2(cin)}), 40.5 (CH_(IHept)), 39.5 (CH_{2(IHept)}), 38.3 (CH_{2(IHept)}), 21.4 (CH_{2(IHept)}), 21.0 (CH_{2(IHept)}), 14.5 (CH_{3(IHept)}), 14.2 (CH_{3(IHept)}).

Elemental analysis: Expected: C 68.59, H 8.86, N 3.08. Found: C 68.75, H 9.03, N 2.96.

9.2.16.10. Synthesis of [INon·H][Pd(η^3 -cin)Cl₂] Pd(ate)-10



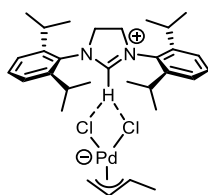
Following the general procedure from INon·HCl (50.00 mg, 0.06 mmol) and [Pd(η^3 -cin)(μ -Cl)]₂ (17.00 mg, 0.03 mmol), the product was obtained as a yellow powder in 99% yield (70.00 mg).

¹H NMR (400 MHz, CDCl₃): δ (ppm) = δ 8.45 (s, 2H, CH_{imid}), 7.94 (s, 1H, C_{NCHN}), 7.61 (t, J = 7.8 Hz, 2H, CH_{Ar}), 7.47 (d, J = 7.6 Hz, 2H, CH_{Ar(cin)}), 7.27 (d, J = 7.9 Hz, 4H, CH_{Ar}), 7.20 (d, J = 7.2 Hz, 3H, CH_{Ar(cin)}), 5.65 (br. s, 1H, CH_(cin)), 4.46 (br. s, 1H, CH_(cin)), 3.84 (br. s, 1H, CH_(cin)), 2.88 (br. s, 1H, CH_(cin)), 2.03-1.94 (m, 4H, CH_(INon)), 1.67-1.52 (m, 16H, CH_{2(INon)}), 1.28-1.20 (m, 20H, CH_{2(INon)}), 1.10-0.91 (m, 12H, CH_{2(INon)}), 0.87 (t, J = 7.1 Hz, 12H, CH_{3(INon)}), 0.79 (t, J = 7.3 Hz, 12H, CH_{3(INon)}).

¹³C {¹H} NMR (100 MHz, CDCl₃): δ (ppm) = δ 143.1 (C_{Ar}), 134.3 (CH_{NCHN}), 132.2 (CH_{Ar}), 132.0 (C_{Ar}), 129.1 (CH_{imid}), 128.6 (CH_{cin}), 128.0 (CH_{cin}), 125.4 (CH_{Ar}), 105.2 (CH_{cin}), 68.9 (CH_{cin}), 58.0 (CH_{2(cin)}), 40.7 (CH_{cin}), 37.0 (CH_{2(INon)}), 35.6 (CH_{2(INon)}), 30.2 (CH_{2(INon)}), 30.0 (CH_{2(INon)}), 23.1 (CH_{2(INon)}), 22.8 (CH_{2(INon)}), 14.1 (CH_{3(INon)}), 13.9 (CH_{3(INon)}).

Elemental analysis: Expected: C 70.60, H 9.28, N 2.74. Found: C 70.42, H 9.48, N 2.81.

9.2.16.11. Synthesis of [SIPr·H][Pd(η^3 -crotyl)Cl₂] Pd(ate)-11



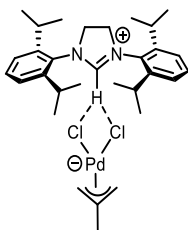
Following the general procedure from SIPr·HCl (86.90 mg, 0.21 mmol) and [Pd(η^3 -crotyl)(μ -Cl)]₂ (40.00 mg, 0.10 mmol), the product was obtained as a yellow powder in a 99% yield (126.00 mg).

¹H NMR (400 MHz, CDCl₃): δ (ppm) = δ 7.75 (s, 1H, C_{NCHN}), 7.47 (t, J = 7.8 Hz, 2H, CH_{imid}), 7.27-7.24 (m, 4H, CH_{Ar}), 5.09 (br.s., 1H, CH_{cin}), 4.97 (s, 4H, CH_{2(SIPr)}), 3.76-3.75 (m, 2H, CH_{crotyl}), 3.15 (dt, J = 13.6, 6.8 Hz, 4H, CH_{SIPr}), 2.63 (d, J = 11.6 Hz, 1H, CH_{crotyl}), 1.41 (d, J = 6.8 Hz, 12H, CH_{3(SIPr)}), 1.34 (d, J = 6.3 Hz, 3H, CH_{3(crotyl)}), 1.22 (d, J = 6.9 Hz, 12H, CH_{3(SIPr)}).

^{13}C { ^1H } NMR (100 MHz, CDCl_3): δ (ppm) = δ 157.1 (CH_{NCN}), 146.5 (C_{Ar}), 131.5 (C_{Ar}), 129.5 (CH_{Ar}), 125.0 (CH_{cin}), 110.0 (C_{cin}), 56.7 ($\text{CH}_2(\text{cin})$), 56.0 ($\text{CH}_2(\text{imid})$), 29.1 ($\text{CH}_3(\text{SIPr})$), 25.6 ($\text{CH}_3(\text{SIPr})$), 24.0 ($\text{CH}_3(\text{SIPr})$), 18.2 ($\text{CH}_3(\text{crotyl})$).

Elemental analysis: Expected C 59.67, H 7.43, N 4.45. Found: C 59.56, H 7.52, N 4.57.

9.2.16.12. Synthesis of $[\text{SIPr-H}][\text{Pd}(\eta^3\text{-2-Me-allyl})\text{Cl}_2] \text{Pd}(\text{ate})\text{-12}$

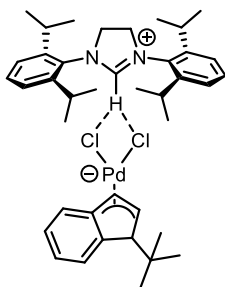


Following the general procedure from SIPr-HCl (86.90 mg, 0.20 mmol) and $[\text{Pd}(\eta^3\text{-2-Me-allyl})(\mu\text{-Cl})_2]$ (40.00 mg, 0.10 mmol), the product was obtained as a yellow powder in 99% yield (125.70 mg).

^1H NMR (400 MHz, CDCl_3): δ (ppm) = δ 7.62 (s, 1H, C_{NCHN}), 7.48 (t, $J = 7.8$ Hz, 2H, CH_{imid}), 7.28 (d, $J = 7.8$ Hz, 4H, CH_{Ar}), 5.01 (s, 4H, $\text{CH}_2(\text{imid})$), 3.73 (s, 2H, $\text{CH}_{\text{crotyl}}$), 3.19 (quant, $J = 6.8$ Hz, 4H, CH_{SIPr}), 2.73 (s, 2H, $\text{CH}_{\text{crotyl}}$), 2.03 (s, 3H, $\text{CH}_3(\text{crotyl})$), 1.43 (d, $J = 6.8$ Hz, 12H, $\text{CH}_3(\text{SIPr})$), 1.23 (d, $J = 6.9$ Hz, 12H, $\text{CH}_3(\text{SIPr})$).

^{13}C { ^1H } NMR (100 MHz, CDCl_3): δ (ppm) = δ 156.9 (C_{Ar}), 146.6 (CH_{NCN}), 131.6 (CH_{Ar}), 129.5 (CH_{Ar}), 125.1 (CH_{Ar}), 107.7 (CH_{allyl}), 60.5 (CH_{allyl}), 56.1 ($\text{CH}_2(\text{imid})$), 29.1 (CH_{SIPr}), 25.6 ($\text{CH}_3(\text{SIPr})$), 24.1 ($\text{CH}_3(\text{SIPr})$), 22.9 ($\text{CH}_3(2\text{-Me-allyl})$).

Elemental analysis: Expected C 59.67, H 7.43, N 4.45. Found: C 59.53, H 7.29, N 4.19.

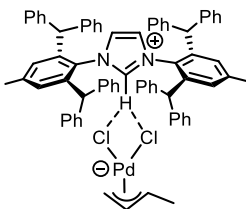
9.2.17.13. Synthesis of [SIPr·H][Pd(η^3 -Ind^{tBu})Cl₂] Pd(ate)-13

Following the general procedure from SIPr·HCl (54.60 mg, 0.13 mmol) and [Pd(η^3 -Ind^{tBu})(μ -Cl)]₂ (40.00 mg, 0.06 mmol), the product was obtained as a yellow powder in 99% yield (94.00 mg).

¹H NMR (400 MHz, CDCl₃): δ (ppm) = δ 7.64 (s, 1H, C_{NCHN}), 7.49 (t, J = 7.8 Hz, 2H, CH_{imid}), 7.29 (d, J = 7.8 Hz, 4H, CH_{Ar}), 7.13-7.09 (m, 1H, CH_{Ind}), 6.80-6.77 (m, 3H, CH_{Ind}), 6.37 (br.s, 1H, CH_{Ind}), 5.50 (br.s, 1H, CH_{Ind}), 4.90 (s, 4H, CH_{SIPr}), 3.10 (quant, J = 7.3 Hz, 4H, CH_{SIPr}), 1.42 (d, J = 6.8 Hz, 12H, CH_{3(SIPr)}), 1.42-1.39 (m, 9H, CH_{3(t-butyl)}), 1.22 (d, J = 6.9 Hz, 12H, CH_{3(SIPr)}).

¹³C {¹H} NMR (100 MHz, CDCl₃): δ (ppm) = δ 157.0 (C_{Ar}), 146.5 (CH_{NCHN}), 131.6 (CH_{Ar}), 129.5 (C_{Ar}), 125.1 (CH_{Ar}), 118.9 (CH_{Ar}), 117.4 (CH_{2(SIPr)}), 107.1 (CH_{2(SIPr)}), 55.9 (CH_{Ind}), 34.3 (CH_{Ind}), 29.2 (CH_{3(t-butyl)}), 29.1 (CH_{3(t-butyl)}), 25.7 (CH_{3(SIPr)}), 24.0 (CH_{3(SIPr)}).

Elemental analysis: Expected C 64.91, H 7.35, N 3.78. Found: C 64.73, H 7.20, N 3.81.

9.2.16.14. Synthesis of [IPr*·H][Pd(η^3 -crotyl)Cl₂] Pd(ate)-14

Following the general procedure from IPr*·HCl (50.00 mg, 0.05 mmol) and [Pd(η^3 -crotyl)(μ -Cl)]₂ (10.30 mg, 0.03 mmol), the product was obtained as a yellow powder in 99% yield (60.00 mg).

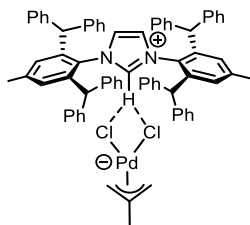
¹H NMR (400 MHz, CDCl₃): δ (ppm) = δ 11.60 (s, 1H, C_{NCHN}), 7.30-7.27 (m, 15H, CH_{Ar}), 7.16-7.10 (m, 16H, CH_{Ar}), 6.79-6.77 (m, 13H, CH_{Ar}), 5.43 (s, 6H, CH_{IPr*}), 5.04 (br.s, 1H, CH_{crotyl}), 3.71-3.69 (m, 2H, CH_{2(crotyl)}), 2.56 (br. s, 1H, CH_{crotyl}), 2.14 (s, 6H, CH_{3(IPr*)}), 1.29 (d, J = 5.6 Hz, 3H, CH_{3(crotyl)}).

¹³C {¹H} NMR (100 MHz, CDCl₃): δ (ppm) = δ 142.6 (C_{Ar}), 142.2 (CH_{NCHN}), 141.4 (C_{Ar}), 141.0 (C_{Ar}), 130.9 (C_{Ar}), 130.3 (CH_{Ar}), 129.2 (CH_{Ar}), 128.6 (CH_{Ar}), 128.5 (CH_{Ar}), 126.9 (CH_{Ar}), 126.7 (CH_{Ar}), 110.3 (CH_{imid}), 79.6 (CH_{crotyl}), 57.3.0 (CH_{crotyl}), 51.1 (CH_{2(crotyl)}), 21.8 (CH_{3(IPr*)}), 18.1 (CH_{3(crotyl)}).

Elemental analysis for C₇₃H₆₄Cl₂N₂Pd CH₂Cl₂: Expected: C 72.32, H 5.50, N 2.48. Found: C 72.11, H 5.44, N 2.78.

ν_{\max} (thin film) 3057 (C-H), 2360 (N=C=N), 1929 (C=C=N), 1494 (C-H), 1029 (C-H).

9.2.16.15. Synthesis of [IPr*·H][Pd(η^3 -2-Me-allyl)Cl₂] Pd(ate)-15



Following the general procedure from IPr*·HCl (50.00 mg, 0.05 mmol) and [Pd(η^3 -2-Me-allyl)(μ -Cl)]₂ (10.30 mg, 0.03 mmol), the product was obtained as a yellow powder in 99% yield (61.00 mg).

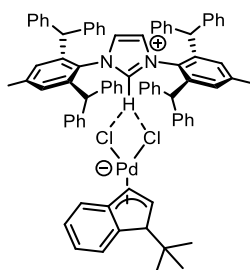
¹H NMR (400 MHz, CDCl₃): δ (ppm) = δ 11.89 (s, 1H, C_{NCHN}), 7.29-7.03 (m, 32H, CH_{Ar}), 6.77-6.76 (m, 8H, CH_{Ar}), 6.71 (s, 4H, CH_{Ar}), 5.44 (s, 4H, CH_(IPr*)), 5.37 (s, 2H, CH_{Imid}), 3.85 (br. s, 2H, CH_{2(allyl)}), 2.81 (br. s, 1H, CH_{allyl}), 2.53 (br. s, 1H, CH_{allyl}), 2.16 (s, 6H, CH_{3(IPr*)}), 2.08 (br. s, 3H, CH_{3(allyl)}).

¹³C {¹H} NMR (100 MHz, CDCl₃): δ (ppm) = δ 142.9 (C_{Ar}), 142.3 (C_{NCHN}), 141.9 (C_{Ar}), 141.1 (C_{Ar}), 140.7 (C_{Ar}), 131.1 (CH_{Ar}), 130.5 (CH_{Ar}), 129.4 (CH_{Ar}), 128.7 (CH_{Ar}), 128.2 (CH_{Ar}), 126.9 (CH_{Ar}), 126.8 (CH_{Ar}), 123.3 (CH_{imid}), 105.9 (CH_{allyl}), 60.5 (CH_{allyl}), 59.5 (CH_{allyl}), 51.3 (CH_(IPr*)), 22.0 (CH_{3(IPr*)}), 14.3 (CH_{3(allyl)}).

Elemental analysis for C₇₃H₆₄Cl₂N₂Pd 2CH₂Cl₂: Expected: C 67.40, H 5.59, N 2.14. Found: C 67.88, H 5.30, N 2.14.

ν_{\max} (thin film) 3055 (C-H), 2206 (N=C=N), 1973 (C=C=N), 1492 (C-H).

9.2.16.16. Synthesis of [IPr*·H][Pd(η^3 -2-Ind^{tBu})Cl₂] Pd(ate)-16



Following the general procedure from IPr*·HCl (50.00 mg, 0.05 mmol) and [Pd(η^3 -Ind^{tBu})(μ -Cl)]₂ (16.30 mg, 0.03 mmol), the product was obtained as a brown powder in 99% yield (67.00 mg).

¹H NMR (400 MHz, CDCl₃): δ (ppm) = δ 12.02 (s, 1H, C_{NCHN}), 7.26-7.09 (m, 34H, CH_{Ar}), 6.91-6.75 (m, 15H, 10 CH_{Ar} + 5 CH_{Ind}), 5.53-5.50 (m, 1H, CH_{Ind}), 5.42 (s, 2H, CH_{Imid}), 5.38 (s, 4H, CH_(IPr*)) 2.16 (s, 6H, CH_{3(IPr*)}), 1.39-1.27 (m, 9H, CH_{3(Ind)}).

^{13}C $\{^1\text{H}\}$ NMR (100 MHz, CDCl_3): δ (ppm) = δ 142.0 (C_{Ar}), 142.3 (CH_{NCN}), 142.1 (C_{Ar}), 141.1 (C_{Ar}), 140.6 (C_{Ar}), 131.1 (CH_{Ar}), 130.4 (CH_{Ar}), 129.4 (CH_{Ar}), 128.6 (CH_{Ar}), 127.6 (CH_{Ind}), 127.3 (CH_{Ind}), 126.9 (CH_{Ar}), 126.8 (CH_{Ar}), 125.4 (CH_{Ind}), 123.2 (CH_{imid}), 120.2 (CH_{Ind}), 118.8 (CH_{Ind}), 118.7 (CH_{Ind}), 107.6 (CH_{Ind}), 73.4 (CH_{Ind}), 51.2 (CH_2), 34.3 (CH_{Ind}), 29.0 ($\text{CH}_3(\text{Ind})$), 28.8 ($\text{CH}_3(\text{Ind})$), 22.0 ($\text{CH}_3(\text{IPr}^*)$).

Elemental analysis for $\text{C}_{82}\text{H}_{72}\text{Cl}_2\text{N}_2\text{Pd}$ CH_2Cl_2 : Expected: C 73.97, H 5.03, N 2.02. Found: C 74.27, H 4.86, N 2.35.

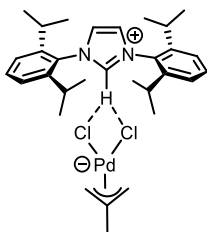
ν_{max} (thin film) 3057 (C-H), 2951 (C-H), 1598 (C-H), 1029 (C-H).

9.3 Chapter 3: Investigation into the catalytic activity of $[\text{NHC}\cdot\text{H}][\text{Pd}(\text{R})\text{Cl}_2]$ complexes in the Suzuki-Miyaura reaction

9.3.1. General procedure of $[\text{NHC}\cdot\text{H}][\text{Pd}(\text{L})\text{Cl}_2]$

In air, the corresponding NHC-HCl (2 equiv.) and $[\text{Pd}(\eta^3\text{-R-allyl})(\mu\text{-Cl})_2]$ (1 equiv.) were added to a mortar. The two solids were mixed and ground using a pestle for 5 min. A crystalline solid was obtained in quantitative yield.

9.3.2. Synthesis of $[\text{IPr}\cdot\text{H}][\text{Pd}(\eta^3\text{-2-Me-allyl})\text{Cl}_2]$ Pd(ate)-17



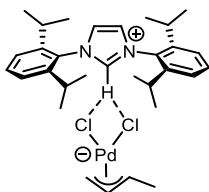
Following the general procedure from IPr-HCl (80.90 mg, 0.19 mmol) and $[\text{Pd}(\eta^3\text{-2-Me-allyl})(\mu\text{-Cl})_2]$ (37.50 mg, 0.09 mmol), the product was obtained as a yellow powder in 99% yield (118.00 mg).

^1H NMR (400 MHz, CDCl_3): δ (ppm) = δ 9.20 (s, 1H, $\text{NCHN}_{\text{imid}}$), 8.36 (s, 2H, CH_{imid}), 7.58 (t, $J = 8.5$ Hz, 2H, CH_{Ar}), 7.36 (d, $J = 9.1$ Hz, 4H, CH_{Ar}), 3.72 (br. s, 2H, $\text{CH}_2(\text{allyl})$), 2.69 (br. s, 2H, $\text{CH}_2(\text{allyl})$), 2.51 (sept, $J = 7.1$ Hz, 4H, CH_{IPr}), 2.03 (br. s, 3H, $\text{CH}_3(\text{allyl})$), 1.31 (d, $J = 6.8$ Hz, 12H, $\text{CH}_3(\text{IPr})$), 1.23 (d, $J = 7.1$ Hz, 12H, $\text{CH}_3(\text{IPr})$).

^{13}C $\{^1\text{H}\}$ NMR (100 MHz, CDCl_3): δ 145.3 (C_{Ar}), 136.9 (CH_{NCN}), 132.2 (CH_{Ar}), 130.0 (C_{Ar}), 127.8 (CH_{imid}), 124.8 (CH_{Ar}), 60.5 ($\text{CH}_2(\text{allyl})$), 29.2 (CH_{IPr}), 24.8 ($\text{CH}_3(\text{IPr})$), 24.1 ($\text{CH}_3(\text{IPr})$), 22.8 ($\text{CH}_3(\text{allyl})$).

Elemental analysis: Expected C 59.86, H 7.13, N 4.50. Found: C 59.58, H 7.19, N 4.67.

9.3.3. Synthesis of [IPr·H][Pd(η^3 -crotyl)Cl₂] Pd(ate)-18



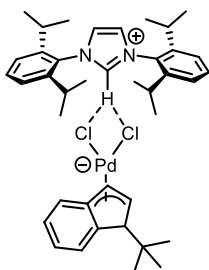
Following the general procedure from IPr·HCl (80.90 mg, 0.19 mmol) and [Pd(η^3 -crotyl)(μ -Cl)]₂ (37.50 mg, 0.09 mmol), the product was obtained as a yellow powder in 99% yield (118.00 mg).

¹H NMR (400 MHz, CDCl₃): δ (ppm) = δ 9.20 (s, 1H, C_{NCHN}), 8.33 (s, 2H, CH_{imid}), 7.56 (t, J = 10.5 Hz, 2H, CH_{Ar}), 7.33 (d, J = 7.3 Hz, 4H, CH_{Ar}), 5.08 (br. s, 1H, CH_(crotyl)), 3.07 (br. s, 2H, CH_{2(crotyl)}), 2.57 (br. s, 1H, CH_(crotyl)), 2.48 (sept, J = 13.5 Hz, 4H, CH_(IPr)), 1.30 (s, 3H, CH_{3(crotyl)}), 1.28 (d, J = 7.2 Hz, 12H, CH_{3(IPr)}), 1.20 (d, J = 7.2 Hz, 12H, CH_{3(IPr)}).

¹³C {¹H} NMR (100 MHz, CDCl₃): δ (ppm) = δ 145.2 (C_{Ar}), 137.0 (CH_{NCHN}), 132.2 (CH_{Ar}), 130.0 (C_{Ar}), 127.7 (CH_{imid}), 124.8 (CH_{Ar}), 110.3 (CH_(allyl)), 79.4 (CH_(allyl)), 57.0 (CH_{2(allyl)}), 29.1 (CH_{3(IPr)}), 24.8 (CH_{3(IPr)}), 24.0 (CH_{3(IPr)}), 18.1 (CH_{3(allyl)}).

Elemental analysis: Expected C 59.86, H 7.13, N 4.50. Found: C 59.70, H 6.95, N 4.69.

9.3.4. Synthesis of [IPr·H][Pd(η^3 -Ind^{tBu})Cl₂] Pd(ate)-19



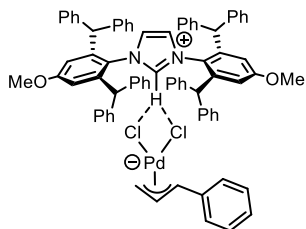
Following the general procedure from IPr·HCl (100.00 mg, 0.23 mmol) and [Pd(η^3 -Ind^{tBu})(μ -Cl)]₂ (74.00 mg, 0.12 mmol), the product was obtained as a brown/beige powder in 99% yield (173.00 mg).

¹H NMR (400 MHz, CDCl₃): δ (ppm) = δ 9.22 (s, 1H, C_{NCHN}), 8.27 (s, 2H, CH_{imid}), 7.57 (t, J = 8.2 Hz, 2H, CH_{Ar}), 7.34 (d, J = 7.8 Hz, 4H, CH_{Ar}), 7.11-7.07 (m, 1H, CH_{Ind}), 6.80-6.57 (m, 4H, CH_{Ind}), 5.51-5.41 (m, 1H, CH_{Ind}), 2.47 (hept, J = 7.2 Hz, 4H, CH_(IPr)), 1.36-1.31 (m, 9H, CH_{3(Ind)}), 1.29 (d, J = 7.2 Hz, 12H, CH_{3(IPr)}), 1.20 (d, J = 6.9 Hz, 12H, CH_{3(IPr)}).

¹³C {¹H} NMR (100 MHz, CDCl₃): δ (ppm) = δ 145.2 (C_{Ar}), 137.0 (CH_{NCHN}), 132.2 (CH_{Ar}), 130.0 (C_{Ar}), 127.7 (CH_{imid}), 127.4 (CH_{Ind}), 125.4 (CH_{Ind}), 125.3 (CH_{Ind}), 124.8 (CH_{Ar}), 124.1 (CH_{Ind}), 120.2-117.7 (CH_{Ind}), 109.1-107.0 (CH_{Ind}), 70.7 (CH_{Ind}), 34.3 (CH_{Ind}), 29.2 (CH_{3(IPr)}), 29.0 (CH_{3(Ind)}), 28.8 (CH_{3(Ind)}), 24.9 (CH_{3(IPr)}), 24.0 (CH_{3(IPr)}).

Elemental Analysis: Expected C 65.08, H 7.10, N 3.79. Found: C 64.87, H 7.17, N 3.94.

9.3.5. Synthesis of [IPr*^{OMe}·H][Pd(η³-cin)Cl₂] Pd(ate)-20



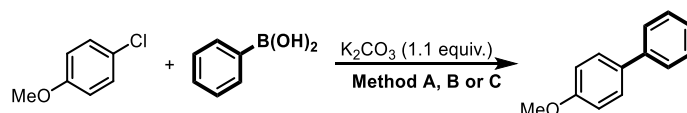
Following the general procedure from IPr*^{OMe}·HCl (50.00 mg, 0.05 mmol) and [Pd(η³-cin)(μ-Cl)₂] (13.00 mg, 0.02 mmol), the product was obtained as a yellow powder in 99% yield (63.00 mg).

¹H NMR (400 MHz, CDCl₃): δ (ppm) = δ 12.29 (s, 1H, C_{NCHN}), 7.34-7.08 (m, 35H, CH_{Ar}), 6.79 (d, *J* = 7.2 Hz, 10H, CH_{Ar}), 6.46 (s, 4H, CH_{Ar}), 5.80-5.60 (br. m, 1H, CH_(cin)), 5.45 (s, 4H, CH_(IPr*OMe)), 5.23 (s, 2H, CH_{imid}), 3.85 (br. s, 1H, CH_(cin)), 3.76 (br. s, 1H, CH_(cin)), 3.51 (s, 6H, CH_{3(IPr*OMe)}), 2.87 (br. s, 1H, CH_(cin)).

¹³C {¹H} NMR (100 MHz, CDCl₃): δ (ppm) = δ 160.5 (C_{Ar}), 143.2 (CH_{NCHN}), 143.0 (C_{Ar}), 142.7 (C_{Ar}), 142.2 (C_{Ar}), 130.4 (CH_{Ar}), 129.3 (CH_{Ar}), 128.6 (CH_{Ar}), 128.6 (CH_{Ar}), 128.2 (CH_{Ar}), 127.0 (CH_{Ar}), 126.9 (CH_{Ar}), 125.8 (CH), 123.1 (CH_{imid}), 115.7 (CH_{Ar}), 105.7 (CH_{cin}), 69.0 (CH_{cin}), 55.2 (OCH_{3(IPr*OMe)}), 51.5 (CH_(IPr*OMe)).

Elemental analysis: Expected: C 75.39, H 5.52, N 2.25. Found: C 75.33, H 5.64, N 2.32.

9.3.6. Preliminary Investigation into the Suzuki-Miyaura reaction



Method A:

The vial containing the pre-catalyst **7a-c** was transferred into the glovebox. Inside the glovebox, the vial was charged with a stirring bar, 4-chloroanisole (0.50 mmol), phenylboronic acid (1.00 equiv.) and K₂CO₃ (1.10 equiv.). The vial was then sealed with a screw cap fitted with a septum. The reaction mixture was taken outside the glovebox. 1 mL of an ethanol/water (1:1) mixture (degassed) was added and the reaction was left to stir at 80 °C for 4 h.

Method B:

The vial containing the pre-catalyst **7a-c** was transferred into the glovebox. Inside the glovebox, the vial was charged with a stirring bar, 4-chloroanisole (0.50 mmol), phenylboronic acid (1.00 equiv.) and K₂CO₃ (1.10 equiv.). The vial was sealed with a screw cap fitted with a septum. The

reaction mixture was taken outside the glovebox. 1 mL of ethanol (degassed) was added and the reaction was left to stir at room temperature for 20 h.

Methods C1, C3:

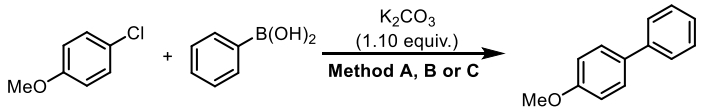
The vial was charged with a stirring bar, **7a-c** (0.30 mol%) and K_2CO_3 (1.10 equiv.) under argon. The mixture was stirred for 1 h at 60 °C (**C1**) or 30 min at 60 °C (**C3**), then 4-chloroanisole (0.50 mmol) and phenylboronic acid (1.00 equiv.) were added and the reaction was left stirring at room temperature for 20 h.

For entries 7-9: Pd dimer (0.15 mol%) and NHC·HCl (0.30 mol%) were used instead of **7a-c**.

Methods C2:

The vial containing the **7a-c** (0.30 mol%) was transferred into the glovebox. Inside the glovebox, the vial was charged with a stirring bar, 4-chloroanisole (0.50 mmol), phenylboronic acid (1.00 equiv.) and K_2CO_3 (1.10 equiv.). The vial was sealed with a screw cap fitted with a septum. The reaction mixture was taken outside the glovebox. 1 mL of ethanol (degassed) was added and the reaction was stirred for 1 h at 60 °C, then 20 h at room temperature (23 °C).

Table S-4: Table for the investigation of the Suzuki-Miyaura coupling of phenylboronic acid and 4-chloroanisole^a



Entry	Catalyst (0.30 mol%)	Meth. A (conv. %)	Meth. B (conv. %)	Meth. C (conv. %)		
				C1	C2	C3
1	[Pd(IPr)(cin)Cl]	71	82			
2	[Pd(IPr)(allyl)Cl]	61	58			
3	[Pd(IPr*)(cin)Cl]	70	73			
4	[IPr-H][Pd(cin)Cl ₂]	NR	NR	82	9	43
5	[IPr-H][Pd(allyl)Cl ₂]	NR	NR	50	NR	13
6	[IPr*-H][Pd(cin)Cl ₂]	NR	NR	83	28	97
7	[Pd(cin)Cl ₂] + 2 IPr-HCl	NR	NR	NR		
8	[Pd(allyl)Cl ₂] + 2 IPr-HCl	NR	NR	NR		
9	[Pd(cin)Cl ₂] + 2 IPr*-HCl	NR	NR	NR		

NR: no reaction. Reaction conditions: 4-chloroanisole (0.50 mmol), phenylboronic acid (1.00 equiv.), K_2CO_3 (1.10 equiv.) in 1 mL of solvent. The reactions were all charged under inert atmosphere and all reagents and catalysts were charged initially except for method C1 and C3. Method A: ethanol/water (1:1) at 80 °C. for 4 h. Method B: ethanol at room temperature for 20 h. Method C: palladate pre-catalysts (entry 4-6) (or Pd dimer, 0.15 mol% and NHC·HCl, 0.30 mol% for entry 7-9), K_2CO_3 and ethanol were heated for 1 h at 60 °C (C1) or 30 min at 60 °C (C3), then the coupling partners were added and the reaction was left stirring at room temperature for 20 h. C2: All reagents and catalysts were added from the start and heated for 1 h at 60 °C then stirred at room temperature for 20 h. Conversion determined by GC.

9.3.7. The effect of different boron sources in the Suzuki-Miyaura reaction

[IPr·H][Pd(η^3 -cin)Cl₂] (0.50 mol%), K₂CO₃ (0.70 mmol) and a stirring bar were added to a screw-cap vial. Ethanol (1 mL) was then added. Afterwards, 4-chloroanisole (0.50 mmol) and the corresponding aryl boron source (0.55 mmol) were added through an ethanol solution (1 mL). The reaction was left to stir at 40 °C for 16 h. The GC yield was determined using mesitylene as internal standard.

Table S-5: Boron Source effect

Entries	Boron source (0.55 mmol)	GC yield (%)	GC yield (%) ^a
1	Phenyl boronic acid	0	99
2	Potassium phenyltrifluoroborate	8	90
3	Aryl boronic pinacol ester	40	94

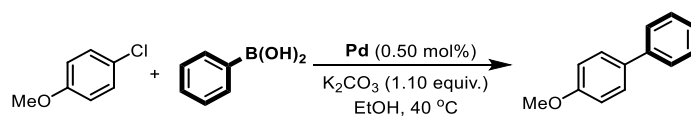
^aAn activation step of 1 h was used: [IPr·H][Pd(η^3 -cin)Cl₂] and K₂CO₃ were stirred for 1 h in ethanol, before the substrates were added.

9.3.8. Optimisation of the Suzuki-Miyaura reaction**9.3.8.1 General procedure**

In air, a vial was charged with [IPr·H][Pd(η^3 -cin)Cl₂], K₂CO₃, ethanol and a magnetic stir bar and sealed with a screw cap. The mixture was allowed to stir at 60 °C for 1h. The vial was removed from the heating block and the corresponding aryl chloride was added, followed by the corresponding aryl boronic acid. The reaction was allowed to stir for the corresponding time at the corresponding temperature.

9.3.8.2 Pre-catalyst optimisation

The general procedure was followed using phenylboronic acid (60.90 mg, 0.50 mmol), 4-chloroanisole (61.00 μ L, 0.50 mmol) with K₂CO₃ (76 mg, 0.55 mmol) in ethanol (1 mL). The GC yield was determined using mesitylene as internal standard.

Table S-5: Pre-catalyst optimisation

[Pd] precatalyst (0.50 mol%)	GC yield ^a (%)
[IPr·H][Pd(η ³ -cin)Cl ₂]	93
[IPr·H][Pd(η ³ -allyl)Cl ₂]	55
[IPr*·H][Pd(η ³ -cin)Cl ₂]	88
[SIPr·H][Pd(η ³ -cin)Cl ₂]	30
[IPr·H][Pd(η ³ -2-Me-allyl)Cl ₂]	80
[IPr·H][Pd(η ³ -crotyl)Cl ₂]	8
[IPr·H][Pd(η ³ -Ind ^{tBu})Cl ₂]	n.r.
[IPr* ^{OMe} ·H][Pd(η ³ -cin)Cl ₂]	20
[IPent·H][Pd(η ³ -cin)Cl ₂]	n.r.
[IPr ^{Cl} ·H][Pd(η ³ -cin)Cl ₂]	60

^a The GC yield was determined using mesitylene as internal standard. Average of two runs. n.r. = no reaction.

9.3.8.3 Solvent optimisation

The general procedure was followed using [IPr·H][Pd(η³-cin)Cl₂] (1.70 mg, 0.50 mol%), phenylboronic acid (61.00 mg, 0.50 mmol), 4-chloroanisole (61.00 μL, 0.50 mmol) with K₂CO₃ (76.00 mg, 0.55 mmol) in the corresponding solvent (1 mL). The GC yield was determined using mesitylene as internal standard.

Table S-6: Solvent optimisation

Entries	Solvent	GC yield (%) ^b
1	Ethanol	92
2	<i>iso</i> -Propanol	45
3	<i>n</i> -Butanol	53
4	Acetone	n.r.
5	Water	<5
6	Toluene	n.r.
7	Dioxane	n.r.
8	THF	n.r.
9	Methanol	5
10	Ethanol:water 1:1	35
11	Ethanol:water 2:1	55
12	Ethanol:water 9:1	73
13 ^a	<i>iso</i> -Propanol	23
14 ^a	<i>n</i> -Butanol	trace
15 ^a	Toluene	n.r.

^a The temperature used in the activation step was altered to the boiling point of the corresponding solvents. ^b The GC yield was determined using mesitylene as internal standard. Average of two runs.

9.3.8.4 Base optimisation

The general procedure was followed using [IPr·H][Pd(η^3 -cin)Cl₂] (1.70 mg, 0.50 mol%), phenylboronic acid (61.00 mg, 0.50 mmol), 4-chloroanisole (61.00 μ L, 0.50 mmol) with the corresponding base (0.55 mmol) in the corresponding solvent (1 mL). The GC yield was determined using mesitylene as internal standard.

Table S-7: Base optimisation in ethanol

Entries	Base (0.55 mmol)	GC yield (%) ^a
1	K ₂ CO ₃	92
2	Na ₂ CO ₃	5
3	Cs ₂ CO ₃	27
4	KHCO ₃	traces
5	NaHCO ₃	traces
6	KOH	72
7	NaOH	80
8	LiOH	20
9	NaHPO ₄	n.r.
10	K ₂ HPO ₄	n.r.
11	K ₃ PO ₄	40
12	KO ^t Am	78
13	KO ^t Bu	75
14	NaOOCH	n.r.
15	Imidazole	n.r.

^a The GC yield was determined using mesitylene as internal standard. Average of two runs.

Table S-8: Base optimisation using *iso*-propanol

Entries	Base (1.10 equiv.)	GC yield (%) ^a
1	K ₂ CO ₃	47
2	Na ₂ CO ₃	0
3	Cs ₂ CO ₃	0
4	KHCO ₃	0
5	NaHCO ₃	0
6	KOH	55
7	NaOH	60
8	LiOH	trace
9	NaHPO ₄	0
10	K ₂ HPO ₄	0
11	K ₃ PO ₄	55
12	KO ^t Am	70
13	KO ^t Bu	72
14	NaOOCH	trace
15	Imidazole	trace

^a The GC yield was determined using mesitylene as internal standard. Average of two runs.

Table S-9: Base optimisation using *n*-butanol

Entries	Base (1.10 equiv.)	GC yield (%) ^a
1	K ₂ CO ₃	53
2	Na ₂ CO ₃	n.r.
3	Cs ₂ CO ₃	17
4	KHCO ₃	traces
5	NaHCO ₃	0
6	KOH	65
7	NaOH	80
8	LiOH	17
9	NaHPO ₄	0
10	K ₂ HPO ₄	0
11	K ₃ PO ₄	traces

^a The GC yield was determined using mesitylene as internal standard. Average of two runs.

9.3.8.5 Optimisation of the aryl boronic acid

The general procedure was followed using [IPr-H][Pd(η^3 -cin)Cl₂] (0.50 mol%), phenylboronic acid (varying equivalents), 4-chloroanisole (61.00 μ L, 0.50 mmol) with K₂CO₃ (76.00 mg, 0.55 mmol) in the corresponding solvent (1 mL). The GC yield was determined using mesitylene as internal standard.

Table S-11: Optimisation of the equivalents of aryl boronic acid.

Entries	PhB(OH) ₂ (equiv.)	GC yield (%) ^a
1	1.00	90
2	1.10	82
3	1.20	87
4	1.30	82
5	1.40	85

^a The GC yield was determined using mesitylene as internal standard. Average of four runs.

9.3.8.6 Optimisation of the equivalence of K₂CO₃

The general procedure was followed using [IPr-H][Pd(η^3 -cin)Cl₂] (0.50 mol%), phenylboronic acid (61.00 mg, 0.50 mmol), 4-chloroanisole (61.00 μ L, 0.50 mmol) with K₂CO₃ (varying equivalents) in the corresponding solvent (1 mL). The GC yield was determined using mesitylene as internal standard.

Table S-11: Optimisation of the equivalents of K₂CO₃

Entries	K ₂ CO ₃ (equiv.)	GC yield (%) ^a
1	1.00	93
2	1.10	95
3	1.20	93
4	1.30	97
5	1.40	99

^a The GC yield was determined using mesitylene as internal standard. Average of four runs.

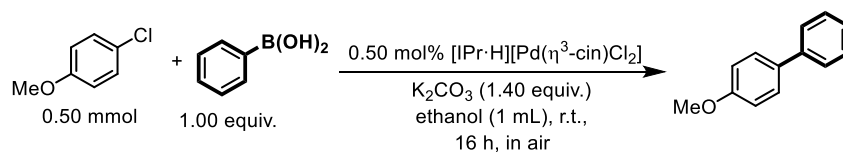
9.3.8.7 Optimisation of the pre-catalyst loading

The general procedure was followed using [IPr-H][Pd(η^3 -cin)Cl₂] (0.10-0.50 mol%), phenylboronic acid (61.00 mg, 0.50 mmol), 4-chloroanisole (61.00 μ L, 0.50 mmol) with K₂CO₃ (97.00 mg, 0.70 mmol) in the corresponding solvent (1 mL). The GC yield was determined using mesitylene as internal standard.

Table S-12: Optimisation of the precatalyst loading

Entries	[IPr-H][Pd(η^3 -cin)Cl ₂] (mol%)	GC yield (%)
1	0.50	99
2	0.30	99
3	0.20	70
4	0.10	31

^a The GC yield was determined using mesitylene as internal standard. Average of four runs.

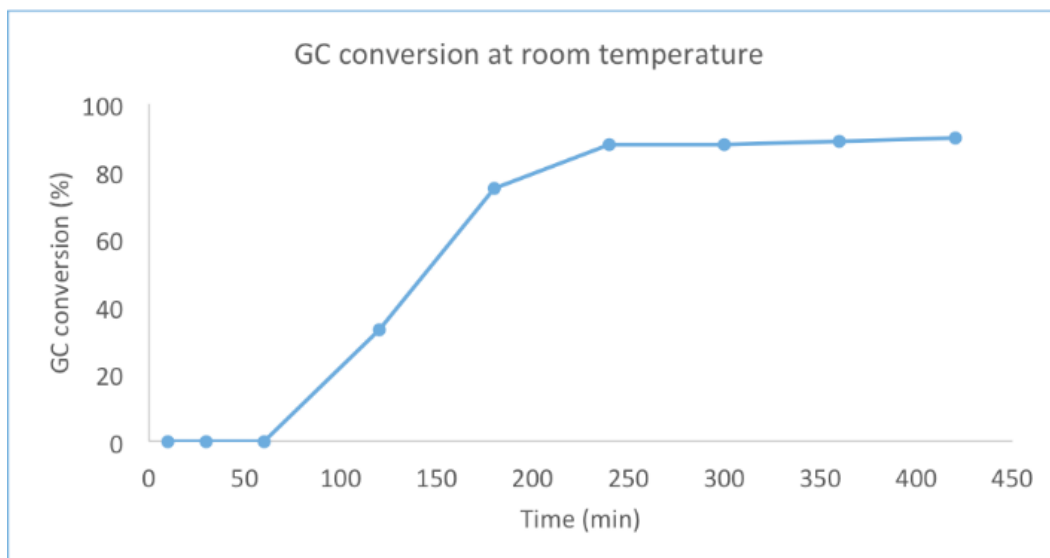
9.3.8.8. Time and temperature optimisation

The general procedure was followed (Section 9.3.9.1) and aliquots were taken and analysed by gas chromatography.

Table S-13: Time optimization at room temperature

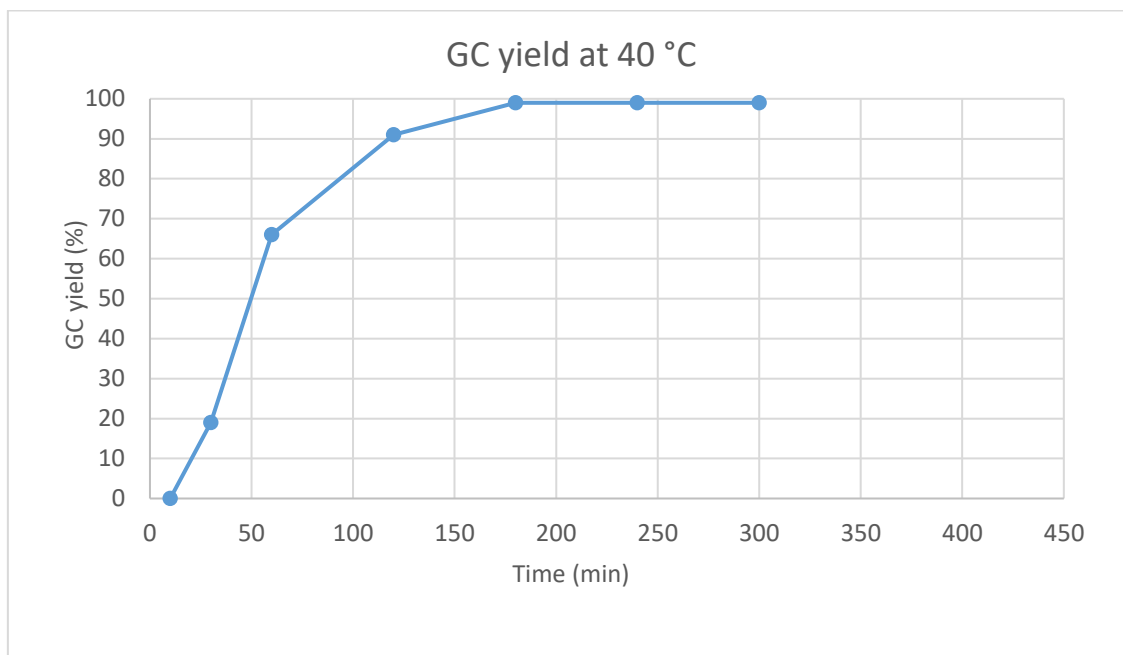
Time (min)	GC yield (%)
10	0
30	0
60	0
120	33
180	75
240	88
300	88
360	89
420	90

^a The GC yield was determined using mesitylene as internal standard. Average of four runs.

Graph 1: Time optimisation at room temperature**Table S-14:** Time optimization at 40 °C

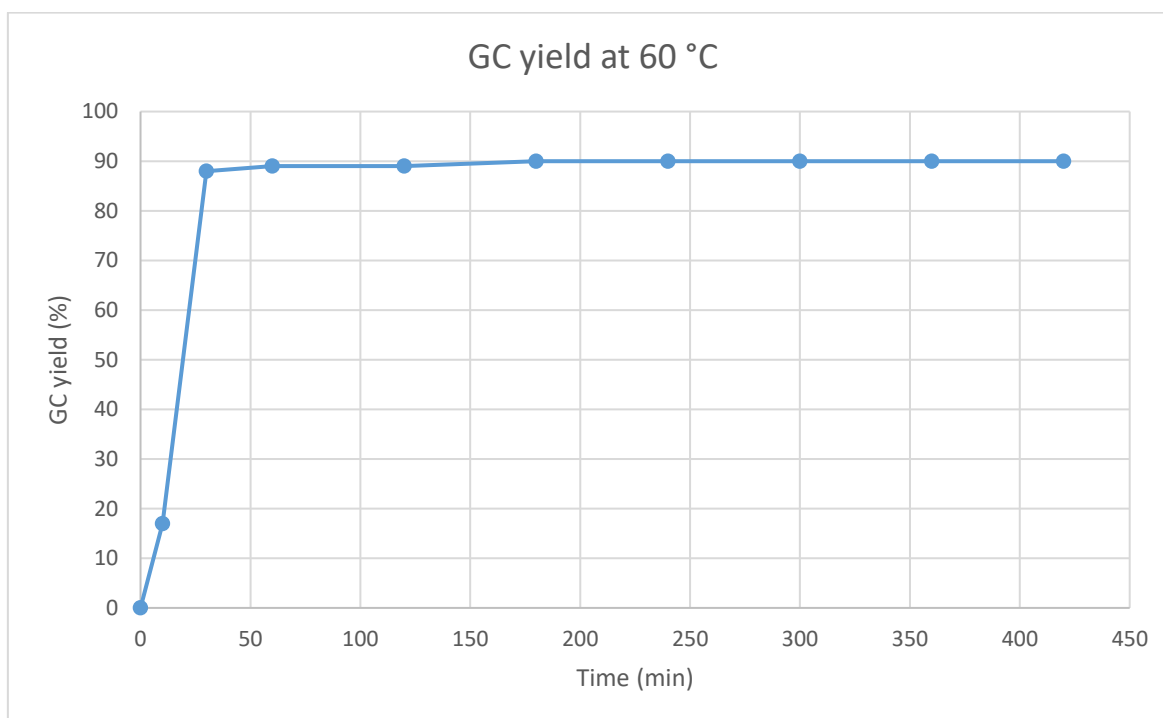
Time (min)	GC yield (%)
10	0
30	19
60	66
120	91
180	99
240	99
300	99

^a The GC yield was determined using mesitylene as internal standard. Average of four runs.

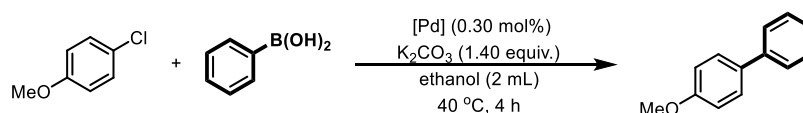
Graph S-2: Time optimisation at 40 °C.**Table S-15:** Time optimization at 60 °C

Time (min)	GC yield (%)
0	0
10	17
30	88
60	89
120	89
180	90
240	90
300	90
360	90
420	90

^a The GC yield was determined using mesitylene as internal standard. Average of four runs.

Graph S-3: Time optimisation at 60 °C.

9.3.8.8. Comparison of different Pd(II)-IPr pre-catalyst in the optimized protocol



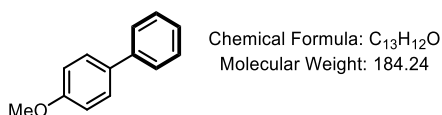
Entries	Pd pre-catalyst	Molecular weight (g/mol)	Mass (mg)	GC conversion (%)
1	[PdCl) ₂ (PEPPSI)(IPr)]	679.9	1.00	79
2	[PdCl(acac)(IPr)]	630.6	0.90	75
3	[PdCl(η ³ -cin)(IPr)]	647.6	1.00	80
4	[PdCl(η ³ -allyl)(IPr)]	578.5	0.90	74

^a The GC yield was determined using mesitylene as internal standard. Average of four runs.

9.3.9. Scope

General procedure: In air, a vial was charged with [IPr-H][Pd(η^3 -cin)Cl₂] (1.70 mg, 0.50 mol%), K₂CO₃ (0.70 mmol, 97.00 mg), ethanol (1 mL) and a magnetic stir bar and sealed with a screw cap. The mixture was left stirring at 60 °C for 1 h. The vial was removed from the heating block and the corresponding aryl chloride (0.50 mmol, 1 equiv.) was added followed by the corresponding aryl boronic acid (0.05 mmol, 1 equiv.). The reaction was left to stir (1000 rpm) for the corresponding time at 40 °C. **Work up:** To the crude mixture, ethyl acetate (10 mL) and water (10 mL) were added. The aqueous phase was extracted 3 times with ethyl acetate (3 x 10 mL). The organic phase was dried over MgSO₄. The resulting crude product was dried under reduced pressure. The crude was filtered through silica gel and recrystallized using dichloromethane and pentane.

4-Methoxybiphenyl, **1a**



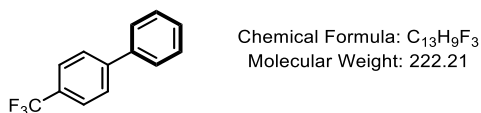
Following the general procedure, from phenylboronic acid (60.90 mg, 0.50 mmol) and 4-chloroanisole (61.00 μ L, 0.50 mmol), the product was obtained in 97% yield (90.00 mg) as a white solid.

¹H NMR (400 MHz, CDCl₃): δ (ppm) = δ 7.57 (t, J = 8.1 Hz, 4H), 7.42 (t, J = 7.3 Hz, 2H), 7.31 (t, J = 7.5 Hz, 1H), 7.00 (t, J = 2.9 Hz, 1H), 6.98 (t, J = 2.1 Hz, 1H), 3.86 (s, 3H).

¹³C {¹H} NMR (100 MHz, CDCl₃): δ (ppm) = δ 159.3 (C_{Ar}), 141.0 (C_{Ar}), 133.9 (C_{Ar}), 128.9 (CH_{Ar}), 128.3 (CH_{Ar}), 126.9 (CH_{Ar}), 126.8 (CH_{Ar}), 114.3 (CH_{Ar}), 55.5 (CH₃).

Analytical data obtained were in agreement with the reported values.⁸

1-phenyl-4-(trifluoromethyl)benzene, **1b**



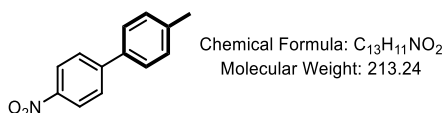
Following the general procedure, from phenylboronic acid (60.90 mg, 0.50 mmol) and 1-chloro-4-trifluoromethyl benzene (122.00 μ L, 0.50 mmol), the product was obtained in 98% yield (109.00 mg) as a white solid.

¹H NMR (400 MHz, CDCl₃): δ (ppm) = δ 7.70 (s, 4H), 7.61-7.60 (m, 2H), 7.50-7.48 (m, 2H), 7.41 (dt, J = 4.7, 1.9 Hz, 1H).

¹³C {¹H} NMR (100 MHz, CDCl₃): δ (ppm) = δ 144.9 (C_{Ar}), 139.9 (C_{Ar}), 129.5 (q, *J* = 32.5 Hz, C_{Ar}-CF₃), 129.1 (2 x CH_{Ar}), 128.3 (2 x CH_{Ar}), 127.6 (CH_{Ar}), 127.4 (CH_{Ar}), 125.9 (q, *J* = 3.8 Hz, CH_{Ar}), 124.5 (q, *J* = 271.8 Hz, CF₃).

Analytical data obtained were in agreement with the reported values.¹⁰

4-methyl,4'-nitrobiphenyl, **1c**



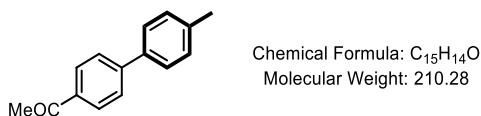
Following the general procedure, from phenylboronic acid (60.90 mg, 0.50 mmol) and 4-chloro-nitrobenzene (79.00 mg, 0.50 mmol), the product was obtained in 89% yield (88.70 mg) as a white solid.

¹H NMR (400 MHz, CDCl₃): δ (ppm) = δ 8.30 (d, *J* = 8.5 Hz, 2H), 7.73 (d, *J* = 9.3 Hz, 2H), 7.54 (d, *J* = 9.3 Hz, 2H), 7.32 (d, *J* = 8.5 Hz, 2H), 2.43 (s, 3H).

¹³C {¹H} NMR (100 MHz, CDCl₃): δ (ppm) = δ 147.7 (C_{Ar}), 147.0 (C_{Ar}), 139.2 (C_{Ar}), 136.0 (C_{Ar}), 130.0 (CH_{Ar}), 127.6 (CH_{Ar}), 127.4 (CH_{Ar}), 124.3 (CH_{Ar}), 21.4 (CH₃).

Analytical data obtained were in agreement with the reported values.¹⁰

1-(4'-methyl-4-biphenyl)ethanone, **1d**

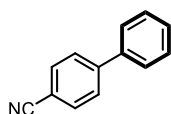


Following the general procedure, from *p*-tolylboronic acid (68.00 mg, 0.50 mmol) and 4-chloroacetophenone (64.00 μL, 0.50 mmol), the product was obtained in 95% yield (100.00 mg) as a white solid.

¹H NMR (400 MHz, CDCl₃): δ (ppm) = δ 8.03 (d, *J* = 8.2 Hz, 2H), 7.69 (d, *J* = 8.6 Hz, 2H), 7.55 (d, *J* = 8.6 Hz, 2H), 7.29 (d, *J* = 8.6 Hz, 2H), 2.64 (s, 3H), 2.41 (s, 3H).

¹³C {¹H} NMR (100 MHz, CDCl₃): δ (ppm) = δ 197.9 (COMe), 145.9 (C_{Ar}), 138.4 (C_{Ar}), 137.1 (C_{Ar}), 135.7 (C_{Ar}), 129.8 (CH_{Ar}), 129.1 (CH_{Ar}), 127.2 (CH_{Ar}), 127.1 (CH_{Ar}), 26.8 (CH₃), 21.3 (CH₃).

Analytical data obtained were in agreement with the reported values.¹⁰

4-cyanobiphenyl, **1e**

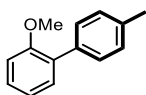
Chemical Formula: C₁₃H₉N
Molecular Weight: 179.22

Following the general procedure, from phenylboronic acid (61.00 mg, 0.50 mmol) and 4-chlorobenzonitrile (69.00 mL, 0.50 mmol), the product was obtained in 89% yield (80.70 mg) as a white solid.

¹H NMR (400 MHz, CDCl₃): δ (ppm) = δ 7.75-7.67 (m, 4H), 7.61-7.58 (m, 2H), 7.52-7.46 (m, 2H), 7.45 (dt, *J* = 5.2, 2.1 Hz, 2H).

¹³C {¹H} NMR (100 MHz, CDCl₃): δ (ppm) = δ 145.8 (C_{Ar}), 139.3 (C_{Ar}), 132.7 (CH_{Ar}), 129.3 (2 x CH_{Ar}), 128.8 (2 x CH_{Ar}), 127.9 (2 x CH_{Ar}), 127.4 (CH_{Ar}), 119.1 (CN), 111.1 (C_{Ar}-CN).

Analytical data obtained were in agreement with the reported values.¹⁰

2-methoxy-4-methylbiphenyl, **1f**

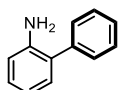
Chemical Formula: C₁₄H₁₄O
Molecular Weight: 198.27

Following the general procedure, from *p*-tolylboronic acid (68.00 mg, 0.50 mmol) and 2-chloroanisole (61.00 μL, 0.50 mmol), the product was obtained in 89% yield (88.40 mg) as a white solid.

¹H NMR (400 MHz, CDCl₃): δ (ppm) = δ 7.49 (d, *J* = 8.7 Hz, 2H), 7.35 (t, *J* = 7.1 Hz, 2H), 7.29 (d, *J* = 8.6 Hz, 2H), 7.09-7.01 (m, 2H), 3.85 (s, 3H), 2.44 (s, 3H).

¹³C {¹H} NMR (100 MHz, CDCl₃): δ (ppm) = δ 156.6 (C_{Ar}), 136.7 (C_{Ar}), 135.7 (C_{Ar}), 130.9 (CH_{Ar}), 130.8 (C_{Ar}), 129.5 (CH_{Ar}), 128.9 (CH_{Ar}), 128.5 (CH_{Ar}), 120.9 (2 x CH_{Ar}), 111.3 (2 x CH_{Ar}), 55.6 (CH₃), 21.3 (CH₃).

Analytical data obtained were in agreement with the reported values.¹⁰

2-aminobiphenyl, **1g**

Chemical Formula: C₁₂H₁₁N
Molecular Weight: 169.23

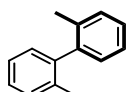
Following the general procedure, from phenylboronic acid (61.00 mg, 0.50 mmol) and 2-chloroaniline (64.00 mg, 0.50 mmol), the product was obtained in 80% yield (68.00 mg) as a brown solid.

¹H NMR (400 MHz, CDCl₃): δ (ppm) = δ 8.27 (d, *J* = 7.1 Hz, 1H), 7.59-7.36 (m, 4H), 7.23-7.04 (m, 2H), 6.86-6.67 (m, 2H), 4.02-4.00 (m, 2H).

¹³C {¹H} NMR (100 MHz, CDCl₃): δ (ppm) = δ 143.6 (C_{Ar}), 139.6 (C_{Ar}), 135.8 (CH_{Ar}), 132.8 (CH_{Ar}), 130.6 (CH_{Ar}), 129.2 (CH_{Ar}), 128.9 (CH_{Ar}), 128.6 (CH_{Ar}), 128.1 (CH_{Ar}), 127.8 (C_{Ar}), 127.3 (CH_{Ar}), 118.8 (CH_{Ar}), 115.8 (CH_{Ar}).

Analytical data obtained were in agreement with the reported values.¹¹

2,2'-methylbiphenyl, **1h**



Chemical Formula: C₁₄H₁₄
Molecular Weight: 182.27

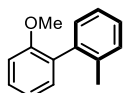
Following the general procedure, from 2-tolylboronic acid (68.00 mg, 0.50 mmol) and 2-chlorotoluene (67.00 μL, 0.50 mmol), the product was obtained in 90% yield (82.50 mg) as a white solid.

¹H NMR (400 MHz, CDCl₃): δ (ppm) = δ 7.28-7.22 (m, 6H), 7.13 (d, *J* = 7.2 Hz, 2H), 2.07 (s, 6H).

¹³C {¹H} NMR (100 MHz, CDCl₃): δ (ppm) = δ 141.7 (2 x C_{Ar}), 135.9 (2 x C_{Ar}), 129.9 (2 x CH_{Ar}), 129.4 (2 x CH_{Ar}), 127.3 (2 x CH_{Ar}), 125.7 (2 x CH_{Ar}), 20.0 (2 x CH₃).

Analytical data obtained were in agreement with the reported values.¹²

2-methoxy-2'-methylbiphenyl, **1i**



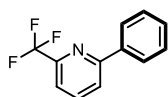
Chemical Formula: C₁₄H₁₄O
Molecular Weight: 198.27

Following the general procedure, from *o*-tolylboronic acid (68.00 mg, 0.50 mmol) and 2-chloroanisole (71.30 mg, 0.50 mmol), the product was obtained in 97% yield (96.70 mg) as a yellowish/white oil.

¹H NMR (400 MHz, CDCl₃): δ (ppm) = δ 7.41-7.35 (m, 1H), 7.29-7.18 (m, 5H), 7.08-6.99 (m, 2H), 3.80 (s, 3H), 2.19 (s, 3H).

¹³C {¹H} NMR (100 MHz, CDCl₃): δ (ppm) = δ 156.7 (C_{Ar}), 138.8 (C_{Ar}), 137.0 (C_{Ar}), 131.1 (CH_{Ar}), 131.0 (C_{Ar}), 130.1 (CH_{Ar}), 129.7 (CH_{Ar}), 128.7 (CH_{Ar}), 127.4 (CH_{Ar}), 125.6 (CH_{Ar}), 120.6 (CH_{Ar}), 110.8 (CH_{Ar}), 55.5 (CH₃), 20.1 (CH₃).

Analytical data obtained were in agreement with the reported values.⁸

2-phenyl-6-(trifluoromethyl)pyridine, **1j**

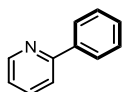
Chemical Formula: C₁₂H₈F₃N
Molecular Weight: 223.20

Following the general procedure, from phenylboronic acid (61.00 mg, 0.50 mmol) and 2-chloro-6-trifluoromethyl pyridine (91.00 mg, 0.50 mmol), the product was obtained in 99% yield (112.00 mg) as a white solid.

¹H NMR (400 MHz, CDCl₃): δ (ppm) = δ 8.09-8.06 (m, 2H), 7.92-7.91 (m, 2H), 7.62-7.60 (m, 1H), 7.52–7.46 (m, 3H).

¹³C {¹H} NMR (100 MHz, CDCl₃): δ (ppm) = δ 157.9 (C_{Ar}), 148.5 (q, J = 34.5 Hz, C_{Py}-CF₃), 138.2 (CH_{Ar}), 137.9 (C_{Ar}), 129.9 (CH_{Ar}), 129.0 (CH_{Ar}), 127.3 (CH_{Ar}), 122.9 (CH_{Ar}), 121.7 (q, J = 274.3 Hz, CF₃), 118.6 (d, J = 2.7 Hz, CH_{Ar}).

Analytical data obtained were in agreement with the reported values.¹³

2-phenylpyridine, **1k**

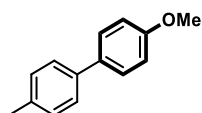
Chemical Formula: C₁₁H₉N
Molecular Weight: 155.20

Following the general procedure, from phenylboronic acid (61.00 mg, 0.50 mmol) and 2-chloropyridine (68.00 μL, 0.50 mmol), the product was obtained in 90% yield (69.00 mg) as a brown solid.

¹H NMR (400 MHz, CDCl₃): δ (ppm) = δ 8.71 (dt, J = 7.8, 4.5 Hz, 1H), 8.01-7.98 (m, 2H), 7.77-7.73 (m, 2H), 7.50-7.48 (m, 2H), 7.45-7.40 (m, 1H), 7.25-7.19 (m, 1H)

¹³C {¹H} NMR (100 MHz, CDCl₃): δ (ppm) = δ 158.0 (C_{Ar}), 148.5 (C_{Ar}), 148.1 (CH_{Ar}), 138.2 (CH_{Ar}), 137.9 (CH_{Ar}), 129.9 (CH_{Ar}), 129.1 (CH_{Ar}), 127.3 (CH_{Ar}), 123.0 (CH_{Ar}), 120.4 (CH_{Ar}), 118.6 (CH_{Ar}).

Analytical data obtained were in agreement with the reported values.¹⁴

4-methoxy-4'-methylbiphenyl, **2a**

Chemical Formula: C₁₄H₁₄O
Molecular Weight: 198.27

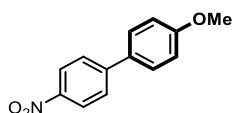
Following the general procedure, from 4-methoxyphenylboronic acid (79.00 mg, 0.50 mmol) and 4-chlorotoluene (67.00 μL, 0.50 mmol), the product was obtained in 85% yield (84.00 mg) as a white solid.

¹H NMR (400 MHz, CDCl₃): δ (ppm) = δ 7.53-7.50 (m, 2H), 7.49-7.44 (m, 2H), 7.24 (d, *J* = 8.5 Hz, 2H), 6.98-6.96 (m, 2H), 3.85 (s, 3H), 2.39 (s, 3H).

¹³C {¹H} NMR (100 MHz, CDCl₃): δ (ppm) = δ 159.1 (C_{Ar}), 138.1 (C_{Ar}), 136.5 (CH_{Ar}), 133.9 (C_{Ar}), 129.6 (CH_{Ar}), 128.1 (CH_{Ar}), 127.9 (C_{Ar}), 126.7 (CH_{Ar}), 114.3 (CH_{Ar}), 55.5 (CH₃), 21.2 (CH₃).

Analytical data obtained were in agreement with the reported values.¹²

4-methoxy-4'-nitro-biphenyl, **2b**



Chemical Formula: C₁₃H₁₁NO₃
Molecular Weight: 229.24

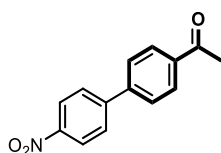
Following the general procedure, from 4-methoxy phenylboronic acid (76.00 mg, 0.50 mmol) and 4-chloro-nitrobenzene (79.00 mg, 0.50 mmol), the product was obtained in 91% yield (105.00 mg) as a beige solid.

¹H NMR (400 MHz, CDCl₃): δ (ppm) = δ 8.82 (d, *J* = 7.8 Hz, 2H), 7.71 (d, *J* = 8.9 Hz, 2H), 7.60 (d, *J* = 6.9 Hz, 2H), 7.03 (d, *J* = 9.7 Hz, 2H), 3.88 (s, 3H).

¹³C {¹H} NMR (100 MHz, CDCl₃): δ (ppm) = δ 160.6 (C_{Ar}), 147.4 (C_{Ar}), 146.7 (C_{Ar}), 131.2 (C_{Ar}), 128.7 (CH_{Ar}), 127.2 (CH_{Ar}), 124.3 (CH_{Ar}), 114.8 (CH_{Ar}), 55.6 (CH₃).

Analytical data obtained were in agreement with the reported values.¹⁵

1-[4-(4-nitrophenyl)phenyl]ethanone, **2c**



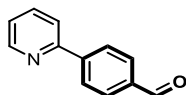
Chemical Formula: C₁₄H₁₁NO₃
Molecular Weight: 241.25

Following the general procedure, from acetylphenyl boronic acid (82.00 mg, 0.50 mmol) and 4-chloro-nitrobenzene (79.00 mg, 0.50 mmol), the product was obtained in 86% yield (103.00 mg) as a beige solid.

¹H NMR (400 MHz, CDCl₃): δ (ppm) = δ 8.32 (d, *J* = 10.8 Hz, 2H), 8.09 (d, *J* = 8.1 Hz, 2H), 7.78 (d, *J* = 9.1 Hz, 2H), 7.73 (d, *J* = 9.1 Hz, 2H), 2.56 (s, 3H).

¹³C {¹H} NMR (100 MHz, CDCl₃): δ (ppm) = δ 197.6 (C_{OMe}), 147.7 (C_{Ar}), 146.3 (C_{Ar}), 143.2 (C_{Ar}), 137.2 (C_{Ar}), 129.2 (CH_{Ar}), 128.2 (CH_{Ar}), 127.7 (CH_{Ar}), 124.3 (CH_{Ar}), 26.8 (CH₃).

Analytical data obtained were in agreement with the reported values.¹⁵

4-(2-pyridinyl)benzaldehyde, **2d**

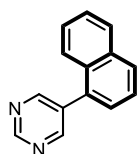
Chemical Formula: C₁₂H₉NO
Molecular Weight: 183.21

Following the general procedure, from 4-formylboronic acid (75.00 mg, 0.50 mmol) and 2-chloropyridine (68.00 μ L, 0.50 mmol), the product was obtained in 70% yield (65.00 mg) as a white solid.

¹H NMR (400 MHz, CDCl₃): δ (ppm) = δ 10.09 (s, 1H), 8.75 (dt, J = 7.7, 4.8 Hz, 1H), 8.19 (d, J = 8.7 Hz, 2H), 8.00 (td, J = 8.7, 5.5 Hz, 2H), 7.82-7.81 (m, 2H), 7.33 (q, J = 4.6 Hz, 1H).

¹³C {¹H} NMR (100 MHz, CDCl₃): δ (ppm) = δ 192.1 (CH_{CHO}), 156.0 (C_{Ar}), 150.1 (CH_{Ar}), 145.0 (C_{Ar}), 137.2 (CH_{Ar}), 136.5 (C_{Ar}), 130.5 (CH_{Ar}), 130.3 (CH_{Ar}), 128.1 (CH_{Ar}), 127.6 (CH_{Ar}), 123.3 (CH_{Ar}), 121.4 (CH_{Ar}).

Analytical data obtained were in agreement with the reported values.¹⁶

5-(naphthalen-1-yl)pyrimidine, **2e**

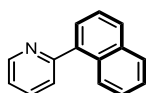
Chemical Formula: C₁₄H₁₀N₂
Molecular Weight: 206.25

Following the general procedure, from 1-naphthalene boronic acid (86.00 mg, 0.50 mmol) and 2-bromopyrimidine (79.50 mL, 0.50 mmol), the product was obtained in 99% (102.30 mg) as a brown oil.

¹H NMR (400 MHz, CDCl₃): δ (ppm) = δ 9.31 (s, 1H), 8.90 (s, 2H), 7.98-7.95 (m, 2H), 7.77 (d, J = 8.9 Hz, 1H), 7.61-7.42 (m, 4H).

¹³C {¹H} NMR (100 MHz, CDCl₃): δ (ppm) = δ 157.7 (C_{Ar}), 157.4 (C_{Ar}), 134.5 (C_{Ar}), 133.9 (C_{Ar}), 132.5 (CH_{Ar}), 131.3 (CH_{Ar}), 129.5 (CH_{Ar}), 128.8 (CH_{Ar}), 127.8 (CH_{Ar}), 127.2 (CH_{Ar}), 126.5 (CH_{Ar}), 125.5 (CH_{Ar}), 124.6 (CH_{Ar}).

Analytical data obtained were in agreement with the reported values.¹⁷

2-(1-naphthyl)pyridine, **2f**

Chemical Formula: C₁₅H₁₁N
Molecular Weight: 205.26

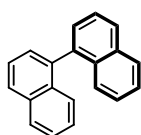
Following the general procedure, from 1-naphthalene boronic acid (86.00 mg, 0.50 mmol) and 2-chloropyridine (68.00 μ L, 0.50 mmol), the product was obtained in 99% (101.90 mg) as a beige oil.

¹H NMR (400 MHz, CDCl₃): δ (ppm) = δ 8.80 (ddd, *J* = 4.9, 1.8, 0.9 Hz, 1H), 8.12-8.05 (m, 1H), 7.95-7.89 (m, 2H), 7.84 (td, *J* = 7.7, 1.8 Hz, 1H), 7.63-7.57 (m, 3H), 7.49 (tt, *J* = 6.8, 5.4 Hz, 3H), 7.34 (ddd, *J* = 7.6, 4.9, 1.2 Hz, 1H).

¹³C {¹H} NMR (100 MHz, CDCl₃): δ (ppm) = δ 159.4 (C_{Ar}), 149.6 (CH_{Ar}), 138.6 (C_{Ar}), 136.5 (CH_{Ar}), 134.0 (C_{Ar}), 131.3 (C_{Ar}), 129.0 (CH_{Ar}), 128.5 (CH_{Ar}), 127.6 (CH_{Ar}), 126.6 (CH_{Ar}), 125.9 (CH_{Ar}), 125.7 (CH_{Ar}), 125.4 (CH_{Ar}), 125.2 (CH_{Ar}), 122.2 (CH_{Ar}).

Analytical data obtained were in agreement with the reported values.¹⁶

1-naphthalen-1-yl-naphthalene, **2g**



Chemical Formula: C₂₀H₁₄
Molecular Weight: 254.33

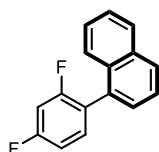
Following the general procedure, from 1-naphthalene boronic acid (86.00 mg, 0.50 mmol) 2-chloronaphthalene (81.30 mg, 0.50 mmol), the product was obtained in 99% yield (126.00 mg) as a brown oil.

¹H NMR (400 MHz, CDCl₃): δ (ppm) = δ 7.96 (dd, *J* = 8.1, 2.6 Hz, 4H), 7.62 (t, *J* = 7.7 Hz, 2H), 7.51-7.45 (m, 4H), 7.41-7.38 (m, 2H), 7.31-7.29 (m, 2H).

¹³C {¹H} NMR (100 MHz, CDCl₃): δ (ppm) = δ 138.6 (C_{Ar}), 133.6 (C_{Ar}), 133.0 (C_{Ar}), 128.3 (CH_{Ar}), 128.0 (CH_{Ar}), 128.0 (CH_{Ar}), 126.7 (CH_{Ar}), 126.1 (CH_{Ar}), 125.9 (CH_{Ar}), 125.5 (CH_{Ar}).

Analytical data obtained were in agreement with the reported values.¹⁸

1-(2,4-difluorophenyl)naphthalene, **2h**



Chemical Formula: C₁₆H₁₀F₂
Molecular Weight: 240.25

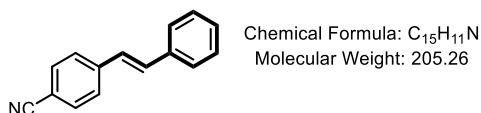
Following the general procedure, from 1-naphthalene boronic acid (86.00 mg, 0.50 mmol) and 1-chloro-2,4-difluorobenzene (74.30 mg, 0.50 mmol), the product was obtained in 80% yield (95.80 mg) as a brown solid.

¹H NMR (400 MHz, CDCl₃): δ (ppm) = δ 7.93 (d, *J* = 8.6 Hz, 2H), 7.64-7.34 (m, 6H), 7.05-6.96 (m, 2H).

¹³C {¹H} NMR (100 MHz, CDCl₃): δ (ppm) = δ 162.76 (dd, J = 253.0, 11.8 Hz, C_{Ar}-F), 160.29 (dd, J = 253.4, 11.7 Hz, C_{Ar}-F), 133.7 (C_{Ar}), 133.2-133.1 (m, C_{Ar} + CH_{Ar}), 132.0 (C_{Ar}), 128.7 (CH_{Ar}), 128.5 (CH_{Ar}), 128.0 (CH_{Ar}), 126.5 (CH_{Ar}), 126.1 (CH_{Ar}), 125.7 (CH_{Ar}), 125.4 (CH_{Ar}), 124.21 (dd, J = 16.7, 3.8 Hz, C_{Ar}), 111.5 (dd, J = 21.0, 3.7 Hz, CH_{Ar}), 104.2 (t, J = 25.8 Hz, CH_{Ar}).

Analytical data obtained were in agreement with the reported values.¹⁹

(E)-4-styrylbenzotrile, 2j



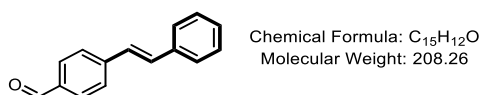
Following the general procedure, from (*E*)-styrylboronic acid (74.00 mg, 0.50 mmol) and 4-chlorobenzotrile (69.00 mg, 0.50 mmol), the product was obtained in 74% yield (76.00 mg) as a yellow solid.

¹H NMR (400 MHz, CDCl₃): δ (ppm) = δ 7.65-7.63 (m, 2H), 7.60-7.58 (m, 2H), 7.55-7.53 (m, 2H), 7.41-7.37 (m, 2H), 7.34-7.30 (t, J = 7.27 Hz, 1H), 7.22 (d, J = 16.3 Hz, 1H), 7.09 (d, J = 16.3 Hz, 1H).

¹³C {¹H} NMR (100 MHz, CDCl₃): δ (ppm) = δ 142.0 (C_{Ar}), 136.4 (C_{Ar}), 132.6 (CH_{Ar}), 132.5 (CH_{Ar}), 129.0 (CH_{Ar}), 128.8 (CH_{Ar}), 127.1 (CH_{Alkene}), 127.0 (CH_{Alkene}), 126.9 (CH_{Ar}), 119.2 (CN), 110.7 (C_{Ar}-CN).

Analytical data obtained were in agreement with the reported values.²⁰

(E)-4-styrylbenzaldehyde, 2k



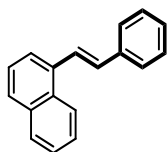
Following the general procedure, from (*E*)-styrylboronic acid (74.00 mg, 0.50 mmol) and 4-chlorobenzaldehyde (70.00 mg, 0.50 mmol), the product was obtained in 96% yield (100.50 mg) as a beige solid.

¹H NMR (400 MHz, CDCl₃): δ (ppm) = δ 10.00 (s, 1H), 7.89 (d, J = 8.7 Hz, 2H), 7.67 (d, J = 8.1 Hz, 2H), 7.56 (d, J = 8.1 Hz, 2H), 7.41 (t, J = 7.5 Hz, 2H), 7.34-7.31 (m, 1H), 7.29 (d, J = 4.9 Hz, 1H), 7.15 (d, J = 16.3 Hz, 1H).

¹³C {¹H} NMR (100 MHz, CDCl₃): δ (ppm) = δ 191.8 (C_{HO}), 143.5 (C_{Ar}), 136.7 (C_{Ar}), 135.4 (C_{Ar}), 132.2 (CH_{Ar}), 130.4 (CH_{Ar}), 129.0 (CH_{Ar}), 128.6 (CH_{Ar}), 127.5 (CH_{Ar}), 127.0 (CH_{Alkene}).

Analytical data obtained were in agreement with the reported values.²¹

(*E*)-1-styrylnaphthalene, **21**



Chemical Formula: C₁₈H₁₄
Molecular Weight: 230.31

Following the general procedure, from (*E*)-styrylboronic acid (74.00 mg, 0.50 mmol) and 1-chloronaphthalene (82.00 mg, 0.50 mmol), the product was obtained in 69% yield (80.00 mg) as a beige solid.

¹H NMR (400 MHz, CDCl₃): δ (ppm) = δ 7.92-7.75 (m, 2H), 7.61-7.15 (m, 10H), 6.99-6.96 (m, 1H), 6.69-6.66 (m, 1H).

¹³C {¹H} NMR (100 MHz, CDCl₃): δ (ppm) = δ 137.8 (C_{Ar}), 137.5 (CH_{Ar}), 135.2 (C_{Ar}), 133.9 (C_{Ar}), 133.0 (CH_{Ar}), 131.9 (CH_{Ar}), 131.5 (C_{Ar}), 129.4 (CH_{Ar}), 128.9 (CH_{Ar}), 128.8 (CH_{Ar}), 127.7 (CH_{Ar}), 126.8 (CH_{Ar}), 126.5 (CH_{Ar}), 126.2 (CH_{Ar}), 126.0 (CH_{Ar}), 125.8 (CH_{Ar}), 123.9 (CH_{alkene}), 123.8 (CH_{alkene}).

Analytical data obtained were in agreement with the reported values.²²

9.4 Chapter 4: Highly catalytically active Pd-NHC pre-catalyst for the formation of C-X bonds

For the synthesis of the pre-catalysts see Section 9.2 and 9.3.

9.4.1. General procedure

In an inert atmosphere, a vial was charged with the pre-catalyst, base, solvent (1 mL) and a magnetic stir bar and sealed with a screw cap. The mixture was left to stir at 110 °C for the stated time (10-60 min, **activation time**). The sample was removed from the heating block and the corresponding aniline was added followed by the corresponding aryl chloride. The reaction was left to stir (910 rpm) for 16 h at varying temperatures.

9.4.2. Catalyst optimisation

The general procedure was followed using 4-fluoroaniline (61.00 mg, 0.55 mmol), 4-chloroanisole (61.00 μ L, 0.50 mmol) with KO^tAm (70.00 mg, 0.55 mmol) in 1,4-dioxane (1 mL) with activation and experimental temperatures at 110 °C. An aliquot was taken to determine the conversion of 4-chloroanisole by GC using mesitylene as internal standard.

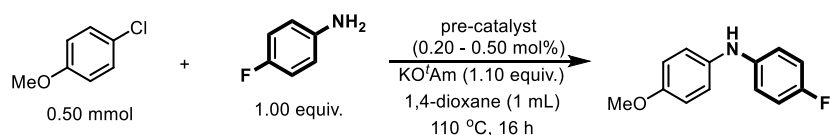


Table S-16: Optimisation of Pd pre-catalyst for 0.20 - 0.50% mol reaction

Entries	Pd pre-catalyst	Mass (mg)	Catalyst loading (mol%)	GC Conversion ^a /Yield ^b (%)
1	[IPent·H][Pd(η^3 -cin)Cl ₂]	2.00	0.50	86 ^a
2	[IHept·H][Pd(η^3 -cin)Cl ₂]	2.30	0.50	88 ^a
3	[INon·H][Pd(η^3 -cin)Cl ₂]	2.60	0.50	93 ^a
4	[IPr*·H][Pd(η^3 -cin)Cl ₂]	3.00	0.50	99 ^a
5	[Pr* ^{OMe} ·H][Pd(η^3 -cin)Cl ₂]	3.10	0.50	95 ^a
6	[IPent ^{Cl} ·H][Pd(η^3 -cin)Cl ₂]	2.20	0.50	87 ^a
7	[IPr·H][Pd(η^3 -cin)Cl ₂]	1.70	0.50	63 ^a
8	[IPr*·H][Pd(η^3 -cin)Cl ₂]	3.00	0.50	99 ^a
9	[IPr*·H][Pd(η^3 -crotyl)Cl ₂]	2.80	0.50	96 ^a
10	[IPr*·H][Pd(η^3 -2-Me-allyl)Cl ₂]	2.80	0.50	95 ^a
11	[IPr*·H][Pd(η^3 -Ind ^{tBu})Cl ₂]	3.20	0.50	87 ^a
12	[INon·H][Pd(η^3 -cin)Cl ₂]	2.70	0.50	98 ^a
13	[IPr*·H][Pd(η^3 -cin)Cl ₂]	1.20	0.20	99 ^a
14	[IPr*·H][Pd(η^3 -crotyl)Cl ₂]	1.20	0.20	90 ^a
15	[IPr*·H][Pd(η^3 -2-Me-allyl)Cl ₂]	1.20	0.20	88 ^a
16	[IPr*·H][Pd(η^3 -Ind ^{tBu})Cl ₂]	1.30	0.20	56 ^a
17	[INon·H][Pd(η^3 -cin)Cl ₂]	1.00	0.20	83 ^a

^a GC conversion based on 4-chloroanisole. Value calculated from an average of two reactions. ^b GC yield, mesitylene is used as internal standard. ^c 0.20 mol% of catalyst used.

9.4.3. Activation time optimisation

The general procedure was followed using [IPr*·H][Pd(η^3 -cin)Cl₂] (0.50 mol%), 4-fluoroaniline (61.00 mg, 0.55 mmol), 4-chloroanisole (61.00 μ L, 0.50 mmol) with KO^tAm (70.00 mg, 0.55 mmol) in 1,4-dioxane at 110 °C with varying activation times. An aliquot was taken to determine the conversion of 4-chloroanisole by GC using mesitylene as internal standard.

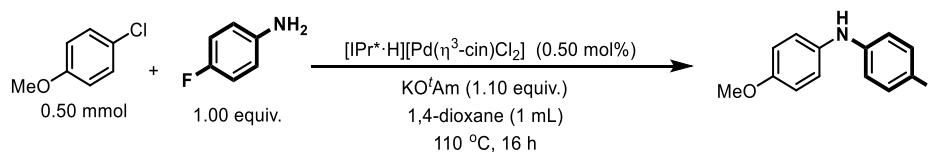


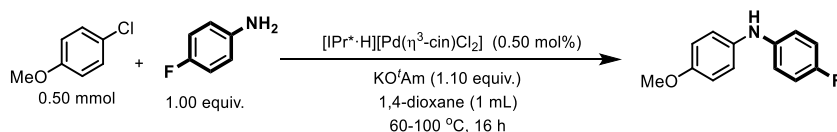
Table S-17: Activation time optimisation

Entries	Time (min)	GC conversion (%) ^a
1	10	88
2	30	80
3	60	99

^a GC conversion is based on 4-chloroanisole. Value calculated from an average of two reactions.

9.4.4. Activation temperature and experimental temperature optimisation

The general procedure was followed using pre-catalyst (0.50 mol%), 4-fluoroaniline (61.00 mg, 0.55 mmol), 4-chloroanisole (61.00 μ L, 0.50 mmol) with KO^tAm (70.00 mg, 0.55 mmol) in 1,4-dioxane (1 mL) at with varying activation temperatures for 1 h and varying experimental temperatures. An aliquot was taken to determine the conversion of 4-chloroanisole by GC using mesitylene as internal standard.

**Table S-18:** Temperature optimisation using $[\text{IPr}^*\cdot\text{H}][\text{Pd}(\eta^3\text{-cin})\text{Cl}_2]$

Entries	Activation Temperature (°C)	Reaction Temperature (°C)	GC conversion (%) ^a
1	60	60	83
2	70	70	80
3	80	80	92
4	90	90	85
5	70	100	76
6	80	100	85
7	90	100	90
8	100	100	95

^a GC conversion is based on 4-chloroanisole. Value calculated from an average of two reactions

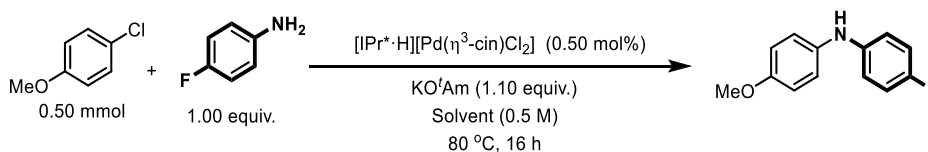
Table S-19: Temperature optimisation using [IPr*·H][Pd(η^3 -cin)Cl₂]

Entries	Activation Temperature (°C)	Reaction Temperature (°C)	GC conversion (%) ^a
1	60	80	99
2	80	80	90
2	90	90	88

^a GC conversion is based on 4-chloroanisole. Value calculated from an average of two reactions

9.4.5. Solvent optimisation

The general procedure was followed using [IPr*·H][Pd(η^3 -cin)Cl₂] (0.50 mol%), 4-fluoroaniline (61.00 mg, 0.55 mmol), 4-chloroanisole (61.00 μ L, 0.50 mmol) with KO^tAm (70.00 mg, 0.55 mmol) in varying solvents (0.5 M), activating at 80 °C for 1 h and running at 80 °C for 16 h. An aliquot was taken to determine the conversion of 4-chloroanisole by GC using mesitylene as internal standard.

**Table S-20:** Solvents used in solvent optimisation in air

Entries	Solvent (0.5 M)	GC conversion (%) ^a
1	Toluene	80
2	THF	64
3	Ethanol	n.r.
4	<i>iso</i> -Propanol	n.r.
5	<i>n</i> -Butanol	n.r.
6	1,4-Dioxane	93

^a GC conversion is based on 4-chloroanisole. Value calculated from an average of two reactions. n.r. = no reaction

Table S-21: Solvents used in solvent optimisation in inert atmosphere

Entries	Solvent (0.5 M)	GC conversion (%) ^a
1	Toluene	90
2	THF	92
3	<i>iso</i> -Propanol	19
4	Acetonitrile	n.r.
5	Hexane	89
6	1,2-Dimethoxyethane	90
7	1,4-Dioxane	90
8	Cyclohexane	94
9	CPME	97
10	2-MeTHF	87
11	Heptane	87
12	1,4-Dioxane ^b	97
13	THF ^b	99
14	CPME ^b	96
15	Cyclohexane ^b	94
16	Ethanol ^c	n.r.

^a GC conversion is based on 4-chloroanisole. Value calculated from an average of two reactions. ^b The substrates were added in reverse from the normal synthesis; 4-fluoroaniline followed by 4-chloroanisole.

^c The reaction was run with K₂CO₃ as the base.

9.4.6. Base optimisation

The general procedure was followed using [IPr*·H][Pd(η³-cin)Cl₂] (0.50 mol%), 4-fluoroaniline (61.00 mg, 0.55 mmol), 4-chloroanisole (61.00 μL, 0.50 mmol) with the corresponding base (0.55 mmol) and corresponding solvent (0.5 M), activating at 80 °C for 1 h and running at 80 °C for 16 h. An aliquot was taken to determine the conversion of 4-chloroanisole by GC using mesitylene as internal standard.

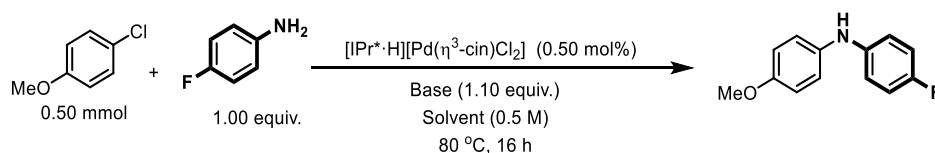


Table S-22: Base optimization in 1,4-dioxane

Entries	Base (0.55 mmol)	GC conversion (%) ^a
1	KO ^t Bu	93
2	K ₂ CO ₃	n.r.
3	K ₃ PO ₄	n.r.
4	KOH	57
5	NaOH	45
6	Cs ₂ CO ₃	<1
7	LiOH	n.r.
8	CsOH	22
9	Na ₂ CO ₃	n.r.
10	NaO ^t Bu	91
11	KF/K ₂ CO ₃ (1:1)	n.r.
12	KO ^t Bu ^b	83

^a GC conversion is based on 4-chloroanisole. Value calculated from an average of two reactions. ^b The substrates were added in reverse from the normal synthesis; 4-fluoroaniline followed by 4-chloroanisole.

Table S-23: Base optimization in THF

Entries	Base (0.55 mmol)	GC conversion (%) ^a
1	KO ^t Am	92
2	KO ^t Bu	98
3	K ₂ CO ₃	n.r.
4	K ₃ PO ₄	n.r.
5	KOH	57
6	NaOH	19
7	Cs ₂ CO ₃	7
8	LiOH	n.r.
9	CsOH	22
10	Na ₂ CO ₃	n.r.
11	KO ^t Bu ^b	99

^a GC conversion is based on 4-chloroanisole. Value calculated from an average of two reactions. ^b The substrates were added in reverse from the normal synthesis; 4-fluoroaniline followed by 4-chloroanisole.

Table S-24: Base optimisation in cyclohexane

Entries	Base (0.55 mmol)	GC conversion (%) ^a
1	KO ^t Am	94
2	KO ^t Bu	86
3	KOH	12
4	NaOH	<1
5	CsOH	n.r.

^a GC conversion is based on 4-chloroanisole. Value calculated from an average of two reactions.

Table S-25: Base optimisation in CPME

Entries	Base (0.55 mmol)	GC Conversion (%) ^a
1	KO ^t Am	99
2	KO ^t Bu	99
3	KOH	42
4	NaOH	32
5	CsOH	38
6	NaO ^t Bu	98

^a GC conversion is based on 4-chloroanisole. Value calculated from an average of two reactions.

9.4.7. Catalyst loading optimisation

The general procedure was followed using [IPr*·H][Pd(η^3 -cin)Cl₂] (mol%), 4-fluoroaniline (61.00 mg, 0.55 mmol), 4-chloroanisole (61.00 μ L, 0.50 mmol) with KO^tBu (62.00 mg, 0.55 mmol) in CPME (0.25 M), activating at 60 °C for 1 h and running at 80 °C for 16 h. An aliquot was taken to determine the conversion of 4-chloroanisole by GC using mesitylene as internal standard.

Table S-26: Catalyst loading optimization

Entries	mol%	GC yield (%)
1	0.50	99
2	0.50 ^a	70
3	0.30	99
4	0.20	99
5	0.10	50

GC yield, internal standard = mesitylene 0.1 mmol. Value calculated from an average of two reactions.

^a no activation step was used.

9.4.8. Time optimisation

The general procedure was followed using [IPr*H][Pd(η^3 -cin)Cl₂] (0.20 mol%), 4-fluoroaniline (61.00 mg, 0.55 mmol), 4-chloroanisole (61.00 μ L, 0.50 mmol) with KO^tBu (62.00 mg, 0.55 mmol) in CPME (0.25 M), activating at 60 °C for 1 h and running at 80 °C for the corresponding time. An aliquot was taken to determine the conversion of 4-chloroanisole by GC using mesitylene as internal standard.

Table S 27: Time optimisation, Part 1

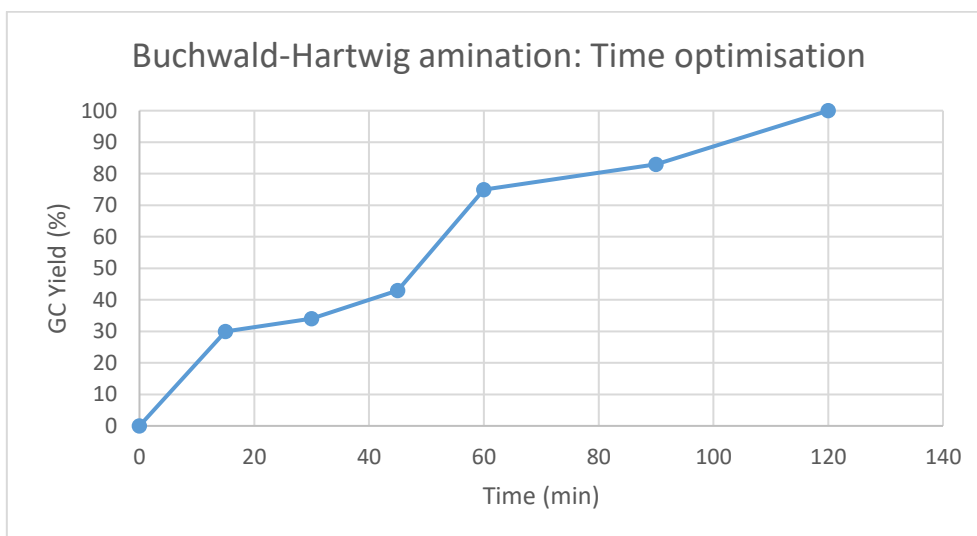
Activation time (min)	Reaction time (min)	GC yield (%)
60	30	30
60	60	71
60	120	99

GC yield, internal standard = mesitylene 0.1 mmol. Value calculated from an average of two reactions.

Table S-28: Time optimisation, Part 2

Activation time (min)	Reaction time (min)	GC yield (%)
60	15	30
60	30	34
60	45	43
60	60	75
60	90	83
60	120	99

GC yield, internal standard = mesitylene 0.10 mmol. Value calculated from an average of two reactions.



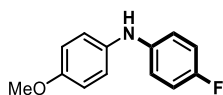
Graph 4: Time optimisation of the Buchwald-Hartwig amination. GC yield, internal standard = mesitylene 0.1mmol. Value calculated from an average of two reactions.

9.4.9. Scope

9.4.9.1 General procedure

A vial was charged with [IPr*H][Pd(η^3 -cin)Cl₂] (1.20 mg, 0.20 mol%), KO^tBu (62.00 mg, 0.55 mmol), CPME (1 mL) and a magnetic stir bar and sealed with a screw cap. The mixture was left to stir at the 60 °C for 1 h. The vial was removed from the heating block and the corresponding solution of aniline and aryl chloride in CPME (1 mL) was added. The reaction was left to stir (910 rpm) at 80 °C for 2 h. The crude mixture was purified by a filtration over silica gel.

4-fluoro-*N*-(4-methoxyphenyl)aniline, **3a**



Chemical Formula: C₁₃H₁₂FNO
Molecular Weight: 217.24

Following the general procedure, from 4-chloroanisole (71.00 mg, 0.50 mmol) and 4-fluoroaniline (56.00 mg, 0.55 mmol), the product was obtained in 99% yield (107.00 mg) as a brown oil.

Large scale:

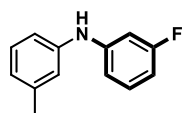
Following the general procedure, from 4-chloroanisole (784.00 mg, 5.50 mmol) and 4-fluoroaniline (672.00 mg, 6.05 mmol), the product was obtained in 99% yield (119.30 mg) as a brown oil.

¹H NMR (400 MHz, CDCl₃): δ (ppm) = δ 7.02 (dt, *J* = 9.1, 4.4 Hz, 2H), 6.95-6.93 (m, 6H), 5.38 (s, 1H), 3.80 (s, 3H).

¹³C {¹H} NMR (100 MHz, CDCl₃): δ (ppm) = δ 157.2 (d, *J* = 238.1, CF), 155.1 (C_{Ar}), 141.2 (d, C_{Ar}, *J* = 1.9 Hz, C_{Ar}), 136.6 (C_{Ar}), 121.3 (2 x CH_{Ar}), 117.9 (d, *J* = 7.6 Hz, CH_{Ar}), 117.9 (2 x CH_{Ar}), 115.9 (d, *J* = 22.4 Hz, CH_{Ar}), 114.9 (CH_{Ar}), 55.7 (CH₃).

¹⁹F NMR (376 MHz, CDCl₃): δ (ppm) = -124.3

Analytical data obtained were in agreement with the reported values.²³

3-fluoro-*N*-(3-methylphenyl)aniline, 3b

Chemical Formula: C₁₃H₁₂FN
Molecular Weight: 201.24

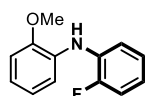
Following the general procedure, from 3-chlorotoluene (63.00 mg, 0.50 mmol) and 3-fluoroaniline (56.00 mg, 0.55 mmol), the product was obtained in 99% yield (99.80 mg) as a brown oil.

¹H NMR (400 MHz, CDCl₃): δ (ppm) = δ 7.28-7.25 (m, 2H), 6.97-6.95 (m, 2H), 6.89 (d, *J* = 8.7 Hz, 1H), 6.81-6.77 (m, 2H), 6.65 (t, *J* = 7.1 Hz, 1H), 5.74 (s, 1H), 2.38 (s, 3H).

¹³C {¹H} NMR (100 MHz, CDCl₃): δ (ppm) = δ 163.9 (d, *J* = 243.8 Hz, CF), 145.6 (d, *J* = 10.55 Hz, C_{Ar}), 142.0 (C_{Ar}), 139.5 (C_{Ar}), 130.5 (d, *J* = 10.0 Hz, CH_{Ar}), 129.4 (CH_{Ar}), 123.1 (CH_{Ar}), 119.9 (CH_{Ar}), 116.2 (CH_{Ar}), 112.6 (CH_{Ar}), 107.0 (d, *J* = 21.5 Hz, CH_{Ar}), 103.6 (d, *J* = 25.1 Hz, CH_{Ar}), 21.6 (CH₃).

¹⁹F NMR (376 MHz, CDCl₃): δ (ppm) = -112.2.

Analytical data obtained were in agreement with the reported values.²⁴

2-fluoro-*N*-(2-methoxyphenyl)aniline, 3c

Chemical Formula: C₁₃H₁₂FNO
Molecular Weight: 217.24

Following the general procedure, from 2-chloroanisole (72.00 mg, 0.50 mmol) and 2-fluoroaniline (56.00 mg, 0.55 mmol), the product was obtained in 80% yield (86.00 mg) as a brown oil.

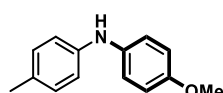
¹H NMR (400 MHz, CDCl₃): δ (ppm) = 7.43 (td, *J* = 8.3, 1.5 Hz, 1H), 7.31-7.29 (m, 1H), 7.13 (ddd, *J* = 11.3, 8.1, 1.4 Hz, 1H), 7.07 (t, *J* = 7.7 Hz, 1H), 6.93-6.86 (m, 4H), 6.23 (s, 1H), 3.91 (s, 3H).

¹³C {¹H} NMR (100 MHz, CDCl₃): δ (ppm) = δ 153.7 (d, *J* = 241.7 Hz, CF), 149.0 (C_{Ar}), 132.0 (C_{Ar}), 131.4 (d, *J* = 11.0 Hz, C_{Ar}), 124.3 (d, *J* = 3.6 Hz, CH_{Ar}), 120.9 (d, *J* = 7.0 Hz, CH_{Ar}), 120.8 (d, *J* = 8.1 Hz, CH_{Ar}), 118.1 (2 x CH_{Ar}), 115.6 (d, *J* = 19.4 Hz, CH_{Ar}), 115.5 (CH_{Ar}), 110.7 (CH_{Ar}), 55.7 (CH₃).

¹⁹F NMR (376 MHz, CDCl₃): δ (ppm) = -131.4

Analytical data obtained were in agreement with the reported values.²⁵

4-methyl-*N*-(4-methoxyphenyl)aniline, **3d**



Chemical Formula: C₁₄H₁₅NO
Molecular Weight: 213.28

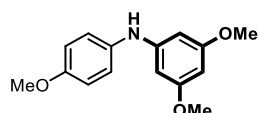
Following the general procedure, from 4-chlorotoluene (63.00 mg, 0.50 mmol) and 4-methoxyaniline (68.00 mg, 0.55 mmol), the product was obtained in 99% yield (105.00 mg) as a black powder.

¹H NMR (400 MHz, CDCl₃): δ (ppm) = δ 7.66-7.60 (m, 4H), 6.88-6.85 (m, 4H), 5.41 (s, 1H), 3.80 (s, 3H), 2.29 (s, 3H).

¹³C {¹H} NMR (100 MHz, CDCl₃): δ (ppm) = δ 154.6 (C_{Ar}), 142.2 (C_{Ar}), 136.5 (C_{Ar}), 129.6 (C_{Ar}), 129.2 (2 x CH_{Ar}), 120.9 (2 x CH_{Ar}), 116.4 (2 x CH_{Ar}), 114.5 (2 x CH_{Ar}), 55.4 (CH₃), 20.4 (CH₃).

Analytical data obtained were in agreement with the reported values.²⁶

3,5-dimethoxy-*N*-(4-methoxyphenyl)aniline, **3e**



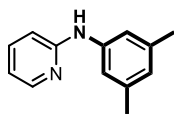
Chemical Formula: C₁₅H₁₇NO₃
Molecular Weight: 259.31

Following the general procedure, from 4-chloroanisole (71.00 mg, 0.50 mmol) and 3,5-dimethoxyaniline (67.00 mg, 0.55 mmol), the product was obtained in 95% yield (122.70 mg) as a yellow oil.

¹H NMR (400 MHz, CDCl₃): δ (ppm) = δ 7.10 (d, *J* = 9.2 Hz, 2H), 6.88 (d, *J* = 8.6 Hz, 2H), 6.07-6.05 (m, 3H), 5.52 (br. s, 1H), 3.80-3.76 (m 9H).

¹³C {¹H} NMR (100 MHz, CDCl₃): δ (ppm) = δ 171.2 (C_{Ar}), 161.3 (C_{Ar}), 155.5 (C_{Ar}), 148.5 (C_{Ar}), 147.4 (C_{Ar}), 135.2 (CH_{Ar}), 123.0 (CH_{Ar}), 114.6 (CH_{Ar}), 93.8 (CH_{Ar}), 93.7 (CH_{Ar}), 91.6 (CH_{Ar}), 90.9 (CH_{Ar}), 60.4 (CH₃), 55.5 (CH₃), 55.1 (CH₃).

Analytical data obtained were in agreement with the reported values.²⁷

***N*-(3,5-dimethylphenyl)pyridin-2-amine, 3f**

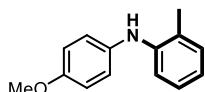
Chemical Formula: C₁₃H₁₄N₂
Molecular Weight: 198.27

Following the general procedure, from 2-chloropyridine (57.00 mg, 0.50 mmol) and 3,5-dimethyl-aniline (67.00 mg, 0.55 mmol), the product was obtained in 75% yield (74.50 mg) as a yellow oil.

¹H NMR (400 MHz, CDCl₃): δ (ppm) = 8.22 (s, 1H), 7.55-7.53 (m, 1H), 6.96-6.92 (m, 3H), 6.77 (br. s, 1H), 6.75-6.70 (m, 2H), 2.34 (s, 6H).

¹³C {¹H} NMR (100 MHz, CDCl₃): δ (ppm) = δ 156.3 (C_{Ar}), 148.4 (CH_{Ar}), 140.4 (C_{Ar}), 139.1 (CH_{Ar}), 137.9 (2 x C_{Ar}), 125.0 (2 x CH_{Ar}), 118.5 (CH_{Ar}), 114.9 (CH_{Ar}), 108.3 (CH_{Ar}), 221.5 (2 x CH₃).

Analytical data obtained were in agreement with the reported values.²⁸

2-methyl-*N*-(4-methoxyphenyl)aniline, 3g

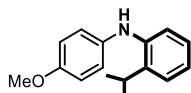
Chemical Formula: C₁₄H₁₅NO
Molecular Weight: 213.28

Following the general procedure, from 4-chloroanisole (63.00 mg, 0.50 mmol) and *o*-toluidine (59.00 mg, 0.55 mmol), the product was obtained in 99% yield (106.00 mg) as an oil.

¹H NMR (400 MHz, CDCl₃): δ (ppm) = δ 7.20 (d, *J* = 8.2 Hz, 1H), 7.14 (t, *J* = 8.3 Hz, 1H), 7.09-7.05 (m, 3H), 6.92-6.88 (m, 3H), 5.25 (s, 1H), 3.84 (s, 3H), 2.29 (s, 3H).

¹³C {¹H} NMR (100 MHz, CDCl₃): δ (ppm) = δ 155.2 (C_{Ar}), 143.4 (C_{Ar}), 136.4 (C_{Ar}), 130.8 (C_{Ar}), 126.9 (2 x CH_{Ar}), 125.4 (2 x CH_{Ar}), 122.2 (CH_{Ar}), 120.1 (CH_{Ar}), 115.2 (CH_{Ar}), 114.8 (CH_{Ar}), 55.7 (CH₃), 17.9 (CH₃).

Analytical data obtained were in agreement with the reported values.²⁶

2-isopropyl-*N*-(4-methoxyphenyl)aniline, 3h

Chemical Formula: C₁₆H₁₉NO
Molecular Weight: 241.33

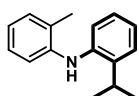
Following the general procedure, from 4-chloroanisole (71.00 mg, 0.50 mmol) and 2-isopropylaniline (75.00 mg, 0.55 mmol), the product was obtained in 99% yield (120.00 mg) as a yellow oil.

¹H NMR (400 MHz, CDCl₃): δ (ppm) = δ 7.20 (d, *J* = 7.5 Hz, 1H), 7.03-6.98 (m, 2H), 6.89-6.83 (m, 3H), 6.79-6.75 (m, 2H), 5.22 (br. s, 1H), 3.72 (s, 3H), 3.05 (sept, *J* = 6.8 Hz, 1H), 1.22 (dd, *J* = 8.9, 5.2 Hz, 6H).

¹³C {¹H} NMR (100 MHz, CDCl₃): δ (ppm) = δ 154.8 (C_{Ar}), 141.8 (C_{Ar}), 137.6 (C_{Ar}), 137.3 (C_{Ar}), 126.5 (CH_{Ar}), 125.9 (CH_{Ar}), 121.4 (CH_{Ar}), 121.1 (CH_{Ar}), 118.1 (CH_{Ar}), 114.8 (CH_{Ar}), 55.7 (CH₃), 27.6 (CH), 22.9 (CH₃), 22.4 (CH₃).

Analytical data obtained were in agreement with the reported values.²⁹

2-isopropyl-*N*-(*o*-tolyl)aniline, **3i**



Chemical Formula: C₁₆H₁₉N
Molecular Weight: 225.34

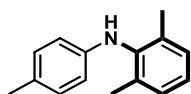
Following the general procedure, from 2-chloroanisole (63.00 mg, 0.50 mmol) and 2-isopropylaniline (71.00 mg, 0.55 mmol), the product was obtained in 99% yield (111.90 mg) as a beige solid.

¹H NMR (400 MHz, CDCl₃): δ (ppm) = δ 7.33 (d, *J* = 8.4 Hz, 1H), 7.21 (d, *J* = 7.2 Hz, 1H), 7.16-7.05 (m, 4H), 6.93-6.89 (m, 2H), 5.24 (s, 1H), 3.17 (q, *J* = 5.8 Hz, 1H), 2.29 (s, 3H), 1.29 (d, *J* = 7.0 Hz, 6H).

¹³C {¹H} NMR (100 MHz, CDCl₃): δ (ppm) = δ 143.2 (C_{Ar}), 140.4 (C_{Ar}), 139.5 (C_{Ar}), 130.8 (CH_{Ar}), 127.0 (C_{Ar}), 126.6 (CH_{Ar}), 126.5 (CH_{Ar}), 126.1 (CH_{Ar}), 122.8 (CH_{Ar}), 121.0 (CH_{Ar}), 120.7 (CH_{Ar}), 119.1 (CH_{Ar}), 117.0 (CH_{Ar}), 27.9 (CH), 23.1 (CH₃), 17.9 (CH₃).

Analytical data obtained were in agreement with the reported values.²⁹

2,6-dimethyl-*N*-(*p*-tolyl)aniline, **3j**



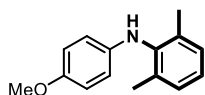
Chemical Formula: C₁₅H₁₇N
Molecular Weight: 211.31

Following the general procedure, from 4-chlorotoluene (63.00 mg, 0.50 mmol) and 2,6-dimethyl-aniline (67.00 mg, 0.55 mmol), the product was obtained in 99% yield (104.00 mg) as a yellow oil.

¹H NMR (400 MHz, CDCl₃): δ (ppm) = δ 7.14-7.08 (m, 3H), 7.00 (d, *J* = 7.8 Hz, 2H); 6.46 (d, *J* = 7.9 Hz, 2H), 5.11 (s, 1H), 2.26 (s, 3H), 2.23 (s, 6H).

¹³C {¹H} NMR (100 MHz, CDCl₃): δ (ppm) = δ 144.0 (C_{Ar}), 138.8 (C_{Ar}), 135.6 (C_{Ar}), 129.8 (2 x CH_{Ar}), 128.6 (2 x CH_{Ar}), 127.5 (2 x C_{Ar}), 125.5 (2 x CH_{Ar}), 113.9 (CH_{Ar}), 20.6 (CH₃), 18.5 (CH₃).

Analytical data obtained were in agreement with the reported values.²⁹

***N*-(4-methoxyphenyl)-2,6-dimethylaniline, 3k**

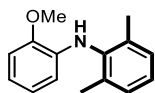
Chemical Formula: C₁₅H₁₇NO
Molecular Weight: 227.31

Following the general procedure, from 4-chloroanisole (71.00 mg, 0.50 mmol) and 2,6-dimethylaniline (67.00 mg, 0.55 mmol), the product was obtained in 99% yield (112.00 mg) as a yellow oil.

¹H NMR (400 MHz, CDCl₃): δ (ppm) = δ 7.12 (d, *J* = 7.1 Hz, 2H), 7.16-7.11 (m, 1H), 6.76 (d, *J* = 8.5 Hz, 2H). 6.51 (d, *J* = 9.4 Hz, 2H), 5.03 (s, 1H), 3.75 (s, 3H), 2.20 (s, 3H).

¹³C {¹H} NMR (100 MHz, CDCl₃): δ (ppm) = δ 152.8 (C_{Ar}), 140.2 (C_{Ar}), 139.4 (C_{Ar}), 135.0 (C_{Ar}), 128.7 (CH_{Ar}), 128.3 (CH_{Ar}), 125.0 (CH_{Ar}), 121.8 (CH_{Ar}), 118.1 (CH_{Ar}), 115.3 (CH_{Ar}), 114.8 (CH_{Ar}), 55.9 (CH₃), 18.5 (CH₃).

Analytical data obtained were in agreement with the reported values.²⁶

***N*-(2-methoxyphenyl)-2,6-dimethylaniline, 3l**

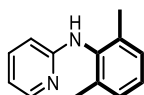
Chemical Formula: C₁₅H₁₇NO
Molecular Weight: 227.31

Following the general procedure, from 2-chloroanisole (71.00 mg, 0.50 mmol) and 2,6-dimethylaniline (67.00 mg, 0.55 mmol), the product was obtained in 80% yield (91.00 mg) as a yellow oil.

¹H NMR (400 MHz, CDCl₃): δ (ppm) = δ 7.13-7.01 (m, 3H), 6.87-6.82 (m, 1H), 6.70-6.68 (m, 2H), 6.14-6.12 (m, 1H), 5.65 (s, 1H), 3.95 (s, 3H), 2.21 (s, 6H).

¹³C {¹H} NMR (100 MHz, CDCl₃): δ (ppm) = δ 146.9 (C_{Ar}), 138.5 (C_{Ar}), 136.3 (C_{Ar}), 136.1 (C_{Ar}), 128.6 (2 x CH_{Ar}), 125.8 (CH_{Ar}), 121.2 (CH_{Ar}), 117.4 (CH_{Ar}), 111.2 (CH_{Ar}), 110 (CH_{Ar}), 55.8 (CH₃), 18.4 (CH₃).

Analytical data obtained were in agreement with the reported values.³⁰

***N*-(2,6-dimethylphenyl)pyridin-2-amine, 3m**

Chemical Formula: C₁₃H₁₄N₂
Molecular Weight: 198.27

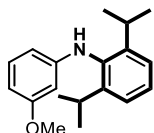
Following the general procedure, from 2-chloropyridine (57.00 mg, 0.50 mmol) and 2,6-dimethylaniline (67.00 mg, 0.55 mmol), the product was obtained in 73% yield (72.00 mg) as a beige solid.

¹H NMR (400 MHz, CDCl₃): δ (ppm) = δ 8.15-8.10 (m, 1H), 7.35 (td, *J* = 6.7, 2.1 Hz, 1H), 7.13 (s, 3H), 6.64 (t, *J* = 6.5 Hz, 1H), 6.27 (br. s, 1H), 6.01 (dt, *J* = 8.5, 3.2 Hz, 1H), 2.23 (s, 6H).

¹³C {¹H} NMR (100 MHz, CDCl₃): δ (ppm) = δ 157.9 (C_{Ar}), 148.6 (CH_{Ar}), 138.0 (C_{Ar}), 136.9 (2 x CH_{Ar}), 136.6 (C_{Ar}), 128.7 (C_{Ar}), 126.9 (2 x CH_{Ar}), 113.8 (CH_{Ar}), 105.8 (CH_{Ar}), 18.5 (2 x CH₃).

Analytical data obtained were in agreement with the reported values.²⁶

2,6-diisopropyl-*N*-(3-methoxyphenyl)aniline, **3n**



Chemical Formula: C₁₉H₂₅NO
Molecular Weight: 283.42

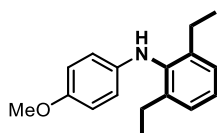
Following the general procedure, from 3-chloroanisole (71.00 mg, 0.50 mmol) and 2,6-diisopropylaniline (98.00 mg, 0.55 mmol), the product was obtained in 99% yield (140.00 mg) as an oil.

¹H NMR (400 MHz, CDCl₃): δ (ppm) = δ 7.39-7.37 (m, 1H), 7.31-7.27 (m, 2H), 7.14 (t, *J* = 8.1 Hz, 1H), 6.37 (dd, *J* = 8.1, 4.1 Hz, 1H), 6.21 (dd, *J* = 8.0, 3.7 Hz, 1H), 6.12 (t, *J* = 2.0 Hz, 1H), 5.23 (s, 1H), 3.78 (s, 3H), 3.34 (q, *J* = 7.2 Hz, 2H), 1.25 (d, *J* = 6.9 Hz, 12H).

¹³C {¹H} NMR (100 MHz, CDCl₃): δ (ppm) = δ 160.9 (C_{Ar}), 149.7 (C_{Ar}), 147.7 (C_{Ar}), 135.1 (2 x C_{Ar}), 130.0 (2 x CH_{Ar}), 127.4 (CH_{Ar}), 123.9 (CH_{Ar}), 106.2 (CH_{Ar}), 103.2 (CH_{Ar}), 99.1 (CH_{Ar}), 55.1 (2 x CH₃), 28.3 (2 x CH), 24.0 (2 x CH₃).

Analytical data obtained were in agreement with the reported values.³¹

2,6-diethyl-*N*-(4-methoxyphenyl)aniline, **3o**



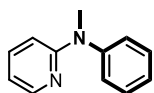
Chemical Formula: C₁₇H₂₁NO
Molecular Weight: 255.36

Following the general procedure, from 4-chloroanisole (71.00 mg, 0.50 mmol) and 2,6-diethylaniline (75.00 mg, 0.55 mmol), the product was obtained in 99% yield (126.00 mg) as a yellow oil.

¹H NMR (400 MHz, CDCl₃): δ (ppm) = δ 7.17-7.13 (m, 3H), 6.76 (dt, *J* = 9.1, 5.3 Hz, 2H), 6.49 (dt, *J* = 8.5, 4.4 Hz, 2H), 5.01 (s, 1H), 3.77 (s, 3H), 2.61 (quant, *J* = 7.5 Hz, 4H), 1.18 (t, *J* = 6.3 Hz, 6H).

¹³C {¹H} NMR (100 MHz, CDCl₃): δ (ppm) = δ 152.6 (C_{Ar}), 141.6 (C_{Ar}), 141.3 (C_{Ar}), 136.0 (2 x C_{Ar}), 126.8 (2 x CH_{Ar}), 126.0 (2 x CH_{Ar}), 114.9 (2 x CH_{Ar}), 114.8 (CH_{Ar}), 55.7 (CH₃), 24.8 (2 x CH₂), 14.8 (2 x CH₃).

Analytical data obtained were in agreement with the reported values.²⁹

***N*-methyl-*N*-phenylpyridin-2-amine, 4a**

Chemical Formula: C₁₂H₁₂N₂
Molecular Weight: 184.24

Following the general procedure, from 2-chloropyridine (57.00 mg, 0.50 mmol) and *N*-methylaniline (59.00 mg, 0.55 mmol), the product was obtained in 99% yield (89.50 mg) as a yellow oil.

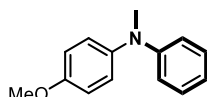
Large scale:

Following the general procedure, from 2-chloropyridine (624.50 mg, 5.50 mmol) and *N*-methylaniline (648.30 mg, 6.05 mmol), the product was obtained in 99% yield (1013.00 mg) as a yellow oil.

¹H NMR (400 MHz, CDCl₃): δ (ppm) = δ 8.24-8.22 (m, 1H), 7.42 (t, *J* = 6.5 Hz, 2H), 7.31-1.22 (m, 4H), 6.62-6.58 (m, 1H), 6.55-6.52 (m, 1H), 3.48 (s, 3H).

¹³C {¹H} NMR (100 MHz, CDCl₃): δ (ppm) = δ 158.9 (C_{Ar}), 147.9 (C_{Ar}), 146.9 (CH_{Ar}), 136.6 (CH_{Ar}), 129.8 (CH_{Ar}), 129.2 (CH_{Ar}), 126.4 (CH_{Ar}), 125.5 (CH_{Ar}), 113.2 (CH_{Ar}), 112.5 (CH_{Ar}), 109.2 (CH_{Ar}), 38.2 (CH₃).

Analytical data obtained were in agreement with the reported values.²³

4-methoxy-*N*-methyl-*N*-phenylaniline, 4b

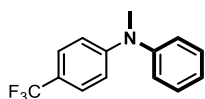
Chemical Formula: C₁₄H₁₅NO
Molecular Weight: 213.28

Following the general procedure, from 4-chloroanisole (71.00 mg, 0.50 mmol) and *N*-methylaniline (59.00 mg, 0.55 mmol), the product was obtained in 99% yield (105.60 mg) as a yellow oil.

¹H NMR (400 MHz, CDCl₃): δ (ppm) = δ 7.23 (t, *J* = 7.9 Hz, 2H), 7.11 (d, *J* = 9.1 Hz, 2H), 6.91 (d, *J* = 9.6 Hz, 2H), 6.81-6.77 (m, 3H), 3.82 (s, 3H), 3.27 (s, 3H).

¹³C {¹H} NMR (100 MHz, CDCl₃): δ (ppm) = δ 156.4 (C_{Ar}), 149.8 (C_{Ar}), 142.3 (C_{Ar}), 129.3 (CH_{Ar}), 129.0 (CH_{Ar}), 126.3 (2 x CH_{Ar}), 118.4 (CH_{Ar}), 115.8 (CH_{Ar}), 114.8 (CH_{Ar}), 114.7 (CH_{Ar}), 112.4 (CH_{Ar}), 55.5 (CH₃), 40.5 (CH₃).

Analytical data obtained were in agreement with the reported values.²³

N-methyl-N-phenyl-4-(trifluoromethyl)aniline, 4c

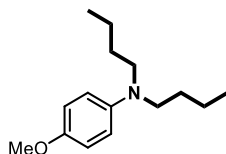
Chemical Formula: C₁₄H₁₂F₃N
Molecular Weight: 251.25

Following the general procedure, from 4-chlorobenzotrifluoride (90.00 mg, 0.50 mmol) and *N*-methylaniline (59.00 mg, 0.55 mmol), the product was obtained in 99% yield (123.90 mg) as a yellow oil.

¹H NMR (400 MHz, CDCl₃): δ (ppm) = δ 7.44-7.38 (m, 4H), 7.21-7.17 (m, 3H), 6.86 (d, *J* = 8.9 Hz, 2H), 3.35 (s, 3H).

¹³C {¹H} NMR (100 MHz, CDCl₃): δ (ppm) = δ 151.6 (C_{Ar}), 147.8 (C_{Ar}), 129.9 (2 x CH_{Ar}), 126.3 (dd, *J* = 3.6, 7.6 Hz, CH_{Ar}), 125.4 (2 x CH_{Ar}), 125.1 (2 x CH_{Ar}), 125.1 (q, *J* = 270.5 Hz, CF₃), 120.1 (q, *J* = 32.6 Hz C-CF₃), 114.9 (CH_{Ar}), 40.2 (CH₃).

Analytical data obtained were in agreement with the reported values.²⁸

***N,N*-dibutyl-4-methoxyaniline, 4d**

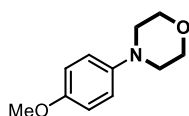
Chemical Formula: C₁₅H₂₅NO
Molecular Weight: 235.37

Following the general procedure, from 4-chloroanisole (71.00 mg, 0.50 mmol) and dibutylamine (71.00 mg, 0.55 mmol), the product was obtained in 80% yield (100.00 mg) as a yellow oil.

¹H NMR (400 MHz, CDCl₃): δ (ppm) = δ 6.83-6.81 (m, 2H), 6.67-6.65 (m, 2H), 3.76 (s, 3H), 3.20 (t, *J* = 7.1 Hz, 4H), 1.56-1.48 (q, *J* = 7.7 Hz, 4H), 1.38-1.29 (sep, *J* = 8.4 Hz, 4H), 0.95 (t, *J* = 7.2 Hz, 6H).

¹³C {¹H} NMR (100 MHz, CDCl₃): δ (ppm) = δ 151.1 (C_{Ar}), 143.5 (C_{Ar}), 115.0 (2 x CH_{Ar}), 114.5 (2 x CH_{Ar}), 56.0 (CH₃), 51.8 (2 x CH₂), 29.6 (2 x CH₂), 20.6 (2 x CH₂), 14.2 (2 x CH₃).

Analytical data obtained were in agreement with the reported values.²⁹

4-(4-methoxyphenyl)morpholine, 4e

Chemical Formula: C₁₁H₁₅NO₂
Molecular Weight: 193.25

Following the general procedure, from 4-chloroanisole (71.00 mg, 0.50 mmol) and morpholine (107.00 mg, 0.55 mmol), the product was obtained in 99% yield (96.00 mg) as a white solid.

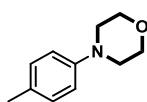
Large scale:

Following the general procedure, from 4-chloroanisole (784.00 mg, 5.50 mmol) and morpholine (1175.40 mg, 6.05 mmol), the product was obtained in 99% yield (1061.00 mg) as a white solid.

^1H NMR (400 MHz, CDCl_3): δ (ppm) = δ 6.91-6.84 (m, 4H), 3.87-3.77 (m, 4H), 3.77 (s, 3H), 3.07-3.05 (m, 4H).

^{13}C { ^1H } NMR (100 MHz, CDCl_3): δ (ppm) = δ 154.1 (C_{Ar}), 145.8 (C_{Ar}), 118.0 (2 x CH_{Ar}), 114.6 (2 x CH_{Ar}), 67.2 (2 x CH_2), 55.7 (CH_3), 51.0 (2 x CH_2)

Analytical data obtained were in agreement with the reported values.²³

4-(*p*-tolyl)morpholine, 4f

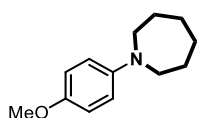
Chemical Formula: $\text{C}_{11}\text{H}_{15}\text{NO}$
Molecular Weight: 177.25

Following the general procedure, from 4-chlorotoluene (63.00 mg, 0.50 mmol) and morpholine (107.00 mg, 0.55 mmol), the product was obtained in 97% yield (86.00 mg) as a white solid.

^1H NMR (400 MHz, CDCl_3): δ (ppm) = δ 7.10 (d, J = 8.7 Hz, 2H), 6.85 (d, J = 7.7 Hz, 2H), 3.87-3.85 (m, 4H), 3.12-3.10 (m, 4H), 2.28 (s, 3H).

^{13}C { ^1H } NMR (100 MHz, CDCl_3): δ (ppm) = δ 149.9 (C_{Ar}), 129.9 (C_{Ar}), 129.7 (2 x CH_{Ar}), 116.2 (2 x CH_{Ar}), 67.1 (2 x CH_2), 50.1 (2 x CH_2), 20.6 (CH_3).

Analytical data obtained were in agreement with the reported values.²⁹

1-(4-methoxyphenyl)azepane, 4g

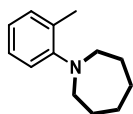
Chemical Formula: $\text{C}_{13}\text{H}_{19}\text{NO}$
Molecular Weight: 205.30

Following the general procedure, from 4-chloroanisole (71.00 mg, 0.50 mmol) and hexamethylene-imine (55.00 mg, 0.55 mmol), the product was obtained in 99% yield (101.00 mg) as a yellow oil.

^1H NMR (400 MHz, CDCl_3): δ (ppm) = δ 6.84 (dt, J = 9.2, 2.4 Hz, 2H), 6.66 (d, J = 8.4 Hz, 2H), 3.76 (s, 3H), 3.43 (t, J = 7.9 Hz, 4H), 1.78-1.75 (m, 4H), 1.56-1.53 (m, 4H).

^{13}C { ^1H } NMR (100 MHz, CDCl_3): δ (ppm) = δ 150.5 (C_{Ar}), 143.9 (C_{Ar}), 115.1 (2 x CH_{Ar}), 112.4 (2 x CH_{Ar}), 56.0 (CH_3), 49.7 (2 x CH_2), 28.1 (2 x CH_2), 27.3 (2 x CH_2).

Analytical data obtained were in agreement with the reported values.³²

1-(*o*-tolyl)azepane, **4h**

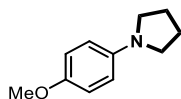
Chemical Formula: C₁₃H₁₉N
Molecular Weight: 189.30

Following the general procedure, from 2-chlorotoluene (57.00 mg, 0.50 mmol) and hexamethylene-imine (55.00 mg, 0.55 mmol), the product was obtained in 99% yield (94.00 mg) as a beige solid.

¹H NMR (400 MHz, CDCl₃): δ (ppm) = 7.16-7.12 (m, 2H), 7.07 (dd, *J* = 8.0, 1.4 Hz, 1H), 6.94 (td, *J* = 7.3, 1.4 Hz, 1H), 3.10 (t, *J* = 5.5 Hz, 4H), 2.33 (s, 3H), 1.80-1.71 (m, 8H).

¹³C {¹H} NMR (100 MHz, CDCl₃): δ (ppm) = δ 155.0 (C_{Ar}), 133.0 (C_{Ar}), 131.0 (CH_{Ar}), 126.5 (CH_{Ar}), 122.4 (CH_{Ar}), 120.9 (CH_{Ar}), 56.0 (CH₂), 29.7 (2 x CH₂), 27.1 (2 x CH₂), 19.0 (CH₃).

Analytical data obtained were in agreement with the reported values.³³

1-(4-methoxyphenyl)pyrrolidine, **4i**

Chemical Formula: C₁₁H₁₅NO
Molecular Weight: 177.25

Following the general procedure, from 4-chloroanisole (71.00 mg, 0.50 mmol) and pyrrolidine (67.00 mg, 0.55 mmol), the product was obtained in 80% yield (71.00 mg) as a yellow oil.

¹H NMR (400 MHz, CDCl₃): δ (ppm) = δ 6.90 (dt, *J* = 8.7, 2.4 Hz, 2H), 6.59 (dt, *J* = 9.5, 2.3 Hz, 2H), 3.79 (s, 3H), 3.29-3.25 (m, 4H), 2.04-2.01 (m, 4H).

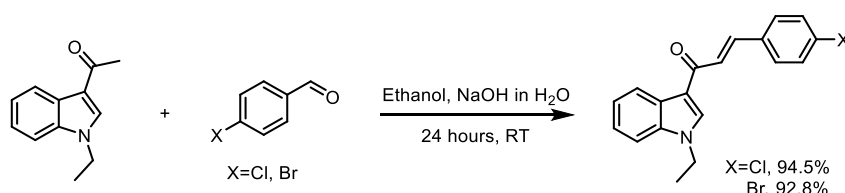
¹³C {¹H} NMR (100 MHz, CDCl₃): δ (ppm) = δ 150.8 (C_{Ar}), 143.3 (C_{Ar}), 115.1 (CH_{Ar}), 112.7 (2 x CH_{Ar}), 56.0 (CH₃), 48.3 (2 x CH₂), 25.2 (2 x CH₂).

Analytical data obtained were in agreement with the reported values.²⁶

9.4.10 Biologically interesting substrates

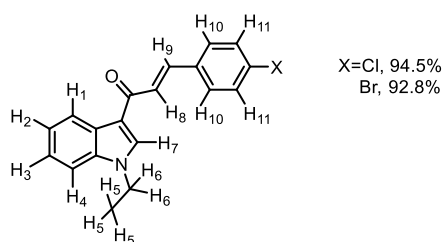
9.4.10.1 Synthesis of the coupling substrates

The synthesis of the coupling substrates were carried out by Abdullah Al.Majid, Assem Barakat and Mohammad Shahidul Islam from King Saud University in Saudi Arabia.



9.4.10.2 General procedure

In a round bottom flask, *N*-ethylacetindole (1.00 g, 5.34 mmol), and the corresponding aldehyde (8.00 mmol, 1.50 equiv.) were dissolved in ethanol (20 mL). Then, NaOH (853.00 mg, 16.00 mmol, 4.00 equiv.) in 10 mL water was added and the mixture was stirred at room temperature for 1 day. The solid was collected by filtration and washed with hexane to give the pure product.



(*E*)-3-(4-chlorophenyl)-1-(1-ethyl-1H-indol-3-yl)prop-2-en-1-one.

Following the general procedure using 4-chloroaldehyde (1.12 g, 8.00 mmol) the product was obtained in 94% (1.56 g) yield. Melting point: 118 – 119 °C.

¹H NMR (400 MHz, CDCl₃): δ (ppm) = 8.54-8.51 (m, 1H, H₁), 7.91 (s, 1H, H₇), 7.76 (d, *J* = 15.6 Hz, 1H, H₄), 7.56 (d, *J* = 7.7 Hz, 2H, H_{8,9}), 7.37-7.31 (m, 6H, H_{2,3,10,11}), 4.26-4.19 (m, 2H, H₆), 1.57 (t, *J* = 7.2 Hz, 3H, H₅)

¹³C {¹H} NMR (100 MHz, CDCl₃): δ (ppm) = δ 184.0 (C=O), 139.6 (C=C), 136.9 (C-N), 135.7 (C_{Ar}), 134.1 (C_{Ar}), 133.9 (C_{Ar}), 129.4 (CH_{Ar}), 129.2 (CH_{Ar}), 127.1 (CHN), 124.5 (CH_{Ar}), 123.7 (CH_{Ar}), 123.2 (CH_{Ar}), 122.9 (CH_{Ar}), 117.8 (CH_{Ar}), 42.0 (CH₂), 15.3 (CH₃).

IR (KBr, cm⁻¹) ν_{max} = 3046, 2971, 2926, 1653, 1595, 1527, 1480, 1464, 1392, 1238, 1200, 1145, 1098, 1089, 1057, 967, 939, 856, 811, 750, 701, 426.

[Anal. Calcd. for C₁₉H₁₆ClNO: C, 73.66; H, 5.21; N, 4.52; Found: C, 73.75; H, 5.42; N, 4.39].

LC/MS (ESI, *m/z*): [M⁺], found 309.10, C₁₉H₁₆ClNO for 309.09.

(E)-3-(4-bromophenyl)-1-(1-ethyl-1H-indol-3-yl)prop-2-en-1-one.

Following the general procedure using 4-bromoaldehyde (1.48 g, 8.00 mmol) the product was obtained in 93% (1.75 g) yield. Melting point: 139 – 140 °C.

¹H NMR (400 MHz, CDCl₃): δ (ppm) = 8.54-8.52 (m, 1H, H₁), 7.93 (s, 1H, H₇), 7.74 (d, *J* = 15.6 Hz, 1H, H₄), 7.53 (d, *J* = 7.7 Hz, 2H, H_{8,9}), 7.40-7.32 (m, 6H, H_{2,3,10,11}), 4.25 (q, *J* = 7.3 Hz, 2H, H₆), 1.57 (t, *J* = 7.2 Hz, 3H, H₅)

¹³C {¹H} NMR (100 MHz, CDCl₃): δ (ppm) = δ 184.0 (C=O), 139.6 (C=C), 136.9 (C-N), 135.7 (C_{Ar}), 134.1 (C_{Ar}), 133.9 (C_{Ar}), 129.4 (CH_{Ar}), 129.2 (CH_{Ar}), 127.1 (CHN), 124.5 (CH_{Ar}), 123.7 (CH_{Ar}), 123.2 (CH_{Ar}), 122.9 (CH_{Ar}), 117.8 (CH_{Ar}), 42.0 (CH₂), 15.3 (CH₃). IR (KBr, cm⁻¹) ν_{max} = 3049, 2977, 1646, 1611, 1588, 1524, 1463, 1449, 1391, 1311, 1268, 1260, 1089, 1062, 993, 975, 858, 835, 779, 741, 717, 671, 561, 520, 478.

[Anal. Calcd. for C₁₉H₁₆BrNO: C 64.42, H 4.55, N 3.95. Found: C 64.31, H 4.67, N 4.15]

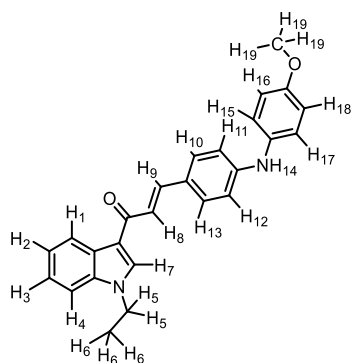
LC/MS (ESI, *m/z*): [M⁺], found 353.00, C₁₉H₁₆BrNO for 353.04.

9.4.10.3 The Buchwald-Hartwig reaction

A vial was charged with [IPr*·H][Pd(η³-cin)Cl₂] (1.20 mg, 2.00 mol%), KO^tBu (11.20 mg, 0.10 mmol), CPME (0.20 mL) and a magnetic stir bar and sealed with a screw cap. The mixture was left to stir at the 60 °C for 1 h. The vial was removed from the heating block and the corresponding solution of aniline and aryl chloride in CPME (0.5 mL) was added. The reaction was left to stir (910 rpm) for 20 h at 80 °C.

The reaction was purified using flash chromatography, gradient from 10:90 to 50:50 ethylacetate/petroleum ether.

Entry 5a and 5b



Following the general procedure, from *N*-Et-Indenone (17.60 mg, 0.05 mmol) and 4-methoxyaniline (6.80 mg, 0.05 mmol), the product yielded 15.60 mg (80%) as an orange/brown oil.

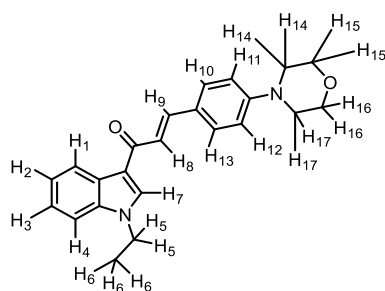
¹H NMR (400 MHz, CDCl₃): δ (ppm) = δ 8.53-8.50 (m, 1H₁), 7.91 (s, 1H₇), 7.79 (d, *J* = 15.5 Hz, 1H₉), 7.53 (d, *J* = 8.6 Hz, 2H_{11 and 12}), 7.39-7.36 (m, 1H₂), 7.33-7.31 (m, 2H_{10 and 13}), 7.29-7.24 (m, 2H_{3 and 4}), 7.14 (d, *J* = 8.9 Hz, 2H_{15 and 17}), 6.91-6.86 (m, 3H_{8, 16 and 18}), 5.77 (br. s, 1H₁₄), 4.25 (q, *J* = 7.3 Hz, 2H₅), 3.82 (s, 3H₁₉), 1.56 (t, *J* = 7.3 Hz, 3H₆).

¹³C {¹H} NMR (100 MHz, CDCl₃): δ (ppm) = δ 184.9 (C=O), 156.2 (C-OMe), 147.3 (C=C), 141.4 (C-NH), 136.8 (C-N), 134.3 (C-NH), 133.4 (CH), 130.1 (CH), 127.2 (CH(N)), 126.4 (CH), 123.7 (CH), 123.5 (CH), 123.3 (C=C), 122.6 (CH), 114.9 (C(C=O)), 114.8 (CH), 109.8 (CH), 55.7 (OCH₃), 41.9 (CH₂), 15.4 (CH₃(CH₂)).

5a HRMS (ESI/Q-TOF) m/z: [M]⁺ Calcd for C₂₆H₂₄N₂O₂ 396.1800. Found: 397.1916.

5b HRMS (ESI/Q-TOF) m/z: [M]⁺ Calcd for C₂₆H₂₄N₂O₂ 396.1800. Found: 397.1916.

Entry 5c



Following the general procedure, from *N*-Et-Indenone (17.60 mg, 0.05 mmol) and morpholine (4.80 mg, 0.05 mmol), the product yielded 13.40 mg (74%) as an orange/brown oil.

¹H NMR (400 MHz, CDCl₃): δ (ppm) = 8.41-8.39 (m, 1H₁), 7.78-7.72 (m, 1H₇), 7.38-7.36 (m, 2H_{8 and 9}), 7.31-7.30 (m, 3H_{2,11 and 12}), 7.19 (d, *J* = 8.4 Hz, 2H_{3 and 4}), 6.87 (d, *J* = 8.5 Hz, 2H_{10 and 13}), 4.22-

4.18 (m, 2H₅), 4.23-4.18 (m, 2H₁₅ and 16), 3.87-3.82 (m, 2H₁₄ and 17), 3.17-3.11 (m, 4H₁₄ and 17; 15 and 16), 1.25 (s, 3H₆).

¹³C {¹H} NMR (100 MHz, CDCl₃): δ (ppm) = 194.9 (C=O), 193.2 (C-N), 149.7 (C=C), 136.7 (C-N), 134.2 (CH), 133.7 (CH), 133.6 (C), 129.2 (CH), 126.6 (C), 124.8 (CH), 123.3 (CH), 122.9 (C=C), 122.7 (CH), 117.2 (C), 116.7 (CH), 116.2 (CH), 109.8 (CH), 67.1 (CH₂), 49.8 (CH₂), 42.1 (CH₂), 41.9 (CH₂), 41.8 (CH₂), 15.3 (CH₃).

HRMS (ESI/Q-TOF) m/z: [M]⁺ Calcd for C₂₃H₂₄N₂O₂ 361.1914. Found: 361.1916.

9.4.11 Optimisation and scope of the α-ketone arylation

9.4.11.1 General procedure

A vial was charged with the pre-catalyst, base, solvent (1 mL) and a magnetic stir bar and sealed with a screw cap. The mixture was left to stir at the 60 °C for 1 h. The sample was removed from the heating block and the corresponding aryl ketone was added followed by the corresponding aryl chloride (0.5 mmol). The reaction was left to stir (910 rpm) at 80 °C for 3 h.

9.4.11.2 Catalyst optimisation

The general procedure was followed using propiophenone (74.00 mg, 0.55 mmol), 4-chloroanisole (63.00 mg, 0.50 mmol) with NaO^tBu (53.00 mg, 0.55 mmol) in CPME (1 mL). A GC sample was taken to determine the GC conversion based on the conversion of 4-chlorotoluene.

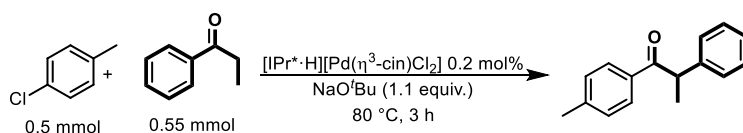


Table S-29: Pre-catalyst optimisation using 0.20 mol%

Entries	Pd Pre-catalyst	GC conversion (%) ^a
1	[IPent·H][Pd(η ³ -cin)Cl ₂]	99
2	[IHept·H][Pd(η ³ -cin)Cl ₂]	99
3	[IPr*·H][Pd(η ³ -cin)Cl ₂]	99
4	[Pr* ^{OMe} ·H][Pd(η ³ -cin)Cl ₂]	99
5	[IPr*·H][Pd(η ³ -crotyl)Cl ₂]	94
6	[IPr*·H][Pd(η ³ -2-Me-allyl)Cl ₂]	99

^a GC conversion is based on 4-chlorotoluene. Value calculated from an average of two reactions.

Table S-30: Pre-catalyst optimization using 0.10 mol%

Entries	Pd Pre-catalyst	GC conversion (%) ^a
1	[IPent·H][Pd(η^3 -cin)Cl ₂]	83
2	[IHept·H][Pd(η^3 -cin)Cl ₂]	77
3	[IPr*·H][Pd(η^3-cin)Cl₂]	86
4	[Pr* ^{OMe} ·H][Pd(η^3 -cin)Cl ₂]	72
5	[IPr*·H][Pd(η^3 -2-Me-allyl)Cl ₂]	79

^a GC conversion is based on 4-chlorotoluene. Value calculated from an average of two reactions.

9.4.11.3 Base/solvent optimisation

The general procedure was followed using [IPr*·H][Pd(η^3 -cin)Cl₂] (1.20 mg, 0.001 mmol), propiophenone (74.00 mg, 0.55 mmol) and 4-chloroanisole (63.00 mg, 0.50 mmol). A GC sample was taken to determine the GC conversion based on the conversion of 4-chlorotoluene.

Table S-31: Base optimisation using cyclopentylmethyl ether (CPME)

Entries	Base (0.55 mmol)	GC conversion (%)
1	KO ^t Bu	n.r.
2	LiO ^t Bu	31
3	NaO ^t Bu	n.r.
4	KOH	n.r.
5	NaOH	99

GC conversion is based on 4-chlorotoluene. Value calculated from an average of two reactions.

Table S-32: Base optimization using toluene

Entries	Base (0.55 mmol)	GC conversion (%)
1	KO ^t Bu	72
2	LiO ^t Bu	5
3	NaO ^t Bu	91
4	KOH	n.r.
5	NaOH	n.r.

GC conversion is based on 4-chlorotoluene. Value calculated from an average of two reactions.

Table S-33: Base optimisation using THF

Entries	Base (0.55 mmol)	GC conversion (%)
1	KO ^t Bu	n.r.
2	LiO ^t Bu	traces
3	NaO ^t Bu	31
4	KOH	n.r.
5	NaOH	n.r.

GC conversion is based on 4-chlorotoluene. Value calculated from an average of two reactions.

Table S-34: Base optimisation using 1,4-dioxane

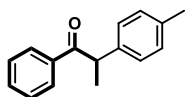
Entries	Base (0.55 mmol)	GC conversion (%)
1	KO ^t Bu	11
2	LiO ^t Bu	n.r.
3	NaO ^t Bu	11
4	KOH	n.r.
5	NaOH	n.r.

GC conversion is based on 4-chlorotoluene. Value calculated from an average of two reactions.

9.4.11.4 Scope

9.4.11.4.1 General procedure

A vial was charged with [IPr*·H][Pd(η^3 -cin)Cl₂] (1.20 mg, 0.20 mol%), NaO^tBu (53.00 mg, 0.55 mmol), CPME (1 mL) and a magnetic stir bar and sealed with a screw cap. The mixture was left to stir at the 60 °C for 1 h. The vial was removed from the heating block and the corresponding solution of aryl ketone and aryl chloride in CPME (1 mL) was added. The reaction was left to stir (910 rpm) for 2 h at 80 °C. The reaction was purified using flash chromatography, 5:95 ethylacetate/pe-troleum ether.

1-phenyl-2-(*p*-tolyl)propan-1-one, **6a**

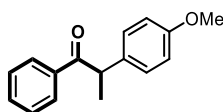
Chemical Formula: C₁₆H₁₆O
Molecular Weight: 224.30

Following the general procedure, from 4-chlorotoluene (63.00 mg, 0.50 mmol) and propiophenone (74.00 mg, 0.55 mmol), the product was obtained in 99% yield (111.00 mg) as a colourless oil.

¹H NMR (400 MHz, CDCl₃): δ (ppm) = δ 7.96 (dd, *J* = 8.4, 1.3 Hz, 2H), 7.49 (tt, *J* = 7.4, 2.2 Hz, 1H), 7.39 (t, *J* = 7.5 Hz, 2H), 7.18 (dt, *J* = 8.1, 2.2 Hz, 2H), 7.11 (d, *J* = 7.9 Hz, 2H), 4.55-4.51 (m, 1H), 2.28 (s, 3H), 1.51 (d, *J* = 6.8 Hz, 3H).

¹³C {¹H} NMR (100 MHz, CDCl₃): δ (ppm) = δ 200.4 (C=O), 138.3 (C_{Ar}), 136.4 (C_{Ar}), 136.4 (C_{Ar}), 132.6 (2 x CH_{Ar}), 129.6 (2 x CH_{Ar}), 128.7 (2 x CH_{Ar}), 128.3 (2 x CH_{Ar}), 127.5 (CH_{Ar}), 47.4 (CH), 20.9 (CH₃), 19.4 (CH₃).

Analytical data obtained were in agreement with the reported values.³⁴

2-(4-methoxyphenyl)-1-phenylpropan-1-one, **6b**

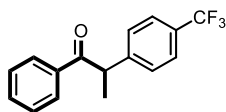
Chemical Formula: C₁₆H₁₆O₂
Molecular Weight: 240.30

Following the general procedure, from 4-chloroanisole (72.00 mg, 0.50 mmol) and propiophenone (74.00 mg, 0.55 mmol), the product was obtained in 98% yield (117.40 mg) as a colourless oil.

¹H NMR (400 MHz, CDCl₃): δ (ppm) = δ 7.98 (d, *J* = 7.1 Hz, 2H), 7.48 (t, *J* = 7.4 Hz, 1H), 7.40 (t, *J* = 7.6 Hz, 2H), 7.23 (d, *J* = 8.7 Hz, 2H), 6.85 (d, *J* = 8.8 Hz, 2H), 4.68-4.62 (m, 1H), 3.74 (s, 3H), 1.53 (d, *J* = 6.9 Hz, 3H).

¹³C {¹H} NMR (100 MHz, CDCl₃): δ (ppm) = δ 200.6 (C=O), 158.5 (C_{Ar}), 136.5 (C_{Ar}), 133.5 (C_{Ar}), 132.8 (2 x CH_{Ar}), 128.8 (2 x CH_{Ar}), 128.8 (2 x CH_{Ar}), 128.5 (2 x CH_{Ar}), 114.4 (CH_{Ar}), 55.2 (CH₃), 47.0 (CH), 19.6 (CH₃).

Analytical data obtained were in agreement with the reported values.³⁴

1-phenyl-2-(4-(trifluoromethyl)phenyl)propan-1-one, **6c**

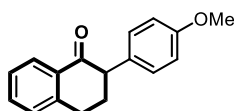
Chemical Formula: C₁₆H₁₃F₃O
Molecular Weight: 278.27

Following the general procedure, from 4-chlorobenzotrifluoride (90.30 mg, 0.50 mmol) and propiophenone (74.00 mg, 0.55 mmol), the product was obtained in 97% yield (134.70 mg) as a colourless oil.

¹H NMR (400 MHz, CDCl₃): δ (ppm) = δ 7.96 (d, *J* = 7.5 Hz, 2H), 7.57 (d, *J* = 8.1 Hz, 2H), 7.53 (t, *J* = 7.4 Hz, 1H), 7.43-7.39 (m, 4H), 4.80 (quant, *J* = 6.9 Hz, 1H), 1.57 (d, *J* = 6.9 Hz, 3H).

¹³C {¹H} NMR (100 MHz, CDCl₃): δ (ppm) = δ 199.8 (C=O), 145.5 (C_{Ar}), 136.2 (C_{Ar}), 133.3 (2 x CH_{Ar}), 129.3 (q, *J* = 32.5 Hz, C(CF₃)), 128.8 (2 x CH_{Ar}), 128.8 (2 x CH_{Ar}), 128.3 (2 x CH_{Ar}), 126.0 (q, *J* = 3.6 Hz, CH_{Ar}), 125.3 (q, *J* = 272.0 Hz, CF₃), 47.6 (CH), 19.5 (CH₃).

Analytical data obtained were in agreement with the reported values.³⁴

2-(4-methoxyphenyl)-3,4-dihydronaphthalen-1(2H)-one, **6d**

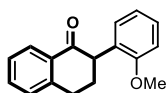
Chemical Formula: C₁₇H₁₆O₂
Molecular Weight: 252.31

Following the general procedure, from 4-chloroanisole (71.00 mg, 0.50 mmol) and α-tetralone (73.10 mg, 0.55 mmol), the product was obtained in 70% yield (88.50 mg) as a colourless oil.

¹H NMR (400 MHz, CDCl₃): δ (ppm) = δ 8.18 (d, *J* = 9.0 Hz, 1H), 7.53 (t, *J* = 7.5 Hz, 1H), 7.40 (t, *J* = 7.6 Hz, 1H), 7.22-7.18 (m, 3H), 6.81 (d, *J* = 8.9 Hz, 2H), 4.13 (s, 1H), 3.75 (s, 3H), 2.94-2.88 (m, 1H), 2.76-2.66 (m, 2H), 2.47-2.40 (m, 1H).

¹³C {¹H} NMR (100 MHz, CDCl₃): δ (ppm) = δ 201.0 (C=O), 159.5 (C_{Ar}), 144.4 (C_{Ar}), 134.3 (CH_{Ar}), 132.9 (C_{Ar}), 131.8 (2 x C_{Ar}), 129.2 (2 x CH_{Ar}), 127.8 (CH_{Ar}), 127.6 (CH_{Ar}), 127.1 (CH_{Ar}), 114.1 (CH_{Ar}), 77.5 (CH), 55.4 (CH₃), 36.5 (CH₂), 26.8 (CH₂).

Analytical data obtained were in agreement with the reported values.³⁵

2-(2-methoxyphenyl)-3,4-dihydronaphthalen-1(2H)-one, **6e**

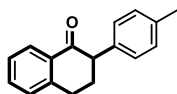
Chemical Formula: C₁₇H₁₆O₂
Molecular Weight: 252.31

Following the general procedure, from 2-chloroanisole (71.00 mg, 0.50 mmol) and α -tetralone (73.10 mg, 0.55 mmol), the product was obtained in 70% yield (88.00 mg) as a colourless oil.

¹H NMR (400 MHz, CDCl₃): δ (ppm) = δ 8.12 (d, J = 7.8 Hz, 1H), 7.52 (t, J = 7.5 Hz, 1H), 7.36 (t, J = 7.5 Hz, 1H), 7.30-7.25 (m, 2H), 7.13 (d, J = 9.1 Hz, 1H), 6.96 (dd, J = 6.8, 1.4 Hz, 2H), 4.08 (dd, J = 12.3, 4.7 Hz, 1H), 3.76 (s, 3H), 3.18-3.14 (m, 1H), 3.04-3.01 (m, 1H), 2.55 (qd, J = 12.2, 4.1 Hz, 1H), 2.30-2.26 (m, 1H).

¹³C {¹H} NMR (100 MHz, CDCl₃): δ (ppm) = δ 198.3 (C=O), 157.2 (C_{Ar}), 144.2 (C_{Ar}), 133.2 (CH_{Ar}), 129.5 (C_{Ar} + CH_{Ar}), 129.3 (C_{Ar}), 128.8 (CH_{Ar}), 128.3 (CH_{Ar}), 127.8 (CH_{Ar}), 126.7 (CH_{Ar}), 120.9 (CH_{Ar}), 111.2 (CH_{Ar}), 55.6 (CH₃), 50.1 (CH), 30.0 (CH₂), 29.6 (CH₂).

Analytical data obtained were in agreement with the reported values.³⁶

2-(*p*-tolyl)-3,4-dihydronaphthalen-1(2H)-one, **6f**

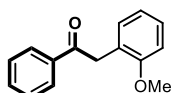
Chemical Formula: C₁₇H₁₆O
Molecular Weight: 236.31

Following the general procedure, from 4-chlorotoluene (63.30 mg, 0.50 mmol) and α -tetralone (73.10 mg, 0.55 mmol), the product was obtained in 95% yield (112.00 mg) as a colourless oil.

¹H NMR (400 MHz, CDCl₃): δ (ppm) = δ 8.18 (dd, J = 7.8, 0.8 Hz, 1H), 7.53 (t, J = 8.1 Hz, 1H), 7.40 (t, J = 7.6 Hz, 1H), 7.20-7.17 (m, 3H), 7.09 (d, J = 8.1 Hz, 2H), 4.17 (s, 1H), 2.93-2.88 (m, 1H), 2.77-2.69 (m, 2H), 2.47-2.41 (m, 1H), 2.29 (s, 3H).

¹³C {¹H} NMR (100 MHz, CDCl₃): δ (ppm) = δ 201.0 (C=O), 144.4 (C_{Ar}), 138.1 (C_{Ar}), 137.9 (C_{Ar}), 134.3 (C_{Ar}), 131.8 (CH_{Ar}), 129.4 (CH_{Ar}), 129.2 (CH_{Ar}), 127.8 (CH_{Ar}), 127.1 (CH_{Ar}), 126.2 (CH_{Ar}), 77.7 (CH), 36.5 (CH₂), 26.8 (CH₂), 21.2 (CH₃).

Analytical data obtained were in agreement with the reported values.³⁷

2-(2-methoxyphenyl)-1-phenylethan-1-one, **6g**

Chemical Formula: C₁₅H₁₄O₂
Molecular Weight: 226.28

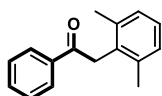
Following the general procedure, from 4-chlorotoluene (63.30 mg, 0.50 mmol) and acetophenone (60.00 mg, 0.55 mmol), the product was obtained in 98% yield (110.00 mg) as a colourless oil.

¹H NMR (400 MHz, CDCl₃): δ (ppm) = δ 8.08 (d, *J* = 7.1 Hz, 2H), 7.57 (t, *J* = 6.8 Hz, 1H), 7.48 (t, *J* = 7.7 Hz, 2H), 7.30 (t, *J* = 8.7 Hz, 1H), 7.22 (d, *J* = 8.9 Hz, 1H), 6.97 (t, *J* = 7.4 Hz, 1H), 6.92 (d, *J* = 8.2 Hz, 1H), 4.31 (s, 2H), 3.80 (s, 3H).

¹³C {¹H} NMR (100 MHz, CDCl₃): δ (ppm) = δ 198.0 (C=O), 157.2 (C_{Ar}), 137.0 (C_{Ar}), 133.0 (CH_{Ar}), 131.1 (CH_{Ar}), 128.6 (CH_{Ar}), 128.5 (CH_{Ar}), 128.4 (CH_{Ar}), 123.7 (C_{Ar}), 120.7 (CH_{Ar}), 110.6 (CH_{Ar}), 55.4 (CH₃), 40.1 (CH₂).

Analytical data obtained were in agreement with the reported values.³⁶

2-(2,6-dimethylphenyl)-1-phenylethan-1-one, **6h**



Chemical Formula: C₁₆H₁₆O
Molecular Weight: 224.30

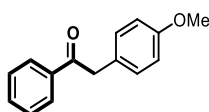
Following the general procedure, from 2-chloro-1,3-dimethylbenzene (70.00 mg, 0.50 mmol) and acetophenone (60.00 mg, 0.55 mmol), the product was obtained in 95% yield (105.00 mg) as a colourless oil.

¹H NMR (400 MHz, CDCl₃): δ (ppm) = δ 8.12 (d, *J* = 7.4 Hz, 2H), 7.64 (t, *J* = 7.0 Hz, 1H), 7.55 (t, *J* = 7.3 Hz, 2H), 7.14-7.10 (m, 3H), 4.40 (s, 2H), 2.24 (s, 6H).

¹³C {¹H} NMR (100 MHz, CDCl₃): δ (ppm) = δ 197.0 (C=O), 137.2 (C_{Ar}), 137.1 (C_{Ar}), 133.3 (CH_{Ar}), 132.5 (2 x C_{Ar}), 128.8 (2 x CH_{Ar}), 128.2 (2 x CH_{Ar}), 128.1 (CH_{Ar}), 127.0 (CH), 39.7 (CH₂), 20.5 (2 x CH₃).

Analytical data obtained were in agreement with the reported values.³⁸

2-(4-methoxyphenyl)-1-phenylethan-1-one, **6i**



Chemical Formula: C₁₅H₁₄O₂
Molecular Weight: 226.28

Following the general procedure, from 4-chloroanisole (72.00 mg, 0.50 mmol) and acetophenone (60.00 mg, 0.55 mmol), the product was obtained in 97% yield (110.00 mg) as a yellow oil.

¹H NMR (400 MHz, CDCl₃): δ (ppm) = δ 8.03-8.01 (m, 2H), 7.58 (tt, *J* = 7.2, 1.3 Hz, 1H), 7.48 (tt, *J* = 6.8, 1.3 Hz, 2H), 7.20-7.18 (m, 2H), 6.89-6.86 (m, 2H), 4.23 (s, 2H), 3.79 (s, 3H).

¹³C {¹H} NMR (100 MHz, CDCl₃): δ (ppm) = δ 198.0 (C=O), 158.6 (C_{Ar}), 136.7 (C_{Ar}), 133.2 (CH_{Ar}), 130.6 (2 x CH_{Ar}), 128.7 (CH_{Ar}), 128.7 (CH_{Ar}), 126.6 (C_{Ar}), 114.3 (CH_{Ar}), 55.3 (CH₃), 44.7 (CH₂).

Analytical data obtained were in agreement with the reported values.³⁷

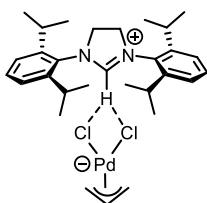
9.5. Study of different throw-away ligands of [NHC·H][Pd(L)Cl₂] complexes and their effect in the Mizoroki-Heck reaction

9.5.1. General procedure of [NHC·H][Pd(L)Cl₂]

In air, the corresponding NHC·HCl (2.00 equiv.) and [Pd(η^3 -R-allyl)(μ -Cl)]₂ (1.00 equiv.) were added to a mortar. The two solids were mixed and grinded using a pestle for 5 min. A crystalline solid was obtained in quantitative yield.

For the synthesis of *pre-catalysts* see Section 9.2 and 9.3

9.5.2 Synthesis of [SIPr·H][Pd(η^3 -allyl)Cl₂] Pd(ate)-21



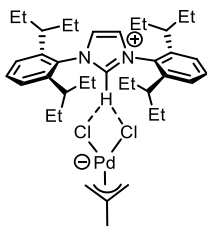
Following the general procedure from SIPr·HCl (65.70 mg, 0.15 mmol) and [Pd(η^3 -allyl)(μ -Cl)]₂ (30.00 mg, 0.07 mmol), the product was obtained as a brown powder in a 99% yield (107.00 mg).

¹H NMR (400 MHz, CDCl₃): δ (ppm) = δ 7.66 (s, 1H, C_{NCHN}), 7.47 (t, J = 7.8 Hz, 2H, CH_{Ar}), 7.28-7.25 (m, 4H, CH_{Ar}), 5.28-5.26 (m, 1H, CH_{cin}), 4.99 (s, 4H, CH_{SIPr}), 3.90 (d, J = 6.6 Hz, 2H, CH_{cin}), 3.18 (dt, J = 13.5, 6.7 Hz, 4H, CH_{IPr}), 2.82 (d, J = 12 Hz, 2H, CH_{cin}), 1.41 (d, J = 6.7 Hz, 12H, CH_{3(IPr)}), 1.22 (d, J = 6.8 Hz, 12H, CH_{3(IPr)}).

¹³C {¹H} NMR (100 MHz, CDCl₃): δ (ppm) = δ 157.0 (C_{Ar}), 146.6 (C_{Ar}), 131.5 (CH_{NCHN}), 129.5 (CH_{Ar}), 125.0 (CH_{Ar}), 109.5 (CH_{2(Imid)}), 61.0 (C_{cin}), 56.0 (CH_{2(cin)}), 29.1 (CH_(IPr)), 25.6 (CH_{3(IPr)}), 24.0 (CH_{3(IPr)}).

Elemental analysis: Expected: C 59.07, H 7.27, N 4.59. Found: C 58.77, H 7.09, N 4.59.

9.5.3. Synthesis of [IPent·H][Pd(η^3 -2-Me-allyl)Cl₂] Pd(ate)-23



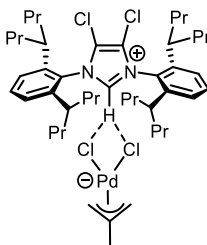
Following the general procedure from IPent·HCl (81.60 mg, 0.15 mmol) and [Pd(η^3 -2-Me-allyl)(μ -Cl)]₂ (30.00 mg, 0.07 mmol), the product was obtained as a brown powder in 99% yield (110.90 mg)

¹H NMR (400 MHz, CDCl₃): δ (ppm) = δ 8.55 (s, 2H, CH_{imid}), 8.05 (s, 1H, C_{NCHN}), 7.59 (t, J = 7.8 Hz, 2H, CH_{Ar}), 7.26-7.24 (m, 3H, CH_{Ar}), 3.71 (br.s, 2H, CH_{allyl}), 2.72 (br.s, 2H, CH_{allyl}), 2.03 (s, 3H, CH_{3(allyl)}), 1.96 (quant, J = 7.9 Hz, 4H, CH_{IPent}), 1.75-1.55 (m, 16H, CH_{2(IPent)}), 0.87 (t, J = 7.4 Hz, 12H, CH_{3(IPent)}), 0.74 (t, J = 7.3 Hz, 12H, CH_{3(IPent)}).

¹³C {¹H} NMR (100 MHz, CDCl₃): δ (ppm) = δ 142.7 (C_{Ar}), 134.4 (CH_{NCHN}), 132.9 (C_{Ar}), 132.0 (C_{Ar}), 129.6 (CH_{Ar}), 125.3 (CH_{IPent}), 60.4 (C_{cin}), 43.5 (CH_{2(cin)}), 29.5 (CH_{2(IPent)}), 28.5 (CH_{3(allyl)}), 22.9 (CH_{3(IPent)}), 12.6 (CH_{3(IPent)}), 12.4 (CH_{3(IPent)}).

Elemental analysis: Expected: C 63.80, H 8.24, N 3.82. Found: C 63.65, H 8.27, N 3.86.

9.5.4. Synthesis of [IHept^{Cl}·H][Pd(η^3 -2-Me-allyl)Cl₂] Pd(ate)-25



Following the general procedure from IHept^{Cl}·HCl (109.20 mg, 0.15 mmol) and [Pd(η^3 -2-Me-allyl)(μ -Cl)]₂ (30.00 mg, 0.07 mmol), the product was obtained as a brown powder in 99% yield (138.00 mg).

¹H NMR (400 MHz, CDCl₃): δ (ppm) = δ 11.02 (s, 1H, C_{NCHN}), 7.60 (br.s, 2H, CH_{imid}), 7.30-7.27 (m, 4H, CH_{Ar}), 7.19 (s, 1H, CH_{allyl}), 3.64 (s, 2H, CH_{allyl}), 2.66 (s, 2H, CH_{allyl}), 2.06-2.04 (m, 4H, CH_{IHept}), 2.00 (s, 3H, CH_{3(allyl)}), 1.65-1.56 (m, 16H, CH_{2(IHept)}), 1.25-1.18 (m, 16H, CH_{2(IHept)}), 0.87-0.83 (m, 24H, CH_{3(IHept)}).

¹³C {¹H} NMR (100 MHz, CDCl₃): δ (ppm) = δ 143.7 (C_{Ar}), 134.5 (C_{Ar}), 132.8 (C_{Ar}), 129.4 (CH_{NCHN}), 128.8 (CH_{Ar}), 126.2 (CH_{Ar}), 125.6 (CH_{Ar}), 122.4 (CH_{cin}), 119.8 (CH_{cin}), 60.7 (C_{imid}), 40.4 (CH_{2(IHept)}),

37.9 (CH₂(IHept)), 37.5 (CH₂(IHept)), 22.7 (CH₂(IHept)), 20.9 (CH₂(IHept)), 20.6 (CH₂(IHept)), 14.7 (CH₃(IHept)), 14.2 (CH₃(IHept)).

Elemental analysis: Expected: C 61.67, H 8.15, N 3.06. Found: C 61.48, H 8.31, N 3.17.

9.5.5 Optimisation of the Mizoroki-Heck reaction

9.5.5.1 General procedure

In an inert atmosphere, a vial was charged with the pre-catalyst, base, solvent and a magnetic stir bar and sealed with a screw cap. The corresponding alkene was added followed by the corresponding aryl bromide (0.5 mmol). The reaction was left to stir (910 rpm) for 16 h at varying temperatures.

9.5.5.2 Preliminary catalyst screening

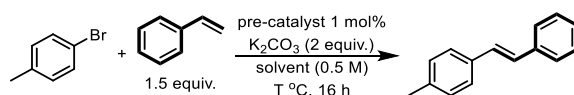
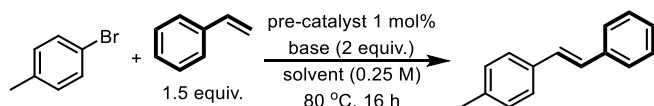


Table S-35

Catalysts (1.00 mol%)	110 °C in <i>n</i> -butanol GC conversion (%)	80 °C in <i>iso</i> -propanol GC conversion (%)
[IPr·H][Pd(η ³ -cin)Cl ₂]	traces	traces
[SIPr·H][Pd(η ³ -cin)Cl ₂]	47	60
[IPr*·H][Pd(η ³ -cin)Cl ₂]	30	40

GC conversion based on 4-bromotoluene. [Pd] and base were added in a vial containing *n*-butanol or *iso*-propanol and left to stir at the stated temperature for 1 h before starting material was added. After addition of starting material, the reaction was left to stir for 16 h at the stated temperature.

9.5.5.3 Catalyst/base/solvent screening



Pre-catalysts used:

[SIMes·H][Pd(η ³ -cin)Cl ₂]	Pd(ate)-2
[SIPr·H][Pd(η ³ -cin)Cl ₂]	Pd(ate)-3
[IPr ^{Cl} ·H][Pd(η ³ -cin)Cl ₂]	Pd(ate)-4
[IPr*·H][Pd(η ³ -cin)Cl ₂]	Pd(ate)-5
[SIPr·H][Pd(η ³ -crotyl)Cl ₂]	Pd(ate)-10
[SIPr·H][Pd(η ³ -2-Me-allyl)Cl ₂]	Pd(ate)-11
[SIPr·H][Pd(η ³ -Ind ^{tBu})Cl ₂]	Pd(ate)-12

Table S-36: Catalyst/base/solvent optimisation

Solvent	Bases	Pd(ate)-2	Pd(ate)-3	Pd(ate)-4	Pd(ate)-5
<i>n</i> -BuOH	K ₂ CO ₃	52	68	58	84
MeTHF		0	0	0	0
PhMe		0	0	28	15
<i>n</i> -BuOH	K ₃ PO ₄	64	50	28	80
MeTHF		47	0	32	0
PhMe		18	0	0	0
<i>n</i> -BuOH	KOH	57	35	26	45
MeTHF		55	65	51	73
PhMe		77	0	19	59
<i>n</i> -BuOH	KO ^t Bu	52	37	27	43
MeTHF		54	0	51	58
PhMe		0	0	55	0

Solvent	Bases	Pd(ate)-10	Pd(ate)-11	Pd(ate)-12	Pd(ate)-3 + TBAB
<i>n</i> -BuOH	K ₂ CO ₃	99	36	99	57
MeTHF		0	0	0	0
PhMe		0	0	0	0
<i>n</i> -BuOH	K ₃ PO ₄	62	63	24	20
MeTHF		17	5	56	79
PhMe		0	45	82	34
<i>n</i> -BuOH	KOH	99	99	99	29
MeTHF		80	99	56	71
PhMe		26	72	51	73
<i>n</i> -BuOH	KO ^t Bu	99	99	99	35
MeTHF		51	62	38	0
PhMe		13	48	0	0

LC yield, internal standard: 4,4-ditertbutylbiphenyl (1.00 mg). Conditions: [Pd] 1.00 mol%, Base (2.00 equiv.), solvent (0.25 M), bromotoluene (0.10 mmol), styrene (1.50 equiv.), 80 °C, 16 h.

Table S-37: Solvent/base screening

Pre-catalysts	Solvents	K ₂ CO ₃	KHCO ₃	Cs ₂ CO ₃	Na ₂ CO ₃
Pd(ate)-10	Iso-propanol	99*	80*	99*	98*
Pd(ate)-11		99*	86*	99*	83*
Pd(ate)-12		98	48*	99*	68*
Pd(ate)-10	2-Butanol	99*	88*	99	82*
Pd(ate)-11		99*	46*	99*	52
Pd(ate)-12		54*	40*	99*	47*
Pd(ate)-10	Ethanol	99*	54*	99	90*
Pd(ate)-11		82*	67*	99*	66*
Pd(ate)-12		88	49	99	37
Pd(ate)-10	2-methylbutan-2-ol	99	99*	99*	99*
Pd(ate)-11		99*	99*	99*	99*
Pd(ate)-12		99*	99*	99*	99*

Pre-catalysts	Solvents	LiOH.H ₂ O	NaOH	KOH	KOAc
Pd(ate)-10	Iso-propanol	95*	99*	99*	98*
Pd(ate)-11		96*	99	99	99*
Pd(ate)-12		86*	99	99*	62*
Pd(ate)-10	2-Butanol	97*	99*	99*	84*
Pd(ate)-11		94*	99	99	85*
Pd(ate)-12		60*	99	99	55*
Pd(ate)-10	Ethanol	99*	99*	99	74*
Pd(ate)-11		99*	99*	99	59*
Pd(ate)-12		99	99	99	71
Pd(ate)-10	2-methylbutan-2-ol	99*	99*	99	99*
Pd(ate)-11		99*	99*	99	99*
Pd(ate)-12		99*	99*	99	99*

LC yield, internal standard: 4,4-ditertbutylbiphenyl (1 mg). Conditions: [Pd] 1 mol%, Base (2. equiv.), solvent (0.25 M), bromotoluene (0.10 mmol), styrene (1.50 equiv.), 80 °C, 16 h.

9.5.5.3 Catalyst loading optimisation

The general procedure was followed using [SIPr·H][Pd(η^3 -R-allyl)Cl₂] (0.10-0.50 mol%) bromotoluene (86.00 mg, 0.50 mmol) and styrene (78.00 mg, 0.75 mmol).

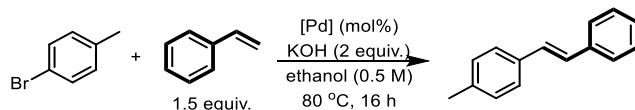


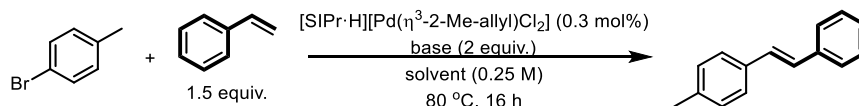
Table S-38: Catalyst loading optimisation

Entries	Catalyst	Catalyst loading (mol%)	GC Yield (%)
1	[SIPr·H][Pd(η^3 -2-Me-allyl)Cl ₂]	0.50	99
2	[SIPr·H][Pd(η^3 -crotyl)Cl ₂]	0.50	99
3	[SIPr·H][Pd(η^3 -Ind ^{tBu})Cl ₂]	0.50	86
4	[SIPr·H][Pd(η^3 -2-Me-allyl)Cl ₂]	0.30	>99
5	[SIPr·H][Pd(η^3 -crotyl)Cl ₂]	0.30	78
6	[SIPr·H][Pd(η^3 -Ind ^{tBu})Cl ₂]	0.30	99
7	[SIPr·H][Pd(η^3 -2-Me-allyl)Cl ₂]	0.10	35
8	[SIPr·H][Pd(η^3 -crotyl)Cl ₂]	0.10	45
9	[SIPr·H][Pd(η^3 -Ind ^{tBu})Cl ₂]	0.10	35

GC yield: Mesitylene 0.01mmol was used as internal standard. Value calculated from an average of two reactions.

9.5.5.4. Base and solvent optimisation

The general procedure was followed using bromotoluene (86.00 mg, 0.50 mmol) and styrene (78.00 mg, 0.75 mmol). [SIPr-H][Pd(η^3 -2-Me-allyl)Cl₂] (0.30 mol%) was used as pre-catalyst.

**Table S-39:** Base/solvent optimisation

Entry	Base (2.0 equiv.)	Solvent (0.25 M)	GC Yield (%)
1	K ₂ CO ₃	<i>iso</i> -Propanol	n.r.
2	K ₂ CO ₃	1-Butanol	n.r.
3	K ₂ CO ₃	2-Methyl-but-2-ol	18
4	NaOH	1-Butanol	>99
5	NaOH	Ethanol	74
6	KOH	1-Butanol	80
7	KOH	2-Methyl-but-2-ol	80
8	KOH	<i>iso</i> -Propanol	>99
9	Cs ₂ CO ₃	1-Butanol	90
10	Cs ₂ CO ₃	Ethanol	70
11	Cs ₂ CO ₃	2-Methyl-but-2-ol	37

GC yield: Mesitylene 0.01 mmol was used as internal standard. Value calculated from an average of two reactions.

Table S-40: Base/solvent optimisation with lowered catalyst loading

Entries	Base (2.00 equiv.)	Solvent (0.25 M)	GC yield (%)
1	Cs ₂ CO ₃	1-Butanol	83
2	KOH	<i>iso</i> -Propanol	98
3	KOH	Ethanol	60
4	NaOH	1-Butanol	85
5	CsOH	<i>iso</i> -Propanol	>99

GC yield: Mesitylene 0.01 mmol was used as internal standard. Value calculated from an average of two reactions.

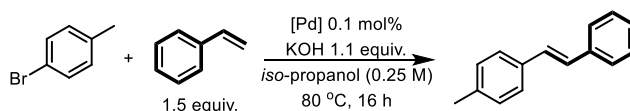
Table S-41: Base equivalent optimisation

Entries	KOH (equiv.)	GC yield (%)
1	1.50	>99
2	1.30	>99
3	1.10	97

GC yield: Mesitylene 0.01 mmol was used as internal standard. Value calculated from an average of two reactions.

9.5.5.5. Catalyst screening

The general procedure was followed using bromotoluene (86.00 mg, 0.50 mmol) and styrene (78.00 mg, 0.75 mmol). [SIPr·H][Pd(η^3 -2-Me-allyl)Cl₂] (0.60 mg, 0.10 mol%) was used as pre-catalyst.

**Table S-42:** Catalyst screening:

Entries	Catalyst 0.10 mol%	GC yield (%)
1 ^a	[SIPr·H][Pd(η^3 -crotyl)Cl ₂]	98
2	[SIPr·H][Pd(η^3 -Ind ^{tBu})Cl ₂]	88
3	[SIPr·H][Pd(η^3 -allyl)Cl ₂]	91
4 ^a	[SIPr·H][Pd(η^3 -cin)Cl ₂]	98
5	[SIPr·H][Pd(η^3 -2-Me-allyl)Cl ₂]	>99

^a Homocoupling in the GC spectrum. GC yield: Mesitylene 0.01 mmol was used as internal standard. Value calculated from an average of two reactions.

Table S-43: Catalyst screening NHC

Entries	Catalyst 0.10 mol%	GC yield (%)
1 ^a	[IPrH][Pd(η^3 -2-Me-allyl)Cl ₂]	98
2 ^a	[IPr ^{Me} H][Pd(η^3 -2-Me-allyl)Cl ₂]	98
3	[IHept ^{Cl} H][Pd(η^3 -2-Me-allyl)Cl ₂]	92
4	[IPentH][Pd(η^3 -2-Me-allyl)Cl ₂]	93
5	[IPr*H][Pd(η^3 -2-Me-allyl)Cl ₂]	>99
6	[SIPrH][Pd(η^3 -2-Me-allyl)Cl ₂]	>99

^a Homocoupling in the GC spectrum. GC yield: Mesitylene 0.01 mmol was used as internal standard. Value calculated from an average of two reactions.

9.5.5.6. Styrene equivalent optimisation

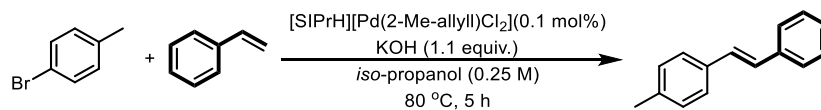


Table S-44: Styrene equivalence optimisation

Entries	Styrene (equiv.)	GC yield (%)
1	1.30	>99
2	1.20	>99
3	1.10	>99

GC yield: Mesitylene 0.01 mmol was used as internal standard. Value calculated from an average of two reactions.

9.5.5.7. Time optimisation

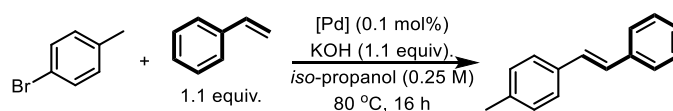


Table S-45: Time optimisation

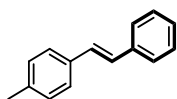
Entries	Time (h)	GC yield (%)
1	15	20
2	30	25
3	45	50
4	60	72
5	120	85
6	180	91
7	240	99
8	300	99

GC yield: Mesitylene 0.01 mmol was used as internal standard. Value calculated from an average of two reactions.

9.5.6 Scope of the Mizoroki-Heck reaction

In air, a vial was charged with [SIPr-H][Pd(η^3 -2-Me-allyl)Cl₂] (0.10 mg, 0.10 mol%), KOH (31.00 mg, 0.55 mmol) and a magnetic stir bar and sealed with a screw cap. The corresponding alkene and the corresponding aryl halide were dissolved in *iso*-propanol (0.25 M). The solution was added to the vial and the reaction was left to stir (910 rpm) for 2 h at 80 °C.

(*E*)-1-methyl-4-styrylbenzene, **7a**



Chemical Formula: C₁₅H₁₄
Molecular Weight: 194.28

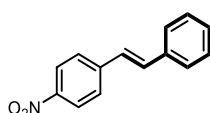
Following the general procedure, from styrene (57.00 mg, 0.55 mmol) and 4-bromotoluene (86.00 mg, 0.50 mmol) the product was obtained in 99% yield (96.40 mg) as a white solid. When 4-chlorotoluene (63.00 mg, 0.50 mmol) was used, the product was obtained in 80% yield (78.00 mg).

¹H NMR (400 MHz, CDCl₃): δ (ppm) = δ 7.55 (d, *J* = 7.2 Hz, 2H), 7.46 (d, *J* = 8.1 Hz, 2H), 7.39 (t, *J* = 7.6 Hz, 2H), 7.30 (t, *J* = 7.5 Hz, 1H), 7.21 (d, *J* = 7.9 Hz, 2H), 7.12 (d, *J* = 2.5 Hz, 2H), 2.40 (s, 3H).

¹³C {¹H} NMR (100 MHz, CDCl₃): δ (ppm) = δ 142.1 (C_{Ar}), 137.6 (C_{Ar}), 134.7 (C_{Ar}), 129.5 (2 x CH_{Ar}), 128.8 (2 x CH_{Ar}), 128.4 (2 x CH_{Ar}), 127.8 (2 x CH_{Ar}), 127.5 (CH_{Ar}), 126.6 (CH_{alkene}), 126.5 (CH_{alkene}), 21.4 (CH₃).

Analytical data obtained were in agreement with the reported values.³⁹

(*E*)-1-nitro-4-styrylbenzene, **7b**



Chemical Formula: C₁₄H₁₁NO₂
Molecular Weight: 225.25

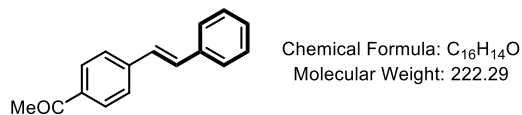
Following the general procedure, from styrene (57.00 mg, 0.55 mmol) and 1-bromo-4-nitrobenzene (101.00 mg, 0.50 mmol) the product was obtained in 98% yield (110.00 mg) as a yellow solid. When 1-chloro-4-nitrobenzene (79 mg, 0.50 mmol) was used the product was obtained in 50% yield (56.00 mg).

¹H NMR (400 MHz, CDCl₃): δ (ppm) = δ 8.24 (dt, *J* = 8.8, 2.1 Hz, 2H), 7.65 (dt, *J* = 9.4, 1.9 Hz, 2H), 7.57 (d, *J* = 7.2 Hz, 2H), 7.42 (t, *J* = 7.4 Hz, 2H), 7.36 (tt, *J* = 6.9, 1.4 Hz, 1H), 7.32-7.29 (m, 1H), 7.17 (d, *J* = 16.7 Hz, 1H).

¹³C {¹H} NMR (100 MHz, CDCl₃): δ (ppm) = δ 146.9 (C_{Ar}), 144.0 (C_{Ar}), 136.3 (C_{Ar}), 133.5 (C_{Ar}), 129.0 (CH_{Ar}), 127.2 (CH_{Ar}), 127.0 (CH_{alkene}), 126.4 (CH_{Ar}), 124.3 (CH_{Ar}).

Analytical data obtained were in agreement with the reported values.⁴⁰

(*E*)-1-(4-styrylphenyl)ethan-1-one, **7c**



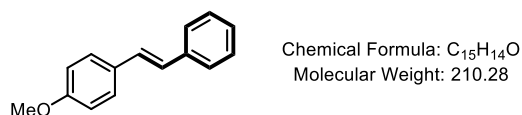
Following the general procedure, from styrene (57.00 mg, 0.55 mmol) and 4-bromoacetophenone (100.00 mg, 0.50 mmol) the product was obtained in 98% yield (110.00 mg) as a white solid. When 4-chloroaceto-phenone (77.00 mg, 0.50 mmol) was used the product was obtained in 50% yield (56.00 mg).

¹H NMR (400 MHz, CDCl₃): δ (ppm) = δ 7.96 (d, *J* = 8.4 Hz, 2H), 7.59 (d, *J* = 8.4 Hz, 2H), 7.55 (d, *J* = 7.2 Hz, 2H), 7.39 (t, *J* = 6.7 Hz, 2H), 7.32 (t, *J* = 6.7 Hz, 1H), 7.18 (dd, *J* = 16.4, 13.2 Hz, 2H), 2.61 (s, 3H).

¹³C {¹H} NMR (100 MHz, CDCl₃): δ (ppm) = δ 197.6 (C(OCH₃)), 142.1 (C_{Ar}), 136.8 (C_{Ar}), 136.1 (C_{Ar}), 131.6 (CH_{Ar}), 129.0 (CH_{Ar}), 128.9 (CH_{Ar}), 128.4 (CH_{Ar}), 127.6 (CH_{Ar}), 126.9 (CH), 126.6 (CH), 26.7 (CH₃).

Analytical data obtained were in agreement with the reported values.³⁹

(*E*)-1-methoxy-4-styrylbenzene, **7d**

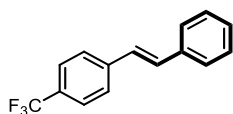


Following the general procedure, from styrene (57.00 mg, 0.55 mmol) and 4-bromanisole (94.00 mg, 0.50 mmol) the product was obtained in 95% yield (99.00 mg) as a white/yellow solid. When 4-chloroanisole (71.00 mg, 0.50 mmol) was used the product was obtained in 61% yield (64.10 mg).

¹H NMR (400 MHz, CDCl₃): δ (ppm) = δ 7.50 (d, *J* = 7.3 Hz, 2H), 7.47 (d, *J* = 8.7 Hz, 2H), 7.37 (t, *J* = 7.7 Hz, 2H), 7.25 (t, *J* = 7.4 Hz, 1H), 7.09-7.06 (m, 2H), 6.92 (d, *J* = 8.8 Hz, 2H), 3.84 (s, 3H).

¹³C {¹H} NMR (100 MHz, CDCl₃): δ (ppm) = δ 159.4 (C_{Ar}), 137.8 (C_{Ar}), 130.3 (C_{Ar}), 128.8 (CH_{Ar}), 128.3 (CH_{Ar}), 127.9 (CH_{Ar}), 127.4 (CH_{Ar}), 126.7 (CH), 126.4 (CH), 114.3 (CH_{Ar}), 55.5 (CH₃).

Analytical data obtained were in agreement with the reported values.³⁹

(E)-1-styryl-4-(trifluoromethyl)benzene, 7e

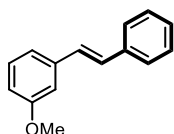
Chemical Formula: C₁₅H₁₁F₃
Molecular Weight: 248.25

Following the general procedure, from styrene (57.00 mg, 0.55 mmol) and 4-bromobenzotrifluoride (112.50 mg, 0.50 mmol) the product was obtained in 98% yield (112.50 mg) as white solid. When 4-chlorobenzotrifluoride (90.20 mg, 0.50 mmol) was used the product was obtained in 70% yield (85.70 mg).

¹H NMR (400 MHz, CDCl₃): δ (ppm) = δ 7.61 (s, 4H), 7.55 (d, *J* = 7.8 Hz, 2H), 7.41 (t, *J* = 7.4 Hz, 2H), 7.30-7.29 (m, 1H), 7.22 (dd, *J* = 16.1, 9.7 Hz, 2H).

¹³C {¹H} NMR (100 MHz, CDCl₃): δ (ppm) = δ 140.9 (CF), 136.8 (C_{Ar}), 131.3 (C_{Ar}), 128.9 (CH_{Ar}), 128.6 (CH_{Ar}), 128.4 (CH_{Ar}), 127.3 (CH_{Ar}), 126.9 (CH_{Ar}), 126.7 (CH_{Alkene}), 125.8 (CH_{Alkene}).

Analytical data obtained were in agreement with the reported values.⁴⁰

(E)-1-methoxy-3-styrylbenzene, 7f

Chemical Formula: C₁₅H₁₄O
Molecular Weight: 210.28

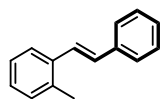
Following the general procedure, from styrene (57.00 mg, 0.55 mmol) and 4-bromoanisole (94.00 mg, 0.50 mmol) the product was obtained in 91% yield (96.00 mg) as a white solid.

When 4-chloroanisole (71.00 mg, 0.50 mmol) was used the product was obtained in 63% yield (65.70 mg).

¹H NMR (400 MHz, CDCl₃): δ (ppm) = 7.61 (d, *J* = 9.3 Hz, 2H), 7.54 (d, *J* = 7.5 Hz, 2H), 7.39-7.32 (m, 2H), 7.29-7.21 (m, 3H), 7.19-7.14 (m, 1H), 7.02 (dd, *J* = 8.6, 3.0 Hz, 1H), 3.86 (s, 3H).

¹³C {¹H} NMR (100 MHz, CDCl₃): δ (ppm) = δ 160.0 (C_{Ar}), 138.9 (C_{Ar}), 137.4 (C_{Ar}), 129.8 (CH_{Ar}), 128.8 (CH_{Ar}), 128.7 (CH_{Ar}), 127.8 (CH_{Ar}), 126.7 (CH_{Ar}), 119.4 (CH_{Ar}), 113.4 (CH_{Alkene}), 111.9 (CH_{Alkene}), 55.4 (CH₃).

Analytical data obtained were in agreement with the reported values.⁴⁰

(E)-1-methyl-2-styrylbenzene, 7g

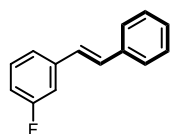
Chemical Formula: C₁₅H₁₄
Molecular Weight: 194.28

Following the general procedure, from styrene (57.00 mg, 0.55 mmol) and 2-bromotoluene (86.00 mg, 0.50 mmol) the product was obtained in 87% yield (84.60 mg) as a white solid.

¹H NMR (400 MHz, CDCl₃): δ (ppm) = δ 7.55 (d, *J* = 7.3 Hz, 1H), 7.53 (d, *J* = 7.3 Hz, 2H), 7.44-7.39 (m, 2H), 7.30 (s, 1H), 7.29-7.27 (m, 2H), 7.21-7.19 (m, 3H), 7.11 (d, *J* = 2.5 Hz, 1H), 2.43 (s, 3H).

¹³C {¹H} NMR (100 MHz, CDCl₃): δ (ppm) = δ 137.8 (C_{Ar}), 136.5 (C_{Ar}), 134.7 (C_{Ar}), 129.5 (2 x CH_{Ar}), 128.8 (2 x CH_{Ar}), 128.7 (2 x CH_{Ar}), 127.8 (2 x CH_{Ar}), 127.5 (CH_{Ar}), 126.6 (CH_{Alkene}), 126.5 (CH_{Alkene}), 21.4 (CH₃).

Analytical data obtained were in agreement with the reported values.³⁹

(E)-1-fluoro-3-styrylbenzene, 7h

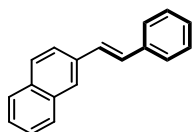
(E)-1-fluoro-3-styrylbenzene
Chemical Formula: C₁₄H₁₁F
Molecular Weight: 198.24

Following the general procedure, from styrene (57.00 mg, 0.55 mmol) and 1-bromo-3-fluorobenzene (88.00 mg, 0.50 mmol) the product was obtained in 95% yield (94.00 mg) as a white solid.

¹H NMR (400 MHz, CDCl₃): δ (ppm) = δ 7.52 (d, *J* = 7.3 Hz, 2H), 7.39 (t, *J* = 7.6 Hz, 2H), 7.32-7.28 (m, 3H), 7.23 (d, *J* = 10.2 Hz, 1H), 7.13-7.11 (m, 2H), 6.96 (t, *J* = 7.5 Hz, 1H).

¹³C {¹H} NMR (100 MHz, CDCl₃): δ (ppm) = δ 164.2 (d, *J* = 309.1 Hz, CF), 139.7 (C_{Ar}), 136.8 (C_{Ar}), 130.1 (CH_{Ar}), 128.8 (CH_{Ar}), 128.0 (CH_{Ar}), 127.5 (CH_{Ar}), 126.7 (CH_{Ar}), 122.5 (CH_{Ar}), 114.5 (CH), 112.9 (CH).

Analytical data obtained were in agreement with the reported values.⁴¹

(E)-2-styrylnaphthalene, 7i

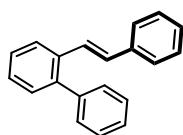
Chemical Formula: C₁₈H₁₄
Molecular Weight: 230.31

Following the general procedure, from styrene (57.00 mg, 0.55 mmol) and 2-bromonaphthalene (103.50 mg, 0.50 mmol) the product was obtained in 91% yield (104.00 mg) as a white solid.

¹H NMR (400 MHz, CDCl₃): δ (ppm) = δ 7.88-7.83 (m, 4H), 7.78 (dd, *J* = 8.6, 1.7 Hz, 1H), 7.60 (d, *J* = 7.2 Hz, 2H), 7.52-7.39 (m, 2H), 7.43 (t, *J* = 7.1 Hz, 2H), 7.33-7.28 (m, 3H), 7.25-7.23 (m, 1H).

¹³C {¹H} NMR (100 MHz, CDCl₃): δ (ppm) = δ 137.5 (C_{Ar}), 134.9 (C_{Ar}), 133.8 (C_{Ar}), 133.2 (C_{Ar}), 129.1 (2 x CH_{Ar}), 128.9 (2 x CH_{Ar}), 128.6 (2 x CH_{Ar}), 128.4 (2 x CH_{Ar}), 128.1 (CH_{Ar}), 127.7 (CH_{Ar}), 126.7 (CH_{Ar}), 126.5 (CH_{Ar}), 126.0 (CH_{Alkene}), 123.6 (CH_{Alkene}).

Analytical data obtained were in agreement with the reported values.³⁹

(E)-2-styrylbiphenyl, 7j

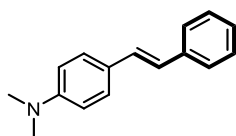
Chemical Formula: C₂₀H₁₆
Molecular Weight: 256.35

Following the general procedure, from styrene (57.00 mg, 0.55 mmol) and 2-bromobiphenyl (116.50 mg, 0.50 mmol) the product was obtained in 90% yield (115.10 mg) as a white solid.

¹H NMR (400 MHz, CDCl₃): δ (ppm) = δ 7.65-7.61 (m, 5H), 7.56 (d, *J* = 7.1 Hz, 2H), 7.48 (t, *J* = 7.9 Hz, 2H), 7.41 (t, *J* = 7.5 Hz, 2H), 7.30-7.22 (m, 2H), 7.17 (s, 2H).

¹³C {¹H} NMR (100 MHz, CDCl₃): δ (ppm) = δ 140.8 (C_{Ar}), 140.5 (C_{Ar}), 137.5 (C_{Ar}), 136.5 (C_{Ar}), 129.0 (CH_{Ar}), 128.9 (CH_{Ar}), 128.6 (CH_{Ar}), 128.6 (CH_{Ar}), 128.3 (CH_{Ar}), 128.1 (CH_{Ar}), 127.8 (CH_{Ar}), 127.5 (CH_{Ar}), 127.2 (CH_{Ar}), 127.1 (CH), 126.7 (CH).

Analytical data obtained were in agreement with the reported values.⁴²

(E)-N,N-dimethyl-4-styrylaniline, 7k

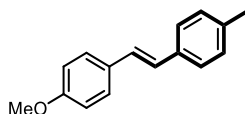
Chemical Formula: C₁₆H₁₇N
Molecular Weight: 223.32

Following the general procedure, from styrene (57.00 mg, 0.55 mmol) and 4-bromo-N,N-dimethyl-aniline (100.00 mg, 0.50 mmol) the product was obtained in 78% yield (87.30 mg) as a white solid.

¹H NMR (400 MHz, CDCl₃): δ (ppm) = δ 7.49 (d, *J* = 7.3 Hz, 2H), 7.44 (d, *J* = 8.8 Hz, 2H), 7.33 (t, *J* = 7.7 Hz, 2H), 7.21 (t, *J* = 6.8 Hz, 1H), 7.06 (d, *J* = 16.3 Hz, 1H), 6.93 (d, *J* = 16.3 Hz, 1H), 6.75 (d, *J* = 7.9 Hz, 2H), 2.99 (s, 6H).

¹³C {¹H} NMR (100 MHz, CDCl₃): δ (ppm) = δ 150.1 (C_{Ar}), 138.3 (C_{Ar}), 128.7 (C_{Ar}), 128.4 (CH_{Ar}), 127.7 (2 x CH_{Ar}), 126.8 (2 x CH_{Ar}), 126.2 (2 x CH_{Ar}), 124.6 (CH_{Ar}), 112.5 (2 x CH_{Alkene}), 40.7 (2 x CH₃).

Analytical data obtained were in agreement with the reported values.⁴³

(E)-1-methoxy-4-(4-methylstyryl)benzene, 7l

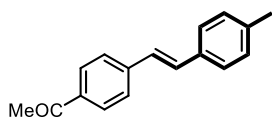
Chemical Formula: C₁₆H₁₆O
Molecular Weight: 224.30

Following the general procedure, from 4-tolylstyrene (65.00 mg, 0.55 mmol) and 4-bromanisole (94.00 mg, 0.50 mmol) the product was obtained in 98% yield (109.00 mg) as a white solid.

¹H NMR (400 MHz, CDCl₃): δ (ppm) = δ 7.45 (d, *J* = 8.7 Hz, 2H), 7.40 (d, *J* = 8.1 Hz, 2H), 7.17 (d, *J* = 7.9 Hz, 2H), 7.04 (quant, *J* = 16.3 Hz, 2H), 6.91 (d, *J* = 8.8 Hz, 2H), 3.83 (s, 3H), 2.33 (s, 3H).

¹³C {¹H} NMR (100 MHz, CDCl₃): δ (ppm) = δ 159.3 (C_{Ar}), 137.2 (C_{Ar}), 135.0 (C_{Ar}), 130.5 (C_{Ar}), 129.5 (2 x CH_{Ar}), 127.7 (2 x CH_{Ar}), 127.4 (2 x CH_{Ar}), 126.7 (2 x CH_{Ar}), 126.3 (CH_{Alkene}), 114.3 (CH_{Alkene}), 55.5 (CH₃), 21.4 (CH₃).

Analytical data obtained were in agreement with the reported values.⁴⁴

(E)-1-(4-(4-methylstyryl)phenyl)ethan-1-one, 7m

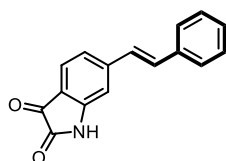
Chemical Formula: C₁₇H₁₆O
Molecular Weight: 236.31

Following the general procedure, from 4-tolylstyrene (65.00 mg, 0.55 mmol) and 4-bromoacetophenone (100.00 mg, 0.50 mmol) the product was obtained in 99% yield (117.00 mg) as a white solid.

¹H NMR (400 MHz, CDCl₃): δ (ppm) = δ 7.96 (d, *J* = 8.4 Hz, 2H), 7.58 (d, *J* = 8.3 Hz, 2H), 7.45 (d, *J* = 8.1 Hz, 2H), 2.61 (s, 3H), 2.38 (s, 3H).

¹³C {¹H} NMR (100 MHz, CDCl₃): δ (ppm) = δ 197.6 (C=O), 142.4 (C_{Ar}), 138.5 (C_{Ar}), 135.9 (C_{Ar}), 134.1 (C_{Ar}), 131.6 (CH_{Ar}), 129.7 (2 x CH_{Ar}), 129.0 (2 x CH_{Ar}), 126.9 (2 x CH), 126.6 (CH_{Alkene}), 126.5 (CH_{Alkene}), 26.7 (CH₃), 21.5 (CH₃).

Analytical data obtained were in agreement with the reported values.⁴⁰

(E)-6-styrylindoline-2,3-dione, 8a

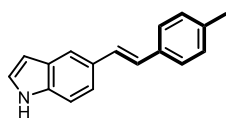
Chemical Formula: C₁₆H₁₁NO₂
Molecular Weight: 249.27

Following the general procedure, from styrene (57.00 mg, 0.55 mmol) and 6-bromoisatin (112.50 mg, 0.50 mmol) the product was obtained in 97% yield (241.00 mg) as a brown oil.

¹H NMR (400 MHz, DMSO-*d*₆): δ (ppm) = δ 7.93 (s, 1H), 7.39 (d, *J* = 8.6 Hz, 2H), 7.16 (br.s., 4H), 6.88 (s, 2H), 6.61 (d, *J* = 6.6 Hz, 3H).

¹³C {¹H} NMR (100 MHz, CDCl₃): δ (ppm) = δ 199.6 (C=O), 170.0 (C=O), 152.7 (C_{Ar}), 151.8 (C_{Ar}), 135.9 (C_{Ar}), 134.0 (C_{Ar}), 127.5 (CH_{Ar}), 126.4 (CH_{Ar}), 123.3 (CH_{Ar}), 118.3 (CH_{Ar}), 116.9 (CH_{Ar}), 116.2 (CH_{Ar}), 115.2 (CH_{Ar}), 113.0 (CH_{Ar}), 112.6 (CH_{Alkene}), 75.5 (CH_{Alkene}).

Analytical data obtained were in agreement with the reported values.⁴¹

(E)-5-styryl-1H-indole, 8b

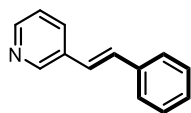
Chemical Formula: C₁₇H₁₅N
Molecular Weight: 233.31

Following the general procedure, from 4-tolylstyrene (61.00 mg, 0.55 mmol) and 4-bromoindone (98.00 mg, 0.50 mmol) the product was obtained in 92% yield (107.00 mg) as a white solid.

¹H NMR (400 MHz, CDCl₃): δ (ppm) = δ 8.11 (br.s., 1H), 7.80 (d, *J* = 9.3 Hz, 1H), 7.47-7.45 (m, 2H), 7.38 (d, *J* = 8.5 Hz, 1H), 7.31-7.26 (m, 2H), 7.21-7.19 (m, 3H), 7.11 (d, *J* = 16.3 Hz, 2H), 2.39 (s, 3H).

¹³C {¹H} NMR (100 MHz, CDCl₃): δ (ppm) = δ 136.9 (C_{Ar}), 135.6 (C_{Ar}), 135.3 (C_{Ar}), 134.5 (C_{Ar}), 129.8 (CH_{Ar}), 129.5 (CH_{Ar}), 129.2 (C_{Ar}), 128.4 (CH_{Ar}), 126.5 (CH), 126.2 (CH), 125.5 (CH_{Ar}), 124.9 (CH_{Ar}), 123.3 (CH_{Ar}), 120.8 (CH_{Ar}), 119.4 (CH_{Ar}), 113.2 (CH_{Ar}), 112.6 (CH_{Ar}), 111.4 (CH_{Ar}), 103.1 (CH_{Alkene}), 102.4 (CH_{Alkene}).

Analytical data obtained were in agreement with the reported values.⁴⁵

(E)-3-styrylpyridine, 8c

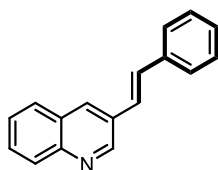
Chemical Formula: C₁₃H₁₁N
Molecular Weight: 181.24

Following the general procedure, from styrene (57.00 mg, 0.55 mmol) and 3-bromopyridine (79.00 mg, 0.50 mmol) the product was obtained in 97% yield (88.00 mg) as a white solid.

¹H NMR (400 MHz, CDCl₃): δ (ppm) = δ 8.73 (s, 1H), 8.49 (d, *J* = 5.8 Hz, 1H), 7.83 (dt, *J* = 8.0, 1.8 Hz, 1H), 7.53 (d, *J* = 7.3 Hz, 2H), 7.40 (t, *J* = 7.5 Hz, 2H), 7.31-7.26 (m, 2H), 7.18 (d, *J* = 16.4 Hz, 1H), 7.09 (d, *J* = 15.9 Hz, 1H).

¹³C {¹H} NMR (100 MHz, CDCl₃): δ (ppm) = δ 150.2 (CH_{Ar}), 148.7 (CH_{Ar}), 147.6 (CH_{Ar}), 136.8 (CH_{Ar}), 133.1 (C_{Ar}), 132.8 (CH_{Ar}), 131.0 (C_{Ar}), 128.6 (CH_{Ar}), 126.8 (CH_{Alkene}), 125.0 (CH_{Alkene}), 123.7 (CH_{Ar}), 123.7 (CH_{Ar}).

Analytical data obtained were in agreement with the reported values.³⁹

(E)-3-styrylquinoline, 8d

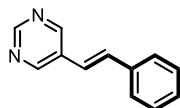
Chemical Formula: C₁₇H₁₃N
Molecular Weight: 231.30

Following the general procedure, from styrene (57.00 mg, 0.55 mmol) and 3-bromoquinoline (104.00 mg, 0.50 mmol) the product was obtained in 81% yield (94.00 mg) as a white solid.

¹H NMR (400 MHz, CDCl₃): δ (ppm) = δ 9.13 (d, *J* = 2.2 Hz, 1H), 8.18 (d, *J* = 2.1 Hz, 1H), 8.10 (d, *J* = 8.3 Hz, 1H), 7.83 (d, *J* = 6.8 Hz, 1H), 7.70 (ddd, *J* = 8.4, 6.9, 1.5 Hz, 1H), 7.59-7.53 (m, 3H), 7.43-7.30 (m, 5H), 7.22 (s, 1H).

¹³C {¹H} NMR (100 MHz, CDCl₃): δ (ppm) = δ 149.6 (C_{Ar}), 147.6 (CH_{Ar}), 136.9 (C_{Ar}), 132.4 (CH_{Ar}), 131.1 (C_{Ar}), 130.4 (CH_{Ar}), 129.4 (CH_{Ar}), 129.4 (CH_{Ar}), 129.0 (CH_{Ar}), 128.6 (CH_{Ar}), 128.4 (CH_{Ar}), 128.0 (CH_{Ar}), 127.2 (CH_{Ar}), 126.8 (CH), 125.3 (CH).

Analytical data obtained were in agreement with the reported values.⁴⁰

(E)-5-styrylpyrimidine, 8f

Chemical Formula: C₁₂H₁₀N₂
Molecular Weight: 182.23

Following the general procedure, from styrene (57.00 mg, 0.55 mmol) and 5-bromopyrimidine (80.00 mg, 0.50 mmol) the product was obtained in 88% yield (80.00 mg) as a white solid.

¹H NMR (400 MHz, CDCl₃): δ (ppm) = δ 9.07 (s, 1H), 8.60 (s, 2H), 7.35 (t, *J* = 7.5 Hz, 3H), 7.26-7.20 (m, 4H).

¹³C {¹H} NMR (100 MHz, CDCl₃): δ (ppm) = δ 156.9 (CH_{Ar}), 156.3 (2 x CH_{Ar}), 143.7 (CH_{Ar}), 139.2 (CH_{Alkene}), 129.0 (C_{Ar}), 127.6 (2 x CH_{Ar}), 127.6 (2 x CH_{Ar}), 127.1 (CH_{Ar}), 127.0 (CH_{Alkene})

Analytical data obtained were in agreement with the reported values.⁴⁵

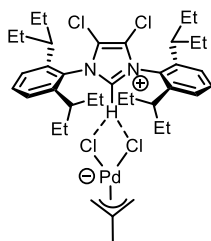
9.6 Chapter 6: Palladium catalysed C-H activation/coupling of alkynes with aryl halides

9.6.1. General procedure of [NHC·H][Pd(L)Cl₂]

In air, the corresponding NHC·HCl (2.00 equiv.) and [Pd(η³-R-allyl)(μ-Cl)]₂ (1.00 equiv.) were added to a mortar. The two solids were mixed and ground using a pestle for 5 min. A crystalline solid was obtained in quantitative yield.

For the synthesis of *palladate pre-catalysts* see Section 9.2., 9.3 and 9.4.

9.6.2. Synthesis of [IPent^{Cl}·H][Pd(η³-2-Me-allyl)Cl₂] Pd(ate)-24



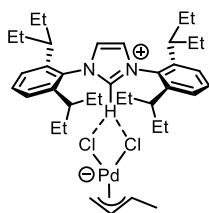
Following the general procedure from IPent^{Cl}·HCl (87.00 mg, 0.15 mmol) and [Pd(η³-2-Me-allyl)(μ-Cl)]₂ (30.00 mg, 0.07 mmol), the product was obtained as a brown powder in 99% yield (124.00 mg).

¹H NMR (400 MHz, CDCl₃): δ (ppm) = δ 11.88 (br.s, 1H, C_{NCHN}), 7.60 (t, *J* = 7.2 Hz, 2H, CH_{imid}), 7.30 (d, *J* = 7.3 Hz, 4H, CH_{Ar}), 3.70 (br.s, 2H, CH_{Ar}), 2.71 (br.s, 2H, CH_{allyl}), 2.02-2.00 (m, 8H, CH_{IPent}), 1.78 (br.s, 7H, CH_{2(IPent)}), 1.66 (t, *J* = 5.3 Hz, 8H, CH_{3(IPent)}), 0.89-0.83 (m, 24H, CH_{3(IPent)}).

¹³C {¹H} NMR (100 MHz, CDCl₃): δ (ppm) = δ 143.3 (C_{Ar}), 142.2 (C_{Ar}), 132.2 (CH_{NCHN}), 129.5 (CH_{Ar}), 126.1 (CH_{Ar}), 121.6 (CH_{allyl}), 61.1 (C_{allyl}), 43.3 (CH_{2(IPent)}), 28.2 (CH_{2(IPent)}), 27.1 (CH_{3(allyl)}), 22.8 (CH_{3(IPent)}), 12.4 (CH_{3(IPent)}), 12.0 (CH_{3(IPent)}).

Elemental analysis: Expected: C 58.33, H 7.28, N 3.49. Found: C 58.27, H 7.53, N 3.44.

9.6.3. Synthesis of [IPent·H][Pd(η^3 -crotyl)Cl₂] Pd(ate)-26



Following the general procedure from IPent·HCl (81.60 mg, 0.15mmol) and [Pd(η^3 -crotyl)(μ -Cl)]₂ (30.00 mg, 0.07 mmol), the product was obtained as a brown powder in a 99% yield (110.80 mg).

¹H NMR (400 MHz, CDCl₃): δ (ppm) = δ 8.55 (d, J = 1.6 Hz, 2H, CH_{imid}), 8.12 (d, J = 1.5 Hz, 1H, CH_{NCHN}), 7.59 (t, J = 7.8 Hz, 2H, CH_{Ar}), 7.25 (s, 2H, CH_{Ar}), 5.12 (br.s, 1H, CH_{allyl}), 3.72 (br.s, 2H, CH_{allyl}), 2.66 (br.s, 1H, CH_{allyl}), 1.94 (quant, J = 9.7 Hz, 4H, CH_{IPent}), 1.75-1.56 (m, 16H, CH_{2(IPent)}), 1.34 (d, J = 6.3 Hz, 3H, CH_{3(allyl)}), 0.87 (t, J = 7.4 Hz, 12H, CH_{3(IPent)}), 0.74 (t, J = 6.7 Hz, 12H, CH_{3(IPent)}).

¹³C {¹H} NMR (100 MHz, CDCl₃): δ (ppm) = δ 142.7 (C_{Ar}), 132.9 (CH_{NCHN}), 132.9 (C_{Ar}), 132.0 (C_{Ar}), 129.5 (CH_{allyl}), 125.3 (CH_{allyl}), 43.5 (CH_{2(IPent)}), 29.4 (CH_{2(IPent)}), 28.5 (CH_{3(allyl)}), 18.2 (CH_{3(IPent)}), 12.6 (CH_{3(IPent)}), 12.4 (CH_{3(IPent)}).

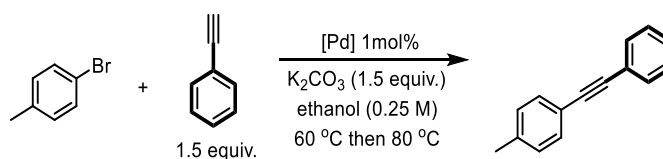
Elemental analysis: Expected: C 63.80, H 8.24, N 3.82. Found: C 63.67, H 8.36, N 3.91.

9.6.4. General procedure

In an inert atmosphere, a vial was charged with the pre-catalyst, base, solvent (0.25 M) and a magnetic stir bar and sealed with a screw cap. The reaction was left to stir for 1 h at 60 °C. Then the corresponding aryl halide (0.50 mmol) was added followed by the corresponding alkyne. The reaction was left to stir for 16 h at varying temperatures.

9.6.5. Catalyst screening

Following the general procedure, 4-bromotoluene (86.00 mg, 0.50 mmol), phenylacetylene (76.50 mg, 0.75 mmol) and K₂CO₃ (104.00 mg, 0.75 mg) in ethanol (0.25 M) were used. The reaction temperature was 80 °C.

Table S-47: Catalyst screening

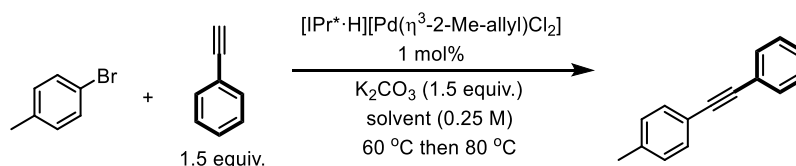
Entries	Pre-catalysts	GC yield
1	[IPr*·H][Pd(η^3 -cin)Cl ₂]	64
2	[SIPr·H][Pd(η^3 -cin)Cl ₂]	29
3	[IPent·H][Pd(η^3 -cin)Cl ₂]	30
4	[IPr·H][Pd(η^3 -crotyl)Cl ₂]	43
5	[IPr ^{Cl} ·H][Pd(η^3 -cin)Cl ₂]	42
6	[IPr·H][Pd(η^3 -Ind ^{tBu})Cl ₂]	16
7	[IPr·H][Pd(η^3 -allyl)Cl ₂]	25
8	[IPr*·H][Pd(η^3 -crotyl)Cl ₂]	87
9	[IPent ^{Cl} ·H][Pd(η^3 -cin)Cl ₂]	73
10	[IHept·H][Pd(η^3 -cin)Cl ₂]	35
11	[INon·H][Pd(η^3 -cin)Cl ₂]	32
12	[IPr* ^{OMe} ·H][Pd(η^3 -cin)Cl ₂]	53
13	[IPr*·H][Pd(η^3 -2-Me-allyl)Cl ₂]	99 (98)
14	[IPent·H][Pd(η^3 -crotyl)Cl ₂]	63
15	[IPr·H][Pd(η^3 -2-Me-allyl)Cl ₂]	90
16	[IPent ^{Cl} ·H][Pd(η^3 -2-Me-allyl)Cl ₂]	86

Average of a minimum of two runs. GC yield, mesitylene 0.1 mmol) used as internal standard. Isolated yield in parenthesis

9.6.6. Solvent and base screening

Table S-48: Solvent optimisation

Following the general procedure [IPr*·H][Pd(η^3 -2-Me-allyl)Cl₂] (5.70 mg, 1.00 mol%), 4-bromotoluene (86.00 mg, 0.50 mmol), phenylacetylene (76.50 mg, 0.75 mmol) and K_2CO_3 (104.00 mg, 0.75 mmol) in the corresponding solvent (0.25 M) was used. The reaction temperature was 80 °C.



Entries	Solvent (0.25 M)	GC yield (%)
1	EtOH/H ₂ O (1:1)	44
2	MeOH	83
3	<i>iso</i> -Propanol	31
4	<i>n</i> -Butanol	75
5	1,4-Dioxane	36
6	Toluene	27
7	CPME	15
8	2-Me-THF	n.r.
9	Cyclohexane	15

Average of a minimum of two runs. GC yield, mesitylene (0.1 mmol) used as internal standard

Table S-49: Base optimisation

Following the general procedure [IPr*·H][Pd(η^3 -2-Me-allyl)Cl₂] (5.70 mg, 1.00 mol%), 4-bromotoluene (86.00 mg, 0.50 mmol), phenylacetylene (76.50 mg, 0.75 mmol) and the corresponding base (0.75 mmol) in ethanol solvent (0.25 M) was used. The reaction temperature was 80 °C.

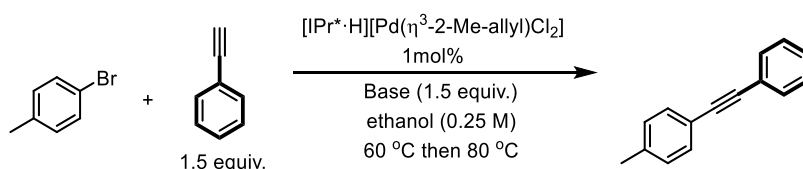


Table S-50: Base optimisation with 1 mol% catalyst loading.

Entries	Base (1.50 equiv.)	GC yield (%)
1	Cs ₂ CO ₃	66
2	Na ₂ CO ₃	47
3	KOH	99
4	NaOH	99
5	CsOH	80
6	KO ^t Bu	99
7	NaO ^t Bu	99
8	K ₃ PO ₄	99

Average of a minimum of two runs. GC yield, mesitylene (0.1 mmol) used as internal standard

Following the general procedure [IPr*·H][Pd(η^3 -2-Me-allyl)Cl₂] (2.90 mg, 0.50 mol%), 4-bromotoluene (86.00 mg, 0.50 mmol), phenylacetylene (76.50 mg, 0.75 mmol) and the corresponding base (0.75 mmol) in ethanol solvent (0.25 M) was used. The reaction temperature was 80 °C.

Table S-51: Base optimisation with 0.50 mol% catalyst loading.

Entries	Base (1.50 equiv.)	GC Yield (%)
1	K ₂ CO ₃	84
2	KOH	96
3	NaOH	99
4	KO ^t Bu	99
5	NaO ^t Bu	99
6	K ₃ PO ₄	99

Average of a minimum of two runs. GC yield, mesitylene (0.10 mmol) used as internal standard

Table S-52: Base optimisation with 0.20 mol% catalyst loading

Following the general procedure [IPr*·H][Pd(η³-2-Me-allyl)Cl₂] (1.20 mg, 0.20 mol%), 4-bromotoluene (86.00 mg, 0.50 mmol), phenylacetylene (76.50 mg, 0.75 mmol) and the corresponding base (0.75 mmol) in ethanol solvent (0.25 M) was used. The reaction temperature was 80 °C.

Entries	Base (1.50 equiv.)	GC Yield (%)
1	NaOH	99
2	KO ^t Bu	62
3	NaO ^t Bu	55
4	K ₃ PO ₄	87

Average of a minimum of two runs. GC yield, mesitylene (0.10 mmol) used as internal standard

Table S-53: Base optimisation with 0.20 mol% catalyst loading with 1.10 equiv of phenylacetylene

Following the general procedure [IPr*·H][Pd(η³-2-Me-allyl)Cl₂] (1.20 mg, 0.20 mol%), 4-bromotoluene (86.00 mg, 0.50 mmol), phenylacetylene (56.00 mg, 0.55 mmol) and the corresponding base (0.75 mmol) in ethanol solvent (0.25 M) was used. The reaction temperature was 80 °C.

Entries	Base (1.50 equiv.)	GC Yield (%)
1	KOH	87
2	NaOH	99
3	KO ^t Bu	72
4	NaO ^t Bu	99
5	K ₃ PO ₄	63
6	K ₂ CO ₃	5
7	NaOMe	99
8	Na ₂ HPO ₄	n.r.
9	NaO ^o CH ₃	n.r.
10	Na ₂ CO ₃	21
11	NaHCO ₃	n.r.

Average of a minimum of two runs. GC yield, mesitylene (0.1 mmol) used as internal standard

Table S-54: Base optimisation with 0.10 mol% catalyst loading

Following the general procedure [IPr*·H][Pd(η³-2-Me-allyl)Cl₂] (0.60 mg, 0.10 mol%), 4-bromotoluene (86.00 mg, 0.50 mmol), phenylacetylene (56.00 mg, 0.55 mmol) and the corresponding base (0.75 mmol) in ethanol solvent (0.25 M) was used. The reaction temperature was 80 °C.

Entries	Base (1.50 equiv.)	GC Yield (%)
1	NaOH	79
2	NaOtBu	82
3	NaOMe	81

Average of a minimum of two runs. GC yield, mesitylene 0.10 mmol used as internal standard

Table S-55: NaOH/solvent optimisation with 0.10 mol% catalyst loading.

Entry	Solvent (0.25 M)	GC yield (%)
1	EtOH/H ₂ O (1:1)	38
2	MeOH	46
3	<i>iso</i> -propanol	19
4	<i>n</i> -butanol	8
5	1,4-dioxane	31
6	Toluene	n.r
7	CPME	27
8	2-Me-THF	4
9	Cyclohexane	3

Average of a minimum of two runs. GC yield, mesitylene (0.10 mmol) used as internal standard

Table S-56: NaO^tBu/solvent optimisation with 0.10 mol% catalyst loading.

Entries	Solvent (0.25 M)	GC yield (%)
1	-	-
2	MeOH	27
3	<i>iso</i> -Propanol	52
4	<i>n</i> -Butanol	19
5	1,4-Dioxane	n.r.
6	Toluene	n.r.
7	CPME	19
8	2-Me-THF	31
9	Cyclohexane	10

Average of a minimum of two runs. GC yield, mesitylene (0.10 mmol) used as internal standard

Table S-57: NaOMe/solvent optimisation with 0.10 mol% catalyst loading.

Entry	Solvent (0.25 M)	GC yield (%)
1	EtOH/H ₂ O (1:1)	n.r.
2	MeOH	39
3	<i>iso</i> -Propanol	87
4	<i>n</i> -Butanol	n.r.
5	1,4-Dioxane	n.r.
6	Toluene	n.r.
7	CPME	24
8	2-Me-THF	35
9	Cyclohexane	n.r.

Average of a minimum of two runs. GC yield, mesitylene (0.10 mmol) used as internal standard

Table S-58: NaOMe equivalent optimisation

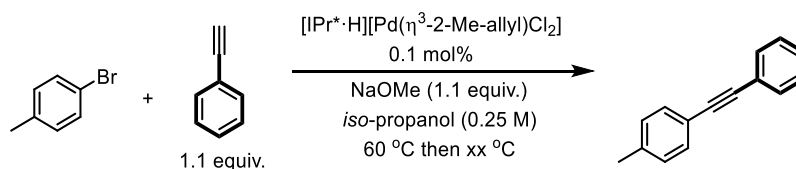
Following the general procedure [IPr*·H][Pd(η^3 -2-Me-allyl)Cl₂] (0.60 mg, 0.10 mol%), 4-bromotoluene (86.00 mg, 0.50 mmol), phenylacetylene (56.00 mg, 0.55 mmol) and NaOMe in the corresponding solvent (0.25 M) was used. The reaction temperature was 80 °C

Entry	Base equiv.	GC Yield (%)
1	1.10	99
2	1.30	99
3	1.50	84
4	2.00	83
5	2.50	25
6	3.00	45

Average of a minimum of two runs. GC yield, mesitylene (0.10 mmol) used as internal standard

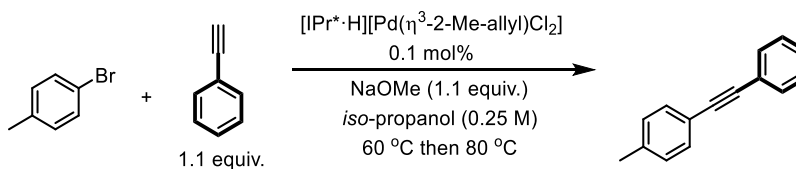
Table S-59: Reaction Temperature optimisation

Following the general procedure $[\text{IPr}^*\text{-H}][\text{Pd}(\eta^3\text{-2-Me-allyl})\text{Cl}_2]$ (0.60 mg, 0.10 mol%), 4-bromotoluene (86.00 mg, 0.50 mmol), phenylacetylene (56.00 mg, 0.55 mmol) and NaOMe (30.00 mg, 0.55 mmol) in *iso*-propanol (0.25 M) was used.



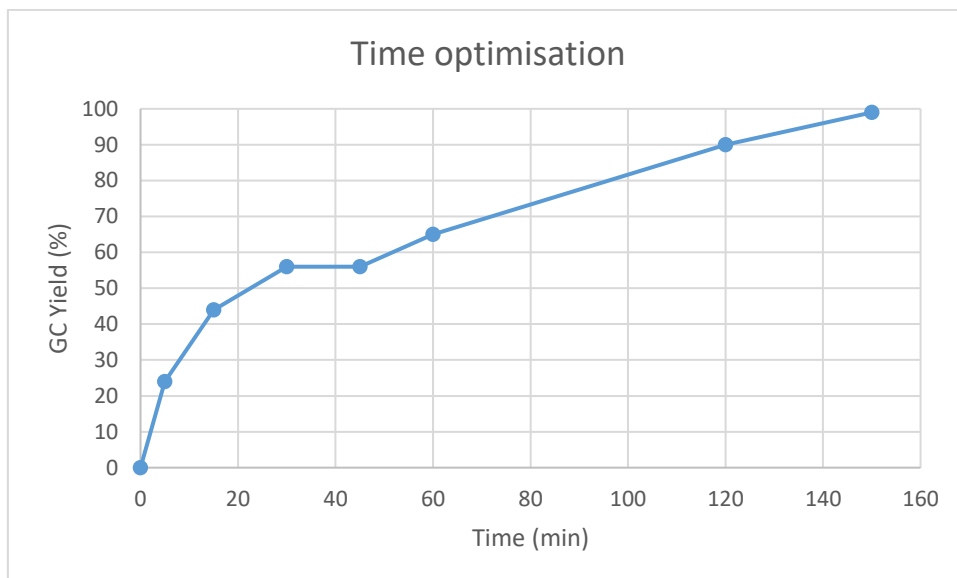
Entries	Reaction temperature (°C)	GC yield (%)
1	40	n.r
2	50	3
3	60	50
4	70	67
5	80	99

Average of a minimum of two runs. GC yield, mesitylene (0.1 mmol) used as internal standard

Table S-60: Time optimisation:

Time (min)	GC yield (%)
5	24
15	44
30	55
45	57
60	66
120	90
150	99

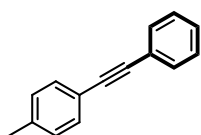
Graph S-4: Time optimisation of the Sonogashira reaction



9.6.7. Scope

Following the general procedure, under inert atmosphere, $[\text{IPr}^*\cdot\text{H}][\text{Pd}(\eta^3\text{-2-Me-allyl})\text{Cl}_2]$ (0.60 mg, 0.10 mol%), the corresponding aryl bromide (0.50 mmol), the corresponding acetylene (0.55 mmol) and NaOMe (30.00 mg, 0.55 mmol) in *iso*-propanol (0.25 M). The reaction was stirred for at 80 °C for 1.30 h.

1-methyl-4-(2-phenylethynyl)benzene, **9a**



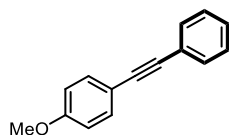
Chemical Formula: $\text{C}_{15}\text{H}_{12}$
Molecular Weight: 192.26

Following the general procedure, from 4-bromotoluene (86.00 mg, 0.50 mmol) and phenylacetylene (56.00 mg, 0.55 mmol) the product was obtained in 99% yield (94.00 mg) as a white solid.

^1H NMR (400 MHz, CDCl_3): δ (ppm) = δ 7.53 (d, J = 7.8 Hz, 2H), 7.43 (d, J = 8.0 Hz, 2H), 7.36-7.31 (m, 3H), 7.17 (d, J = 7.9 Hz, 2H), 2.37 (s, 3H).

^{13}C $\{^1\text{H}\}$ NMR (100 MHz, *d*-benzene): δ (ppm) = δ 138.5 (C_{Ar}), 131.6 (2 x CH_{Ar}), 129.3 (2 x CH_{Ar}), 128.5 (2 x CH_{Ar}), 128.2 (2 x CH_{Ar}), 123.6 (CH_{Ar}), 120.6 (C_{Ar}), 89.7 (C_{Alkyne}), 88.9 (C_{Alkyne}), 21.7 (CH_3).

Analytical data obtained were in agreement with the reported values.⁴⁶

1-methoxy-4-(phenylethynyl)benzene, **9b**

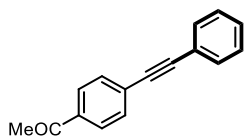
Chemical Formula: C₁₅H₁₂O
Molecular Weight: 208.26

Following the general procedure, from 4-bromoanisole (94.00 mg, 0.50 mmol) and phenylacetylene (56.00 mg, 0.55 mmol) the product was obtained in 86% yield (89.00 mg) as a white solid.

¹H NMR (400 MHz, CDCl₃): δ (ppm) = δ 7.53–7.50 (m, 2H), 7.49 (dt, *J* = 8.9, 2.2 Hz, 2H), 7.36–7.31 (m, 3H), 6.88 (d, *J* = 8.9 Hz, 2H), 3.83 (s, 3H).

¹³C {¹H} NMR (100 MHz, CDCl₃): δ (ppm) = δ 159.7 (C_{OMe}), 133.2 (C_{Ar}), 131.6 (C_{Ar}), 128.5 (C_{Ar}), 128.1 (C_{Ar}), 123.7 (C_{Ar}), 115.5 (C_{Ar}), 114.7 (C_{Ar}), 89.5 (C_{Alkyne}), 88.2 (C_{Alkyne}), 55.5 (CH₃).

Analytical data obtained were in agreement with the reported values.⁴⁶

1-(4-(phenylethynyl)phenyl)ethan-1-one, **9c**

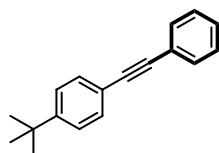
Chemical Formula: C₁₆H₁₂O
Molecular Weight: 220.27

Following the general procedure, from 4-bromoacetophenone (99.50 mg, 0.50 mmol) and phenylacetylene (56.00 mg, 0.55 mmol) the product was obtained in 92% yield (101.00 mg) as an off-white solid.

¹H NMR (400 MHz, CDCl₃): δ (ppm) = δ 7.53 (dd, *J* = 7.9, 1.6 Hz, 2H), 7.49 (d, *J* = 8.8 Hz, 2H), 7.35–7.32 (m, 3H), 6.89 (d, *J* = 8.8 Hz, 2H), 3.83 (s, 3H).

¹³C {¹H} NMR (100 MHz, CDCl₃): δ (ppm) = δ 159.7 (C_{OMe}), 133.2 (C_{Ar}), 131.6 (C_{Ar}), 128.5 (C_{Ar}), 128.1 (C_{Ar}), 123.7 (C_{Ar}), 115.8 (C_{Ar}), 114.1 (C_{Ar}), 89.5 (C_{Alkyne}), 88.2 (C_{Alkyne}), 55.5 (CH₃).

Analytical data obtained were in agreement with the reported values.⁴⁷

1-(*tert*-butyl)-4-(phenylethynyl)benzene, **9d**

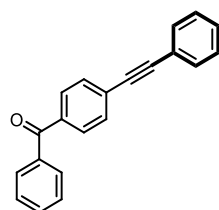
Chemical Formula: C₁₈H₁₈
Molecular Weight: 234.34

Following the general procedure, from 1-bromo-4-*tert*-butylbenzene (106.50 mg, 0.50 mmol) and phenylacetylene (56.00 mg, 0.55 mmol) the product was obtained in 89% yield (104.00 mg) as an off-white solid.

¹H NMR (400 MHz, CDCl₃): δ (ppm) = δ 7.54 (dd, *J* = 7.8, 1.8 Hz, 2H), 7.48 (d, *J* = 8.4 Hz, 2H), 7.38-7.33 (m, 5H), 1.33 (s, 9H).

¹³C {¹H} NMR (100 MHz, CDCl₃): δ (ppm) = δ 151.7 (C_{Ar}), 132.7 (CH_{Ar}), 131.7 (CH_{Ar}), 131.5 (CH_{Ar}), 129.4 (CH_{Ar}), 128.5 (CH_{Ar}), 128.2 (CH_{Ar}), 125.5 (CH_{Ar}), 125.5 (CH_{Ar}), 123.6 (C_{Ar}), 120.4 (C_{Ar}), 89.7 (C_{Alkyne}), 88.8 (C_{Alkyne}), 34.9 (C(CH₃)₃), 31.3 (CH₃).

Analytical data obtained were in agreement with the reported values.⁴⁸

Phenyl(4-(phenylethynyl)phenyl)methanone, **9f**

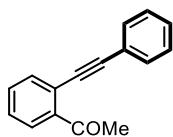
Chemical Formula: C₂₁H₁₄O
Molecular Weight: 282.34

Following the general procedure, from 4-bromobenzophenone (130.50 mg, 0.50 mmol) and phenylacetylene (56.00 mg, 0.55 mmol) the product was obtained in 90% yield (127.00 mg) as a light yellow solid.

¹H NMR (400 MHz, CDCl₃): δ (ppm) = δ 7.83 (d, *J* = 8.2 Hz, 1H), 7.61 (t, *J* = 7.4 Hz, 1H), 7.52 (t, *J* = 7.7 Hz, 1H), 7.40 (d, *J* = 7.5 Hz, 4H), 7.35 (t, *J* = 7.6 Hz, 4H), 7.29-7.26 (m, 3H).

¹³C {¹H} NMR (100 MHz, CDCl₃): δ (ppm) = δ 196.9 (C=O), 143.9 (C_{Ar}), 137.7 (C_{Ar}), 132.6 (2 x CH_{Ar}), 132.6 (2 x CH_{Ar}), 130.2 (2 x CH_{Ar}), 130.2 (CH_{Ar}), 128.6 (2 x CH_{Ar}), 128.6 (CH_{Ar}), 128.4 (2 x CH_{Ar}), 128.3 (2 x CH_{Ar}), 127.7 (C_{Ar}), 126.7 (C_{Ar}), 76.4 (2 x C_{alkyne}).

Analytical data obtained were in agreement with the reported values.⁴⁹

1-(2-(phenylethynyl)phenyl)ethan-1-one, **9e**

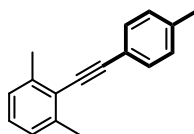
Chemical Formula: C₁₆H₁₂O
Molecular Weight: 220.27

Following the general procedure, from 2-bromoacetophenone (99.50 mg, 0.50 mmol) and phenylacetylene (56.00 mg, 0.55 mmol) the product was obtained in 92% yield (100.50 mg) as a light yellow solid.

¹H NMR (400 MHz, CDCl₃): δ (ppm) = δ 7.62-7.59 (m, 2H), 7.52 (d, *J* = 8.0 Hz, 2H), 7.47 (d, *J* = 7.1 Hz, 2H), 7.39-7.30 (m, 3H).

¹³C {¹H} NMR (100 MHz, CDCl₃): δ (ppm) = δ 201.6 (C_{COMe}), 134.0 (C_{Ar}), 132.8 (C_{Ar}), 131.9 (2 x CH_{Ar}), 129.1 (2 x CH_{Ar}), 128.9 (2 x CH_{Ar}), 128.5 (CH_{Ar}), 128.0 (CH_{Ar}), 127.6 (CH_{Ar}), 126.8 (C_{Ar}), 119.1 (C_{Alkyne}), 69.3 (C_{Alkyne}), 30.5 (CH₃).

Analytical data obtained were in agreement with the reported values.⁵⁰

1,3-dimethyl-2-(*p*-tolylethynyl)benzene, **9h**

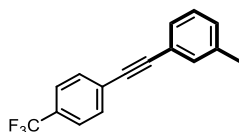
Chemical Formula: C₁₇H₁₆
Molecular Weight: 220.32

Following the general procedure, from 2-bromo-1,3-dimethylbenzene (92.50 mg, 0.50 mmol) and 4-tolylacetylene (64.00 mg, 0.55 mmol) the product was obtained in 88% yield (97.00 mg) as a white solid.

¹H NMR (400 MHz, CDCl₃): δ (ppm) = δ 7.46 (d, *J* = 7.9 Hz, 2H), 7.18 (d, *J* = 7.8 Hz, 2H), 7.13-7.07 (m, 3H), 2.52 (s, 6H), 2.39 (s, 3H).

¹³C {¹H} NMR (100 MHz, CDCl₃): δ (ppm) = δ 140.3 (C_{Ar}), 138.4 (2 x C_{Ar}), 131.4 (2 x CH_{Ar}), 129.3 (2 x CH_{Ar}), 127.7 (CH_{Ar}), 126.8 (2 x CH_{Ar}), 123.3 (C_{Ar}), 120.9 (C_{Ar}), 98.2 (C_{alkyne}), 86.6 (C_{alkyne}), 21.7 (CH₃), 21.3 (CH₃).

Analytical data obtained were in agreement with the reported values.⁵¹

1-methyl-3-((4-(trifluoromethyl)phenyl)ethynyl)benzene, **9i**

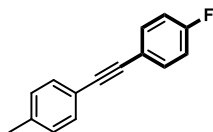
Chemical Formula: C₁₆H₁₁F₃
Molecular Weight: 260.26

Following the general procedure, from 1-bromo-4-(trifluoromethyl)benzene (112.50 mg, 0.50 mmol) and 3-tolylacetylene (64.00 mg, 0.55 mmol) the product was obtained in 71% yield (92.00 mg) as a white solid.

¹H NMR (400 MHz, CDCl₃): δ (ppm) = δ 7.64-7.59 (m, 4H), 7.39-7.35 (m, 2H), 7.28-7.25 (m, 1H), 7.19 (d, *J* = 7.6 Hz, 1H), 2.37 (s, 3H).

¹³C {¹H} NMR (100 MHz, CDCl₃): δ (ppm) = δ 138.3 (C_{Ar}), 132.4 (d, *J* = 66.3 Hz, CF₃), 131.9 (C_{Ar}), 129.9 (2 x CH_{Ar}), 129.0 (2 x CH_{Ar}), 128.5 (CH_{Ar}), 127.4 (CH_{Ar}), 125.4 (CH_{Ar}), 123.0 (CH_{Ar}), 122.5 (C_{Ar}), 92.1 (C_{Alkyne}), 87.8 (C_{Alkyne}), 21.4 (CH₃).

Analytical data obtained were in agreement with the reported values.⁵²

1-fluoro-4-(*p*-tolylethynyl)benzene, **9j**

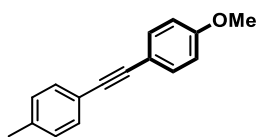
Chemical Formula: C₁₅H₁₁F
Molecular Weight: 210.25

Following the general procedure, from 4-bromotoluene (86.00 mg, 0.50 mmol) and 4-fluorophenyl-acetylene (64.00 mg, 0.55 mmol) the product was obtained in 65% yield (69.00 mg) as a white solid.

¹H NMR (400 MHz, CDCl₃): δ (ppm) = δ 7.51 (dd, *J* = 8.8, 5.4 Hz, 2H), 7.42 (d, *J* = 8.1 Hz, 2H), 7.17 (d, *J* = 7.9 Hz, 2H), 7.05 (t, *J* = 8.7 Hz, 2H), 2.37 (s, 3H).

¹³C {¹H} NMR (100 MHz, CDCl₃): δ (ppm) = δ 163.5-161.5 (d, *J* = 248.8 Hz, CF), 140.2 (C_{Ar}), 138.6 (CH_{Ar}), 133.6 (CH_{Ar}), 131.6 (CH_{Ar}), 129.3 (CH_{Ar}), 128.1 (CH_{Ar}), 128.0 (CH_{Ar}), 120.1 (CH_{Ar}), 116.0 (C_{Ar}), 115.9 (CH_{Ar}), 115.7 (C_{Ar}), 89.3 (C_{alkyne}), 87.8 (C_{alkyne}), 21.7 (CH₃).

Analytical data obtained were in agreement with the reported values.⁴⁶

1-methoxy-4-(*p*-tolylethynyl)benzene, **9k**

Chemical Formula: C₁₆H₁₄O
Molecular Weight: 222.29

Following the general procedure, from 4-bromotoluene (86.00 mg, 0.50 mmol) and 4-methoxyphenylacetylene (73.00 mg, 0.55 mmol) the product was obtained in 60% yield (67.00 mg) as a white solid.

¹H NMR (400 MHz, CDCl₃): δ (ppm) = δ 7.47 (d, *J* = 8.9 Hz, 2H), 7.41 (d, *J* = 8.1 Hz, 2H), 7.15 (d, *J* = 7.9 Hz, 2H), 6.88 (d, *J* = 8.9 Hz, 2H), 3.83 (s, 3H), 2.36 (s, 3H).

¹³C {¹H} NMR (100 MHz, CDCl₃): δ (ppm) = δ 159.6 (C_{Ar}), 138.2 (C_{Ar}), 133.1 (2 x CH_{Ar}), 131.5 (2 x CH_{Ar}), 129.2 (2 x CH_{Ar}), 120.6 (C_{Ar}), 115.7 (2 x CH_{Ar}), 114.1 (C_{Ar}), 88.8 (C_{Alkyne}), 88.3 (C_{Alkyne}), 55.4 (CH₃), 21.6 (CH₃). Analytical data obtained were in agreement with the reported values.⁵¹

9.6.8. Catalytic dimerization of terminal alkynes

9.6.8.1 General procedure

In air, a vial was charged with [IPr*·H][Pd(η³-2-Me-allyl)Cl₂] (0.60 mg, 0.10 mol%), NaOMe, *iso*-propanol (0.5 M) and a magnetic stir bar and sealed with a screw cap. The reaction was left to stir at 60 °C for 1 h. Then the corresponding alkyne was added. The reaction was left to stir at 80 °C for 16 h.

9.6.8.2 Preliminary results

Following the general procedure, from phenylacetylene (51.00 mg, 0.50 mmol), the following yields were obtained.

Table S-61: Preliminary results

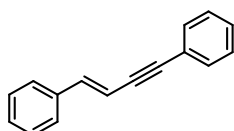
Entries	NaOMe (mmol)	GC conversion (%)
1	0.75	99
2	0.50	99
3	0.06	99

An average of a minimum of two runs.

9.6.8.3 Scope

In air, a vial was charged with [IPr*·H][Pd(η^3 -2-Me-allyl)Cl₂] (0.60 mg, 0.10 mol%), NaOMe (1 mg, 0.06 mmol), *iso*-propanol (0.5 M) and a magnetic stir bar and sealed with a screw cap. The reaction was left to stir at 60 °C for 1 h. Then the corresponding alkyne was added. The reaction was left to stir at 80 °C for 1 h.

(*E*)-but-1-en-3-yne-1,4-diyl dibenzene, **10a**



Chemical Formula: C₁₆H₁₂
Molecular Weight: 204.27

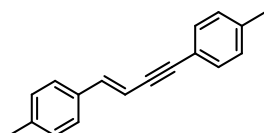
Following the general procedure, from phenylacetylene (51.00 mg, 0.50 mmol), the product was obtained in 99% yield (51.00 mg) as a white solid.

¹H NMR (400 MHz, CDCl₃): δ (ppm) = δ 7.51-7.48 (m, 2H), 7.42-7.38 (m, 2H), 7.38-7.29 (m, 6H), 7.09 (d, *J* = 16.2 Hz, 1H), 6.43 (d, *J* = 16.2 Hz, 1H).

¹³C {¹H} NMR (100 MHz, d-benzene): δ (ppm) = δ 141.4 (CH_{Alkene}), 136.5 (C_{Ar}), 131.7 (2 x CH_{Ar}), 128.9 (CH_{Ar}), 128.8 (2 x CH_{Ar}), 128.5 (CH_{Ar}), 128.3 (2 x CH_{Ar}), 126.5 (CH_{Ar}), 123.6 (C_{Ar}), 108.3 (CH_{Alkene}), 91.9 (C_{Alkyne}), 89.0 (C_{Alkyne}).

Analytical data obtained were in agreement with the reported values.⁵³

(*E*)-4,4'-(but-1-en-3-yne-1,4-diyl)bis(methylbenzene), **10b**



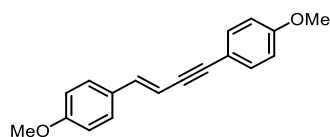
Chemical Formula: C₁₈H₁₆
Molecular Weight: 232.33

Following the general procedure, from 4-tolylacetylene (58.00 mg, 0.50 mmol), the product was obtained in 99% yield (58.00 mg) as a white solid.

¹H NMR (400 MHz, CDCl₃): δ (ppm) = δ 7.37 (d, *J* = 8.1 Hz, 2H), 7.33 (d, *J* = 8.1 Hz, 2H), 7.16 (t, *J* = 7.7 Hz, 4H), 7.10 (d, *J* = 16.2 Hz, 1H), 6.35 (d, *J* = 16.2 Hz, 1H), 2.36 (s, 6H).

¹³C {¹H} NMR (100 MHz, CDCl₃): δ (ppm) = δ 141.0 (CH_{Alkene}), 138.8 (C_{Ar}), 138.4 (C_{Ar}), 133.8 (2 x CH_{Ar}), 131.5 (2 x CH_{Ar}), 129.6 (2 x CH_{Ar}), 129.3 (CH_{Ar}), 126.3 (CH_{Ar}), 120.5 (C_{Ar}), 107.3 (CH_{Alkene}), 91.7 (C_{Alkyne}), 88.6 (C_{Alkyne}), 21.7 (CH₃), 21.5 (CH₃).

Analytical data obtained were in agreement with the reported values.⁵³

(E)-4,4'-(but-1-en-3-yne-1,4-diyl)bis(methoxybenzene), 10c

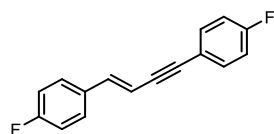
Chemical Formula: C₁₈H₁₆O₂
Molecular Weight: 264.32

Following the general procedure, from 4-methoxyphenylacetylene (66.00 mg, 0.50 mmol), the product was obtained in 98% yield (65.00 mg) as a white solid.

¹H NMR (400 MHz, CDCl₃): δ (ppm) = δ 7.47 (d, *J* = 8.9 Hz, 1H), 7.42 (d, *J* = 9.1 Hz, 2H), 7.37 (d, *J* = 8.7 Hz, 1H), 6.96 (d, *J* = 16.2 Hz, 1H), 6.88 (t, *J* = 9.2 Hz, 4H), 6.26 (d, *J* = 16.2 Hz, 1H), 3.82 (s, 6H).

¹³C {¹H} NMR (100 MHz, CDCl₃): δ (ppm) = δ 160.3 (C_{Ar}), 160.1 (C_{Ar}), 159.6 (CH_{Alkene}), 140.2 (CH_{Ar}), 134.2 (CH_{Ar}), 133.0 (CH_{Ar}), 129.5 (C_{Ar}), 127.7 (CH_{Ar}), 115.8 (CH_{Ar}), 114.3 (CH_{Ar}), 114.1 (CH_{Ar}), 106.1 (CH_{Alkene}), 91.2 (C_{Alkyne}), 88.4 (C_{Alkyne}), 55.5 (CH₃), 55.4 (CH₃).

Analytical data obtained were in agreement with the reported values.⁵³

(E)-4,4'-(but-1-en-3-yne-1,4-diyl)bis(fluorobenzene), 10d

Chemical Formula: C₁₆H₁₀F₂
Molecular Weight: 240.25

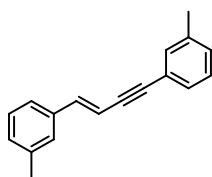
Following the general procedure, from 4-fluorophenylacetylene (60.00 mg, 0.50 mmol), the product was obtained in 98% yield (58.00 mg) as a white solid.

¹H NMR (400 MHz, CDCl₃): δ (ppm) = δ 7.46 (dd, *J* = 8.7, 5.4 Hz, 2H), 7.41 (dd, *J* = 8.7, 5.4 Hz, 2H), 7.06-6.98 (m, 5H), 6.29 (d, *J* = 16.2 Hz, 1H).

¹³C {¹H} NMR (100 MHz, CDCl₃): δ (ppm) = δ 164.1 (d, *J* = 61.5 Hz, CF), 162.1 (d, *J* = 62.3 Hz, CF), 140.2 (CH_{Ar}), 133.5 (C_{Ar}), 132.6 (CH_{Ar}), 128.1 (CH_{Ar}), 128.0 (CH_{Ar}), 116.0 (CH_{Ar}), 115.9 (CH_{Ar}), 115.8 (CH_{Ar}), 115.7 (CH_{Alkene}), 107.8 (CH_{Alkene}), 90.7 (C_{Alkyne}), 88.5 (C_{Alkyne}).

Analytical data obtained were in agreement with the reported values.⁵⁴

(E)-3,3'-(but-1-en-3-yne-1,4-diyl)bis(methylbenzene), 10e



Chemical Formula: C₁₈H₁₆
Molecular Weight: 232.33

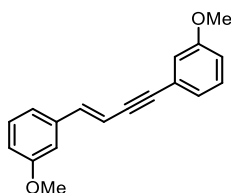
Following the general procedure, from 3-tolylacetylene (58.00 mg, 0.50 mmol), the product was obtained in 99% yield (57.00 mg) as a white solid.

¹H NMR (400 MHz, CDCl₃): δ (ppm) = δ 7.34-7.31 (m, 2H), 7.27-7.23 (m, 4H), 7.17-7.13 (m, 2H), 7.05 (d, *J* = 16.2 Hz, 1H), 6.42 (d, *J* = 16.2 Hz, 1H), 2.39 (d, *J* = 9.3 Hz, 6H).

¹³C {¹H} NMR (100 MHz, CDCl₃): δ (ppm) = δ 141.4 (CH_{Alkene}), 138.5 (C_{Ar}), 138.1 (C_{Ar}), 136.4 (C_{Ar}), 132.2 (CH_{Ar}), 129.6 (CH_{Ar}), 129.2 (CH_{Ar}), 128.7 (CH_{Ar}), 128.4 (CH_{Ar}), 127.1 (CH_{Ar}), 123.6 (C_{Ar}), 123.4 (C_{Ar}), 108.1 (CH_{Alkene}), 91.9 (C_{Alkyne}), 88.8 (C_{Alkyne}), 21.5 (CH₃), 21.4 (CH₃).

Analytical data obtained were in agreement with the reported values.⁵⁴

(*E*)-3,3'-(but-1-en-3-yne-1,4-diyl)bis(methoxybenzene), **10f**



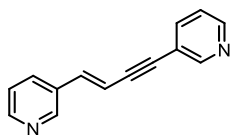
Chemical Formula: C₁₈H₁₆O₂
Molecular Weight: 264.32

Following the general procedure, from 3-methoxyphenylacetylene (73.00 mg, 0.50 mmol), the product was obtained in 97% yield (72.00 mg) as a white solid.

¹H NMR (400 MHz, CDCl₃): δ (ppm) = δ 7.28-7.22 (m, 3H), 7.08 (d, *J* = 7.6 Hz, 1H), 7.04-7.00 (m, 2H), 6.95 (br.s, 1H), 6.89 (ddd, *J* = 13.7, 8.2, 2.4 Hz, 2H), 6.39 (d, *J* = 16.2 Hz, 1H), 3.83 (s, 3H), 3.82 (s, 3H).

¹³C {¹H} NMR (100 MHz, CDCl₃): δ (ppm) = δ 160.0 (C_{Ar}), 159.5 (C_{Ar}), 141.4 (CH_{Alkene}), 137.8 (C_{Ar}), 129.9 (CH_{Ar}), 129.6 (CH_{Ar}), 129.6 (CH_{Ar}), 124.5 (CH_{Ar}), 124.3 (C_{Ar}), 119.2 (CH_{Ar}), 116.3 (CH_{Ar}), 115.1 (CH_{Ar}), 114.4 (CH_{Ar}), 111.7 (CH_{Ar}), 108.5 (CH_{Alkene}), 92.0 (C_{Alkyne}), 88.8 (C_{Alkyne}), 55.4 (CH₃).

Analytical data obtained were in agreement with the reported values.⁵⁵

(E)-3,3'-(but-1-en-3-yne-1,4-diyl)dipyridine, 10g

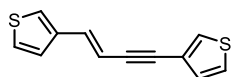
Chemical Formula: C₁₄H₁₀N₂
Molecular Weight: 206.25

Following the general procedure, from 3-ethynylpyridine (52.00 mg, 0.5 mmol), the product was obtained in 98% yield (50.00 mg) as a white solid.

¹H NMR (400 MHz, CDCl₃): δ (ppm) = δ 8.72 (dd, *J* = 2.1, 0.8 Hz, 1H), 8.66 (d, *J* = 2.2 Hz, 1H), 8.54 (ddd, *J* = 4.7, 3.1, 1.6 Hz, 2H), 7.78-7.74 (m, 2H), 7.32-7.28 (m, 2H), 7.09 (d, *J* = 16.3 Hz, 1H), 6.48 (d, *J* = 16.3 Hz, 1H).

¹³C {¹H} NMR (100 MHz, CDCl₃): δ (ppm) = δ 152.4 (CH_{Ar}), 150.0 (CH_{Ar}), 148.9 (CH_{Ar}), 148.5 (CH_{Ar}), 138.7 (CH_{Alkene}), 138.5 (CH_{Ar}), 138.5 (CH_{Ar}), 132.7 (C_{Ar}), 132.7 (CH_{Ar}), 123.8 (C_{Ar}), 123.2 (C_{Ar}), 109.9 (CH_{Alkene}), 91.5 (C_{Alkyne}), 89.4 (C_{Alkyne}).

Analytical data obtained were in agreement with the reported values.⁵³

(E)-3,3'-(but-1-en-3-yne-1,4-diyl)dithiophene, 10h

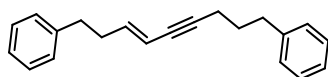
Chemical Formula: C₁₂H₈S₂
Molecular Weight: 216.32

Following the general procedure, from 3-ethynylthiophene (52.00 mg, 0.50 mmol), the product was obtained in 98% yield (50.00 mg) as a white solid.

¹H NMR (400 MHz, CDCl₃): δ (ppm) = δ 7.46 (dd, *J* = 3.0, 1.1 Hz, 1H), 7.32-7.24 (m, 4H), 7.15 (dd, *J* = 5.0, 1.2 Hz, 1H), 7.04 (d, *J* = 16.4 Hz, 1H), 6.21 (d, *J* = 16.1 Hz, 1H).

¹³C {¹H} NMR (100 MHz, CDCl₃): δ (ppm) = δ 139.4 (C_{Ar}), 135.2 (CH_{Ar}), 129.9 (CH_{Alkene}), 128.5 (CH_{Ar}), 126.7 (CH_{Ar}), 125.5 (CH_{Ar}), 124.5 (CH_{Ar}), 123.7 (CH_{Ar}), 122.6 (CH_{Alkene}), 107.9 (C_{Ar}), 88.4 (C_{Alkyne}), 86.9 (C_{Alkyne}).

Analytical data obtained were in agreement with the reported values.⁵³

(E)-non-3-en-5-yne-1,9-diyl dibenzene, 10i

Chemical Formula: C₂₁H₂₂
Molecular Weight: 274.41

Following the general procedure, from 4-phenyl-1-butyne (65.00 mg, 0.50 mmol) the product was obtained in 98% yield (50.00 mg) as a white solid.

¹H NMR (400 MHz, CDCl₃): δ (ppm) = δ 7.32-7.18 (m, 10H), 6.13-6.04 (m, 1H), 5.49 (d, *J* = 16.2 Hz, 1H), 2.87 (t, *J* = 7.5 Hz, 2H), 2.72 (t, *J* = 7.5 Hz, 2H), 2.60 (td, *J* = 7.6, 1.7 Hz, 2H), 2.41 (dd, *J* = 14.9, 7.5 Hz, 2H).

¹³C {¹H} NMR (100 MHz, CDCl₃): δ (ppm) = δ 142.5 (CH_{Alkene}), 141.5 (C_{Ar}), 140.9 (C_{Ar}), 128.6 (2 x CH_{Ar}), 128.5 (2 x CH_{Ar}), 126.4 (2 x CH_{Ar}), 126.1 (2 x CH_{Ar}), 110.5 (CH_{Alkene}), 88.4 (C_{Alkyne}), 79.8 (C_{Alkyne}), 35.4 (CH₂), 35.4 (CH₂), 34.9 (CH₂), 21.8 (CH₂), 20.7 (CH₂).

Analytical data obtained were in agreement with the reported values.⁵⁶

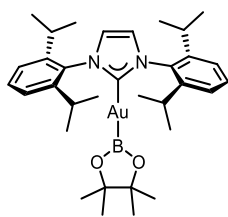
9.7 Chapter 7: Synthesis and application of [Au(NHC)(Bpin)] complexes

9.7.1. Synthesis of [Au(NHC)(Bpin)] complexes.

9.7.1.1 General procedure

A vial was charged with the corresponding [Au(OH)(NHC)] complex and anhydrous methanol (0.16 M) was added. The solvent was evaporated off under reduced pressure and 50 °C. This was repeated 5 times. The vial was taken into the glovebox, where the vial was charged with a stirring bar, bis(pinacolato)diboron (B₂pin₂) (1.10 equiv.) and benzene (0.16 M). The reaction mixture was stirred for 20 h. Work up: In the glovebox the solvent was removed under reduced pressure. The solid was washed with cold hexane. [Au(NHC)(Bpin)] was obtained as a white solid.

9.7.1.2 [Au(IPr)(Bpin)]



Following the general procedure [Au(OH)(IPr)] (300.00 mg, 0.49 mmol) was dissolved in anhydrous methanol (3.00 mL). B₂pin₂ (138.80 mg, 0.55 mmol) and benzene (3.00 mL) was charged into the vial. [Au(IPr)(Bpin)] was obtained as a white crystalline solid in 84% yield (302.00 mg).

¹H NMR (400 MHz, benzene-d₆): δ (ppm) = δ 7.12-7.10 (m, 2H, CH_{Ar}), 7.04-7.02 (m, 4H, CH_{Ar}), 6.27 (s, 2H, CH_{Imid}), 2.67 (sep, *J* = 6.8 Hz, 4H, CH_{IPr}), 1.53 (d, *J* = 7.5 Hz, 12 H, CH_{3(IPr)}), 1.08 (d, *J* = 6.1 Hz, 12 H, CH_{3(IPr)}), 0.98 (s, 12H, CH_{3(Bpin)}).

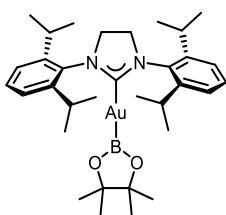
^{13}C $\{^1\text{H}\}$ NMR (100 MHz, benzene- d_6): δ (ppm) = δ 216.7 ($\text{C}_{\text{carbene}}$), 145.8 (C_{Ar}), 135.0 (C_{Ar}), 130.4 (C_{Ar}), 124.1 (C_{Ar}), 122.6 ($\text{C}_{\text{imid.}}$), 79.8 (C_{Bpin}), 29.0 ($\text{CH}_3(\text{Bpin})$), 25.8 ($\text{CH}_3(\text{Bpin})$), 25.1 ($\text{CH}_3(\text{Bpin})$), 24.8 ($\text{CH}_3(\text{IPr})$), 23.9 ($\text{CH}_3(\text{IPr})$).

^{11}B NMR (400 MHz, benzene- d_6): δ (ppm) 49.87.

Elemental analysis: Expected: C 55.55, H 6.92, N 3.93. Found: C 55.62, H 6.85, N 3.82.

ν_{max} (thin film) = 2960 (C-H_{alkane} stretching), 1458 (C-H_{alkane} bending), 1363 (C=C_{aromatic} bending), 1128 (C-O stretching).

9.7.1.3 [Au(SIPr)(Bpin)]



Following the general procedure [Au(OH)(SIPr)] (100.00 mg, 0.16 mmol) was dissolved in anhydrous methanol (1.00 mL). B₂pin₂ (46.10 mg, 0.18 mmol) and benzene (3.00 mL) was charged into the vial. [Au(SIPr)(Bpin)] was obtained as a white crystalline solid in 65% yield (77.00 mg).

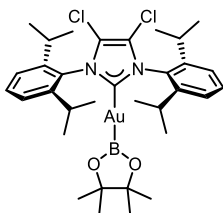
^1H NMR (400 MHz, benzene- d_6): δ (ppm) = δ 7.10 – 7.01 (m, 6H, CH_{Ar}), 3.11 (s, 4H, $\text{CH}_2(\text{imid.})$), 3.04 (sep, J = 6.8 Hz, 4H, $\text{CH}_{(\text{SIPr})}$), 1.65 (d, J = 7.2 Hz, 12H, $\text{CH}_3(\text{SIPr})$), 1.20 (d, J = 8.1 Hz, 12H, $\text{CH}_3(\text{SIPr})$), 0.95 (s, 12H, $\text{CH}_3(\text{Bpin})$).

^{13}C $\{^1\text{H}\}$ NMR (100 MHz, benzene- d_6): δ (ppm) = δ 146.8 (C_{Ar}), 135.1 (C_{Ar}), 129.7 (C_{Ar}), 128.6 (CH_{Ar}), 124.4 (CH_{Ar}), 79.7 (C_{Bpin}), 53.9 (C_{Bpin}), 29.2 ($\text{CH}_3(\text{Bpin})$), 25.7 ($\text{CH}_3(\text{Bpin})$), 25.7 ($\text{CH}_3(\text{IPr})$), 24.1 ($\text{CH}_3(\text{IPr})$).

^{11}B NMR (400 MHz, benzene- d_6): δ (ppm): 49.16.

Elemental analysis: Expected: C 55.47, H 7.05, N 3.92. Found: C 55.80, H 7.05, N 4.06.

ν_{max} (thin film) = 2962 (C-H_{alkane} stretching), 1483 (C-H_{alkane} bending), 1456 (C-H_{alkane} bending), 1363 (C=C_{aromatic} bending), 1126 (C-O stretching).

9.7.1.4 [Au(IPr^{Cl})(Bpin)]

Following the general procedure [Au(OH)(IPr^{Cl})] (100.00 mg, 0.15 mmol) was dissolved in anhydrous methanol (1 mL). B₂pin₂ (41.60 mg, 0.16 mmol) and benzene (2 mL) was charged into the vial. [Au(IPr^{Cl})(Bpin)] was obtained as a white crystalline solid in 56% yield (65.00 mg).

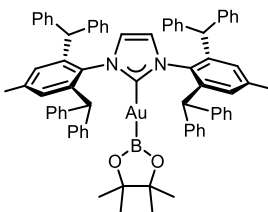
¹H NMR (400 MHz, benzene-d₆): δ (ppm) = δ 7.12-7.08 (m, 3H, CH_{Ar}), 7.02-7.00 (m, 3H, CH_{Ar}), 2.67 (sep, *J* = 7.3 Hz, 4H, CH_(IPr)), 1.53 (d, *J* = 7.5 Hz, 12H, (CH₃(IPr))), 1.10 (d, *J* = 7.5 Hz, 12H, CH₃(IPr)), 0.96 (s, 12H, CH₃(Bpin)).

¹³C {¹H} NMR (100 MHz, benzene-d₆): δ (ppm) = δ 216.5 (C_{carbene}), 146.3 (C_{Ar}), 131.7 (C_{Ar}), 131.3 (C_{Ar}), 128.6 (C_{Ar}), 124.4 (C_{Ar}), 119.2 (CH_{Ar}), 80.0 (C_{Bpin}), 29.5 (CH₃(Bpin)), 25.7 (CH₃(Bpin)), 25.0 (CH₃(IPr)), 23.4 (CH₃(IPr)).

¹¹B NMR (400 MHz, benzene-d₆): δ (ppm): 50.99.

Elemental analysis: Expected: C 50.72, H 5.93, N 3.59. Found: C 50.81, H 5.86, N 3.59.

v_{max} (thin film) = 2960 (C-H_{alkane} stretching), 1583 (C-H_{alkane} bending), 1463 (C-H_{alkane} bending), 1372 (C=C_{aromatic} bending), 1128 (C-O stretching), 850 (C-Cl stretch).

9.7.1.4 [Au(IPr^{*})(Bpin)]

Following the general procedure [Au(OH)(IPr^{*})] (100.00 mg, 0.09 mmol) was dissolved in anhydrous methanol (2 mL). B₂pin₂ (24.60 mg, 0.097 mmol) and benzene (5 mL) was charged into the vial. [Au(IPr^{*})(Bpin)] was obtained as a white crystalline solid in 70% yield (76.00 mg).

¹H NMR (400 MHz, benzene-d₆): δ (ppm) = δ 7.82-7.80 (m, 4H, CH_{Ar}), 7.41-7.37 (m, 6H, CH_{Ar}), 6.99 (br.s., 35H, CH_{Ar}), 5.84 (s, 2H, CH_(IPr*)), 5.58 (s, 2H, CH_(IPr*)), 1.54 (s, 6H, CH₃(IPr^{*})), 1.15 (s, 12H, CH₃(Bpin)).

¹³C {¹H} NMR (100 MHz, benzene-d₆): δ (ppm) = δ 215.0 (C_{carbene}), 143.9 (C_{Ar}), 143.2 (C_{Ar}), 141.3 (C_{Ar}), 140.1 (C_{Ar}), 134.6 (CH_{Ar}), 130.7 (CH_{Ar}), 130.3 (CH_{Ar}), 129.7 (CH_{Ar}), 128.7 (CH_{Ar}), 127.6 (CH_{Ar}),

126.6 (CH_{Ar}), 126.4 (CH_{Ar}), 123.2 (CH_{Ar}), 110.1 (CH_{Ar}), 79.9 (C_{Bpin}), 51.3 (CH_{Imid}), 25.9 (CH_{3(Bpin)}), 20.9 (CH_{3(IPr*)}).

¹¹B NMR (400 MHz, benzene-d₆): δ (ppm): 49.26.

Elemental analysis: C₇₅H₆₉AuBN₂O₂ CH₂Cl₂: C 68.99 H 5.42 N 2.21. Found C 69.84 H 5.94 N 2.32

v_{max} (thin film) = 3059 (C-H_{alkane} stretching), 1598 (C-H_{alkane} bending), 1492 (C-H_{alkane} bending), 1444 (C=C_{aromatic} bending), 1105 (C-O stretching).

9.7.2 Preliminary experiments

[Au(IPr)(Bpin)] (0.11 mmol, 8.00 mg) was transferred to a NMR tube inside the glovebox, benzene-d₆ was added followed by R (0.11 mmol). The NMR tube was stirred for 5 min, and then a ¹H NMR spectrum was recorded. The NMR tube was heated to 60 °C for 16 h, and then a ¹H NMR was recorded.

R = *p*-tolylaldehyde (0.011 mmol, 1.35 mg)

R = diphenylacetylene (0.11 mmol, 2.00 mg)

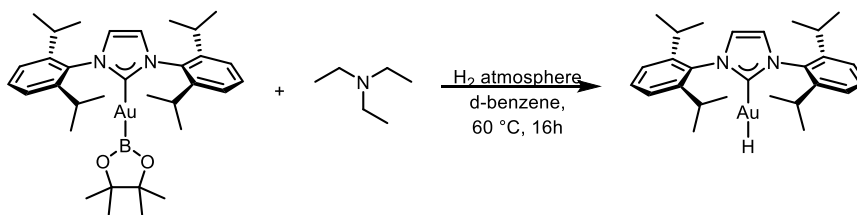
R = phenylacetylene (0.11 mmol, 1.90 mg)

R = styrene (0.11 mmol, 1.00 mg)

9.7.2.1 *In situ* experiment with *p*-tolylaldehyde:

[Au(IPr)(OH)] (0.11 mmol, 7.00 mg) was transferred to a vial and anhydrous methanol (0.5 mL) was added. The solvent was removed under reduced pressure at 50 °C. This was repeated 4 times. The vial was transferred to the glovebox where benzene-d₆ (0.4 mL) was added followed by B₂pin₂ (0.01 mmol, 3.12 mg) and *p*-tolylaldehyde (0.11 mmol, 1.30 mg). The mixture was transferred to a NMR tube and the tube was shaken for 5 min. The first ¹H NMR spectrum was taken. Next the tube was heated to 50 °C for 1.30 h. Second ¹H NMR was taken. Next the NMR tube was heated to 60°C for 16 h. The third NMR spectrum was taken. The solution changed colour from colourless to reddish/brown.

No change in ¹H NMR spectra observed

9.7.3 Activation of H₂

In the glovebox, [Au(IPr)(Bpin)] and triethylamine were added to a J Young NMR tube followed by benzene-d₆.

A ¹H NMR spectrum was recorded and no change was observed. The J Young NMR tube was exposed to H₂ via freeze pumping 3 times on the Schlenk line, no change was observed via ¹H NMR spectroscopy. Then the tube was heated to 60 °C for 16 h. No change was observed for reaction a), b) and c). A new complex was observed for reaction d). [AuH(IPr)] was synthesised quantitatively. The reaction mixture was concentrated and washed with pentane. [AuH(IPr)] was isolated in 97% yield (5.00 mg).

Table S-62: Activation of H₂

Entry		Mr	Mass	Moles	Equiv.
	[Au(IPr)(Bpin)]	713.54 mg/mol	7.00 mg	0.009 mmol	1.00
a)	NEt ₃	101.19 mg/mol	0.50 mg	0.0045 mmol	0.50
b)	NEt ₃	101.19 mg/mol	1.00 mg	0.009 mmol	1.00
c)	NEt ₃	101.19 mg/mol	2.00 mg	0.019 mmol	2.00
d)	NEt ₃	101.19 mg/mol	2.70 mg	0.027 mmol	3.00

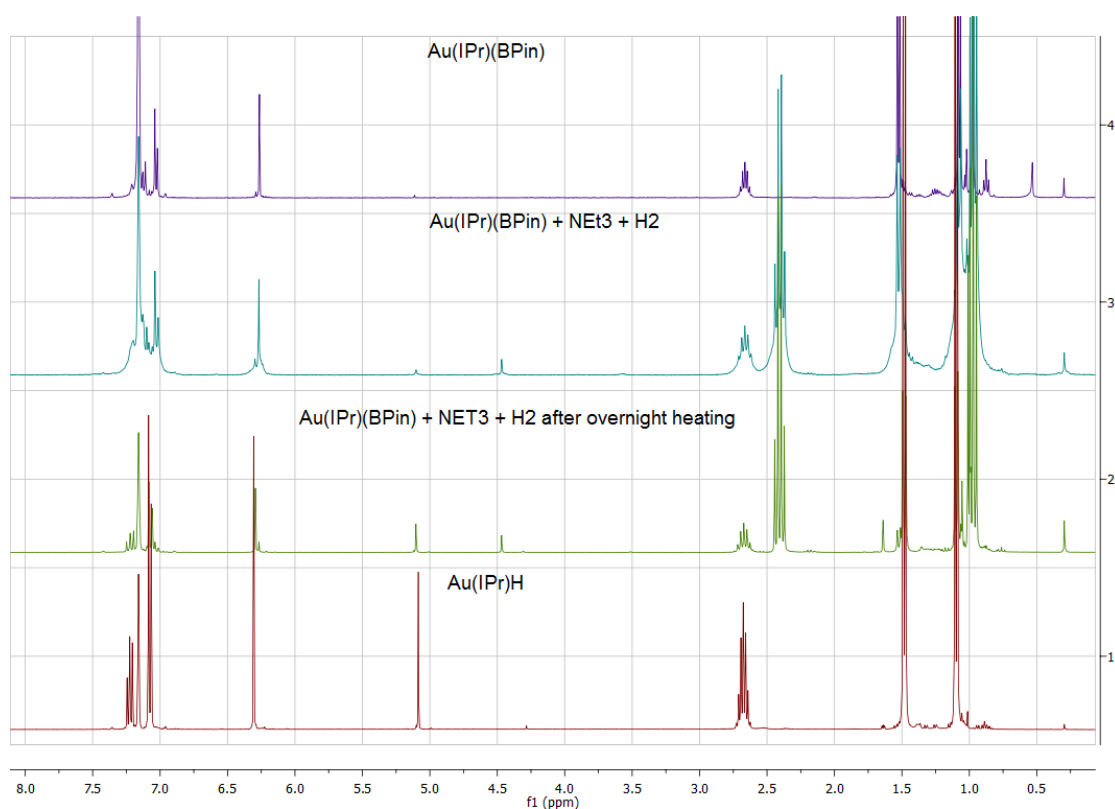


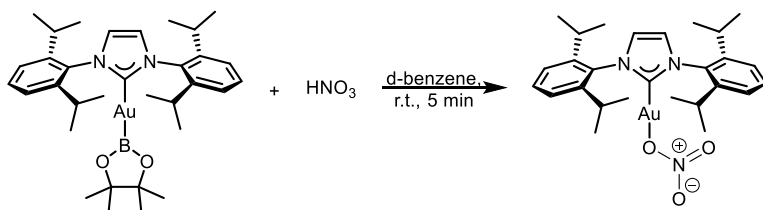
Figure S-1: ^1H NMR spectra of the activation of H_2

9.7.3.1 [AuH(IPr)]

^1H NMR (400 MHz, benzene- d_6): δ (ppm) = δ 7.24 (t, $J = 7.9$ Hz, 2H, CH_{Ar}), 7.09 (d, $J = 7.9$ Hz, 4H, CH_{Ar}), 6.31 (s, 2H, CH_{imid}), 5.09 (s, 1H, Au-H), 2.70 (sept., $J = 7.4$ Hz, 4H, CH_{IPr}), 1.49 (d, $J = 6.8$ Hz, 12H, $\text{CH}_3(\text{IPr})$), 1.11 (d, $J = 6.4$ Hz, 12H, $\text{CH}_3(\text{IPr})$).

^{13}C $\{^1\text{H}\}$ NMR (100 MHz, benzene- d_6): δ (ppm) = δ 204.5 ($\text{C}_{\text{carbene}}$), 145.9 (C_{Ar}), 135.1 (C_{Ar}), 130.5 (CH_{Ar}), 124.1 (CH_{Ar}), 122.4 (CH_{Ar}), 29.1 (CH_{IPr}), 25.0 ($\text{CH}_3(\text{IPr})$), 23.9 ($\text{CH}_3(\text{IPr})$).

Analytical data obtained is in agreement with literature.⁵⁷

9.7.4 Reaction with HNO₃

In the glovebox, [Au(IPr)(Bpin)] (10.00 mg, 0.01 mmol) and HNO₃ (0.88 mg, 0.01 mmol) were added to a J Young NMR tube followed by benzene-d₆. The tube was shaken for 5 min at room temperature.

¹H NMR spectrum was recorded and a new complex was detected. The crude mixture was concentrated and washed with hexane. The solid was identified as [Au(IPr)(ONO₂)], which is in agreement with the literature.⁵⁸ The complex was isolated in 98% yield (8.80 mg). The hexane filtrate was concentrated and identified as B₂pin₂.

[Au(IPr)(ONO₂)]

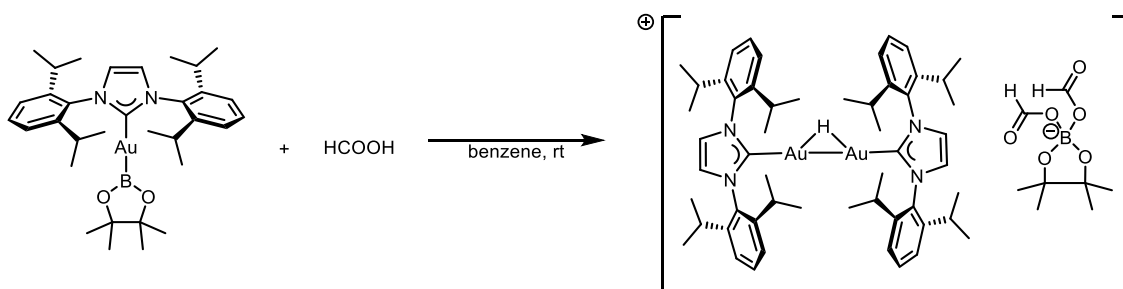
¹H NMR (400 MHz, benzene-d₆): δ (ppm) = δ 7.16-7.10 (m, 2H, CH_{Ar}), 7.03 (d, *J* = 12.4 Hz, 4H, CH_{Ar}), 6.27 (s, 2H, CH_{Imid}), 2.45 (sept, *J* = 8.7 Hz, 4H, CH_{IPr}), 1.36 (d, *J* = 7.8 Hz, 12H, CH_{3(IPr)}), 1.04 (d, *J* = 7.8 Hz, 12H, CH_{3(IPr)}).

¹³C {¹H} NMR (100 MHz, benzene-d₆): δ (ppm) = δ 175.3 (C_{carbene}), 164.7 (C_{Ar}), 145.7 (C_{Ar}), 134.1 (CH_{Ar}), 133.7 (CH_{Ar}), 131.1 (CH_{Ar}), 130.9 (CH_{Ar}), 124.5 (CH_{Ar}), 123.7 (CH_{Ar}), 123.2 (CH_{Ar}), 28.9 (CH_{3(IPr)}), 24.6 (CH_{3(IPr)}), 24.4 (CH_{3(IPr)}), 24.1 (CH_{3(IPr)}).

B₂pin₂

¹H NMR (400 MHz, benzene-d₆): δ (ppm) = δ 1.01 (s, 12H).

9.7.5 Reaction with HCOOH



In the glovebox, [Au(IPr)(Bpin)] (10.00 mg, 0.01 mmol) and HCOOH (1.90 mg, 0.04 mmol) were added to a J Young NMR tube followed by benzene-d₆. The reaction was monitored for 3 h. ¹H NMR were recorded after 5 min, 1 h, 2 h and 3 h. Crystals were grown using benzene in pentane.

¹H NMR (400 MHz, benzene-d₆): δ (ppm) = δ 13.33 (s, 2H_{formato}), 8.62 (s, 4H_{imid}), 7.31 (t, *J* = 8.4 Hz, 4H_{aryl}), 7.06 (d, *J* = 7.4 Hz, 8H_{aryl}), 2.44-2.40 (m, 8H_{IPr(CH)}), 1.25 (s, 10H_{IPr(CH₃)}), 1.16 (d, *J* = 7.2 Hz, 21H_{IPr(CH₃)}), 1.04-1.01 (m, 30H_{IPr and Bpin}).

¹³C {¹H} NMR (100 MHz, benzene-d₆): δ (ppm) = δ 186.5 (COH_{formato}), 164.8 (C), 145.7 (C), 133.6 (C), 131.1 (CH_{Ar}), 131.0 (CH_{Ar}), 124.7 (CH_{Ar}), 124.5 (CH_{Ar}), 124.4 (CH_{Ar}), 29.0 (CH_{IPr}), 28.9 (CH_{IPr}), 25.0 (CH_{3(IPr)}), 24.7 (CH_{3(IPr)}), 24.5 (CH_{3(IPr)}), 23.9 (CH_{3(IPr)}), 23.7 (CH_{3(IPr)}).

Elemental Analysis for C₃₃H₄₈AuBN₂O₂ 2CH₂Cl₂: C 49.24 H 6.00 N 3.59. Found C 49.55 H 6.04 N 3.60

V_{max} (thin film) = 2962.66 (C-H(OCOH)stretching), 1610.20 (C=O stretching), 1458.18 (CH₂ bending), 1384.89 (CH₃ bending), 1263.37 (C-O stretching).

9.7.5.1 Mechanistic studies

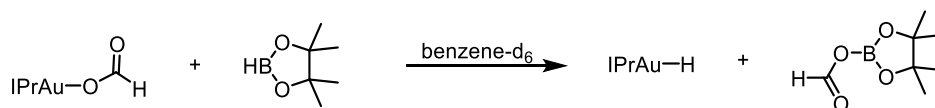
a)



Procedure: In the glovebox, [Au(IPr)H] (15 mg, 0.025 mmol) was transferred into a J-Young NMR tube, followed by HCOOH (1.2 mg, 0.025 mmol) in benzene-d₆ (0.5 mL). The NMR tube was shaken for 5 min and a ¹H NMR spectrum was taken, confirming the formation of [Au(IPr)(OCOH)].

¹H NMR (400 MHz, benzene-d₆): δ (ppm) = δ 9.23 (s, 1H, CH_{formato}), 7.18-7.16 (m, 2H, CH_{Ar}), 7.00 (d, *J* = 7.6 Hz, 4H, CH_{Ar}), 6.22 (s, 2H, CH_{imid}), 2.57 (sept, *J* = 6.5 Hz, 4H, CH_{IPr}), 1.45 (d, *J* = 7.6 Hz, 12H, CH_{3(IPr)}), 1.03 (d, *J* = 8.1 Hz, 12H, CH_{3(IPr)}).

b)

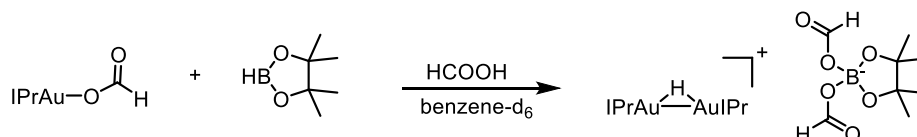


Procedure: In the glovebox, [Au(IPr)(OCOH)] (10 mg, 0.015 mmol) was transferred into a J-Young NMR tube, followed by 4,4,5,5-tetramethyl-1,3,2-dioxaborolane (HBpin) (2 mg, 0.015 mmol) in

benzene- d_6 (0.5 mL). The NMR tube was shaken and a ^1H NMR was taken, confirming the formation of $[\text{Au}(\text{IPr})\text{H}]$.

^1H NMR (400 MHz, benzene- d_6): δ (ppm) = δ 7.24 (t, $J = 7.9$ Hz, 2H, CH_{Ar}), 7.09 (d, $J = 7.9$ Hz, 4H, CH_{Ar}), 6.31 (s, 2H, CH_{imid}), 5.09 (s, 1H, Au-H), 2.70 (sept., $J = 6.4$ Hz, 4H, CH_{IPr}), 1.49 (d, $J = 6.8$ Hz, 12H, $\text{CH}_3(\text{IPr})$), 1.11 (d, $J = 6.4$ Hz, 12H, $\text{CH}_3(\text{IPr})$).

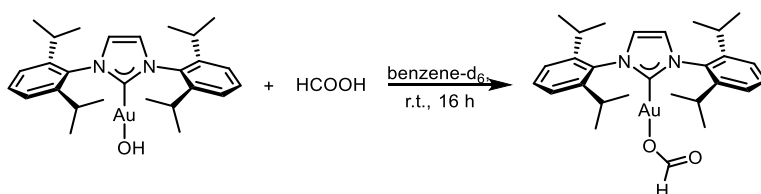
c)



Procedure: In the glovebox, $[\text{Au}(\text{IPr})(\text{OCOH})]$ (20 mg, 0.032 mmol) was transferred into a J-Young NMR tube, followed by HBpin (4 mg, 0.032 mmol) and benzene- d_6 (0.5 mL). Afterwards, HCOOH (2.9 mg, 0.032 mmol) was added. The NMR tube was shaken and a ^1H NMR was taken after 16 h, confirming the formation of $[\text{Au}_2(\text{IPr})_2(\mu\text{-H})][(\text{OCOH})_2\text{Bpin}]$.

^1H NMR (400 MHz, benzene- d_6): δ (ppm) = δ 13.33 (s, $2\text{H}_{\text{formato}}$), 8.62 (s, 4H_{imid}), 7.31 (t, $J = 8.4$ Hz, 4H_{aryl}), 7.06 (d, $J = 7.4$ Hz, 8H_{aryl}), 2.44-2.40 (m, $8\text{H}_{\text{IPr}(\text{CH})}$), 1.25 - 1.01 (m, $60\text{H}_{\text{IPr and Bpin}}$).

9.7.7 Synthesis of $[\text{Au}(\text{IPr})(\text{OCOH})]$ from $[\text{Au}(\text{IPr})(\text{OH})]$



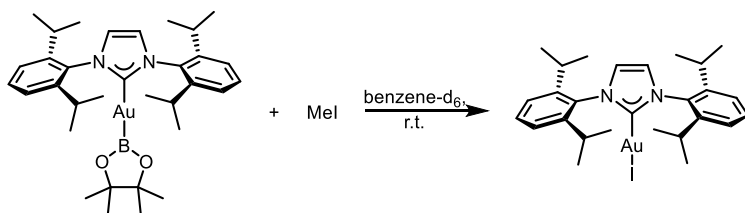
Outside the glovebox $[\text{Au}(\text{IPr})(\text{OH})]$ (200.00 mg, 0.33 mmol) was added to a round bottom flask, followed by formic acid (12.50 μL , 0.33 mmol). The mixture was dissolved in anhydrous toluene (50 mL) and left to stir for 16 h. The crude product was concentrated and washed with pentane. $[\text{Au}(\text{IPr})(\text{OCOH})]$ was obtained as a white powder in 92% isolated yield (192.00 mg).

^1H NMR (400 MHz, benzene- d_6): δ (ppm) = δ 9.26 (s, 1H, $\text{CH}_{\text{formato}}$), 7.21-7.19 (m, 2H, CH_{Ar}), 7.04 (d, $J = 8.2$ Hz, 4H, CH_{Ar}), 6.25 (s, 2H, CH_{imid}), 2.55 (sept., $J = 8.7$ Hz, 4H, CH_{IPr}), 1.48 (d, $J = 7.5$ Hz, 12H, $\text{CH}_3(\text{IPr})$), 1.06 (d, $J = 8.2$ Hz, 12H, $\text{CH}_3(\text{IPr})$).

^{13}C $\{^1\text{H}\}$ NMR (100 MHz, benzene- d_6): δ (ppm) = δ 175.6 (COH), 168.4 (C), 166.7 (C), 145.8 (C), 134.1 (CH_{Ar}), 130.9 (CH_{Ar}), 124.4 (CH_{Ar}), 123.3 (CH_{Ar}), 123.2 (CH_{Ar}), 29.0 (CH_{IPr}), 24.6 ($\text{CH}_3(\text{IPr})$), 24.5 ($\text{CH}_3(\text{IPr})$), 24.2 ($\text{CH}_3(\text{IPr})$).

ν_{max} (thin film) 2960 (O-H stretch), 1641 (C=O stretch), 1469 (O-H bend).

9.7.9 Reactions with MeI



9.7.9.1 Time optimisation

Inside the glovebox, [Au(IPr)(Bpin)] (50.00 mg, 0.07 mmol) was added to a NMR tube, followed by methyl iodide (9.95 mg, 0.07 mmol) and the mixture was dissolved in benzene-d₆ (0.6 mL).

¹H NMR spectra were taken over 16 h.

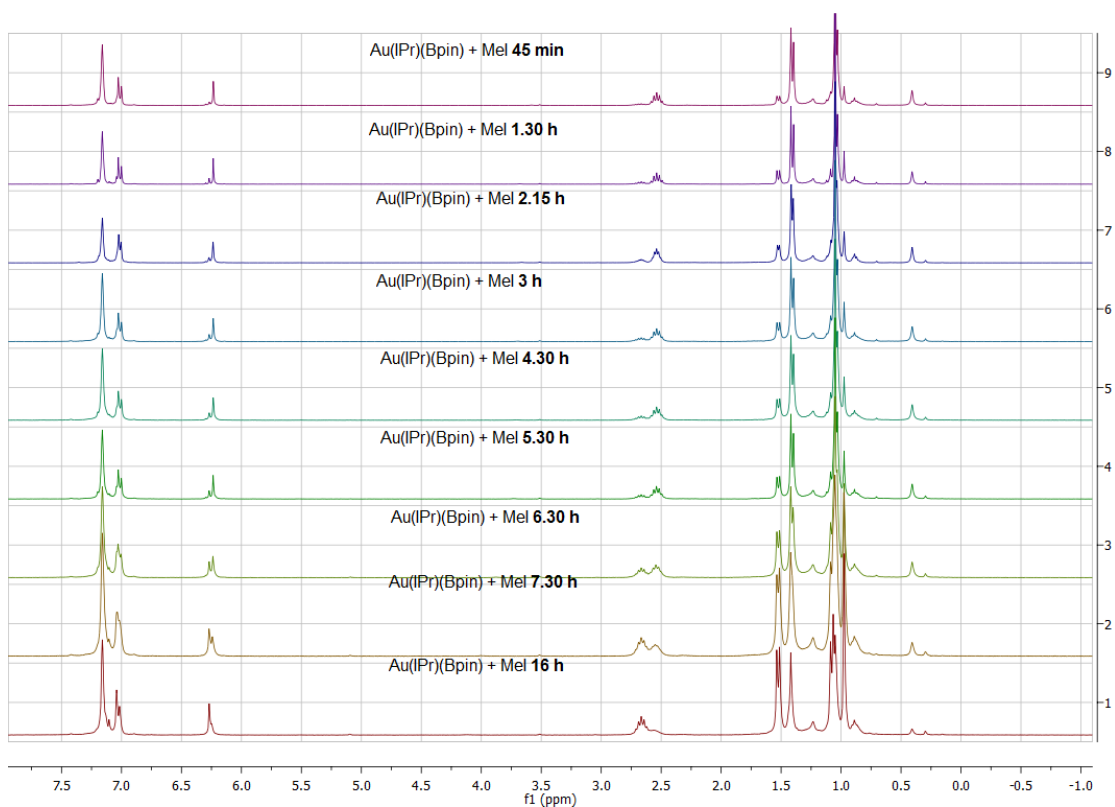
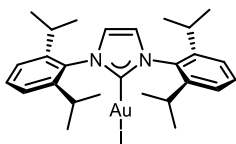


Figure S-2: Time optimisation of [Au(IPr)].

The crude mixture was concentrated and washed with pentane. ¹H NMR of the solid was recorded and identified as [Au(IPr)].

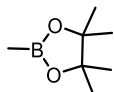
[Au(IPr)]



^1H NMR (400 MHz, benzene- d_6): δ (ppm) = δ 7.20-7.18 (m, 2H, CH_{Ar}), 7.03 (t, $J = 7.8$ Hz, 4H, CH_{Ar}), 6.23 (s, 2H, CH_{Imid}), 2.55 (sept, $J = 6.8$ Hz, 4H, $\text{CH}_{(\text{IPr})}$), 1.42 (d, $J = 6.8$ Hz, 12H, $\text{CH}_3(\text{IPr})$), 1.05 (d, $J = 7.5$ Hz, 12H, $\text{CH}_3(\text{IPr})$).

^{13}C { ^1H } NMR (100 MHz, benzene- d_6): δ (ppm) = δ 187.3 ($\text{C}_{\text{carbene}}$), 145.7 (C_{Ar}), 134.3 (C_{Ar}), 131.0 (C_{Ar}), 124.4 (CH_{Ar}), 122.4 (CH_{Ar}), 82.8 (CH_{Imid}), 29.0 (CH_{IPr}), 25.0 ($\text{CH}_3(\text{IPr})$), 24.7 ($\text{CH}_3(\text{IPr})$), 24.0 ($\text{CH}_3(\text{IPr})$). This is in agreement with the literature.⁵⁹

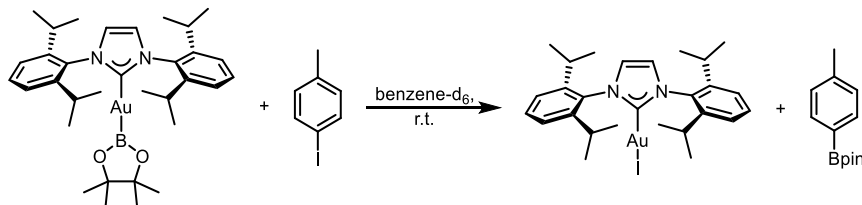
2,4,4,5,5-pentamethyl-1,3,2-dioxaborolane



^1H NMR (400 MHz, benzene- d_6): δ (ppm) = δ 1.05 (s, 12H, CH_3), 0.39 (s, 3H, CH_3)

NMR analysis was in agreement with a commercially available sample.

9.7.10 Reaction with tolyl iodide



Outside the glovebox [Au(IPr)(Bpin)] (10.00 mg, 0.01 mmol) was added to a NMR tube, followed by methyl iodide (6.10 mg, 0.03 mmol) and the mixture was dissolved in benzene- d_6 (0.6 mL). The reaction was left to stir for 48 h in air. The crude product was concentrated and washed with pentane. ^1H NMR spectrum of the solid was recorded and the compound identified as [Au(IPr)].

[Au(IPr)]

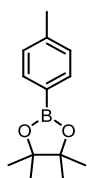
^1H NMR (400 MHz, benzene- d_6): δ (ppm) = δ 7.20-7.18 (m, 2H), 7.02 (d, $J = 8.1$ Hz, 4H), 6.23 (s, 2H), 2.55 (sept, $J = 9.2$ Hz, 4H), 1.42 (d, $J = 6.9$ Hz, 12H), 1.05 (d, $J = 6.8$ Hz, 12H)

This is in agreement with the literature.⁵⁹

9.7.10.1 Catalytic borylation of tolyl iodide

Outside the glovebox, a vial was charged with [Au(NHC)(Bpin)] (5 mol%), iodotoluene (55.00 mg, 0.25 mmol), B₂pin₂ (95.00 mg, 0.38 mmol), NaOMe (21.00 mg, 0.38 mmol), THF (1 mL), a magnetic stirring bar and sealed with a septum cap. The reaction was stirred at room temperature (24 °C) for 16 h. A sample was taken and analysed via GC analysis and the conversion was based on iodotoluene. No side products were detected via GC analysis and NMR analysis.

4,4,5,5-tetramethyl-2-(p-tolyl)-1,3,2-dioxaborolane



Chemical Formula: C₁₃H₁₉BO₂
Molecular Weight: 218.10

¹H NMR (400 MHz, CDCl₃): δ (ppm) = δ 7.75 (d, *J* = 7.6 Hz, 2H), 7.21 (d, *J* = 7.7 Hz, 2H), 2.39 (s, 3H), 1.37 (s, 12H).

¹³C {¹H} NMR (100 MHz, CDCl₃): δ (ppm) = δ 141.5 (C_{Ar}), 134.9 (CH_{Ar}), 128.6 (CH_{Ar}), 83.7 (C_{Bpin}), 25.0 (CH_{3(Bpin)}), 21.8 (CH₃).

Table S-62: Preliminary results for the catalytic borylation of tolyl iodide.

Entries	[Au(NHC)(Bpin)] (mol%)	GC conversion (%)
1	[Au(IPr)(Bpin)] (5 mol%)	n.r.
2	[Au(IPr ^{Cl})(Bpin)] (5 mol%)	n.r.
3	[Au(IPr*)(Bpin)] (5 mol%)	6.
4	[Au(SIPr)(Bpin)] (5 mol%)	99
5	[Au(SIPr)(Bpin)] (3 mol%)	62
6	[Au(SIPr)(Bpin)] (1.5 mol%)	53

GC conversion was based on 4-iodotoluene, average of two runs.

9.7.11 Computational analysis

Results were obtained by Laura Falivene and Luigi Cavallo

Computational details. Dissociation free energies have been calculated using the Gaussian09 package. The BP86 GGA functional of Becke and Perdew was used. Geometry optimizations were performed with the standard split-valence basis set with a polarization function of Ahlrichs and coworkers for H, C, N, O, F and B atoms (SVP keyword in Gaussian), while the quasi relativistic small-core Stuttgart effective core potential (ECP) was used for Gold (SDD keyword in Gaussian09). The reported free energies have been obtained via single point energy calculations with the triple- ζ basis set of Ahlrichs for H, C, N, O, F and B atoms (TZVP keyword in Gaussian09). Solvent effects, CH₂Cl₂, were included using the PCM method. The dissociation free energies reported have been computed as the free energy difference between the fully optimized IPr-Au-L (L = BPin, F, OH) complexes and the optimized fragments corresponding to IPr-Au⁺ and L⁻ fragments for the gold-anion bond, and to the IPr and Au-L fragments for the gold-IPr bond.

To have a better understanding of the bonding in the three complexes, energy decomposition analysis (EDA) has been performed using the Amsterdam Density Functional (ADF) program. The analysis was performed starting from the ADF optimized structure of the IPr-Au-L complexes, by rigid fragmentation of the complex. The electronic configuration of the molecular systems was described by a triple- ζ STO basis set with a polarization function (ADF basis set TZP). Relativistic effects have been included via ZORA approximation. The local exchange-correlation potential by Vosko *et al.*, augmented in a self-consistent manner with Becke's exchange gradient correction and Perdew's correlation gradient correction, was used in this analysis.

The energy decomposition analysis (EDA) has been performed computing the bond snapping energy (BSE) corresponding to the interaction of two rigid fragments that both possess the local equilibrium geometry of the final molecule and which both have an electronic structure suitable for bond formation.

Although BSE does not always correlate with the bond dissociation enthalpies, since reorganization and relaxation of the fragments are not taken into account, BSE is closely related to bond enthalpy terms, which in turn provide a good approximation to bond strength values. In addition, BSE can be decomposed into two main components, namely steric interaction ΔE_0 and orbital interaction ΔE_{int} (eqn (1)):

$$BSE = -[\Delta E_0 + \Delta E_{int}] \quad (1)$$

The steric interaction term ΔE_0 can be split further into an electrostatic interaction term ΔE_{Elstat} and a Pauli repulsion term ΔE_{Pauli} , which is directly related to the two-orbital electron interactions between occupied orbitals on both interacting fragments (eqn (2)):

$$\Delta E_0 = \Delta E_{Elstat} + \Delta E_{Pauli} \quad (2)$$

where ΔE_{Elstat} constitutes a stabilizing contribution to BSE, ΔE_{Pauli} constitutes a destabilizing contribution, and it is the relative size of electrostatic interaction and Pauli repulsion that determines the overall character of the steric interaction term.

The total orbital interaction energy ΔE_{int} can be broken down further into contributions from the orbital interactions within the various irreducible representations τ of the overall symmetry group of the system (eqn (3)):

$$\Delta E_{int} = \sum_{\tau} \Delta E_{int}^{\tau} \quad (3)$$

All the molecules studied in the present work possess C_s symmetry; the NHC and the BPin ligands are located in the σ_{xy} mirror plane of the molecule. Therefore, A' contributions to the orbital interaction energy are associated with σ -bonding and A'' contributions represent π -bonding. The A' and A'' contributions of the orbital interaction energy are further divided into both σ/π -donation and σ/π -backdonation.

In order to estimate these interactions, additional constrained space orbital variation (CSOV) calculations have been performed. In particular, to assess the contribution of σ/π -donation, the bond decomposition analysis was performed by again considering the interaction of the fragments, but now excluding the set of virtual a' and a'' orbitals of the ligand from the variational space. This way, the A'/A'' contribution of the orbital interaction energy can be associated only with the ligand to metal fragment donation. Similarly, the amount of σ/π -backdonation is determined explicitly excluding all virtual a' and a'' orbitals on the [Au] fragment.

Results. As a first step, we calculated the accurate dissociation free energy in CH_2Cl_2 of both the anionic ligand L (L = BPin⁻, F⁻, OH⁻) and of IPr from the IPr-Au-L systems. The energy to dissociate the anionic ligand L increases in the order F (212 kJ/mol) < OH (263 kJ/mol) < BPin (376 kJ/mol). Conversely, the energy to dissociate IPr decreases upon moving from F⁻ to OH⁻ to BPin⁻, with 272, 236 and 105 kJ/mol, respectively. These results indicate that BPin⁻ is a ligand clearly

different from F^- and OH^- , and that it remarkably weakens the Au-IPr bond. To have a better understanding of the differences between the Au-BPin and the Au-F and Au-OH bonds, as well as of the different impact of $BPi\bar{n}$ on the Au-IPr bond compared to that of F^- and OH^- , we performed an energy decomposition analysis (EDA).

In these calculations, the geometry of the metal fragment is kept rigid and we calculated the heterolytic BSE, which means fragmenting the complex into cationic $[IPr-Au]^+$ and anionic $[BPi\bar{n}]^-$ fragments. As expected, electrostatic interaction is the most important attractive bonding force, since the fragments are ions. The total steric interaction ΔE_0 is stabilizing, indicating that the attractive electrostatic interaction overcompensates the Pauli repulsive term (-1740 vs. +1320 kJ/mol). The orbital term is mainly constituted by σ interaction consisting for the 60% of filled molecular orbitals on the ligand interacting with empty orbitals on the metal (ligand-to-metal σ -donation), the remaining 40% deriving from interaction of filled molecular orbitals on the metal interacting with empty orbitals on the ligand (metal-to-ligand σ -backdonation). As regard the smaller in magnitude π interaction, it is ascribed both to donation from the ligand to the metal (55%) and to the retro-donation from the metal to the ligand (45%). Overall the bond strength of 837 kJ/mol is almost 50%-50% shared between the steric and orbital terms (-420 vs -417 kJ/mol).

Table C-1. Bond decomposition analysis (in kJ/mol) of the (IPr)Au-L and IPr-Au(L) bonds for L = BPin, F, OH.

	(IPr)Au-BPin	(IPr)Au-F	(IPr)Au-OH	IPr-Au(BPin)	IPr-Au(F)	IPrAu(OH)
ΔE_{elstat}	-1740	-800	-947	-619	-923	-882
ΔE_{Pauli}	1320	408	547	670	887	877
ΔE_0	-420	-392	-399	52	-36	-5
$\Delta E_{int}(\sigma)$	-366	-243	-276	-188	-264	-249
$\Delta E_{int}(\pi)$	-52	-62	-81	-34	-71	-71
ΔE_{int}	-418	-305	-357	-222	-335	-320
BSE	-838	-696	-756	-170	-371	-325

As comparison, we considered the IPr-Au-F and the IPr-Au-OH systems and we performed the BSE analysis of the Au-F and Au-OH bond, see Table C-1. The data reported in Table C-1 indicate that the decreased strength of the Au-X (X= F, OH) bond, 696 and 756 kJ/mol, compared with the Au-BPin bond, 838 kJ/mol, is mainly ascribed to the much lower orbital interaction term ΔE_{int} , which is 113 and 61 kJ/mol weaker for the Au-F and the Au-OH bonds, respectively, while the steric term ΔE_0 is substantially the same for both systems (oscillating in a 20 kJ/mol window). Interestingly, despite of the similar magnitude in ΔE_0 , the ΔE_{elstat} and ΔE_{Pauli} components of ΔE_0

are remarkably lower in the Au-F and Au-OH bonds, which indicates that these bonds are less polarized than the Au-BPin bond.

This result is confirmed by the Hirshfeld charge analysis showing a charge of -0.71 and -0.38e on F and OH, respectively, versus a charge of -0.82e on BPin. Correspondingly, the positive charge on Au is larger in the F and OH systems (0.75 and 0.52e for X = F and OH, respectively) than in the BPin system (0.83e). As for the orbital interaction term, the π contribution is marginally larger in the Au-F and Au-OH system, while the σ term is clearly larger in the Au-BPin complex due to the strong σ -back-donation [Au] \rightarrow ligand (the first empty σ orbital on Bin⁻ is clearly more stable than that on F⁻ and OH⁻). Overall, these results suggest that the increased strength of the Au-BPin bond is a consequence of its high ionic character, leading to stronger electrostatic interaction, and of increased orbital interaction correlated to a stronger σ -backdonation from the metal to the ligand.

Moving to the Au-IPr bond, we performed a bond decomposition analysis fragmenting the complex into the neutral Au[L] and [IPr] fragments. The BSE analysis shows the opposite trend relative to that reported for the Au-BPin/FL bond. In fact, the Au-IPr bond is 200 and 155 kJ/mol stronger in the Au-F and Au-OH systems, relative to the Au-BPin system. The clearly weaker IPr-Au bond in presence of BPin is almost equally distributed in the overall steric interaction term ΔE_0 and the overall orbital interaction term ΔE_{int} . In the following we report the HOMO and LUMO analysis, see Figure C-1.

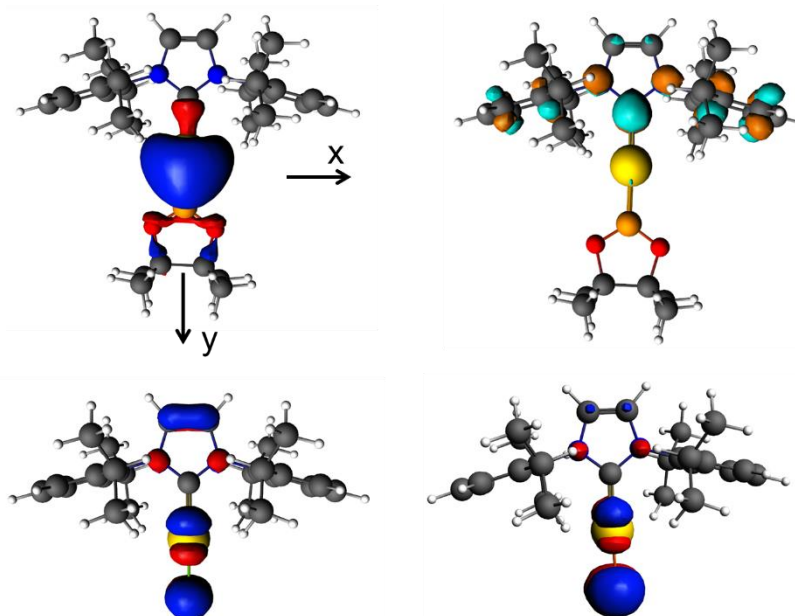


Figure C-1. Images of HOMO and LUMO for IPr-Au-BPin at top and of HOMO for IPr-Au-F (on the left) and IPr-Au-OH (on the right) at bottom.

The LUMO arising from the NHC π moiety, with contribution of orbitals on the aryl N-substituents, is almost identical for the three systems. As an example, the LUMO of the IPr-Au-BPin system is reported in Figure 1. Moving to the HOMO, the Au-F and Au-OH complexes differ significantly from the Au-BPin one. The Au contribution is clearly higher in the BPin system, 47.6% vs 31.5% and 19.4% in the F and OH systems, respectively. The orbitals involved are the Au $d_{x^2-y^2}$, mainly, with a small contribution from the Au d_{z^2} for the BPin system, and the HOMO results in a strong bonding interaction from the Au center to the O-B-O moiety, with the B atom mainly participating with the s and p_y orbitals. Differently, in the F and OH complexes the HOMO corresponds to an antibonding interaction between the Au d_{yz} and the p_z of F and OH.

References:

- (1) N. Marion, O. Navarro, J. Mei, E. D. Stevens, N. M. Scott and S. P. Nolan, *J. Am. Chem. Soc.*, **2006**, *128*, 4101–11.
- (2) M. S. Viciu, O. Navarro, R. F. Germaneau, R. A. K. Iij, W. Sommer, N. Marion, E. D. Stevens, L. Cavallo and S. P. Nolan, *Organometallics*, **2004**, *23*, 1629–1635.
- (3) A. Chartoire, M. Lesieur, L. Falivene, A. M. Z. Slawin, L. Cavallo, C. S. J. Cazin and S. P. Nolan, *Chem. Eur. J.*, **2012**, *18*, 4517–21.
- (4) N. Marion, O. Navarro, J. Mei, E. D. Stevens, N. M. Scott and S. P. Nolan, *J. Am. Chem. Soc.*, **2006**, *128*, 4101–4111.
- (5) S. Dierick, D. F. Dewez and E. Marko, *Organometallics*, **2014**, *33*, 677–683.
- (6) S. Meiries, G. Le Duc, A. Chartoire, A. Collado, K. Speck, K. S. Athukorala Arachchige, A. M. Z. Slawin and S. P. Nolan, *Chemistry*, **2013**, *19*, 17358–68.
- (7) G. Bastug and S. P. Nolan, *Organometallics*, **2014**, *33*, 1253–1258.
- (8) F. Izquierdo, C. Zinser, Y. Minenkov, D. B. Cordes, A. M. Z. Slawin, L. Cavallo, F. Nahra, C. S. J. Cazin and S. P. Nolan, *ChemCatChem*, **2017**, 1–12.
- (9) P. R. Melvin, A. Nova, D. Balcells, W. Dai, N. Hazari, D. P. Hruszkewycz, H. P. Shah and M. T. Tudge, *ACS Catal.*, **2015**, *5*, 3680–3688.
- (10) F. Izquierdo, M. Corpet and S. P. Nolan, *European J. Org. Chem.*, **2015**, 1920–1924.
- (11) S. Ando, H. Matsunaga and T. Ishizuka, *J. Org. Chem.*, **2017**, acs.joc.6b02666.
- (12) J.-S. Ouyang, Y.-F. Li, F.-D. Huang, D.-D. Lu and F.-S. Liu, *ChemCatChem*, **2018**, *10*, 371–375.
- (13) P. Petiot and A. Gagnon, *European J. Org. Chem.*, **2013**, 5282–5289.

- (14) V. Ramakrishna, M. J. Rani and N. D. Reddy, *European J. Org. Chem.*, **2017**, 2017, 7238–7255.
- (15) L. Y. Xu, C. Y. Liu, S. Y. Liu, Z. G. Ren, D. J. Young and J. P. Lang, *Tetrahedron*, **2017**, 73, 3125–3132.
- (16) M. R. Yadav, M. Nagaoka, M. Kashihara, R.-L. Zhong, T. Miyazaki, S. Sakaki and Y. Nakao, *J. Am. Chem. Soc.*, **2017**, jacs.7b03159.
- (17) Y. Zou, G. Yue, J. Xu and J. Zhou, *European J. Org. Chem.*, **2014**, 2014, 5901–5905.
- (18) K. Yasamut, J. Jongcharoenkamol, S. Ruchirawat and P. Ploypradith, *Tetrahedron*, **2016**, 72, 5994–6000.
- (19) L. Niu, H. Zhang, H. Yang and H. Fu, *Synlett*, **2014**, 25, 995–1000.
- (20) M. A. Zolfigol, T. Azadbakht, V. Khakyzadeh, R. Nejatyami and D. M. Perrin, *RSC Adv.*, **2014**, 4, 40036.
- (21) H. Firouzabadi, N. Iranpoor, M. Gholinejad, S. Akbari and N. Jeddi, *RSC Adv.*, **2014**, 4, 17060.
- (22) A. R. Hajipour, F. Rezaei and Z. Khorsandi, *Green Chem.*, **2017**, 19, 1353–1361.
- (23) S. Meiries, K. Speck, D. B. Cordes, A. M. Z. Slawin and S. P. Nolan, *Organometallics*, **2013**, 32, 330–339.
- (24) R. D. Hreha, Y.-D. Zhang, B. Domercq, N. Larribeau, J. N. Haddock, B. Kippelen and S. R. Marder, *Synthesis (Stuttg.)*, **2002**, 1201–1212.
- (25) M. Pompeo, J. L. Farmer, R. D. J. Froese and M. G. Organ, *Angew. Chem. Int. Ed.*, **2014**, 53, 3223–3226.
- (26) A. Rühling, L. Rakers and F. Glorius, *ChemCatChem*, **2017**, 9, 547–550.
- (27) A. K. Mishra, A. Verma and S. Biswas, *J. Org. Chem.*, **2017**, 82, 3403–3410.
- (28) B. J. Tardiff and M. Stradiotto, *European J. Org. Chem.*, **2012**, 3972–3977.
- (29) D. C. Samblanet and J. A. R. Schmidt, *J. Organomet. Chem.*, **2012**, 720, 7–18.
- (30) X. B. Lan, Y. Li, Y. F. Li, D. S. Shen, Z. Ke and F. S. Liu, *J. Org. Chem.*, **2017**, 82, 2914–2925.
- (31) X. Ding, M. Huang, Z. Yi, D. Du, X. Zhu and Y. Wan, *J. Org. Chem.*, **2017**, 82, 5416–5423.
- (32) C. Deldaele and G. Evano, *ChemCatChem*, **2016**, 8, 1319–1328.
- (33) Y. He, F. Wang, X. Zhang and X. Fan, *Chem. Commun.*, **2017**, 53, 4002–4005.
- (34) J. A. Fernández-Salas, E. Marelli, D. B. Cordes, A. M. Z. Slawin and S. P. Nolan, *Chem. Eur. J.*, **2015**, 21, 3906–3909.
- (35) C. C. C. J. Seechurn, S. L. Parisel and T. J. Colacot, *J. Org. Chem.*, **2011**, 76, 7918–7932.
- (36) O. Navarro, N. Marion, Y. Oonishi, R. A. Kelly and S. P. Nolan, *J. Org. Chem.*, **2006**, 71,

- 685–692.
- (37) J. Li and Z.-X. Wang, *Org. Biomol. Chem.*, **2016**, *14*, 7579–7584.
- (38) S. M. Raders, J. M. Jones, J. G. Semmes, S. P. Kelley, R. D. Rogers and K. H. Shaughnessy, *European J. Org. Chem.*, **2014**, *2014*, 7395–7404.
- (39) U. I. Tessin, X. Bantreil, O. Songis and C. S. J. Cazin, *Eur. J. Inorg. Chem.*, **2013**, 2007–2010.
- (40) N. Sun, M. Chen, L. Jin, W. Zhao, B. Hu, Z. Shen and X. Hu, *Beilstein J. Org. Chem.*, **2017**, *13*, 1735–1744.
- (41) X. Li, X. Gong, Z. Li, H. Chang, W. Gao and W. Wei, *RSC Adv.*, **2017**, *7*, 2475–2479.
- (42) K. W. Quasdorf, A. Antoft-Finch, P. Liu, A. L. Silberstein, A. Komaromi, T. Blackburn, S. D. Ramgren, K. N. Houk, V. Snieckus and N. K. Garg, *J. Am. Chem. Soc.*, **2011**, *133*, 6352–6363.
- (43) F. M. Moghaddam, R. Pourkaveh and A. Karimi, *J. Org. Chem.*, **2017**, *82*, 10635–10640.
- (44) A. K. Yadav and K. N. Singh, *New J. Chem.*, **2017**, *41*, 14914–14917.
- (45) K. Kanagaraj and K. Pitchumani, *Chem. Eur. J.*, **2013**, *19*, 14425–14431.
- (46) L. N. R. Maddali and S. Meka, *New J. Chem.*, **2018**, *42*, 4412–4418.
- (47) S. Sadjadi, *Appl. Organomet. Chem.*, **2018**, 1–16.
- (48) Z. Y. Tian, S. M. Wang, S. J. Jia, H. X. Song and C. P. Zhang, *Org. Lett.*, **2017**, *19*, 5454–5457.
- (49) S. N. Jadhav, A. S. Kumbhar, S. S. Mali, C. K. Hong and R. S. Salunkhe, *New J. Chem.*, **2015**, *39*, 2333–2341.
- (50) A. G. Krishna Reddy and G. Satyanarayana, *Synth.*, **2017**, *49*, 5149–5158.
- (51) E. Buxaderas, D. a. Alonso and C. Nájera, *European J. Org. Chem.*, **2013**, *2013*, 5864–5870.
- (52) H. Zhong, J. Wang, L. Li and R. Wang, *Dalton Trans.*, **2014**, *43*, 2098–103.
- (53) O. S. Morozov, A. F. Asachenko, D. V. Antonov, V. S. Kochurov, D. Y. Paraschuk and M. S. Nechaev, *Adv. Synth. Catal.*, **2014**, *356*, 2671–2678.
- (54) D. Xu, Q. Sun, Z. Quan, X. Wang and W. Sun, *Asian J. Org. Chem.*, **2018**, *7*, 155–159.
- (55) E. Buxaderas, D. A. Alonso and C. Nájera, *RSC Adv.*, **2014**, *4*, 46508–46512.
- (56) X. F. Wei, X. W. Xie, Y. Shimizu and M. Kanai, *J. Am. Chem. Soc.*, **2017**, *139*, 4647–4650.
- (57) E. Y. Tsui, P. Müller and J. P. Sadighi, *Angew. Chem. Int. Ed.*, **2008**, *47*, 8937–8940.
- (58) M. Brill, F. Nahra, A. Gómez-Herrera, C. Zinser, D. B. Cordes, A. M. Z. Slawin and S. P. Nolan, *ChemCatChem*, **2017**, *9*, 117–120.

- (59) N. H. C. N-heterocyclic, X. Cl, O. Santoro, A. Collado, A. M. Z. Slawin, S. P. Nolan and C. S. J. Cazin, *Chem. Commun.*, **2013**, 49, 10483–10485.